BERGISCHE
UNIVERSITÄT
WUPPERTAL

Multiobjective Optimization in the Parameterization of Gas Heating Devices

Dissertation
zur Erlangung des Doktorgrades (Dr. rer. nat.)
Fakultät für Mathematik und Naturwissenschaften
Bergische Universität Wuppertal

vorgelegt von
Tobias Suszka

Wuppertal, Oktober 2024

Acknowledgments

I would like to express my appreciation to my supervisor Kathrin Klamroth who provided invaluable support and infinite patience and I am truly grateful for her inspiration and guidance. My sincere thanks also go to the Vaillant GmbH for their financial support of this project. I am particularly grateful to Matthias Stursberg who initiated the cooperation with Vaillant and made this project possible. Furthermore, I would like to express my deepest gratitude to Thomas Ernst whose expertise and knowledge were invaluable during this dissertation. I would also like to recognize Michael Stiglmayr for being the second reviewer and Britta Efkes for providing the Latex template for this dissertation.
Lastly, I would like to mention the people who supported me outside of academia. I am grateful to Patrick Bruseberg. His way of seeing things in a positive light has always built me up. I also thank Morre for always having a caffeinated drink ready for me. Last but not least, I would like to extend my deepest gratitude to Yvonne. Your unwavering support and encouragement have been invaluable to me throughout this journey. Thank you for your love and for always being by my side.

Contents

List of Tables iii

List of Figures iii

Abbreviations and Acronyms v

1. Introduction 1

I. Technical and Mathematical Foundations 5

2. Technical Background 7
2.1. Basics of Control Theory . . . 7
2.2. Basics of Combustion . . . 9
2.3. Combustion Control System IoniDetect . . . 11
2.4. Mathematical Heat Engine Model . . . 18

3. ADA: Automatic Drift Adaption 29
3.1. Modeling of Drift . . . 29
3.2. The Notion of ADA . . . 37
3.3. Sequence of ADA Iterations . . . 43
3.4. Plurality of ADA Pairs . . . 46
3.5. Goal of This Thesis: Optimize ADA Parameters . . . 51

4. Basic Mathematical Concepts 53
4.1. Multiobjective Optimization . . . 53
4.2. Evolutionary Multiobjective Optimization . . . 61
4.3. Fixed Point Iteration Procedures . . . 69

II. Mathematical Analysis of ADA 77

5. Mathematical Formulation of ADA 79
5.1. Formalism: Required Sets and Functions . . . 80
5.2. The ADA Algorithm . . . 86

6. ADA Procedure with a Single ADA Pair **91**
6.1. Ioni Current Based ADA Algorithm with a Single ADA Pair 91
6.2. Resistance Based Iteration Function with a Single ADA Pair 94
6.3. Convergence Characteristics of the Picard Iteration Associated to the Drift Resistance Iteration Function 102
6.4. Conclusion of Analysis with Respect to a Single ADA Pair 113

7. ADA Procedure with a Plurality of ADA Pairs **115**
7.1. The Super Fixed Point Vector 116
7.2. Resistance Based Approach 124
7.3. Convergence Characteristics of the ADA Algorithm with a Plurality of ADA Pairs 139
7.4. Approximation Quality: Relation Between the Drift Resistance and the Super Fixed Point Vector 150
7.5. Conclusion and Considerations for Optimization 157

III. Optimization of the ADA Parameters **159**

8. Optimization Models **161**
8.1. Description of the ADA Optimization Problem 162
8.2. Convergence Related Requirements 166
8.3. Optimization Objective: Fast Rate of Convergence 174
8.4. Conflicting Objectives: Small L^p Versus a Small Start Point Increment of ADA Pair p 179
8.5. Constraints 186
8.6. Optimization Model for the Nominal Case Without Tolerances 192
8.7. Optimization Model for the Case with Tolerances 197
8.8. Comparison of the Two Optimization Models 209

9. Solving the ADA Optimization Problems **211**
9.1. Solving the Nominal ADA Optimization Problem 211
9.2. Solving the ADA Optimization Problem with Tolerances 228

10. Conclusion **239**

Bibliography **243**

A. Examples with Respect to the ADA Iteration Functions **247**

List of Tables

9.1. Aggregated Objective Function Values Versus Individual Objective Function Values 236

List of Figures

2.1. Closed-loop and Open-loop Control 8
2.2. Basic Feedback Control System 9
2.3. CO Emission Versus Equivalence AFR 11
2.4. Principle of Ionization Current Measurement 12
2.5. Basic Principle of the IoniDetect Combustion Control 14
2.6. Ioni Current Setpoints 15
2.7. λ-Target Curve and Control Curve 17
2.8. Extended Concept of IoniDetect Combustion Control 18
2.9. Brennfeld Static Signals 20
2.10. Ioni Current Versus GVP and Equivalence AFR Versus GVP 21
2.11. CO Emission Versus GVP 22

3.1. Equivalence Circuit Diagram of the Ioni Current Measurement Circuit . . 30
3.2. Impact of Drift 36
3.3. Selection of Start Point and Test Point 39
3.4. Approximation of the Start Point's GVP 40
3.5. Approximation of the Drifted Test Ioni Current 41
3.6. Impact of Drift Adaption 42
3.7. Drift Resistance Approximation Function 48
3.8. Overlapping ADA Pairs 50

4.1. Pareto Dominance 55
4.2. Connected Pareto Front 57
4.3. Nondominated Sorting in Combination with Crowding Distance Operator 68

5.1. Drift Resistance Approximation at the Start Fan Speeds 83

6.1. Impact of Tolerances with Respect to the Position of the Ioni Electrode . 104
6.2. Impact of Tolerances on the ADA Iteration Function's Fixed Point 105

8.1. Impact of Start Ioni Current on Start Equivalence AFR 181
8.2. Impact of Start Ioni Current on Lipschitz Constant of Iteration Function 184

9.1. Exemplary Objective Functions of Scalarized Problem 221
9.2. Decision and Objective Space for the Case $p = 2$ in the Use Case Without Tolerances 224
9.3. Decision and Objective Space for the Case $p = 1$ in the Use Case Without Tolerances 226
9.4. Objective Space in the Use Case with Tolerances 235
9.5. Nondominated Sets from Two Different Runs with NSGA-II 237

Abbreviations and Acronyms

AC alternating current. 12

ADA automatic drift adaption. 1, 7, 13, 29

AFR air-fuel ratio. 9

CDP constrained dominance principle. 68, 232

CHT constraint handling technique. 68, 232

CO carbon monoxide. 10

DC direct current. 30

DM decision maker. 161

ERC electronic fuel/air ratio control system. 13

GA genetic algorithm. 61

HE heat engine. 13

ioni ionization. 12

MOO multiobjective optimization. 53, 54

NSGA-II Nondominated Sorting Genetic Algorithm-II. 3, 61, 240

SBX simulated binary crossover. 62

1. Introduction

Common heating systems in Germany are gas-fired boilers, oil heaters, heat pumps and biomass heating systems [BDH24]. The heating system with the largest market share are gas-fired condensing boilers. For instance, gas-fired condensing boilers had a market share of over 50 percent in the German market for heating systems in 2023 [BDH23]. The global market leader in the field of central heating is the Vaillant Group [Vai24]. The Vaillant Group is a family-owned German company with its headquarters in Remscheid. The German brand of the Vaillant Group is Vaillant. In 2019, Vaillant presented its new generation of gas-fired condensing boilers. The centerpiece of these boilers is Vaillant's combustion control system IoniDetect [Wic19]. A core element of IoniDetect is the so-called automatic drift adaption (ADA) procedure, which makes sure that the appliances operate with a high combustion quality [LS17].
This study is conducted in cooperation with Vaillant and investigates the ADA procedure from a mathematical point of view. ADA is an iterative procedure and requires a set of parameters, the so-called ADA parameters or ADA pairs. The aim of this work is to find optimized ADA parameters by computer simulation and optimization. This chapter gives an introduction to this thesis by briefly presenting the ADA procedure, stating the research problem, the research aims and the research questions as well as the significance of the topic. Finally, the scope of this work is briefly outlined.

In IoniDetect, flame ionization is used to control combustion, which is the state of the art [Car+18, p. 49]. Flames are ionized and thus they have an electric conductivity. This conductivity depends on the gas/air-mixture, which allows indirect control of the gas/air-mixture. For this purpose, an electrode is placed inside the flames that measures the flames' conductivity. However, flames are a hostile environment for the electrode and an oxide layer accrues on the electrode's surface during boiler operation. This additional oxide layer alters the measurement of the flames' conductivity and the gas/air-mixture cannot be properly controlled anymore. Therefore, a steady self-recalibration of the system is required that adapts to the accrued oxide layer [Car+18]. One solution to this problem is the ADA procedure [LS17]. The ADA procedure requires two operating points, the so-called start point and test point, which are both specified by a fan speed and an electric current. These four values (two fan speeds and two currents) constitute a so-called ADA pair.

Suitable ADA pairs must be selected for each "boiler class" so that the ADA procedure can work as desired. Typically, five to seven ADA pairs are specified for each "boiler class" [Sch15, p. 35]. However, the documentation of the IoniDetect system provides only little information on how to select suitable ADA pairs. Some particularities with respect to

the selection of the fan speeds of the test points are stated in [Sch15]. A more detailed description of the selection of the ADA pairs as well as a corresponding theoretical reasoning are provided in [Loc18]. However, in [Loc18] only the special case with a single ADA pair for the situation without tolerances is considered. Therefore, the theoretical understanding of the ADA procedure can be considered as incomplete. Accordingly, in practice, the ADA parameters are selected based on experience as well as by trial and error in the lab. These approaches are time consuming and do not guarantee that the selected ADA parameters are optimal with respect to the rate of convergence of the ADA procedure and under the influence of tolerances. In contrast, a systematic approach to the ADA parameterization as well as the application of computer simulations can considerably save development time and supports the identification of close to optimal ADA parameters.

The aim of this work is to provide such a systematic approach to the ADA parameterization. To achieve this, the following research objectives are considered:

- To provide an algorithmic formulation of the ADA procedure and a corresponding mathematical framework.
- To analyze the convergence properties of the ADA procedure.
- To state what optimal ADA parameters are and to formulate corresponding optimization problems.
- To propose methods for solving the ADA optimization problems.

The following research questions are addressed in this thesis:

- What are conditions that guarantee convergence of the ADA procedure to a desired limit with a high rate of convergence?
- How can these convergence conditions be modeled in an optimization problem?
- What are suitable methods to solve the proposed optimization models?

The analysis of the ADA procedure in this thesis contributes to the understanding of its convergence properties. It is shown that the basic ADA procedure with a single ADA pair implements the Picard iteration fixed point procedure. According to Banach's fixed point theorem, its convergence properties are closely related to the corresponding iteration function's Lipschitz constant. However, in the general ADA procedure with a plurality of ADA pairs, the Picard iteration is not applicable anymore, because the ADA pairs influence each other in a certain sense. The corresponding convergence analysis is rather complicated, but it is still possible to derive conditions that guarantee convergence of the ADA procedure with a plurality of ADA pairs. Another result of this analysis is that tolerances with respect to the ioni electrode's position usually alter the convergence characteristics of the ADA procedure. In particular, such tolerances might cause that the limit of the ADA procedure

is outside of a desired tolerance band, i.e., the corresponding gas appliance might leave the region of feasible combustion states.
Furthermore, this work shows that optimizing the ADA pairs is a multiobjective problem, i.e., in general we have conflicting objectives when optimizing the ADA pairs. To put it simply, a high rate of convergence of the ADA procedure is conflicting with a short duration of a single ADA iteration. Considering the multiobjective aspect of the ADA optimization problem allows the decision makers to select the solution that fits their preferences best.
It is proposed to solve the ADA optimization problem with respect to tolerances with the Nondominated Sorting Genetic Algorithm-II (NSGA-II), which is demonstrated in a use case. Therefore, this work also contributes an example for the application of NSGA-II in practice.
In total, this work provides both, a thorough theoretical understanding of the ADA procedure from a mathematical point of view as well as a support for the ADA parameterization problem in practice.

Note that this thesis focuses on the algorithmic part of the ADA procedure. Other aspects that also have an effect on the ADA procedure, such as the material of the ionization electrode, are not in the scope of this work. Furthermore, this work is based on measurement data provided by Vaillant. As a consequence, some aspects of modeling the combustion process are already predetermined. For instance, the provided measurement data is based on static signals and thus the dynamic behavior of the gas appliances is disregarded to a certain degree.

This thesis is divided into three parts. Part I lays the technical and mathematical foundations required for this work. The technical and combustion related backgrounds are presented in Chapter 2. In Chapter 3, the ADA procedure is presented based on technical documentation provided by Vaillant and Siemens. The latter is the company where the ADA procedure was invented [LS17]. In Chapter 4, the required mathematical concepts are presented. These are multiobjective optimization, evolutionary multiobjective optimization and fixed point iteration procedures.
Part II thoroughly analyzes the ADA procedure from a mathematical point of view. For this, a required formalism is first introduced and then used to formulate the ADA Algorithm 5.2 in Chapter 5. This algorithm is then analyzed for the special case that a single ADA pair is considered in Chapter 6. The general case with a plurality of ADA pairs is considered in Chapter 7.
In Part III, optimization problems for the ADA parameterization and methods to solve these problems are proposed based on the analysis in the preceding part. In Chapter 8, two ADA optimization problems are proposed. One problem for the case without tolerances and one problem for the case with tolerances. Finally, suitable methods for solving these problems are presented in Chapter 9 and demonstrated in a use case.

Remark 1.1 *To help readers to keep a better overview on the notation used in this thesis, a notation cheat sheet is included with the printed version of this work as a bookmark. In the digital version, the notation cheat sheet can be found at the very end of the document.*

Remark 1.2 *If not otherwise stated, all vectors in this thesis are row vectors.*

Part I.

Technical and Mathematical Foundations

2. Technical Background

This thesis is about the optimization of the ADA parameters with computer simulation. ADA is a part of the combustion control system IoniDetect from Vaillant. This chapter is intended to provide the necessary technical basics to describe and understand the ADA procedure. First, some basic concepts of control theory and combustion are explained. Then the combustion control system IoniDetect is presented. Finally, a mathematical model is presented for modeling gas appliances with IoniDetect.
While some details and data of this chapter are confidential, we present most of the axis labeling in figures without any numbers. Every graph presented in this chapter is created with linearly interpolated measurement data provided by Vaillant.

2.1. Basics of Control Theory

This section provides the basic concepts and terms of control systems that are required to describe and explain IoniDetect and ADA. In this thesis, 'control theory' refers to the engineering discipline. It does not refer to the mathematical branch 'optimal control theory'.
The definition of the term 'control system' is imprecise. Åström and Murray define control "to be the use of algorithms and feedback in engineered systems." [ÅM09, p. 3]. Doyle, Francis, and Tannenbaum state that "Control systems are what make machines, in the broadest sense of the term, function as intended." [DFT90, p. 1]. In this context, the machines are gas-fired heating devices and they function as intended if they satisfy a given heat demand while they combust gas at a desired operating point.
Control systems can be categorized as open loop and closed loop control [Wes06, p. 6]. A closed loop system contains a feedback loop, such that the controller gets information about the actual value of the machine's process variable. In this context the process variable conveys information about the combustion process. An open loop system does not contain such a feedback loop and the controller does not have any information about the process variable [ÅM09, p. 2]. In Figure 2.1, closed loop and open loop control are illustrated as block diagrams. IoniDetect is a closed loop control system and thus the focus of this section lies on such systems. Closed loop control is also referred to as feedback control.
In a minimalist setup, a feedback control system consists of three components, which are denoted as plant, controller and sensor. The plant is "the object that is to be controlled" [DFT90, p. 27], no matter if the object is a plant or something else. The controller is the entity that controls the plant. The sensor measures the plant's output and provides a

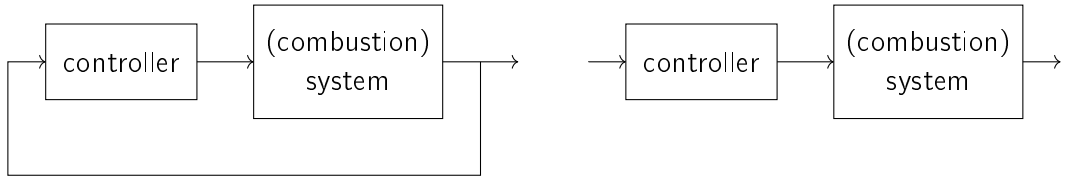

(a) Closed-loop (combustion) control (b) Open-loop (combustion) control

Figure 2.1.: In closed loop control there is a feedback loop that provides information about the current output of the (combustion) system to the controller. In open loop control this information is not available to the controller. Adapted from [ÅM09, p. 1].

feedback signal to the controller [Wes06, pp. 2–4], [DFT90, p. 27].
The plant usually contains one or more actuators. An actuator transforms the commands of the controller to physical actions [Wes06, p. 4]. For instance, the gas valve of a gas-fired heating device is an actuator. Depending on the controller's commands, it is moved to a more open or more closed position, which alters the gas volume flow and thus the combustion process.
As a real world machine a plant is prone to external disturbances. The goal of a feedback control system is that the output of the plant follows a desired reference signal and that external disturbances are compensated. The sensor measures the plant's output and provides it to the controller, which compares the sensor's output to the reference value. The difference between output and reference is called error. Depending on the error the controller determines a drive command for the actuators, such that (ideally) the absolute value of the error is reduced, i.e., the plant's output gets closer to the reference [ÅM09, p. 4].

Remark 2.1 *In this thesis, the value of a reference signal is referred to as* setpoint*, which is the term used by Vaillant.*

Because no sensor is perfect, every sensor is prone to noise. Therefore, sensor noise can be considered as an additional input of control systems [DFT90, p. 28]. This completes the basic setup of a feedback control system, which is shown in Figure 2.2.
The ADA procedure is related to the sensor and the sensor noise of the IoniDetect combustion control system. In this context, the plant is a gas-fired heating device, whose actuators are a fan and a gas valve. Its sensor is an electrode that is used to measure an electric current that depends on the gas flame in the heating device [Sch15, p. 7]. The electrode is positioned in the flames, which causes oxidation at the electrode. With increasing operation time an oxide layer builds up on the electrode, which alters the electrode's electrical characteristic and distorts the measured current. This distortion can be interpreted as sensor noise. But in contrast to white noise, this is not a stochastic phenomenon. It is rather a systematic sensor error of unknown size and the ADA procedure is intended to compensate this systematic error. The ADA procedure is described in Chapter 3. A mathematical formulation of the ADA procedure is provided in Chapter 5.

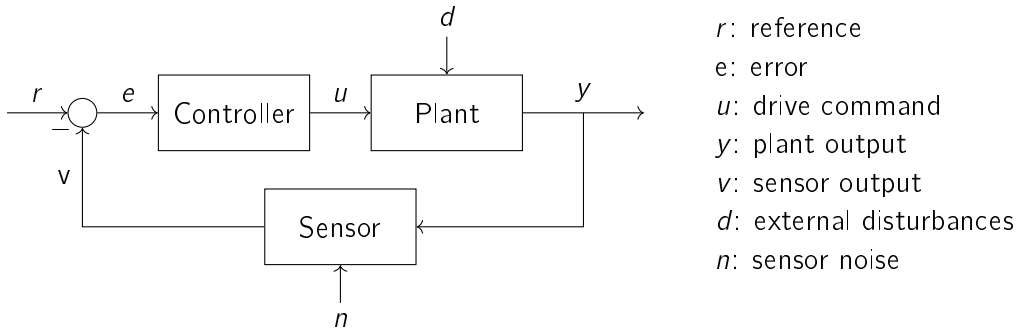

Figure 2.2.: Basic feedback control system. A sensor measures the plant's output y, which is compared to a given reference value r. Depending on the error $e := r - v$, the controller gives a drive command u to the plant's actuators, which influences the plant's output and closes the feedback loop. The plant and the sensor are prone to external influences, which are denoted by d and n, respectively. Adapted from [DFT90, p. 27].

Control system design deals with stability, robustness etc. These are not in the scope of this work. The IoniDetect control system and its design are considered as given.
For this thesis the notion of feedback control and the concept of the basic control system as shown in Figure 2.2 are relevant. The following section presents the basics of combustion theory related to gas-fired heating devices. Thereafter, combustion control based on ionization is explained.

2.2. Basics of Combustion

This section deals with the basics of combustion processes in gas-fired appliances. Because this thesis is about optimization and not about combustion, the level of detail is kept at a minimum. More detailed information can be found in the given references.
Combustion "is a complex sequence of chemical reactions between a fuel and oxygen" [Tan14, p. 59]. In gas-fired heating devices the fuel is usually natural gas or liquid petroleum gas [MCF11, p. 1]. But also hydrogen enriched natural gas is gaining in importance [Wis19]. The oxygen is provided by the ambient air [MCF11, p. 6].
The products of a combustion process depend on the mixture of fuel and oxygen, which is usually described by the air-fuel ratio (AFR) [Tan14, p. 60]. The following definition is taken from [Tan14, p. 59].

Definition 2.2 *The (mole) air-fuel ratio is defined by* $(A/F) := \frac{n_a}{n_f}$*, where* n_a *denotes the mole amount of air and* n_f *the mole amount of fuel.*

A particular mixture is the so-called stoichiometric mixture. It contains exactly the amount of fuel and air, such that fuel and oxygen are consumed completely during combustion [MCF11, p. 17].

Definition 2.3 *If a combustion process consumes all fuel and oxygen atoms, the mixture is called* stoichiometric. *The according AFR is denoted by* $(A/F)_s$.

In combustion engineering, it is useful and common to normalize the AFR by the stoichiometric AFR [MCF11, p. 20].

Definition 2.4 *The* equivalence air-fuel ratio *is defined by* $\lambda := \frac{(A/F)}{(A/F)_s}$.

Remark 2.5 *Combustion always requires fuel and oxygen. Therefore, the stoichiometric AFR* $(A/F)_s$ *is always greater than zero and no corresponding case distinction in the definition of* λ *is required. Furthermore, the equivalence AFR is dimensionless by construction.*

A distinction with respect to λ is made between the three following cases [Tan14, p. 60].

- The AFR is stoichiometric, i.e., $(A/F) = (A/F)_s \Leftrightarrow \lambda = 1$.
- The AFR is smaller than the stoichiometric AFR. Then we have $(A/F) < (A/F)_s \Leftrightarrow \lambda < 1$. This case is called *fuel rich combustion*, because some of the fuel atoms are not consumed during combustion and will be left.
- The AFR is larger than the stoichiometric AFR. Then we have $(A/F) > (A/F)_s \Leftrightarrow \lambda > 1$. This case is called *fuel lean combustion*, because some of the oxygen atoms are not consumed during combustion and will be left.

A combustion with a fuel rich mixture ($\lambda < 1$) has an excessive emission of carbon monoxide (CO) and some of the chemical energy contained in the fuel is not used and wasted [BK16, p. 444] [MCF11, p. 180]. Therefore, a fuel rich combustion is avoided. Theoretically, a stoichiometric AFR is sufficient and considered ideal [Tan14, p. 60]. But the mixture in a burning chamber is usually not absolutely homogeneous and some fuel molecules might not have reacted with oxygen. Thus an additional amount of air is required and the combustion process shall be fuel lean [BK16, p. 447], i.e., the equivalence AFR λ shall be greater than one.
On the other hand, if λ gets too large, the efficiency decreases again due to so-called exhaust gas losses [CL17, p. 119], i.e., the exhaust gas contains heat energy that is not used and released into the environment. In addition, the flame temperature decreases and as a consequence the emission of CO increases [MCF11, p. 180]. Furthermore, the flame length might get too large and the flame might hit the opposite wall of an appliance's heat exchanger. Then the temperature of the flame rapidly decreases, which also causes a large emission of CO [Mer+06, p. 118].
The emission of CO is critical, because inhaled CO is toxic for organisms and is lethal even at relatively low doses [MCF11, p. 177]. Figure 2.3 shows the curve of CO emission versus equivalence AFR for a certain constant air mass flow. The graph was created with linearly interpolated Vaillant measurement data and has the typical "inverted bell shape" [MCF11, p. 180]. Around $\lambda = 1.4$ the CO emission is low. But if the AFR gets more fuel lean or more fuel rich, the CO emission increases very fast.

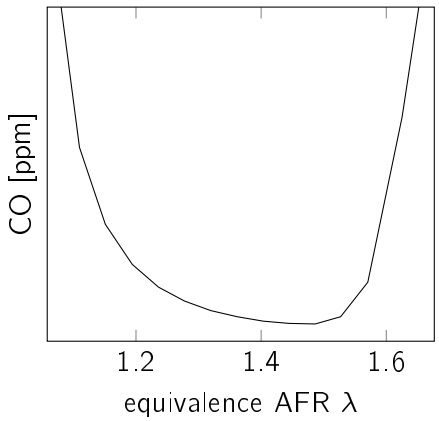

Figure 2.3.: The emission of CO versus the equivalence AFR at a constant air mass flow. Around $\lambda = 1.4$ the emission of CO is low. Outside the interval $[1.2, 1.55]$ the emission of CO increases very fast.

In addition to CO emissions, the flame speed and the flame temperature also depend on λ [MCF11, p. 122]. Furthermore, there are lower and upper flammability limits with respect to λ [MCF11, p. 125].
In summary, λ plays a central role in controlling and monitoring combustion [BK16, p. 448]. The desired equivalence AFR of gas-fired heating devices is usually $1.24 \leq \lambda \leq 1.44$ [CL17, p. 381]. Therefore, the amount of air and gas used for combustion has to be adjusted accordingly, which is usually done with a combustion control system.

2.3. Combustion Control System IoniDetect

Combustion control means controlling the mixture of fuel and air in order to obtain an optimal AFR. A common approach is an open loop control with pneumatic gas valves, where the air flow rate and the gas flow rate are pneumatically coupled. There is no feedback of the combustion process and the actual AFR is unknown. The gas valves are adjusted once during installation of the appliances to the prevailing conditions. If thereafter the gas quality changes, the appliances do not operate at an optimal AFR anymore [Kie+12, pp. 1, 2]. This is becoming problematic, because the gas quality is expected to fluctuate more and more [Kie+12, p. 2] [Car+18, p. 21]. A solution is a closed loop and gas adaptive combustion control. Measuring the AFR directly is expensive and not applicable in gas-fired appliances. Therefore, indirect methods were developed. There are mainly three approaches to closed loop combustion control. The most used and state of the art technology is based on ionization of the flame [Car+18, pp. 45, 49]. It is also used in the newest generation of Vaillant's gas-fired boilers. Vaillant's corresponding combustion control system is called IoniDetect [Wic19]. The ionization technology and IoniDetect are central for this thesis. They are described in more detail in the following subsections.

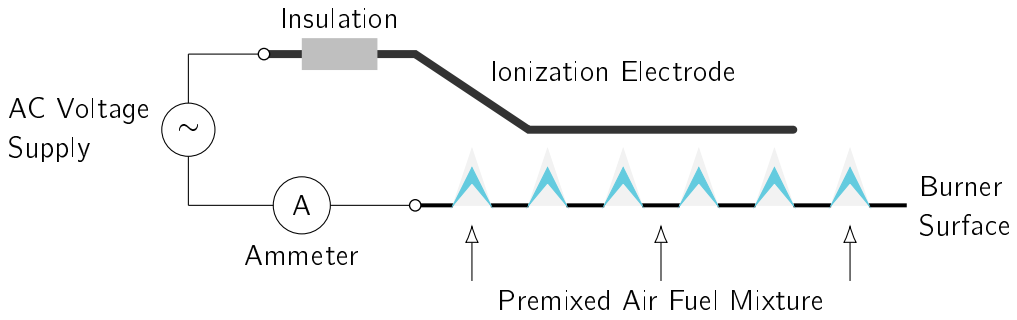

Figure 2.4.: Principle of ionization current measurement. An electrode is placed inside or close to the flames. An AC voltage supply is connected to this electrode and to the burner. Because flames have an electric conductivity the voltage results in an electric current that can be measured with an ammeter. Adapted from [Res19] and [Kie+12].

2.3.1. Combustion Control Based on Ionization

In *Compendium of Chemical Terminology* ionization is defined as "the generation of one or more ions" [Gol14]. Ions are atoms or particles "having a net electric charge" [Gol14, p. 759]. Ionization takes place in flames, i.e., free electrons and ions are generated in flames. Therefore, a flame has an electric conductivity and can become a part of an electric network [Res19, p. 7]. By applying a voltage across the flame an electric current flows through the flame and can be measured. This is the so-called ionization current [Kie+12, p. 3]. To measure the ionization current an electrode has to be placed inside or close to the flames. An alternating current (AC) voltage supply is connected to the electrode and to the burner. This electric circuit is closed by the flames and the applied voltage causes the ionization current, which can be measured. Figure 2.4 gives a schematic illustration of this principle.

Remark 2.6 *In an electric circuit flames are far more complex than a simple ohmic resistance. They have a rectifying behavior like a diode. Furthermore, they have a large resistance and the ionization current has a small magnitude. Therefore, specialized measurement setups with operational amplifiers are used to measure and process the ionization current [Loc16]. A thorough analysis of the physical and chemical processes inside flames and of their electric properties was done by Resch in her dissertation "Voruntersuchungen für eine mechatronische Produktentwicklung von elektronischen Gas-Luft-Verbünden" [Res19].*

Remark 2.7 *From now on ionization is abbreviated by ioni.*

The ioni current depends on several factors like the AFR and the load of the appliance [Kie+12, p. 3] [Res19, pp. 7, 8]. Therefore, it can be used as a feedback signal to control the mixture and thus the combustion process.
But the setup with an electrode positioned in the flames has a major drawback. Flames are a hostile environment for the material of the electrode. The electrode suffers from

oxidation and its electric properties change constantly. This process is also called *drift* of the electrode. Because of the electrode's drift a steady self-recalibration of the system is required [Car+18, pp. 42, 44]. The graph of ioni current versus λ has a characteristic shape. Oxidation of the electrode might shift this graph, but its shape stays similar. This is the basis for many self-recalibration methods [Car+18, p. 42].
Vaillant decided to use the Sitherm Pro combustion control concept by Siemens. In this thesis, Vaillant's term IoniDetect is used synonymously to Sitherm Pro. The self-recalibration method in IoniDetect is called automatic drift adaption (ADA) [Sch15]. ADA requires up to 28 parameters, that have to be determined for each heat engine (HE).

Remark 2.8 *The HE is the module of a Vaillant gas heating device that is responsible for the combustion. "The primary function of the heat engine ... is to combust gas in order to generate heat" [PHE]. Its main components are a heat exchanger, a gas valve, a fan, a burner, electrodes and an ignitor [PHE, Module Specification Peec Heat Engines].*
In contrast, a boiler, for example, also has a hydraulic for the central heating and a cover for mounting. In particular, different boilers can have the same heat engine. Some detailed schematic illustrations of a Vaillant boiler can be found in the dissertation of Resch [Res19, pp. 5, 6].

This thesis is about determining optimized ADA parameters. Therefore, the IoniDetect concept is described in detail in the following subsections. The ADA procedure is presented in Chapter 3.

2.3.2. Basic Concept of IoniDetect

In 2019 Vaillant presented its new generation of gas-fired condensing boilers, called ecoTEC exclusive. They use a combustion control based on ionization and are gas adaptive. Vaillant named their combustion control IoniDetect [Wic19]. The kernel of IoniDetect is Sitherm Pro by Siemens. The information presented in this section is based on the corresponding patent "Control Facility For a Burner System" [LS17] and on the Vaillant intern document *Konzept Sitherm Pro* [Sch15]. IoniDetect is used in premixed burners only [Sch15, p. 7]. In a premixed burner fuel and air are mixed first and thereafter the combustion takes place. The counterpart to premixed burners are diffusion burners, where no separate mixing of fuel and air takes place [CL17, p. 349].

Remark 2.9 *For completeness it is mentioned that IoniDetect is an electronic fuel/air ratio control system (ERC). In the European standard EN 12067-2:2022 an ERC is defined as a "closed loop system consisting of the electronic control unit, actuating elements for the fuel flow and the air flow as a minimum, and allocated feedback signal(s)" [Eur22, p. 9]. IoniDetect was developed in accordance with this standard and meets these requirements.*

The task of the IoniDetect control system is to adjust the mixture of gas and air such that two objectives are met. First, a given heat demand has to be satisfied. A higher heat demand requires more air and gas. A smaller heat demand, on the other hand, requires

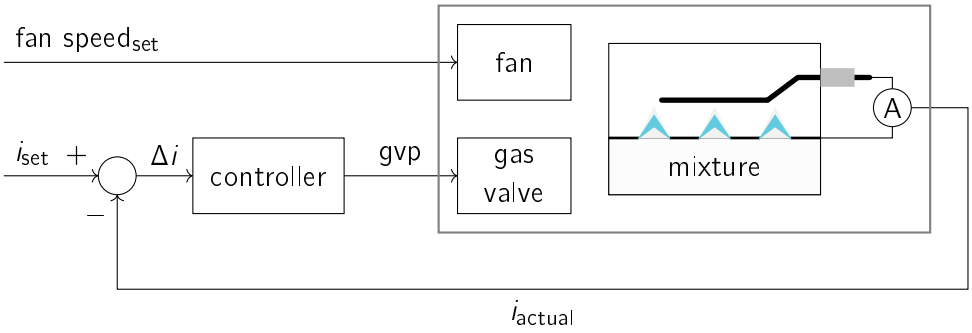

Figure 2.5.: Basic principle of the IoniDetect combustion control. Control of air volume flow and of gas volume flow is decoupled to a certain degree. The air volume flow is controlled by the fan speed. The gas volume flow is controlled with a feedback loop based on the ioni current. Illustration based on [Sch15, p. 7].

less air and gas. Second, the combustion process shall have an optimal AFR [Sch15, p. 7]. Note that both objectives can be met simultaneously.
The mixture is adjusted by IoniDetect via two actuators, which are a fan and a gas valve [Sch15, p. 7]. The fan delivers fresh air to the mixing chamber. The air volume flow depends on the fan speed. A larger fan speed usually results in a larger air volume flow. The gas volume flow, on the other hand, is controlled by the position of the gas valve. A more open position usually results in a larger gas volume flow.
In IoniDetect the two objectives satisfying a heat demand and keeping the combustion at the desired AFR are decoupled to a certain degree. The fan speed is linked to the heat demand, while the gas valve adjusts the AFR. An ioni electrode is used as a sensor to control the AFR [Sch15, p. 7]. The basic principle of the IoniDetect control system is shown in Figure 2.5. The gas valve position, and thus to a certain degree also the gas volume flow, is controlled with a feedback loop that is based on the ioni current. A desired ioni current setpoint i_{set} is compared to the actual current i_{actual}. A controller permanently attempts to drive the difference $\Delta i := i_{set} - i_{actual}$ to zero. It moves the gas valve according to the difference and the gas volume flow changes. This changes the mixture and thus also the AFR. A change in the AFR causes a change in the ioni current and the feedback loop is closed. The following example demonstrates this principle in more detail.

Example 2.10 *Let us assume a given heat demand and that the fan runs at the corresponding fan speed, which is denoted by* $\overline{\text{fs}}$ *in this example. Let* λ_{target} *be the desired equivalence AFR. Figure 2.6(a) shows the ioni current versus* λ *graph with the fan speed fixed at* $\overline{\text{fs}}$*. The setpoint is marked by the dot, which is the unique ioni current such that* λ *equals* λ_{target}*.*
Let us further assume that the combustion is not optimal and we have $\lambda_{actual} < \lambda_{target}$*, i.e., the mixture is too fuel rich. According to the curve in Figure 2.6(a), we have* $i_{actual} > i_{set}$ *in this case. Because* $\Delta i := i_{set} - i_{actual} < 0$*, the controller commands a more closed gas valve position and the gas volume flow decreases. Since the fan speed is still at* $\overline{\text{fs}}$*,*

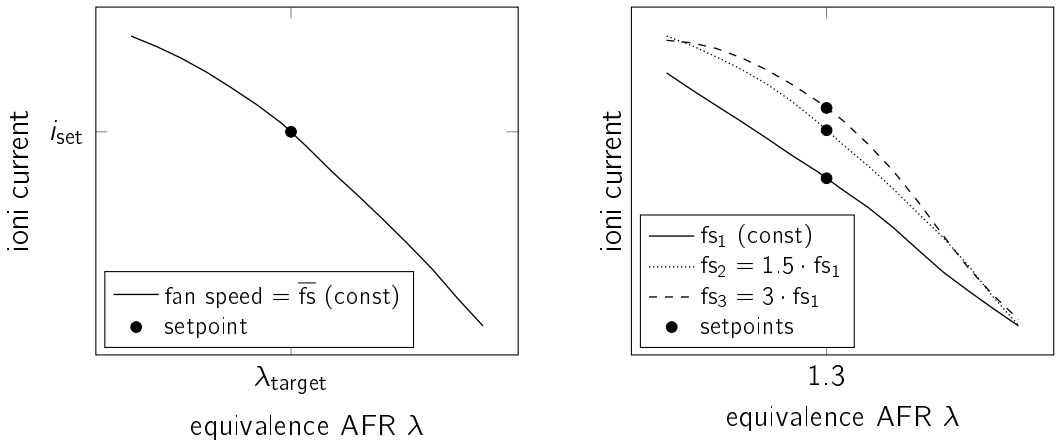

(a) The fan speed is fixed at $\overline{fs}$. There exists a unique ioni current setpoint for the given target λ.

(b) The target λ is assumed to be fixed at 1.3. If the fan speed changes, the ioni current setpoint also changes.

Figure 2.6.: The graphs are created with measurement data of the same Vaillant HE. Each curve contains (λ, ioni current) points with identical fan speed. The dots mark the setpoints for given target λ values at different fan speeds.

the air volume flow remains approximately unchanged, see also Remark 2.11 below. An unchanged amount of air and a decreased amount of gas result in an increased AFR, i.e., λ increases.
On the other hand, if the AFR is too large and therefore the ioni current is less than i_{set}, the gas valve is further opened and the AFR decreases.

Remark 2.11 *If the fan speed is constant, then the air volume flow is only approximately constant. It also depends on the amount of gas that is sucked through the gas valve into the mixing chamber and on pressure changes in the burner and the flue system [AR24, 0018].*
If several gas-fired boilers are connected to the same flue system, which is sometimes done to increase a system's heating power, there might be larger fluctuations in a boiler's air volume flow although its fan speed is constant. A safe combustion is not always guaranteed in such a situation. As a mitigation, Vaillant has developed heat engines based on IoniDetect that are equipped with a mass flow sensor to measure the air mass flow. In such a heat engine the air mass flow is the process variable and the fan speed is adjusted such that the air mass flow follows the desired air mass flow setpoints. This ensures safe combustion, even if several appliances are connected to the same flue system.
Note that for the remainder of this thesis we consider only heat engines that are not equipped with a mass flow sensor. However, all the results in this thesis can also be applied to IoniDetect heat engines equipped with a mass flow sensor by replacing the fan speed with the so-called virtual fan speed. The virtual fan speed is an artificial value, which in a certain sense is equivalent to the air mass flow [PHE, Item 3728, Item 3733].

Example 2.10 demonstrates that the controller of the gas valve requires two parameters that define the setpoint. They are the desired equivalence AFR λ_{target} and the corresponding ioni current i_{set}. Figure 2.6(a) indicates that the ioni current setpoint is a function of the fan speed. This is indeed the case, as shown in Figure 2.6(b). It is based on measurement data of a Vaillant HE. The data were recorded at three different fan speeds fs_1, fs_2 and fs_3. Each of the three ioni current versus λ graphs consists of points with identical fan speed. For each fan speed let the desired equivalence AFR be $\lambda_{\text{target}} = 1.3$. The corresponding setpoints are marked by the dots. It is apparent that each fan speed has a different ioni current setpoint. Therefore, the controller requires a function that maps every feasible fan speed fs to its corresponding ioni current setpoint $i_{\text{set}}(\text{fs})$. This function is called control curve. It is relevant for the ADA algorithm and for the construction of the optimization models later on and thus it is explained in detail in the following subsection.

2.3.3. Control Curve and λ-Target Curve

To control the gas valve properly, an ioni current setpoint is required. As shown at the end of the preceding subsection, the ioni current depends on the AFR and on the fan speed. The determination of the ioni current setpoint(s) is based on measurement data of the respective HEs and can be divided into two steps. Because the optimal AFR usually depends on the load, i.e., on the fan speed, a desired equivalence AFR $\lambda_{\text{target}}(\text{fs})$ has to be determined for each feasible fan speed fs first. Thereafter, the corresponding ioni current setpoints $i_{\text{set}}\big(\text{fs}, \lambda_{\text{target}}(\text{fs})\big)$ are determined [Sch15, pp. 14–16]. Of course, this cannot be done for every fan speed in the interval of feasible fan speeds $[\text{fs}_{\min}, \text{fs}_{\max}]$. Rather, one chooses a suitable finite subset of fan speeds and only determines $\lambda_{\text{target}}(\text{fs})$ and $i_{\text{set}}\big(\text{fs}, \lambda_{\text{target}}(\text{fs})\big)$ for these fan speeds. The chosen fan speeds and the according ioni current setpoints are stored in a look up table. The controller linearly interpolates between the entries of this table. The first and the last entry are extrapolated using the slopes defined by their neighbored entries [Sch15, p. 15]. This interpolated and extrapolated function is the so-called *control curve*. Analogously, the so-called λ-*target curve* is the linear interpolation of the λ_{target} versus fan speed values. However, the λ-target curve is extrapolated as a constant function.
Figure 2.7 shows an exemplary λ-target curve and the corresponding control curve. It is important to emphasize that the controller works with the control curve only. As already mentioned, the controller does not have the capability to measure the equivalence AFR directly, i.e., IoniDetect is blind with regard to the equivalence AFR. Therefore, the λ-target curve is irrelevant to the controller. It only represents the desired equivalence AFR and it is only used to determine the control curve.

Remark 2.12 *Because the controller is blind with regard to the equivalence AFR, the HEs usually operate with some deviation to the target λ. E.g., the electrode's position has some tolerances and thus the measured ioni currents of two identical HEs usually differ from each other. Another example is the influence of weather. Depending on the atmospheric pressure or the wind conditions, the pressure in the flue system differs and the*

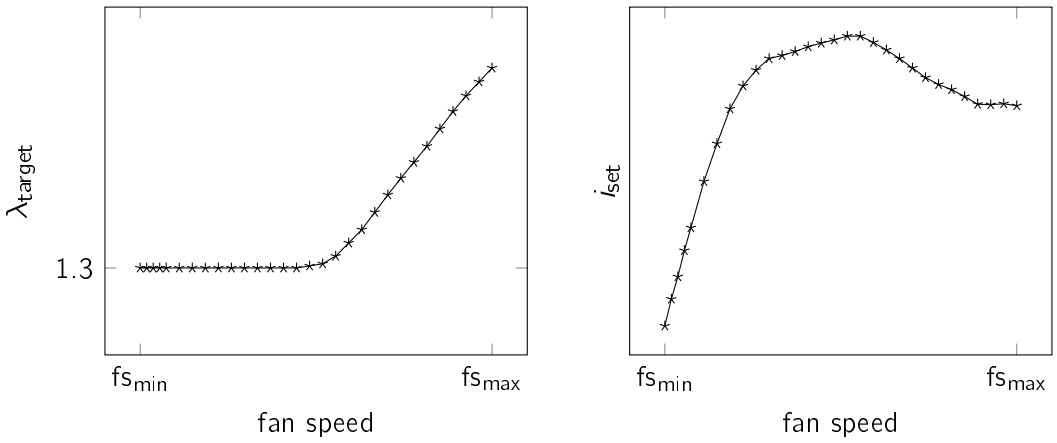

(a) λ-target curve

(b) Control curve

Figure 2.7.: Both curves are the linear interpolation of 32 supporting points. The λ-target curve represents the desired λ as a function of the fan speed. The control curve maps any feasible fan speed fs to an ioni current $i_{\text{set}}(\text{fs})$ such that $\lambda\big(\text{fs}, i_{\text{set}}(\text{fs})\big) = \lambda_{\text{target}}(\text{fs})$ (under ideal conditions).

air mass flow varies, although the fan speed remains unchanged. Therefore, the design of the control curve parameters has to take these and some other tolerances into account. This is an optimization problem on its own, but it is beyond the scope of this thesis. In the context of the ADA problem, the control curve and the λ-target curve are always assumed to be given.

By integrating the control curve into the model of the IoniDetect combustion control system as described in the preceding Section 2.3.2 and as illustrated in Figure 2.5, we obtain a more complete model of IoniDetect. The resulting extended model is illustrated in Figure 2.8. This system has only one input, which is the fan speed setpoint. The control curve transforms the fan speed setpoint to an ioni current setpoint, which is used to control the gas valve. Based on this extended model of IoniDetect, the ADA optimization problem is formulated and analyzed in the course of this thesis.

Remark 2.13 *Note that the model of IoniDetect according to Figure 2.8 is still basic. There are far more details related to the control of the fan speed and the gas valve. Especially in the context of the dynamic behavior of the combustion system, there is more to consider. For example, there exists a feed forward control for the gas valve that allows the system to react quickly to major load changes [Sch15, pp. 16 sq.]. Because these are not relevant with respect to the ADA problem, they are omitted in the following. A more detailed introduction to IoniDetect can be found in [Sch15].*

Next, we define a mathematical model of HEs with IoniDetect. This model is used to explain and analyze the ADA procedure as well as to design ADA optimization models in the course of this thesis.

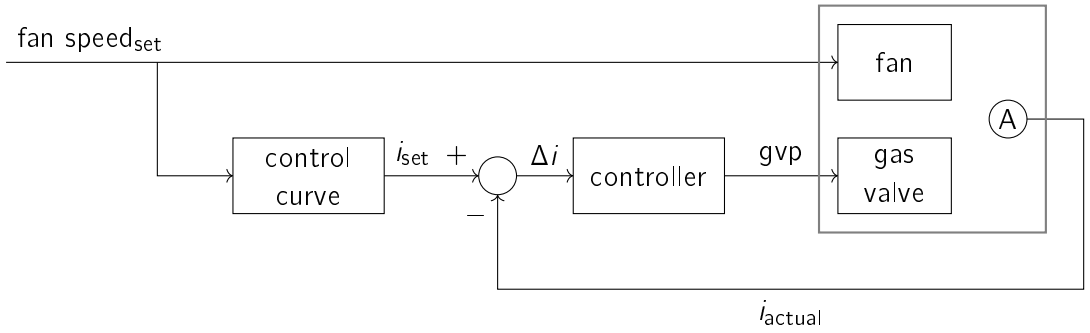

Figure 2.8.: This is an extension of the concept shown in Figure 2.5. The extended system has only one input, which is the fan speed setpoint. It is transformed by the control curve to an ioni current setpoint, which is used to control the gas valve. Based on [Sch15, p. 7].

2.4. Mathematical Heat Engine Model

We want to optimize the ADA parameters with computer simulations. For this, we need an appropriate mathematical model of the IoniDetect HEs. The relevant physical sizes with respect to the ADA procedure are the fan speed, the gas valve position, the ioni current, the equivalence AFR and the CO emission. The goal of this section is to formulate a mathematical model of the HE that represents these sizes as well as their relations and interdependence appropriately.
For this, we have to take two aspects into account. First, the model has to be based on the measurement data provided by Vaillant. The second aspect results from the fact that all considered HEs follow some physical laws and thus have some combustion system behavior in common. This common behavior can be derived from combustion theory and is also present in measurement data. Thus it is postulated as universal HE properties below. The HE model should reflect these universal properties.

2.4.1. Measurement Data Provided by Vaillant

This subsection is based on the Vaillant intern documentation [PHE, Item 1608], where the measurement process is described in detail. The key points are summarized in the following.
The basic notion is that an HE is considered as a system that has two inputs and several outputs. The inputs correspond to the positions of the two actuators, i.e., the inputs are the fan speed and the gas valve position. The outputs are several resulting physical sizes. Regarding the ADA problem, we are only interested in the ioni current, the equivalence AFR and the CO emission. The latter two are indicators for the combustion quality, see also Section 2.2. The ioni current is used to control the combustion as delineated in Section 2.3. Other outputs like the thermal load are not relevant for the ADA problem and thus they are ignored in the following.

The measurement process can be summarized as follows.

- A sample set S of n, $n \in \mathbb{N}$, fan speed and gvp combinations is specified, i.e., $S = \{(\mathrm{fs}_k, g_k) : k \in [n]\}$ with $[n] := \{1, \ldots, n\}$.
- For each sample point $(\mathrm{fs}_k, g_k) \in S$ the fan speed is fixed at fs_k and the gvp is fixed at g_k.
- Because the inputs are fixed at fs_k and g_k, the combustion process eventually stabilizes, i.e., the output variables no longer change after a certain time. Then the corresponding ioni current i_k, the equivalence AFR λ_k and the CO emission co_k are recorded.

With this, one obtains n five-dimensional data points $(\mathrm{fs}_k, g_k, i_k, \lambda_k, \mathrm{co}_k)$, $k \in [n]$. These n data points constitute a set of HE measurement data, which is called *Brennfeld static signals* by Vaillant.

Remark 2.14 *Brennfeld is a coinage in the German language. It is a combination of the two words Brenner and Kennfeld.*

Remark 2.15 *An HE system has a thermal inertia and thus it takes a certain time until the combustion process and the corresponding outputs have stabilized while the inputs are kept constant. Because the outputs are only recorded once the system has stabilized, the recorded data contains no information about the corresponding HE system's dynamic behavior. Therefore, the denotation of the HE measurement data contains the term* static signals. *A detailed introduction to signal, systems and dynamics can be found in [LJ19] and [Ada22].*
To consider only static signals reduces a system's complexity and is a simplification. The underlying assumption made by Vaillant is that an HE's dynamics are sufficiently approximated by the Brennfeld static signals.

Figure 2.9 shows the Brennfeld static signals of a Vaillant HE [PHE, Item 6371]. The upper left part shows the sample set S that contains a total of $n = 304$ fan speed and gvp combinations. The upper right part shows the recorded ioni currents against the sample points S, i.e., the set $\{(\mathrm{fs}_k, g_k, i_k) : k \in [304]\}$ is shown. Analogously, the recorded equivalence AFRs and the recorded CO emissions against S are shown in the lower left and lower right part of Figure 2.9, respectively.
The data shown in the upper right part of Figure 2.9 suggests that the ioni current is strictly increasing with the gvp if the fan speed is kept fixed. The data shown in the lower left part of Figure 2.9 suggests that the equivalence AFR is strictly decreasing with the gvp if the fan speed is kept fixed. This is indeed always the case and allows us to propose universal HE properties. These properties are then used to formulate the HE model in Section 2.4.3.

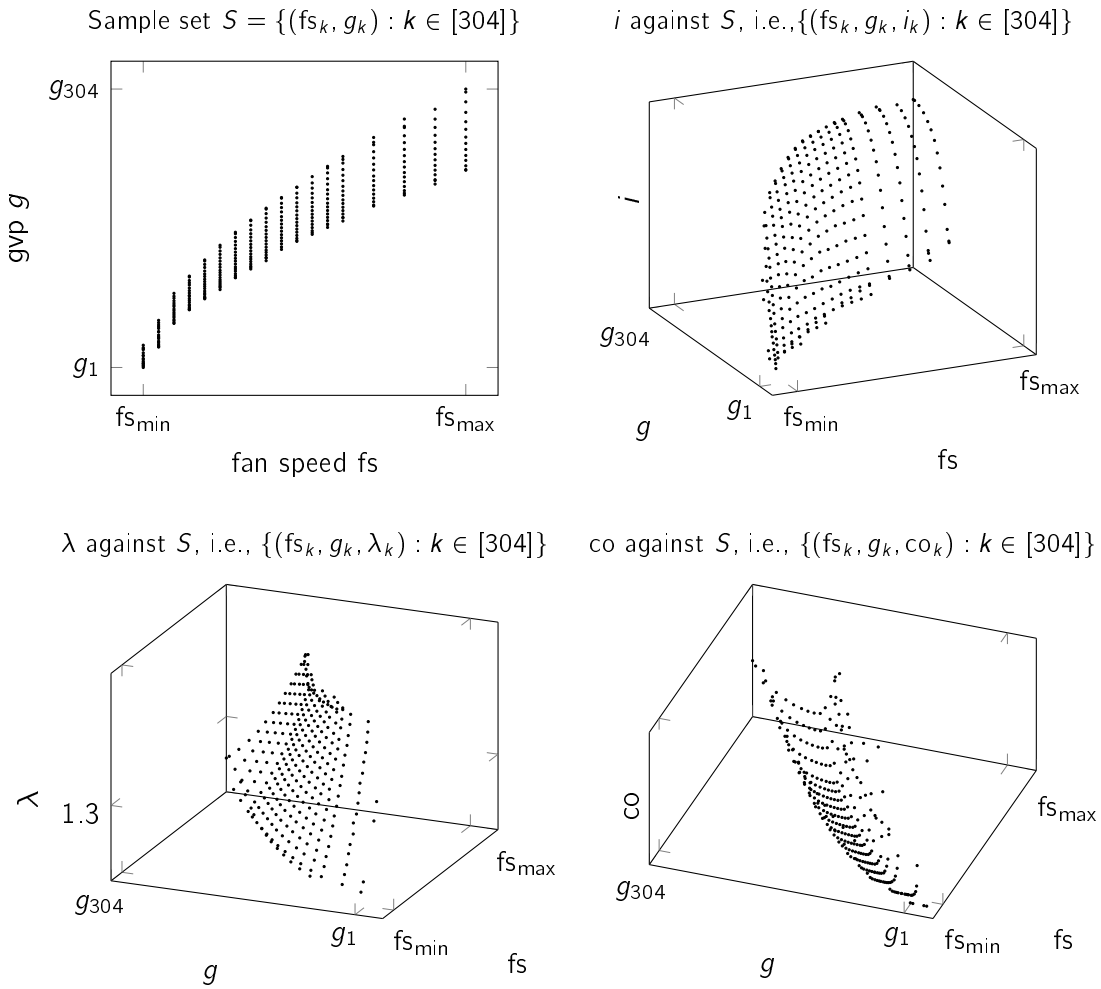

Figure 2.9.: Brennfeld static signals of the Vaillant HE according to [PHE, Item 6371] are shown. The figure is intended to give an intuition of the Brennfeld static signals. The details and scaling of the shown graphs are not important.
In the upper left part, the sample set S consisting of 304 fan speed and gvp combinations is shown. The upper right part shows the recorded ioni currents against the sample set S. In the lower part, the equivalence AFR λ and the CO emission co against S are shown.

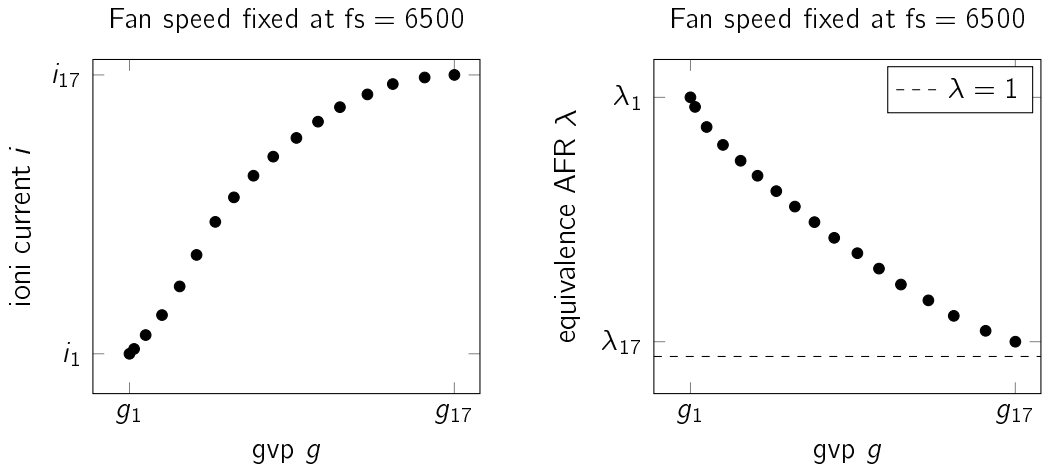

Figure 2.10.: A total of 17 data points of the Brennfeld static signals according to [PHE, Item 6371] are shown. All data points have the same fan speed fs = 6500. In the left part, the ioni current i against the gvp g is shown. The ioni current is strictly increasing with the gvp. In the right part, the equivalence AFR λ against g is shown. The equivalence AFR is strictly decreasing with the gvp.

2.4.2. Universal HE Properties

The first universal property is based on the fact that every HE has a minimum and a maximum fan speed, both of which are positive.

Definition 2.16 *The minimum and the maximum fan speed of an HE are denoted by* $\mathrm{fs}_{\min}$ *and* $\mathrm{fs}_{\max}$*, respectively. The set of all feasible fan speeds is the closed interval* $\mathrm{FS} := [\mathrm{fs}_{\min}, \mathrm{fs}_{\max}] \subset \mathbb{R}_{>0} := \{x \in \mathbb{R} : x > 0\}$.

Remark 2.17 *In practice, the fan speed can only be changed in discrete steps [WHB, Item 4196]. Therefore, assuming that every* $\mathrm{fs} \in \mathrm{FS}$ *is feasible is a simplification. However, because the step size between two fan speeds is sufficiently small in practice, it is assumed that this simplification does not affect the ADA optimization later on.*

Next, we consider some monotonicity properties of the ioni current and of the equivalence AFR with respect to the gvp. The left part of Figure 2.10 shows the ioni current against the gvp of 17 sample points (fs_k, g_k), $k \in [17]$, where all sample points have the same fan speed fs, i.e., $\mathrm{fs}_k = \mathrm{fs}$ for all $k \in [17]$. In the right part of Figure 2.10, the equivalence AFR λ against the gvp g for the same 17 sample points is shown. Note that the ioni current i is strictly increasing with the gvp g and that the equivalence AFR λ is strictly decreasing with g. Furthermore, the "slope" of the ioni current "curve" reduces with increasing gvp and the 17-th data point seems to constitute an ioni current maximum. In addition, the equivalence AFR of the 17-th data point is close to one.
All these observations are no coincidence. This behavior can be observed not only in this example but in all measurement data. Apart from the empirical findings, a theoretical

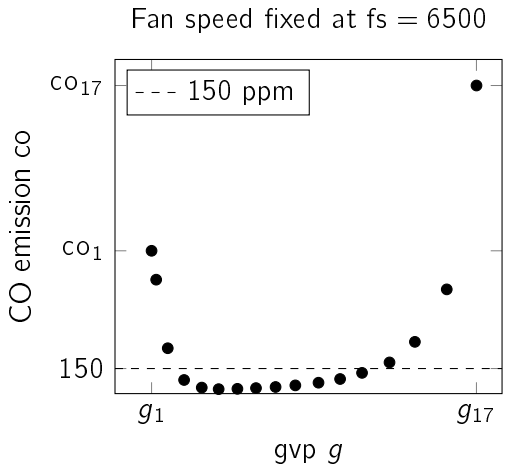

Figure 2.11.: The CO emission co against the gvp g for 17 data points of the Brennfeld static signals according to [PHE, Item 6371] are shown. All data points have the same fan speed fs = 6500. The CO emission curve is convex. In addition, the 150 ppm line is shown, which is usually the CO limit for the ADA procedure, see also Section 8.1 below.

derivation is also possible. The monotonicity of the ioni current as well as that the ioni current's maximum is close to $\lambda = 1$ can be found in the dissertation by Resch [Res19]. That λ is strictly decreasing with g while fs is fixed can be explained as follows. Let us consider two actuator positions (fs_1, g_1) and (fs_2, g_2) with $\mathrm{fs}_1 = \mathrm{fs}_2$. Without loss of generality let $g_1 < g_2$. Because the fan speeds are identical but g_2 is greater than g_1, (fs_2, g_2) results in a mixture that contains more gas than the mixture of (fs_1, g_1) while the amount of air is (approximately[1]) identical. Therefore, the AFR of (fs_2, g_2) is smaller than the AFR of (fs_1, g_1), i.e., $\lambda_2 < \lambda_1$. In addition to the monotonicity properties, it is reasonable to assume that the graphs of i against g and of λ against g with the fan speed fixed are continuous. An actuator position (fs, g) corresponds to a certain amount of oxygen and gas that are mixed. Their mixture results in a certain equivalence AFR during combustion. If the fan speed or the gvp is changed slightly, the AFR also changes only slightly. The continuity of i versus g is justified analogously.
Regarding the CO emission, there exists no monotonicity property. Figure 2.11 shows the CO emission versus the gvp for the same data points (fs_k, g_k), $k \in [17]$, whose corresponding ioni currents and equivalence AFRs have already been considered above. It is apparent that the curve of co versus g is convex. Again, this is no coincidence, see also Section 2.2 and [MCF11, p. 180]. Therefore, the convexity of the CO emission curve is also considered as a universal HE property. In addition, it is also reasonable to assume that the CO emissions change continuously with the gvp.
The monotonicity, convexity and continuity properties motivate the definition of the mathematical HE model given below.

[1] That the air volume flow is only approximately constant while the fan speed is fixed is detailed in Remark 2.11.

2.4.3. The HE Model

Based on the kind of measurement data provided by Vaillant, i.e., we consider static signals and no dynamic behavior, and based on the universal HE properties delineated in the preceding subsection, a mathematical HE model is formulated. The following definition as well as the results derived in this subsection are from the author of this thesis.

Definition 2.18 *An* HE model *is a* 5*-tuple* $\mathcal{H} = (\mathrm{FS}, G, \iota, \Lambda, \zeta)$*, where* $\mathrm{FS} = [\mathrm{fs}_{\min}, \mathrm{fs}_{\max}] \subset \mathbb{R}_{>0}$ *is the set of feasible fan speeds of the HE and:*

- $G = (G_{\mathrm{fs}})_{\mathrm{fs}\in\mathrm{FS}}$ *is an indexed family of closed and bounded intervals that contains for each* $\mathrm{fs} \in \mathrm{FS}$ *exactly one closed and bounded interval* G_{fs}*, i.e.,*

  $$G_{\mathrm{fs}} \in G \;\Rightarrow\; G_{\mathrm{fs}} \subset \mathbb{R} \text{ is a closed and bounded interval.}$$

  A set $G_{\mathrm{fs}} \in G$ *is called the* set of gas valve positions with respect to fs.

- $\iota = (\iota_{\mathrm{fs}})_{\mathrm{fs}\in\mathrm{FS}}$ *is an indexed family of functions* $\iota_{\mathrm{fs}} : G_{\mathrm{fs}} \to \mathbb{R}_{>0}$ *that are strictly increasing as well as continuous and where* $G_{\mathrm{fs}} \in G$*, i.e.,*

  $$\iota_{\mathrm{fs}} \in \iota \;\Rightarrow\; \iota_{\mathrm{fs}} : G_{\mathrm{fs}} \to \mathbb{R}_{>0} \text{ s.t. } G_{\mathrm{fs}} \in G \text{ and } \iota_{\mathrm{fs}} \text{ strictly increasing and continuous.}$$

  A function $\iota_{\mathrm{fs}} \in \iota$ *is called the* ioni current function with respect to fs.

- $\Lambda = (\Lambda_{\mathrm{fs}})_{\mathrm{fs}\in\mathrm{FS}}$ *is an indexed family of functions* $\Lambda_{\mathrm{fs}} : G_{\mathrm{fs}} \to \mathbb{R}_{>0}$ *that are strictly decreasing as well as continuous and where* $G_{\mathrm{fs}} \in G$*, i.e.,*

  $$\Lambda_{\mathrm{fs}} \in \Lambda \;\Rightarrow\; \Lambda_{\mathrm{fs}} : G_{\mathrm{fs}} \to \mathbb{R}_{>0} \text{ s.t. } G_{\mathrm{fs}} \in G \text{ and } \Lambda_{\mathrm{fs}} \text{ strictly decreasing and continuous.}$$

  A function $\Lambda_{\mathrm{fs}} \in \Lambda$ *is called the* equivalence AFR function with respect to fs.

- $\zeta = (\zeta_{\mathrm{fs}})_{\mathrm{fs}\in\mathrm{FS}}$ *is an indexed family of functions* $\zeta_{\mathrm{fs}} : G_{\mathrm{fs}} \to \mathbb{R}_{>0}$ *that are convex as well as continuous and where* $G_{\mathrm{fs}} \in G$*, i.e.,*

  $$\zeta_{\mathrm{fs}} \in \zeta \;\Rightarrow\; \zeta_{\mathrm{fs}} : G_{\mathrm{fs}} \to \mathbb{R}_{>0} \text{ s.t. } G_{\mathrm{fs}} \in G \text{ and } \zeta_{\mathrm{fs}} \text{ convex and continuous.}$$

  A function $\zeta_{\mathrm{fs}} \in \zeta$ *is called the* CO emission function with respect to fs.

Remark 2.19 *According to Definition 2.18, the images of all ioni current functions* ι_{fs}*, of all equivalence AFR functions* Λ_{fs} *and of all CO emission functions* ζ_{fs}*,* $\mathrm{fs} \in \mathrm{FS}$*, are contained in* $\mathbb{R}_{>0}$*. This condition is justified, because the ioni current is always positive (Remark 3.5 below), the equivalence AFR is always positive (Remark 2.5) and burning natural gas always produces* CO*, i.e., there is no negative emission of CO.*

The following example presents an HE model according to Definition 2.18.

Example 2.20 *We set* $\mathrm{FS} := [1, 2]$ *and* $G_{\mathrm{fs}} := [10\,\mathrm{fs}, 20\,\mathrm{fs}]$ *for all* $\mathrm{fs} \in \mathrm{FS}$. *Furthermore, we define for all* $\mathrm{fs} \in \mathrm{FS}$ *functions* $\iota_{\mathrm{fs}} : G_{\mathrm{fs}} \to \mathbb{R}_{>0}$, $\Lambda_{\mathrm{fs}} : G_{\mathrm{fs}} \to \mathbb{R}_{>0}$ *and* $\zeta_{\mathrm{fs}} : G_{\mathrm{fs}} \to \mathbb{R}_{>0}$ *by*

$$\iota_{\mathrm{fs}}(g) := 10g, \quad \Lambda_{\mathrm{fs}}(g) := -g + 100 \quad \text{and} \quad \zeta_{\mathrm{fs}}(g) := g^2.$$

Then, $\mathcal{H} = \left(\mathrm{FS}, (G_{\mathrm{fs}})_{\mathrm{fs}\in\mathrm{FS}}, (\iota_{\mathrm{fs}})_{\mathrm{fs}\in\mathrm{FS}}, (\Lambda_{\mathrm{fs}})_{\mathrm{fs}\in\mathrm{FS}}, (\zeta_{\mathrm{fs}})_{\mathrm{fs}\in\mathrm{FS}}\right)$ *satisfies all conditions of Definition 2.18, because* G_{fs} *is a closed and bounded interval,* ι_{fs} *is strictly increasing and continuous,* Λ_{fs} *is strictly decreasing and continuous and* ζ_{fs} *is convex and continuous for all* $\mathrm{fs} \in \mathrm{FS}$. *Furthermore, the images of all functions are contained in* $\mathbb{R}_{>0}$. *Therefore,* $\mathcal{H}$ *is an HE model according to Definition 2.18. However, the model* $\mathcal{H}$ *in this example is artificial and not related to a set of measurement data.*

Definition 2.18 of $\mathcal{H}$ is abstract in the sense that it is possible to build an HE model without regarding any measurement data at all as demonstrated in Example 2.20. The abstraction from measurement data allows to argue with the HE related properties according to Definition 2.18 only, i.e., the argumentation in this thesis are (almost) independent of a particular set of measurement data or a particular regression or interpolation method.
Of course, when solving the ADA optimization problems in practice, the HE models must be in accordance with the corresponding measurement data. How an HE model may be generated from measurement data is discussed in the following Subsection 2.4.4. But first, we derive some further mathematical properties of the HE model.

Lemma 2.21 *The functions* ι_{fs} *and* Λ_{fs} *of an HE model* $\mathcal{H}$ *are homeomorphisms. Their images* $\iota_{\mathrm{fs}}(G_{\mathrm{fs}})$ *and* $\Lambda_{\mathrm{fs}}(G_{\mathrm{fs}})$ *are closed intervals.*

Proof. Let $\mathcal{H} = \left(\mathrm{FS}, (G_{\mathrm{fs}})_{\mathrm{fs}\in\mathrm{FS}}, (\iota_{\mathrm{fs}})_{\mathrm{fs}\in\mathrm{FS}}, (\Lambda_{\mathrm{fs}})_{\mathrm{fs}\in\mathrm{FS}}, (\zeta_{\mathrm{fs}})_{\mathrm{fs}\in\mathrm{FS}}\right)$ be an HE model. Let $\mathrm{fs} \in \mathrm{FS}$. According to Definition 2.18, the function ι_{fs} is strictly increasing and continuous. Therefore, ι_{fs} is bijective, i.e., its inverse ι_{fs}^{-1} exists. Because ι_{fs} is strictly increasing and its domain is an interval, ι_{fs}^{-1} is also continuous [Gar13, p. 163]. In total, ι_{fs} is a homeomorphism. As the image of a closed interval under a homeomorphism, the set $\iota_{\mathrm{fs}}(G_{fs})$ is a closed interval as well.
The statements with respect to Λ_{fs} are shown analogously. □

The images of the HE model functions are essential for formulating and analyzing the ADA algorithm below. Thus they are denoted as follows.

Definition 2.22 *Let* $\mathcal{H} = \left(\mathrm{FS}, (G_{\mathrm{fs}})_{\mathrm{fs}\in\mathrm{FS}}, (\iota_{\mathrm{fs}})_{\mathrm{fs}\in\mathrm{FS}}, (\Lambda_{\mathrm{fs}})_{\mathrm{fs}\in\mathrm{FS}}, (\zeta_{\mathrm{fs}})_{\mathrm{fs}\in\mathrm{FS}}\right)$ *be an HE model and let* $\mathrm{fs} \in \mathrm{FS}$. *The* set of ioni currents with respect to fs *is* $I_{\mathrm{fs}} := \iota_{\mathrm{fs}}(G_{\mathrm{fs}})$. *The* set of equivalence AFRs with respect to fs *is* $L_{\mathrm{fs}} := \Lambda_{\mathrm{fs}}(G_{\mathrm{fs}})$. *The* set of CO emissions with respect to fs *is* $\mathrm{CO}_{\mathrm{fs}} := \zeta_{\mathrm{fs}}(G_{\mathrm{fs}})$.

Corollary 2.23 *The sets* I_{fs} *and* L_{fs} *are closed intervals in* $\mathbb{R}_{>0}$ *for all* $\mathrm{fs} \in \mathrm{FS}$.

As already mentioned, the mathematical modeling and analysis of the ADA procedure in this thesis is based on the properties of the HE model according to Definition 2.18 and Lemma 2.21. In order to obtain meaningful HE models, we briefly discuss how to generate an HE model from measurement data.

2.4.4. Generating an HE Model from Measurement Data

Let us suppose that we have a set of HE measurement data, i.e., we have some Brennfeld static signals of an HE specimen, and we are interested in an HE model that reflects the measurement data. This corresponds to performing a curve fitting with the measurement data.
To illustrate the curve fitting process, let us suppose that we have a set of n data points $\{(\mathrm{fs}_k, g_k, i_k, \lambda_k, \mathrm{co}_k) : k \in [n]\}$. An exemplary set of measurement data with $n = 304$ data points is shown in Figure 2.9 above. Because each of the three outputs i, λ and co is obtained from the same two inputs fs and g, we perform three curve fittings, one for each of the data sets $\{(\mathrm{fs}_k, g_k, i_k) : k \in [n]\}$, $\{(\mathrm{fs}_k, g_k, \lambda_k) : k \in [n]\}$ and $\{(\mathrm{fs}_k, g_k, \mathrm{co}_k) : k \in [n]\}$. Regarding the exemplary data shown in Figure 2.9, these sets correspond to the upper right part, to the lower left part and to the lower right part of Figure 2.9, respectively.
Let $\hat{\imath}$, $\hat{\Lambda}$ and $\hat{\zeta}$ denote the resulting fits, respectively. Each fit is a function from a subset of $\mathbb{R}^2$, which corresponds to the fan speeds and gas valve positions, to a subset of $\mathbb{R}$, which corresponds to the ioni current, the equivalence AFR and the CO emission, respectively. From these fits the corresponding HE model can be derived as follows.

- For each $\mathrm{fs} \in \mathrm{FS}$, we specify a closed interval G_{fs}. This must be done such that (fs, g) is in the domain of each of the three fits $\hat{\imath}$, $\hat{\Lambda}$ and $\hat{\zeta}$ for all $g \in G_{\mathrm{fs}}$. Usually, this is done by considering a suitable hull (not necessarily convex) of the sample set $S = \{(\mathrm{fs}_k, g_k) : k \in [n]\}$. For instance, in Matlab this corresponds to the function *boundary(S)*.

- In order to obtain the HE model functions ι_{fs}, Λ_{fs} and ζ_{fs}, the domains of the fitted functions $\hat{\imath}$, $\hat{\Lambda}$ and $\hat{\zeta}$ are restricted to $\{\mathrm{fs}\} \times G_{\mathrm{fs}}$ for all $\mathrm{fs} \in \mathrm{FS}$. I.e., for all $\mathrm{fs} \in \mathrm{FS}$ we set
$$\iota_{\mathrm{fs}} := \hat{\imath}|_{\{\mathrm{fs}\}\times G_{\mathrm{fs}}}, \quad \Lambda_{\mathrm{fs}} := \hat{\Lambda}|_{\{\mathrm{fs}\}\times G_{\mathrm{fs}}} \quad \text{and} \quad \zeta_{\mathrm{fs}} := \hat{\zeta}|_{\{\mathrm{fs}\}\times G_{\mathrm{fs}}}.$$
Note that all these functions are well-defined according to the selection of the sets G_{fs} in the previous step.

- Care must be taken to ensure that all these functions satisfy the conditions of Definition 2.18. This means that ι_{fs} must be strictly increasing and continuous, Λ_{fs} must be strictly decreasing and continuous and ζ_{fs} must be convex and continuous for all $\mathrm{fs} \in \mathrm{FS}$. To achieve this, the boundaries of some of the intervals G_{fs} may have to be selected tighter or a different regression or interpolation method may have to be selected.

The approach with the HE model proposed in Section 2.4.3 allows flexibility in the choice of regression method. Any interpolation or regression method is feasible as long as the corresponding model $\mathcal{H}$ satisfies the conditions of Definition 2.18. Because the data of the Brennfeld static signals are already mean values, the Vaillant engineers prefer interpolation of the data [PHE, Item 16668]. Two common interpolation methods are thin plate splines and linear interpolation. If not otherwise stated, all graphs presented in this thesis as well

as the use cases presented in Chapter 9 below are based on a variant of linear interpolation. This is done for the following reasons. Linear interpolations are usually computationally less expensive, i.e., they are fast to evaluate. Furthermore, with linear interpolations it is "easier" to adhere to the monotonicity conditions according to Definition 2.18. Finally, the ADA procedure requires certain inverse ioni current functions ι_{fs}^{-1}, see for instance Definition 6.5 below, and the inverse functions are more easy to determine/evaluate in the case of a linear interpolation. However, whether interpolation or regression is more appropriate and which is the best suited interpolation/regression method for generating an HE model from Brennfeld static signals remain open questions and are left for future research.

Next, we explain how the combustion control system IoniDetect can be simulated with the proposed HE model. This is relevant when the ADA procedure is presented in the following Chapter 3.

2.4.5. Relation Between the Proposed HE Model and IoniDetect

In the proposed HE model, an HE is modeled as a system with the two inputs fan speed and gvp and the three outputs ioni current, equivalence AFR and CO emission, which follows in a certain sense the "physical logic". This means that a fan speed and a gvp result in a certain mixture. The combustion process corresponding to this mixture has a certain equivalence AFR, a certain ioni current and a certain CO emission.
However, IoniDetect works the other way around. As detailed in Section 2.3, IoniDetect is neither able to control the gas valve position directly nor to measure the equivalence AFR. Instead, the ioni current is used as an indirect measure of the equivalence AFR to control the gas valve, i.e., the inputs of IoniDetect are the fan speed and the ioni current. Its outputs are the gvp, the equivalence AFR and the CO emission. The following example demonstrates how this is modeled with the proposed HE model.

Example 2.24 *Let an HE model* $\mathcal{H} = \left(\mathsf{FS}, (G_{\mathsf{fs}})_{\mathsf{fs}\in\mathsf{FS}}, (\iota_{\mathsf{fs}})_{\mathsf{fs}\in\mathsf{FS}}, (\Lambda_{\mathsf{fs}})_{\mathsf{fs}\in\mathsf{FS}}, (\zeta_{\mathsf{fs}})_{\mathsf{fs}\in\mathsf{FS}}\right)$ *be given. Furthermore, let* $\mathsf{fs} \in \mathsf{FS}$ *be a given fan speed setpoint and let* $i \in I_{\mathsf{fs}}$ *be a given ioni current setpoint. Then, IoniDetect works as follows.*
The fan speed is fixed at fs *and the gas valve is adjusted such that the resulting ioni current is equal to* i*. The corresponding gvp is* $g := \iota_{\mathsf{fs}}^{-1}(i)$*. With the gvp at hand, we can then calculate the resulting equivalence AFR and CO emission via* $\lambda = \Lambda_{\mathsf{fs}}(g)$ *and* $\mathsf{co} = \zeta_{\mathsf{fs}}(g)$.

Remark 2.25 *It is important to emphasize that IoniDetect can only evaluate the inverse ioni current function* ι_{fs}^{-1} *but not the "non-inverted" ioni current function* ι_{fs}, $\mathsf{fs} \in \mathsf{FS}$. *This is particularly relevant for the ADA procedure, which is explained in the following chapter.*

2.4.6. Discussion of the Proposed HE Model

As all models, the proposed HE model makes some simplifications, which are discussed in this subsection.

Black box model The proposed HE model is a black box model in the sense that it obscures the underlying physics [FSK08, p. 33]. It transforms the two inputs fan speed and gvp to an equivalence AFR, an ioni current and a CO emission value without explicitly considering physical laws. The combustion process as well as the ionization processes in the flame are only approximated on a macroscopic level. Because Vaillant only provides this kind of measurement data, the black box approach is predetermined. Therefore, considering different modeling approaches is not in the scope of this work.
Challenges in modeling combustion processes based on physical laws, in particular the ionization of flames, are explained in [Son23, p. 63].

Static signals versus dynamic behavior As mentioned in Remark 2.15, considering only an HE system's static signals and not its dynamic behavior is a simplification. Again, because Vaillant only provides this kind of measurement data, the restriction to static signals is predetermined. However, simulating dynamic HE properties with so-called Hammerstein-Wiener models is promising as demonstrated by Sonnenschein in his dissertation [Son23, pp. 64 sqq.]. Whether this is also a suitable approach in the context of the ADA optimization problem is an open question and left for future research.

Atmospheric conditions and other impacts The comparison of several Brennfeld static signals indicates that the ioni current depends not only on the fan speed and the gvp but also on other influences such as the gas pressure and temperature or atmospheric conditions like the air pressure and humidity. This is also pointed out by Sonnenschein [Son23, pp. 80 sqq.]. Nevertheless, the fan speed and the gvp have the largest influence on the ioni current and regarding the ADA optimization the HE model according to Definition 2.18 has a sufficient approximation quality. But in order to obtain more precise HE models and better simulation results, it might be worth to further investigate the influence of environmental conditions on the ioni current.

Continuous fan speed and gas valve position As delineated in Remark 2.17, the fan speed can only change in discrete steps. The same is true for the gvp. In contrast, the proposed HE model assumes a continuous fan speed and gvp for simplification. While the step size of the fan speed is rather small, the step size of the gvp is rather large. It is shown in Section 3.2 below that the gvp is central for the ADA procedure. Whether better simulation results regarding the ADA optimization can be achieved by considering a discrete gvp instead of a continuous gvp is an open question and left for future research.

To conclude the discussion of the proposed HE model, we briefly consider its simulation quality.

Simulation Quality of the HE Model

Before ADA parameters are ultimately selected and stored in the combustion control software, they are tested in the lab with a particular test procedure, which is described in [PHE, Item 1618]. Therefore, this test procedure was also implemented with the proposed HE model to assess ADA parameters with computer simulation. However, there is a certain discrepancy between measured values in the lab and their simulated counterparts [PHE, Item 16770]. For example, in one use case, the deviation of the resulting equivalence AFR between the measured values and the simulated counterparts after 15 ADA iterations with each ADA pair was approximately 0.1 at smaller fan speeds and approximately -0.05 at larger fan speeds [PHE, Item 16770]. This indicates a potential shortcoming of the HE model. Because the decision makers are nevertheless satisfied with the ADA parameters obtained by the methods proposed in this study [PHE, Items 3124 and 7082], the simulation quality is considered to be sufficient. However, further modeling work will have to be conducted in order to obtain better simulation quality.

This concludes the presentation of the proposed HE model and also the presentation of the technical background required to comprehend the ADA procedure, which is presented next.

3. ADA: Automatic Drift Adaption

In this chapter, the automatic drift adaption (ADA) procedure is presented based on the United States patent "Control Facility For a Burner System" [LS17] as well as on the Vaillant intern documentations *Konzept Sitherm Pro* [Sch15], [WHB] and [PHE]. The patent [LS17] was filed by Lochschmied and Schmiederer and contains the invention of the ADA concept. In this thesis it is referred to as the 'ADA patent'. The examples and figures in this chapter, which are used to demonstrate and explain the ADA procedure, as well as all formulations with respect to the HE model, are added by the author of this thesis.

Remark 3.1 *Note that the ADA patent [LS17] as well as the Vaillant intern documentations [Sch15], [WHB] and [PHE] are technical documents. They do not always provide mathematically exact statements. Some of their statements may be based on experience and on trial and error. In this sense, ADA is a technical procedure and can be considered as a heuristic to compensate the drift.*
Although ADA is an algorithm, the aforementioned documentations contain only a partial algorithmic description. Therefore, the mathematical and algorithmic aspects of ADA are secondary in this chapter. Rather it is considered a technical description of ADA. A mathematical description of the ADA algorithm and an analysis of its convergence properties are provided in Chapters 5 to 7 below.

As stated in Section 2.3.1, combustion control based on ionization has a large drawback. The ioni electrode has to be positioned in the flames, but there it is prone to oxidation processes. With increasing operating time an oxide layer accrues on the electrode's surface. This oxide layer has the effect of an electrical insulation and reduces the conductivity of the electrode [LS17, p. 5]. This alters the electrical characteristics of the ioni current measurement circuit.

Remark 3.2 *In the context of an ioni electrode, the process of oxidation is also called* aging *or* drift. *In thesis, the term drift is mostly used.*

We first describe how drift is modeled. Then, the notion behind the ADA procedure is illustrated. Finally, the more advanced concepts of a sequence of ADA iterations and a plurality of ADA pairs are presented.

3.1. Modeling of Drift

The influence of drift on combustion control is closely related to the ioni current measurement circuit.

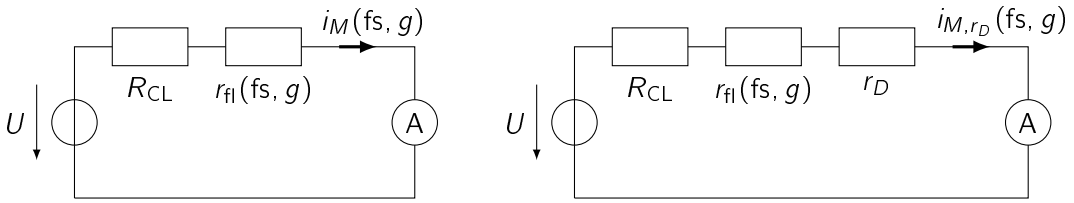

Figure 3.1.: In the left part, the equivalence circuit diagram of the ioni current measurement circuit is shown. It consists of a DC voltage source, a current limiting resistance, the flame resistance and an ammeter to measure the resulting current. The occurrence of drift is modeled by an additional resistance r_D that is connected in series. This situation is depicted in the right part. Adapted from [LS17].

3.1.1. Ioni Current Measurement Circuit

The ioni current measurement circuit is one of the key components of IoniDetect. It is explained in detail in the corresponding ADA patent [LS17, p. 5] and in the Vaillant intern documentation [Loc16]. Both documents also contain a much simpler equivalent circuit diagram of the measurement circuit. An equivalent circuit is "a simpler but functionally equivalent form for complicated systems" [Joh03, p. 1]. The equivalent circuit corresponding to the ioni current measurement circuit is illustrated in the left part of Figure 3.1. It consists of a direct current (DC) voltage source with a known voltage U, an ammeter and two resistances that are connected in series. The ammeter is used to measure the circuit's current i_M. This current is the ioni current that is used in IoniDetect to control the AFR as described in Section 2.3.2. The two resistances are a current limiting resistance R_{CL} and the flame resistance r_{fl}.
The current limiting resistance is an ohmic resistance with a constant size. As the name suggests it is included in the circuit to reduce and limit the current i_M. The flame resistance depends on the electric conductivity of the flame and is a function of the air quantity and of the fuel quantity [LS17, p. 5]. Because in IoniDetect the mixture of air and fuel is adjusted via the fan speed and the gvp, the flame resistance is considered as a function of the fan speed and the gvp in following. Details about the electrical characteristics of flames are stated in Remark 2.6.
For the subsequent analysis of the ADA optimization problem, it is convenient to combine the current limiting resistance and the flame resistance to $r_F(\mathrm{fs}, g) := R_{\mathrm{CL}} + r_{\mathrm{fl}}(\mathrm{fs}, g)$. Because the two resistances are connected in series, the measured current is (by applying Ohm's law)

$$i_M(\mathrm{fs}, g) = \frac{U}{r_F(\mathrm{fs}, g)}. \tag{3.1}$$

Remark 3.3 *For the remainder of this thesis, U corresponds to the DC voltage of the equivalent circuit of the ioni current measurement circuit. As a DC voltage, U is constant. Furthermore, U is positive, i.e., $U > 0$.*

Remark 3.4 *Let the fan speed* fs *and the gvp* g *be such that we have a stable combustion. Then, the total resistance* $r_F(\text{fs}, g)$ *is always greater than zero and bounded. Even if there was a short circuit because the electrode was in contact with the burner, the current limiting resistance would still be present and limit the current and thus* $r_F(\text{fs}, g) > 0$.
On the other hand, because we have a stable combustion, the flame is an electrical conductor and its resistance $r_{\text{fl}}(\text{fs}, g)$ *is finite and thus* $r_F(\text{fs}, g) < \infty$. *If the electrode was bent such that it is far away from the flame, an electric current could not flow. But such a scenario is beyond the scope of this work.*

Remark 3.5 *Let the fan speed* fs *and the gvp* g *be such that we have a stable combustion. Then, the ioni current* $i_M(\text{fs}, g)$ *is always greater than zero and finite. According to Remark 3.4, we have* $0 < r_F(\text{fs}, g) < \infty$. *Therefore, the ioni current* $i_M(\text{fs}, \lambda) = \frac{U}{r_F(\text{fs},\lambda)}$ *is well-defined and because* $U > 0$, *we have* $0 < i_M < \infty$.

In the equivalent circuit of the measurement circuit, the phenomenon of drift, i.e., an accretion of oxide on the electrode, is modeled as an additional resistance that is connected in series [LS17, p. 5]. This situation is depicted in the right part of Figure 3.1, where the additional resistance r_D is connected in series in the equivalent circuit of the measurement circuit. This is the so-called drift resistance.

Definition 3.6 *The additional resistance that models the electrode's drift in the equivalent circuit is called* drift resistance.

With the drift resistance present, the total resistance of the circuit is $r(\text{fs}, g) = R_{\text{cl}} + r_{\text{fl}}(\text{fs}, g) + r_D = r_F(\text{fs}, g) + r_D$. The measured ioni current is (by applying Ohm's law)

$$i_{M,r_D}(\text{fs}, g) = \frac{U}{r(\text{fs}, g)} = \frac{U}{r_F(\text{fs}, g) + r_D}. \tag{3.2}$$

The influence of drift on the measured ioni current corresponds to comparing (3.1) with (3.2). We have

$$r_D \neq 0 \;\Rightarrow\; i_M(\text{fs}, g) \neq i_{M,r_D}(\text{fs}, g),$$

which has an impact on the combustion quality as it is shown in Section 3.1.4 below. But first, we take a closer look at the assumptions with respect to the drift resistance made in this thesis.

3.1.2. Assumptions with Respect to the Drift Resistance

A central assumption made by Vaillant is that the drift resistance does not depend on the fan speed or the gvp, i.e., r_D is not a function of the fan speed or the gvp [PHE, Item 1618]. An ohmic resistance is (almost) constant and does not depend on the fan speed or the equivalence AFR and is therefore suitable for simulating a constant drift. Accordingly, Vaillant simulates drift in the laboratories by connecting an additional ohmic resistance in series in the measuring circuit [PHE, Item 1618].

Remark 3.7 *The ADA patent [LS17] assumes the more general case that the resistance depends on the fan speed and possibly also on the gas valve position [LS17, p. 9]. However, practical experience by Vaillant has shown that the simplified assumption of r_D not being a function of* fs *or g is sufficient.*

Another aspect related to assumptions on the drift resistance is time dependency. According to the ADA patent, "drift only takes place as a creeping phenomenon" [LS17, p. 3], i.e., the drift resistance changes slowly over time. In the simulations, we consider rather small period of times. Therefore, the simplifying assumption is made that the drift resistances is not a function of the time. This assumption is consistent with the already mentioned approach to simulate drift in the lab, because the ohmic resistances used to simulate drift are constant and thus are not time depended. The only way to simulate a change of drift in the lab is to replace the used ohmic resistance. This is actually done when testing ADA parameters with a certain test pattern in the lab, where three different drift resistances $r_{D,1} < r_{D,2} < r_{D,3}$ are considered [PHE, Item 1618]. The following assumption summarizes the considerations made so far.

Assumption 3.8 *The drift resistance is always assumed to be a constant, i.e., $r_D \in \mathbb{R}$. In particular, it is assumed to be not a function of the fan speed, of the gvp or of time.*

An aspect that is important in practice is the definition of the reference point for no drift. A natural definition for *no drift* would be the situation that a brand new electrode and burner are used, i.e., if the HE has zero operating hours. But Vaillant defines a situation as no drift, where the ioni electrode has already been exposed to oxidation for a period of 90 hours and the burner was exposed to oxidation for a period of 20 hours. This is done, because the effect of drift is particularly noticeable at the first hundred hours of operating time [PHE, Item 1618]. Thereafter, the oxidation process takes place at a much slower rate and eventually stabilizes at a certain point.
All measured ioni currents that are considered in this work were recorded according to Vaillant's definition of no drift. This motivates the following definition.

Definition 3.9 *The term* no drift*, i.e., the case $r_D = 0$, corresponds to the situation that the ioni electrode has already been exposed to oxidation for a period of* 90 *hours and the burner was exposed to oxidation for a period of* 20 *hours.*

A consequence of Definition 3.9 is that a negative drift resistance is possible. This might happen if an installer mistakenly cleans the ioni electrode with a wire brush. Then, the oxide layer is removed and the ioni current measurement circuit's total resistance is smaller than in the situation according to Definition 3.9. Because this is an unintended and unlikely case, it was decided to consider only nonnegative drift resistances in this work.

Assumption 3.10 *The drift resistance is always assumed to be a nonnegative constant, i.e., $r_D \in \mathbb{R}_{\geq 0} := \{x \in \mathbb{R} : x \geq 0\}$.*

Remark 3.11 *According to the ADA patent [LS17], "[b]ending or displacement respectively of the ionization electrode" might have the effect of a negative drift resistance [LS17, p. 6].*

This seems to be a contradiction to Assumption 3.10. But these geometric tolerances with respect to the ioni electrode have the effect of an additional drift resistance. This additional resistance is independent of the considered r_D. It can even be present if we actually have a situation with no drift. This is detailed in Sections 6.3.2 and 7.4.1 below.

We summarize that the drift of the ioni electrode is modeled as a nonnegative and constant ohmic resistor r_D that is connected in series in the equivalence circuit diagram of the ioni current measurement circuit. The resulting drifted ioni current is calculated by (3.2). Therefore, Equation 3.2 is added to the HE model presented in Section 2.4 to represent drift in the HE model.

3.1.3. Drifted HE Model

The measured ioni current $i_M(\mathrm{fs}, g)$ in the equivalence circuit diagram corresponds to $\iota_{\mathrm{fs}}(g)$ in the HE model, see also Section 2.4. In this subsection, we add the drifted ioni current $i_{M,r_D}(\mathrm{fs}, g)$ to the HE model. Note that we only need to adjust the ioni current functions in the HE model in the event of drift. The other variables and functions of the HE model remain unchanged. The equivalence AFR and the CO emission depend on the mixture of air and gas and thus they depend only on the fan speed and the gvp and not on the drift resistance.
It is possible to express the drifted ioni current as a function of the ioni current without drift. The corresponding ioni current without drift is $i_M(\mathrm{fs}, g) = \frac{U}{r_F(\mathrm{fs},g)}$ according to (3.1). Let $r_D \geq 0$ be a drift resistance. Then, the corresponding ioni current with drift is $i_{M,r_D}(\mathrm{fs}, g) = \frac{U}{r_F(\mathrm{fs},g)+r_D}$ according to (3.2). By plugging $r_F(\mathrm{fs}, g) = \frac{U}{i_M(\mathrm{fs},g)}$ into (3.2), we obtain

$$i_{M,r_D}(\mathrm{fs}, g) = \frac{U}{r_F(\mathrm{fs}, g) + r_D} = \frac{U}{\frac{U}{i_M(\mathrm{fs},g)} + r_D} = \frac{U i_M(\mathrm{fs}, g)}{r_D i_M(\mathrm{fs}, g) + U}. \tag{3.3}$$

Equation 3.3 motivates the following definition the drifted HE model.

Definition 3.12 *Let $\mathcal{H} = \big(\mathrm{FS}, (G_{\mathrm{fs}})_{\mathrm{fs}\in\mathrm{FS}}, (\iota_{\mathrm{fs}})_{\mathrm{fs}\in\mathrm{FS}}, (\Lambda_{\mathrm{fs}})_{\mathrm{fs}\in\mathrm{FS}}, (\zeta_{\mathrm{fs}})_{\mathrm{fs}\in\mathrm{FS}}\big)$ be an HE model according to Definition 2.18 and let $r_D \geq 0$ be a drift resistance. The corresponding* drifted HE model *is the 5-tuple $\mathcal{H}_{r_D} = \big(\mathrm{FS}, (G_{\mathrm{fs}})_{\mathrm{fs}\in\mathrm{FS}}, (\iota_{\mathrm{fs},r_D})_{\mathrm{fs}\in\mathrm{FS}}, (\Lambda_{\mathrm{fs}})_{\mathrm{fs}\in\mathrm{FS}}, (\zeta_{\mathrm{fs}})_{\mathrm{fs}\in\mathrm{FS}}\big)$, where $(\iota_{\mathrm{fs},r_D})_{\mathrm{fs}\in\mathrm{FS}}$ is an indexed family of functions $\iota_{\mathrm{fs},r_D} : G_{\mathrm{fs}} \to \mathbb{R}_{>0}$ that are defined by*

$$\iota_{\mathrm{fs},r_D}(g) := \frac{U\iota_{\mathrm{fs}}(g)}{r_D\iota_{\mathrm{fs}}(g) + U} \;\forall\; g \in G_{\mathrm{fs}}. \tag{3.4}$$

The functions ι_{fs,r_D} are called the drifted ioni current functions with respect to fs and r_D.

Lemma 3.13 *Let $r_D \geq 0$. Then, the drifted ioni current functions ι_{fs,r_D} are well-defined for all* $\mathrm{fs} \in \mathrm{FS}$.

Proof. Let $r_D \geq 0$ and let $\mathrm{fs} \in \mathrm{FS}$. According to Definition 2.18, we have $\iota_{\mathrm{fs}}(g) > 0$ for all $g \in G_{\mathrm{fs}}$. In addition $r_D \geq 0$ and $U > 0$, thus we have $r_D\iota_{\mathrm{fs}}(g) + U > 0$, i.e., the denominator of (3.4) is greater than zero and the fraction is well-defined. Because

the nominator $U\iota_{\text{fs}}(g)$ is positive as well, we have $\iota_{\text{fs},r_D}(g) > 0$ for all $g \in G_{\text{fs}}$, i.e, $\iota_{\text{fs},r_D}(G_{\text{fs}}) \subset \mathbb{R}_{>0}$. □

Analogous to the undrifted ioni current function ι_{fs}, the drifted functions ι_{fs,r_D} are also strictly increasing homeomorphisms. To show this, we consider the following auxiliary function, which is motivated by (3.4).

Definition 3.14 *Let $r_D \geq 0$. We define the auxiliary function*

$$h_{r_D} : \mathbb{R}_{>0} \to \mathbb{R}_{>0}, \quad h_{r_D}(x) := \frac{Ux}{U + r_D x}.$$

Lemma 3.15 *The function h_{r_D} is well-defined, continuous and strictly increasing.*

Proof. That h_{r_D} is well-defined follows from the fact that its domain is $\mathbb{R}_{>0}$ (analogous to the proof of Lemma 3.13). Because h_{r_D} is composed of continuous operations, it is continuous as well. The function h_{r_D} is even differentiable. Its derivative is

$$\frac{d}{dx} h_{r_D}(x) = \frac{U(U + r_D x) - Uxr_D}{(U + r_D x)^2} = \frac{U^2}{(U + r_D x)^2}.$$

We have $\frac{d}{dx} h_{r_D}(x) > 0$ for all $x \in \mathbb{R}_{>0}$, i.e., h_{r_D} is strictly increasing on $\mathbb{R}_{>0}$. □

Lemma 3.16 *Let $r_D \geq 0$ and let* $\text{fs} \in \text{FS}$. *The drifted ioni current function ι_{fs,r_D} according to* (3.4) *is a strictly increasing homeomorphism.*

Proof. By construction, we have $\iota_{\text{fs},r_D} = h \circ \iota_{fs}$. The functions ι_{fs} and h are both strictly increasing and continuous (Definition 2.18 and Lemma 3.15, respectively). As a composition of strictly increasing and continuous functions, ι_{fs,r_D} is also strictly increasing and continuous. In particular, ι_{fs,r_D} is bijective and thus its inverse function $\iota^{-1}_{\text{fs},r_D}$ exists. Because ι_{fs,r_D} is strictly increasing and its domain is an interval (the set G_{fs} is an interval according to Definition 2.18), $\iota^{-1}_{\text{fs},r_D}$ is also continuous [Gar13, p. 163]. In total, ι_{fs,r_D} is a strictly increasing homeomorphism. □

The images of the drifted ioni current functions ι_{fs,r_D}, $\text{fs} \in \text{FS}$, play a central role in the ADA procedure and thus they are denoted as follows.

Notation 3.17 *Let $\mathcal{H}_{r_D} = \left(\text{FS}, (G_{\text{fs}})_{\text{fs}\in\text{FS}}, (\iota_{\text{fs},r_D})_{\text{fs}\in\text{FS}}, (\Lambda_{\text{fs}})_{\text{fs}\in\text{FS}}, (\zeta_{\text{fs}})_{\text{fs}\in\text{FS}}\right)$ be a drifted HE model. The images of the drifted ioni current functions ι_{fs,r_D} are called* the sets of drifted ioni currents (with respect to fs and r_D) *and are denoted by $I_{\text{fs},r_D} := \iota_{\text{fs},r_D}(G_{\text{fs}})$ for all* $\text{fs} \in \text{FS}$.

Corollary 3.18 *Let* $\text{fs} \in \text{FS}$. *The set of drifted ioni currents I_{fs,r_D} is a closed interval in $\mathbb{R}_{>0}$.*

Proof. As the image of a closed interval under a homeomorphism, I_{fs,r_D} is a closed interval as well. □

Recall from Section 2.4.5 that IoniDetect can only evaluate the inverse ioni current functions ι_{fs}^{-1}, $\mathsf{fs} \in \mathsf{FS}$. This also applies to the situation with drift. The following remark is analogous to Remark 2.25.

Remark 3.19 *It is important to emphasize that if a drift resistance r_D is present, IoniDetect can only evaluate the inverse of the drifted ioni current function $\iota_{\mathsf{fs},r_D}^{-1}$, $\mathsf{fs} \in \mathsf{FS}$. It can neither evaluate the "non-inverted" drifted ioni current function ι_{fs,r_D} nor the ioni current functions with no drift, i.e., ι_{fs} and ι_{fs}^{-1}.*

With the drift included into the HE model, we show the influence of drift on the combustion control in the following subsection.

3.1.4. Impact of Drift

To illustrate the impact of drift, recall from Section 2.3.2 that the combustion control system IoniDetect is blind with respect to the equivalence AFR and to the gvp. Instead, the ioni current is used as an indirect measure of the equivalence AFR to control the gas valve. For this, the ioni current setpoints of an HE must be determined with special equipment to measure the equivalence AFR in the lab as stated in Section 2.3.3. It is important to emphasize that the ioni current setpoints are determined under the condition of no drift.
But with increasing operating time an oxide layer accrues on the electrode and we have an additional drift resistance r_D in the measurement circuit, which alters the ioni current according to (3.3). The following example demonstrates how this change in ioni current caused by drift influences combustion control and the AFR.

Example 3.20 *Let $\mathcal{H} = \left(\mathsf{FS}, (G_{\mathsf{fs}})_{\mathsf{fs}\in\mathsf{FS}}, (\iota_{\mathsf{fs}})_{\mathsf{fs}\in\mathsf{FS}}, (\Lambda_{\mathsf{fs}})_{\mathsf{fs}\in\mathsf{FS}}, (\zeta_{\mathsf{fs}})_{\mathsf{fs}\in\mathsf{FS}}\right)$ be an HE model based on Vaillant measurement data according to [PHE, Item 6371]. Let us suppose that a fan speed setpoint* $\mathsf{fs} \in \mathsf{FS}$ *is given. Let the corresponding ioni current setpoint according to the control curve be i_{set}. Then, the combustion control by IoniDetect works as follows. The fan speed is fixed at* fs*. The gas valve is then moved such that the resulting ioni current is i_{set}. Using the HE model, this corresponds to calculating the gvp $g_n := \iota_{\mathsf{fs}}^{-1}(i_{\mathsf{set}})$, which is equivalent to $\iota_{\mathsf{fs}}(g_n) = i_{\mathsf{set}}$. The subscript n refers to the situation with no drift. The fan speed* fs *and the gvp g_n in turn result in the equivalence AFR $\lambda_n = \Lambda_{\mathsf{fs}}(g_n)$.*
This situation is illustrated in Figure 3.2. The solid curve in the left part of Figure 3.2 corresponds to the inverse ioni current function ι_{fs}^{-1}. With this function the gvp corresponding to the ioni current setpoint i_{set} is determined by IoniDetect, see also Section 2.4.5. This gvp is denoted by g_n and the corresponding point is marked by the dot in the left part of Figure 3.2. The right part of Figure 3.2 shows the equivalence AFR function Λ_{fs}. The equivalence AFR resulting from fs *and g_n is $\Lambda_{\mathsf{fs}}(g_n) = 1.3$. The corresponding point is marked by the dot in the right part of Figure 3.2. An equivalence AFR of* 1.3 *is a common value for normal HE operation, see also Section 2.2.*
We further assume that some drift has taken place and that a drift resistance $r_D = 140k\Omega$ is present, which is a common value [PHE, Item 1618]. In the HE model, the drifted ioni

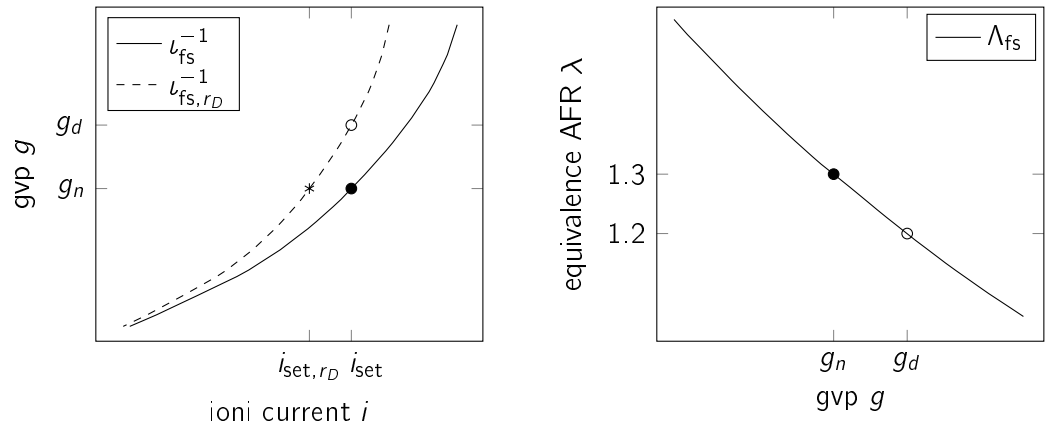

Figure 3.2.: The impact of drift is illustrated for a given fan speed setpoint fs and an ioni current setpoint i_{set} as well as the drift resistance $r_D = 140k\Omega$. The dot corresponds to the situation with no drift. The circle corresponds to the situation with drift. In the case of drift, the resulting equivalence AFR decreases from $\Lambda_{\mathsf{fs}}(g_n) = \Lambda_{\mathsf{fs}} \circ \iota_{\mathsf{fs}}^{-1}(i_{\mathsf{set}}) = 1.3$ to $\Lambda_{\mathsf{fs}}(g_d) = \Lambda_{\mathsf{fs}} \circ \iota_{\mathsf{fs},r_D}^{-1}(i_{\mathsf{set}}) = 1.2$. The asterisk corresponds to the setpoint that is perfectly adapted to r_D, because $\Lambda_{\mathsf{fs}} \circ \iota_{\mathsf{fs},r_D}^{-1}(i_{\mathsf{set},r_D}) = 1.3$.

current is represented by the function ι_{fs,r_D}, which is calculated from ι_{fs} by (3.4). *Its inverse function $\iota_{\mathsf{fs},r_D}^{-1}$ is represented by the dashed curve in the left part of Figure 3.2. Recall that the controller does not have any direct information about the AFR. It just follows the control curve, i.e., it controls the gas valve such that the ioni current equals i_{set}. In the drifted case, this results in the gvp $g_d = \iota_{\mathsf{fs},r_D}^{-1}(i_{\mathsf{set}})$. The subscript d refers to the situation with drift. This is illustrated by the circle in the left part of Figure 3.2. Note that the resulting gvp is larger than the gvp in the case with no drift, i.e., $g_d > g_n$. The increased gvp results in the reduced AFR $\Lambda_{\mathsf{fs}}(g_d) = 1.2$, which is represented by the circle in the right part of Figure 3.2. The combustion process is not optimal anymore.*
In order to operate at the desired AFR $\lambda_n = 1.3$ also in the drifted case, the ioni current setpoint has to be corrected. This corrected ioni current setpoint is denoted by i_{set,r_D} and is marked by the asterisk in the left part of Figure 3.2. Then, the resulting gvp is $\iota_{\mathsf{fs},r_D}^{-1}(i_{\mathsf{set},r_D}) = g_n$ and the resulting equivalence AFR equals $\lambda_n = \Lambda_{\mathsf{fs}}(g_n) = 1.3$ again.

As demonstrated in Example 3.20, if no correction is made, then the AFR becomes more and more fuel rich with increasing drift resistance. As a consequence, the emission of CO increases and in the worst case the appliances become toxic. Therefore, every ioni current setpoint of the control curve has to be corrected according to Equation (3.4). But the value of r_D is unknown in general and it is hardly possible and not practical to measure it directly. The ADA procedure is a solution to this problem. According to the ADA patent [LS17], ADA corrects the measured current "simply and reliably" without "exceeding predetermined limits for the combustion values" [LS17, p. 2]. The ADA procedure is presented in the following sections.

3.2. The Notion of ADA

As illustrated in the previous section, in order to ensure a safe combustion, we need the drifted ioni currents ι_{fs,r_D} according to (3.4). For this, we require the unknown drift resistance r_D. The goal of ADA is to approximate r_D. In this section, we illustrate how this is done by ADA. For this, we assume for the remainder of this chapter that an HE model $\mathcal{H} = \big(\mathsf{FS}, (G_{\mathsf{fs}})_{\mathsf{fs}\in\mathsf{FS}}, (\iota_{\mathsf{fs}})_{\mathsf{fs}\in\mathsf{FS}}, (\Lambda_{\mathsf{fs}})_{\mathsf{fs}\in\mathsf{FS}}, (\zeta_{\mathsf{fs}})_{\mathsf{fs}\in\mathsf{FS}}\big)$ and a drift resistance $r_D \geq 0$ are given.
As a first step, we solve (3.4) for r_D.

Lemma 3.21 *Let* $\mathsf{fs} \in \mathsf{FS}$ *and* $g \in G_{\mathsf{fs}}$*, then*

$$r_D = U\big(\frac{1}{\iota_{\mathsf{fs},r_D}(g)} - \frac{1}{\iota_{\mathsf{fs}}(g)}\big). \tag{3.5}$$

Proof. Let $\mathsf{fs} \in \mathsf{FS}$ and let $g \in G_{\mathsf{fs}}$. Note that $\iota_{\mathsf{fs}}(g) > 0$ and $\iota_{\mathsf{fs},r_D}(g) > 0$ according to Definitions 2.18 and 3.12, respectively. We have

$$\begin{aligned}(3.4) \;&\Leftrightarrow\; \frac{1}{\iota_{\mathsf{fs},r_D}(g)} = \frac{r_D\iota_{\mathsf{fs}}(g) + U}{U\iota_{\mathsf{fs}}(g)} \;\Leftrightarrow\; \frac{1}{\iota_{\mathsf{fs},r_D}(g)} = \frac{r_D}{U} + \frac{1}{\iota_{\mathsf{fs}}(g)} \\ &\Leftrightarrow\; r_D = U\big(\frac{1}{\iota_{\mathsf{fs},r_D}(g)} - \frac{1}{\iota_{\mathsf{fs}}(g)}\big).\end{aligned}$$

□

Lemma 3.21 states that if we know the undrifted and the drifted ioni current of a certain actuator position (fs, g), then we also know r_D.
In ADA, this is done at a specific operating point that is called *test point* [LS17, p. 7] [Sch15] [WHB, Item 4229]. The test point is specified by a fan speed and an ioni current. The fan speed is called *test fan speed* and denoted by t in the following. The ioni current is called *test ioni current* and is denoted by i_t in the following. It is important to emphasize that the test ioni current corresponds to the situation with no drift.
The fan speed t and the ioni current i_t correspond to a unique gvp. In relation to the HE model, the corresponding gvp of the test point is $g_A := \iota_t^{-1}(i_t)$. The subscript A stands for ADA. To comply with the HE model, we require that $t \in \mathsf{FS}$ and $i_t \in I_t = \iota_t(G_t)$. Then, $\iota_t^{-1}(i_t)$ is well-defined (Definitions 2.18 and 2.22). In particular, $g_A \in G_t$ holds.
By plugging the data of the test point into (3.5), the drift resistance is calculated by

$$r_D = \frac{U}{\iota_{t,r_D}(g_A)} - \frac{U}{i_t}. \tag{3.6}$$

The test fan speed t and the test ioni current i_t are selected in the lab and thus they are known. However, the drifted test ioni current $\iota_{t,r_D}(g_A)$ is unknown, because r_D is unknown. If we could set the gvp to g_A, then IoniDetect could simply measure the resulting ioni current $\iota_{t,r_D}(g_A)$. But IoniDetect can only evaluate the inverse drifted ioni current function $\iota_{\mathsf{fs},r_D}^{-1}$, see also Remark 3.19.

There is one small exception. Let us suppose that we have a given fan speed fs $\in$ FS and a given ioni current i. Once the gas valve has moved to the position $g = \iota^{-1}_{\text{fs},r_D}(i)$ (well-defined if $i \in I_{\text{fs},r_D}$), IoniDetect can fix the gvp at g. Then, this particular g can be considered as known to IoniDetect and the drifted ioni current $\iota_{t,r_D}(g)$ can be determined (if $g \in G_t$). I.e., while the gvp is fixed at g, the fan speed is changed from fs to t and then the resulting ioni current is measured. The ADA procedure uses this small exception to approximate $\iota_{t,r_D}(g_A)$, which in turn is plugged into (3.6) in order to approximate r_D. The approximation of $\iota_{t,r_D}(g_A)$ is a key component of ADA and is described in detail next.

3.2.1. Approximation of the Drifted Test Ioni Current and of the Drift Resistance

In order to approximate $\iota_{t,r_D}(g_A)$, a second operating point, the so-called *start point*, is required [LS17, p. 7]. The start point is also specified by a fan speed and an ioni current. These are denoted by s and i_s, respectively, in the following. The start fan speed has to be larger than the test fan speed, i.e., $s > t$ [LS17, p. 7] [WHB, Item 4228]. Furthermore, the test point and the start point must have the same gvp [LS17, p. 7], i.e., the start ioni current must be selected such that $\iota_s^{-1}(i_s) = g_A = \iota_t^{-1}(i_t)$. Note that the start point is specified for the case with no drift, i.e., $\iota_s(g_A) = i_s$ (and not $\iota_{s,r_D}(g_A) = i_s$). To comply with the HE model, we require that $s \in$ FS and $g_A \in G_s$, because $i_s = \iota_s(g_A)$, or equivalently $g_A = \iota_s^{-1}(i_s)$, is well-defined in this case.
Now, let us suppose that an oxide layer has accrued on the ioni electrode that corresponds to an unknown drift resistance $r_D \geq 0$. We want to approximate r_D according to (3.6) and require the value of $\iota_{t,r_D}(g_A)$. With the start and the test point at hand, $\iota_{t,r_D}(g_A)$ is approximated in two steps. First, the gvp g_A is approximated by $\hat{g}_A := \iota^{-1}_{s,r_D}(i_s)$, i.e., the fan speed is fixed at s and the gas valve is moved such that the resulting drifted ioni current corresponds to i_s. Then, the gvp is fixed at $\hat{g}_A$ and the fan speed is reduced from s to t. The resulting ioni current $\iota_{t,r_D}(\hat{g}_A)$ is the approximation of $\iota_{t,r_D}(g_A)$, which is then plugged into (3.6) to approximate r_D. In total, we perform the steps

$$\hat{g}_A := \iota^{-1}_{s,r_D}(i_s), \quad \hat{i}_{t,r_D} := \iota_{t,r_D}(\hat{g}_A) \quad \text{and} \quad \hat{r}_D := \frac{U}{\hat{i}_{t,r_D}} - \frac{U}{i_t}. \tag{3.7}$$

The following example demonstrates the approximation of r_D according to (3.7).

Example 3.22 *The HE model considered in this example is based on Vaillant measurement data according to [PHE, Item 6371]. Let us suppose that we have already selected a start point with the fan speed $s \in$ FS and the ioni current $i_s \in I_s$ as well as a test point with the fan speed $t \in$ FS and the ioni current $i_t \in I_t$, where $s > t$. Furthermore, the start and the test point are selected such that they have the same gvp, i.e., $\iota_s^{-1}(i_s) = \iota_t^{-1}(i_t) = g_A$ or equivalently $\iota_s(g_A) = i_s$ and $\iota_t(g_A) = i_t$.*
The start and the test point as well as the corresponding ioni current functions are shown in Figure 3.3. The solid orange curve corresponds to the ioni current function at the start

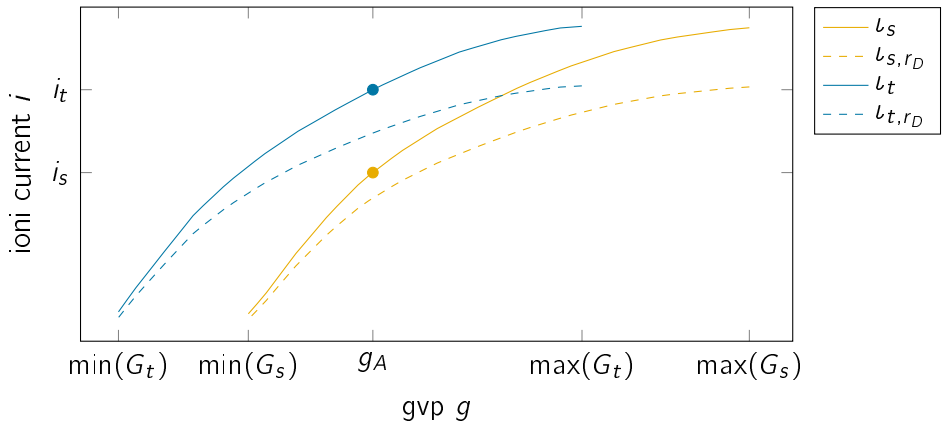

Figure 3.3.: The start point (s, i_s) and the test point (t, i_t) as selected in Example 3.22 are shown. Their ioni currents are selected such that both points have the identical gvp g_A, i.e., $\iota_s^{-1}(i_s) = \iota_t^{-1}(i_t) =: g_A$. In particular, $g_A \in G_s \cap G_t$ holds.

fan speed and the solid blue curve corresponds to the ioni current function at the test fan speed. The start and test ioni current are selected such that both points have the same gvp g_A and such that g_A complies with the HE model, i.e., $g_A \in G_s$ and $g_A \in G_t$. The corresponding start ioni current is $i_s = \iota_s(g_A)$ and the start point is marked by the orange dot in Figure 3.3. Analogously, we have $i_t = \iota_t(g_A)$ and the test point is marked by the blue dot. Note that the start point and test point are specified for the case with no drift. Let us further suppose that a drift resistance $r_D = 140k\Omega$ is present. The corresponding drifted ioni current functions according to (3.4) *at the start fan speed and at the test fan speed are represented by the dashed orange and blue curve, respectively, in Figure 3.3. In the following, we demonstrate the approximation of r_D according to* (3.7).
First, the gvp g_A is approximated with the start point, i.e., with the start fan speed s and the start ioni current i_s. This corresponds to evaluating $\iota_{s,r_D}^{-1}(i_s)$. This situation is depicted in Figure 3.4. The solid curve corresponds to the inverse ioni current at the start fan speed s with no drift, ι_s^{-1}. The dashed curve corresponds to the inverse drifted ioni current function at s, ι_{s,r_D}^{-1}. In the case of no drift, the start ioni current i_s corresponds to the gvp g_A, i.e., $\iota_s^{-1}(i_s) = g_A$. This is marked by the dot in Figure 3.4. However, because r_D is present, IoniDetect can only evaluate $\iota_{s,r_D}^{-1}(i_s)$, see also Remark 3.19. Therefore, the gvp is approximated by $\hat{g}_A := \iota_{s,r_D}^{-1}(i_s)$. This is marked by the circle in Figure 3.4.
To approximate the drifted test ioni current $i_{t,r_D} := \iota_{t,r_D}(g_A)$, the gvp is fixed at $\hat{g}_A$ and the fan speed is reduced from s to t. This situation is depicted in Figure 3.5. Analogously to Figure 3.3, the solid and dashed blue curve correspond to ι_t and ι_{t,r_D}, respectively. The test point with the ioni current i_t and the gvp $g_A = \iota_t^{-1}(i_t)$ is marked by the dot. The drifted test ioni current $i_{t,r_D} := \iota_{t,r_D}(g_A)$ is marked by the asterisk. Recall that the goal of ADA is to approximate i_{t,r_D}. With the approximation $\hat{g}_A$ of g_A, we obtain the approximation $\hat{i}_{t,r_D} = \iota_{t,r_D}(\hat{g}_A)$. This point is marked by the circle in Figure 3.5.
With this, we can finally approximate the drift resistance according to (3.7). *In this*

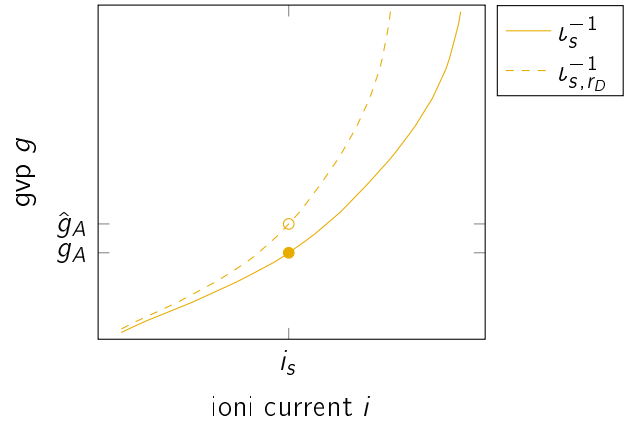

Figure 3.4.: The approximation of the gvp $g_A = \iota_s^{-1}(i_s)$ by using the start point is shown. The dot corresponds to the undrifted start point (i_s, g_A). Because IoniDetect can only evaluate ι_{s,r_D}^{-1}, the gvp g_A is approximated by $\hat{g}_A = \iota_{s,r_D}^{-1}(i_s)$, which is represented by the circle.

example, we obtain $\hat{r}_D \approx 84k\Omega$. *Because* $r_D = 140k\Omega$, *this means that the drift resistance was approximated by approximately* 60 *percent of its true value.*

Approximating the drift resistance is only an intermediate step. Our ultimate goal is to obtain the drifted ioni currents according to (3.4).

3.2.2. Approximation of Arbitrary Drifted Ioni Currents

Equation (3.4) can be interpreted as a transformation, where a given ioni current $\iota_{\mathsf{fs}}(g)$ is transformed to its drifted counterpart $\iota_{\mathsf{fs},r_D}(g)$ for a given drift resistance $r_D \geq 0$. By plugging the approximated drift resistance $\hat{r}_D$ into (3.4), we obtain the approximation

$$\iota_{\mathsf{fs},\hat{r}_D}(g) = \frac{U\iota_{\mathsf{fs}}(g)}{\hat{r}_D\iota_{\mathsf{fs}}(g) + U} \tag{3.8}$$

of the drifted ioni current $\iota_{\mathsf{fs},r_D}(g)$ for $\mathsf{fs} \in \mathsf{FS}$ and $g \in G_{\mathsf{fs}}$.

Remark 3.23 *To avoid case distinctions, we suppose that* (3.8) *is well-defined for all considered drift resistance approximations* $\hat{r}_D$ *for the moment. A function corresponding to* (3.8) *and an appropriate domain for the case* $\mathsf{fs} = s$ *are formally defined in Chapter 5 when a mathematical formulation of the ADA algorithm is presented.*

Equation (3.8) is used to approximate the drifted counterparts of the ioni current setpoints of the control curve. For instance, let $\mathsf{fs} \in \mathsf{FS}$ and let i_{set} be the corresponding ioni current setpoint according to the control curve. If i_{set} is not adapted with respect to r_D, the combustion quality is not optimal anymore as demonstrated in Example 3.20. Therefore, i_{set} is updated according to (3.8) as soon as a drift resistance approximation $\hat{r}_D$ is available. Then, $i_{\mathsf{set},\hat{r}_D} := \frac{Ui_{\mathsf{set}}}{\hat{r}_D i_{\mathsf{set}} + U}$ is the updated ioni current setpoint of the control curve for the fan speed fs and the combustion quality usually improves.

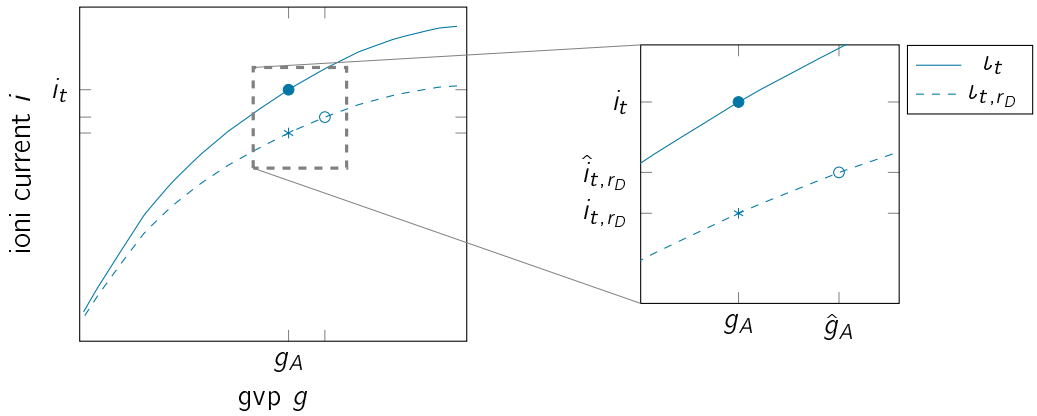

Figure 3.5.: The approximation of the drifted test ioni current $i_{t,r_D} = \iota_{t,r_D}(g_A)$ by using the approximation $\hat{g}_A$ of g_A is shown. The gvp is fixed at $\hat{g}_A$ and the fan speed is adjusted to t. This corresponds to evaluating $\iota_{t,r_D}(\hat{g}_A) =: \hat{i}_{t,r_D}$, which is represented by the circle. The undrifted test point is represented by the dot and the drifted test point is marked by the asterisk. It is apparent that $|\hat{i}_{t,r_D} - i_{t,r_D}| < |i_t - i_{t,r_D}|$, i.e., the determined $\hat{i}_{t,r_D}$ is a better approximation of i_{t,r_D} than i_t is.

Example 3.24 *This Example continues Examples 3.20 and 3.22. We consider the situation as in Example 3.20, i.e., we have the fan speed setpoint* fs *and the ioni current setpoint* i_{set}*. In the case with no drift, the resulting equivalence AFR is* $\lambda_n = \Lambda_{\text{fs}} \circ \iota_{\text{fs}}^{-1}(i_{\text{set}}) = 1.3$ *as shown in Figure 3.2.*
Furthermore, we suppose that the drift resistance $r_D = 140k\Omega$ *is present. If* i_{set} *is not corrected with respect to* r_D*, then the resulting equivalence AFR is* $\lambda_d = \Lambda_{\text{fs}} \circ \iota_{\text{fs},r_D}^{-1}(i_{\text{set}}) = 1.2$ *as demonstrated in Example 3.20 and according to Figure 3.2, i.e., the combustion quality has deteriorated.*
Now, let us suppose that the drift resistance is approximated by $\hat{r}_D = 84k\Omega$ *as done in Example 3.22, i.e., the drift resistance is approximated by approximately* 60 *percent of its true value. With this, we approximate the drifted ioni current setpoint* $i_{\text{set},r_D} := \frac{U i_{\text{set}}}{r_D i_{\text{set}} + U}$ *by* $i_{\text{set},\hat{r}_D} := \frac{U i_{\text{set}}}{\hat{r}_D i_{\text{set}} + U}$ *according to* (3.8)*. With this, we obtain the (not perfectly) corrected gvp* $g_c = \iota_{\text{fs},r_D}^{-1}(i_{\text{set},\hat{r}_D})$*, which in turn results in the equivalence AFR* $\Lambda_{\text{fs}}(g_c) = 1.27$ *and the combustion quality has improved.*
This situation is depicted in Figure 3.6. The left part of Figure 3.6 is an enlarged section of the left part of Figure 3.2. The point resulting from the correction with the drift resistance approximation $\hat{r}_D$ *is represented by the square. The drifted ioni current setpoint approximation* $i_{\text{set},\hat{r}_D}$ *results in the corrected gvp* g_c*. Analogously, the right part of Figure 3.6 is an enlarged section of the right part of Figure 3.2. The corrected gvp* g_c *results in the equivalence AFR* $\Lambda_{\text{fs}}(g_c) = 1.27$*, which is again represented by the square. This is closer to the desired equivalence AFR* $\lambda_n = 1.3$ *than* $\lambda_d = 1.2$ *to* λ_n *is, i.e, the combustion quality has improved compared to the case with drift but without a correction.*

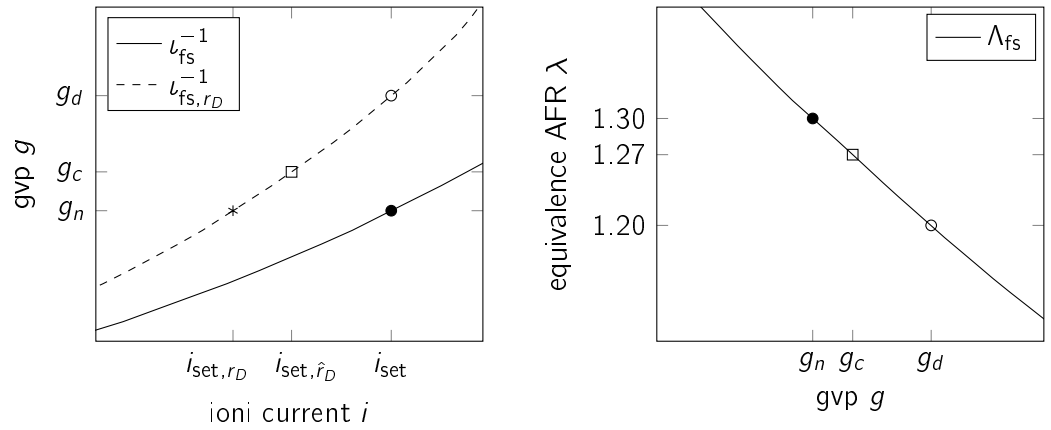

Figure 3.6.: The left and the right part of this figure show an enlarged section of the left part and of the right part of Figure 3.2, respectively. The square in the left part represents the approximation of i_{set,r_D} that is determined by applying (3.8) with $\hat{r}_D = 84k\Omega$ from Example 3.22 and i_{set} from Example 3.20. The resulting equivalence AFR is represented by the square in the right part of this figure. Because $\Lambda_{\mathrm{fs}}(g_c) = \Lambda_{\mathrm{fs}} \circ \iota_{\mathrm{fs},r_D}^{-1}(i_{\mathrm{set},\hat{r}_D}) = 1.27$, the situation has improved compared to $\Lambda_{\mathrm{fs}}(g_d) = \Lambda_{\mathrm{fs}} \circ \iota_{\mathrm{fs},r_D}^{-1}(i_{\mathrm{set}}) = 1.2$.

Next, we briefly discuss the selection of the start and the test point. In particular, we consider how their selection is related to the approximation quality of $\hat{i}_{t,r_D}$ and $\hat{r}_D$ according to (3.7).

3.2.3. Approximation Quality and Selection of the Start and Test Point

The start point (s, i_s) and the test point (t, i_t) are essential for the approximation of r_D according to (3.7). The following definition states how s, t, i_s and i_t have to be selected in order to comply with the HE model and with the considerations made so far. Because a start point and a test point are assigned to each other, the combination of both is denoted as an ADA pair in this thesis.

Definition 3.25 *Let* $\mathcal{H} = \left(\mathrm{FS}, (G_{\mathrm{fs}})_{\mathrm{fs}\in\mathrm{FS}}, (\iota_{\mathrm{fs}})_{\mathrm{fs}\in\mathrm{FS}}, (\Lambda_{\mathrm{fs}})_{\mathrm{fs}\in\mathrm{FS}}, (\zeta_{\mathrm{fs}})_{\mathrm{fs}\in\mathrm{FS}}\right)$ *be an HE model. A quadruple* (s, t, i_s, i_t) *is called* well-defined ADA pair with respect to $\mathcal{H}$, *if*

$$s, t \in \mathrm{FS} : s > t, \quad i_s \in I_s \quad \text{and} \quad i_t \in I_t.$$

It is called well-selected ADA pair with respect to $\mathcal{H}$, *if in addition* $\iota_s^{-1}(i_s) = \iota_t^{-1}(i_t) =: g_A$ *holds.*

Remark 3.26 *Note that an ADA pair is only well-defined or well-selected in relation to an HE model* $\mathcal{H}$. *For instance, if a well-selected ADA pair is considered with a different HE model* $\overline{\mathcal{H}} \neq \mathcal{H}$, *then it might not be well-selected anymore. Such a situation is often caused by tolerances with respect to the position of the ioni electrode relative to the burner. Then, the condition* $\iota_s^{-1}(i_s) = \iota_t^{-1}(i_t)$ *of Definition 3.25 is usually not satisfied anymore. This*

is detailed in Section 6.3.2 below. For the moment, we consider only well-selected ADA pairs. When there is no risk of confusion, the HE model related to a well-selected ADA pair is not explicitly stated for the remainder of this thesis.

Let (s, t, i_s, i_t) be a well-selected ADA pair. Its approximation quality of r_D according to (3.7) depends on two aspects. First, we need a good approximation of g_A, i.e.,

$$|\hat{g}_A - g_A| = |\iota_{s,r_D}^{-1}(i_s) - \iota_s^{-1}(i_s)|$$

should be small. Therefore, the start point should be selected such that $\iota_{s,r_D}^{-1}(i_s)$ and $\iota_s^{-1}(i_s)$ are close to each other. For instance, in Example 3.22 this can be achieved by selecting a smaller start ioni current i_s according to Figure 3.4. Note that this would result in a smaller ADA gvp $g_A = \iota_s^{-1}(i_s)$, because ι_s^{-1} is strictly increasing.
Second, we want that $\iota_{t,r_D}(\hat{g}_A)$ is close to $\iota_{t,r_D}(g_A)$. Therefore, the test point should be selected such that the absolute value of the gradient of ι_{t,r_D} is small in the vicinity of g_A (under the assumption that ι_{t,r_D} is differentiable), i.e.,

$$\left|\frac{d}{dg}\iota_{t,r_D}(g)\right| \text{ is small } \forall\ g \in [g_A - \delta, g_A + \delta],\ \delta := |g_A - \hat{g}_A|.$$

For instance, in Example 3.22 this can be achieved by selecting a larger test ioni current i_t according to Figure 3.5. However, this results in a larger ADA gvp $g_A = \iota_t^{-1}(i_t)$. This contradicts the selection of a smaller start ioni current i_s, because a smaller i_s results in a smaller g_A.
Note that a different drift resistance $\bar{r}_D \neq r_D$ results in different drifted ioni current functions $\iota_{t,\bar{r}_D} \neq \iota_{t,r_D}$ and $\iota_{s,\bar{r}_D}^{-1} \neq \iota_{s,r_D}^{-1}$ in general, which makes the selection of an ADA pair more complicated.
These considerations illustrate the challenges when selecting an ADA pair with respect to the approximation quality. In addition, certain combustion limits must not be exceeded during the function evaluations according to (3.7). This work addresses the challenge of selecting optimized ADA pairs. The goal as well as the scope of this work are formulated in more detail in Section 3.5.

The approximation of the drifted test ioni current and of the drift resistance according to (3.7) as well as the approximation of arbitrary drifted ioni currents according to (3.8) are the core of the ADA procedure. By applying a combination of (3.7) and (3.8) successively, the approximation quality can be improved. This gives us a sequence of approximations, which is detailed next.

3.3. Sequence of ADA Iterations

Equation (3.7) usually only partially approximates the drift resistance. For instance, in Example 3.22 we obtained $\hat{r}_D = 0.6 r_D$. Of course, we are interested in a perfect approximation of r_D, which can be achieved by successively applying (3.7).

To illustrate this, we require the drifted start and test ioni current. These correspond to the transformation of the start and test ioni current to their drifted counterparts according to (3.4).

Definition 3.27 *Let (s, t, i_s, i_t) be a well-defined ADA pair. The* drifted start ioni current *and the* drifted test ioni current *are defined by*

$$i_{s,r_D} := \iota_{s,r_D}(g_s) \text{ with } g_s = \iota_s^{-1}(i_s) \quad \text{and} \quad i_{t,r_D} := \iota_{t,r_D}(g_t) \text{ with } g_t = \iota_t^{-1}(i_t),$$

respectively.

Remark 3.28 *Note that the drifted test ioni current i_{t,r_D} according to Definition 3.27 corresponds to the drifted test ioni current $\iota_{t,r_D}(g_A)$ used to illustrate the notion of ADA in Section 3.2.*

Lemma 3.29 *Let (s, t, i_s, i_t) be a well-defined ADA pair. Then, the drifted start and test ioni current are well-defined. Furthermore, we have*

$$i_{s,r_D} = \frac{U i_s}{r_D i_s + U} \quad \text{and} \quad i_{t,r_D} = \frac{U i_t}{r_D i_t + U}.$$

In particular, we have $i_{s,r_D} > 0$ and $i_{t,r_D} > 0$.

Proof. Because (s, t, i_s, i_t) is a well-defined ADA pair, we have $i_s \in I_s = \iota_s(G_s)$ (Definition 3.25) and thus $g_s = \iota_s^{-1}(i_s) \in G_s$ (Definition 2.22), i.e., g_s is well-defined. Because G_s is the domain of ι_{s,r_D} (Definition 3.12), $\iota_{s,r_D}(g_s)$ is well-defined as well.
By construction, we have $\iota_s(g_s) = \iota_s \circ \iota_s^{-1}(i_s) = i_s$ and thus

$$i_{s,r_D} = \iota_{s,r_D}(g_s) = \frac{U \iota_s(g_s)}{r_D \iota_s(g_s) + U} = \frac{U i_s}{r_D i_s + U}.$$

Finally, $U > 0$, $r_D \geq 0$ and $i_s \in I_s \subset \mathbb{R}_0$ imply that $i_{s,r_D} > 0$.
The statements with respect to i_{t,r_D} are shown analogously. □

To motivate the sequence of ADA iterations, let us consider a well-defined ADA pair (s, t, i_s, i_t). In addition, let the ADA pair be well-selected, i.e., let $\iota_s^{-1}(i_s) = \iota_t^{-1}(i_t) =: g_A$. If we plug the drifted start ioni current i_{s,r_D} into (3.7), then the drifted test ioni current and the drift resistance are perfectly approximated, because

$$\hat{i}_{t,r_D} = \iota_{t,r_D} \circ \iota_{s,r_D}^{-1}(i_{s,r_D}) = \iota_{t,r_D} \circ \iota_{s,r_D}^{-1} \circ \iota_{s,r_D}(g_A) = \iota_{t,r_D}(g_A) = i_{t,r_D}$$

and

$$\hat{r}_D = \frac{U}{\hat{i}_{t,r_D}} - \frac{U}{i_t} = \frac{U}{i_{t,r_D}} - \frac{U}{i_t} = \frac{r_D i_t + U}{i_t} - \frac{U}{i_t} = r_D \tag{3.9}$$

in this case. However, i_{s,r_D} is usually unknown. Therefore, the idea is to approximate i_{s,r_D} by applying (3.8) with the incumbent drift resistance approximation $\hat{r}_D$, i.e., we calculate

$i_{s,\hat{r}_D} = \frac{U i_s}{\hat{r}_D i_s + U}$. Equation (3.7) is then applied with $i_{s,\hat{r}_D}$ instead of i_s. With this, we obtain an updated approximation of the drifted test ioni current, i.e., we update

$$\hat{i}_{t,r_D} \leftarrow \iota_{t,r_D} \circ \iota_{s,r_D}^{-1}(i_{s,\hat{r}_D}), \quad \text{where} \quad i_{s,\hat{r}_D} = \frac{U i_s}{\hat{r}_D i_s + U} \quad \text{and} \quad \hat{r}_D = \frac{U}{\hat{i}_{t,r_D}} - \frac{U}{i_t}.$$

One such update of $\hat{i}_{t,r_D}$ is a so-called *ADA iteration*.

Definition 3.30 *Let (s, t, i_s, i_t) be a well-defined ADA pair (not necessarily well-selected). Let $\hat{i}_{t,r_D}$ be the incumbent approximation of the drifted test ioni current i_{t,r_D}. An* ADA iteration *is an update of $\hat{i}_{t,r_D}$ according to the following three steps.*

Approximate the drifted start ioni current *We approximate i_{s,r_D} by*

$$i_{s,\hat{r}_D} \coloneqq \frac{U i_s}{\hat{r}_D i_s + U} \quad \text{with} \quad \hat{r}_D = \frac{U}{\hat{i}_{t,r_D}} - \frac{U}{i_t}.$$

Move to approximated drifted start point *The fan speed is fixed at s and the gvp is adjusted such that the resulting ioni current equals $i_{s,\hat{r}_D}$. This results in the gvp $\hat{g} \coloneqq \iota_{s,r_D}^{-1}(i_{s,\hat{r}_D})$.*

Approximate the drifted test ioni current *The gvp is fixed at $\hat{g}$ and the fan speed is reduced from s to t. The resulting ioni current is the updated approximation of the drifted test ioni current, i.e., $\hat{i}_{t,r_D} \leftarrow \iota_{t,r_D}(\hat{g})$.*

Remark 3.31 *In the first iteration, usually no approximation of the drifted test ioni current is available. Then, the undrifted test ioni current i_t is used as the approximation of i_{t,r_D}, i.e., $\hat{i}_{t,r_D} = i_t$ is initially used [LS17, p. 10]. Note that this corresponds to the drift resistance approximation $\hat{r}_D = 0$, because $\hat{r}_D = \frac{U}{\hat{i}_{t,r_D}} - \frac{U}{i_t} = \frac{U}{i_t} - \frac{U}{i_t} = 0$ in this case.*

Remark 3.32 *Definition 3.30 is based on the technical documentation according to [LS17], [Sch15] and [WHB, Item 4228]. Therefore, Definition 3.30 is rather a technical description than a mathematical definition of an ADA iteration.*
An algorithmic description of an ADA iteration in a mathematical sense is given in Section 5.2.1 below after a corresponding formalism is introduced. This includes conditions such that the function evaluations in Definition 3.30 are well-defined.

By successively performing ADA iterations, we obtain a sequence of drifted test ioni current approximations $(\hat{i}_{t,r_D}^k)_{k \in \mathbb{N}}$. Ideally, this sequence converges to the true drifted test ioni current i_{t,r_D}, because then $\hat{r}_D = r_D$ according to (3.9). In addition, we are interested in a high rate of convergence.
According to the ADA patent [LS17] both aspects are fulfilled: "By means of iterative execution of the aforesaid test [...], there is rapid convergence" [LS17, p. 8]. And "following one or two iterations, there is practically no deviation present any more" [LS17, p. 9]. But the patent [LS17] gives only little information if there are certain conditions required for convergence. Conditions related to convergence are only stated in the ADA patent's

section about the selection of the test point: "The only pre-condition is that the function is uniformly rising or falling in the measurement range of the test point" [LS17, p. 8]. The term function in the citation refers to the ioni current versus λ curve with the fan speed fixed at the test fan speed t. If $\lambda \geq 1.05$, then this monotony "conditions are typically in effect" [LS17, p. 8]. Other aspects of this function are not relevant and the "shape and profile of the function remain unknown in this respect" [LS17, p. 8].
In Section 6.3, an analysis of the sequence's convergence behavior is done. One result is that it is required that an ADA pair is well-selected, otherwise the sequence of ADA iterations has not the true drifted test ioni current i_{t,r_D} as its limit (if it converges at all). In Section 6.3.4, the results of this analysis are compared to the aforementioned statements made in the patent [LS17].

Remark 3.33 *An aspect related to the sequence of drifted test ioni current approximations $(\hat{i}^k_{t,r_D})_{k\in\mathbb{N}}$ is the possibility to smoothen the results. The authors of the ADA patent propose to average the measured drifted test ioni currents approximations and thus "reduce scatter" [LS17, p. 9]. In IoniDetect, this is achieved by using two filter values, which are applied in two steps at the end of an ADA iteration [Sch15, p. 39]. Note that the term 'filter' is used in the sense of smoothing. It is used in the ADA patent and also by Vaillant. Essentially, the proposed filtering limits the step size when updating the drifted test ioni current approximation. In Section 6.2.2, it is shown that the sequence of drifted test ioni current approximations is a monotonic sequence. Thus, limiting the step size does not affect the sequence's limit, only its rate of convergence. Therefore, for the sake of simplicity, filtering of the ADA results is not considered in this study.*

3.4. Plurality of ADA Pairs

So far, only one ADA pair (s, t, i_s, i_t) was considered. However, the documentation suggests to use a plurality of ADA pairs [Sch15, p. 35]. On the one hand, tolerances with respect to the ioni electrode's position relative to the burner may affect the ioni current measurement in a way that has the effect of an additional drift resistance that depends on the fan speed and that can even be negative [LS17, p. 6]. A plurality of ADA pairs whose test fan speeds are distributed in the set of feasible fan speeds $\mathrm{FS} = [\mathrm{fs}_{\min}, \mathrm{fs}_{\max}]$ is better suited to detect and compensate this dependency on the fan speed. On the other hand, it is useful in practice to be able to perform an ADA iteration at different burner loads. During an ADA iteration, the appliances produce heat, which must be dissipated. The amount of produced heat depends on the fan speeds during the iteration. A small fan speed corresponds to a small burner load and a large fan speed corresponds to a large burner load, see also Section 2.3.2. If there is only a small heat demand, it is not possible to perform an ADA iteration at ADA pairs with large fan speeds, because the produced heat cannot be dissipated. This is mitigated by a plurality of ADA pairs, which allows to perform an ADA iteration at different burner loads [Sch15, p. 35].

3.4.1. Numbering of ADA Pairs and Corresponding Notation

To distinguish the ADA pairs, they are numbered. The numbering begins with 1 and follows a descending order with respect to the fan speed of the test points. For example, if we have a set of N ADA pairs, then the test point with the largest fan speed has the number 1 and the test point with the smallest fan speed has the number N. The start points get the same number as their associated test points. The descending order is counter-intuitive but it is a convention by Siemens and Vaillant [PHE, Item 3280] and thus it is also used in this thesis.

Notation 3.34 *Let $N \in \mathbb{N}$ be the total number of ADA pairs. We define $[N] := \{1, \dots, N\}$. The number of an ADA pair is indicated by a superscript. The p-th ADA pair is denoted by (s^p, t^p, i_s^p, i_t^p), $p \in [N]$.*
Analogously, the drifted test ioni current (Definition 3.27) of the p-th ADA pair is denoted by i_{t,r_D}^p, $p \in [N]$.

Recall from Definition 3.25 that an ADA pair is well-defined if it complies with the considered HE model and if its start fan speed is larger than its test fan speed.

Remark 3.35 *From now on, it is generally assumed that we have N well-defined ADA pairs (s^p, t^p, i_s^p, i_t^p), $p \in [N]$, in a descending order with respect to their test fan speeds, i.e., $t^1 > t^2 > \dots > t^N$.*

3.4.2. Drift Resistance Approximation Function

The ADA procedure approximates the drifted test ioni current i_{t,r_D} of an ADA pair, which in turn is used to approximate the drift resistance by applying (3.7). In the case of a plurality of ADA pairs, the ADA procedure provides an approximation of the drifted test ioni current for each of the N ADA pairs and thus also N approximations of the drift resistance. Each drift resistance approximation is associated to the corresponding ADA pair's test fan speed. Then, we have N data points $(t^p, \hat{r}_D^p)$ with $\hat{r}_D^p = \frac{U}{\hat{i}_{t,r_D}^p} - \frac{U}{i_t^p}$, where $\hat{i}_{t,r_D}^p$ denotes the incumbent approximation of i_{t,r_D}^p, $p \in [N]$.
By interpolating these data points we obtain a drift resistance approximation function that depends on the fan speed. Any suitable form of interpolation is possible [LS17, p. 11]. In IoniDetect a linear interpolation is used, which is extrapolated as a constant function beyond the smallest and the largest test fan speed, t^N and t^1, respectively [Sch15, p. 35] [WHB, Item 4268]. In order to formulate the corresponding drift resistance approximation function, it is convenient to combine the drifted test ioni current approximations of each ADA pair into a single vector.

Definition 3.36 *Let N ADA pairs be given and for each ADA pair let $i_p \in \mathbb{R}_{>0}$ be an approximation of the drifted test ioni current i_{t,r_D}^p, $p \in [N]$. We define the corresponding* vector of drifted test ioni current approximations *by $\hat{\boldsymbol{i}}_{t,r_D} := (i_1, \dots, i_N)$.*

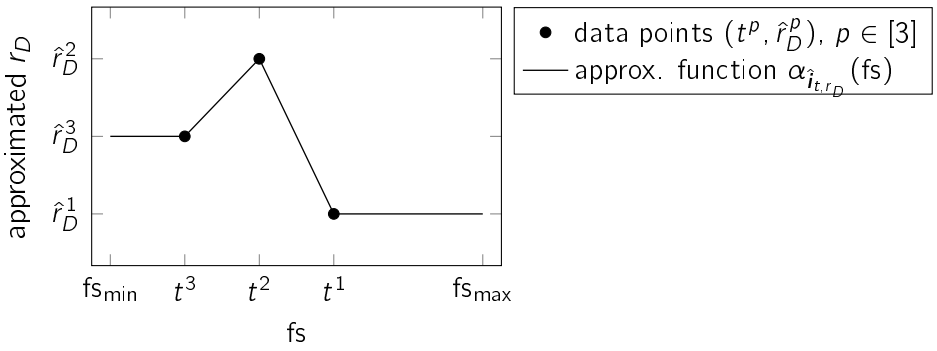

Figure 3.7.: Example of a drift resistance approximation function $\alpha_{\hat{\boldsymbol{i}}_{t,r_D}}(\mathrm{fs})$ with three data points. For each $p \in [3]$, the data point is a combination of the test fan speed t^p and the drift resistance approximation $\hat{r}_D^p := \frac{U}{i_p} - \frac{U}{i_t^p}$. The approximation function is a linear interpolation of the data points. It is extrapolated as a constant function.

Remark 3.37 *By construction, we have* $\hat{\boldsymbol{i}}_{t,r_D} \in \mathbb{R}^N_{>0} := \{x \in \mathbb{R}^N : x_i > 0 \ \forall\ i \in [N]\}$. *This is consistent with the considerations made so far. According to Definition 3.30, every drifted test ioni current approximation* $\hat{i}_{t,r_D}$ *is determined by evaluating* $\iota_{t,r_D}(\hat{g})$ *for a certain* $\hat{g}$. *Because the image of* ι_{t,r_D} *is always greater than zero (Definition 3.12), every drifted test ioni current approximation determined by ADA is greater than zero.*

Definition 3.38 *Let* N *ADA pairs* (s^p, t^p, i_s^p, i_t^p), $p \in [N]$, *be given. Furthermore, let* $\hat{\boldsymbol{i}}_{t,r_D} = (i_1, \ldots, i_N)$ *be a vector of drifted test ioni current approximations as defined in Definition 3.36.*
The drift resistance approximation function given $\hat{\boldsymbol{i}}_{t,r_D}$ *is the function* $\alpha_{\hat{\boldsymbol{i}}_{t,r_D}} : \mathrm{FS} \to \mathbb{R}$ *defined by*

$$\alpha_{\hat{\boldsymbol{i}}_{t,r_D}}(\mathrm{fs}) := \begin{cases} \frac{U}{i_N} - \frac{U}{i_t^N} & \text{if } \mathrm{fs} < t^N, \\ w\left(\frac{U}{i_p} - \frac{U}{i_t^p}\right) + (1-w)\left(\frac{U}{i_{p-1}} - \frac{U}{i_t^{p-1}}\right) & \text{if } \mathrm{fs} = wt^p + (1-w)t^{p-1},\ w \in (0,1], \\ \frac{U}{i_1} - \frac{U}{i_t^1} & \text{if } \mathrm{fs} \geq t^1. \end{cases}$$

(Memory aid: α *like (a)pproximation function.)*

Figure 3.7 shows an example of a drift resistance approximation function $\alpha_{\hat{\boldsymbol{i}}_{t,r_D}}(\mathrm{fs})$ with three data points, i.e., for the case $N = 3$ and a certain $\hat{\boldsymbol{i}}_{t,r_D} = (i_1, i_2, i_3)$. The black dots correspond to the data points $\left(t^p, \hat{r}_D^p\right)$ with $\hat{r}_D^p := \frac{U}{i_p} - \frac{U}{i_t^p}$, $p \in [3]$, and the black line is the corresponding drift resistance approximation function $\alpha_{\hat{\boldsymbol{i}}_{t,r_D}}(\mathrm{fs})$.

Remark 3.39 *Although the drift resistance is assumed to be a constant* $r_D \in \mathbb{R}_{\geq 0}$ *according to Assumption 3.10, the drift resistance approximation function* $\alpha_{\hat{\boldsymbol{i}}_{t,r_D}}(\mathrm{fs})$ *determined by ADA is usually not constant if a plurality of ADA pairs is used. In general the quality of the approximation is different for each ADA pair and also the number of ADA iterations performed is different for each ADA pair. Therefore, the values of the data points usually differ and thus their linear interpolation is not constant.*

Recall from Section 3.2.2 that the drift resistance approximation is used to correct the ioni currents according to (3.8). With a plurality of ADA pairs, however, the drift resistance approximation is no longer constant, but generally depends on the fan speed. Therefore, we have to adapt (3.8) accordingly.

Definition 3.40 *Let* $\mathcal{H} = \big(\mathrm{FS}, (G_{\mathsf{fs}})_{\mathsf{fs}\in\mathrm{FS}}, (\iota_{\mathsf{fs}})_{\mathsf{fs}\in\mathrm{FS}}, (\Lambda_{\mathsf{fs}})_{\mathsf{fs}\in\mathrm{FS}}, (\zeta_{\mathsf{fs}})_{\mathsf{fs}\in\mathrm{FS}}\big)$ *be an HE model and let* $\alpha_{\hat{i}_{t,r_D}} : \mathrm{FS} \to \mathbb{R}$ *be a drift resistance approximation function according to Definition 3.38. For all* $\mathsf{fs} \in \mathrm{FS}$*, the corresponding drifted ioni current approximation function is defined by*

$$\iota_{\mathsf{fs},\alpha_{\hat{i}_{t,r_D}}}(g) := \frac{U\iota_{\mathsf{fs}}(g)}{\alpha_{\hat{i}_{t,r_D}}(\mathsf{fs})\iota_{\mathsf{fs}}(g) + U} \;\forall\; g \in G_{\mathsf{fs}}. \tag{3.10}$$

Remark 3.41 *In general, it is not excluded that the drift resistance approximation function* $\alpha_{\hat{i}_{t,r_D}}$ *is negative. Because only positive ioni currents are permitted by IoniDetect [Sch15], it must be ensured that the result is positive when evaluating* (3.10).

Remark 3.42 *Regarding the ADA iteration according to Definition 3.30, Equation* (3.10) *is relevant in the first step, where the drifted start ioni current is approximated. With a plurality of ADA pairs, the approximation has to be determined by applying* (3.10)*. Let* $p \in [N]$*, then the drifted start ioni current of the p-th ADA pair is approximated by*

$$i^p_{s,\hat{r}_D} := \frac{U i^p_s}{\hat{r}_D i^p_s + U} \quad \textit{with} \quad \hat{r}_D = \alpha_{\hat{i}_{t,r_D}}(s^p). \tag{3.11}$$

A suited domain such that the result of (3.11) *is always positive is defined in Section 5.1 below. For the moment, we suppose that all evaluations of* (3.11) *considered in this chapter are positive.*

A consequence of (3.11) is that ADA pairs must not be overlapping.

3.4.3. ADA Pairs Must Not Be Overlapping

Each ADA pair (s^p, t^p, i^p_s, i^p_t) can be associated with the interval $[t^p, s^p]$ defined by its test and start fan speed. Note that the test fan speed is always smaller than the start fan speed because we consider only well-defined ADA pairs (Definition 3.25). An overlap occurs, if the fan speed intervals of two ADA pairs intersect.

Definition 3.43 *Let* (s^k, t^k, i^k_s, i^k_t) *and* $(s^\ell, t^\ell, i^\ell_s, i^\ell_t)$*,* $k \neq \ell$*, be two ADA pairs. They are called* overlapping *if*

$$[t^k, s^k] \cap [t^\ell, s^\ell] \neq \emptyset.$$

If ADA pairs are not overlapping, then the start fan speed of ADA pair p lies between two test fan speeds for all $p \in \{2, \ldots, N\}$, which is stated in the following lemma.

Lemma 3.44 *If (well-defined) ADA pairs are not overlapping, then* $t^p < s^p < t^{p-1}$ *holds for all* $p \in \{2, \ldots, N\}$.

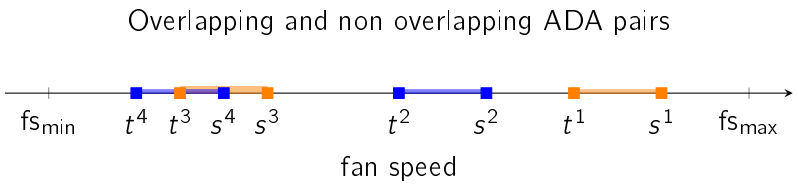

Figure 3.8.: The start and test fan speeds as well as the corresponding fan speed intervals of four ADA pairs are shown. The ADA pairs $p = 4$ and $p = 3$ are overlapping, because $[t^4, s^4] \cap [t^3, s^3] \neq \emptyset$ holds. In contrast, the ADA pairs $p = 2$ and $p = 1$ have no overlap with any other ADA pair, because all possible intersections with their respective fan speed intervals are empty.

Proof. Let $p \in \{2, \dots, N\}$ and assume that ADA pairs are not overlapping. Because we consider only well-defined ADA pairs, we have $t^p < s^p$. Next, let us suppose that $t^{p-1} \leq s^p$. Then, we have $t^{p-1} \in [t^p, s^p]$ and $t^{p-1} \in [t^{p-1}, s^{p-1}]$, i.e., the pairs p and $p-1$ are overlapping. This is a contradiction and thus we have $s^p < t^{p-1}$. □

The statement of Lemma 3.44 is illustrated in the following example.

Example 3.45 *Let us consider a situation with four ADA pairs and let their fan speeds be* $t^4 = 3$, $s^4 = 4$, $t^3 = 3.5$, $s^3 = 4.5$, $t^2 = 6$, $s^2 = 7$, $t^1 = 8$ *and* $s^1 = 9$. *The fan speeds and their corresponding fan speed intervals* $[t^p, s^p]$, $p \in [4]$, *are depicted in Figure 3.8. They are alternately colored blue and orange.*
Because $[t^4, s^4] \cap [t^3, s^3] = [t^3, s^4] \neq \emptyset$, *the ADA pairs* $p = 4$ *and* $p = 3$ *are overlapping. In particular* $t^4 < s^4 < t^3$ *does not hold. In contrast, the ADA pairs* $p = 2$ *and* $p = 1$ *are not overlapping and* $t^2 < s^2 < t^1$ *holds.*

In Example 3.45, we have overlapping ADA pairs and thus $t^4 < t^3 < s^4 < s^3 < t^2$. This situation is problematic, for the following reason. Let us suppose that we perform an ADA iteration with ADA pair $p = 4$ according to Definition 3.30. In the first step, we approximate the drifted start ioni current of ADA pair $p = 4$. For this, we need the drift resistance approximation $\alpha_{\hat{i}_{t,r_D}}(s^4)$ according to (3.11). Recall from Definition 3.38 that $\alpha_{\hat{i}_{t,r_D}}(\mathrm{fs})$ interpolates linearly between the drift resistance approximations of two adjacent test fan speeds. Because $t^4 < t^3 < s^4 < t^2$, the approximation $\alpha_{\hat{i}_{t,r_D}}(s^4)$ depends on the drift resistance approximations at t^3 and at t^2. It does not depend on the drift resistance approximation at t^4, although this is the drift resistance approximation to be updated in the considered ADA iteration. This might cause undesired behavior and increases complexity. In contrast, if ADA pairs must not be overlapping, we have $t^4 < s^4 < t^3$ and $\alpha_{\hat{i}_{t,r_D}}(s^4)$ depends on the drift resistance approximations at t^4 and at t^3. Therefore, Vaillant's engineers decided to avoid overlapping ADA pairs [PHE, Item 3280]. As a consequence, the maximum number of ADA pairs is limited.

3.4.4. Recommended Number of ADA Pairs

The number of specified ADA pairs has to be balanced between having a good covering of the set of feasible fan speeds FS by the test fan speeds t^p, $p \in [N]$, on the one hand, and taking restrictions into account on the other hand. As stated at the beginning of Section 3.4, tolerances with respect to the position of the ioni electrode might have the effect of an additional drift resistance that depends on the fan speed. Too few data points might miss fan speed regions of larger changes of this additional drift resistance. On the other hand, because ADA pairs must not be overlapping and the interval of feasible fan speeds is bounded, the number of ADA pairs is limited. As a compromise, up to seven ADA pairs are used in IoniDetect [Sch15, p. 35]. If appropriate, it is possible to use less than seven ADA pairs.

3.4.5. Selection of ADA Pair for Next ADA Update

With a plurality of ADA pairs, we have to specify which ADA pair p shall be selected for the next update. However, the selection of an ADA update sequence is done automatically by the IoniDetect system according to certain rules [WHB, Item 4228]. For instance, if no update of ADA pair p was performed for more than 100 operating hours, an update of p is forced [PHE, Item 12678].
Furthermore, there is no stopping criterion for ADA specified, i.e., there exists no number of maximum ADA iterations. A stopping criterion is not required in practice for two reasons. First, the ADA algorithm is rarely executed at an interval of several hours. In IoniDetect, the minimum time span between two subsequent ADA updates of the same ADA pair is 48 operating hours [WHB, Item 8529]. Second, drift is a "creeping phenomenon" [LS17, p. 3] as stated in Section 3.1.2. Accordingly, the drift resistance changes steadily and therefore its approximation is never completed.
To summarize, we have no influence on which ADA pair is updated next. Therefore, we suppose that the ADA update sequences follow certain random distributions when analyzing the ADA procedure from a mathematical point of view. This is detailed in Section 7.3 below.

This concludes the introduction to the ADA procedure. We can now formulate the goals of this work in the following section.

3.5. Goal of This Thesis: Optimize ADA Parameters

As detailed in this chapter, each ADA pair is defined by four values. They are the fan speeds and the ioni currents of the pair's start and test point. These values are refereed to as ADA parameters in this thesis. IoniDetect uses up to seven ADA pairs. Therefore, up to 28 ADA parameters are required.

Remark 3.46 *The controller of IoniDetect requires a lot more parameters related to ADA. For instance, one such parameter is the time to wait until the ioni current at the test point is measured [Sch15, p. 35]. These additional parameters are mostly related to the dynamic behavior of the combustion system. Because only static signals are used in this thesis, see for instance Remark 2.15, these parameters are disregarded.*

As stated in Section 3.2.3, the effectiveness of ADA and the quality of the approximated drift resistances strongly depend on the ADA parameters. Therefore, a good design of the ADA parameters is essential. In the past, the parameterization of ADA was done mostly in the lab. But this is expensive and time consuming. In addition, the results were not very robust against tolerances such as tolerances regarding the position of the electrode relative to the burner.
Therefore, some Vaillant employees proposed to use computer simulations for the parameterization of ADA. Usually, simulations are less expensive and take less time to find results. In addition they offer a good environment for optimization.
That is the starting point of this work. The goal of this thesis is to find optimized ADA parameters based on computer simulations in the sense that the drift resistance is approximated with a high quality while certain constraints are respected.
There are many other parameters that influence the function of IoniDetect, the implications of drift and the effectiveness of ADA. Some of them are

- electrode related like the material, size or shape of the electrode,
- measurement setup related like the frequency and amplitude of the applied voltage,
- parameters related like the control curve and
- design related like the position of the electrode relative to the burner.

All these aspects are not in the scope of this thesis. Although they might offer further potential for optimization, they are assumed to be given.
The optimization of the ADA parameters requires a thorough analysis of the ADA algorithm, which is covered in Chapters 5 to 7. Based on this analysis suitable optimization models are developed in Chapter 8. The optimization models are multiobjective. An introduction to multiobjective optimization is given in the following chapter, where the basic mathematical concepts required for this thesis are presented.

4. Basic Mathematical Concepts

This chapter deals with the mathematical concepts required to work on the task of finding optimized ADA parameters. In the course of this thesis, we show that the ADA optimization problem contains conflicting objectives. Optimization problems with conflicting objectives are called multiobjective optimization problems and are studied in the field of multiobjective optimization (MOO). Therefore, the basics of MOO are covered in the following section. A common approach to solve multiobjective optimization problems are evolutionary algorithms, which are presented thereafter. As ADA is a fixed point iteration procedure, the basics of fixed point iteration procedures are also presented.

4.1. Multiobjective Optimization

This section is based on the books *Multicriteria Optimization* [Ehr05], *Multi-Objective Optimization using Evolutionary Algorithms* [Deb01] and *Nonlinear Multiobjective Optimization* [Mie98]. If not otherwise stated, all definitions, concepts and results presented in this section are detailed in one of these books.

In optimization, one is interested in minimizing or maximizing a function for a given feasible set. This function is called objective function. In single objective optimization, the image space of the objective function is one-dimensional. For instance, let us suppose that we have a feasible set X and an objective function $f : X \to \mathbb{R}$, which we want to minimize. Then, we are interested in an element $x^* \in X$ such that $f(x^*)$ is minimal in $f(X) \subset \mathbb{R}$, i.e., $f(x^*) = \min_{x \in X} f(x)$. The set $\mathbb{R}$ has a natural total order and thus we can always state whether $f(x_1) \leq f(x_2)$, $f(x_1) \geq f(x_2)$ or $f(x_1) = f(x_2)$ for all $x_1, x_2 \in X$. If we have multiple objective functions, i.e., we have p objectives, $p \geq 2$, then we have a p-dimensional objective function $f : X \to \mathbb{R}^p$. Let us suppose that we want to minimize this function f, i.e, we are interested in an element $x^* \in X$ such that $f(x^*)$ is minimal in $f(X) \subset \mathbb{R}^p$. However, in contrast to $\mathbb{R}$, the space $\mathbb{R}^p$, $p \geq 2$, does not have a natural total order. Therefore, we must also specify an order on $\mathbb{R}^p$. This leads to the concept of Pareto optimality, which is introduced in the following.

Remark 4.1 *Without loss of generality, we consider only minimization problems for the remainder of this thesis. This is no restriction, because a maximization problem can be converted into an equivalent minimization problem by multiplying the objective function with* (-1) *[Deb01, p. 14].*

4.1.1. Pareto Optimality

For the remainder of this section, let X be a nonempty set and let $f : X \to \mathbb{R}^p$ with $p \geq 2$. We first define the componentwise order on $\mathbb{R}^p$. We then introduce Pareto optimality and define related terms.

Definition 4.2 *Let $y, \bar{y} \in \mathbb{R}^p$. The* componentwise order *is the binary relation $\leq$ on $\mathbb{R}^p$ defined by*

$$y \leq \bar{y} \;\Leftrightarrow\; y_i \leq \bar{y}_i \;\forall\, i \in [p] \text{ and } \exists\, j \in [p] : y_j < \bar{y}_j.$$

If $y \leq \bar{y}$, one also says y (Pareto) dominates *$\bar{y}$.*

With the componentwise order at hand, we can specify an optimality notion for multi-objective optimization problems, which are defined by

$$\min_{x \in X} \; f(x) = \big(f_1(x), \ldots, f_p(x)\big). \tag{MOP}$$

Definition 4.3 *A solution $x^* \in X$ is called* Pareto optimal *or* efficient *for* (MOP)*, if there exists no $x \in X$ such that $f(x) \leq f(x^*)$.*
The set of all Pareto optimal solutions for (MOP) *is called the* efficient set *and is denoted by X_{eff}.*

Remark 4.4 *The terms* Pareto optimal *and* efficient *are used interchangeably in this thesis.*

Remark 4.5 *The interpretation of Pareto optimality is as follows: Let x^* be an efficient solution. Then it is not possible to improve an objective function value of x^* without deteriorating the function value of another objective.*

Remark 4.6 *Other orders, such as the lexicographic order, are also studied in MOO. This is detailed in [Ehr05, pp. 16–19]. The most common order used in MOO is the componentwise order, which is also relevant for the ADA optimization. Therefore, only Pareto optimality is considered for the remainder of this thesis.*

By definition, the efficient points are a subset of the feasible set X. The space containing X is called the decision space. In MOO, one is also interested in the images of X and X_{eff}. Because the images of X_{eff} under f are not Pareto dominated in $f(X)$, the set $f(X_{\text{eff}})$ is called the nondominated set.

Definition 4.7 *We denote $Y := f(X)$. The* set of nondominated points *of* (MOP) *is defined by $Y_{\text{nd}} := f(X_{\text{eff}})$.*

Remark 4.8 *An alternative term for the* set of nondominated points *is* Pareto front. *Both terms are used interchangeably in this thesis.*

Remark 4.9 *The image space of f, $\mathbb{R}^p$, is called the objective space of* (MOP).

The concept of Pareto optimality as well as the related terms are briefly demonstrated in the following example.

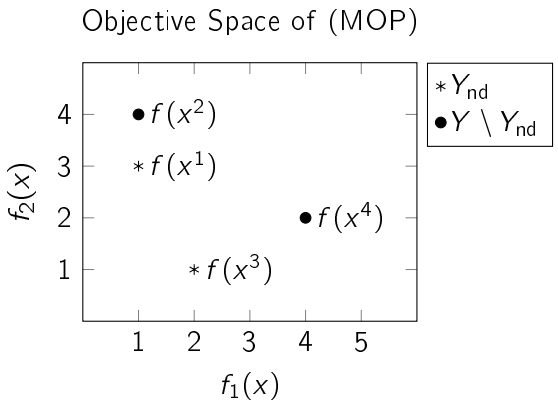

Figure 4.1.: The image set Y of the problem (MOP) presented in Example 4.10 is illustrated. The point $f(x^1)$ dominates $f(x^2)$ and the point $f(x^3)$ dominates $f(x^4)$. The points $f(x^1)$ and $f(x^3)$ are nondominated in Y.

Example 4.10 *Let us consider a feasible set with four elements, i.e., let* $X = \{x^1, x^2, x^3, x^4\}$. *Furthermore, let us consider the two-dimensional objective function* $f : X \to \mathbb{R}^2$ *specified by*

$$f(x^1) := (1,3), \quad f(x^2) := (1,4), \quad f(x^3) := (2,1) \quad \textit{and} \quad f(x^4) := (4,2).$$

Figure 4.1 shows the image set $Y = \{f(x^1), \ldots, f(x^4)\}$ *in the objective space of* (MOP). *It is apparent that* $f(x^1) \leq f(x^2)$ *and that* $f(x^3) \leq f(x^4)$, *i.e.,* $f(x^1)$ *Pareto dominates* $f(x^2)$ *and* $f(x^3)$ *Pareto dominates* $f(x^4)$. *Therefore,* x^2 *and* x^4 *cannot be efficient. In contrast, there is no point in* Y *that dominates* $f(x^1)$ *and there is no point in* Y *that dominates* $f(x^3)$. *Therefore, the efficient set for* (MOP) *is* $X_{\text{eff}} = \{x^1, x^3\}$ *and the nondominated set is* $Y_{\text{nd}} = \{f(x^1), f(x^3)\} = \{(1,3), (2,1)\}$.

As demonstrated in Example 4.10, the Pareto optimal set and the nondominated set usually contain more than one element (if they are not empty). This reflects the nature of the conflicting objectives, i.e., we usually have a trade-off between the individual objectives. Therefore, after the set of Pareto optimal solutions is determined, decision makers are required who select the Pareto optimal solution that best fits their needs. The decision making process regarding the ADA optimization problem as well as some details about the decision makers are presented in the introduction to Chapter 8.

From a mathematical point of view, we are interested in finding the set of efficient solutions. An important aspect is the existence of efficient solutions. The main idea behind all existence statements is that the nondominated points must be located on the boundary of the image set Y, which is denoted by $\text{bd}(Y)$ in the following. Because if $y \notin \text{bd}(Y)$, then we can always find a $\bar{y} \in Y$ that dominates y.

Lemma 4.11 $Y_{\text{nd}} \subset \text{bd}(Y)$.

Proof. See [Ehr05, p. 28]. □

Therefore, if Y is open, then the nondominated set is empty, i.e., there exists no efficient solution for (MOP). In contrast, if Y is nonempty and compact, then $Y_{\text{nd}} \neq \emptyset$.

Lemma 4.12 *Let Y be nonempty and compact. Then, $Y_{\text{nd}} \neq \emptyset$.*

Proof. The statement follows from Theorem 2.19 in [Ehr05, p. 33]. □

For instance, if the feasible set X is nonempty and compact and the objective function f is continuous, then $Y = f(X)$ is also compact and there exist efficient solutions, i.e., $X_{\text{eff}} \neq \emptyset$.

Remark 4.13 *The requirements in Lemma 4.12 are rather strong. Some weaker conditions for the existence of efficient solutions are discussed in detail in [Ehr05, pp. 24 sqq.].*

"[T]he range of the values which nondominated points can attain" [Ehr05, p. 33] is indicated by the so-called ideal point and nadir point. The ideal point can be interpreted as the largest lower bound for Y_{nd} and the nadir point can be interpreted as the smallest upper bound for Y_{nd}.

Definition 4.14 *Let $\min_{x \in X} f_i(x)$ exist for all $i \in \{1, \ldots, p\}$. The* ideal point *of* (MOP) *is the point $y^I = (y_1^I, \ldots, y_p^I)$ defined by*

$$y_i^I := \min_{x \in X} f_i(x) = \min_{y \in Y} y_i, \ \ i = 1, \ldots, p.$$

Let $\max_{x \in X_{\text{eff}}} f_i(x)$ exist for all $i \in \{1, \ldots, p\}$. The nadir point *of* (MOP) *is the point $y^N = (y_1^N, \ldots, y_p^N)$ defined by*

$$y_i^N := \max_{x \in X_{\text{eff}}} f_i(x) = \max_{y \in Y_{\text{nd}}} y_i, \ \ i = 1, \ldots, p.$$

Example 4.15

1. *We determine the ideal point and the nadir point of the problem* (MOP) *presented in Example 4.10. We have $Y_{\text{nd}} = \{(1, 3), (2, 1)\}$ and thus $y^I = (1, 1)$ as well as $y^N = (2, 3)$.*

2. *Figure 4.2 below shows the ideal point and the nadir point for another exemplary problem* (MOP).

A further characterization of the set of nondominated points, which is needed in the context of the ADA optimization, is connectedness. The following definition of a connected set is taken from [Ehr05, p. 86]. For this, the closure of a set S is denoted by $\text{cl}(S)$.

Definition 4.16 *A set $S \subset \mathbb{R}^p$ is called* not connected, *if there exist $S_1, S_2 \subset \mathbb{R}^p$, $S_1 \neq \emptyset$, $S_2 \neq \emptyset$ such that $S = S_1 \cup S_2$ and $\text{cl}(S_1) \cap S_2 = S_1 \cap \text{cl}(S_2) = \emptyset$.*
If there exist no such S_1 and S_2, then S is called connected.

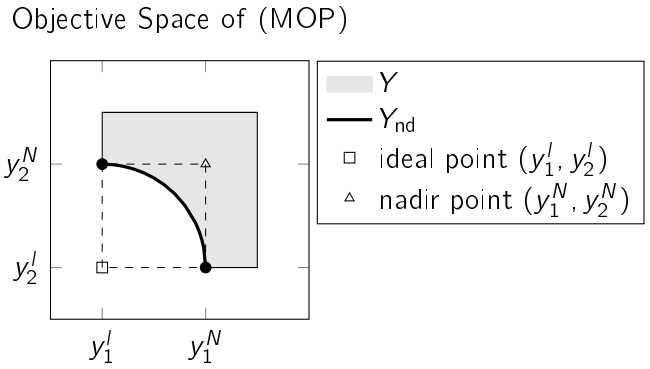

Figure 4.2.: The image set Y of a two-dimensional problem (MOP) is shown. The thick curve corresponds to the Pareto front, which is connected and nonconvex.

Example 4.17 *Figure 4.2 shows the image set Y of a not further specified two-dimensional problem* (MOP). *The problem's nondominated set Y_{nd} is marked by the thick curve. It is connected and nonconvex. In addition, the ideal point (y_1^I, y_2^I) and the nadir point (y_1^N, y_2^N) as well as the two extreme points (y_1^I, y_2^N) and (y_1^N, y_2^I) of Y_{nd} are shown. Note that Y_{nd} is a continuous curve between the two extreme points.*
In contrast, the nondominated set $Y_{\text{nd}} = \{(1,3),(2,1)\}$ in Example 4.10 is not connected. By selecting $S_1 = \{(1,3)\}$ and $S_2 = \{(2,1)\}$, we have $Y_{\text{nd}} = S_1 \cup S_2$ and $\text{cl}(S_1) \cap S_2 = S_1 \cap \text{cl}(S_2) = S_1 \cap S_2 = \emptyset$.

In Example 4.17, Y_{nd} is a continuous curve between the two extreme points (y_1^I, y_2^N) and (y_1^N, y_2^I). This is always the case if Y_{nd} is connected, closed and bounded as well as (MOP) is two-dimensional, i.e., $p = 2$. This is the statement of the following lemma, which is required to prove Lemma 9.18 below. Although this can be considered as a basic statement, it is not explicitly contained in any of the books mentioned at the beginning of this Section 4.1. Therefore, the following proof is from the author of this thesis.

Lemma 4.18 *Let $p = 2$ and let Y_{nd} be nonempty, closed and bounded. If Y_{nd} is connected, then*

$$\forall\, z_1 \in [y_1^I, y_1^N]\ \exists\, y = (y_1, y_2) \in Y_{\text{nd}} : y_1 = z_1 \text{ and}$$
$$\forall\, z_2 \in [y_2^I, y_2^N]\ \exists\, y = (y_1, y_2) \in Y_{\text{nd}} : y_2 = z_2.$$

Proof. Let Y_{nd} be nonempty, closed, bounded and connected. Then, Y_{nd} is nonempty and compact and thus the ideal point (y_1^I, y_2^I) as well as the nadir point (y_1^N, y_2^N) exist. In particular, there exist $y = (y_1, y_2) \in Y_{\text{nd}}$ and $\bar{y} = (\bar{y}_1, \bar{y}_2) \in Y_{\text{nd}}$ such that $y_1 = y_1^I$ and $\bar{y}_1 = y_1^N$.
If $y_1^I = y_1^N$, then there is nothing to show. Therefore, let $y_1^I \neq y_1^N$. Let us assume that there exists $z_1 \in (y_1^I, y_1^N)$ such that there exists no $y = (y_1, y_2) \in Y_{\text{nd}}$ with $y_1 = z_1$. We

show that this leads to a contradiction with respect to Y_{nd} being connected. We select

$$S_1 := \{y = (y_1, y_2) \in Y_{\text{nd}} : y_1 \in [y_1^l, z_1)\} \text{ and } S_2 := \{y = (y_1, y_2) \in Y_{\text{nd}} : y_1 \in (z_1, y_1^N]\}.$$

Note that $S_1 \neq \emptyset$ and $S_2 \neq \emptyset$ as well as $S_1 \cup S_2 = Y_{\text{nd}}$. It remains to show that $\text{cl}(S_1) \cap S_2 = S_1 \cap \text{cl}(S_2) = \emptyset$.
For this, we show that $(y_1, y_2) \in \text{cl}(S_1)$ implies $y_1 \leq z_1$. Let us suppose that there exists $(\bar{y}_1, \bar{y}_2) \in \text{cl}(S_1)$ such that $\bar{y}_1 > z_1$. We select $\varepsilon := \frac{1}{2}(\bar{y}_1 - z_1)$. Note that $\varepsilon > 0$. But we have $S_1 \cap B_\varepsilon(\bar{y}_1, \bar{y}_2) = \emptyset$ and thus $(\bar{y}_1, \bar{y}_2) \notin \text{cl}(S_1)$. This is a contradiction and thus $(y_1, y_2) \in \text{cl}(S_1)$ implies $y_1 \leq z_1$. Furthermore, $(y_1, y_2) \in S_2$ implies $y_1 > z_1$. Therefore, we have $\text{cl}(S_1) \cap S_2 = \emptyset$. The equation $S_1 \cap \text{cl}(S_2) = \emptyset$ is shown analogously.
In total, we have shown that Y_{nd} is not connected. This is a contradiction and thus no such z_1 can exist.
The lemma's second statement for all $z_2 \in [y_2^l, y_2^N]$ is shown analogously. □

Depending on the structure of a multiobjective problem (MOP), there exist different approaches for solving (MOP). For instance, if (MOP) has linear objective functions and linear constraints, then (MOP) can be solved with a multiobjective simplex method [Ehr05, pp. 171 sqq.]. If (MOP) has no structure that can be exploited in a direct approach or if one is interested in a particular solution of (MOP) only, then a common approach for generating Pareto optimal solutions of (MOP) are scalarization methods. Depending on a parameter P, a scalarization method converts the multiobjective problem (MOP) into a single objective problem, which is then solved with corresponding single objective optimization methods. Depending on the selected scalarization method, P has a different meaning like, for instance, a weight or a budget restriction for each objective function. The two most popular scalarization methods are the weighted sum scalarization and the ε-constraint scalarization. Both methods are briefly presented in the following.

4.1.2. Weighted Sum Scalarization

The idea behind the weighted sum scalarization is straightforward. Each objective is weighted with an individual weight and the weighted objectives are summed up to a single objective function. Since we consider minimization problems, we allow only nonnegative weights. Furthermore, without loss of generality we normalize the weights such that their sum is always one.

Definition 4.19 *Let* $\lambda = (\lambda_1, \ldots, \lambda_p) \in \mathbb{R}^p_{\geq 0} := \{x \in \mathbb{R}^p : x_i \geq 0\}$ *such that* $\sum_{i=1}^p \lambda_i = 1$. *The corresponding weighted sum scalarization of* (MOP) *is the problem*

$$\min_{x \in X} \sum_{i=1}^{p} \lambda_i f_i(x). \qquad (\text{MOP}_w(\lambda))$$

A thorough analysis of the weighted sum scalarization is given in [Ehr05, pp. 65 sqq.]. In the following, the most important results are briefly summarized. For this, we require the concept of weak efficiency.

Definition 4.20 *A solution $x^* \in X$ is called* weakly efficient *for* (MOP)*, if there exists no $x \in X$ such that $f_i(x) < f_i(x^*)$ for all $i \in [p]$.*

Example 4.21 *We consider once more the problem* (MOP) *from Example 4.10 with the feasible set $X = \{x^1, x^2, x^3, x^4\}$ and $f(x^1) := (1,3)$, $f(x^2) := (1,4)$, $f(x^3) := (2,1)$ as well as $f(x^4) := (4,2)$. Recall that x^1 and x^3 are the efficient points for* (MOP)*. Therefore, x^1 and x^3 are also weakly efficient. But x^2 is also weakly efficient, although it is not efficient. In contrast, the solution x^4 is not weakly efficient, because $f_1(x^2) = 2 < 4 = f_1(x^4)$ and $f_2(x^2) = 1 < 2 = f_2(x^4)$.*

The following theorem summarizes the major results regarding the weighted sum scalarization.

Theorem 4.22 *1. Let $\lambda \in \mathbb{R}^p_{\geq 0}$. If x^* is optimal for* ($\mathrm{MOP}_w(\lambda)$)*, then x^* is weakly efficient for* (MOP)*. If in addition all optimal solutions for* ($\mathrm{MOP}_w(\lambda)$) *are mapped to the same image $f(x^*) \in Y$, then x^* is efficient for* (MOP)*.*

2. Let $\lambda \in \mathbb{R}^p_{>0}$. If x^* is optimal for ($\mathrm{MOP}_w(\lambda)$)*, then x^* is efficient for* (MOP)*.*

3. If (MOP) *is convex, i.e., the set X is convex and the objective functions f_i, $i \in [p]$, are convex, then for each $x^* \in X_{\mathrm{eff}}$ there exists $\lambda^* \in \mathbb{R}^p_{\geq 0}$ such that x^* is optimal for* ($\mathrm{MOP}_w(\lambda)$) *with $\lambda = \lambda^*$.*

Proof. The statements follow from Theorem 3.4, Theorem 3.5, Theorem 3.6, Corollary 3.7 and Proposition 3.8 in [Ehr05, pp. 69, 70]. □

Remark 4.23 *It is important to emphasize that in general not all efficient solutions can be found with the weighted sum scalarization if the problem* (MOP) *is nonconvex. This is detailed in [Ehr05, p. 73] or [Deb01, pp. 53, 54].*

According to Theorem 4.22, several (weakly) efficient solutions of (MOP) may be found by varying the parameter $\lambda \in \mathbb{R}^p_{\geq 0}$. But this requires solving various single objective optimization problems of the type ($\mathrm{MOP}_w(\lambda)$), which might be computationally expensive. The major advantages of the weighted sum scalarization are its simplicity and that no additional constraints are added to the problem formulation. In addition, if the problem is convex, then all efficient solutions can be found by varying the parameter $\lambda \in \mathbb{R}^p_{\geq 0}$ appropriately.
However, specifying appropriate weight vectors λ can be challenging in practice. For instance, two different weight vectors $\lambda^1 \neq \lambda^2$ might yield the same (weakly) efficient solution. Another disadvantage of the weighted sum scalarization is that for nonconvex problems it is in general impossible to find all efficient solutions. In contrast, the ε-constraint scalarization, which is presented in the following, is able to find all efficient solutions also for a nonconvex problem.

4.1.3. ε-Constraint Scalarization

As delineated in the preceding subsection, the weighted sum scalarization aggregates all objectives into a single objective function. In contrast, in the ε-constraint scalarization "only one of the original objectives is minimized, while the others are transformed to constraints."[Ehr05, p. 98]. For this, we require two parameters. First, an index $k \in [p]$ that indicates which of the p objective functions is minimized. Second, a vector $\varepsilon = (\varepsilon_1, \ldots, \varepsilon_p) \in \mathbb{R}^p$ that represents the upper bounds for the objectives that are transformed to constraints. Note that the component ε_k is not required and irrelevant, because f_k is kept as the single objective function to be minimized and not transformed to a constraint. However, it is a convention to include it [Ehr05, p. 99].

Definition 4.24 *Let $k \in [p]$ and let $\varepsilon = (\varepsilon_1, \ldots, \varepsilon_p) \in \mathbb{R}^p$. The corresponding ε-constraint scalarization of* (MOP) *is the problem*

$$\min_{x \in X} f_k(x), \ \text{s.t.} \ f_i(x) \leq \varepsilon_i \ \forall \ i \in [p] \setminus \{k\}. \qquad (\text{MOP}_c(\varepsilon, k))$$

The functional principle of the ε-constraint scalarization is, for instance, illustrated in [Ehr05, p. 99] or [Deb01, p. 55].
The following theorem summarizes the major results regarding the ε-constraint scalarization.

Theorem 4.25
1. *If x^* is an optimal solution of* ($\text{MOP}_c(\varepsilon, k)$) *for some ε and k, then x^* is weakly efficient for* (MOP).
2. *If x^* is the unique solution of* ($\text{MOP}_c(\varepsilon, k)$), *then x^* is efficient for* (MOP).
3. *A solution $x^* \in X$ is efficient for* (MOP) *if and only if there exists $\varepsilon^* \in \mathbb{R}^p$ such that x^* is optimal for* ($\text{MOP}_c(\varepsilon, k)$) *for all $k \in [p]$ with $\varepsilon = \varepsilon^*$.*

Proof. The statements follow from Proposition 4.3, Proposition 4.4 and Theorem 4.5 in [Ehr05, pp. 99, 100]. □

According to Theorem 4.25, the ε-constraint scalarization is able to find all Pareto optimal solutions for an arbitrary problem (MOP) by using appropriate vectors $\varepsilon \in \mathbb{R}^p$. This is also true for nonconvex problems, which is the major advantage of the ε-constraint scalarization compared to the weighted sum scalarization.
However, just as with the weighted sum scalarization it might be challenging to find appropriate vectors $\varepsilon \in \mathbb{R}^p$ for the ε-constraint scalarization in practice. For instance, it may be difficult to select $\varepsilon \in \mathbb{R}^p$ such that the resulting problem ($\text{MOP}_c(\varepsilon, k)$) has a feasible solution at all [Bra+08, p. 13]. Therefore, "information about the ranges of objective functions in the Pareto optimal set is useful" in selecting appropriate vectors $\varepsilon \in \mathbb{R}^p$ [Bra+08, p. 13].
In Section 9.1 below, we deal with the nominal ADA optimization problem with a single ADA pair, which is a two-dimensional optimization problem. A particularity of this

problem is that information about the range of its second objective function is available. Furthermore, this problem is nonconvex in general. Therefore, a variant of the ε-constraint scalarization is proposed in Section 9.1.2 to solve this problem.

In addition to the scalarization methods and the briefly mentioned direct approaches to solve (MOP), there exists also a variety of approximation methods and (meta)heuristic approaches. One popular class of metaheuristics are evolutionary algorithms. These are introduced in the following, because we propose solving the ADA optimization problem with respect to tolerances by using evolutionary algorithms in Section 9.2.2 below.

4.2. Evolutionary Multiobjective Optimization

This section is based on the books *Multi-Objective Optimization using Evolutionary Algorithms* [Deb01] and *Multiobjective Optimization* [Bra+08]. The main idea behind evolutionary optimization algorithms is to imitate the evolution process in nature [Deb01, p. 77]. Regarding multiobjective optimization, some of the most popular approaches are genetic algorithms and particle swarm algorithms [Bra+08, p. 78].
A popular multiobjective genetic algorithm is the NSGA-II. "In fact, in a wide range of benchmarks and application problems, NSGA-II was reported to yield good approximations of Pareto fronts, in particular for the 2-D case." [CEM12, p. 21] Thus, it is proposed to use NSGA-II to solve the ADA optimization problem with tolerances in Section 9.2.2 below. For this, the basics of genetic algorithms in general as well as some particularities of the NSGA-II are briefly presented in the following.

4.2.1. Genetic Algorithms

A genetic algorithm (GA) is a population based and iterative procedure. The term population refers to a sample set of solutions that is considered in the current iteration. The iterations of a GA are also called generations. In each generation, three operators are successively applied to the population, which are reproduction, crossover and mutation. These operators modify the solutions within the populations and (ideally) drive the solutions from generation to generation towards optimality. After a maximum number of generations specified by the user, the procedure terminates and the solutions with the best fitness values within the incumbent population are the approximations of the optimal solution(s). The initial population is usually randomly generated.
For this, a fitness assignment function is required that assigns a fitness value to each solution. The fitness value of a solution represents its degree of optimality. A feasible solution with a better objective function value should have a better fitness value than an infeasible solution or than a solution with a worse objection function value. If we have no constraints, then, in the single objective case, the fitness assignment function usually corresponds to the objective function [Deb01, p. 83].

A flow chart of this working principle is, for instance, illustrated in Figure 41 in [Deb01, p. 83]. The three operators as well as some related particularities like binary representation of a solution are introduced in the following.

Reproduction This operator "mimics Darwin's survival of the fittest principle by making duplicate copies of above-average solutions in the population at the expense of deleting below-average solutions" [Bra+08, p. 66]. One of the most common methods is tournament selection. As the name suggests, in tournament selection two solutions are (randomly) picked from the population and their fitness values are compared to each other. The solution with the larger fitness value is placed in the mating pool. This procedure is repeated until the mating pool is filled. The mating pool is an intermediate population from which new solutions are created by applying the crossover and the mutation operator. A common mating pool size is half of the population size [Ses09].
There exist several other reproduction methods like proportionate selection or ranking selection [Deb01, p. 84]. But "[i]t has been shown ... that the tournament selection has better or equivalent convergence and computational time complexity properties when compared to any other reproduction operator that exists in the literature." [Deb01, p. 85]. Tournament selection is also used in NSGA-II as the reproduction operator.

Crossover In the crossover operator "two or more parent solutions are used to create (through recombination) one or more child solutions" [Bra+08, p. 64], where the parent solutions are randomly selected from the mating pool. Most crossover methods exchange some "portions" of the two parent solutions. This requires a representation of the parent solutions that allows a meaningful and reasonable exchange. A common representation are binary strings. For instance, if we have a 10 bit representation for a decision variable, then 1024 different values for this decision variable are possible. The binary string representation is usually combined with a single-point crossover. Then, the crossover "is performed by randomly choosing a crossing site along the strings and by exchanging all bits on the right side of the crossing site" [Deb01, p. 89]. In this way, two child solutions are created. However, if the search space is continuous, a major disadvantage of the binary representation "is the inability to achieve any arbitrary precision in the optimal solution" [Deb01, p. 106]. To overcome this problem a method called simulated binary crossover (SBX) was developed. "As the name suggests, the SBX operator simulates the working principle of the single-point crossover operator on binary strings" [Deb01, p. 109]. To illustrate how SBX is applied, let us suppose that we have two parent solutions $x^{1,t}$ and $x^{2,t}$, where t denotes the current generation. Let us further suppose that we want to perform a crossover of the i-th component. First, a number $u_i \in [0, 1)$ is drawn randomly. Then u_i is used to calculate

$$q_i = \begin{cases} (2u_i)^{\frac{1}{\eta_c+1}} & \text{if } u_i \leq \frac{1}{2}, \\ \left(\frac{1}{2(1-u_i)}\right)^{\frac{1}{\eta_c+1}} & \text{otherwise,} \end{cases} \tag{4.1}$$

where $\eta_c \geq 0$ is the so-called distribution index. The resulting q_i in turn is used to calculate the offspring's i-th component via

$$x_i^{1,t+1} := \frac{1}{2}\big((1+q_i)x_i^{1,t} + (1-q_i)x_i^{2,t}\big) \text{ and } x_i^{2,t+1} := \frac{1}{2}\big((1-q_i)x_i^{1,t} + (1+q_i)x_i^{2,t}\big).$$

The role of the distribution index η_c is as follows. "A large value of η_c gives a higher probability for creating 'near-parent' solutions and a small value of η_c allows distant solutions to be selected as offspring" [Deb01, p. 110]. Common values are $\eta_c \in [10, 20]$ [Bra+08, p. 76] [Ses09]. The relation between u_i, q_i and η_c as well as the derivation of (4.1) are detailed in [Deb01, pp. 109–112].
SBX is a popular crossover operator [Bra+08, p. 64] and it is also used in NSGA-II. An overview of alternative crossover operators is given in [Deb01, pp. 107 sqq.].

Mutation The mutation operator perturbs single solutions in the mating pool to hopefully obtain a better solution. "The need for mutation is to keep diversity in the population" [Deb01, p. 91]. Note that "[a] fundamental difference with a crossover operator is that mutation is applied to a single solution, whereas crossover is applied to more than one solution." [Bra+08, p. 66].
In binary representation, the bit-wise mutation operator is common. This operator "changes a 1 to a 0 and vice versa, with a mutation probability of p_m" [Deb01, p. 91]. In real-coded GAs, the bit-wise mutation is not applicable. A common mutation operator for real-coded GAs is the so-called polynomial mutation, which is based on a polynomial probability distribution.
To illustrate how the polynomial mutation is applied, let us suppose that we want to mutate the i-th component of a solution x. Let us further suppose that the i-th component of the feasible set is bounded by x_i^L and x_i^U. First, a number $u_i \in [0, 1]$ is drawn randomly. Then u_i is used to calculate

$$q_i = \begin{cases} (2u_i)^{\frac{1}{\eta_m+1}} - 1 & \text{if } u_i < \frac{1}{2}, \\ 1 - \big(2(1-u_i)\big)^{\frac{1}{\eta_m+1}} & \text{otherwise,} \end{cases} \tag{4.2}$$

where $\eta_m \geq 0$ is the so-called mutation distribution index. The resulting q_i in turn is used to calculate the i-th component of the perturbed solution, denoted by $\tilde{x}$, via

$$\tilde{x}_i = x_i + (x_i^U - x_i^L)q_i. \tag{4.3}$$

Note that $\tilde{x}_i$ must not be smaller than x_i^L and it must not be greater than x_i^U in order to obtain a feasible solution, which is in general not guaranteed by the formula according to (4.2) and (4.3).
The perturbation of x_i can be controlled with the distribution index η_m. A smaller η_m produces a greater perturbation and vice versa [Deb01, p. 120]. A common value is $\eta_m = 20$ [Bra+08, p. 76] [Ses09]. The relation between u_i, q_i and η_m as well as the derivation of (4.2) are detailed in [Deb01, p. 120].
The polynomial mutation is also used in NSGA-II. An overview of alternative mutation operators is given in [Deb01, pp. 118 sqq.].

Properties of Genetic Algorithms

We briefly discuss some of the properties of GAs. Because GAs are population based and process several solutions simultaneously, "it is likely that the expected GA solution may be a global solution" [Deb01, p. 92]. In addition, GAs usually do not require any further information than objective function evaluations. In particular, no gradients are required in general. Furthermore, because of "probabilistic transition rules and an initial random population", GAs are able "to recover from early mistakes" [Deb01, p. 92]. Therefore, GAs can be applied to a wide class of optimization problems including multimodal problems.
However, the three evolutionary operators and their parameters must be selected such that the "extent of exploration ... through recombination and mutation operators" is balanced "with the extent of exploitation through the selection[1] operator" [Deb01, p. 93].
Selecting the right operators and parameters may be challenging in practice. In particular because the approximation quality of a GA is in general unknown, i.e., it is unknown how close the output of a GA is to the true optimal solution(s) and to the true Pareto front.

This concludes the introduction to GAs. As mentioned at the beginning of Section 4.2, we next introduce a GA specifically designed for solving multiobjective optimization problems.

4.2.2. Nondominated Sorting Genetic Algorithm (NSGA) II

Recall from Section 4.1.1 that a multiobjective optimization problem in general does not have one optimal solution. Rather, there usually exist several Pareto optimal solutions, the so-called Pareto optimal set. In continuous optimization, the Pareto optimal set is often an infinite set. Therefore, we are usually interested in finding a finite set of solutions that is a good representation of the Pareto optimal set. This can be characterized by two goals. First, the found solutions shall be close to the Pareto front (ideally their images are elements of the Pareto front). Second, the found solutions shall be "as diverse as possible" [Deb01, p. 22].
An evolutionary algorithm works with populations and thus it has a "tremendous advantage for ... solving multi-objective optimization problems", because "a population of Pareto-optimal solutions can be captured in a single simulation run of an [evolutionary algorithm]" [Deb01, p. 161]. To make use of this advantage, a fitness assignment function is required that produces selection pressure towards Pareto optimality and diversity.
This also applies to NSGA-II, a popular genetic algorithm for solving multiobjective optimization problems. As a genetic algorithm its basic working principle is as described in Section 4.2.1, i.e., in each generation the reproduction, the crossover and the mutation operators are applied to the incumbent population. However, the particularity of NSGA-II is its fitness assignment function, which is presented in the following. All concepts and results presented in this subsection are based on the article “A fast and elitist multiobjective

[1] The term selection operator is synonymous to the reproduction operator introduced above.

genetic algorithm: NSGA-II" [Deb+02].

Fitness Assignment Function

The main idea behind NSGA-II is that a solution is assigned a large fitness if it is not Pareto dominated by another solution in the population and if there are no other nondominated solutions in its vicinity in the objective space. In contrast, if a solution is dominated by another solution in the population or if two nondominated solutions in the population are close to each other in the objective space, then these are assigned a small fitness. Therefore, the fitness assignment is composed of the two parts Pareto dominance and diversity. The fitness of a solution with respect to Pareto dominance is determined by nondominated sorting. The fitness with respect to diversity is determined with the so-called crowding distance. In addition, NSGA-II is an elitist algorithm. All three concepts are detailed in the following.

Nondominated sorting Let us suppose that we are in the t-th iteration and let X_t be the set of incumbent solutions, i.e., X_t denotes the population in the t-th generation. Let $Y_t := f(X_t)$ denote the image of X_t under the multiobjective function f. The idea behind nondominated sorting is that the solutions in X_t are sorted for their "degree of nondominance" in Y_t. This is done iteratively. Let F_1 denote the set of all points that are nondominated in Y_t. The set F_1 is also called front 1 and its preimages in X_t are assigned the rank 1. We remove the points in F_1 from Y_t and filter again for nondominance. This gives us the set F_2 that contains all nondominated points in $Y_t \setminus F_1$. The preimages of F_2 in X_t are assigned the rank 2. This is continued iteratively, i.e.,

$$F_{i+1} = \left\{ y \in Y_t \setminus \bigcup_{k=1}^{i} F_k : y \text{ is nondominated in } Y_t \setminus \bigcup_{k=1}^{i} F_k \right\},$$

until all elements in X_t are assigned a rank. This gives us a partition of X_t and Y_t. Each $x \in X_t$ is assigned exactly one rank and each $y \in Y_t$ is contained in exactly one front.

Remark 4.26 *By using an efficient bookkeeping it is possible to perform the nondominated sorting of X_t and Y_t with a time complexity of $\mathcal{O}(pN^2)$ and a storage requirement of $\mathcal{O}(N^2)$, where p is the number of objectives and N is the population size. The corresponding algorithm is detailed in [Deb01, pp. 42–44] and [Deb+02, pp. 183–184].*

The fitness assignment with nondominated sorting is straightforward. A solution with a smaller rank is preferred over a solution with a larger rank. If two solutions have the same rank, the solution that makes a greater contribution to diversity (within the front that contains both solutions) is preferred. An indicator for the contribution of a solution to a front's diversity is the crowding distance.

Crowding distance Only the basic idea behind the crowding distance is presented. Details as well as an algorithmic description can be found in [Deb01, pp. 236–240] and [Deb+02, pp. 185–186]. Note that the crowding distance is only computed for solutions within the same front F_k, because otherwise the solution with the lower rank is preferred. To illustrate how the crowding distance is calculated, let us suppose that our multiobjective problem has p, $p \geq 2$, objectives and that the front F_k has ℓ elements, i.e., $F_k = \{y^1, \ldots, y^\ell\}$. Then, we have to compute ℓ crowding distances d_i, $i \in [\ell]$.
First, the crowding distances are initialized with zero, i.e., we set $d_i := 0$ for all $i \in [\ell]$.
Next, we proceed component by component of the objective space. For each $m \in [p]$, we sort the m-th component of the elements in F_k in increasing order. For the moment, let us suppose that these components are unique, i.e., we only have strict inequalities and thus a unique order. Let σ_m be the corresponding permutation, i.e., we have $y_m^{\sigma_m(1)} < y_m^{\sigma_m(2)} < \ldots < y_m^{\sigma_m(\ell)}$. In particular, we have $y_m^{\sigma_m(1)} = \min\{y_m^1, \ldots, y_m^\ell\}$ and $y_m^{\sigma_m(\ell)} = \max\{y_m^1, \ldots, y_m^\ell\}$.
The boundaries of F_k are most important for diversity and thus we assign $d_{\sigma_m(1)} \leftarrow \infty$ as well as $d_{\sigma_m(\ell)} \leftarrow \infty$. The remaining crowding distances are updated by

$$d_{\sigma_m(i)} \leftarrow d_{\sigma_m(i)} + \frac{y_m^{\sigma_m(i+1)} - y_m^{\sigma_m(i-1)}}{f_m^{\max} - f_m^{\min}} \quad \forall\, i \in \{2, \ldots, \ell - 1\}.$$

Remark 4.27 *The parameters $f_m^{\min}$ and $f_m^{\max}$ are used to normalize the componentwise contributions to the crowding distance. But the literature does not clearly state how $f_m^{\min}$ and $f_m^{\max}$ should be selected. In [Deb01], it is suggested to select $f_m^{\min}$ and $f_m^{\max}$ "as the population-minimum and population-maximum values of the m-th objective function" [Deb01, p. 236]. However, in a subsequent example in [Deb01], $f_m^{\min}$ and $f_m^{\max}$ are selected as the m-th components of the ideal point and of the nadir point, respectively [Deb01, p. 238].*
In contrast, the NSGA-II implementation by Seshadri [Ses09], which is used in the use case in Section 9.2.4 below, uses the minimum and the maximum of the m-th component of the elements in F_k only (and not of the whole population), i.e., $f_m^{\min} = y_m^{\sigma_m(1)}$ and $f_m^{\max} = y_m^{\sigma_m(\ell)}$.

Remark 4.28 *The literature ([Deb01] and [Deb+02]) does not state how to deal with the case that the ordering of the m-th component of the elements in F_k is not unique, i.e., if there exist $y^i, y^j \in F_k$, $i \neq j$, such that $y_m^i = y_m^j$. Because all ADA optimization problems are continuous, it is considered very unlikely that two or more solutions within a front have an identical component in the objective space. Therefore, this case is ignored in the following.*

An example where the crowding distance is determined step by step with hand calculations is given in [Deb01, pp. 237–240].

Elitism Elitism is "[a]n operator which preserves the better of parent and child solutions (or populations) so that a previously found better solution is never deleted" [Bra+08,

p. 65]. Elitism is also implemented in NSGA-II. The elite-preserving operator in NSGA-II is straightforward. Let N denote the population size. Let us suppose that the three evolutionary operators presented in the preceding Subsection 4.2.1, reproduction, crossover and mutation, have already been applied in the current generation. This gives us two populations, the original parents as well as the offspring generated by crossover and mutation. We combine both populations to an intermediate population, which has typically the size $2N$ (N parents and N offspring). From this combined intermediate population the N solutions with the best fitness values constitute the population for the subsequent iteration, i.e., the N solutions with the smallest rank and the largest crowding distance are selected.
For instance, let us suppose that F_1 contains $N - 10$ elements and that F_2 contains 20 elements. Then all elements of F_1 as well as the ten elements of F_2 with the largest crowding distance in F_2 constitute the new population, which again has the size N.
Because all parent solutions are considered as candidates for the new population, the new population cannot be "less optimal" than the preceding population.

The interaction of nondominated sorting, crowding distance and elitism is briefly illustrated in the following example.

Example 4.29 *We consider the t-th generation of a run with NSGA-II for a not further specified two-dimensional problem* (MOP). *The tournament, the crossover and the mutation operator have already been applied in this generation. This gives us a combined population that consists of the N parents (the incumbent population in generation t) and of N offspring generated by crossover and mutation. In this example, we have* $N = 6$ *and the combined population consists of* $2N = 12$ *solutions. In Figure 4.3, the combined population is shown in the objective space. Because it is not relevant for the following, the parents and the offspring are not visually distinguished, i.e., it is not apparent which solution is a parent and which solution is an offspring. Note that each point has a unique preimage in the combined population under f (because exactly* 12 *points are shown).*
We apply nondominated sorting to find the "best" $N = 6$ *solutions in the combined population. We filter the combined population for nondominance and obtain the front* F_1. *Next, we filter the combined population without (the preimages of)* F_1 *for nondominance and obtain the front* F_2 *and so on. In total, we have the four fronts* F_1 *to* F_4.
We start to fill the new population, denoted by P_{t+1} *in the following. The front* F_1 *contains three elements and thus we can add all solutions corresponding to* F_1 *to* P_{t+1}. *With this, we have* $6 - 3 = 3$ *spaces left in* P_{t+1}. *However, the next front,* $F_2 = \{a, b, c, d\}$, *has four elements. Therefore, we use the crowding distance operator to determine which three solutions from* F_2 *we add to* P_{t+1}. *Without explicitly calculating the crowding distance it is apparent from Figure 4.3 that b has the smallest crowding distance in* F_2. *Therefore, the solutions corresponding to a, c and d are added to* P_{t+1}. *With this, the population for the subsequent* $(t + 1)$*st generation is constituted and the remaining solutions of the intermediate population are discarded.*

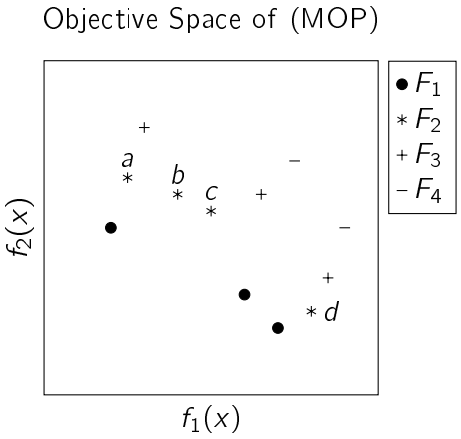

Figure 4.3.: The image of a combined population consisting of 6 parents and 6 offspring under a two-dimensional objective function f is shown (parents and offspring are not visually distinguished). The four ranked fronts F_1 to F_4 are a partition of the combined population's image. Furthermore, it is apparent that the point b has the smallest crowding distance in the front $F_2 = \{a, b, c, d\}$. Adapted from Figure 139 in [Deb01, p. 237].

Remark 4.30 *The computational complexity of one iteration with NSGA-II is* $\mathcal{O}(pN^2)$*, where* p *denotes the number of objective functions of* (MOP) *and* N *denotes the population size [Deb01, p. 240]. This results from the nondominated sorting of the intermediate population with the size* $2N$*, see also Remark 4.26.*

This concludes the introduction to NSGA-II. A more detailed introduction as well as a detailed algorithmic description of NSGA-II can be found in [Deb01, pp. 233–236] and [Deb+02].

Most multiobjective evolutionary algorithms are designed for unconstrained or box constrained problems. Therefore, an additional constraint handling technique (CHT) is required for solving a constrained optimization problem with such algorithms [DD15, p. 1]. This also applies to NSGA-II and thus a small overview of CHTs in evolutionary multiobjective optimization is given.

4.2.3. Constraint Handling Techniques

There exists a variety of CHTs for solving constrained multiobjective optimization problems with evolutionary algorithms. A survey and taxonomy of CHTs in evolutionary multiobjective optimization is given in [Lia+23].
For this study, we are particularly interested in CHTs for NSGA-II. Deb et al. suggest to combine NSGA-II with a CHT based on a separation of objectives and constraints [Deb+02]. This method is called constrained dominance principle (CDP).

Constrained Dominance Principle

If two solutions are compared, then either both solutions are feasible, one is feasible and the other is not or both are infeasible. The idea behind CDP is to modify the Pareto dominance relation between two solutions and include their "degree of (in)feasibility". The following definition is taken from [Deb+02, p. 192].

Definition 4.31 *Let x^i and x^j be two solutions for* (MOP) *(x^i and x^j not necessarily elements of X). The solution x^i* constrained-dominates *x^j if any of the following conditions is satisfied.*

- *x^i and x^j are both feasible and x^i Pareto dominates x^j, i.e., $x^i, x^j \in X$ and $f(x^i) \leq f(x^j)$.*
- *x^i is feasible and x^j is not, i.e., $x^i \in X$ and $x^j \notin X$.*
- *x^i and x^j are both not feasible, but x^i has the smaller overall constraint violation, where the overall constraint violation is the sum of the absolute values of all constraint violations.*

"The effect of using this constrained-domination principle is that any feasible solution has a better nondomination rank than any infeasible solution" and that "among two infeasible solutions, the solution with a smaller constraint violation has a better rank" [Deb+02, p. 192]. With this, NSGA-II and CDP are combined by replacing the Pareto dominance with the constrained dominance when applying NSGA-II.
The advantages of CDP are that it does not require any additional parameters, it is simple and it is easy to implement [Deb+02, p. 196]. Furthermore, in several tests the combination of NSGA-II with CDP provided good results [Deb+02, p. 196]. However, if an optimization problem has discrete feasible regions or infeasible barriers, then CDP might "cause the population to fall into some local feasible regions" [Lia+23, p. 4].
Experiments have shown that satisfactory results are achieved when the ADA optimization problems are solved by combining NSGA-II with CDP. Therefore, CDP is the only CHT considered in this work. As already mentioned, an overview of alternative CHTs for evolutionary multiobjective optimization is given in [Lia+23].

This concludes the introduction to evolutionary multiobjective optimization. In the following section, some basics of fixed point iteration procedures are presented.

4.3. Fixed Point Iteration Procedures

In Chapter 6, it is shown that the ADA procedure with a single ADA pair corresponds to the Picard iteration, which is a fixed point iteration procedure. Therefore, this subsection deals with the terms fixed point and iteration procedure and is based on the book *Iterative Approximation of Fixed Points* written by Berinde [Ber07]. The term fixed point and the Picard iteration are introduced first. Thereafter, some convergence results are presented.

4.3.1. Fixed Points and the Picard Iteration

As the name suggests, a fixed point of a function is an element that is mapped to itself. The definition of a fixed point is very general, i.e., the underlying set and the corresponding function do not have to have any structure.

Definition 4.32 *Let X be a nonempty set. A function f that maps the set X to X is called* selfmap.
Let $f : X \to X$ be a selfmap. An element $x \in X$ with $f(x) = x$ is called fixed point of f. *The* set of fixed points of f *is denoted by* $\mathrm{Fix}(f)$.

The following example shows that $\mathrm{Fix}(f)$ can be empty, contain a certain number of elements or can be the whole underlying set X.

Example 4.33 *1. Let X be an arbitrary nonempty set and $f := \mathrm{id}$ the identity. Then, we have $\mathrm{Fix}(f) = X$, because $f(x) = x \; \forall \; x \in X$.*

2. Let $X = \mathbb{R}$ and $f(x) := \frac{1}{2}x + 5$. Then $\mathrm{Fix}(f) = \{10\}$, because

$$\frac{1}{2}x + 5 = x \;\Leftrightarrow\; 5 = \frac{1}{2}x \;\Leftrightarrow\; 10 = x.$$

3. Let $X = \mathbb{R}$ and $f(x) := x + 1$. Suppose f has a fixed point x^*. Then, we have $x^* + 1 = x^*$, which implies $1 = 0$. That is a contradiction and thus we have $\mathrm{Fix}(f) = \emptyset$.

It is not always possible to explicitly calculate the set of fixed points like in Example 4.33. Rather one has to rely on iterative approximation procedures [Ber07, p. 20]. Such procedures are based on consecutive function evaluations, so we introduce a notation for that.

Notation 4.34 *Let $f : X \to X$ be a selfmap with a nonempty set X. Then, $f^n(x)$ is the n-th* iterate of x under f. *It is recursively defined by $f^0(x) := x$ and $f^{n+1}(x) := f\left(f^n(x)\right)$.*

Remark 4.35 *The part $f^0(x) := x$ looks similar to the definition of a fixed point. But the term $f^0(x)$ simply denotes the element x itself.*

The most basic iterative fixed point method is the so-called Picard iteration [Ber07, p. 3].

Definition 4.36 *The sequence $\{f^n(x_0)\}_{n \in N_0} \subset X$ is called the* Picard iteration associated to f starting at x_0. *It is also denoted by $\{x_n\}_{n \in \mathbb{N}_0}$, where $x_n := f^n(x_0)$.*

If $x_0 \in \mathrm{Fix}(f)$, then we obviously have $f^n(x_0) = x_0$ for all $n \in \mathbb{N}_0$. A major result with respect to the Picard iteration for arbitrary starting points $x_0 \in X$ is Banach's fixed point theorem. It is one of the most important theorems in the metrical fixed point theory [Ber07, p. 6]. However, Banach's fixed point theorem requires that X is a complete

metric space. A complete metric space is a metric space in which every Cauchy sequence is convergent [Ber07, p. 5]. This is no restriction to us, since the ADA iteration function A_i, which is defined and analyzed in Chapter 6 below, lives on $\mathbb{R}$ and it is well known that $\mathbb{R}$ together with the metric $d(x, y) := |x - y|$ is a complete metric space. Therefore, the following definitions and theorems are stated for subsets of $\mathbb{R}$ only, although more general versions exist.
In order to formulate Banach's fixed point theorem, we need the concept of Lipschitz continuity. We also introduce the closely related term *contractive function*.

Definition 4.37 *Let $X \subset \mathbb{R}$ and let $f : X \to \mathbb{R}$. The function f is called* L-Lipschitzian, *if there exists $L > 0$ such that*

$$|f(x) - f(y)| \leq L|x - y| \ \forall\ x, y \in X.$$

The corresponding constant L is called Lipschitz constant.
The function f is called contractive, *if*

$$|f(x) - f(y)| < |x - y| \ \forall\ x, y \in X,\ x \neq y.$$

Remark 4.38 *There exists a more general definition of Lipschitz continuity that is defined for functions between two metric spaces (X_1, d_1) and (X_2, d_2). However, Definition 4.37 is sufficient for the ADA optimization.*

Theorem 4.39 (Banach's fixed point theorem) *Let $X \subset \mathbb{R}$ and let $f : X \to X$ be L-Lipschitzian with $L < 1$. Then*

1. *f has a unique fixed point $x^* \in X$.*
2. *The Picard iteration associated to f converges to x^* for an arbitrary starting point $x_0 \in X$.*
3. *The a priori error estimate $|x_n - x^*| \leq \frac{L^n}{1-L} \cdot |x_1 - x_0|$ holds for all $n \in \mathbb{N}_0$.*
4. *The a posteriori error estimate $|x_n - x^*| \leq \frac{L}{1-L} \cdot |x_n - x_{n-1}|$ holds for all $n \in \mathbb{N}_0$.*
5. *The rate of convergence can be estimated by $|x_n - x^*| \leq L \cdot |x_n - x_{n-1}| \leq L^n \cdot |x_0 - x^*|$ for all $n \in \mathbb{N}$.*

Proof. See [Ber07, p. 32]. □

The existence of a Lipschitz constant $L < 1$ is a strict requirement for Banach's fixed point theorem. If the condition is slightly weakened to f being only contractive, then the conclusions of Banach's fixed point theorem are not valid in general. The following example is taken from [Ber07, p. 34]. The proof presented in the example is added by the author of this thesis.

Example 4.40 *Let $X := [1, \infty)$ and $f : X \to X$ be defined by $f(x) := x + \frac{1}{x}$. Then*

1. *$|f(x) - f(y)| < |x - y|$ for all $x, y \in X$ with $x \neq y$.*
2. *There exists no $L < 1$ such that $|f(x) - f(y)| \leq L \cdot |x - y|$ for all $x, y \in X$.*
3. *$\mathrm{Fix}(f) = \emptyset$ and the Picard iteration associated to f does not converge for any starting point $x_0 \in X$.*

Proof. 1. First, we show that f is strictly increasing. Let $x, y \in X$ and $x < y$. Then we have

$$\begin{aligned} 1 \leq x < y \;&\Rightarrow\; 1 < x \cdot y \;\Rightarrow\; \frac{1}{xy} < 1 \;\Rightarrow\; 0 < 1 - \frac{1}{xy} \\ &\Rightarrow\; 0 < (y - x)(1 - \frac{1}{xy}) \quad (\text{because } y - x > 0) \\ &\Rightarrow 0 < y - x - \frac{y}{xy} + \frac{x}{xy} = y + \frac{1}{y} - x - \frac{1}{x} = f(y) - f(x) \Rightarrow f(x) < f(y). \end{aligned}$$

Now, we are able to prove the first statement. Let $x, y \in X$ with $x \neq y$. Without loss of generality, let $x < y$. That implies $\frac{1}{y} - \frac{1}{x} < 0$ and $f(x) < f(y)$, since f is strictly increasing. Thus, we have

$$|f(x) - f(y)| = f(y) - f(x) = y + \frac{1}{y} - (x + \frac{1}{x}) = y - x + (\frac{1}{y} - \frac{1}{x}) < y - x = |x - y|.$$

2. Let us suppose that there exists a constant $L < 1$ such that $|f(x) - f(y)| \leq L \cdot |x - y|$ for all $x, y \in X$. Let x be an arbitrary element of X. We set $y := x + \frac{1}{(1-L)x}$. Then, we have $1 \leq x < y$ and thus

$$\begin{aligned} |f(x) - f(y)| &= y + \frac{1}{y} - x - \frac{1}{x} \\ &> y - x - \frac{1}{x} = x + \frac{1}{(1-L)x} - x - \frac{1}{x} = \frac{1}{(1-L)x} - \frac{1-L}{(1-L)x} \\ &= L\frac{1}{(1-L)x} = L\left(x + \frac{1}{(1-L)x} - x\right) = L(y - x) = L \cdot |x - y|. \end{aligned}$$

That is a contradiction and the second statement is proven.
3. Let us suppose that the Picard iteration associated to f converges for some starting point $x \in X$. Let x^* be the limit. That gives us $f(x^*) = x^* + \frac{1}{x^*} = x^*$, what implies $1 = 0$. Thus, the Picard iteration does not converge and the set of fixed points is empty. □

However, if the ambient space has more structure than simply being a subset of $\mathbb{R}$, then even the weaker property 'contractive' is sufficient to guarantee that the Picard iteration converges for an arbitrary starting point.

Theorem 4.41 *Let $X \subset \mathbb{R}$ be compact and let $f : X \to X$ be contractive. Then*

1. *f has a unique fixed point $x^* \in X$ and*
2. *the Picard iteration associated to f converges to x^* for any starting point $x_0 \in X$.*

Proof. See [Ber07, p. 35]. □

Remark 4.42 *The theorem and proof in [Ber07, p. 35] are formulated for the more general case that X is a compact metric space.*

Remark 4.43 *Because there does not exist a Lipschitz constant smaller than one for a contractive function in general, it is not possible to make a statement about the convergence rate or about the error estimates of the Picard iteration in this case [Ber07, p. 35].*

So far, one can guess that the Lipschitz constant plays a central in this thesis. If differentiable functions are considered, there is a link between the absolute value of a function's derivative and its Lipschitz constant. The following lemma is a well-known result of mathematical analysis, see for instance [For23, p. 250].

Lemma 4.44 *Let $I \subset \mathbb{R}$ be an interval and let $f : I \to \mathbb{R}$ be a differentiable function.*

1. *If there exists $L > 0$, such that $|f'(x)| \leq L$ for all $x \in I$, then f is L-Lipschitzian.*
2. *If $|f'(x)| < 1$ for all $x \in I$, then f is contractive.*

There exist a lot more iterative fixed point procedures with according convergence results. But they usually require an extended structure of the ambient space X or there are some more specific requirements to the function f. But they are not applicable in the case of the ADA procedure. However, the ADA iteration functions have a certain structure, which allows to make some ADA specific fixed point iteration statements. These are presented in the following subsection.

4.3.2. Fixed Point Related Results Required for the Convergence Analysis of the ADA Procedure

The results presented in the preceding subsection are very general. However, the ADA iterations have a certain structure. In Chapter 6, we show that the ADA iteration functions are strictly increasing and that they are defined on closed intervals. This information is used to make some more specific statements with respect to the corresponding Picard iteration in this subsection. All statements and proofs in this subsection were developed by the author of this thesis.

If f is strictly increasing, contractive and has a fixed point, then $f(x)$ is limited by x and the fixed point. Note that f is not required to be a selfmap.

Lemma 4.45 *Let $X \subset \mathbb{R}$. Let $f : X \to \mathbb{R}$ be contractive and strictly increasing and let $x^* \in X$ be a fixed point of f. For $x \in X$, we have*

$$x < x^* \;\Rightarrow x < f(x) < x^* \quad \text{and} \quad x^* < x \;\Rightarrow\; x^* < f(x) < x.$$

Proof. Let $x \in X$ such that $x < x^*$. Because f is strictly increasing and x^* is a fixed point of f, we have

$$x < x^* \;\Rightarrow\; f(x) < f(x^*) = x^*.$$

Next, let us assume that $f(x) \leq x$. But then

$$f(x) \leq x < x^* = f(x^*) \;\Rightarrow\; 0 < x^* - x \leq f(x^*) - f(x) \;\Rightarrow\; |f(x) - f(x^*)| \geq |x - x^*|,$$

which is a contradiction to f being contractive. Thus, we have $x < f(x)$.
The second statement is shown analogously. □

With this, we can state that if f is a strictly increasing and contractive function on a closed and bounded interval I, then f is a selfmap if and only if f has a fixed point.

Lemma 4.46 *Let $I \subset \mathbb{R}$ be a closed and bounded interval. Let $f : I \to \mathbb{R}$ be contractive and strictly increasing. Then, f has a fixed point if and only if f is a selfmap, i.e.,*

$$\exists\, x^* \in I : f(x^*) = x^* \;\Leftrightarrow\; f(I) \subset I.$$

Furthermore, if f has a fixed point, then it is unique and the Picard iteration associated to f converges to this fixed point for an arbitrary starting point $x \in I$.

Proof. "⇒" Let there exist $x^* \in I$ such that $f(x^*) = x^*$. Let $x \in I$. We have to show that $f(x) \in I$. For this, we do a case distinction with respect to x. If $x = x^*$, then $f(x) = x^* \in I$. If $x < x^*$, then $x < f(x) < x^*$ according to Lemma 4.45. Because $x, x^* \in I$ and I is a closed interval, $f(x)$ is also an element of I. Analogously, $x^* < x$ implies that $x^* < f(x) < x$ and thus $f(x) \in I$.
"⇐" Let f be a selfmap. The set I is a closed and bounded interval by assumption and thus compact. Therefore, f is a contractive selfmap on a compact set and thus we can apply Theorem 4.41, which states that f has a unique fixed point $x^* \in I$ and that the Picard iteration associated to f converges to x^* for an arbitrary starting point $x \in I$. □

Finally, the following lemma states monotonicity properties of the Picard iterations associated to strictly increasing functions f.

Lemma 4.47 *Let $X \subset \mathbb{R}$ be nonempty, let $f : X \to X$ be strictly increasing and let $x \in X$. Then, the following holds:*

1. *If $f(x) > x$, then the Picard iteration associated to f starting at x is strictly increasing.*
2. *If $f(x) < x$, then the Picard iteration associated to f starting at x is strictly decreasing.*

3. *If $f(x) = x$, then $x \in \mathrm{Fix}(f)$ and the Picard iteration associated to f starting at x is constant.*

Proof. We show the first statement by induction. So let $x \in X$ and let $f(x) > x$.
Base case:
For $n = 1$ the claim follows from the assumption $f(x) > x$.
Induction hypothesis:
Let the statement hold for $n = 1, \ldots, k$, i.e., we have $f^n(x) > f^{n-1}(x)$ for all $n = 1, \ldots, k$.
Induction step:
We consider $n = k + 1$. According to the induction hypothesis, we have $f^k(x) > f^{k-1}(x)$. Because f is strictly increasing, we have $f^{k+1}(x) = f\big(f^k(x)\big) > f\big(f^{k-1}(x)\big) = f^k(x)$. This proves the first statement. The second statement is shown analogously. The third statement follows from the definition of a fixed point. □

With this we have all the statements together that are required for the convergence analysis in Chapters 6 and 7 below.

Part II.

Mathematical Analysis of ADA

5. Mathematical Formulation of ADA

In this chapter, the ADA procedure is presented from a mathematical point of view. First, a corresponding formalism is introduced and all the required sets and functions are defined. This formalism is then used to formulate the full ADA Algorithm 5.2 below. "Good" convergence characteristics of this algorithm are an objective in the optimization later on. Therefore, the convergence characteristics of Algorithm 5.2 are thoroughly analyzed in Chapters 6 and 7. The findings are used to develop the optimization models in Chapter 8.

The ADA procedure is presented in detail in Chapter 3. As explained there, it requires certain parameters, the so-called ADA pairs. Each ADA pair consists of a start and a test point. Each start and test point consists of a fan speed and of an ioni current. The following notation briefly summarizes the notation introduced in Definition 3.25 and Notation 3.34 above.

Notation 5.1 *Let $N \in \mathbb{N}$ be the total number of ADA pairs. We define $[N] := \{1, \dots, N\}$. The ADA parameters of the p-th ADA pair, $p \in [N]$, are denoted by*

s^p and t^p: the ADA pair's start and test fan speed, respectively,

i_s^p and i_t^p: the ADA pair's start and test ioni current, respectively.

There are certain requirements with respect to the ADA pairs. The following definition extends Definition 3.25 of a well-defined ADA pair.

Definition 5.2 *Let $\mathcal{H} = \left(\mathsf{FS}, (G_{\mathsf{fs}})_{\mathsf{fs}\in\mathsf{FS}}, (\iota_{\mathsf{fs}})_{\mathsf{fs}\in\mathsf{FS}}, (\Lambda_{\mathsf{fs}})_{\mathsf{fs}\in\mathsf{FS}}, (\zeta_{\mathsf{fs}})_{\mathsf{fs}\in\mathsf{FS}}\right)$ be an HE model and let $p \in [N]$. A quadruple (s^p, t^p, i_s^p, i_t^p) is called* feasible ADA pair with respect to $\mathcal{H}$, *if*

$$s^p, t^p \in \mathsf{FS} : s^p > t^p, \quad i_s^p \in I_{s^p}, \quad i_t^p \in I_{t^p} \quad \text{and} \quad G_{s^p} \cap G_{t^p} \neq \emptyset.$$

Remark 5.3 *This remark is analogous to Remark 3.26. When there is no risk of confusion, the HE model related to a feasible ADA pair is not explicitly stated for the remainder of this thesis.*

Remark 5.4 *An ADA pair (s^p, t^p, i_s^p, i_t^p) is feasible if and only if it is well-defined and in addition $G_{s^p} \cap G_{t^p} \neq \emptyset$ holds. The condition $G_{s^p} \cap G_{t^p} \neq \emptyset$ is included to avoid case distinctions in the following. From a practical point of view, if $G_{s^p} \cap G_{t^p} = \emptyset$, then feasible combustion limits are exceeded during an ADA iteration.*

Remark 5.5 *If an ADA pair (s^p, t^p, i_s^p, i_t^p) is feasible, then its ioni currents are positive, i.e., $i_s^p > 0$ and $i_t^p > 0$. This follows from $I_{s^p} \subset \mathbb{R}_{>0}$ and $I_{t^p} \subset \mathbb{R}_{>0}$ (Definitions 2.18 and 2.22).*

Assumption 5.6 *To avoid case distinctions, it is implicitly assumed that all considered ADA pairs are feasible for the remainder of this part.*

During the course of this part, we often switch between ioni currents and corresponding resistances. This is done by applying Ohm's law with the voltage U. Recall from Remark 3.3 that U is a positive constant, i.e., $U > 0$. It is convenient to define resistances that correspond to the start and test ioni currents.

Definition 5.7 *For all $p \in [N]$ we define the p-th ADA pair's start and test resistance, respectively, by*

$$r_s^p := \frac{U}{i_s^p} \quad \text{and} \quad r_t^p := \frac{U}{i_t^p}.$$

Remark 5.8 *Because $i_t^p > 0$ and $i_t^p > 0$, we have $r_s^p > 0$ and $r_t^p > 0$ for all $p \in [N]$.*

In the following section, a formalism is introduced that allows to formulate the ADA procedure as an algorithm. For this, we implicitly assume that a drift resistance $r_D \geq 0$, an HE model $\mathcal{H} = \big(\mathrm{FS}, (G_{\mathrm{fs}})_{\mathrm{fs}\in\mathrm{FS}}, (\iota_{\mathrm{fs}})_{\mathrm{fs}\in\mathrm{FS}}, (\Lambda_{\mathrm{fs}})_{\mathrm{fs}\in\mathrm{FS}}, (\zeta_{\mathrm{fs}})_{\mathrm{fs}\in\mathrm{FS}}\big)$ and N feasible ADA pairs (s^p, t^p, i_s^p, i_t^p), $p \in [N]$, are given.

5.1. Formalism: Required Sets and Functions

Let $\hat{\boldsymbol{i}}_{t,r_D} = (i_1, \ldots, i_N)$ be the incumbent vector of drifted test ioni current approximations. According to Definition 3.30 and Remark 3.42, an ADA iteration with the p-th ADA pair, i.e., an update of i_p, $p \in [N]$, is composed of the following four steps.

(A1) $\hat{r}_D \leftarrow \alpha_{\hat{\boldsymbol{i}}_{t,r_D}}(s^p)$

(A2) $i^p_{s,\hat{r}_D} \leftarrow \frac{U i_s^p}{\hat{r}_D i_s^p + U}$

(A3) $\hat{g} \leftarrow \iota^{-1}_{s^p,r_D}(i^p_{s,\hat{r}_D})$

(A4) $i_p \leftarrow \iota_{t^p,r_D}(\hat{g})$.

The aim of this section is to provide a formalism such that we can express steps (A1) to (A4) with functions. We begin with step (A1) and take a closer look at the drift resistance approximations at the start fan speeds, i.e., we take a closer look at $\alpha_{\hat{\boldsymbol{i}}_{t,r_D}}(s^p)$, $p \in [N]$. Thereafter, we consider steps (A2) to (A4).

5.1.1. Drift Resistance Approximations at the Start Fan Speeds

In step (A1), we calculate $\alpha_{\hat{\boldsymbol{i}}_{t,r_D}}(s^p)$, which corresponds to calculating the incumbent drift resistance approximation at the start fan speed s^p. Recall from Definition 3.38 that for a given vector $\hat{\boldsymbol{i}}_{t,r_D} = (i_1, \ldots, i_N)$ the function $\alpha_{\hat{\boldsymbol{i}}_{t,r_D}}(\mathrm{fs})$ is a linear interpolation combined with a constant extrapolation of the N data points $(t^p, \hat{r}_D^p)$ with $\hat{r}_D^p = \frac{U}{i_p} - \frac{U}{i_t^p}$, $p \in [N]$.

Calculating $\frac{U}{i_p} - \frac{U}{i_t^p}$ is essential for the ADA procedure and thus we define corresponding functions.

Definition 5.9 *For $p \in [N]$ we define*

$$\beta^p : \mathbb{R}_{>0} \to (-r_t^p, \infty), \quad \beta^p(i) := \frac{U}{i} - \frac{U}{i_t^p} = \frac{U}{i} - r_t^p$$

and

$$\left(\beta^p\right)^{-1} : (-r_t^p, \infty) \to \mathbb{R}_{>0}, \quad \left(\beta^p\right)^{-1}(r) := \frac{U}{r + r_t^p}.$$

Lemma 5.10 *The functions β^p and $\left(\beta^p\right)^{-1}$ are well-defined.*

Proof. Let $i \in \mathbb{R}_{>0}$. Then, $\frac{U}{i}$ is defined and $\beta^p(i)$ can be evaluated. Furthermore, we have (because $U > 0$)

$$i \in \mathbb{R}_{>0} \;\Rightarrow\; i > 0 \;\Rightarrow\; \frac{U}{i} > 0 \;\Rightarrow\; \beta^p(i) = \frac{U}{i} - r_t^p > -r_t^p \;\Rightarrow\; \beta^p(i) \in (-r_t^p, \infty).$$

On the other hand, let $r \in (-r_t^p, \infty)$. Then we have $r > -r_t^p$ and thus $r + r_t^p > 0$ holds and $\frac{U}{r+r_t^p} = \left(\beta^p\right)^{-1}(r)$ is defined. Furthermore, $\left(\beta^p\right)^{-1}(r) > 0$ holds (because $U > 0$). □

Lemma 5.11 *Let $p \in [N]$. The function β^p is a homeomorphism. Its inverse function is $\left(\beta^p\right)^{-1}$. Furthermore, both functions are strictly decreasing.*

Proof. The functions β^p and $\left(\beta^p\right)^{-1}$ are each a composition of continuous operations on their respective domains and thus they are continuous as well. Next, we show that they are inverse of each other. Let $i \in \mathbb{R}_{>0}$, then we have

$$\left(\beta^p\right)^{-1} \circ \beta^p(i) = \left(\beta^p\right)^{-1}\left(\frac{U}{i} - r_t^p\right) = \frac{U}{\frac{U}{i} - r_t^p + r_t^p} = i.$$

Let $r \in (-r_t^p, \infty)$, then we have

$$\beta^p \circ \left(\beta^p\right)^{-1}(r) = \beta^p\left(\frac{U}{r + r_t^p}\right) = \frac{U}{\frac{U}{r+r_t^p}} - r_t^p = r + r_t^p - r_t^p = r.$$

To show that β^p is strictly decreasing, let $i_1, i_2 \in \mathbb{R}_{>0}$ such that $i_1 < i_2$. Then,

$$0 < i_1 < i_2 \;\Rightarrow\; \frac{U}{i_2} < \frac{U}{i_1} \;\Rightarrow\; \frac{U}{i_2} - r_t^p < \frac{U}{i_1} - r_t^p \;\Rightarrow\; \beta^p(i_2) < \beta^p(i_1)$$

and thus β^p is strictly decreasing. As the inverse function of a strictly decreasing function, $\left(\beta^p\right)^{-1}$ is also strictly decreasing. □

Before we use β^p to reformulate the calculation of $\alpha_{\hat{i}_{t,r_D}}(s^p)$, we take a closer look at the relation between the start and the test fan speed of an ADA pair. Recall from Section 3.4.1 that the numbering of the ADA pairs follows a descending order with respect

to their test fan speeds, i.e., $t^p < t^{p-1}$ for all $p \in \{2, \dots, N\}$. In addition, ADA pairs must not be overlapping as stated in Section 3.4.3. Then, the start fan speed of ADA pair p lies between the test fan speeds of the ADA pairs p and $p-1$ for all $p \in \{2, \dots, N\}$ according to Lemma 3.44 (if the ADA pairs are well-defined), i.e., $t^p < s^p < t^{p-1}$ for all $p \in \{2, \dots, N\}$. Recall that all ADA pairs considered in this work are required to be not overlapping. Therefore, we can express s^p by a weighted sum of t^p and t^{p-1} with weights w^p and $1 - w^p$ between 0 and 1 for all $p \in \{2, \dots, N\}$.

Definition 5.12 *Let $p \in \{2, \dots, N\}$. We define*

$$w^p := \frac{t^{p-1} - s^p}{t^{p-1} - t^p}.$$

Lemma 5.13 *Let $p \in \{2, \dots, N\}$. Then, we have*

$$0 < w^p < 1 \quad \textit{and} \quad s^p = w^p t^p + (1 - w^p) t^{p-1}.$$

Proof. Let $p \in \{2, \dots, N\}$. According to Lemma 3.44, we have $t^{p-1} > s^p > t^p$ and thus

$$t^{p-1} > s^p > t^p \;\Rightarrow\; t^{p-1} - t^p > t^{p-1} - s^p > 0 \;\Rightarrow\; 1 > \frac{t^{p-1} - s^p}{t^{p-1} - t^p} = w^p > 0.$$

Regarding the second statement, let us consider

$$\begin{aligned} w^p t^p + (1 - w^p) t^{p-1} &= \frac{t^{p-1} - s^p}{t^{p-1} - t^p} t^p + \Big(1 - \frac{t^{p-1} - s^p}{t^{p-1} - t^p}\Big) t^{p-1} \\ &= \frac{t^{p-1} - s^p}{t^{p-1} - t^p} t^p + \frac{t^{p-1} - t^p - (t^{p-1} - s^p)}{t^{p-1} - t^p} t^{p-1} \\ &= \frac{t^{p-1} - s^p}{t^{p-1} - t^p} t^p + \frac{s^p - t^p}{t^{p-1} - t^p} t^{p-1} \\ &= \frac{-s^p t^p + s^p t^{p-1}}{t^{p-1} - t^p} = \frac{(t^{p-1} - t^p) s^p}{t^{p-1} - t^p} = s^p. \end{aligned}$$

□

With this, we can state an equation for $\alpha_{\hat{\boldsymbol{i}}_{t,r_D}}(s^p)$, $p \in [N]$, that depends on the incumbent drifted test ioni current approximations.

Lemma 5.14 *Let $\hat{\boldsymbol{i}}_{t,r_D} = (i_1, \dots, i_N) \subset \mathbb{R}^N_{>0}$ be a given vector of drifted test ioni current approximations. The corresponding drift resistance approximations at the start fan speeds are*

$$\alpha_{\hat{\boldsymbol{i}}_{t,r_D}}(s^p) = \begin{cases} \beta^1(i_1) & \text{if } p = 1, \\ w^p \beta^p(i_p) + (1 - w^p) \beta^{p-1}(i_{p-1}) & \text{if } p \geq 2. \end{cases} \tag{5.1}$$

An equivalent but less concise expression is

$$\alpha_{\hat{\boldsymbol{i}}_{t,r_D}}(s^p) = \begin{cases} \frac{U}{i_1} - \frac{U}{i_t^1} & \text{if } p = 1, \\ w^p \big(\frac{U}{i_p} - \frac{U}{i_t^p}\big) + (1 - w^p) \big(\frac{U}{i_{p-1}} - \frac{U}{i_t^{p-1}}\big) & \text{if } p \geq 2. \end{cases} \tag{5.2}$$

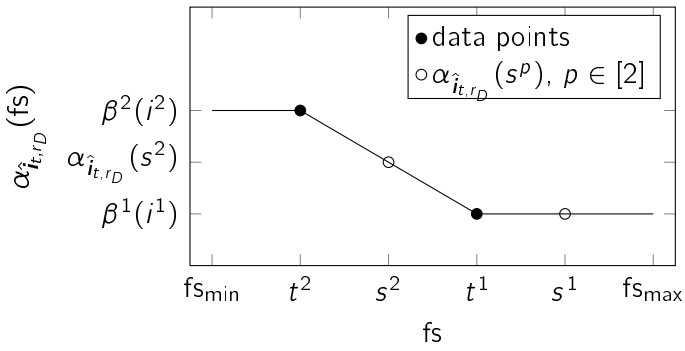

Figure 5.1.: The drift resistance approximation function $\alpha_{\hat{\boldsymbol{i}}_{t,r_D}}(\mathrm{fs})$ for a situation with two ADA pairs and a given vector of drifted test ioni current approximations $\hat{\boldsymbol{i}}_{t,r_D} = (i_1, i_2)$ is shown. The black dots correspond to the data point $\left(t^p, \beta^p(i_p)\right)$, $p \in \{1,2\}$. The rings mark the corresponding drift resistance approximations at the start fan speeds s^1 and s^2.

Proof. The statement follows from Definitions 3.38 and 5.9 as well as from Lemma 5.13. □

Remark 5.15 *Equation* (5.2) *of Lemma 5.14 is also found in the Vaillant documentation [WHB, Items 4267 and 4268].*

The following example demonstrates the statements of Lemma 5.14.

Example 5.16 *We consider a situation with two ADA pairs, i.e., we have* $N = 2$*. For this, let us assume that two ADA pairs* (s^1, t^1, i_s^1, i_t^1) *and* (s^2, t^2, i_s^2, i_t^2) *are given. In accordance with the convention of the ADA pair numbering, let* $t^2 < t^1$*. Let us further assume, that we have a vector of incumbent drifted test ioni current approximations* $\hat{\boldsymbol{i}}_{t,r_D} = (i_1, i_2)$*. Then, we have two data points* $\left(t^2, \beta^2(i_2)\right)$ *and* $\left(t^1, \beta^1(i_1)\right)$ *for the drift resistance approximation function* $\alpha_{\hat{\boldsymbol{i}}_{t,r_D}}(\mathrm{fs})$*.*
In this example, let $\beta^2(i_2) > \beta^1(i_1)$*. This situation is depicted in Figure 5.1, where the two data point are marked by dots. The black line is the corresponding drift resistance approximation function* $\alpha_{\hat{\boldsymbol{i}}_{t,r_D}}(\mathrm{fs})$*, which is a linear interpolation of these data points combined with a constant extrapolation. The drift resistance approximations at the start fan speeds are marked by rings. The start fan speed of ADA pair* 2*,* s^2*, lies in the middle between the two test fan speeds, i.e, we have* $s^2 = \frac{1}{2}(t^1 + t^2)$*, in this example. Therefore, ADA pair* 2 *has the weight* $w^2 = \frac{1}{2}$ *(Definition 5.12) and we have* $\alpha_{\hat{\boldsymbol{i}}_{t,r_D}}(s^2) = \frac{1}{2}\beta^2(i_2) + \frac{1}{2}\beta^1(i_1)$ *(Lemma 5.14). Because of* $\beta^2(i_2) \neq \beta^1(i_1)$*, we have* $\alpha_{\hat{\boldsymbol{i}}_{t,r_D}}(s^2) \neq \beta^2(i_2)$*.*
In contrast, the drift resistance approximation at the start fan speed of pair 1 *is identical to the drift resistance approximation at the pair's test fan speed, because the drift resistance approximation function is extrapolated as a constant function beyond the data point* $\left(t^1, \beta^1(i_1)\right)$*. Therefore,* $\alpha_{\hat{\boldsymbol{i}}_{t,r_D}}(s^1) = \alpha_{\hat{\boldsymbol{i}}_{t,r_D}}(t^1) = \beta^1(i_1)$ *holds, which is in accordance with Lemma 5.14.*
This demonstrates the big difference between the cases $N = 1$ *and* $N \geq 2$*. In the case*

$N = 1$, we only have one data point and thus the drift resistance approximation function $\alpha_{\hat{\boldsymbol{i}}_{t,r_D}}(\mathrm{fs})$ is constant and we always have $\alpha_{\hat{\boldsymbol{i}}_{t,r_D}}(s^1) = \beta^1(i_1)$. In the case $N \geq 2$, we have $\alpha_{\hat{\boldsymbol{i}}_{t,r_D}}(s^p) \neq \beta^p(i_p)$ for $p \geq 2$ in general.

The weighted sum in Lemma 5.14 plays a central role. We thus introduce the following notation.

Definition 5.17 *Let $p \in \{2, \ldots, N\}$, let w^p be according to Definition 5.12 and let $x, y \in \mathbb{R}$. We define*

$$\omega^p(x, y) := w^p x + (1 - w^p) y.$$

(Memory aid: ω stands for '(w)eighted sum'.)

Definition 5.17 gives us a concise expression for the drift resistance approximations at the start fan speeds.

Corollary 5.18 *Let $\hat{\boldsymbol{i}}_{t,r_D} = (i_1, \ldots, i_N)$ be a given vector of drifted test ioni current approximations. We have*

$$\alpha_{\hat{\boldsymbol{i}}_{t,r_D}}(s^p) = \begin{cases} \beta^1(i_1) & \text{if } p = 1, \\ \omega^p\big(\beta^p(i_p), \beta^{p-1}(i_{p-1})\big) & \text{if } p \geq 2. \end{cases}$$

Proof. The statement follows from Lemma 5.14 and Definition 5.17. □

A major conclusions from Corollary 5.18 is that in the case $p = 1$ the approximated drift resistance at the start fan speed $s^p = s^1$ depends only on i_1. In the case $p \geq 2$, the approximated drift resistance at the start fan speed s^p depends on i_p and on i_{p-1}. This is also the reason, why the ADA procedure with a single ADA pair is less complicated than the ADA procedure with a plurality of ADA pairs. In the case of a single ADA pair, i.e., in the case $N = 1$, the drift resistance approximation function is constant with $\alpha_{\hat{\boldsymbol{i}}_{t,r_D}}(\mathrm{fs}) = \beta^1(i_1)$ for all $\mathrm{fs} \in \mathrm{FS}$. In contrast, in the case $N \geq 2$, the drift resistance at the start fan speed of the p-th ADA pair is also influenced by its upper neighbor $p - 1$ for all $p \geq 2$. Accordingly, the cases $N = 1$ and $N \geq 2$ are dealt with separately. The case $N = 1$ is detailed in Chapter 6 and the case $N \geq 2$ is detailed in Chapter 7.
But first, we formulate the ADA procedure as an algorithm. In doing so, we must ensure that the corresponding function evaluations are well-defined. We specify suitable domains for this.

5.1.2. Set of Feasible Drift Resistance Approximations

In this subsection, we specify a domain such that the successive execution of steps (A2) to (A4) is well-defined. Definition 5.19 of the set $\hat{R}^p_{r_D}$ below is motivated by the following two considerations.

- Because $\iota_{s^p,r_D} : G_{s^p} \to I_{s^p,r_D}$ is a homeomorphism (Lemma 3.16), step (A3) is well-defined if and only if $i_{s,\hat{r}_D} \in I_{s^p,r_D} = \iota_{s^p,r_D}(G_{s^p})$ if and only if $\hat{g} := \iota^{-1}_{s^p,r_D}(i_{s,\hat{r}_D}) \in G_{s^p}$.

- Because G_{t^p} is the domain of ι_{t^p,r_D} (Definition 3.12), the function evaluation $\iota_{t^p,r_D}(\hat{g})$ in step (A4) is well-defined if and only if $\hat{g} \in G_{t^p}$.

Definition 5.19 *Let $p \in [N]$ and let (s^p, t^p, i_s^p, i_t^p) be the p-th ADA pair. Furthermore, let $r_D \in \mathbb{R}_{\geq 0}$ be a drift resistance and let $\mathcal{H} = \big(\mathsf{FS}, (G_{\mathsf{fs}})_{\mathsf{fs}\in\mathsf{FS}}, (\iota_{\mathsf{fs}})_{\mathsf{fs}\in\mathsf{FS}}, (\Lambda_{\mathsf{fs}})_{\mathsf{fs}\in\mathsf{FS}}, (\zeta_{\mathsf{fs}})_{\mathsf{fs}\in\mathsf{FS}}\big)$ be an HE model. The* set of feasible drift resistance approximations of ADA pair p with respect to r_D and $\mathcal{H}$ *is defined by*

$$\hat{R}^p_{r_D} := \frac{U}{\iota_{s^p,r_D}(G_{s^p} \cap G_{t^p})} - r_s^p := \left\{ r \in \mathbb{R} : \ \exists\ g \in G_{s^p} \cap G_{t^p} \ \text{s.t.}\ r = \frac{U}{\iota_{s^p,r_D}(g)} - r_s^p \right\}.$$

Lemma 5.20 *The set $\hat{R}^p_{r_D}$ is well-defined.*

Proof. According to Definition 3.12, all images of ι_{s^p,r_D} are greater than zero and thus $\hat{R}^p_{r_D}$ is well-defined. □

Remark 5.21 *When there is no risk of confusion, the HE model $\mathcal{H}$ and the drift resistance $r_D \geq 0$ related to $\hat{R}^p_{r_D}$ are not explicitly stated for the remainder of this thesis. I.e., if not otherwise stated, we implicitly assume that an HE model $\mathcal{H}$ and a drift resistance $r_D \geq 0$ are given.*

With the set $\hat{R}^p_{r_D}$ as a domain, we can now specify a function that corresponds to the step (A2).

Definition 5.22 *Let (s^p, t^p, i_s^p, i_t^p) be the p-th ADA pair and let $\hat{R}^p_{r_D}$ be the set of feasible drift resistance approximations of ADA pair p, $p \in [N]$. We define*

$$\gamma^p : \hat{R}^p_{r_D} \to \iota_{s^p,r_D}\big(G_{s^p} \cap G_{t^p}\big), \quad \gamma^p(r) := i_s^p \frac{U}{i_s^p \cdot r + U}. \tag{5.3}$$

Lemma 5.23 *The function γ^p is well-defined, continuous, bijective and strictly decreasing.*

Proof. By Definition 5.19, we have

$$\begin{aligned} r \in \hat{R}^p_{r_D} \ &\Rightarrow\ \exists\ g \in G_{s^p} \cap G_{t^p} : r = \frac{U}{\iota_{s^p,r_D}(g)} - r_s^p = \frac{U}{\iota_{s^p,r_D}(g)} - \frac{U}{i_s^p} \\ &\Rightarrow\ \exists\ g \in G_{s^p} \cap G_{t^p} : i_s^p r + U = \frac{i_s^p U}{\iota_{s^p,r_D}(g)} \\ &\Rightarrow\ \exists\ g \in G_{s^p} \cap G_{t^p} : \iota_{s^p,r_D}(g) = \frac{i_s^p U}{i_s^p r + U} = \gamma^p(r). \end{aligned}$$

Therefore, $\gamma^p(r)$ exists and $\gamma^p(r) \in \iota_{s^p,r_D}\big(G_{s^p} \cap G_{t^p}\big)$ holds, i.e., γ^p is well-defined.
As a composition of continuous operations, γ^p is also continuous.
Injectivity: Let $r_1, r_2 \in \hat{R}^p_{r_D}$ such that $\gamma^p(r_1) = \gamma^p(r_2)$. Then, we have

$$\gamma^p(r_1) = \gamma^p(r_2) \ \Rightarrow\ \gamma^p(r_1) := i_s^p \frac{U}{i_s^p \cdot r_1 + U} = \gamma^p(r_2) := i_s^p \frac{U}{i_s^p \cdot r_2 + U} \ \Rightarrow\ r_1 = r_2.$$

Surjectivity: Let $i \in \iota_{s^p,r_D}(G_{s^p} \cap G_{t^p})$. We define $r := \frac{U}{i} - r_s^p$. Then, $r \in \hat{R}_{r_D}^p$ holds and we have

$$\gamma^p(r) = i_s^p \frac{U}{i_s^p\left(\frac{U}{i} - \frac{U}{i_s^p}\right) - U} = \frac{i_s^p U}{\frac{i_s^p U}{i}} = i.$$

Finally, let $r_1, r_2 \in \hat{R}_{r_D}^p$ such that $r_1 < r_2$. Because $\gamma^p(r) = i_s^p \frac{U}{i_s^p \cdot r + U} \in \iota_{s^p,r_D}(G_{s^p}) \subset \mathbb{R}_{>0}$ as well as $U > 0$ and $i_s^p > 0$, we have $i_s^p r + U > 0$ for all $r \in \hat{R}_{r_D}^p$. Therefore,

$$r_1 < r_2 \;\Rightarrow\; 0 < i_s^p r_1 + U < i_s^p r_2 + U \;\Rightarrow\; \frac{i_s^p U}{i_s^p r_2 + U} < \frac{i_s^p U}{i_s^p r_1 + U} \;\Rightarrow\; \gamma^p(r_2) < \gamma^p(r_1)$$

and thus γ^p is strictly decreasing. □

Corollary 5.24 *The successive execution of steps* (A2) *to* (A4) *with ADA pair p, $p \in [N]$, is well-defined if and only if $\hat{r}_D \in \hat{R}_{r_D}^p$, i.e.,*

$$\iota_{t^p,r_D} \circ \iota_{s^p,r_D}^{-1}\left(\frac{U i_s^p}{\hat{r}_D i_s^p + U}\right) = \iota_{t^p,r_D} \circ \iota_{s^p,r_D}^{-1} \circ \gamma^p(\hat{r}_D) \text{ is well-defined } \Leftrightarrow\; \hat{r}_D \in \hat{R}_{r_D}^p.$$

With this, we have all the parts together to formulate the ADA algorithm in the following section.

5.2. The ADA Algorithm

We first formulate an algorithm for a single ADA iteration, i.e., an algorithm that corresponds to steps (A1) to (A4). Based on this algorithm, we then present the full ADA Algorithm 5.2 that corresponds to a sequence of ADA iterations with a plurality of ADA pairs.

5.2.1. Algorithm for a Single ADA Iteration with ADA Pair *p*

An ADA iteration with ADA pair p is composed of the steps (A1) to (A4) presented at the beginning of Section 5.1. Corollary 5.18 reformulates step (A1) such that it is expressed as a function of the incumbent drifted test ioni current approximations. Steps (A2) to (A4) are covered by Corollary 5.24. The following Algorithm 5.1 combines the statements of both corollaries.

Remark 5.25 *If the drift resistance approximation determined in Line 7 or 9 in Algorithm 5.1 is such that the subsequent calculations are not well-defined, then the output is $i_j = \mathrm{NaN}$ for all $j \in [N]$. This indicates that the ADA iteration could not be carried out successfully, see also Remark 5.33 below.*

Lemma 5.26 *Let $p \in [N]$ and let $\hat{\boldsymbol{i}}_{\boldsymbol{t},\mathrm{in}} = (i_1, \ldots, i_N) \in \mathbb{R}_{>0}^N$ be a given vector of drifted test ioni current approximations. The execution of Algorithm 5.1 corresponds to an ADA iteration of ADA pair p according to Definition 3.30 and Remark 3.42. Furthermore, all calculations in Algorithm 5.1 are well-defined.*

Algorithm 5.1 ADA Update of the p-th Entry of the Vector $\hat{\boldsymbol{i}}_{t,r_D}$

Input:

$\mathcal{H} = \left(\mathsf{FS}, (G_{\mathsf{fs}})_{\mathsf{fs}\in\mathsf{FS}}, (\iota_{\mathsf{fs}})_{\mathsf{fs}\in\mathsf{FS}}, (\Lambda_{\mathsf{fs}})_{\mathsf{fs}\in\mathsf{FS}}, (\zeta_{\mathsf{fs}})_{\mathsf{fs}\in\mathsf{FS}}\right)$ // *HE model*

(s^j, t^j, i_s^j, i_t^j), $j \in [N]$ // *ADA parameters of N ADA pairs*

$r_D \in \mathbb{R}_{\geq 0}$ // *drift resistance*

$\hat{\boldsymbol{i}}_{t,r_D} = (i_1, \ldots, i_N) \subset \mathbb{R}_{>0}^N$ // *incumbent drifted test ioni current approximations*

$p \in [N]$ // *selected ADA pair for update*

Calculations:

if $p = 1$ **then**

  $\hat{r}_D = \beta^1(i_1)$ // *drift resistance approximation at* s^1

else if $p \geq 2$ **then**

  $\hat{r}_D = \omega^p\left(\beta^p(i_p), \beta^{p-1}(i_{p-1})\right)$ // *drift resistance approximation at* s^p, $p \geq 2$

end if

if $\hat{r}_D \in \hat{R}_{r_D}^p$ **then**

  $i_p \leftarrow \iota_{t^p,r_D} \circ \iota_{s^p,r_D}^{-1} \circ \gamma^p(\hat{r}_D)$

else

  $i_j \leftarrow \mathrm{NaN}\ \ \forall\, j \in [N]$ // *mark results as not valid*

end if

Output:

$\hat{\boldsymbol{i}}_{t,r_D} = (i_1, \ldots, i_N)$ // *updated drifted test ioni current approximations*

Proof. The statement follows from Definition 3.30, Remark 3.42 as well as from Corollaries 5.18 and 5.24. □

Example 5.27 *In Example 3.22 above, the notion of the ADA procedure is demonstrated. The calculations carried out there correspond to execute Algorithm 5.1 with a single ADA pair, i.e., for the case $N = 1$, and thus with $p = 1$. The undrifted test ioni current i_t is used as the incumbent drifted test ioni current approximation, i.e., $\hat{\boldsymbol{i}}_{t,r_D} = (i_t)$. Note that the superscript p and the subscript p are not used in Example 3.22, because only a single ADA pair is considered there. All in all, the ADA iteration demonstrated in Example 3.22 corresponds to the update $i \leftarrow \iota_{t,r_D} \circ \iota_{s,r_D}^{-1} \circ \gamma \circ \beta(i)$ with $i = i_t$.*

Algorithm 5.1 is not yet the full ADA algorithm, because usually sequences of ADA iterations are used to approximate the drifted test ioni currents, see also Section 3.3. The full ADA algorithm is presented below.

5.2.2. Full ADA Algorithm with a Sequence of ADA Iterations

Algorithm 5.1 states how to perform a single ADA update of the p-th entry of the vector $\hat{\boldsymbol{i}}_{t,r_D}$. But it does not contain any instructions on which ADA pair p shall be selected for the next update or on how many updates of the p-th entry shall be performed. Therefore, we delineate an algorithm that provides a framework for a sequence of ADA updates, i.e.,

we delineate a coordination algorithm that is wrapped around Algorithm 5.1. This requires the term ADA update sequence.

Definition 5.28 *Let $\ell \in \mathbb{N}$ and let $[\ell] := \{1, \dots, \ell\}$. A sequence $(u_k)_{k\in[\ell]}$ with $u_k \in [N]$ for all $k \in [\ell]$ is called an* ADA update sequence of length ℓ.

Example 5.29 *Let $N = 3$ and let $\ell = 6$. Then $(u_k^1)_{k\in[\ell]} := (1, 2, 3, 1, 2, 3)$ and $(u_k^2)_{k\in[\ell]} := (1, 1, 2, 2, 3, 3)$ are both ADA update sequences of length ℓ.*

Remark 5.30 *Infinite ADA update sequences are also possible. For instance, $(u_k = 1)_{k\in\mathbb{N}}$ is the infinite ADA update sequence whose entries are all one.*

Remark 5.31 *If there is no risk of confusion, an ADA update sequence $(u_k)_{k\in K}$ is abbreviated and denoted by u in the following.*

Let us suppose that an ADA update sequence $u = (u_k)_{k\in[\ell]}$ of length ℓ is given. Then, the k-th entry of u, denoted by u_k, corresponds to the ADA pair that is selected for the ADA update with Algorithm 5.1 in the k-th iteration. A corresponding framework is provided by Algorithm 5.2.

Algorithm 5.2 ADA Update for a given ADA Update Sequence u

Input:

$\mathcal{H} = \big(\mathrm{FS}, (G_{\mathrm{fs}})_{\mathrm{fs}\in\mathrm{FS}}, (\iota_{\mathrm{fs}})_{\mathrm{fs}\in\mathrm{FS}}, (\Lambda_{\mathrm{fs}})_{\mathrm{fs}\in\mathrm{FS}}, (\zeta_{\mathrm{fs}})_{\mathrm{fs}\in\mathrm{FS}}\big)$ // *HE model*

(s^j, t^j, i_s^j, i_t^j), $j \in [N]$ // *ADA parameters of N ADA pairs*

$r_D \in \mathbb{R}_{\geq 0}$ // *drift resistance*

$\hat{\boldsymbol{i}}_{t,\mathrm{in}} = (i_1, \dots, i_N) \in \mathbb{R}_{>0}^N$ // *initial drifted test ioni current approximations*

$(u_k)_{k\in[\ell]}$ // *ADA update sequence of length ℓ*

Calculations:

for $k = 1$ to ℓ **do**

  $p = u_k$

  if $p = 1$ and $\beta^1(i_1) \in \hat{R}_{r_D}^1$ **then**

    $i_1 \leftarrow \iota_{t^1,r_D} \circ \iota_{s^1,r_D}^{-1} \circ \gamma^1 \circ \beta^1(i_1)$ // *Algorithm 5.1 with $p = 1$*

  else if $p \geq 2$ and $\omega^p\big(\beta^p(i_p), \beta^{p-1}(i_{p-1})\big) \in \hat{R}_{r_D}^p$ **then**

    $i_p \leftarrow \iota_{t^p,r_D} \circ \iota_{s^p,r_D}^{-1} \circ \gamma^p \circ \omega^p\big(\beta^p(i_p), \beta^{p-1}(i_{p-1})\big)$ // *Algorithm 5.1 with $p \geq 2$*

  else

    $i_j \leftarrow \mathrm{NaN}$ for all $j \in [N]$ // *mark results as not valid*

    break // *leave for-loop early*

  end if

end for

Output:

$\hat{\boldsymbol{i}}_{t,\mathrm{out}} = (i_1, \dots, i_N)$ // *updated drifted test ioni current approximations*

Lemma 5.32 *All function evaluations in Algorithm 5.2 are well-defined. Furthermore, if it is executed with $u = (p)$ (the ADA update sequence of length one with the entry p), $p \in [N]$, then its output vector is identical to that of Algorithm 5.1.*

Proof. The statements follow from Lemma 5.26 and by construction. □

Remark 5.33 *If an incumbent approximation i_p is such that the subsequent calculations are not well-defined, then the for-loop is left early and $i_j = \mathrm{NaN}$ is returned for all $j \in [N]$. This indicates that the ADA iterations could not be carried out successfully. From a practical point of view, if a calculation in Algorithm 5.2 is not well-defined, then combustion limits are exceeded during the corresponding ADA iteration.*
In practice, if the ADA procedure could not be successfully carried out for a larger period of time and an oxide layer accrues on the ioni electrode without being corrected, the so-called ADA supervision function will eventually lock the appliance [WHB, Items 4228 and 24108].

Remark 5.34 *A common vector of initial approximations is $\hat{\boldsymbol{i}}_{\boldsymbol{t},\mathrm{in}} = (i_t^1, \ldots, i_t^N)$, i.e., the undrifted test ioni currents are usually the initial approximations of the drifted test ioni currents, see also Remark 3.31. However, the vector $\hat{\boldsymbol{i}}_{\boldsymbol{t},\mathrm{in}}$ is not restricted to these values. A typical situation with a different initial vector is if approximations of the drifted test ioni currents are already available.*

Remark 5.35 *As stated in Section 3.4.5, the selection of an ADA update sequence is done automatically by the IoniDetect system. Therefore, we have no influence on the ADA update sequence and the selection of when to update which ADA pair is not in the scope of this study. Instead, we suppose that the ADA update sequences follow certain random distributions. This is detailed in Section 7.3.*

For the optimization of the ADA parameters we are interested in the convergence characteristics of Algorithm 5.2. In particular, we are interested in the conditions under which Algorithm 5.2 converges to a limit (if certain infinite ADA update sequences are considered) and, if this is the case, what the rate of convergence is and whether the limit corresponds to the sought drifted test ioni currents. These questions are addressed in the following chapters. For this, we are interested in how the output of Algorithm 5.2 changes if its inputs change. In particular, we are interested in $\hat{\boldsymbol{i}}_{\boldsymbol{t},\mathrm{out}}$ as a function of the starting vector $\hat{\boldsymbol{i}}_{\boldsymbol{t},\mathrm{in}}$ and the ADA update sequence u. Therefore, if not otherwise stated, we always implicitly assume that a certain HE model $\mathcal{H}$, a drift resistance $r_D \geq 0$ and N ADA pairs (s^j, t^j, i_s^j, i_t^j), $j \in [N]$, are given in the following.

Definition 5.36 *Let $\mathcal{H}$, $r_D \geq 0$, and (s^j, t^j, i_s^j, i_t^j), $j \in [N]$, be given and fixed. Let $\hat{\boldsymbol{i}}_{\boldsymbol{t},\mathrm{in}}$ be an input vector, i.e., a vector with initial drifted test ioni current approximations, and let $u = (u_k)_{k \in [\ell]}$ be an ADA update sequence whose entries u_k are an element of $[N]$ for all $k \in [\ell]$. The corresponding output of Algorithm 5.2 is denoted by $\hat{\boldsymbol{i}}_{\boldsymbol{t},\mathrm{out}}(\hat{\boldsymbol{i}}_{\boldsymbol{t},\mathrm{in}}, u)$.*

In the following, we consider the cases $N = 1$ and $N \geq 2$ separately. This is done for two reasons. First, in the case $N = 1$, there is no choice to be made what ADA pair

shall be updated next, i.e., we consider only ADA update sequences whose entries are all one. Second, by comparing Line 9 of Algorithm 5.2 with Line 11, it is apparent that the resulting iteration function is less complicated in the case $N = 1$. However, some convergence results can be transferred from the case $N = 1$ to the case $N \geq 2$.

6. ADA Procedure with a Single ADA Pair

In this chapter, we analyze the ADA Algorithm 5.2 for the special case $N = 1$, i.e., we consider a single ADA pair only. A plurality of ADA pairs is considered in Chapter 7. We present an algorithm that corresponds to Algorithm 5.2 in the case $N = 1$ first. Thereafter, the convergence properties of this algorithm are analyzed.

6.1. Ioni Current Based ADA Algorithm with a Single ADA Pair

In the case $N = 1$, there is no choice with respect to what pair is selected for the next ADA update, i.e., we consider only ADA update sequences whose entries are all one. Therefore, Line 9 is executed in each iteration of the for-loop of Algorithm 5.2 (if $\beta^1(i_1) \in \hat{R}^1_{r_D}$ holds). The composite function in Line 9 of Algorithm 5.2 is essential and thus it is considered in detail.

6.1.1. Ioni Current Based ADA Iteration Function

Before we define a function that corresponds to Line 9 of Algorithm 5.2, we specify a suitable domain. Line 9 is executed if $\beta^1(i_1) \in \hat{R}^1_{r_D}$, which motivates the following approach.

Remark 6.1 *The following motivations and statements are made for the more general case that an ADA pair (s^p, t^p, i_s^p, i_t^p), $p \in [N]$, is considered, i.e., we do not restrict the considerations to the ADA pair $p = 1$. This is done, because the following definitions are also essential when a plurality of ADA pairs is considered in Chapter 7.*

Since β^p is a homeomorphism (Lemma 5.11), $\left(\beta^p\right)^{-1}\left(\hat{R}^p_{r_D}\right)$ is a candidate for the sought domain. However, we have to make an assumption to ensure that $\hat{R}^p_{r_D}$ is a subset of the domain of $\left(\beta^p\right)^{-1}$, i.e., we have to make sure that $\hat{R}^p_{r_D} \subset (-r_t^p, \infty)$ holds.

Assumption 6.2 *We assume that for all $p \in [N]$ and for all $i \in I_{s^p,r_D} = \iota_{s^p,r_D}(G_{s^p})$ the inequality $\frac{U}{i} > r_s^p - r_t^p$ holds. Practical experience has shown that*

- *$1.5M\Omega > r_s^p > r_t^p > 0.9M\Omega$ and thus $0.6M\Omega > r_s^p - r_t^p > 0$ as well as*
- *$\frac{U}{\iota_{s^p,r_D}(g)} > 0.8M\Omega$ for all $g \in G_{s^p}$ and for all considered drift resistances.*

Thus, the assumption $\frac{U}{\iota_{s^p,r_D}(g)} > r_s^p - r_t^p$ for all $g \in G_{s^p}$ is reasonable from a practical point of view.

Definition 6.3 *Let $p \in [N]$ and let Assumption 6.2 hold. By considering $\hat{R}^p_{r_D}$ from Definition 5.19, we define*

$$\hat{I}^p_{r_D} := \left(\beta^p\right)^{-1}(\hat{R}^p_{r_D}).$$

Lemma 6.4 *If Assumption 6.2 holds, then $\hat{I}^p_{r_D}$ is well-defined. In particular, $\hat{I}^p_{r_D} \subset \mathbb{R}_{>0}$ and $\hat{R}^p_{r_D} \subset (-r^p_t, \infty)$ hold in this case.*

Proof. Let $p \in [N]$ and let Assumption 6.2 hold. We show that $\hat{R}^p_{r_D} \subset (-r^p_t, \infty)$ holds. Because $(-r^p_t, \infty)$ is the domain of $\left(\beta^p\right)^{-1}$ (Definition 5.9), $\left(\beta^p\right)^{-1}(\hat{R}^p_{r_D})$ is well-defined in this case. Let $r \in \hat{R}^p_{r_D}$. Then, there exists $g \in G_{s^p} \cap G_{t^p} \subset G_{s^p}$ such that $r = \frac{U}{i} - r^p_s$ with $i = \iota_{s^p, r_D}(g)$. According to Assumption 6.2, $\frac{U}{i} > r^p_s - r^p_t$ holds and thus we have

$$r = \frac{U}{i} - r^p_s >= r^p_s - r^p_t - r^p_s = -r^p_t \;\Rightarrow\; r \in (-r^p_t, \infty) \;\Rightarrow\; \left(\beta^p\right)^{-1}(r) \text{ is defined.}$$

Because the codomain of $\left(\beta^p\right)^{-1}$ is the set of positive real numbers, $\hat{I}^p_{r_D} := \left(\beta^p\right)^{-1}(\hat{R}^p_{r_D}) \subset \mathbb{R}_{>0}$ holds. □

Next, we define the iteration function that corresponds to Line 9 of Algorithm 5.2.

Definition 6.5 *Let $\mathcal{H}$ be an HE model, let $r_D \geq 0$ be a drift resistance and let (s^p, t^p, i^p_s, i^p_t) be a given ADA pair. We define the corresponding* ioni current based ADA iteration function *by*

$$A^p_{i,r_D} : \hat{I}^p_{r_D} \to \mathbb{R}_{>0},\; A^p_{i,r_D}(i) := \iota_{t^p, r_D} \circ \iota^{-1}_{s^p, r_D} \circ \gamma^p \circ \beta^p(i). \tag{6.1}$$

Remark 6.6 *The subscript i of A^p_{i,r_D} indicates that this is the ioni current based ADA iteration function. This is done to distinguish it from the resistance based version that is presented in Section 6.2.*

Remark 6.7 *According to* (3.4)*, the functions ι_{t^p, r_D} and ι_{s^p, r_D} depend on the drift resistance r_D. Therefore, the iteration function A^p_{i,r_D} also depends on the drift resistance. If we have two different drift resistances $r_{D,1} \neq r_{D,2}$, then we have $A^p_{i,r_{D,1}} \neq A^p_{i,r_{D,2}}$ in general.*

Lemma 6.8 *The ioni current based ADA iteration function A^p_{i,r_D} is well-defined, i.e., the function A^p_{i,r_D} can be evaluated for all $i \in \hat{I}^p_{r_D}$. Furthermore, $A^p_{i,r_D}(i) > 0$ holds for all $i \in \hat{I}^p_{r_D}$.*

Proof. Let $i \in \hat{I}^p_{r_D}$. According to Definition 6.3, we have $\beta^p(i) \in \hat{R}^p_{r_D}$. With this, the statement follows by applying Corollary 5.24 and from Definition 6.5. □

The ioni current based ADA iteration function A^p_{i,r_D} is used to formulate an algorithm that is a special case of Algorithm 5.2 for the case $N = 1$.

Algorithm 6.1 Ioni Current Based ADA Algorithm in the Case $N = 1$

Input:
- $\mathcal{H}$ // *HE model*
- (s, t, i_s, i_t) // *ADA parameters of a single ADA pair*
- $r_D \geq 0$ // *drift resistance*
- $\ell \in \mathbb{N}$ // *length of ADA update sequence, i.e., number of iterations*
- $i \in \hat{I}_{r_D}$ // *initial approximation of the drifted test ioni current*

Calculations:
- $k = 1$
- **while** $k \leq \ell$ **and** $i \in \hat{I}_{r_D}$ **do**
  - $i \leftarrow A_{i,r_D}(i)$
  - $k \leftarrow k + 1$
- **end while**
- **if** $i \notin \hat{I}_{r_D}$ **then**
  - $i \leftarrow \mathrm{NaN}$ // *no valid output*
- **end if**

Output:
- i // *approximation of the drifted test ioni current* i_{t,r_D}

6.1.2. Ioni Current Based ADA Algorithm

Since we consider a single ADA pair only, we omit the superscript p in the following. Furthermore, we consider only ADA update sequences whose entries are all one. Thus, only their length ℓ is of interest. Keeping this in mind, we formulate Algorithm 6.1.

Remark 6.9 *The second condition in the header of the while-loop, $i \in \hat{I}_{r_D}$, together with Lemma 6.8, guarantees that the function evaluations in Algorithm 6.1 are always well-defined. This is required, because there might exist $i \in \hat{I}_{r_D}$ such that $A_{i,r_D}(i) \notin \hat{I}_{r_D}$, i.e., the ADA function A_{i,r_D} is not a selfmap in general and a consecutive evaluation of A_{i,r_D} is not always possible. The conditions under which A_{i,r_D} is a selfmap are closely related to the convergence characteristics of Algorithm 6.1. This is discussed in Section 6.2.2.*

Algorithm 6.1 is indeed a special case of Algorithm 5.2.

Lemma 6.10 *If Algorithm 6.1 and Algorithm 5.2 are executed with the same inputs, i.e., with the same $\mathcal{H}$, r_D, (s^1, t^1, i_s^1, i_t^1), $\hat{\boldsymbol{i}}_{\boldsymbol{t},\mathrm{in}} = (i)$ and $u = (u_k)_{k\in[\ell]}$, $u_k = 1$ for all $k \in [\ell]$, then their outputs are identical.*

Proof. The statement follows from Definition 6.3 of $\hat{I}_{r_D}$ as well as from Definition 6.5 of A_{i,r_D} and from the construction of Algorithm 6.1. □

It is apparent that Algorithm 6.1 implements a fixed point iteration. It corresponds to the first ℓ iterations of the Picard iteration associated to A_{i,r_D} starting at i. The Picard iteration is introduced in Section 4.3. Analyzing the convergence properties and

approximation quality of Algorithm 6.1 means analyzing the fixed point characteristics of A_{i,r_D}. For this, we consider the domain of A_{i,r_D} first.

Lemma 6.11 *The sets $\hat{I}_{r_D}$ and $\hat{R}_{r_D}$ are closed, bounded and nonempty intervals. In particular, they are compact.*

Proof. We have $\hat{R}_{r_D} = \frac{U}{\iota_{s,r_D}(G_s \cap G_t)} - r_s$ (Definition 5.19). The sets G_s and G_t are closed and bounded intervals (Definition 2.18) and thus $G_s \cap G_t$ is also a closed and bounded interval. Because we consider only feasible ADA pairs (Assumption 5.6), the intersection $G_s \cap G_t$ is nonempty (Definition 5.2). Furthermore, the function ι_{s,r_D} is continuous (Definition 2.18). In total, $\hat{R}_{r_D}$ is the image of a closed, bounded and nonempty interval under a continuous function. Thus, $\hat{R}_{r_D}$ is a closed, bounded and nonempty interval as well.
According to Lemma 5.11, the function $\beta : \hat{I}_{r_D} \to \hat{R}_{r_D}$ is a homeomorphism. Therefore, $\hat{I}_{r_D} = (\beta)^{-1}(\hat{R}_{r_D})$ is also a closed, bounded and nonempty interval.
Finally, because both sets are bounded and closed, they are compact. □

By applying Banach's fixed point theorem, we can state the following convergence properties.

Lemma 6.12 *Let A_{i,r_D} be a contractive selfmap on $\hat{I}_{r_D}$. Then, A_{i,r_D} has a unique fixed point and the Picard iteration associated to A_{i,r_D} starting at i converges to this fixed point for every $i \in \hat{I}_{r_D}$.*

Proof. Because the set $\hat{I}_{r_D}$ is compact (Lemma 6.11), we can apply Theorem 4.41. □

Remark 6.13 *Note that A_{i,r_D} being contractive is not a necessary condition for the statement of Lemma 6.12. In Appendix A, Example A.1 presents an iteration function A_{i,r_D} that is not contractive but that still has a unique fixed point and for all $i \in \hat{I}_{r_D}$ the Picard iteration associated to A_{i,r_D} starting at i converges to this fixed point.*

As a consequence of Lemma 6.12, we are particularly interested in when A_{i,r_D} is a contractive selfmap. According to Definition 6.5, the function A_{i,r_D} is composed of ι_{s,r_D}^{-1} and ι_{t,r_D}, among others. The functions ι_{s,r_D} and ι_{t,r_D} are the drifted versions of ι_s and ι_t, respectively. According to (3.4), the drifted functions $\iota_{\mathrm{fs},r_D}(g)$ can be considered as rational functions with $\iota_{\mathrm{fs}}(g)$ as the argument. This makes the convergence analysis rather complicated. By shifting the focus from ioni current to resistance, it is possible to express the iteration function by ι_t and ι_s^{-1} instead of ι_{t,r_D} and ι_{s,r_D}^{-1}, respectively, which facilitates the fixed point analysis. Therefore, the resistance based approach is first presented and afterwards analyzed in the following section.

6.2. Resistance Based Iteration Function with a Single ADA Pair

In this section, we derive an iteration function that is in a certain sense "equivalent" to the ioni current based iteration function A_{i,r_D} but that is more accessible to a convergence

analysis. From a physical point of view, this approach is motivated by applying Ohm's law to the equivalent circuit illustrated in Section 3.1.1. Instead of considering ioni currents i, we consider corresponding resistances r by calculating $r = \frac{U}{i}$, where U is the DC voltage of the aforementioned equivalent circuit, see also Remark 3.3. For this, we define corresponding sets of resistances and resistance functions.

Definition 6.14 *Let* $\mathcal{H} = \big(\mathsf{FS}, (G_{\mathsf{fs}})_{\mathsf{fs}\in\mathsf{FS}}, (\iota_{\mathsf{fs}})_{\mathsf{fs}\in\mathsf{FS}}, (\Lambda_{\mathsf{fs}})_{\mathsf{fs}\in\mathsf{FS}}, (\zeta_{\mathsf{fs}})_{\mathsf{fs}\in\mathsf{FS}}\big)$ *be an HE model and let* $r_D \geq 0$. *For* $\mathsf{fs} \in \mathsf{FS}$ *let* I_{fs} *be the sets of ioni currents according to Definition 2.22 and let* I_{fs,r_D} *be the set of drifted ioni currents according to Notation 3.17. For* $\mathsf{fs} \in \mathsf{FS}$, *we define:*

- $R_{\mathsf{fs}} := \frac{U}{I_{\mathsf{fs}}} := \{r \in \mathbb{R} : \ \exists\, i \in I_{\mathsf{fs}} \text{ such that } r = \frac{U}{i}\}$ *(*set of resistances with respect to fs*),*
- *analogously* $R_{\mathsf{fs},r_D} := \frac{U}{I_{\mathsf{fs},r_D}}$ *(*set of drifted resistances with respect to fs*),*
- $\rho_{\mathsf{fs}} : G_{\mathsf{fs}} \to R_{\mathsf{fs}}$, $\rho_{\mathsf{fs}}(g) := \frac{U}{\iota_{\mathsf{fs}}(g)}$ *(*resistance function with respect to fs*) and*
- $\rho_{\mathsf{fs},r_D} : G_{\mathsf{fs}} \to R_{\mathsf{fs},r_D}$, $\rho_{\mathsf{fs},r_D}(g) := \frac{U}{\iota_{\mathsf{fs},r_D}(g)}$ *(*drifted resistance function with respect to fs*).*

Lemma 6.15 *The sets* R_{fs} *and* R_{fs,r_D} *as well as the resistance functions* ρ_{fs} *and* ρ_{fs,r_D} *are well-defined for all* $\mathsf{fs} \in \mathsf{FS}$.

Proof. Let $\mathsf{fs} \in \mathsf{FS}$. We have $I_{\mathsf{fs}} \subset \mathbb{R}_{>0}$ (Corollary 2.23) and $I_{\mathsf{fs},r_D} \subset \mathbb{R}_{>0}$ (Corollary 3.18). Thus, the sets R_{fs} and R_{fs,r_D} are well-defined. Furthermore, we have $\iota_{\mathsf{fs}} : G_{\mathsf{fs}} \to I_{\mathsf{fs}}$ (Definition 2.18) and $\iota_{\mathsf{fs},r_D} : G_{\mathsf{fs}} \to I_{\mathsf{fs},r_D}$ (Notation 3.17). Therefore, the functions ρ_{fs} and ρ_{fs,r_D} are well-defined by construction of the sets R_{fs} and R_{fs,r_D}. □

Remark 6.16 *Recall that the functions* ι_{fs} *and* ι_{fs,r_D} *correspond to the ioni current in the equivalent circuit depicted in Figure 3.1 without drift resistance and with drift resistance, respectively. The functions* ρ_{fs} *and* ρ_{fs,r_D} *correspond to the circuit's total resistance without drift resistance and with drift resistance, respectively.*

Lemma 6.17 *Let* $\mathsf{fs} \in \mathsf{FS}$. *The functions* ρ_{fs} *and* ρ_{fs,r_D} *are strictly decreasing homeomorphisms. Their inverse functions are*

$$\rho_{\mathsf{fs}}^{-1}(r) = \iota_{\mathsf{fs}}^{-1}\Big(\frac{U}{r}\Big) \quad \text{and} \quad \rho_{\mathsf{fs},r_D}^{-1}(r) = \iota_{\mathsf{fs},r_D}^{-1}\Big(\frac{U}{r}\Big).$$

Proof. Let $\mathsf{fs} \in \mathsf{FS}$. Recall that ι_{fs} and ι_{fs,r_D} are homeomorphisms (Lemmas 2.21 and 3.16, respectively). Therefore, ρ_{fs} and ρ_{fs,r_D} are a composition of bijective and continuous functions and thus they are bijective and continuous as well. To show the statement with respect to ρ_{fs}^{-1}, let $r \in R_{\mathsf{fs}}$. Then, we have $g := \rho_{\mathsf{fs}}^{-1}(r) \in G_{\mathsf{fs}}$ as well as $r = \rho_{\mathsf{fs}}(g)$ and thus

$$r = \rho_{\mathsf{fs}}(g) = \frac{u}{\iota_{\mathsf{fs}}(g)} \ \Rightarrow\ \iota_{\mathsf{fs},r_D}(g) = \frac{U}{r} \ \Rightarrow\ g = (\iota_{\mathsf{fs}})^{-1}\Big(\frac{U}{r}\Big) = (\rho_{\mathsf{fs}})^{-1}(r).$$

The statement $\rho_{\mathsf{fs},r_D}^{-1}(r) = \iota_{\mathsf{fs},r_D}^{-1}\left(\frac{U}{r}\right)$ is shown analogously.
Because ι_{fs}^{-1} and $\iota_{\mathsf{fs},r_D}^{-1}$ are continuous, the compositions $\rho_{\mathsf{fs}}^{-1}(r) = \iota_{\mathsf{fs}}^{-1}\left(\frac{U}{r}\right)$ and $\rho_{\mathsf{fs},r_D}^{-1}(r) = \iota_{\mathsf{fs},r_D}^{-1}\left(\frac{U}{r}\right)$ are also continuous.
It remains to show that ρ_{fs} and ρ_{fs,r_D} are strictly decreasing. Let $g_1, g_2 \in G_{\mathsf{fs}}$ such that $g_1 < g_2$. Because ι_{fs} is strictly increasing (Definition 2.18) and $U > 0$, we have

$$g_1 < g_2 \;\Rightarrow\; \iota_{\mathsf{fs}}(g_1) < \iota_{\mathsf{fs}}(g_2) \;\Rightarrow\; \rho_{\mathsf{fs}}(g_2) = \frac{U}{\iota_{\mathsf{fs}}(g_2)} < \frac{U}{\iota_{\mathsf{fs}}(g_1)} = \rho_{\mathsf{fs}}(g_1).$$

Analogously, ρ_{fs,r_D} is strictly decreasing because ι_{fs,r_D} is strictly increasing (Lemma 3.16).
□

In the following, we often add or subtract constants. It is convenient to have a corresponding auxiliary function.

Definition 6.18 *For $c \in \mathbb{R}$, we define*

$$\sigma_c^+ : \mathbb{R} \to \mathbb{R}, \quad \sigma_c^+(x) \coloneqq x + c,$$
$$\sigma_c^- : \mathbb{R} \to \mathbb{R}, \quad \sigma_c^-(x) \coloneqq x - c.$$

Lemma 6.19 *Let $c \in \mathbb{R}$. The functions σ_c^+ and σ_c^- are homeomorphisms. Their inverse functions are $\left(\sigma_c^+\right)^{-1} = \sigma_c^-$ and $\left(\sigma_c^-\right)^{-1} = \sigma_c^+$.*

Proof. Let $c \in \mathbb{R}$. The continuity of σ_c^+ and σ_c^- follows from the fact that sum is a continuous operation. Regarding the inverse functions, let $x \in \mathbb{R}$. Then, we have

$$\sigma_c^+ \circ \sigma_c^-(x) = (x - c) + c = x = (x + c) - c = \sigma_c^- \circ \sigma_c^+(x).$$

□

The function ρ_{fs} can be transformed to its drifted counterpart by simply adding r_D.

Lemma 6.20 *Let* $\mathsf{fs} \in \mathsf{FS}$ *and let $r_D \geq 0$, then*

$$\rho_{\mathsf{fs},r_D} = \sigma_{r_D}^+ \circ \rho_{\mathsf{fs}} \quad \textit{and} \quad \rho_{\mathsf{fs},r_D}^{-1} = \rho_{\mathsf{fs}}^{-1} \circ \sigma_{r_D}^-.$$

Proof. Let $g \in G_{\mathsf{fs}}$. By applying (3.4), we have

$$\rho_{\mathsf{fs},r_D}(g) = \frac{U}{\iota_{\mathsf{fs},r_D}(g)} = U\frac{r_D\iota_{\mathsf{fs}}(g) + U}{\iota_{\mathsf{fs}}(g)U} = r_D + \frac{U}{\iota_{\mathsf{fs}}(g)} = r_D + \rho_{\mathsf{fs}}(g) = \sigma_{r_D}^+ \circ \rho_{\mathsf{fs}}(g)$$

and thus

$$\mathrm{id}_{R_{\mathsf{fs}}} = \rho_{\mathsf{fs},r_D} \circ \rho_{\mathsf{fs},r_D}^{-1} = \sigma_{r_D}^+ \circ \rho_{\mathsf{fs}} \circ \rho_{\mathsf{fs},r_D}^{-1} \;\Leftrightarrow\; \sigma_{r_D}^- = \rho_{\mathsf{fs}} \circ \rho_{\mathsf{fs},r_D}^{-1} \;\Leftrightarrow\; \rho_{\mathsf{fs}}^{-1} \circ \sigma_{r_D}^- = \rho_{\mathsf{fs},r_D}^{-1}.$$

□

Lemma 6.20 reveals the advantage of considering the resistance functions. Then, the influence of drift is modeled by simply adding the drift resistance, which is in accordance with the corresponding assumption made in the ADA patent [LS17, p. 5], see also Section 3.1. In contrast, if ioni currents are considered, the influence of drift is modeled by (3.4), which is a rational function and thus more complicated to handle. This motivates considering the resistance based iteration function that is defined below.

6.2.1. Drift Resistance Iteration Function

Recall that the ioni current based iteration function A^p_{i,r_D} has approximations of the drifted test ioni current as inputs and outputs. The resistance based iteration function will be constructed such that it has approximations of the drift resistance as inputs and outputs. We define the iteration function first. Its physical interpretation is presented thereafter. For the following definition, recall that $r^p_s = \frac{U}{i^p_s}$ and $r^p_t = \frac{U}{i^p_t}$ (Definition 5.7).

Definition 6.21 *Let $\mathcal{H} = \big(\mathrm{FS}, (G_{\mathrm{fs}})_{\mathrm{fs}\in\mathrm{FS}}, (\iota_{\mathrm{fs}})_{\mathrm{fs}\in\mathrm{FS}}, (\Lambda_{\mathrm{fs}})_{\mathrm{fs}\in\mathrm{FS}}, (\zeta_{\mathrm{fs}})_{\mathrm{fs}\in\mathrm{FS}}\big)$ be an HE model, let $r_D \geq 0$ and let (s^p, t^p, i^p_s, i^p_t) be a feasible ADA pair with respect to $\mathcal{H}$. The corresponding* drift resistance iteration function *is defined by*

$$A^p_{r_D} : \hat{R}^p_{r_D} \to \mathbb{R}, \quad A^p_{r_D} := \sigma^-_{r^p_t} \circ \rho_{t^p,r_D} \circ \rho^{-1}_{s^p,r_D} \circ \sigma^+_{r^p_s}. \tag{6.2}$$

Lemma 6.22 *The function $A^p_{r_D}$ is well-defined, i.e., we can evaluate $A^p_{r_D}(r)$ for all $r \in \hat{R}^p_{r_D}$.*

Proof. Let $r \in \hat{R}^p_{r_D}$. According to Definition 5.19, there exists $g \in G_{s^p} \cap G_{t^p}$ such that $r = \frac{U}{\iota_{s^p,r_D}(g)} - r^p_s = \rho_{s^p,r_D}(g) - r^p_s$. This is equivalent to $r + r^p_s = \rho_{s^p,r_D}(g)$ and thus $g = \rho^{-1}_{s^p,r_D} \circ \sigma^+_{r^p_s}(r) \in G_{s^p} \cap G_{t^p}$. Because $g \in G_{t^p}$ and G_{t^p} is the domain of ρ_{t^p,r_D}, the evaluation $\rho_{t^p,r_D}(g) = \rho_{t^p,r_D} \circ \rho^{-1}_{s^p,r_D} \circ \sigma^+_{r^p_s}(r)$ is well-defined. Finally, subtracting the constant r^p_t from $\rho_{t^p,r_D}(g)$ is also well-defined. In total, the element $A^p_{r_D}(r)$ exists. □

The drift resistance iteration function $A^p_{r_D}$ is composed of four functions. This composition can be physically interpreted as follows. For this, let $\hat{r}_D \in \hat{R}^p_{r_D}$ be the incumbent drift resistance approximation.

1. $\sigma^+_{r^p_s}(\hat{r}_D)$: The drifted start resistance is $r^p_{s,r_D} := r^p_s + r_D$ according to Lemma 6.20. This value is approximated by $\hat{r}^p_{s,r_D} = r^p_s + \hat{r}_D$.

2. $\rho^{-1}_{s^p,r_D}(\hat{r}^p_{s,r_D})$: The fan speed is set to s^p and the gas valve is moved such that the measurement circuit's resistance stabilizes at $\hat{r}^p_{s,r_D}$, i.e., such that the measured ioni current is $\frac{U}{\hat{r}^p_{s,r_D}}$. Then, the gas valve position $\hat{g} \in G_{s^p}$ is determined, such that $\rho_{s^p,r_D}(\hat{g}) = \hat{r}^p_{s,r_D}$.

3. $\rho_{t^p,r_D}(\hat{g})$: The gas valve position is fixed at $\hat{g}$ and the fan speed is reduced from s^p to t^p. Then, the corresponding drifted resistance is measured. With this, the drifted test resistance is approximated, i.e., the drifted test resistance $r^p_{t,r_D} = r^p_t + r_D$ is approximated by $\hat{r}^p_{t,r_D} := \rho_{t^p,r_D}(\hat{g})$.

4. $\sigma^-_{r^p_t}(\hat{r}_{t^p,r_D})$: Because $\hat{r}^p_{t,r_D}$ is the approximation of $r^p_{t,r_D} = r^p_t + r_D$, we approximate r_D by $\hat{r}^p_{t,r_D} - r^p_t$, i.e., the new approximation of the drift resistance at the test fan speed is $\hat{r}_D \leftarrow \hat{r}_{t^p,r_D} - r^p_t$.

One iteration with the drift resistance iteration function $A^p_{r_D}$ is demonstrated in Example 6.26 below.
Our goal is to analyze the convergence properties of Algorithm 6.1 using $A^p_{r_D}$. For this, we first show how the iteration functions A^p_{i,r_D} and $A^p_{r_D}$ are related.

6.2.2. Relation Between the Iteration Functions A^p_{i,r_D} and $A^p_{r_D}$

In order to state how A^p_{i,r_D} and $A^p_{r_D}$ are related, we need some preliminary work. For this, we implicitly assume that an HE model $\mathcal{H}$, a drift resistance $r_D \geq 0$ and a feasible ADA pair (s^p, t^p, i^p_s, i^p_t) are given for the remainder of this section. We begin with some relations between the drifted ioni current and the drifted resistance functions.

Lemma 6.23 *Let $r \in \hat{R}^p_{r_D}$, then $\iota^{-1}_{s^p,r_D} \circ \gamma^p(r) = \rho^{-1}_{s^p,r_D} \circ \sigma^+_{r^p_s}(r)$.*

Proof. Let $r \in \hat{R}^p_{r_D}$. By applying Definition 5.22 of γ^p, we have

$$\begin{aligned}\iota^{-1}_{s^p,r_D} \circ \gamma^p(r) &= \iota^{-1}_{s^p,r_D}\left(i^p_s \frac{U}{i^p_s r + U}\right) = \iota^{-1}_{s^p,r_D}\left(\frac{U}{r + \frac{U}{i^p_s}}\right) = \iota^{-1}_{s^p,r_D}\left(\frac{U}{r + r^p_s}\right) = \rho^{-1}_{s^p,r_D}(r + r^p_s) \\ &= \rho^{-1}_{s^p,r_D} \circ \sigma^+_{r^p_s}(r),\end{aligned}$$

where we used that $\iota^{-1}_{s^p,r_D}\left(\frac{U}{r}\right) = \rho^{-1}_{s^p,r_D}(r)$ (Lemma 6.17). □

Lemma 6.24 *Let $g \in G_{t^p}$, then $\iota_{t^p,r_D}(g) = \left(\beta^p\right)^{-1} \circ \sigma^-_{r^p_t} \circ \rho_{t^p,r_D}(g)$.*

Proof. Let $g \in G_{t^p}$. Because $\iota_{t^p,r_D}(g) \in \mathbb{R}_{>0}$ (Definition 3.12), we can apply β^p to $\iota_{t^p,r_D}(g)$ (Definition 5.9) and obtain

$$\beta^p \circ \iota_{t^p,r_D}(g) = \frac{U}{\iota_{t^p,r_D}(g)} - r^p_t = \rho_{t^p,r_D}(g) - r^p_t = \sigma^-_{r^p_t} \circ \rho_{t^p,r_D}(g).$$

Because β^p is bijective (Lemma 5.11), $\iota_{t^p,r_D}(g) = \left(\beta^p\right)^{-1} \circ \sigma^-_{r^p_t} \circ \rho_{t^p,r_D}(g)$ holds. □

With this, we are able to state and prove the relation between A^p_{i,r_D} and $A^p_{r_D}$.

Lemma 6.25 *We have*

$$A^p_{i,r_D} = (\beta^p)^{-1} \circ A^p_{r_D} \circ \beta^p.$$

Proof. By using that $\iota^{-1}_{s^p,r_D} \circ \gamma(r) = \rho^{-1}_{s^p,r_D} \circ \sigma^+_{r^p_s}(r)$ for all $r \in \hat{R}^p_{r_D}$ (Lemma 6.23) and that $\iota_{t^p,r_D}(g) = (\beta^p)^{-1} \circ \sigma^-_{r_t} \circ \rho_{t^p,r_D}(g)$ for all $g \in G_t$ (Lemma 6.24), we have

$$\begin{aligned}A^p_{i,r_D} &= \iota_{t^p,r_D} \circ \iota^{-1}_{s^p,r_D} \circ \gamma^p \circ \beta^p = \left((\beta^p)^{-1} \circ \sigma^-_{r^p_t} \circ \rho_{t^p,r_D}\right) \circ \left(\rho^{-1}_{s^p,r_D} \circ \sigma^+_{r^p_s}\right) \circ \beta^p \\ &= (\beta^p)^{-1} \circ \left(\sigma^-_{r^p_t} \circ \rho_{t^p,r_D} \circ \rho^{-1}_{s^p,r_D} \circ \sigma^+_{r^p_s}\right) \circ \beta^p = (\beta^p)^{-1} \circ A^p_{r_D} \circ \beta^p.\end{aligned}$$

□

We demonstrate the statement of Lemma 6.25 in an example.

Example 6.26 *In this example, we evaluate the iteration function $A^p_{r_D}(r)$ at $r = 0$ by evaluating $\beta^p \circ A^p_{i,r_D} \circ (\beta^p)^{-1}(r)$. According to Definition 6.5 of A^p_{i,r_D}, we have*

$$A^p_{i,r_D} \circ (\beta^p)^{-1}(0) = \iota_{t^p,r_D} \circ \iota^{-1}_{s^p,r_D} \circ \gamma^p \circ \beta^p \circ (\beta^p)^{-1}(r) = \iota_{t^p,r_D} \circ \iota^{-1}_{s^p,r_D} \circ \gamma^p(0).$$

By applying Definition 5.22 of γ^p, we obtain

$$\gamma^p(r) = \frac{U i_s^p}{r i_s^p + U} \;\Rightarrow\; \gamma^p(0) = i_s^p \;\Rightarrow\; A^p_{i,r_D} \circ (\beta^p)^{-1}(0) = \iota_{t^p,r_D} \circ \iota^{-1}_{s^p,r_D}(i_s^p).$$

Let us consider the same ADA pair (s, t, i_s, i_t), the same drift resistance $r_D = 140k\Omega$ and the same HE model as in Example 3.22, where $\hat{i}_{t,r_D} := \iota_{t,r_D} \circ \iota^{-1}_{s,r_D}(i_s)$ is determined. Note that the superscript p notation for a plurality of ADA pairs has not yet been introduced when Example 3.22 was presented. Thus, the superscript p is omitted for the remainder of this example. By combining everything, we have

$$A_{r_D}(0) = \beta \circ A_{i,r_D} \circ (\beta)^{-1}(0) = \beta \circ \iota_{t,r_D} \circ \iota^{-1}_{s,r_D}(i_s) = \beta(\hat{i}_{t,r_D}) = \frac{U}{\hat{i}_{t,r_D}} - \frac{U}{i_t}.$$

This value is presented at the end of Example 3.22, which is $A_{r_D}(0) = \frac{U}{\hat{i}_{t,r_D}} - \frac{U}{i_t} \approx 0.6 r_D$. In other words, one iteration with A_{r_D} improves the drift resistance approximation from $r = 0$ to $r \approx 0.6 r_D$ in this example.

We are interested in the Picard iterations associated to the iteration functions A^p_{i,r_D} and $A^p_{r_D}$. For this, we take a look at the successive evaluation of both functions, respectively, which requires the application of Lemma 6.25. At this point, we must make sure that the iteration functions can be successively evaluated. According to Remark 6.9 this is not always the case, because A^p_{i,r_D} and $A^p_{r_D}$ are not selfmaps in general. However, A^p_{i,r_D} is a selfmap if and only if $A^p_{r_D}$ is a selfmap as is shown in the following.

Remark 6.27 *If there is no risk of confusion, the subscript r_D and the superscript p of A^p_{i,r_D} and $A^p_{r_D}$ as well as of $\hat{I}^p_{r_D}$ and $\hat{R}^p_{r_D}$ are omitted in the following.*

Lemma 6.28 *We have $A_i(\hat{I}) \subset \hat{I}$ if and only if $A(\hat{R}) \subset \hat{R}$.*

Proof. "⇒" Let $A_i(\hat{I}) \subset \hat{I}$. Because $\beta : \hat{I} \to \hat{R}$ is bijective, we have

$$\begin{aligned} r \in \hat{R} \;&\Rightarrow\; \beta^{-1}(r) \in \hat{I} \;\Rightarrow\; A_i \circ \beta^{-1}(r) \in \hat{I} \;\Rightarrow\; \beta \circ A_i \circ \beta^{-1}(r) \in \beta(\hat{I}) \\ &\Rightarrow\; A(r) \in \beta(\hat{I}) = \hat{R}. \end{aligned}$$

The last implication is taken from the statement of Lemma 6.25.
"⇐" Let $A(\hat{R}) \subset \hat{R}$. Analogous to "⇒", we have that $i \in \hat{I}$ implies $A_i(i) \in \hat{I}$. □

Assumption 6.29 *To avoid case distinctions, the iteration functions A_i and A are assumed to be selfmaps for the remainder of this section, i.e., we assume that $A_i : \hat{I} \to \hat{I}$ and $A : \hat{R} \to \hat{R}$. Under which conditions they are actually selfmaps is stated in Lemma 6.35 below.*

Lemma 6.30 *Let $n \in \mathbb{N}$, then we have*

$$A_i^n = \beta^{-1} \circ A^n \circ \beta.$$

Proof. By induction.
Base case:
For $n = 1$ the claim follows from Lemma 6.25.
Induction step:
Let the statement hold for $n = 1, \ldots, k$. We consider $n = k + 1$.

$$\begin{aligned} A_i^{k+1} = A_i \circ A_i^k = A_i \circ \beta^{-1} \circ A^k \circ \beta = \beta^{-1} \circ A \circ \beta \circ \beta^{-1} \circ A^k \circ \beta \\ = \beta^{-1} \circ A \circ A^k \circ \beta = \beta^{-1} \circ A^{k+1} \circ \beta. \end{aligned}$$

□

Lemma 6.30 states how the Picard iterations associated to A_i and A are related. This relation is used to derive some statements with respect to the limits of these Picard iterations.

Theorem 6.31 *Let $i \in \hat{I}$, then the following holds*

$$\lim_{n\to\infty} A_i^n(i) = i^* \;\Rightarrow\; \lim_{n\to\infty} A^n\big(\beta(i)\big) = \beta(i^*).$$

Let $r \in \hat{R}$, then the following holds

$$\lim_{n\to\infty} A^n(r) = r^* \;\Rightarrow\; \lim_{n\to\infty} A_i^n\big(\beta^{-1}(r)\big) = \beta^{-1}(r^*).$$

Proof. Let $i \in \hat{I}$ and let $\lim_{n\to\infty} A_i^n(i) = i^*$. First, we show that $\beta(i^*)$ is well-defined, i.e., we show that i^* is an element of the domain of β, which is $\hat{I}$. Because $(A_i^n)_{n\in\mathbb{N}} \subset \hat{I}$ and $\hat{I}$ is closed according to Lemma 6.11, the sequence's limit i^* is also an element of $\hat{I}$. Analogously, we have $r^* \in \hat{R}$ and thus $\beta^{-1}(r^*)$ is well-defined.
Next, we show the first implication of the theorem. According to Lemma 6.30, we have $A^n \circ \beta = \beta \circ A_i^n$ for all $n \in \mathbb{N}$ and thus

$$\begin{aligned} \lim_{n\to\infty} \big(A^n \circ \beta(i)\big) = \lim_{n\to\infty} \big(\beta \circ A_i^n(i)\big) = \lim_{n\to\infty} \Big(\frac{U}{A_i^n(i)} - r_t\Big) \\ = \frac{U}{\lim_{n\to\infty} A_i^n(i)} - r_t = \frac{U}{i^*} - r_t = \beta(i^*). \end{aligned}$$

Now, let $r \in \hat{R}$ and let $\lim_{n\to\infty} A(r) = r^*$. It is $A_i^n \circ \beta^{-1} = \beta^{-1} \circ A^n$ according to Lemma 6.30. Analogous to the first part of the proof, we have

$$\lim_{n\to\infty} \big(A_i^n \circ \beta^{-1}(r)\big) = \lim_{n\to\infty} \big(\beta^{-1} \circ A^n(r)\big) = \frac{U}{\lim_{n\to\infty}\big(A^n(r)\big) + r_t} = \frac{U}{r^* + r_t} = \beta^{-1}(r^*).$$

The last part of the equation follows from $\beta^{-1}(r) = \frac{U}{r+r_t}$ (Definition 5.9). □

Theorem 6.32 *Let $i \in \hat{I}$, then the Picard iteration associated to A_i starting at i converges to a fixed point i^* if and only if the Picard iteration associated to A starting at $\beta(i)$ converges to the fixed point $\beta(i^*)$.*

Proof. The statements follows directly from Theorem 6.31. □

As an important consequence, the iteration function A_i converges to the sought drifted test ioni current if and only if the iteration A converges to the drift resistance.

Corollary 6.33 *Let $r_D \geq 0$ and let $i_{t,r_D} := \frac{Ui_t}{r_D i_t + U}$ be the drifted test ioni current according to Lemma 3.29. Then*

$$\lim_{n\to\infty} A_i^n(i) = i_{t,r_D} \;\Leftrightarrow\; \lim_{n\to\infty} A^n\big(\beta(i)\big) = r_D.$$

In particular, i_{t,r_D} is a fixed point of A_i if and only if r_D is a fixed point of A.

Proof. The statement follows from Theorem 6.32 and the fact that

$$\beta(i_{t,r_D}) = \frac{U}{i_{t,r_D}} - \frac{U}{i_t} = \frac{U(r_D i_t + U)}{U i_t} - \frac{U}{i_t} = r_D + \frac{U}{i_t} - \frac{U}{i_t} = r_D.$$

□

Theorem 6.32 and Corollary 6.33 legitimate the approach to analyze the Picard iteration associated to A in order to obtain the convergence characteristics of the Picard iteration associated to A_i. But first, to conclude this subsection about the relation between the iteration functions A_i and A, we show that both functions are strictly increasing. Note that the following result is also valid if they are not selfmaps.

Lemma 6.34 *The ADA iteration functions $A_i : \hat{I} \to \mathbb{R}$ and $A : \hat{R} \to \mathbb{R}$ are strictly increasing.*

Proof. Let $i_1, i_2 \in \hat{I}$ such that $i_1 < i_2$. Because β and γ are strictly decreasing (Lemma 5.11 and 5.23, respectively) as well as $(\iota_{s,r_D})^{-1}$ and ι_{t,r_D} are strictly increasing (Lemma 3.16), we have

$$\begin{aligned} i_1 < i_2 \;&\Rightarrow\; \beta(i_1) > \beta(i_2) \;\Rightarrow\; \gamma\circ\beta(i_1) < \gamma\circ\beta(i_2) \\ &\Rightarrow\; A_i(i_1) = \iota_{t,r_D}\circ(\iota_{s,r_D})^{-1}\circ\gamma\circ\beta(i_1) < \iota_{t,r_D}\circ(\iota_{s,r_D})^{-1}\circ\gamma\circ\beta(i_2) = A_i(i_2). \end{aligned}$$

Furthermore, let $r_1, r_2 \in \hat{R}$ such that $r_1 < r_2$. By applying $A = \beta\circ A_i\circ\beta^{-1}$ (consequence of Lemma 6.25) and using that β as well as β^{-1} are strictly decreasing, we have

$$\begin{aligned} r_1 < r_2 \;&\Rightarrow\; \beta^{-1}(r_1) > \beta^{-1}(r_2) \;\Rightarrow\; A_i\circ\beta^{-1}(r_1) > A_i\circ\beta^{-1}(r_2) \\ &\Rightarrow\; A(r_1) = \beta\circ A_i\circ\beta^{-1}(r_1) < \beta\circ A_i\circ\beta^{-1}(r_2) = A(r_2). \end{aligned}$$

□

6.3. Convergence Characteristics of the Picard Iteration Associated to the Drift Resistance Iteration Function

In this section, we analyze the Picard iteration associated to A_{r_D}. The analysis addresses two questions. Under which conditions does the Picard iteration associated to A_{r_D} converge to a (unique) fixed point? And how is this fixed point related to the drift resistance?
The approach to answer the first question is to apply Lemma 4.46 and Theorem 4.41 from Section 4.3 about fixed point iteration procedures. The second answer is deduced from the construction of the drift resistance iteration function A_{r_D}.
First, we state conditions that guarantee that A_{r_D} has a fixed point and analyze for what starting points the Picard iteration associated to A_{r_D} converges to this fixed point. This requires the concept of being contractive from Definition 4.37.

Lemma 6.35 *Let A_{r_D} be contractive, then the following statements are equivalent:*

1. *A_{r_D} has at least one fixed point.*
2. *A_{r_D} has a unique fixed point.*
3. *A_{r_D} is a selfmap.*

Furthermore, if one of the three statements holds, then the Picard iteration associated to A_{r_D} converges for every starting point $r \in \hat{R}_{r_D}$.

Proof. Let A_{r_D} be contractive. We know that A_{r_D} is strictly increasing (Lemma 6.34) and that the domain of A_{r_D} is a closed interval (Lemma 6.11). Therefore, we can apply Lemma 4.46 which proves the equivalence of the three statements.
As a consequence, if one of the three items holds, then A_{r_D} is a contractive selfmap on a compact set and we can apply Theorem 4.41, which proves the convergence statement. □

Remark 6.36 *Note that A_{r_D} being contractive is not a necessary condition for the statement of Lemma 6.35. In Appendix A, Example A.2 presents an iteration function A_{r_D} that is not contractive but that still has a unique fixed point and for all $r \in \hat{R}_{r_D}$ the Picard iteration associated to A_{r_D} starting at r converges to this fixed point. Furthermore, this example demonstrates that A_{i,r_D} being contractive does not imply that A_{r_D} is contractive. The converse implication is also not true in general, i.e., A_{r_D} being contractive does not imply that A_{i,r_D} is contractive, which is demonstrated in Example A.1 in Appendix A.
Therefore, focusing on contractive iteration functions A_{r_D} might exclude some cases that still result in convergent Picard iterations. However, practical experience has shown that such cases are not very likely. In addition, focusing on contractive iteration functions A_{r_D} facilitates a corresponding convergence analysis.*

Lemma 6.35 states that if A_{r_D} has a fixed point and is contractive, then the Picard iteration associated to A_{r_D} converges for an arbitrary starting point $r \in \hat{R}_{r_D}$. We first analyze under which condition the fixed point of A_{r_D} corresponds to the drift resistance r_D. Thereafter, we analyze conditions such that A_{r_D} is contractive.

6.3.1. Relation Between the Fixed Point of A_{r_D} and the Drift Resistance

The following lemma states conditions such that the fixed point of A_{r_D} is the sought drift resistance.

Lemma 6.37 *Let $r_D \geq 0$, then*

$$A_{r_D}(r_D) = r_D \;\Leftrightarrow\; \rho_s^{-1}(r_s) = \rho_t^{-1}(r_t) \;\Leftrightarrow\; \iota_s^{-1}(i_s) = \iota_t^{-1}(i_t).$$

In particular, if one of the three statements holds, then $r_D \in \hat{R}_{r_D}$.

Proof. Let $r_D \geq 0$, then

$$\begin{aligned} r_D = A_{r_D}(r_D) &\;\Leftrightarrow\; \sigma_{r_t}^- \circ \rho_{t,r_D} \circ \rho_{s,r_D}^{-1} \circ \sigma_{r_s}^+(r_D) = r_D \;\Leftrightarrow\; \rho_{t,r_D} \circ \rho_{s,r_D}^{-1} \circ \sigma_{r_s}^+(r_D) = \sigma_{r_t}^+(r_D) \\ &\;\Leftrightarrow\; \rho_{s,r_D}^{-1} \circ \sigma_{r_s}^+(r_D) = \rho_{t,r_D}^{-1} \circ \sigma_{r_t}^+(r_D) \;\Leftrightarrow\; \rho_{s,r_D}^{-1}(r_s + r_D) = \rho_{t,r_D}^{-1}(r_t + r_D) \\ &\;\Leftrightarrow\; \rho_{s,r_D}^{-1} \circ \sigma_{r_D}^+(r_s) = \rho_{t,r_D}^{-1} \circ \sigma_{r_D}^+(r_t) \;\Leftrightarrow\; \rho_s^{-1}(r_s) = \rho_t^{-1}(r_t) \\ &\;\Leftrightarrow\; \iota_s^{-1}\Big(\frac{U}{r_s}\Big) = \iota_t^{-1}\Big(\frac{U}{r_t}\Big) \;\Leftrightarrow\; \iota_s^{-1}(i_s) = \iota_t^{-1}(i_t), \end{aligned}$$

where the last two lines follow from Lemmas 6.20 and 6.17 as well as from Definition 5.7. □

Lemma 6.37 states that whether the drift resistance is a fixed point of A_{r_D} depends on the ADA parameters and the HE model. If s, t, i_s and i_t are selected such that $\iota_s^{-1}(i_s) = \iota_t^{-1}(i_t)$ holds, then the drift resistance is a fixed point of A_{r_D}. If in addition A_{r_D} is contractive, then the Picard iteration associated to A_{r_D} converges to r_D for an arbitrary starting point $r \in \hat{R}_{r_D}$ according to Lemma 6.35. Therefore, the ADA parameters are ideally selected such that A_{r_D} is contractive and $\iota_s^{-1}(i_s) = \iota_t^{-1}(i_t)$ holds. However, because of manufacturing tolerances, the condition $\iota_s^{-1}(i_s) = \iota_t^{-1}(i_t)$ cannot always be satisfied. This is detailed in the following subsection.

6.3.2. Impact of Tolerances

The following example demonstrates the impact of tolerances with respect to the position of the ioni electrode relative to the burner.

Example 6.38 *This example is an extension of Example 3.22 and is also based on Vaillant measurement data. Let $\mathcal{H} = \big(\mathrm{FS}, (G_{\mathrm{fs}})_{\mathrm{fs}\in\mathrm{FS}}, (\iota_{\mathrm{fs}})_{\mathrm{fs}\in\mathrm{FS}}, (\Lambda_{\mathrm{fs}})_{\mathrm{fs}\in\mathrm{FS}}, (\zeta_{\mathrm{fs}})_{\mathrm{fs}\in\mathrm{FS}}\big)$ be the same HE model as considered in Example 3.22, i.e., $\mathcal{H}$ is based on the Vaillant measurement data according to [PHE, Item 6371]. Furthermore, let (s, t, i_s, i_t) be the ADA pair as selected in Example 3.22, i.e., we have $s, t \in \mathrm{FS}$ such that $s > t$ and $\iota_s^{-1}(i_s) = \iota_t^{-1}(i_t) =: g_A$.*
The corresponding ioni current functions ι_s and ι_t are depicted in Figure 6.1. The solid orange curve corresponds to ι_s and the solid blue curve corresponds to ι_t. The orange and the blue dot correspond to the start point and to the test point, respectively. Note that both points have the identical gvp g_A. Because $\iota_s^{-1}(i_s) = \iota_t^{-1}(i_t)$, the ADA pair's

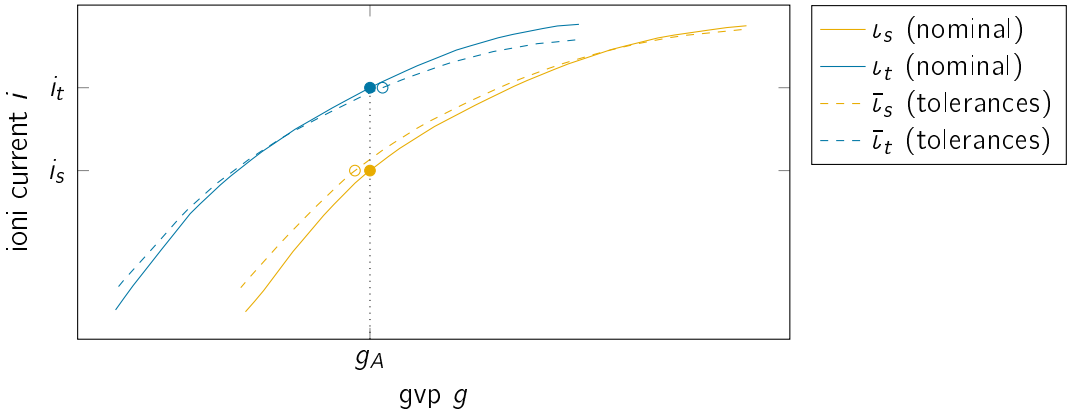

Figure 6.1.: The impact of tolerances with respect to the position of the ioni electrode is shown. The functions ι_s and ι_t correspond to measurement data with the ioni electrode in nominal position. In contrast, the functions $\bar{\iota}_s$ and $\bar{\iota}_t$ correspond to measurement data of the same HE but with the ioni electrode displaced from the nominal position, which is usually caused by manufacturing tolerances. Note that $\iota_s^{-1}(i_s) = \iota_t^{-1}(i_t) =: g_A$ but $\bar{\iota}_s^{-1}(i_s) \neq \bar{\iota}_t^{-1}(i_t)$.

iteration function $A_{r_D} = \sigma_{r_t}^- \circ \rho_{t,r_D} \circ \rho_{s,r_D}^{-1} \circ \sigma_{r_s}^+$ has the desired fixed point r_D according to Lemma 6.37.

We consider a second HE model $\overline{\mathcal{H}} = \left(\overline{\mathrm{FS}}, (\overline{G}_{\mathrm{fs}})_{\mathrm{fs}\in\overline{\mathrm{FS}}}, (\bar{\iota}_{\mathrm{fs}})_{\mathrm{fs}\in\overline{\mathrm{FS}}}, (\bar{\Lambda})_{\mathrm{fs}\in\overline{\mathrm{FS}}}, (\bar{\zeta})_{\mathrm{fs}\in\overline{\mathrm{FS}}}\right)$, which is based on Vaillant measurement data according to [PHE, Item 6344]. The Brennfeld static signals of [PHE, Item 6344] and [PHE, Item 6371] belong to the same HE. However, with [PHE, Item 6371] the ioni electrode is in the nominal position, while with [PHE, Item 6344] the ioni electrode is deliberately not in the nominal position in order to simulate manufacturing tolerances. The HE model $\overline{\mathcal{H}}$ is referred to as the tolerance model for the remainder of this example. Note that the ADA pair (s, t, i_s, i_t) remains unchanged, because an ADA pair is only selected once for an HE.

The start ioni current function $\bar{\iota}_s$ and the test ioni current function $\bar{\iota}_t$ of the tolerance model are represented by the dashed orange and blue curve, respectively, in Figure 6.1. It is apparent that the non-nominal position of the electrode has slightly changed the start and test ioni current functions. The corresponding start point $(\bar{\iota}_s^{-1}(i_s), i_s)$ and test point $(\bar{\iota}_t^{-1}(i_t), i_t)$ are marked with the orange and blue circle, respectively. In contrast to the nominal case, we have $\bar{\iota}_s^{-1}(i_s) \neq \bar{\iota}_t^{-1}(i_t)$ and thus r_D is not a fixed point of the iteration function $\bar{A}_{r_D} := \sigma_{r_t}^- \circ \bar{\rho}_{t,r_D} \circ \bar{\rho}_{s,r_D}^{-1} \circ \sigma_{r_s}^+$ according to Lemma 6.37.

This can be verified with Figure 6.2, which shows the iteration functions A_{r_D} and $\bar{A}_{r_D}$ for $r_D = 140k\Omega$. The solid black curve corresponds to A_{r_D} and the dashed black curve corresponds to $\bar{A}_{r_D}$. Note that both iteration functions are strictly increasing, which is in accordance with Lemma 6.34. In addition, the identity function is represented by the dotted line to illustrate the fixed points of A_{r_D} and $\bar{A}_{r_D}$, which are marked by the dot and the circle, respectively. While the fixed point of A_{r_D} is the desired value r_D, the fixed point

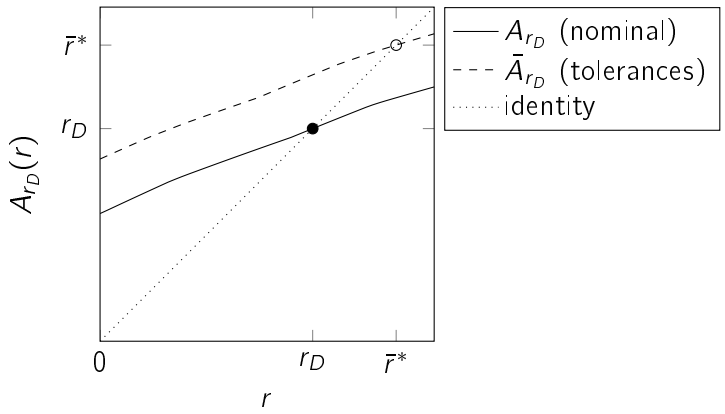

Figure 6.2.: In the nominal case, r_D is a fixed point of A_{r_D}, which is marked by the dot. In contrast, in the case with tolerances with respect to the position of the ioni electrode, the fixed point of $\bar{A}_{r_D}$ is $\bar{r}^* \neq r_D$, which is marked by the circle.

of $\bar{A}_{r_D}$ is $\bar{r}^*$, which is $\bar{r}^* = 195k\Omega > 140k\Omega = r_D$ in this example.
In conclusion, tolerances might shift the fixed point of an iteration function $\bar{A}_{r_D}$ away from r_D, i.e., we might have $\bar{r}^* \neq r_D$. In the extreme case, the fixed point is shifted "outside" of the set $\hat{R}_{r_D}$ and the corresponding iteration function $\overline{A}_{r_D}$ is not a selfmap anymore and thus the Picard iteration does not converge anymore (within the set $\hat{R}_{r_D}$). But even if $\overline{A}_{r_D}$ has a fixed point $\bar{r}^* \in \hat{R}_{r_D}$, it might be outside of feasible combustion limits. Therefore, the aspect tolerances has to be considered in the ADA parameterization.

Example 6.38 demonstrates that manufacturing tolerances might influence the fixed point characteristics of the selected ADA parameters. We can derive two corresponding cases from Lemma 6.37. In the first case, (s, t, i_s, i_t) are selected such that $\iota_s^{-1}(i_s) = \iota_t^{-1}(i_t)$. Then r_D is a fixed point of A_{r_D}. This is considered as the standard or nominal situation. Accordingly, the second case is $\iota_s^{-1}(i_s) \neq \iota_t^{-1}(i_t)$, which might be caused by tolerances with respect to the ioni electrode's position. Then, r_D is not a fixed point of A_{r_D}. This is considered as a non-standard situation. These two cases motivate the following definition.

Definition 6.39 *Let $\mathcal{H} = \left(\mathrm{FS}, (G_{\mathrm{fs}})_{\mathrm{fs}\in\mathrm{FS}}, (\iota_{\mathrm{fs}})_{\mathrm{fs}\in\mathrm{FS}}, (\Lambda_{\mathrm{fs}})_{\mathrm{fs}\in\mathrm{FS}}, (\zeta_{\mathrm{fs}})_{\mathrm{fs}\in\mathrm{FS}}\right)$ be an HE model and let (s, t, i_s, r_s) be an ADA pair. If $\iota_s^{-1}(i_s) = \iota_t^{-1}(i_t)$, then $\mathcal{H}$ and the ADA pair are considered to be* nominal.
If $\iota_s^{-1}(i_s) \neq \iota_t^{-1}(i_t)$, then $\mathcal{H}$ and the ADA pair are considered to be non-standard.

Remark 6.40 *Note that the definition of the terms nominal and non-standard requires an HE model and an ADA pair. This is required, because the ioni current functions ι_s and ι_t are taken from the HE model $\mathcal{H}$, while s, t, i_s and i_t are the ADA pair's parameters. As a consequence, if an ADA pair is designed with an HE model $\mathcal{H}$ such that they are nominal, the same ADA pair with a different HE model $\overline{\mathcal{H}} \neq \mathcal{H}$ might be non-standard as demonstrated in Example 6.38.*

Corollary 6.41 *Let $r_D \geq 0$. Let $\mathcal{H}$ be an HE model and (s, t, i_s, r_s) be an ADA pair. Then,*

$$A_{r_D}(r_D) = r_D \;\Leftrightarrow\; \mathcal{H} \text{ and } (s, t, i_s, i_t) \text{ are nominal.}$$

Proof. The statement follows from Lemma 6.37 and from Definition 6.39. □

The distinction between the two cases nominal and non-standard according to Definition 6.39 and Corollary 6.41 plays a central role when developing the ADA optimization models in Chapter 8 below.

So far, we have analyzed the fixed points of the iteration function A_{r_D}. To guarantee convergence of the Picard iteration associated to A_{r_D} to its fixed point (if it exists), it is required that A_{r_D} is contractive according to Lemma 6.35. Therefore, conditions such that A_{r_D} is contractive are detailed next.

6.3.3. Conditions Such That A_{r_D} Is Contractive

The function A_{r_D} is composed of the resistance functions $\rho_{t,r_D}(g) = \frac{U}{\iota_t(g)} + r_D$ and $\rho_{s,r_D}^{-1}(r) = \iota_s^{-1}\left(\frac{U}{r - r_D}\right)$, among others. According to Definition 2.18 of the HE model, the functions ι_{fs} are continuous and strictly increasing, but these requirements are in general not sufficient to ensure that A_{r_D} is contractive. I.e., in general, we are not able to tell whether A_{r_D} is contractive or not. However, if A_{r_D} is differentiable, it is possible to estimate the Lipschitz constant of A_{r_D} by considering the absolute value of its derivative. This is the approach in this subsection.
We have to be aware of the fact that the HE model does not require that the functions ι_{fs} are differentiable and thus A_{r_D} is not differentiable in general. Rather, the differentiability of A_{r_D} depends on the selected regression method of the HE model. For instance, the ioni current functions are differentiable if Gaussian processes are used. On the other hand, piecewise linearly interpolated functions are not everywhere differentiable in general.
For the following analysis it is assumed that the ioni current functions ι_{fs} are everywhere differentiable. This is done in the knowledge that the analysis is only valid for differentiable HE models. This is reasonable, because the real physical ioni current functions are assumed to be differentiable [Loc18, p. 11].

Lemma 4.44 from Section 4.3 states that a differentiable function f is contractive if the absolute value of its derivative is bounded by 1. This motivates the following approach. First, the derivative of A_{r_D} is determined. Thereafter, we analyze under what conditions the derivative's absolute value is smaller than 1.

Theorem 6.42 *Let ι_s and ι_t be differentiable and let $r_D \geq 0$. Then A_{r_D} is also differentiable and for all $\bar{r} \in \hat{R}_{r_D}$ we have*

$$\frac{d}{dr} A_{r_D}(\bar{r}) = \frac{\frac{d}{dg}\rho_t\left(\hat{g}(\bar{r})\right)}{\frac{d}{dg}\rho_s\left(\hat{g}(\bar{r})\right)} \tag{6.3}$$

$$= \frac{\frac{d}{dg}\iota_t\big(\hat{g}(\bar{r})\big)}{\frac{d}{dg}\iota_s\big(\hat{g}(\bar{r})\big)} \cdot \frac{\iota_s^2\big(\hat{g}(\bar{r})\big)}{\iota_t^2\big(\hat{g}(\bar{r})\big)}, \tag{6.4}$$

where

$$\hat{g}(\bar{r}) \coloneqq \rho_{s,r_D}^{-1} \circ \sigma_{r_s}^{+}(\bar{r}) = \rho_s^{-1} \circ \sigma_{r_D}^{-} \circ \sigma_{r_s}^{+}(\bar{r}) = \rho_s^{-1}(\bar{r} + r_s - r_D). \tag{6.5}$$

Proof. Let ι_s and ι_t be differentiable. Then the corresponding resistance functions $\rho_t = \frac{U}{\iota_t}$ and $\rho_s^{-1} = \left(\frac{U}{\iota_s}\right)^{-1}$ are also differentiable. According to Definition 6.21, A_{r_D} is a composition that contains the drifted resistance functions ρ_{t,r_D} and ρ_{s,r_D}^{-1}. We can transform the drifted resistance functions to the corresponding resistance functions without drift by Lemma 6.20 and we get

$$A_{r_D} = \sigma_{r_t}^{-} \circ \rho_{t,r_D} \circ \rho_{s,r_D}^{-1} \circ \sigma_{r_s}^{+} = \sigma_{r_t}^{-} \circ \sigma_{r_D}^{+} \circ \rho_t \circ \rho_s^{-1} \circ \sigma_{r_D}^{-} \circ \sigma_{r_s}^{+}. \tag{6.6}$$

As a composition of differentiable functions, A_{r_D} is also differentiable.
We apply the chain rule to the right hand side of (6.6) to deduce the derivative of A_{r_D}. We consider single parts of the composition first and combine them at the end of the proof.
We define $\hat{r}_{s,r_D}(r) \coloneqq \sigma_{r_D}^{-} \circ \sigma_{r_s}^{+}(r) = r - r_D + r_s$. Its derivative is $\frac{d}{dr}\hat{r}_{s,r_D}(r) = 1$.
Next, we are interested in the derivative $\frac{d}{dr}\rho_s^{-1}\big(\hat{r}_{s,r_D}(r)\big)$, which is obtained by applying the inverse function rule. For this, we define $\hat{g}(r) \coloneqq \rho_s^{-1} \circ \sigma_{r_D}^{-} \circ \sigma_{r_s}^{+}(r) = \rho_s^{-1} \circ \hat{r}_{s,r_D}(r)$. Note that $\hat{g}(r)$ refers to a gas valve position, because ρ_s is a function from gvp to resistance and thus its inverse is a function from resistance to gvp. Let $\bar{r} \in \hat{R}_{r_D}$, then we have $\rho_s^{-1}\big(\hat{r}_{s,r_D}(\bar{r})\big) = \hat{g}(\bar{r})$. By applying the inverse function rule and the chain rule, we have

$$\frac{d}{dr}\rho_s^{-1}\big(\hat{r}_{s,r_D}(\bar{r})\big) = \frac{1}{\frac{d}{dg}\rho_s\big(\hat{g}(\bar{r})\big)}\frac{d}{dr}\hat{r}_{s,r_D}(\bar{r}) = \frac{1}{\frac{d}{dg}\rho_s\big(\hat{g}(\bar{r})\big)}.$$

Before we combine everything, we consider the derivative of $\sigma_{r_t}^{-} \circ \sigma_{r_D}^{+}\big(x(r)\big)$, which corresponds to the most left part of the composition in the right hand side of (6.6). We have $\frac{d}{dr}(\sigma_{r_t}^{-} \circ \sigma_{r_D}^{+})\big(x(r)\big) = \frac{d}{dr}\big(x(r) - r_t + r_D\big) = \frac{d}{dr}x(r)$. Everything combined and applying the chain rule results in

$$\begin{aligned}\frac{d}{dr}A_{r_D}(\bar{r}) = \frac{d}{dr}\big(\sigma_{r_t}^{-} \circ \sigma_{r_D}^{+} \circ \rho_t \circ \rho_s^{-1} \circ \hat{r}_{s,r_D}\big)(\bar{r}) &= \frac{d}{dr}\big(\rho_t \circ \rho_s^{-1} \circ \hat{r}_{s,r_D}\big)(\bar{r}) \\ &= \frac{d}{dg}\rho_t\big(\hat{g}(\bar{r})\big) \cdot \frac{d}{dr}\rho_s^{-1}\big(\hat{r}_{s,r_D}(\bar{r})\big) \\ &= \frac{d}{dg}\rho_t\big(\hat{g}(\bar{r})\big) \cdot \frac{1}{\frac{d}{dg}\rho_s\big(\hat{g}(\bar{r})\big)}, \end{aligned} \tag{6.7}$$

which is the Theorem's first statement.
To prove the second statement, we express (6.7) with the ioni current functions ι_{fs}. We have $\rho_{\mathrm{fs}}(g) = \frac{U}{\iota_{\mathrm{fs}}(g)}$ and thus its derivative is

$$\frac{d}{dg}\rho_{\mathrm{fs}}(g) = \frac{d}{dg}\frac{U}{\iota_{\mathrm{fs}}(g)} = -U\frac{1}{\iota_{\mathrm{fs}}^2(g)}\frac{d}{dg}\iota_{\mathrm{fs}}(g). \tag{6.8}$$

The theorem's second statement, i.e., Equation (6.4), follows by plugging (6.8) into (6.7). □

Recall that we are interested in the case that $|\frac{d}{dr}A_{r_D}(r)| < 1$ or equivalently $-1 < \frac{d}{dr}A_{r_D}(r) < 1$. According to Lemma 6.34, A_{r_D} is strictly increasing and thus we always have $0 < \frac{d}{dr}A_{r_D}(r)$. Therefore, it is sufficient to consider the upper boundary of $\frac{d}{dr}A_{r_D}(r)$ only.

Theorem 6.43 *As in Theorem 6.42, we define $\hat{g}(r) := \rho_s^{-1}(r + r_s - r_D)$ for $r \in \hat{R}_{r_D}$. Let ι_s and ι_t be differentiable and let $r_D \geq 0$. If*

$$\frac{d}{dg}\rho_t\big(\hat{g}(r)\big) > \frac{d}{dg}\rho_s\big(\hat{g}(r)\big) \;\forall\; r \in \hat{R}_{r_D} \quad \text{or} \tag{6.9}$$

$$\frac{d}{dg}\iota_t\big(\hat{g}(r)\big) < \frac{\iota_t^2\big(\hat{g}(r)\big)}{\iota_s^2\big(\hat{g}(r)\big)} \cdot \frac{d}{dg}\iota_s\big(\hat{g}(r)\big) \;\forall\; r \in \hat{R}_{r_D}, \tag{6.10}$$

then A_{r_D} is contractive on $\hat{R}_{r_D}$.

Proof. For $r \in \hat{R}_{r_D}$ let $\hat{g}(r) := \rho_s^{-1}(r + r_s - r_D)$. We show that (6.9) holds if and only if (6.10) holds if and only if $A'_{r_D}(r) < 1$ for all $r \in \hat{R}_{r_D}$.
According to Lemma 6.17, the functions ρ_s and ρ_t are strictly decreasing, i.e., their derivatives are negative. By applying (6.3) of Theorem 6.42, we have

$$\frac{d}{dr}A_{r_D}(r) = \frac{\frac{d}{dg}\rho_t\big(\hat{g}(r)\big)}{\frac{d}{dg}\rho_s\big(\hat{g}(r)\big)} < 1 \;\Leftrightarrow\; \frac{d}{dg}\rho_t\big(\hat{g}(r)\big) > \frac{d}{dg}\rho_s\big(\hat{g}(r)\big).$$

In contrast, the ioni current functions ι_s and ι_t are strictly increasing according to Definition 2.18, i.e., their derivatives are greater than zero. By applying (6.4) of Theorem 6.42, we have

$$\frac{d}{dr}A_{r_D}(r) = \frac{\frac{d}{dg}\iota_t\big(\hat{g}(r)\big)}{\frac{d}{dg}\iota_s\big(\hat{g}(r)\big)} \cdot \frac{\iota_s^2\big(\hat{g}(r)\big)}{\iota_t^2\big(g\hat{(}r)\big)} < 1 \;\Leftrightarrow\; \frac{d}{dg}\iota_t\big(\hat{g}(r)\big) < \frac{\iota_t^2\big(\hat{g}(r)\big)}{\iota_s^2\big(g\hat{(}r)\big)} \cdot \frac{d}{dg}\iota_s\big(\hat{g}(r)\big).$$

On the other hand, the derivative of A_{r_D} is always greater than zero according to Lemma 6.34. Therefore, we have

$$|A'_{r_D}(r)| < 1 \;\forall\; r \in \hat{R}_{r_D} \;\Leftrightarrow\; (6.9) \;\Leftrightarrow\; (6.10)$$

and the statement follows from Lemma 4.44. □

Remark 6.44 *The gas valve positions $\hat{g}(r) := \rho_s^{-1}(r + r_s - r_D)$ with $r \in \hat{R}_{r_D}$ in Theorems 6.42 and 6.43 correspond to the set $G_s \cap G_t$. According to Definitions 5.19 and 6.14 as well as to Lemma 6.20, we have $\hat{R}_{r_D} = \rho_s(G_s \cap G_t) - r_s + r_D$ and thus*

$$\begin{aligned} r \in \hat{R}_{r_D} &\;\Leftrightarrow\; \exists\; g \in G_s \cap G_t : \rho_s(g) - r_s + r_D = r \\ &\;\Leftrightarrow\; \exists\; g \in G_s \cap G_t : g = \rho_s^{-1}(r - r_D + r_s) = \hat{g}(r). \end{aligned}$$

So far, we have the statement that $A_{r_D}(r)' < 1$ implies that A_{r_D} is contractive. We get an even stronger statement, if we additionally assume that A_{r_D} is continuously differentiable.

Lemma 6.45 *Let A_{r_D} be continuously differentiable. If $A'_{r_D} < 1$, then there exists $L < 1$ such that A_{r_D} is L-Lipschitzian.*

Proof. Let A_{r_D} be continuously differentiable and let $A'_{r_D} < 1$. The domain of A_{r_D} is a closed and bounded interval according to Lemma 6.11. Thus A'_{r_D} is a continuous mapping on a compact set. By applying the extreme value theorem, we know that A'_{r_D} attains its maximum and minimum on its domain $\hat{R}_{r_D}$. Because $A'_{r_D} < 1$, there exists $L < 1$ such that $A'_{r_D} \leq L$. On the other hand, we have $A'_{r_D} > 0$ according to Lemma 6.34 and thus $|A'_{r_D}| \leq L$. The statement follows by applying Lemma 4.44. □

Being L-Lipschitzian with $L < 1$ is a stronger statement in the sense that it implies being contractive. Furthermore, in the context of ADA and the corresponding Picard iteration, it has the advantage that we get rate of convergence estimations from Banach's fixed point theorem.

Lemma 6.46 *Let A_{r_D} be L-Lipschitzian with $L < 1$. If A_{r_D} has a fixed point r^*, then the following rate of convergence estimations for a starting point $r \in \hat{R}_{r_D}$ hold:*

$$|r_n - r^*| \leq L \cdot |r_n - r_{n-1}| \leq L^n \cdot |r - r^*| \ \forall\ n \in \mathbb{N},$$

where $r_n := A^n_{r_D}(r)$.

Proof. Let A_{r_D} be L-Lipschitzian with $L < 1$. Then A_{r_D} is contractive. Furthermore, let A_{r_D} have a fixed point. Then A_{r_D} is a selfmap according to Lemma 6.35. But then we can apply Banach's fixed point theorem and the rate of convergence statement follows from Theorem 4.39. □

Remark 6.47 *At this point, we can analyze the influence that the selection of the ADA parameters s, t, i_s and i_t has on the fixed point convergence characteristics of A_{r_D}. Recall that the iteration function A_{r_D} depends on the start and test ioni current functions ι_s and ι_t, respectively. Therefore, by selecting s and t, the corresponding iteration function A_{r_D} might have a smaller or larger Lipschitz constant. In the worst case, the resulting iteration function is not contractive and the ADA algorithm might not be convergent. On the other hand, if the Lipschitz constant of A_{r_D} is small, we have a fast rate of convergence according to Lemma 6.46.*
By selecting the start and the test ioni current i_s and i_t, respectively, the fixed point is determined (if it exists), see also Lemma 6.37. If the ioni currents are not properly selected, the fixed point of A_{r_D} might differ significantly from the drift resistance or the HE might leave feasible combustion limits while performing an ADA iteration, which both might result in undesired outcomes of the ADA algorithm.

Therefore, the question whether the ADA procedure is capable to successfully compensate possible drift resistances depends to a large extent on the selection of the ADA parameters. This is the motivation to develop and solve a corresponding optimization model in this thesis.

So far, we have deduced conditions such that the ADA algorithm with a single ADA pair is convergent. There exists a document by Siemens that also states some conditions for convergence of the ADA algorithm with a single ADA pair. In the following subsection, these conditions are compared to the results presented in this subsection.

6.3.4. Comparison with the Documentation by Siemens

As stated in Section 2.3.2, the combustion control system IoniDetect, and as a part of it also the ADA procedure, were developed by Siemens. Siemens provides a document with the title *Funktionsweise ADA* [Loc18] that contains a brief description of the ADA concept and also conditions for the convergence of the ADA procedure [Loc18, p. 8]. In this subsection, we compare the convergence conditions stated in the Siemens document [Loc18] with the results of the preceding subsection. For the remainder of this subsection, the term "Siemens document" refers to [Loc18].
The approach in the Siemens document to state some convergence conditions for the ADA procedure is similar to the approach taken in this thesis. The authors of the Siemens document also begin with the equivalence circuit of the ioni current measurement circuit and state that the measured ioni current corresponds to the circuit's resistance by applying Ohm's law, i.e., $r = \frac{U}{i}$. However, they discuss the ADA procedure with ioni currents and the resistances considered as functions of the equivalence AFR λ. In contrast, in this thesis the ioni currents and the resistances are considered as functions of the gas valve position. In this subsection, it will be shown that both approaches can be considered as equivalent under the conditions of Assumption 6.48 given below.
To illustrate the approach of the Siemens document, let us assume that an ADA pair (s, t, i_s, i_t) is given. We further assume that we have a nominal situation, i.e., $\iota_s^{-1}(i_s) = \iota_t^{-1}(i_t) =: g_A$ holds. Let Λ_s and Λ_t be the corresponding equivalence AFR functions according to Definition 2.18 of the HE model. With this, we can determine the equivalence AFR of the start and of the test point, which are $\lambda_s := \Lambda_s(g_A)$ and $\lambda_t := \Lambda_t(g_A)$, respectively. In the Siemens document, the following assumption with respect to the relation between the gas valve position and the equivalence AFR λ is made.

Assumption 6.48 *For all feasible gas valve positions, we assume that if the gas valve position is kept constant and the fan speed is reduced from s to t, then the difference of the corresponding λ values is always $\Delta\lambda := \lambda_s - \lambda_t$ [Loc18, p. 6].*
Expressed in the notation of the HE model, this reads

$$\Lambda_s(g) - \Lambda_t(g) = \Delta\lambda \ \forall\ g \in G_s \cap G_t, \ \textit{where } \Delta\lambda := \lambda_s - \lambda_t. \tag{6.11}$$

Remark 6.49 *Assumption 6.48 is also mentioned in the ADA patent [LS17]. The ADA patent states that if the fan speed is reduced from s to t with the gvp kept constant, then "the air coefficient is lowered by a more or less constant change in the air coefficient $\Delta\lambda$" [LS17, p. 7].*

By composing certain functions of the HE model, we can define the functions that correspond to the approach in the Siemens document. I.e., we consider the resistance as a function of λ instead of the gvp g. Recall from Definitions 2.18 and 2.22 that for all $\mathrm{fs} \in \mathrm{FS}$ the function $\Lambda_{\mathrm{fs}} : G_{\mathrm{fs}} \to L_{\mathrm{fs}}$ is a homeomorphism between the set of gas valve positions G_{fs} and the set of their corresponding equivalence AFRs L_{fs}.

Definition 6.50 *Let $\mathcal{H} = \left(\mathrm{FS}, (G_{\mathrm{fs}})_{\mathrm{fs}\in\mathrm{FS}}, (\iota_{\mathrm{fs}})_{\mathrm{fs}\in\mathrm{FS}}, (\Lambda_{\mathrm{fs}})_{\mathrm{fs}\in\mathrm{FS}}, (\zeta_{\mathrm{fs}})_{\mathrm{fs}\in\mathrm{FS}}\right)$ be an HE model and let $\rho_{\mathrm{fs}} : G_{\mathrm{fs}} \to R_{\mathrm{fs}}$, $\mathrm{fs} \in \mathrm{FS}$, be the homeomorphism according to Definition 6.14. For $\mathrm{fs} \in \mathrm{FS}$, we define*

$$\rho_{\lambda,\mathrm{fs}} : L_{\mathrm{fs}} \to R_{\mathrm{fs}} \quad \text{by} \quad \rho_{\lambda,\mathrm{fs}} := \rho_{\mathrm{fs}} \circ \Lambda_{\mathrm{fs}}^{-1}. \tag{6.12}$$

Remark 6.51 *The function $\rho_{\lambda,\mathrm{fs}}$ is well-defined by construction.*

The central statement of the Siemens document is, that the ADA algorithm converges if the derivatives of $\rho_{\lambda,s}$ and $\rho_{\lambda,t}$ fulfill certain conditions [Loc18, p. 9].

Statement 6.52 *Let Assumption 6.48 hold. If*

$$\frac{d}{d\lambda}\rho_{\lambda,s}(\overline{\lambda}_s) > \frac{d}{d\lambda}\rho_{\lambda,t}(\overline{\lambda}_t) \ \forall \text{ feasible } \overline{\lambda}_s = \overline{\lambda}_t + \Delta\lambda, \tag{6.13}$$

then the ADA procedure with a single ADA pair converges.

Remark 6.53 *From a mathematical point of view, Statement 6.52 is imprecise.*

- *The Siemens document does not explicitly state that the functions $\rho_{\lambda,s}$ and $\rho_{\lambda,t}$ are differentiable. The differentiability is assumed only implicitly.*
- *The Siemens document does not specify the sets of feasible $\overline{\lambda}_s$ and $\overline{\lambda}_t$. They just state that only such $\overline{\lambda}_t$ in the neighborhood of λ_t shall be considered, that can be realistically reached by drift [Loc18, p. 11].*
- *No statement with respect to the existence and uniqueness of the fixed point is done.*

Remark 6.54 *Although the content of Statement 6.52 can be considered as central with respect to the ADA procedure, it is not formulated as a theorem in this thesis. This is done, because from a mathematical point of view, the Siemens document does not provide a corresponding proof. The authors provide a sketch of proof only.*
In the opinion of the author of this thesis, a corresponding complete proof of Statement 6.52 would be no shorter and similarly elaborate as the proofs presented so far.

In the following, we show that if Assumption 6.48 holds, then Statement 6.52 can be considered to be equivalent to Theorem 6.43.

Theorem 6.55 *Let ι_s, ι_t, Λ_s and Λ_t be differentiable. Furthermore, let Assumption 6.48 hold. For $\overline{g} \in G_s \cap G_t$, we define $\overline{\lambda}_s := \Lambda_s(\overline{g})$ and $\overline{\lambda}_t := \Lambda_t(\overline{g})$. Then, we have*

$$\frac{d}{d\lambda}\rho_{\lambda,s}(\overline{\lambda}_s) > \frac{d}{d\lambda}\rho_{\lambda,t}(\overline{\lambda}_t) \;\Leftrightarrow\; \frac{d}{dg}\rho_t(\overline{g}) > \frac{d}{dg}\rho_s(\overline{g}).$$

Proof. According to Definition 6.50, we have $\rho_{\lambda,\mathrm{fs}} = \rho_{\mathrm{fs}} \circ \Lambda_{\mathrm{fs}}^{-1}$ and thus we apply the chain rule to show the statement.
First, we focus on the derivatives of Λ_s^{-1} and Λ_t^{-1}. By Assumption 6.48, we have $\Lambda_s(g) = \Lambda_t(g) + \Delta\lambda$ for all $g \in G_s \cap G_t$. Furthermore, Λ_s and Λ_t are strictly decreasing according to Definition 2.18. Hence, we have

$$\frac{d}{dg}\Lambda_s(g) = \frac{d}{dg}\Lambda_t(g) < 0 \;\forall\; g \in G_s \cap G_t. \tag{6.14}$$

As a consequence, the inverse functions $\Lambda_s(g)^{-1}$ and $\Lambda_t(g)^{-1}$ are also differentiable. By applying the inverse function rule, we obtain

$$\frac{d}{d\lambda}\Lambda_s^{-1}(\overline{\lambda}_s) = \frac{1}{\frac{d}{dg}\Lambda_s(\overline{g})} \quad \text{and} \quad \frac{d}{d\lambda}\Lambda_t^{-1}(\overline{\lambda}_t) = \frac{1}{\frac{d}{dg}\Lambda_t(\overline{g})},$$

with $\overline{g} \in G_s \cap G_t$ and $\overline{\lambda}_s = \Lambda_s(\overline{g})$ as well as $\overline{\lambda}_t = \Lambda_t(\overline{g})$.
Now, we apply the chain rule to $\rho_{\lambda,s}$ and $\rho_{\lambda,t}$, which gives us

$$\begin{aligned}\frac{d}{d\lambda}\rho_{\lambda,s}(\overline{\lambda}_s) > \frac{d}{d\lambda}\rho_{\lambda,t}(\overline{\lambda}_t) \;&\Leftrightarrow\; \frac{d}{dg}\rho_s(\overline{g}) \cdot \frac{1}{\frac{d}{dg}\Lambda_s(\overline{g})} > \frac{d}{dg}\rho_t(\overline{g}) \cdot \frac{1}{\frac{d}{dg}\Lambda_t(\overline{g})} \\ &\Leftrightarrow\; \frac{d}{dg}\rho_s(\overline{g}) < \frac{d}{dg}\rho_t(\overline{g}),\end{aligned}$$

where the second equivalence results from (6.14). □

Corollary 6.56 *Let ι_s, ι_t, Λ_s and Λ_t be differentiable and let A_{r_D} have a fixed point. Furthermore, let Assumption 6.48 hold. If for all $\overline{g} \in G_s \cap G_t$*

$$\frac{d}{d\lambda}\rho_{\lambda,s}(\overline{\lambda}_s) > \frac{d}{d\lambda}\rho_{\lambda,t}(\overline{\lambda}_t), \quad \textit{with } \overline{\lambda}_s := \Lambda_s(\overline{g}) \textit{ and } \overline{\lambda}_t := \Lambda_t(\overline{g}),$$

then A_{r_D} is contractive and the ADA algorithm converges to the fixed point for an arbitrary starting point $r \in \hat{R}_{r_D}$.

Corollary 6.56 is a nice result in the sense that the convergence conditions presented in the Siemens document are consistent with the results of the analysis in this thesis. However, similar to the ADA patent [Loc16], the Siemens document can be considered rather a technical document and less a mathematical paper, as already mentioned in Remarks 6.53 and 6.54.
A drawback of the approach in the Siemens document is, that the stated convergence conditions require that Assumption 6.48 is met. In contrast, the convergence conditions

deduced in this thesis and stated in Theorem 6.43 do not require that Assumption 6.48 is met. Therefore, Theorem 6.43 can be considered as a more general result.
The Siemens document considers the nominal situation and a single ADA pair only. Results with respect to the non-standard situation or to a plurality of ADA pairs are not provided. Therefore, a comparison of results related to a non-standard situation or to a plurality of ADA pairs cannot be done.

Another document that contains some statements about convergence conditions of ADA is the ADA patent [LS17], which was filed by Siemens. In Chapter 3 above, the ADA algorithm is presented in detail based on this patent. As mentioned in Section 3.3, the ADA patent contains only little information about convergence conditions. The ADA patent's authors state that "[t]he only pre-condition is that the function is uniformly rising or falling in the measurement range of the test point" [LS17, p. 8]. The term function in the citation refers to the ioni current versus λ curve with the fan speed fixed at the test fan speed t. Furthermore, they state that other aspects of this function are not relevant and the "shape and profile of the function remain unknown in this respect" [LS17, p. 8]. At this point, we can conclude that the convergence conditions stated in the patent are not sufficient in general. Because in order to guarantee convergence, the gradient at the test and at the start point have to be considered according to Theorem 6.43, Statement 6.52 and Corollary 6.56.

This concludes the analysis of the ADA algorithm with respect to a single ADA pair. The next section briefly summarizes the results so far.

6.4. Conclusion of Analysis with Respect to a Single ADA Pair

In this chapter, we have analyzed the ADA algorithm with a single ADA pair. The following list briefly recaps the findings.

- The ADA algorithm is based on a Picard iteration (Algorithm 6.1).
- The goal of ADA is to approximate the drifted test ioni current. The corresponding iteration function is A_{i,r_D} (Definition 6.5). By applying Ohm's law, a resistance based variant of the ADA algorithm can be deduced that approximates the drift resistance and has the iteration function A_{r_D} (Definition 6.21). Both variants are "equivalent" in the sense that their fixed point characteristics are identical (Theorem 6.32). The resistance based variant is more accessible to a theoretical analysis.
- If A_{r_D} is contractive, then it is a selfmap if and only if it has a unique fixed point. Then, the Picard iteration associated to A_{r_D} converges to this fixed point for an arbitrary feasible starting point (Lemma 6.35).
- If $\iota_s^{-1}(i_s) = \iota_t^{-1}(i_t)$ holds, then the sought drift resistance r_D is a fixed point of A_{r_D} (Lemma 6.37). This case is considered to be the nominal case. A situation with

$\iota_s^{-1}(i_s) \neq \iota_t^{-1}(i_t)$ is considered to be non-standard (Definition 6.39). Tolerances with respect to the ioni electrode's position cause non-standard situations. This becomes relevant in the following chapter, where a plurality of ADA pairs is considered.

- Under which conditions is A_{r_D} contractive? Some statements are possible if A_{r_D} is differentiable, which is the case if the ioni current functions ι_s and ι_t of the corresponding HE model are differentiable. If the absolute value of the derivative of A_{r_D} is smaller than one, then A_{r_D} is contractive (Lemma 4.44). This is the case, if $\frac{d}{dg}\rho_t(g) > \frac{d}{dg}\rho_s(g)$ for all $g \in G_s \cap G_t$ (Theorem 6.43). This result is consistent with convergence statements provided by Siemens (Section 6.3.4).

- A major conclusion is that the selection of the ADA parameters has a big influence on the convergence characteristics and thus on the success of the ADA procedure. Therefore, the optimization of the ADA parameters is closely related to their corresponding convergence characteristics (Remark 6.47).

The results so far can only partially be generalized to the case that a plurality of ADA pairs is considered. This is delineated in the following chapter.

7. ADA Procedure with a Plurality of ADA Pairs

In the preceding chapter, the convergence characteristics of the ADA Algorithm 5.2 in the case of a single ADA pair are thoroughly analyzed. However, as stated in Section 3.4.4, up to seven ADA pairs are usually used by Vaillant [Sch15, p. 35]. In this chapter, we analyze the fixed point and convergence characteristics of Algorithm 5.2 if a plurality of ADA pairs is considered, i.e., we consider the case $N \geq 2$. For this, let $N \in \mathbb{N}$, $N \geq 2$, be arbitrary but fixed.

The difficulty in the analysis of Algorithm 5.2 in the case of a plurality of ADA pairs is that an ADA update of ADA pair p, $p \geq 2$, depends on the values of i_p and i_{p-1}, which is $i_p \leftarrow \iota_{t^p,r_D} \circ \iota^{-1}_{s^p,r_D} \circ \gamma^p \circ \omega^p\big(\beta^p(i_p), \beta^{p-1}(i_{p-1})\big)$ according to Line 11 of Algorithm 5.2. In contrast, an update of ADA pair $p = 1$ depends on i_1 only according to Line 9.

This problem can be partly overcome by considering a situation where the incumbent drifted test ioni current approximation of ADA pair $p-1$ is constant. For instance, such a situation occurs if the ioni current iteration function of ADA pair one, A^1_{i,r_D}, has a unique fixed point i_1^* and the first component of the incumbent drifted test ioni current vector i_1 is equal to i_1^*. Because i_1^* is the fixed point of A^1_{i,r_D}, $i_1 = A^1_{i,r_D}(i_1)$ holds in each iteration of Algorithm 5.2 with $p = 1$ in this case. Then, in each update with ADA pair $p = 2$ the same $i_1 = i_1^*$ is used and the update function corresponding to Line 11 of Algorithm 5.2 can be considered as a one-dimensional iteration function that depends on i_2 only, which is

$$i_2 \leftarrow \iota_{t^2,r_D} \circ \iota^{-1}_{s^2,r_D} \circ \gamma^2 \circ \omega^2\big(\beta^2(i_2), \beta^1(i_1^*)\big). \tag{7.1}$$

Let us suppose, that the iteration function corresponding to (7.1) is a contractive self-map. Then, it has a certain unique fixed point i_2^* and the Picard iteration associated to this function converges to i_2^* for an arbitrary (feasible) starting point. Thus, after sufficiently many subsequent updates of ADA pair $p = 2$, the second component of the incumbent vector, i_2, gets arbitrary close to i_2^*. When thereafter ADA pair $p = 3$ is updated, we can assume i_2 to be (almost) fixed at i_2^* and so on, i.e., we can recursively construct a vector of corresponding fixed points.

The major result of this chapter is Theorem 7.68, which states that the output of Algorithm 5.2, $\hat{\boldsymbol{i}}_{\boldsymbol{t},\text{out}}(\hat{\boldsymbol{i}}_{\boldsymbol{t},\text{in}}, u)$, converges to the aforementioned vector of fixed points if the considered ADA update sequence u contains sufficiently many iterations with each ADA pair and the considered input vector $\hat{\boldsymbol{i}}_{\boldsymbol{t},\text{in}}$ is "feasible". Similar to the case $N = 1$, this convergence property is shown by considering a resistance based approach that is in a certain sense equivalent but more accessible to a convergence analysis.

The aforementioned vector of fixed points and a required corresponding formalism are detailed in the following section. This includes the definition of the iteration function corresponding to (7.1) and its domain for the more general case $p \geq 2$. Thereafter, a resistance based approach is introduced and finally the convergence statement is proven.

Recall that Algorithm 5.2 also has the inputs $\mathcal{H}$, (s^j, t^j, i_s^j, i_t^j), $j \in [N]$, and r_D in addition to $\hat{\boldsymbol{i}}_{\boldsymbol{t},\text{in}}$ and u. Therefore, we implicitly assume that an HE model $\mathcal{H}$, N ADA pairs (s^j, t^j, i_s^j, i_t^j), $j \in [N]$, as well as a drift resistance $r_D \geq 0$ are given for the remainder of this chapter.

7.1. The Super Fixed Point Vector

The goal of this section is to define the vector of fixed points mentioned in the introduction to this chapter. Because the components of this vector are fixed points that are recursively constructed from preceding fixed points, this vector is called the super fixed point vector in Definition 7.14 below. In the course of this chapter it is shown that under certain conditions the super fixed point vector is the limit of the ADA Algorithm 5.2 and thus it is essential for the analysis of the ADA algorithm's convergence characteristics. The definition of the super fixed point vector requires a certain formalism, which is delineated in the following.
According to Line 11 of Algorithm 5.2, an update with ADA pair p, $p \geq 2$, is done by calculating

$$i_p \leftarrow \iota_{t^p,r_D} \circ \iota_{s^p,r_D}^{-1} \circ \gamma^p \circ \omega^p\big(\beta^p(i_p), \beta^{p-1}(i_{p-1})\big) \tag{7.2}$$

If we suppose that i_{p-1} is fixed, we can treat (7.2) as a one-dimensional iteration function with i_p as the only argument. This motivates the following definition, where the weighted sum function $\omega^p(x, y) = w^p x + (1 - w^p)y$ from Definition 5.17 is considered as a function of the first argument x only.

Definition 7.1 *Let $p \in \{2, \ldots, N\}$ and let $y \in \mathbb{R}$. We define*

$$\omega_y^p : \mathbb{R} \to \mathbb{R}, \quad \omega_y^p(x) \coloneqq w^p x + (1 - w^p)y,$$

where w^p is the weight according to Definition 5.12.

Lemma 7.2 *The function ω_y^p is a homeomorphism. Its inverse function is $\big(\omega_y^p\big)^{-1}(z) = \frac{1}{w^p}\big(z - (1 - w^p)y\big)$. Furthermore, both functions are strictly increasing.*

Proof. According to Lemma 5.13, we have $0 < w^p < 1$ and thus

$$\begin{aligned} z = \omega_y^p(x) \;&\Leftrightarrow\; z = w^p x + (1 - w^p)y \;\Leftrightarrow w^p x = z - (1 - w^p)y \\ &\Leftrightarrow\; x = \frac{1}{w^p}\big(z - (1 - w^p)y\big) =: \big(\omega_y^p\big)^{-1}(z) \;\forall\, x \in \mathbb{R}. \end{aligned}$$

As linear functions, ω_y^p and $\big(\omega_y^p\big)^{-1}$ are continuous. Their slopes are w^p and $\frac{1}{w^p}$, respectively. Since $0 < w^p < 1$, both functions are strictly increasing. □

We use ω_y^p to reformulate (7.2) to a function with a single argument. For this, let us assume that $i_{p-1} \in \mathbb{R}_{>0}$ is given and fixed. Then, $\beta^{p-1}(i_{p-1}) = \frac{U}{i_{p-1}} - \frac{U}{i_t^p}$ exists and we have $\omega^p\big(\beta^p(i_p), \beta^{p-1}(i_{p-1})\big) = \omega^p_{\beta^{p-1}(i_{p-1})} \circ \beta^p(i_p)$. Therefore, the composition $\iota_{t^p,r_D} \circ \iota^{-1}_{s^p,r_D} \circ \gamma^p \circ \omega^p_{\beta^{p-1}(i_{p-1})} \circ \beta^p$ is the resulting iteration function if i_{p-1} is fixed. Before we formally define a corresponding function, we specify an appropriate domain.
Recall from Lemma 5.32 and Line 10 of Algorithm 5.2 that an update of the p-th component of the incumbent drifted test ioni current vector $\hat{\boldsymbol{i}}_{t,r_D} = (i_1, \ldots, i_N)$ is well-defined, if $\omega^p\big(\beta^p(i_p), \beta^{p-1}(i_{p-1})\big) \in \hat{R}^p_{r_D}$ holds. Expressed in the notation with i_{p-1} fixed, we are interested in elements i_p such that $\omega^p_{\beta^{p-1}(i_{p-1})} \circ \beta^p(i_p) \in \hat{R}^p_{r_D}$. Because $\omega^p_{\beta^{p-1}(i_{p-1})}$ and β^p are homeomorphisms, the set $\big(\beta^p\big)^{-1} \circ \big(\omega^p_{\beta^{p-1}(i_{p-1})}\big)^{-1}(\hat{R}^p_{r_D})$ is a candidate for the sought domain. However, we have to make sure that this set is well-defined. This is not always the case and depends on the element $\beta^{p-1}(i_{p-1})$. The following definition reflects this fact. Recall that the sets $\hat{R}^p_{r_D}$ are nonempty, closed and bounded intervals (Lemma 6.11) and thus their minima exist.

Remark 7.3 *In the following Definition 7.4, the physical interpretation of the real number v is $v = \beta^{p-1}(i_{p-1})$, i.e., v corresponds to the drift resistance approximation of ADA pair $p-1$ if the drifted test ioni current approximation i_{p-1} is given. In other words, the elements v are abbreviations for elements of the type $\beta^{p-1}(i_{p-1})$.*
Furthermore, because the fan speeds of ADA pair $p-1$ are greater than the fan speeds of ADA pair p, the ADA pair $p-1$ is also referred to as the upper neighbor of ADA pair p.

Definition 7.4 *Let $p \in \{2, \ldots, N\}$ and let $r_D \geq 0$. The* set of feasible upper neighbor drift resistance approximations of ADA pair p with respect to r_D *is defined by*

$$V^p_{r_D} := \left\{ v \in \mathbb{R} : v < \frac{\min \hat{R}^p_{r_D} + w^p r_t^p}{1 - w^p} \right\},$$

where $0 < w^p < 1$ are the weights from Definition 5.12.
Let $v \in V^p_{r_D}$ be fixed. The set of feasible drift resistance approximations of ADA pair p given v *is defined by*

$$\hat{R}^p_{r_D,v} := \big(\omega^p_v\big)^{-1}(\hat{R}^p_{r_D}) = \left\{ \frac{1}{w^p}\big(r - (1-w^p)v\big) : r \in \hat{R}^p_{r_D} \right\} =: \frac{1}{w^p}\big(\hat{R}^p_{r_D} - (1-w^p)v\big).$$

The set of feasible drifted test ioni current approximations of ADA pair p given v *is defined by*

$$\hat{I}^p_{r_D,v} := \big(\beta^p\big)^{-1}(\hat{R}^p_{r_D,v}) = \left\{ \frac{U}{r + r_t^p} : r \in \hat{R}^p_{r_D,v} \right\} =: \frac{U}{\hat{R}^p_{r_D,v} + r_t^p}.$$

Lemma 7.5 *The sets $V^p_{r_D}$, $\hat{R}^p_{r_D,v}$ and $\hat{I}^p_{r_D,v}$ are well-defined. Furthermore, $\hat{R}^p_{r_D,v} \subset (-r_t^p, \infty)$ and $\hat{I}^p_{r_D,v} \subset \mathbb{R}_{>0}$ hold.*

Proof. Let $p \in \{2, \ldots, N\}$. Because $\hat{R}^p_{r_D}$ is a closed and nonempty interval (Lemma 6.11), its minimum $\min \hat{R}^p_{r_D}$ exists. Furthermore, $0 < w^p < 1$ holds (Lemma 5.13) and thus the

set $V_{r_D}^p$ is well-defined.
Let $v \in V_{r_D}^p$. Because $\omega_v^p : \mathbb{R} \to \mathbb{R}$ is a homeomorphism (Lemma 7.2), the set $\hat{R}_{r_D,v}^p := \left(\omega_v^p\right)^{-1}(\hat{R}_{r_D}^p)$ is well-defined.
To show that $\hat{I}_{r_D,v}^p := \left(\beta^p\right)^{-1}(\hat{R}_{r_D,v}^p)$ is well-defined, we have to show that $\hat{R}_{r_D,v}^p \subset (-r_t^p, \infty)$, because $(-r_t^p, \infty)$ is the domain of $\left(\beta^p\right)^{-1}$ (Definition 5.9). So, let $r_v \in \hat{R}_{r_D,v}^p$. Then, there exists $r \in \hat{R}_{r_D}^p$ such that $r_v = \left(\omega_v^p\right)^{-1}(r) = \frac{1}{w^p}\big(r - (1 - w^p)v\big)$. Because $v \in V_{r_D}^p$ and $r \geq \min \hat{R}_{r_D}^p$, we have

$$
\begin{aligned}
& v < \frac{\min \hat{R}_{r_D}^p + w^p r_t^p}{1 - w^p} \leq \frac{r + w^p r_t^p}{1 - w^p} \\
\Rightarrow\ & (1 - w^p)v < r + w^p r_t^p \\
\Rightarrow\ & -w^p r_t^p < r - (1 - w^p)v \\
\Rightarrow\ & -r_t^p < \frac{1}{w^p}\big(r - (1 - w^p)v\big) = \left(\omega_v^p\right)^{-1}(r) = r_v \ \Rightarrow\ r_v \in (-r_t^p, \infty).
\end{aligned}
$$

Furthermore, we have

$$
i \in \hat{I}_{r_D,v}^p \ \Rightarrow\ \exists\, r_v \in \hat{R}_{r_D,v}^p : i = (\beta^p)^{-1}(r_v) = \frac{U}{r_v + r_t^p} \ \Rightarrow\ i > 0,
$$

where the last implication follows from $\hat{R}_{r_D,v}^p \subset (-r_t, \infty)$ and $U > 0$. □

Remark 7.6 *The sets $V_{r_D}^p$, $\hat{R}_{r_D,v}^p$ and $\hat{I}_{r_D,v}^p$ are abstract in the sense that they are only introduced to guarantee that the following steps are well-defined. For instance, for the optimization models that are developed in Chapter 8 the set $V_{r_D}^p$ is not required anymore, see also Remark 8.8. From a practical point of view, they are irrelevant, because drifted test ioni current approximations not contained in $\hat{I}_{r_D,v}^p$ usually correspond to infeasible combustion states.*

Lemma 7.7 *Let $p \in \{2, \dots, N\}$ and let $v \in V_{r_D}^p$. The sets $\hat{R}_{r_D,v}^p$ and $\hat{I}_{r_D,v}^p$ are closed, bounded and nonempty intervals.*

Proof. The set $\hat{R}_{r_D}^p$ is a closed, bounded and nonempty interval (Lemma 6.11) and the functions β^p and ω_v^p are homeomorphisms (Lemmas 5.11 and 7.2, respectively). Therefore, $\hat{R}_{r_D,v}^p = \left(\omega_v^p\right)^{-1}(\hat{R}_{r_D}^p)$ and $\hat{I}_{r_D,v}^p = \left(\beta^p\right)^{-1}(\hat{R}_{r_D,v}^p) = \left(\beta^p\right)^{-1} \circ \left(\omega_v^p\right)^{-1}(\hat{R}_{r_D}^p)$ are also closed, bounded and nonempty intervals. □

Now, we have all the parts together to define the aforementioned iteration function that corresponds to (7.2) with i_{p-1} fixed.

Definition 7.8 *Let $p \in \{2, \dots, N\}$, let $r_D \geq 0$ and let $i_{p-1} \in \mathbb{R}_{>0}$ such that $v := \beta^{p-1}(i_{p-1}) \in V_{r_D}^p$. The* ioni current based iteration function of ADA pair p given v *is defined by*

$$
B_{r_D,v}^p : \hat{I}_{r_D,v}^p \to \mathbb{R}_{>0}, \quad B_{r_D,v}^p(i) := \iota_{t^p,r_D} \circ \iota_{s^p,r_D}^{-1} \circ \gamma^p \circ \omega_v^p \circ \beta^p(i).
$$

Remark 7.9 *Note that the superscript p indicates the ADA pair number. It does not indicate the successive evaluation of the function in the context of the Picard iteration.*

Lemma 7.10 *The function $B^p_{r_D,v}$ is well-defined, i.e., it can be evaluated for all $i \in \hat{I}^p_{r_D,v}$. Furthermore, $B^p_{r_D,v}(i) > 0$ holds for all $i \in \hat{I}^p_{r_D,v}$.*

Proof. Let $i \in \hat{I}^p_{r_D,v}$. By Definition 7.4, we have $\hat{I}^p_{r_D,v} = \left(\beta^p\right)^{-1} \circ \left(\omega^p_v\right)^{-1}(\hat{R}^p_{r_D})$ and thus

$$i \in \hat{I}^p_{r_D,v} \;\Rightarrow\; \exists\, r \in \hat{R}^p_{r_D} : i = \left(\beta^p\right)^{-1} \circ \left(\omega^p_v\right)^{-1}(r) \;\Rightarrow\; \omega^p_v \circ \beta^p(i) \in \hat{R}^p_{r_D}.$$

Because $\iota_{t^p,r_D} \circ \iota^{-1}_{s^p,r_D} \circ \gamma^p(r)$ is well-defined for all $r \in \hat{R}^p_{r_D}$ (Corollary 5.24) and the image of ι_{t^p,r_D} is a subset of $\mathbb{R}_{>0}$ (Notation 3.17 and Corollary 3.18), we have $B^p_{r_D,v}(i) := \iota_{t^p,r_D} \circ \iota^{-1}_{s^p,r_D} \circ \gamma^p \circ \omega^p_v \circ \beta^p(i) > 0$. □

We use the domains $\hat{I}^p_{r_D,v}$ according to Definition 7.4 and the functions $B^p_{r_D,v}$ according to Definition 7.8 and reformulate Algorithm 5.2 to Algorithm 7.1, which facilitates the analysis of its convergence characteristics later on.

Algorithm 7.1 Reformulated Version of Algorithm 5.2

Input:

$\mathcal{H} = \left(\mathrm{FS}, (G_{\mathrm{fs}})_{\mathrm{fs}\in\mathrm{FS}}, (\iota_{\mathrm{fs}})_{\mathrm{fs}\in\mathrm{FS}}, (\Lambda_{\mathrm{fs}})_{\mathrm{fs}\in\mathrm{FS}}, (\zeta_{\mathrm{fs}})_{\mathrm{fs}\in\mathrm{FS}}\right)$ // *HE model*

(s^j, t^j, i^j_s, i^j_t), $j \in [N]$ // *ADA parameters of N ADA pairs*

$r_D \in \mathbb{R}_{\geq 0}$ // *drift resistance*

$\hat{\boldsymbol{i}}_{\boldsymbol{t},\mathrm{in}} = (i_1, \ldots, i_N) \in \mathbb{R}^N_{>0}$ // *initial drifted test ioni current approximations*

$(u_k)_{k\in[\ell]}$ // *ADA update sequence of length ℓ*

Calculations:

for $k = 1$ to ℓ **do**
  $p = u_k$
  if $p = 1$ and $i_1 \in \hat{I}^1_{r_D}$ **then**
    $i_1 \leftarrow A^1_{i,r_D}(i_1)$
  else if $p \geq 2$ and $i_p \in \hat{I}^p_{r_D,\beta^{p-1}(i_{p-1})}$ **then**
    $i_p \leftarrow B^p_{r_D,\beta^{p-1}(i_{p-1})}(i_p)$
  else
    $i_j \leftarrow$ NaN for all $j \in [N]$ // *mark results as not valid*
    break // *leave for-loop early*
  end if
end for

Output:

$\hat{\boldsymbol{i}}_{\boldsymbol{t},\mathrm{out}} = (i_1, \ldots, i_N)$ // *updated drifted test ioni current approximations*

Lemma 7.11 *Given the same inputs, the outputs of Algorithm 5.2 and Algorithm 7.1 are identical.*

Proof. The framework around the for-loops of both algorithms is identical. It remains to show that the calculations within both for-loops are identical.

- Definition 6.3: $i_1 \in \hat{I}^1_{r_D} \Leftrightarrow \beta^1(i_1) \in \hat{R}^1_{r_D}$ and thus Line 8 of Algorithm 7.1 corresponds to Line 8 of Algorithm 5.2.

- Definition 6.5: $A^p_{i,r_D}(i) := \iota_{t^p,r_D} \circ \iota^{-1}_{s^p,r_D} \circ \gamma^p \circ \beta^p(i) \; \forall \; i \in \hat{I}^p_{r_D}$ and thus Line 9 of Algorithm 7.1 corresponds to Line 9 of Algorithm 5.2.

- Definition 7.4: $\hat{I}^p_{r_D,\beta^{p-1}(i_{p-1})} = \left(\beta^p\right)^{-1}\left(\hat{R}^p_{r_D,\beta^{p-1}(i_{p-1})}\right) = \left(\beta^p\right)^{-1} \circ \left(\omega^p_{\beta^{p-1}(i_{p-1})}\right)^{-1}(\hat{R}^p_{r_D})$, i.e., $i_p \in \hat{I}^p_{\beta^{p-1}(i_{p-1})} \Leftrightarrow \omega^p_{\beta^{p-1}(i_{p-1})} \circ \beta^p(i_p) = \omega^p\left(\beta^p(i_p), \beta^{p-1}(i_{p-1})\right) \in \hat{R}^p_{r_D}$, and thus Line 10 of Algorithm 7.1 corresponds to Line 10 of Algorithm 5.2.

- Definition 7.8: $B^p_{r_D,v}(i) := \iota_{t^p,r_D} \circ \iota^{-1}_{s^p,r_D} \circ \gamma^p \circ \omega^p_v \circ \beta^p(i) = \iota_{t^p,r_D} \circ \iota^{-1}_{s^p,r_D} \circ \gamma^p \circ \omega^p\left(\beta^p(i), v\right) \; \forall \; i \in \hat{I}^p_{r_D,v}$ and thus Line 11 of Algorithm 7.1 corresponds to Line 11 of Algorithm 5.2.

The subsequent lines are identical in both for-loops. □

Remark 7.12 *Aiming at a better readability, when there is no risk of confusion, the subscript r_D of the sets $\hat{R}^p_{r_D}$, $\hat{I}^p_{r_D}$, $V^p_{r_D}$, $\hat{R}^p_{r_D,v}$ and $\hat{I}^p_{r_D,v}$ as well as of the iteration functions $A^p_{r_D}$, A^p_{i,r_D} and $B^p_{r_D,v}$ is omitted for the remainder of this chapter.*

Now, we have all the parts together to define the aforementioned super fixed point vector. The basic idea behind this vector is presented in the introduction to this chapter. At this point, this idea is briefly repeated but this time by utilizing the iteration functions B^p_v and the reformulated Algorithm 7.1. For this, we introduce a notation for the situation that a function f has a unique fixed point.

Notation 7.13 *Let $X \subset \mathbb{R}$ and let $f : X \to X$ be a selfmap. If f has a* **unique** *fixed point $x^* \in X$, then this fixed point is denoted by* $\mathrm{fix}(f)$*, i.e.,* $\mathrm{fix}(f) := x^*$.

Let the ioni current iteration function of the first ADA pair, A^1_i, have the unique fixed point $\mathrm{fix}(A^1_i)$. If the first component of the incumbent drifted test ioni current vector is $i_1 = \mathrm{fix}(A^1_i)$, then i_1 does not change anymore independent of arbitrary subsequent ADA iterations. Therefore, we can consider $i_1 = \mathrm{fix}(A^1_i)$ as constant. In this case, the iteration function for ADA updates with the second ADA pair is $B^2_{\beta^1(i_1)} = B^2_{\beta^1\left(\mathrm{fix}(A^1_i)\right)}$. If in addition the second component of the incumbent vector is $i_2 = \mathrm{fix}\left(B^2_{\beta^1\left(\mathrm{fix}(A^1_i)\right)}\right)$, then i_2 also remains constant independent of arbitrary subsequent ADA iterations and so on. This recursive construction is formally defined in the following. The corresponding vector is called super fixed point vector, because its components are fixed points of functions that are related to the fixed points of the preceding components.

Definition 7.14 *Let N ADA pairs (s^p, t^p, i_s^p, i_t^p), $p \in [N]$, an HE model $\mathcal{H}$ and a drift resistance $r_D \geq 0$ be given. The corresponding* super fixed point vector $\boldsymbol{i}^{**} = (i_1^{**}, \ldots, i_N^{**})$ *is recursively defined by*

$$i_1^{**} := \begin{cases} \mathrm{fix}(A_i^1) & \text{if } \mathrm{fix}(A_i^1) \text{ exists,} \\ \mathrm{NaN} & \text{else,} \end{cases}$$

and for $p \in \{2, \ldots, N\}$ by

$$i_p^{**} := \begin{cases} \mathrm{fix}\big(B^p_{\beta^{p-1}(i_{p-1}^{**})}\big) & \text{if } i_{p-1}^{**} \neq \mathrm{NaN} \text{ and } \mathrm{fix}\big(B^p_{\beta^{p-1}(i_{p-1}^{**})}\big) \text{ exists,} \\ \mathrm{NaN} & \text{else.} \end{cases}$$

The super fixed point vector is called feasible*, if $\boldsymbol{i}^{**} \in \mathbb{R}^N$ holds, i.e., if none of its components is* NaN*.*

Remark 7.15 *The definition of the super fixed point vector depends on the iteration functions A^1_{i,r_D} and $B^p_{r_D,v}$, $p \in \{2, \ldots, N\}$. Therefore, it is implicitly related to the ADA pairs, to the HE model $\mathcal{H}$ and to the drift resistance r_D.*

Definition 7.16 *The consideration of N ADA pairs (s^p, t^p, i_s^p, i_t^p), $p \in [N]$, an HE model $\mathcal{H}$ and a drift resistance $r_D \geq 0$ such that $\boldsymbol{i}^{**}$ is feasible is referred to as a* feasible scenario*. In other words, we a have a feasible scenario if and only if $\boldsymbol{i}^{**} \in \mathbb{R}^N$.*

Lemma 7.17 *The super fixed point vector is unique.*

Proof. According to Notation 7.13, $\mathrm{fix}(f)$ implies that $\mathrm{fix}(f)$ is the unique fixed point of f. With this, the uniqueness of $\boldsymbol{i}^{**}$ follows by construction. □

Lemma 7.18 *If the super fixed point vector is feasible, then $\boldsymbol{i}^{**} \in \mathbb{R}^N_{>0}$, i.e., all components of $\boldsymbol{i}^{**}$ are positive.*

Proof. Let $\boldsymbol{i}^{**} = (i_1^{**}, \ldots, i_N^{**})$ be feasible, i.e., $i_p^{**} \in \mathbb{R}$ for all $p \in [N]$. Then, we have $i_1^{**} \in \hat{I}^1$. Because $\hat{I}^1 \subset \mathbb{R}_{>0}$ (Lemma 6.4), $i_1^{**} > 0$ holds. For $p \geq 2$, we have $i_p^{**} \in \hat{I}_v^p$ and $\hat{I}_v^p \subset \mathbb{R}_{>0}$ (Lemma 7.5) with $v = \beta^{p-1}(i_{p-1}^{**})$. Therefore, $i_p^{**} > 0$ holds for all $p \in \{2, \ldots, N\}$ as well. □

Remark 7.19 *An example of a super fixed point vector is given in Example 7.44 below, after the drift resistance based iteration function $C^p_{r_D,v}$ is introduced in Definition 7.36 below. This is done, because a corresponding example with drift resistance iteration functions is more straightforward.*

As already mentioned, under certain conditions the super fixed point vector is the limit of the output of Algorithm 5.2 according to Theorem 7.68 below. However, Algorithm 5.2 is only defined for finite ADA update sequences, because otherwise its for-loop would not terminate. A concept to consider the output of Algorithm 5.2 for infinite ADA update sequences is to consider the first n elements of an infinite ADA update sequence. Then, we can analyze the behavior of the Algorithm's output if n is successively increased. This motivates the following definitions.

Definition 7.20 *Let $u = (u_n)_{n\in[\ell]}$ be an ADA update sequence of length ℓ, $\ell \in \mathbb{N}$. The* ADA subsequence *that contains the first k elements of u is denoted by $u(k)$, $k \in [\ell]$. It is element-wise defined by $u(k)_n := u_n$ for all $n \in [k]$. This definition is also valid for infinite ADA update sequences $u = (u_n)_{n\in\mathbb{N}}$.*

Example 7.21 *Let $N = 3$ and let $u := (1, 2, 3, 1, 2, 3, 1, 2, 3)$ be an ADA sequence of length $\ell = 9$. Then, the ADA subsequence corresponding to $k = 4$ is $u(k) = (1, 2, 3, 1)$.*

Definition 7.22 *Let $\hat{\boldsymbol{i}}_{\boldsymbol{t},\text{in}} \in \mathbb{R}^N_{>0}$ be an input vector and let u be an ADA update sequence (finite or infinite). The n-th* ADA iterate with respect to $\hat{\boldsymbol{i}}_{\boldsymbol{t},\text{in}}$ and u *is defined by*

$$\boldsymbol{i}^n(\hat{\boldsymbol{i}}_{\boldsymbol{t},\text{in}}, u) := \hat{\boldsymbol{i}}_{\boldsymbol{t},\text{out}}\big(\hat{\boldsymbol{i}}_{\boldsymbol{t},\text{in}}, u(n)\big), \text{ where } n \begin{cases} \leq \ell & \text{if } u \text{ is of length } \ell \\ \in \mathbb{N} & \text{if } u \text{ is an infinite sequence,} \end{cases}$$

where $\hat{\boldsymbol{i}}_{\boldsymbol{t},\text{out}}\big(\hat{\boldsymbol{i}}_{\boldsymbol{t},\text{in}}, u(n)\big)$ is the output of Algorithm 5.2 given the inputs $\hat{\boldsymbol{i}}_{\boldsymbol{t},\text{in}}$ and $u(n)$ according to Definition 5.36. The components of the n-th ADA iterate are denoted by $\boldsymbol{i}^n(\hat{\boldsymbol{i}}_{\boldsymbol{t},\text{in}}, u) = (i^n_1, \ldots, i^n_N)$.

Corollary 7.23 *By construction, the n-th ADA iterate $\boldsymbol{i}^n(\hat{\boldsymbol{i}}_{\boldsymbol{t},\text{in}}, u)$ corresponds to the incumbent drifted test ioni current vector after the n-th iteration with the for-loop of Algorithm 7.1 given the inputs $\hat{\boldsymbol{i}}_{\boldsymbol{t},\text{in}}$ and u.*

The ADA iterates can be recursively calculated, if the corresponding outputs of Algorithm 5.2 are valid, i.e., if no component of the corresponding output vectors is NaN. To avoid case distinctions with respect to such a situation a feasibility condition is introduced before the recursive formula to calculate the ADA iterates is presented.

Definition 7.24 *An input vector $\hat{\boldsymbol{i}}_{\boldsymbol{t},\text{in}} \in \mathbb{R}^N_{>0}$ and an ADA update sequence u are called* feasible input combination, *if all ADA iterates $\boldsymbol{i}^n = (i^n_1, \ldots, i^n_N)$ are an element of $\mathbb{R}^N$, i.e., if $i^n_p \neq$ NaN for all $p \in [N]$ and for all $n \in [\ell]$ (u of length ℓ) or for all $n \in \mathbb{N}$ (u infinite sequence).*

Remark 7.25 *Note that Definition 7.24 is implicitly related to an HE model $\mathcal{H}$, the ADA parameters (s^j, t^j, i^j_s, i^j_t), $j \in [N]$, and the drift resistance r_D. For instance, let $\overline{\mathcal{H}} \neq \mathcal{H}$ be two different HE models. Then, $\hat{\boldsymbol{i}}_{\boldsymbol{t},\text{in}}$ and u being a feasible input combination for $\mathcal{H}$, (s^j, t^j, i^j_s, i^j_t), $j \in [N]$, and r_D does not imply that they are a feasible input combination for $\overline{\mathcal{H}}$, (s^j, t^j, i^j_s, i^j_t), $j \in [N]$, and r_D.*

Remark 7.26 *As already mentioned at the introduction to this Chapter 7, it is implicitly assumed that an HE model $\mathcal{H}$, a drift resistance $r_D \geq 0$ and N ADA pairs (s^p, t^p, i^p_s, i^p_t), $p \in [N]$, are given for the remainder of this chapter.*

For feasible input combinations the ADA iterates can be recursively calculated as follows.

Lemma 7.27 *Let $\hat{\boldsymbol{i}}_{\boldsymbol{t},\text{in}} \in \mathbb{R}^N_{>0}$ be an input vector and let $u = (u_n)_{n\in[\ell]}$ ($n \in \mathbb{N}$) be a finite (infinite) ADA update sequence such that they are a feasible input combination. Let $\boldsymbol{i}^n(\hat{\boldsymbol{i}}_{\boldsymbol{t},\text{in}}, u) = (i_1^n, \ldots, i_N^n)$ be the corresponding n-th ADA iterate. Then, the following recursion with $\boldsymbol{i}^0(\hat{\boldsymbol{i}}_{\boldsymbol{t},\text{in}}, u) := \hat{\boldsymbol{i}}_{\boldsymbol{t},\text{in}}$ holds for all $n \in [\ell]$ ($n \in \mathbb{N}$):*

$$\boldsymbol{i}^n(\hat{\boldsymbol{i}}_{\boldsymbol{t},\text{in}}, u) = \begin{cases} \left(A_i^1(i_1^{n-1}), i_2^{n-1}, \ldots, i_N^{n-1}\right) & \text{if } u_n = 1, \\ \left(i_1^{n-1}, \ldots, i_{p-1}^{n-1}, B^p_{\beta^{p-1}(i_{p-1}^{n-1})}(i_p^{n-1}), i_{p+1}^{n-1}, \ldots, i_N^{n-1}\right) & \text{if } u_n =: p \geq 2. \end{cases} \tag{7.3}$$

In particular, $\boldsymbol{i}^n(\hat{\boldsymbol{i}}_{\boldsymbol{t},\text{in}}, u) \in \mathbb{R}^N_{>0}$ holds.

Proof. Let $i^{\text{in}} = (i_1^{\text{in}}, \ldots, i_N^{\text{in}})$ be an input vector and let $u = (u_n)_{n\in[\ell]}$ be an ADA update sequence of length ℓ such that $\hat{\boldsymbol{i}}_{\boldsymbol{t},\text{in}}$ and u are a feasible input combination. Because $\hat{\boldsymbol{i}}_{\boldsymbol{t},\text{in}}$ and u are a feasible input combination, the conditions $i_1^{n-1} \in \hat{I}^1$ (if $u_n = 1$) and $i_p^n \in \hat{I}^p_{\beta^{p-1}(i_{p-1}^{n-1})}$ (if $u_n \geq 2 =: p$) are met for all $n \in [\ell]$ (Definition 7.24), i.e., all considered function evaluations are well-defined in this proof. In the following, the statement is shown by induction over the length n of the ADA subsequences $u(n)$, i.e., over the first n entries of u, $n \in [\ell]$.

Base case:

Let $n = 1$, then $u(n) = (u_1)$ with $u_1 \in [N]$. The corresponding output of Algorithm 7.1 is

$$\hat{\boldsymbol{i}}_{\boldsymbol{t},\text{out}}\left(\hat{\boldsymbol{i}}_{\boldsymbol{t},\text{in}}, u(1)\right) = \begin{cases} \left(A_i^1(i_1^{\text{in}}), i_2^{\text{in}}, \ldots, i_N^{\text{in}}\right) & \text{if } u_1 = 1, \\ \left(i_1^{\text{in}}, \ldots, i_{p-1}^{\text{in}}, B^p_{\beta^{p-1}(i_{p-1}^{\text{in}})}(i_p^{\text{in}}), i_{p+1}^{\text{in}}, \ldots, i_N^{\text{in}}\right) & \text{if } u_1 =: p \geq 2. \end{cases}$$

Because $\boldsymbol{i}^1(\hat{\boldsymbol{i}}_{\boldsymbol{t},\text{in}}, u) = \hat{\boldsymbol{i}}_{\boldsymbol{t},\text{out}}\left(\hat{\boldsymbol{i}}_{\boldsymbol{t},\text{in}}, u(1)\right)$ according to Definition 7.22, (7.3) hods for $n = 1$.

Induction hypothesis:

For a certain $k < \ell$ let (7.3) hold for all $n \leq k$.

Induction step:

Let u_{k+1} be the $(k+1)$st entry of the ADA update sequence u. According to Corollary 7.23, the incumbent vector after the k-th iteration of the for-loop of Algorithm 7.1 is the k-th ADA iterate $\boldsymbol{i}^k(\hat{\boldsymbol{i}}_{\boldsymbol{t},\text{in}}, u) = (i_1^k, \ldots, i_N^k)$, which is recursively calculated by (7.3) according to the induction hypothesis. In the $(k+1)$st iteration, the for-loop is executed with $(i_1, \ldots, i_N) = (i_1^k, \ldots, i_N^k)$ and with $p = u_{k+1}$. Only the p-th component is updated by

$$i_p \leftarrow \begin{cases} A_i^1(i_1) & \text{if } p = 1 \\ B^p_{\beta^{p-1}(i_{p-1})}(i_p) & \text{if } p \geq 2, \end{cases} \quad \text{i.e.,} \quad i_p^{k+1} = \begin{cases} A_i^1(i_1^k) & \text{if } p = 1 \\ B^p_{\beta^{p-1}(i_{p-1}^k)}(i_p^k) & \text{if } p \geq 2. \end{cases}$$

The remaining components are not updated in the $(k+1)$st iteration and thus $i_{\bar{p}}^{k+1} = i_{\bar{p}}^k$ holds for $\bar{p} \in [N] \setminus \{p\}$. In total, (7.3) also holds for $n = k+1$.

The base case and the induction step are also valid for infinite ADA update sequences and thus (7.3) holds for infinite ADA update sequences as well.

Because the codomains of all considered iteration functions are $\mathbb{R}_{>0}$ (Lemmas 6.8 and 7.10), $\boldsymbol{i}^n(\hat{\boldsymbol{i}}_{\boldsymbol{t},\text{in}}, u) \in \mathbb{R}^N_{>0}$ holds for all $n \in [\ell]$.

□

With the concept of ADA iterates at hand, we can consider the output of Algorithm 5.2 for infinite ADA update sequences. Let u be an infinite ADA update sequence and let $\hat{\boldsymbol{i}}_{\boldsymbol{t},\text{in}}$ be an input vector such that $\hat{\boldsymbol{i}}_{\boldsymbol{t},\text{in}}$ and u are a feasible input combination. Then, we are interested in whether $\lim_{n\to\infty} \boldsymbol{i}^n(\hat{\boldsymbol{i}}_{\boldsymbol{t},\text{in}}, u)$ exists and if so, does $\lim_{n\to\infty} \boldsymbol{i}^n(\hat{\boldsymbol{i}}_{\boldsymbol{t},\text{in}}, u) = \boldsymbol{i}^{**}$ hold? Similar to the case $N = 1$, we consider a resistance based variant to answer these questions. In the following section we define and analyze a resistance based iteration function that is closely related to B_v^p but that is more accessible to a corresponding fixed point analysis.

7.2. Resistance Based Approach

As detailed in Section 5.1.1, the drifted test ioni current approximation i_p and the corresponding drift resistance approximation $\hat{r}_D^p$ at the test fan speed t^p of ADA pair p, $p \in [N]$, are related by $\hat{r}_D^p = \beta^p(i_p)$, see also Definition 5.9. This relation is used to construct the resistance based approach in this section.

7.2.1. Drift Resistance Super Fixed Point Vector

In the previous section, the (ioni current based) ADA iterate $\boldsymbol{i}^n(\hat{\boldsymbol{i}}_{\boldsymbol{t},\text{in}}, u)$ and the super fixed point vector $\boldsymbol{i}^{**}$ are defined. In this subsection, their resistance based counterparts are defined. The p-th component of $\boldsymbol{i}^n(\hat{\boldsymbol{i}}_{\boldsymbol{t},\text{in}}, u)$ corresponds to the incumbent drifted test ioni current approximation of ADA pair p after the n-th iteration. This approximation can be transformed to the corresponding drift resistance approximation by applying the function β^p.

Definition 7.28 *Let $\hat{\boldsymbol{i}}_{\boldsymbol{t},\text{in}} \in \mathbb{R}_{>0}^N = (i_1^{\text{in}}, \ldots, i_N^{\text{in}})$ be an input vector and let u be a finite or infinite ADA update sequence such that $\hat{\boldsymbol{i}}_{\boldsymbol{t},\text{in}}$ and u are a feasible input combination. For $n \in [\ell]$ (u has length ℓ) or $n \in \mathbb{N}$ (u is an infinite sequence) let $\boldsymbol{i}^n(\hat{\boldsymbol{i}}_{\boldsymbol{t},\text{in}}, u) = (i_1^n, \ldots, i_N^n)$ be the corresponding n-th ADA iterate.*
The n-th resistance based ADA iterate with respect to $\hat{\boldsymbol{i}}_{\boldsymbol{t},\text{in}}$ and *u is the vector*

$$\boldsymbol{r}^n(\hat{\boldsymbol{i}}_{\boldsymbol{t},\text{in}}, u) = (r_1^n, \ldots, r_N^n) \text{ defined by } r_p^n := \beta^p(i_p^n) \;\forall\; p \in [N].$$

Lemma 7.29 *The n-th resistance based ADA iterate is well defined for all $n \in [\ell]$ ($n \in \mathbb{N}$, if u is an infinite ADA update sequence).*

Proof. Let $\hat{\boldsymbol{i}}_{\boldsymbol{t},\text{in}}$ be an input vector and let u be an ADA update sequence such that $\hat{\boldsymbol{i}}_{\boldsymbol{t},\text{in}}$ and u are a feasible input combination. Let $\boldsymbol{i}^n(\hat{\boldsymbol{i}}_{\boldsymbol{t},\text{in}}, u) = (i_1^n, \ldots, i_N^n)$ be the corresponding n-th ADA iterate. According to Lemma 7.27, $i_p^n > 0$ holds for all $p \in [N]$. Because $\mathbb{R}_{>0}$ is the domain of β^p (Definition 5.9), $\beta^p(i_p^n)$ is defined for all $p \in [N]$. □

If the limit of the ioni current based ADA iterates exists, it is related to the limit of the resistance based ADA iterates.

Theorem 7.30 *Let u be an infinite ADA update sequence and let $\hat{\boldsymbol{i}}_{\boldsymbol{t},\text{in}}$ be an input vector such that $\hat{\boldsymbol{i}}_{\boldsymbol{t},\text{in}}$ and u are a feasible input combination. Let $\boldsymbol{i}^* = (i_1^*, \dots, i_N^*) \in \mathbb{R}_{>0}^N$. Then, the following holds:*

$$\lim_{n\to\infty} \boldsymbol{i}^n(\hat{\boldsymbol{i}}_{\boldsymbol{t},\text{in}}, u) = \boldsymbol{i}^* \;\Leftrightarrow\; \lim_{n\to\infty} \boldsymbol{r}^n(\hat{\boldsymbol{i}}_{\boldsymbol{t},\text{in}}, u) = \big(\beta^1(i_1^*), \dots, \beta^N(i_N^*)\big).$$

Proof. Let u be an infinite ADA update sequence and let $\hat{\boldsymbol{i}}_{\boldsymbol{t},\text{in}}$ be an input vector such that $\hat{\boldsymbol{i}}_{\boldsymbol{t},\text{in}}$ and $u(n)$ are a feasible input combination for all $n \in \mathbb{N}$ and let $\boldsymbol{i}^* = (i_1^*, \dots, i_N^*) \in \mathbb{R}_{>0}^N$. Aiming at a better readability, the n-th ADA iterate $\boldsymbol{i}^n(\hat{\boldsymbol{i}}_{\boldsymbol{t},\text{in}}, u)$ is abbreviated by $\boldsymbol{i}^n$. Analogously, the n-th resistance based ADA iterate is abbreviated by $\boldsymbol{r}^n$. The components of the n-th iterates are denoted by $\boldsymbol{i}^n = (i_1^n, \dots, i_N^n)$ and $\boldsymbol{r}^n = (r_1^n, \dots, r_N^n)$. Recall from Definition 7.28 that $r_p^n = \beta^p(i_p^n)$ for all $p \in [N]$ and for all $n \in \mathbb{N}$.
"$\Rightarrow$" Let $\lim_{n\to\infty} \boldsymbol{i}^n = \boldsymbol{i}^*$. According to Lemma 7.27, we have $(\boldsymbol{i}^n)_{n\in\mathbb{N}} \in \mathbb{R}_{>0}^N$ for all $n \in \mathbb{N}$. Furthermore, $\lim_{n\to\infty} \boldsymbol{i}^n \in \mathbb{R}_{>0}^N$ holds by assumption. Therefore, for all $p \in [N]$ there exists $i_{\min,p} > 0$ such that $i_{\min,p} \le i_p^n$ for all $n \in \mathbb{N}$ as well as $i_{\min,p} \le i_p^*$. We set $i_{\min} := \min_{p\in[N]}(i_{\min,p})$. Then, we have

$$0 < i_{\min} \le i_p^n \;\forall\, p \in [N] \;\forall\, n \in \mathbb{N} \quad \text{and} \quad i_{\min} \le i_p^* \;\forall\, p \in [N].$$

Let $\varepsilon > 0$ arbitrary but fixed. We set $\overline{\varepsilon} := \frac{i_{\min}^2}{U}\varepsilon$. Note that $i_{\min} > 0$ and thus $\overline{\varepsilon} > 0$ and therefore

$$\begin{aligned}\lim_{n\to\infty} \boldsymbol{i}^n = \boldsymbol{i}^* \;&\Rightarrow\; \exists\, \bar{n} \in \mathbb{N} : \|\boldsymbol{i}^n - \boldsymbol{i}^*\|_{\max} < \overline{\varepsilon} \;\forall\, n \ge \bar{n} \\ &\Rightarrow\; |i_p^n - i_p^*| < \overline{\varepsilon} \;\forall\, p \in [N] \;\forall\, n \ge \bar{n}.\end{aligned}$$

In total, for $p \in [N]$ and for $n \ge \bar{n}$, we have

$$\begin{aligned}\big|r_p^n - \beta^p(i_p^*)\big| &= \big|\beta^p(i_p^n) - \beta^p(i_p^*)\big| = \Big|\frac{U}{i_p^n} - r_t^p - \big(\frac{U}{i_p^*} - r_t^p\big)\Big| = U\Big|\frac{1}{i_p^n} - \frac{1}{i_p^*}\Big| \\ &= U\Big|\frac{i_p^*}{i_p^n i_p^*} - \frac{i_p^n}{i_p^n i_p^*}\Big| = \frac{U}{i_p^n i_p^*}|i_p^* - i_p^n| \le \frac{U}{i_p^n i_p^*}\|\boldsymbol{i}^n - \boldsymbol{i}^*\|_{\max} \\ &< \frac{U}{i_p^n i_p^*}\overline{\varepsilon} = \frac{U}{i_p^n i_p^*}\frac{{i_{\min}}^2}{U}\varepsilon \le \varepsilon.\end{aligned}$$

Therefore, $\big\|\boldsymbol{r}^n - \big(\beta^1(i_1^*), \dots, \beta^N(i_N^*)\big)\big\|_{\max} < \varepsilon$ for all $n \ge \bar{n}$ and thus $\lim_{n\to\infty} \boldsymbol{r}^n(\hat{\boldsymbol{i}}_{\boldsymbol{t},\text{in}}, u) = \big(\beta^1(i_1^*), \dots, \beta^N(i_N^*)\big)$ holds.
"$\Leftarrow$" Let $\lim_{n\to\infty} \boldsymbol{r}^n(\hat{\boldsymbol{i}}_{\boldsymbol{t},\text{in}}, u) = \big(\beta^1(i_1^*), \dots, \beta^N(i_N^*)\big)$. Recall that $\beta^p : \mathbb{R}_{>0} \to (-r_t^p, \infty)$ is bijective (Lemma 5.11). Because $r_p^n = (\beta^p)^{-1}(i_p^n)$, we have $r_p^n > -r_t^p$ for all $p \in [N]$ and for all $n \in \mathbb{N}$. Furthermore, $i_p^* > 0$ by assumption and thus $\beta^p(i_p^*) > -r_t$ holds for all $p \in [N]$ as well. Therefore, for all $p \in [N]$ there exists $r_{\min,p} > -r_t^p$ such that $r_{\min,p} \le r_p^n$ for all $n \in \mathbb{N}$ and $r_{\min,p} \le \beta^p(i_p^*)$. We set $r_{\min} := \min_{p\in[N]}(r_{\min,p} + r_t^p)$. Then, we have $r_{\min} > 0$ and

$$r_{\min} \le r_{\min,p} + r_t^p \le r_p^n + r_t^p \;\forall\, p \in [N] \;\forall\, n \in \mathbb{N} \quad \text{as well as} \quad r_{\min} \le \beta^p(i_p^*) + r_t^p \;\forall\, p \in [N].$$

Let $\varepsilon > 0$ arbitrary but fixed. We set $\overline{\varepsilon} := \frac{r_{\min}^2}{U}\varepsilon$. Note that $r_{\min} > 0$ and thus $\overline{\varepsilon} > 0$. By using the abbreviation $\boldsymbol{r}^* = \big(\beta^1(i_1^*), \ldots, \beta^N(i_N^*)\big)$, we have

$$\begin{aligned}\lim_{n\to\infty} \boldsymbol{r}^n = \boldsymbol{r}^* \;&\Rightarrow\; \exists\, \bar{n} \in \mathbb{N} : \|\boldsymbol{r}^n - \boldsymbol{r}^*\|_{\max} < \overline{\varepsilon}\ \forall\ n \geq \bar{n} \\ &\Rightarrow\; \left|r_p^n - \beta^p(i_p^*)\right| < \overline{\varepsilon}\ \forall\ p \in [N]\ \forall\ n \geq \bar{n}.\end{aligned}$$

With this, we can state that for all $p \in [N]$ and for all $n \geq \bar{n}$

$$\begin{aligned}|i_p^n - i_p^*| &= \left|(\beta^p)^{-1} \circ \beta^p(i_p^n) - (\beta^p)^{-1} \circ \beta^p(i_p^*)\right| = \left|(\beta^p)^{-1}(r_p^n) - (\beta^p)^{-1} \circ \beta^p(i_p^*)\right| \\ &= \left|\frac{U}{r_p^n + r_t^p} - \frac{U}{\beta^p(i_p^*) + r_t^p}\right| = \frac{U}{(r_p^n + r_t^p)(\beta^p(i_p^*) + r_t^p)}|\beta^p(i_p^*) - r_p^n| \\ &< \frac{U}{(r_p^n + r_t^p)(\beta^p(i_p^*) + r_t^p)}\overline{\varepsilon} = \frac{U}{(r_p^n + r_t^p)(\beta^p(i_p^*) + r_t^p)}\frac{r_{\min}^2}{U}\varepsilon \\ &= \frac{r_{\min}}{r_p^n + r_t^p} \cdot \frac{r_{\min}}{\beta^p(i_p^*) + r_t^p} \cdot \varepsilon \leq 1 \cdot 1 \cdot \varepsilon = \varepsilon.\end{aligned}$$

Therefore, $\left\|\boldsymbol{i}^n - \boldsymbol{i}^*\right\|_{\max} < \varepsilon$ for all $n \geq \bar{n}$ and thus $\lim_{n\to\infty} \boldsymbol{i}^n(\hat{\boldsymbol{i}}_{\boldsymbol{t},\mathrm{in}}, u) = \boldsymbol{i}^*$ holds. □

Remark 7.31 *From a practical point of view, the requirement of Theorem 7.30 that the limit $\boldsymbol{i}^*$ is an element of $\mathbb{R}_{>0}^N$, i.e., $i_p^* > 0$ for all $p \in [N]$, is not restrictive. Indeed, in practice every drifted and undrifted ioni current is greater than zero, see also Remarks 3.4 and 3.5.*

Theorem 7.30 motivates the following definition of the drift resistance super fixed point vector.

Definition 7.32 *Let $\boldsymbol{i}^{**} = (i_1^{**}, \ldots, i_N^{**})$ be the super fixed point vector of a feasible scenario according to Definition 7.16. The corresponding* drift resistance super fixed point vector *is defined by*

$$\boldsymbol{r}^{**} := \big(\beta^1(i_1^{**}), \ldots, \beta^N(i_N^{**})\big).$$

Lemma 7.33 *The vector $\boldsymbol{r}^{**}$ is well-defined.*

Proof. Let $\boldsymbol{i}^{**} = (i_1^{**}, \ldots, i_N^{**})$ be feasible. Then, $i_p^{**} > 0$ holds for all $p \in [N]$ (Lemma 7.18). Because $(0, \infty)$ is the domain of β^p, $r_p^{**} = \beta^p(i_p^{**})$ is well-defined for all $p \in [N]$. □

Remark 7.34 *The drift resistance super fixed point vector $\boldsymbol{r}^{**}$ is defined for the case of a feasible scenario only.*

Corollary 7.35 *Let there be a feasible scenario, i.e., let $\boldsymbol{i}^{**} \in \mathbb{R}_{>0}^N$. Furthermore, let u be a given infinite ADA update sequence and let $\hat{\boldsymbol{i}}_{\boldsymbol{t},\mathrm{in}}$ be a given input vector. If $\hat{\boldsymbol{i}}_{\boldsymbol{t},\mathrm{in}}$ and u are a feasible input combination, then*

$$\lim_{n\to\infty} \boldsymbol{i}^n(\hat{\boldsymbol{i}}_{\boldsymbol{t},\mathrm{in}}, u) = \boldsymbol{i}^{**} \;\Leftrightarrow\; \lim_{n\to\infty} \boldsymbol{r}^n(\hat{\boldsymbol{i}}_{\boldsymbol{t},\mathrm{in}}, u) = \boldsymbol{r}^{**}.$$

Proof. The statement follows from Theorem 7.30 and Definition 7.32. □

Corollary 7.35 legitimates the approach to consider the resistance based iterates in order to analyze the convergence characteristics of Algorithm 5.2 in the case $N \geq 2$. There exists a resistance based iteration function $C^p_{r_D,v}$ that allows to recursively calculate the drift resistance super fixed point vector and to recursively calculate the resistance based ADA iterates. This function is essential for the analysis of the fixed point characteristics of Algorithm 5.2 and thus it is detailed in the following.

7.2.2. Resistance Based ADA Iteration Function with a Plurality of ADA Pairs

The resistance based iteration function for the case $N \geq 2$ is based on the iteration function $A^p_{r_D} : \hat{R}^p_{r_D} \to \mathbb{R}$ for the case $N = 1$. The function $A^p_{r_D}$ is introduced in Definition 6.21 and its fixed point characteristics are thoroughly analyzed in Chapter 6. The domain of the resistance based iteration function for the case $N \geq 2$ is the set $\hat{R}^p_{r_D,v}$ from Definition 7.4.

Definition 7.36 *Let $r_D \geq 0$ and let $p \in \{2, \dots, N\}$. Furthermore, let $i_{p-1} \in \mathbb{R}_{>0}$ such that $v := \beta^{p-1}(i_{p-1}) \in V^p_{r_D}$. The* resistance based iteration function of ADA pair p given v *is defined by*

$$C^p_{r_D,v} : \hat{R}^p_{r_D,v} \to \mathbb{R}, \quad C^p_{r_D,v} := A^p_{r_D} \circ \omega^p_v = \sigma^-_{r^p_t} \circ \rho_{t^p,r_D} \circ \rho^{-1}_{s^p,r_D} \circ \sigma^+_{r^p_s} \circ \omega^p_v.$$

Remark 7.37 *The physical interpretation of $C^p_{r_D,v}$ is as follows. According to Remark 7.3, $v := \beta^{p-1}(i_{p-1})$ corresponds to the drift resistance approximation at the test fan speed of ADA pair $p-1$. Then, $\omega^p_v(r) = w^p r + (1-w^p)v$ is the weighted sum of r and v, where r is an approximation of the drift resistance at the test fan speed of ADA pair p. This weighted sum corresponds to the drift resistance approximation at the start fan speed s^p of ADA pair p (Lemmas 5.13 and 5.14). Thereafter, this drift resistance approximation is plugged into the drift resistance iteration function $A^p_{r_D}$, which is detailed in Section 6.2. In contrast, in the case $N = 1$, the drift resistance approximation function is constant with the fan speed, because only a single ADA pair is considered. Accordingly, the drift resistance approximation at the fan speed s^p corresponds to the drift resistance approximation at the test fan speed of ADA pair p in this case. Therefore, the drift resistance approximation r of pair p is plugged directly into $A^p_{r_D}$, i.e., the weighted sum is omitted in the case $N = 1$. In Example 7.44, the function $C^p_{r_D,v}$ is illustrated in the context of the drift resistance super fixed point vector $\boldsymbol{r}^{**}$.*

Remark 7.38 *Analogously to Remark 7.12, if there is no risk of confusion, the subscript r_D of $C^p_{r_D,v}$ is omitted in the following.*

Lemma 7.39 *The function C^p_v is well-defined, i.e., it can be evaluated for all $r \in \hat{R}^p_v$.*

Proof. Let $r \in \hat{R}^p_v$. Because $\hat{R}^p_v = \left(\omega^p_v\right)^{-1}(\hat{R}^p)$ (Definition 7.4), we have $q := \omega^p_v(r) \in \hat{R}^p$. The set $\hat{R}^p$ is the domain of A^p and thus $C^p_v(r) = A^p \circ \omega^p_v(r) = A^p(q)$ exists. □

The following lemma states how the resistance based iteration function C_v^p and the ioni current based iteration function B_v^p are related.

Lemma 7.40 *Let $p \in \{2, \dots, N\}$ and let $v \in V^p$. Then, we have*

$$C_v^p = \beta^p \circ B_v^p \circ (\beta^p)^{-1}.$$

Proof. Using that

- $C_v^p = A^p \circ \omega_v^p$ (Definition 7.36),
- $A^p = \beta^p \circ A_i^p \circ \left(\beta^p\right)^{-1}$ (Lemma 6.30),
- $A_i^p = \iota_{t^p, r_D} \circ \iota_{s^p, r_D}^{-1} \circ \gamma^p \circ \beta^p$ (Definition 6.5),
- $\beta^p \circ \left(\beta^p\right)^{-1} = \mathrm{id}_{(-r_t^p, \infty)}$ (Lemma 5.11),
- $B_v^p = \iota_{t^p, r_D} \circ \iota_{s^p, r_D}^{-1} \circ \gamma^p \circ \omega_v^p \circ \beta^p$ (Definition 7.8),

we have

$$\begin{aligned} C_v^p &= A^p \circ \omega_v^p = \left(\beta^p \circ A_i^p \circ (\beta^p)^{-1}\right) \circ \omega_v^p \\ &= \beta^p \circ (\iota_{t^p, r_D} \circ \iota_{s^p, r_D}^{-1} \circ \gamma^p \circ \beta^p) \circ (\beta^p)^{-1} \circ \omega_v^p \\ &= \beta^p \circ \iota_{t^p, r_D} \circ \iota_{s^p, r_D}^{-1} \circ \gamma^p \circ \omega_v^p \circ \left(\beta^p \circ (\beta^p)^{-1}\right) \\ &= \beta^p \circ (\iota_{t^p, r_D} \circ \iota_{s^p, r_D}^{-1} \circ \gamma^p \circ \omega_v^p \circ \beta^p) \circ \left(\beta^p\right)^{-1} = \beta^p \circ B_v^p \circ \left(\beta^p\right)^{-1}. \end{aligned}$$

In the third line, we used that $\hat{R}_v^p$ is the domain of C_v^p and that $\beta^p \circ \left(\beta^p\right)^{-1}(\hat{R}_v^p) = \hat{R}_v^p$ holds (Lemma 7.5). □

The fixed points of B_v^p and C_v^p are also related (if they exist).

Lemma 7.41 *Let $p \in \{2, \dots, N\}$ and let $v \in V^p$. Then i^* is a fixed point of B_v^p if and only if $\beta^p(i^*)$ is a fixed point of C_v^p.*

Proof. According to Lemma 7.40, we have $B_v^p = (\beta^p)^{-1} \circ C_v^p \circ \beta^p$ and thus

$$B_v^p(i^*) = i^* \;\Leftrightarrow\; (\beta^p)^{-1} \circ C_v^p \circ \beta^p(i^*) = i^* \;\Leftrightarrow\; C_v^p \circ \beta^p(i^*) = \beta^p(i^*).$$

□

Recall from Definition 7.14 that the components of the super fixed point vector $\boldsymbol{i}^{**}$ are fixed points of certain ioni current based iteration functions B_v^p. Because the fixed points of B_v^p and C_v^p are related according to Lemma 7.41, the components of the drift resistance super fixed point vector $\boldsymbol{r}^{**}$ are fixed points of certain associated resistance based iteration functions C_v^p.

Lemma 7.42 *Let there be a feasible scenario, i.e., let* $\boldsymbol{i}^{**} = (i_1^{**}, \ldots, i_N^{**}) \in \mathbb{R}_{>0}^N$*, and let* $\boldsymbol{r}^{**} = (r_1^{**}, \ldots, r_N^{**})$ *be the corresponding drift resistance super fixed point vector. Then, the following recursion holds:*

$$r_1^{**} = \mathrm{fix}(A^1) \quad \textit{and} \quad r_p^{**} = \mathrm{fix}\big(C^p_{r_{p-1}^{**}}\big) \;\forall\; p \in \{2, \ldots, N\}.$$

Proof. For this proof, recall that $r_p^{**} = \beta^p(i^{**})$ for all $p \in [N]$ (Definition 7.32). We begin with $p = 1$. By considering that $i_1^{**} = \mathrm{fix}(A_i^1)$ (Definition 7.14) and $A_i^1 = \big(\beta^1\big)^{-1} \circ A^1 \circ \beta^1$ (Lemma 6.25), we have

$$i_1^{**} = A_i^1(i_1^{**}) = \big(\beta^1\big)^{-1} \circ A^1 \circ \beta^1(i_1^{**}) \;\Leftrightarrow\; r_1^{**} = \beta^1(i_1^{**}) = A^1 \circ \beta^1(i_1^{**}) = A^1(r_1^{**}).$$

Next, let $p \in \{2, \ldots, N\}$. By considering that $i_p^{**} = \mathrm{fix}\big(B^p_{\beta^{p-1}(i_{p-1}^{**})}\big)$ (Definition 7.14), $\beta^{p-1}(i_{p-1}^{**}) = r_{p-1}^{**}$ (Definition 7.32), $B_v^p(i^*) = i^*$ if and only if $C_v^p \circ \beta^p(i^*) = \beta^p(i^*)$ (Lemma 7.41) and $r_p^{**} = \beta^p(i_p^{**})$ (Definition 7.32), we have

$$i_p^{**} = B^p_{\beta^{p-1}(i_{p-1}^{**})}(i_p^{**}) = B^p_{r_{p-1}^{**}}(i_p^{**}) \;\Leftrightarrow\; \beta^p(i_p^{**}) = C^p_{r_{p-1}^{**}} \circ \beta^p(i_p^{**}) \;\Leftrightarrow\; r_p^{**} = C^p_{r_{p-1}^{**}}(r_p^{**}).$$

□

Lemma 7.42 gives us a resistance based condition to check whether a scenario is feasible or not.

Lemma 7.43 *A scenario is feasible if and only if the* N *fixed points recursively defined by*

$$r_1 = \mathrm{fix}(A^1) \quad \textit{and} \quad r_p = \mathrm{fix}\big(C^p_{r_{p-1}}\big) \;\forall\; p \in \{2, \ldots, N\}$$

exist.

Proof. "⇒" Let there be a feasible scenario. Then the super fixed point $\boldsymbol{r}^{**} = (r_1^{**}, \ldots, r_N^{**})$ exists (Definition 7.32) and $r_p = r_p^{**}$ holds for all $p \in [N]$ (Lemma 7.42).
"⇐" Let the N fixed points recursively defined by $r_1 = \mathrm{fix}(A^1)$ and $r_p = \mathrm{fix}\big(C^p_{r_{p-1}}\big)\ \forall\ p \in \{2, \ldots, N\}$ exist. Then, r_p, $p \in [N]$, must be an element of the domain of the corresponding function, i.e., $r_1 \in \hat{R}^1$ and $r_p \in \hat{R}^p_{r_{p-1}}$ for $p \in \{2, \ldots, N\}$. As a consequence, $(\beta^p)^{-1}(r_p)$ exists for all $p \in [N]$ and $(\beta_p)^{-1}(r_p) > 0$ holds (Lemmas 6.4 and 7.5). We set $i_p := (\beta^p)^{-1}(r_p)$ for all $p \in [N]$. In the following, we show by induction that $\boldsymbol{i}^{**} = (i_1, \ldots, i_p)$ holds, where $\boldsymbol{i}^{**}$ is the super fixed point vector according to Definition 7.14. Because $i_p > 0$ for all $p \in [N]$, the scenario is feasible in this case.
Base case: By applying Lemma 6.25, we have

$$r_1 = A^1(r_1) \;\Rightarrow\; \beta^1 \circ A_i^1 \circ (\beta^1)^{-1}(r_1) \;\Rightarrow\; (\beta^1)^{-1}(r_1) = A_i^1 \circ (\beta^1)^{-1}(r_1) \;\Rightarrow\; i_1 = \mathrm{fix}(A_i^1).$$

Because $i_1^{**} = \mathrm{fix}(A_i^1)$ (Definition 7.14), $i_1^{**} = i_1$ holds. In particular, we have $i_1^{**} = i_1 > 0$.
Induction hypothesis: Let there exist $k \in [N-1]$ such that $i_p^{**} = i_p = (\beta^p)^{-1}(r_p)$ for all $p \in [k]$.

Induction step: Let $p = k + 1$. By applying Lemma 7.40, we have

$$r_p = C^p_{r_{p-1}}(r_p) = \beta^p \circ B^p_{r_{p-1}} \circ (\beta^p)^{-1}(r_p) \;\Rightarrow\; (\beta^p)^{-1}(r_p) = B^p_{r_{p-1}}(\beta^p)^{-1}(r_p) \;\Rightarrow\; i_p = B^p_{r_{p-1}}(i_p).$$

Because $r_{p-1} = \beta^{p-1}(i^{**}_{p-1})$ (induction hypothesis), we have $i_p = \mathrm{fix}\big(B^p_{\beta^{p-1}(i^{**}_{p-1})}\big)$ and thus $i^{**}_p = i_p$ according to Definition 7.14. In particular, $i^{**}_p > 0$ holds and the induction step is completed. In total, we have $i^{**}_p \neq \mathrm{NaN}$ for all $p \in [N]$ and thus the scenario is feasible. □

The recursive construction of the drift resistance super fixed point vector according to Lemma 7.42 is demonstrated in the following example. This also includes a demonstration of the corresponding iteration functions C^p_v.

Example 7.44 *In this example, we determine the drift resistance super fixed point vector* $\boldsymbol{r}^{**} = (r^{**}_1, r^{**}_2, r^{**}_3)$ *of a feasible scenario with three ADA pairs, i.e, we have* $N = 3$. *For the sake of simplicity, the considered functions and values are artificial. Furthermore, we assume that the domains* $\hat{R}^p$, $p \in [3]$, *as well as the sets* V^2 *and* V^3 *are sufficiently large such that all considered function evaluations are well-defined. Therefore, no domains or other sets are specified in this example. Let us suppose that*

$$A^1(r) := \frac{1}{2}r + \frac{1}{2}, \quad A^2(r) := \frac{1}{3}r, \quad \textit{and} \quad A^3(r) := \frac{1}{4}r.$$

Then, A^p *is strictly increasing, contractive and a selfmap for* $p \in [3]$ *(if the domains contain the corresponding fixed points). Because* $A^1(1) = \frac{1}{2} + \frac{1}{2} = 1$, *we have* $\mathrm{fix}(A^1) = 1$. *According to Lemma 7.42, the first component of the drift resistance super fixed point vector is* $r^{**}_1 = \mathrm{fix}(A^1) = 1$.
For the second and third component of $\boldsymbol{r}^{**}$, *we need the weights of the corresponding weighted sums. In this example, let the weights be* $w^2 = \frac{1}{2}$ *and* $w^3 = \frac{4}{5}$, *i.e., we have*

$$\omega^2_v(r) = w^2 r + (1 - w^2)v = \frac{1}{2}r + \frac{1}{2}v \quad \textit{and} \quad \omega^3_v(r) = w^3 r + (1 - w^3)v = \frac{4}{5}r + \frac{1}{5}v.$$

Because $C^p_v = A^p \circ \omega^p_v$ *(Definition 7.36), we have*

$$C^2_{v_1} = \frac{1}{3}(\frac{1}{2}r + \frac{1}{2}v_1) = \frac{1}{6}r + \frac{1}{6}v_1,\ v_1 \in V^2 \quad \textit{and} \quad C^3_{v_2} = \frac{1}{4}(\frac{4}{5}r + \frac{1}{5}v_2) = \frac{1}{5}r + \frac{1}{20}v_2,\ v_2 \in V^3.$$

To avoid confusions with the used indices, recall from Remark 7.3 that V^p *is the set of feasible drift resistance approximations of the upper neighbor of ADA pair p. I.e., the physical interpretation of* $v_{p-1} \in V^p$ *is that* v_{p-1} *is the incumbent drift resistance approximation of ADA pair* $p - 1$, *which influences the drift resistance approximation of ADA pair p.*
Note that C^2_v *and* C^3_v *are both strictly increasing and contractive. This is no coincident. Corresponding statements is presented in Lemmas 7.46 and 7.48 below. In particular, Lemma 4.46 can be applied, which states that both functions are selfmaps if and only if*

their (unique) fixed points exist. Because we assume that the domains $\hat{R}_v^2$ and $\hat{R}_v^3$ as well as the sets of feasible upper neighbors V^2 and V^3 are sufficiently large in this example, the fixed points $\mathrm{fix}(C_{v_1}^2)$ *and* $\mathrm{fix}(C_{v_2}^3)$ *exist.*
We continue to recursively determine the drift resistance fixed point vector $\boldsymbol{r}^{**}$. According to Lemma 7.42, $r_2^{**} = \mathrm{fix}(C_{r_1^{**}}^2)$ holds. Because $r_1^{**} = 1$, we have

$$C_{r_1^{**}}^2(r) = \frac{1}{6}r + \frac{1}{6}r_1^{**} = \frac{1}{6}r + \frac{1}{6} \;\Rightarrow\; \mathrm{fix}(C_{r_1^{**}}^2) = \frac{1}{5} \;\left(\textit{since } C_{r_1^{**}}^2(\frac{1}{5}) = \frac{1}{30} + \frac{1}{6} = \frac{6}{30} = \frac{1}{5}\right)$$

and thus $r_2^{**} = \frac{1}{5}$. Analogously, we have

$$C_{r_2^{**}}^3(r) = \frac{1}{5}r + \frac{1}{20}r_2^{**} = \frac{1}{5}r + \frac{1}{100} \;\Rightarrow\; \mathrm{fix}(C_{r_2^{**}}^3) = \frac{1}{80} \;\left(\textit{since } C_{r_2^{**}}^3(\frac{1}{80}) = \frac{1}{400} + \frac{1}{100} = \frac{5}{400}\right)$$

and thus $r_3^{**} = \frac{1}{80}$. With this, the drift resistance super fixed point vector is fully determined as $\boldsymbol{r}^{**} = \left(1, \frac{1}{5}, \frac{1}{80}\right)$. The corresponding super fixed point vector $\boldsymbol{i}^{**} = (i_1^{**}, \ldots, i_N^{**})$ can be calculated from $\boldsymbol{r}^{**}$ with $i_p^{**} = \left(\beta^p\right)^{-1}(r_p^{**})$ (Definition 7.32). However, this requires the voltage U and the test ioni current i_t^p of each ADA pair p, $p \in [3]$. Because U and the test ioni currents are only implicitly given in this example, we refrain from calculating $\boldsymbol{i}^{**}$.

A further benefit from the fact that C_v^p and B_v^p are related by $C_v^p = \beta^p \circ B_v^p \circ (\beta^p)^{-1}$ is that the resistance based ADA iterates $\boldsymbol{r}^n(\hat{\boldsymbol{i}}_{\boldsymbol{t},\mathrm{in}}, u)$ can also be recursively calculated by certain functions C_v^p.

Lemma 7.45 *Let $\hat{\boldsymbol{i}}_{\boldsymbol{t},\mathrm{in}} \in \mathbb{R}_{>0}^N = (i_1^{\mathrm{in}}, \ldots, i_N^{\mathrm{in}})$ be an input vector and let $u = (u_n)_{n\in[\ell]}$ be an ADA update sequence of length ℓ, $\ell \in \mathbb{N}$, such that $\hat{\boldsymbol{i}}_{\boldsymbol{t},\mathrm{in}}$ and u are a feasible input combination. For $n \in [\ell]$ let $\boldsymbol{r}^n(\hat{\boldsymbol{i}}_{\boldsymbol{t},\mathrm{in}}, u) = (r_1^n, \ldots, r_N^n)$ be the corresponding $n-th$ resistance based ADA iterate. With $r_p^0 := \beta^p(i_p^{\mathrm{in}})$ for all $p \in [N]$ the following recursion holds:*

$$\boldsymbol{r}^n(\hat{\boldsymbol{i}}_{\boldsymbol{t},\mathrm{in}}, u) = \begin{cases} \left(A^1(r_1^{n-1}), r_2^{n-1}, \ldots, r_N^{n-1}\right) & \textit{if } u_n = 1, \\ \left(r_1^{n-1}, \ldots, r_{p-1}^{n-1}, C_{r_{p-1}^{n-1}}^p(r_p^{n-1}), r_{p+1}^{n-1}, \ldots, r_N^{n-1}\right) & \textit{if } u_n =: p \geq 2. \end{cases} \tag{7.4}$$

This recursion also holds for infinite ADA update sequences.

Proof. The statement is shown by induction over n.
Base case:
Let $n = 1$ and let $\boldsymbol{r}^1(\hat{\boldsymbol{i}}_{\boldsymbol{t},\mathrm{in}}, u) = (r_1^1, \ldots, r_N^1)$ be the corresponding first resistance based ADA iterate as well as $\boldsymbol{i}(\hat{\boldsymbol{i}}_{\boldsymbol{t},\mathrm{in}}, u) = (i_1^1, \ldots, i_N^1)$ the corresponding first ioni current based ADA iterate. Then, $r_p^1 = \beta^1(i_p^1)$ holds for all $p \in [N]$ (Definition 7.28). According to Lemma 7.27, we have

$$\boldsymbol{i}^1\left(\hat{\boldsymbol{i}}_{\boldsymbol{t},\mathrm{in}}, u\right) = \begin{cases} \left(A_i^1(i_1^{\mathrm{in}}), i_2^{\mathrm{in}}, \ldots, i_N^{\mathrm{in}}\right) & \text{if } u_1 = 1, \\ \left(i_1^{\mathrm{in}}, \ldots, i_{p-1}^{\mathrm{in}}, B_{\beta^{p-1}(i_{p-1}^{\mathrm{in}})}^p(i_p^{\mathrm{in}}), i_{p+1}^{\mathrm{in}}, \ldots, i_N^{\mathrm{in}}\right) & \text{if } u_1 =: p \geq 2. \end{cases}$$

Let $u_1 = 1$. Then, we have

$$r_1^1 = \beta^1 \circ A_i^1(i_1^{\text{in}}) = \beta^1 \circ A_i^1 \circ (\beta^1)^{-1} \circ (\beta^1)(i_1^{\text{in}}) = \beta^1 \circ A_i^1 \circ (\beta^1)^{-1}(r_1^0) = A^1(r_1^0),$$

where the last equality follows from Lemma 6.25. For $\bar{p} \in \{2, \ldots, N\}$, we have $r_{\bar{p}}^1 = \beta^{\bar{p}}(i_{\bar{p}}^1) = \beta^{\bar{p}}(i_{\bar{p}}^{\text{in}}) = r_{\bar{p}}^0$. Therefore, (7.4) holds for $n = 1$ and $u_1 = 1$.
Now, let $u_1 = p$, $p \geq 2$. By construction, we have $\beta^{p-1}(i_{p-1}^{\text{in}}) = r_{p-1}^0$ and thus

$$\begin{aligned} r_p^1 &= \beta^p(i_p^1) = \beta^p \circ B^p_{\beta^{p-1}(i_{p-1}^{\text{in}})}(i_p^{\text{in}}) = \beta^p \circ B_{r_{p-1}^0}(i_p^{\text{in}}) = \beta^p \circ B_{r_{p-1}^0} \circ (\beta^p)^{-1} \circ \beta^p(i_p^{\text{in}}) \\ &= \beta^p \circ B_{r_{p-1}^0} \circ (\beta^p)^{-1}(r_p^0) = C^p_{r_{p-1}^0}(r_p^0), \end{aligned}$$

where the last equality follows from Lemma 7.40. With this, (7.4) also holds in the case $u_1 \geq 2$ and the base case is proved.
Induction hypothesis:
For a certain $k < \ell$, $k \in \mathbb{N}$, let (7.4) hold for all $n \leq k$.
Induction step:
According to Lemma 7.27, the $(k+1)$st ADA iterate is

$$\boldsymbol{i}^{k+1}(\hat{\boldsymbol{i}}_{\boldsymbol{t},\text{in}}, u) = \begin{cases} (A_i^1(i_1^k), i_2^k, \ldots, i_N^k) & \text{if } u_{k+1} = 1, \\ (i_1^k, \ldots, i_{p-1}^k, B^p_{\beta^{p-1}(i_{p-1}^k)}(i_p^k), i_{p+1}^k, \ldots, i_N^k) & \text{if } u_{k+1} =: p \geq 2. \end{cases}$$

Analogous to the base case, we have

$$\boldsymbol{r}^{k+1}(\hat{\boldsymbol{i}}_{\boldsymbol{t},\text{in}}, u) = \begin{cases} (A^1(r_1^k), r_2^k, \ldots, r_N^k) & \text{if } u_{k+1} = 1, \\ (r_1^k, \ldots, r_{p-1}^k, C^p_{r_{p-1}^k}(r_p^k), r_{p+1}^k, \ldots, r_N^k) & \text{if } u_{k+1} =: p \geq 2. \end{cases}$$

Therefore, by considering the induction hypothesis, (7.4) holds for all $n \leq k+1$ and the induction is completed.
Because the base case and the induction step are also valid for infinite ADA update sequences, (7.4) holds for infinite ADA update sequences as well. □

Our goal is to show that $\lim_{n\to\infty} \boldsymbol{r}^n(\hat{\boldsymbol{i}}_{\boldsymbol{t},\text{in}}, u) = \boldsymbol{r}^{**}$ for certain inputs $\hat{\boldsymbol{i}}_{\boldsymbol{t},\text{in}}$ and u. Because $\boldsymbol{r}^n(\hat{\boldsymbol{i}}_{\boldsymbol{t},\text{in}}, u)$ and $\boldsymbol{r}^{**}$ can be calculated by functions C_v^p according to Lemmas 7.45 and 7.42, respectively, the resistance based iteration function is considered in more detail in the following subsection.

7.2.3. Properties of the Resistance Based ADA Iteration Function C_v^p

Since C_v^p is a composite function that contains A^p, C_v^p inherits some of the properties of A^p. Because C_v^p is only defined for $p \geq 2$, we assume that $p \in \{2, \ldots, N\}$ for the remainder of this subsection.

Lemma 7.46 *The function C_v^p is strictly increasing.*

Proof. The functions ω_v^p and A^p are strictly increasing according to Lemmas 7.2 and 6.34, respectively. As a composition of strictly increasing functions, $C_v^p = A^p \circ \omega_v^p$ is also strictly increasing. □

A benefit of the fact that C_v^p is strictly increasing is that Lemma 4.46 can be applied.

Corollary 7.47 *Let $C_v^p : \hat{R}_v^p \to \mathbb{R}$ be contractive. Then, C_v^p is a selfmap if and only if C_v^p has a fixed point. Furthermore, if C_v^p has a fixed point, it is unique, and the Picard iteration associated to C_v^p converges to this fixed point for an arbitrary starting point $r \in \hat{R}_v^p$.*

Proof. Because C_v^p is strictly increasing (Lemma 7.46) and its domain $\hat{R}_v^p$ is a closed and bounded interval (Lemma 7.7), Lemma 4.46 can be applied. □

Since we are interested in "good" convergence characteristics of the Picard iteration associated to C_v^p, we are interested in conditions that guarantee that C_v^p is contractive and that C_v^p is a selfmap. These are closely related to the corresponding conditions for A^p.

Lemma 7.48 *If A^p is contractive, then C_v^p is contractive.*

Proof. Let A^p be contractive and let $r_1, r_2 \in \hat{R}_v^p$ with $r_1 \neq r_2$. We have to show that $|C_v^p(r_1) - C_v^p(r_2)| < |r_1 - r_2|$. According to Lemma 5.13, we have $0 < w^p < 1$ and thus

$$\left|\omega_v^p(r_1) - \omega_v^p(r2)\right| = \left|w^p r_1 + (1-w^p)v - \left(w^p r_2 + (1-w^p)v\right)\right| = w^p|r_1 - r_2| < |r_1 - r_2|.$$

Furthermore, A^p is contractive by assumption and thus

$$|C_v^p(r_1) - C_v^p(r_2)| = |A^p \circ \omega_v^p(r_1) - A^p \circ \omega_v^p(r_2)| < |\omega_v^p(r_1) - \omega_v^p(r_2)| < |r_1 - r_2|.$$

□

The converse is not true in general, i.e., if C_v^p is contractive, then this does not imply that A^p is contractive. This is briefly demonstrated in the following counterexample.

Example 7.49 *Let A^p be defined by $A^p(r) = 2r$ and let $w^p = \frac{1}{3}$, i.e., $\omega_v^p(r) = \frac{1}{3}r + \frac{2}{3}v$. Then, A^p is not contractive, because $|A(r_1) - A(r_2)| = 2|r_1 - r_2| > |r_1 - r_2|$ for all $r_1 \neq r_2$. However, $C_v^p(r) = A^p \circ \omega_v^p(r) = 2\left(\frac{1}{3}r + \frac{2}{3}v\right)$ is contractive, because*

$$\left|C_v^p(r_1) - C_v^p(r_2)\right| = \left|\frac{2}{3}r_1 + \frac{4}{3}v - (\frac{2}{3}r_2 + \frac{4}{3}v)\right| = \frac{2}{3}|r_1 - r_2| < |r_1 - r_2| \ \forall\ r_1 \neq r_2.$$

Furthermore, if A^p has a fixed point, then this does in general not imply that C_v^p has a fixed point. As a consequence, if A^p is a selfmap, then this does in general not imply that C_v^p is a selfmap. Both aspects are demonstrated in the following counterexample.

Example 7.50 *Let $\hat{R}^p = [-1, 1]$ and let $A^p : \hat{R}^p \to \mathbb{R}$ be defined by $A^p(r) := \frac{1}{2}r$. Furthermore, let $w^p = \frac{1}{2}$, which is in accordance with Lemma 5.13. In this example, the*

test resistance r_t^p is not further specified. However, $r_t^p > 0$ holds according to Remark 5.8. Because

$$r_t^p > 0 \;\Rightarrow\; \frac{\min \hat{R}^p + w^p r_t^p}{1 - w^p} = 2\big(-1 + \frac{1}{2} r_t^p\big) = -2 + r_t^p > -2,$$

we can state that $(-\infty, -2] \subset V^p := \big\{v \in \mathbb{R} : v < \frac{\min \hat{R}^p + w^p r_t^p}{1 - w^p}\big\}$ (Definition 7.4). We select $v := -2$. Because $v \in V^p$ in this example, the corresponding set $\hat{R}_v^p$ and function C_v^p are well-defined. We have $\omega_v^p(x) = w^p x + (1 - w^p)v = \frac{1}{2}x + \frac{1}{2}(-2)$ and thus

$$C_v^p(r) = A^p \circ w^p(r) = \frac{1}{2}(\frac{1}{2}r - 1) = \frac{1}{4}r - \frac{1}{2}.$$

According to Definition 7.4, the domain of C_v^p is

$$\hat{R}_v^p = \big(\omega_v^p\big)^{-1}(\hat{R}^p) = \frac{1}{w^p}\big(\hat{R}^p - (1 - w^p)v\big) = 2\big(\hat{R}^p - \frac{1}{2}(-2)\big) = 2\big([-1, 1] + 1\big) = [0, 4].$$

Let us consider A^p first. The absolute value of its gradient is $\big|\frac{d}{dr}A(r)\big| = \frac{1}{2}$ and thus smaller than one and therefore A^p is contractive. Furthermore, A^p has the fixed point $r^* = 0$. Thus, A^p is a selfmap according to Lemma 6.35.
Next, we consider the function C_v^p. Note that C_v^p is also contractive, which is in accordance with Lemma 7.48. If C_v^p was considered as a function over $\mathbb{R}$, then it would have the unique fixed point $r_v^* := -\frac{2}{3}$. But r_v^* is not an element of $\hat{R}_v^p = [0, 4]$ and thus C_v^p does not have a fixed point (within its domain). As a consequence, according to Corollary 7.47 we see that C_v^p is not a selfmap, i.e., we have $C_v^p(\hat{R}_v^p) \not\subseteq \hat{R}_v^p$.

The drift resistance iteration function C_v^p is introduced to facilitate the convergence analysis of Algorithm 5.2. In order to prove the convergence statements of Theorem 7.68 below, it is required that C_v^p is a selfmap for all v within a certain ε-ball centered at r_{p-1}^{**} for all $p \in \{2, \ldots, N\}$. However, as demonstrated in Example 7.50, it is not sufficient to require that A^p is a selfmap to guarantee that C_v^p is a selfmap for all $v \in V^p$. Furthermore, it is also not sufficient to require that a single $C_{\bar{v}}^p$, $\bar{v} \in V^p$, is a contractive selfmap to guarantee that C_v^p is a contractive selfmap for all $v \in V^p$. In general, if C_v^p is a contractive selfmap, then there might exist $x \in V^p$, $x \neq v$, such that C_x^p is not a selfmap. This is demonstrated in the following example.

Example 7.51 *Let us consider $\hat{R}^p := [-\frac{1}{2}, 1]$ and let $A^p(r) := \frac{1}{2}r$ for all $r \in \hat{R}^p$. Note that A^p is strictly increasing, contractive and has the fixed point $r^* = 0 \in \hat{R}^p$. Thus, A^p is also a selfmap according to Lemma 6.35. Let us consider a weight of $w^p = \frac{1}{2}$ and let us assume that $v := 1$ and $x := -1$ are elements of V^p. This gives us $\big(\omega_v^p\big)^{-1}(r) = \frac{1}{w^p}\big(r - (1 - w^p)v\big) = 2(r - \frac{1}{2} \cdot 1) = 2r - 1$. Because $\hat{R}_v^p = \big(\omega_v^p\big)^{-1}(\hat{R}^p)$, we have $\hat{R}_v^p = [-2, 1]$ Analogously, we have $\big(\omega_x^p\big)^{-1}(r) = 2r + 1$ and $\hat{R}_x^p = [0, 3]$.*
Considering the iteration functions C_v^p and C_x^p, we have

$$C_v^p(r) = A^p \circ \omega_v^p(r) = \frac{1}{2}\big(w^p r + (1 - w^p)v\big) = \frac{1}{2}\big(\frac{1}{2}r + \frac{1}{2} \cdot 1\big) = \frac{1}{4}r + \frac{1}{4}$$

and analogously $C_x^p(r) = \frac{1}{4}r - \frac{1}{4}$. Both functions are strictly increasing and contractive, which is consistent with Lemmas 7.46 and 7.48. However, C_v^p is a selfmap on its domain $\hat{R}_v^p$, whereas C_x^p is not a selfmap on its domain $\hat{R}_x^p$, which is shown in the following. Note that $r_v^* = \frac{1}{3} \in \hat{R}_v^p$ is a fixed point of C_v^p and thus C_v^p is a selfmap according to Corollary 7.47. On the other hand, for $r := 0 \in \hat{R}_x^p$, we have $C_x^p(r) = -\frac{1}{4} \notin \hat{R}_x^p$ and thus C_x^p is not a selfmap on its domain.

However, if $I = [v_1, v_2] \subset V^p$, then it is sufficient to check that C_v^p is a selfmap for the boundaries v_1 and v_2 to guarantee that C_v^p is a selfmap for all $v \in I$. To prove this, some preliminary work must be done. Some of this preliminary work is also used to prove the convergence statements in the following section. We begin with some monotonicity properties of C_v^p.

Lemma 7.52 *Let $v_1, v_2 \in V^p$ such that $v_1 < v_2$. Then, the following statements hold:*

- $\omega_{v_1}^p(r) < \omega_{v_2}^p(r) \;\forall\; r \in \mathbb{R}$,
- $C_{v_1}^p(r) < C_{v_2}^p(r) \;\forall\; r \in \hat{R}_{v_1}^p \cap \hat{R}_{v_2}^p$.

Proof. Let $r \in \mathbb{R}$. Because $0 < w^p < 1$ (Lemma 5.13), we have

$$\begin{aligned} v_1 < v_2 \;&\Rightarrow\; (1-w^p)v_1 < (1-w^p)v_2 \;\Rightarrow\; w^p r + (1-w^p)v_1 < w^p r + (1-w^p)v_2 \\ &\Rightarrow\; \omega_{v_1}^p(r) < \omega_{v_2}^p(r). \end{aligned}$$

Furthermore, because A^p is strictly increasing (Lemma 6.34), we have

$$C_{v_1}^p(r) = A^p \circ \omega_{v_1}^p(r) < A^p \circ \omega_{v_2}^p(r) = C_{v_2}^p(r)$$

for all $r \in \hat{R}_{v_1}^p \cap \hat{R}_{v_2}^p$. □

The following lemma is an auxiliary statement.

Lemma 7.53 *Let $v, x \in V^p$. Then, the following holds:*

$$\hat{R}_v^p = \left(\omega_v^p\right)^{-1} \circ \omega_x^p(\hat{R}_x^p) \quad \textit{and} \quad r \in \hat{R}_x^p \;\Leftrightarrow\; r + \frac{1-w^p}{w^p}(x-v) \in \hat{R}_v^p.$$

Proof. By Definition 7.4, we have $\hat{R}_v^p = \left(\omega_v^p\right)^{-1}(\hat{R}^p)$ and $\hat{R}_x^p = \left(\omega_x^p\right)^{-1}(\hat{R}^p)$. Therefore, we have $\hat{R}^p = \omega_x^p(\hat{R}_x^p)$ and thus $\hat{R}_v^p = \left(\omega_v^p\right)^{-1}(\hat{R}^p) = \left(\omega_v^p\right)^{-1} \circ \omega_x^p(\hat{R}_x^p)$.
Let $r \in \hat{R}_x^p$. According to Lemma 7.2, we have

$$\begin{aligned} \left(\omega_v^p\right)^{-1} \circ \omega_x^p(r) = \left(\omega_v^p\right)^{-1}\left(w^p r + (1-w^p)x\right) &= \frac{1}{w^p}\Big(\left(w^p r + (1-w^p)x\right) - (1-w^p)v\Big) \\ &= r + \frac{1-w^p}{w^p}(x-v) \end{aligned}$$

and thus $r \in \hat{R}_x^p$ if and only if $r + \frac{1-w^p}{w^p}(x-v) \in \hat{R}_v^p$. □

If two iteration functions C_v^p and C_x^p are contractive selfmaps, then their fixed points $\mathrm{fix}(C_v^p)$ and $\mathrm{fix}(C_x^p)$, respectively, exist (Corollary 7.47). The following lemma states that the fixed point of C_v^p is contained in the domain of C_x^p and vice versa.

Lemma 7.54 *Let $v, x \in V^p$ and let C_v^p as well as C_x^p be contractive selfmaps on $\hat{R}_v^p$ and $\hat{R}_x^p$, respectively. Then, we have*

$$\mathrm{fix}(C_v^p) \in \hat{R}_v^p \cap \hat{R}_x^p \quad \textit{and} \quad \mathrm{fix}(C_x^p) \in \hat{R}_v^p \cap \hat{R}_x^p.$$

Proof. Because C_v^p and C_x^p are contractive selfmaps, their unique fixed points $\mathrm{fix}(C_v^p) \in \hat{R}_v^p$ and $\mathrm{fix}(C_x^p) \in \hat{R}_x^p$, respectively, exist (Corollary 7.47). Let us consider $\bar{r} := \left(\omega_v^p\right)^{-1} \circ \omega_x^p\big(\mathrm{fix}(C_x^p)\big)$, which is an element of $\hat{R}_v^p$ (Lemma 7.53). Therefore, we have

$$\begin{aligned} C_v^p(\bar{r}) &= A^p \circ \omega_v^p(\bar{r}) = A^p \circ \omega_v^p \circ \left(\omega_v^p\right)^{-1} \circ \omega_x^p\big(\mathrm{fix}(C_x^p)\big) \\ &= A^p \circ \omega_x^p\big(\mathrm{fix}(C_x^p)\big) = C_x^p\big(\mathrm{fix}(C_x^p)\big) = \mathrm{fix}(C_x^p). \end{aligned}$$

Because C_v^p is a selfmap on $\hat{R}_v^p$, $\mathrm{fix}(C_x^p) = C_v^p(\bar{r}) \in \hat{R}_v^p$ holds. The statement $\mathrm{fix}(C_v^p) \in \hat{R}_x^p$ is shown analogously by swapping the roles of v and x. □

A consequence of Lemma 7.54 is that if a starting point $r \in \hat{R}_v^p \cap \hat{R}_x^p$ is considered, then each iterate of the Picard iteration associated to C_v^p starting at r and each iterate of the Picard iteration associated to C_x^p starting at r is contained in this intersection.

Corollary 7.55 *Let $v, x \in V^p$ and let C_v^p as well as C_x^p be contractive selfmaps on $\hat{R}_v^p$ and $\hat{R}_x^p$, respectively. Furthermore, let $r \in \hat{R}_v^p \cap \hat{R}_x^p$. Then, we have*

$$\forall\, n \in \mathbb{N}: \quad \left(C_v^p\right)^n(r) \in \hat{R}_v^p \cap \hat{R}_x^p \quad \textit{and} \quad \left(C_x^p\right)^n(r) \in \hat{R}_v^p \cap \hat{R}_x^p.$$

Proof. We begin with the first part and show $\left(C_v^p\right)^n(r) \in \hat{R}_v^p \cap \hat{R}_x^p$ for all $n \in \mathbb{N}$. Because $r \in \hat{R}_v^p$ and C_v^p is a selfmap on $\hat{R}_v^p$ by assumption, $\left(C_v^p\right)^n(r) \in \hat{R}_v^p$ holds for all $n \in \mathbb{N}$. To show $\left(C_v^p\right)^n(r) \in \hat{R}_x^p$, we have to consider the fixed point of C_v^p. Because C_v^p and C_x^p are contractive selfmaps (by assumption), their fixed points $\mathrm{fix}(C_v^p)$ and $\mathrm{fix}(C_x^p)$, respectively, exist and $\mathrm{fix}(C_v^p) \in \hat{R}_x^p$ holds (Lemma 7.54). In the following, we distinguish three cases. First, let $r = \mathrm{fix}(C_v^p)$. Then, $\left(C_v^p\right)^n(r) = r \in \hat{R}_x^p$ holds for all $n \in \mathbb{N}$. Next, let $r < \mathrm{fix}(C_v^p)$. Because $\hat{R}_x^p$ is a closed interval (Lemma 7.7) and $r \in \hat{R}_x^p$ as well as $\mathrm{fix}(C_v^p) \in \hat{R}_x^p$, we have $[r, \mathrm{fix}(C_v^p)] \subset \hat{R}_x^p$. By applying Lemma 4.45 inductively, $r < \left(C_v^p\right)^n(r) < \mathrm{fix}(C_v^p)$ holds for all $n \in \mathbb{N}$ and thus $\left(C_v^p\right)^n(r) \in [r, \mathrm{fix}(C_v^p)] \subset \hat{R}_x^p$ for all $n \in \mathbb{N}$. The third case, $r > \mathrm{fix}(C_v^p)$, is shown analogously to the second case, $r < \mathrm{fix}(C_v^p)$. In total, $\left(C_v^p\right)^n(r) \in \hat{R}_x^p$ holds for all $n \in \mathbb{N}$ in all three cases.
The second part of the statement, $\left(C_x^p\right)^n(r) \in \hat{R}_v^p \cap \hat{R}_x^p$ for all $n \in \mathbb{N}$, is shown analogously by swapping the roles of v and x. □

Next, we show a monotonicity property between elements $v \in V^p$ and the fixed points of the corresponding iteration functions, $\mathrm{fix}(C_v^p)$.

Lemma 7.56 *Let $v, x \in V^p$ and let C_v^p as well as C_x^p be contractive selfmaps. Then,*

$$v < x \;\Rightarrow\; \mathrm{fix}(C_v^p) < \mathrm{fix}(C_x^p)$$

holds.

Proof. Let $v < x$, then we have $C_v^p(r) < C_x^p(r)$ for all $r \in \hat{R}_v^p \cap \hat{R}_x^p$ (Lemma 7.52). Furthermore, we have $\mathrm{fix}(C_v^p), \mathrm{fix}(C_x^p) \in \hat{R}_v^p \cap \hat{R}_x^p$ (Lemma 7.54) and thus $C_x^p\big(\mathrm{fix}(C_v^p)\big) > C_v^p\big(\mathrm{fix}(C_v^p)\big) = \mathrm{fix}(C_v^p)$. Then, the Picard iteration associated to C_x^p starting at $\mathrm{fix}(C_v^p)$ is strictly increasing according to Lemma 4.47. Because the Picard iteration associated to C_x^p converges to $\mathrm{fix}(C_x^p)$ for an arbitrary starting point in $\hat{R}_x^p$ (Corollary 7.47), $\mathrm{fix}(C_x^p) > \mathrm{fix}(C_v^p)$ holds. □

There is also a relation between elements $v \in V^p$ and the domains $\hat{R}_v^p$ of the corresponding iteration functions C_v^p.

Lemma 7.57 *Let $v_1, v_2 \in V^p$ with $v_1 \leq v_2$. Then, the following holds:*

$$x \in [v_1, v_2] \;\Rightarrow\; \hat{R}_{v_1}^p \cap \hat{R}_{v_2}^p \subset \hat{R}_x^p$$

Proof. By Definition 7.4, we have $\hat{R}_{v_1}^p = \big(\omega_{v_1}^p\big)^{-1}(\hat{R}^p)$ and $\hat{R}_{v_2}^p = \big(\omega_{v_2}^p\big)^{-1}(\hat{R}^p)$. Let $\bar{r} \in \hat{R}_{v_1}^p \cap \hat{R}_{v_2}^p$, then there exist $r_1, r_2 \in \hat{R}^p$ such that $\bar{r} = \big(\omega_{v_1}^p\big)^{-1}(r_1)$ and $\bar{r} = \big(\omega_{v_2}^p\big)^{-1}(r_2)$. By considering Lemma 7.52, we have

$$v_1 \leq x \leq v_2 \;\Rightarrow\; r_1 = \omega_{v_1}^p(\bar{r}) \leq \omega_x^p(\bar{r}) \leq \omega_{v_2}^p(\bar{r}) = r_2.$$

Recall that $\hat{R}^p$ is a closed interval (Lemma 6.11) and thus we have

$$\omega_x^p(\bar{r}) \in [r_1, r_2] \subset \hat{R}^p \;\Rightarrow\; \omega_x^p(\bar{r}) \in \hat{R}^p \;\Rightarrow\; \bar{r} \in \big(\omega_x^p\big)^{-1}(\hat{R}^p) = \hat{R}_x^p \;\forall\; x \in [v_1, v_2].$$

□

With this, we can finally state that if $C_{v_1}^p$ and $C_{v_2}^p$ are both (contractive) selfmaps, where v_1 and v_2 are the boundaries of an interval $I = [v_1, v_2] \subset V^p$, then C_v^p is a selfmap for all $v \in I$.

Theorem 7.58 *Let A^p be contractive. Let $v_1, v_2 \in V^p$ with $v_1 \leq v_2$ and let $C_{v_1}^p$ as well as $C_{v_2}^p$ be selfmaps. Then,*

$$x \in [v_1, v_2] \;\Rightarrow\; C_x^p \text{ is contractive selfmap}$$

holds.

Proof. Let $x \in [v_1, v_2]$. Because V^p is an interval (Definition 7.4) and $v_1, v_2 \in V^p$ by assumption, $[v_1, v_2] \subset V^p$ holds and the function $C_x^p : \hat{R}_x^p \to \mathbb{R}$ exists (Definition 7.36). Furthermore, $C_{v_1}^p$, C_x^p and $C_{v_2}^p$ are contractive, because A^p is contractive (Lemma 7.48). Because $C_{v_1}^p$ and $C_{v_2}^p$ are contractive selfmaps, the fixed points $\mathrm{fix}(C_{v_1}^p)$ and $\mathrm{fix}(C_{v_2}^p)$ exist

(Corollary 7.47) and $\mathrm{fix}(C^p_{v_1}) \leq \mathrm{fix}(C^p_{v_2})$ holds (Lemma 7.56). Furthermore, according to Lemmas 7.54 and 7.57,

$$\left[\mathrm{fix}(C^p_{v_1}), \mathrm{fix}(C^p_{v_2})\right] \subset \hat{R}^p_{v_1} \cap \hat{R}^p_{v_2} \subset \hat{R}^p_x$$

holds and thus we can evaluate $C^p_x\big(\mathrm{fix}(C^p_{v_1})\big)$ and $C^p_x\big(\mathrm{fix}(C^p_{v_2})\big)$.
In the following, we show that the Picard iteration associated to C^p_x starting at $\mathrm{fix}(C^p_{v_1})$ is strictly increasing and is bounded from above by $\mathrm{fix}(C^p_{v_2})$. Because $x \in [v_1, v_2]$, we have $v_1 \leq x$. If $v_1 = x$ there is nothing to show, because $C^p_x = C^p_{v_1}$ in this case. Therefore, let $v_1 < x$. Then, we have $\mathrm{fix}(C^p_{v_1}) = C^p_{v_1}\big(\mathrm{fix}(C^p_{v_1})\big) < C^p_x\big(\mathrm{fix}(C^p_{v_1})\big)$ (Lemma 7.52). Therefore, the Picard iteration associated to C^p_x starting at $\mathrm{fix}(C^p_{v_1})$ is strictly increasing (Lemma 4.47). Next, we show that this Picard iteration is bounded from above by $\mathrm{fix}(C^p_{v_2})$. This is done by induction over the number of iterations n. But first, we consider the following auxiliary statement. Because $x \leq v_2$, A^p as well as ω^p_v are both strictly increasing and according to Lemma 7.52, the following holds for all $r \in \hat{R}^p_x \cap \hat{R}^p_{v_2}$:

$$\begin{aligned} r \leq \mathrm{fix}(C^p_{v_2}) \;&\Rightarrow\; \omega^p_x(r) \leq \omega^p_{v_2}(r) \leq \omega^p_{v_2}\big(\mathrm{fix}(C^p_{v_2})\big) \\ &\Rightarrow\; A^p \circ \omega^p_x(r) \leq A^p \circ \omega^p_{v_2}(r) \leq A^p \circ \omega^p_{v_2}\big(\mathrm{fix}(C^p_{v_2})\big) \\ &\Rightarrow\; C^p_x(r) \leq C^p_{v_2}\big(\mathrm{fix}(C^p_{v_2})\big) = \mathrm{fix}(C^p_{v_2}). \end{aligned} \tag{7.5}$$

Base case:
For $n = 0$, we have $\big(C^p_x\big)^0\big(\mathrm{fix}(C^p_{v_1})\big) = \mathrm{fix}(C^p_{v_1}) \leq \mathrm{fix}(C^p_{v_2})$.
Induction hypothesis:
Let the statement hold for $n = 0, \ldots, m$.
Induction step:
We consider $n = m+1$. The inequality $\big(C^p_x\big)^m\big(\mathrm{fix}(C^p_{v_1})\big) \leq \mathrm{fix}(C^p_{v_2})$ holds according to the induction hypothesis. By considering (7.5), we have

$$\big(C^p_x\big)^m\big(\mathrm{fix}(C^p_{v_1})\big) \leq \mathrm{fix}(C^p_{v_2}) \;\Rightarrow\; \big(C^p_x\big)^{m+1}\big(\mathrm{fix}(C^p_{v_1})\big) = C^p_x\Big(\big(C^p_x\big)^m\big(\mathrm{fix}(C^p_{v_1})\big)\Big) \leq \mathrm{fix}(C^p_{v_2}).$$

As a strictly increasing and bounded sequence, the considered Picard iteration converges to a point $r^*_x := \lim_{n\to\infty}\big(C^p_x\big)^n\big(\mathrm{fix}(C^p_{v_1})\big) \in \left[\mathrm{fix}(C^p_{v_1}), \mathrm{fix}(C^p_{v_2})\right] \subset \hat{R}^p_x$. The following argument why r^*_x is a fixed point of C^p_x is taken from [Ber07, p. 32]:

$$C^p_x(r^*_x) = \lim_{n\to\infty}\big(C^p_x\big)^{n+1}\big(\mathrm{fix}(C^p_{v_1})\big) = \lim_{n\to\infty}\big(C^p_x\big)^{n}\big(\mathrm{fix}(C^p_{v_1})\big) = r^*_x.$$

Because C^p_x is contractive, the existence of a fixed point of C^p_x implies that C^p_x is a selfmap (Corollary 7.47) and the statement is shown.

□

As already mentioned, the importance of Theorem 7.58 is that it reduces the list of requirements of the convergence theorem that is presented in the following section. Because if $C^p_{r^{**}_{p-1}-\varepsilon}$ and $C^p_{r^{**}_{p-1}+\varepsilon}$ are selfmaps and A^p is contractive, then C^p_v is a contractive selfmap for all v that are an element of the closed ε-ball centered at r^{**}_{p-1}.
As a final preparation, we consider the intersection of two resistance based domains.

Lemma 7.59 *Let $p \in \{2, \dots, N\}$ and let $v_1, v_2 \in V^p$. Furthermore, let $\hat{R}^p_{v_1} = [r^{\min}_{v_1}, r^{\max}_{v_1}]$ and let $\hat{R}^p_{v_2} = [r^{\min}_{v_2}, r^{\max}_{v_2}]$. Then, the following holds:*

$$v_1 < v_2 \;\Rightarrow\; \hat{R}^p_{v_1} \cap \hat{R}^p_{v_2} = [r^{\min}_{v_1}, r^{\max}_{v_2}].$$

Proof. According to Lemma 7.7, the domains $\hat{R}^p_{v_1}$ and $\hat{R}^p_{v_2}$ are nonempty and closed intervals and thus there exist $r^{\min}_{v_1} \le r^{\max}_{v_1}$ and $r^{\min}_{v_2} \le r^{\max}_{v_2}$ such that $\hat{R}^p_{v_1} = [r^{\min}_{v_1}, r^{\max}_{v_1}]$ and $\hat{R}^p_{v_2} = [r^{\min}_{v_2}, r^{\max}_{v_2}]$. Let $v_1 < v_2$. First, we show that $r^{\min}_{v_2} < r^{\min}_{v_1}$ and $r^{\max}_{v_2} < r^{\max}_{v_1}$, which is somehow counter-intuitive. Let us consider

$$0 < w^p < 1 \;\Rightarrow\; 1 < \frac{1}{w^p} \;\Rightarrow\; 0 < \frac{1}{w^p} - 1 = \frac{1 - w^p}{w^p} \;\Rightarrow\; \frac{1 - w^p}{w^p}(v_1 - v_2) < 0.$$

With this and by applying Lemma 7.53, we have

$$r^{\min}_{v_2} = r^{\min}_{v_1} + \frac{1 - w^p}{w^p}(v_1 - v_2) < r^{\min}_{v_1} \quad \text{and} \quad r^{\max}_{v_2} = r^{\max}_{v_1} + \frac{1 - w^p}{w^p}(v_1 - v_2) < r^{\max}_{v_1}.$$

Therefore, $r \in \hat{R}^p_{v_1} \cap \hat{R}^p_{v_2}$ if and only if $r \in [r^{\min}_{v_1}, r^{\max}_{v_2}]$. □

This completes the analysis of the properties of the resistance based iteration function C^p_v and we finally have all the parts together to state and prove the convergence characteristics of Algorithm 5.2 with a plurality of ADA pairs.

7.3. Convergence Characteristics of the ADA Algorithm with a Plurality of ADA Pairs

In this section, we state conditions that guarantee that the output of Algorithm 5.2 converges to the super fixed point vector $\boldsymbol{i}^{**}$. For this, we require the concept of a sufficiently well distributed ADA update sequence. We consider an ADA update sequence as sufficiently well distributed, if after each entry of the sequence there follows an infinite number of entries of each $p \in [N]$.

Definition 7.60 *An infinite ADA update sequence $u = (u_n)_{n \in \mathbb{N}}$ is called* sufficiently well distributed *if for all $\bar{n} \in \mathbb{N}$ and for all $p \in [N]$ there exist an infinite subsequence $(u_{n_k})_{k \in \mathbb{N}}$ such that $n_1 \ge \bar{n}$ and $u_{n_k} = p$ for all $k \in \mathbb{N}$.*

Example 7.61 *Let $u = (u_n)_{n \in \mathbb{N}}$ be an infinite ADA update sequence defined by*

$$u_n := \begin{cases} 1, & \text{if } \exists\, k \in \mathbb{N}_0 : n = kN + 1 \\ \vdots & \\ N, & \text{if } \exists\, k \in \mathbb{N}_0 : n = kN + N, \end{cases} \qquad \text{i.e.,} \quad u = (1, 2, \dots, N, 1, 2, \dots, N, \dots).$$

Let $\bar{n} \ge 1$ and let $p \in [N]$. Then, u_{n_k} with $n_k := (k + \bar{n})N + p$ is a subsequence of u whose entries are all p such that $n_1 \ge \bar{n}$. Therefore, u is a sufficiently well distributed ADA update sequence.

In contrast, let $v = (v_n)_{n\in\mathbb{N}}$ be the infinite ADA update sequence whose entries are all one, i.e., $v_n = 1$ for all $n \in \mathbb{N}$. The sequence v is not sufficiently well distributed because, for example, there does not exist a subsequence whose entries are all two.

We continue with an important auxiliary statement. Recall from Remark 7.3 that $v \in V^p$ denotes the incumbent drift resistance approximation of ADA pair $p-1$ and that we are interested in the fixed points of C_v^p for certain $v \in V^p$ according to Lemma 7.42. We define an auxiliary function that provides a link between the neighborhood of the drift resistance super fixed point r_{p-1}^{**} of ADA pair $p-1$, which is a subset of V^p, and the fixed points of C_v^p for elements v taken from this neighborhood. This function is contractive, which is essential for the proof of the major convergence Theorem 7.68 below and the reason why the resistance based approach was taken in the first place.

Definition 7.62 *Let $\boldsymbol{i}^{**} \in \mathbb{R}_{>0}^N$ and let $\boldsymbol{r}^{**} = (r_1^{**}, \ldots, r_N^{**})$ be the corresponding drift resistance super fixed point vector. Let $p \in \{2, \ldots, N\}$ and let $\varepsilon > 0$. We set $m(\varepsilon) := r_{p-1}^{**} - \varepsilon$ and $M(\varepsilon) := r_{p-1}^{**} + \varepsilon$. If*

- *$m(\varepsilon) \in V^p$ and $M(\varepsilon) \in V^p$,*
- *A^p is a contractive selfmap and*
- *$C_{m(\varepsilon)}^p$ as well as $C_{M(\varepsilon)}^p$ are selfmaps,*

then we define

$$\varphi_\varepsilon^p : [m(\varepsilon), M(\varepsilon)] \to [\mathrm{fix}(C_{m(\varepsilon)}^p), \mathrm{fix}(C_{M(\varepsilon)}^p)], \quad \varphi_\varepsilon^p(v) := \mathrm{fix}(C_v^p).$$

Theorem 7.63 *The function φ_ε^p is well-defined, strictly increasing and contractive.*

Proof. Let $p \in \{2, \ldots, N\}$, let $m := r_{p-1}^{**} - \varepsilon$ and $M := r_{p-1}^{**} + \varepsilon$. To show that φ_ε^p is well-defined, we have to show that for all $v \in [m, M]$

- the function C_v^p is well-defined,
- the function C_v^p is a contractive selfmap (and thus $\mathrm{fix}(C_v^p)$ exists),
- the image of $[m, M]$ under φ_ε^p is a subset of $[\mathrm{fix}(C_m^p), \mathrm{fix}(C_M^p)]$.

Because V^p is an interval (Definition 7.4), $m, M \in V^p$ implies that $[m, M] \subset V^p$. Therefore, the function C_v^p is well-defined for all $v \in [m, M]$ (Definition 7.36). By assumption, A^p is contractive and the functions C_m^p as well as C_M^p are both selfmaps. Then, the function C_v^p is also a contractive selfmap for all $v \in [m, M]$ (Theorem 7.58). Therefore, the unique fixed point $\mathrm{fix}(C_v^p)$ exists for all $v \in [m, M]$ (Corollary 7.47). To show that $\varphi_\varepsilon^p\big([m, M]\big) \subset [\mathrm{fix}(C_m^p), \mathrm{fix}(C_M^p)]$, we first show that φ_ε^p is strictly increasing. For this, let $v, x \in [m, M]$ such that $v < x$. Then, $\varphi_\varepsilon^p(v) = \mathrm{fix}(C_v^p) < \mathrm{fix}(C_x^p) = \varphi_\varepsilon^p(x)$ holds according to Lemma 7.56 and thus φ_ε^p is strictly increasing. With this, we have

$$v \in [m, M] \;\Rightarrow m \le v \le M \;\Rightarrow\; \varphi_\varepsilon^p(m) \le \varphi_\varepsilon^p(v) \le \varphi_\varepsilon^p(M) \;\Rightarrow\; \varphi_\varepsilon^p(v) \in \big[\varphi_\varepsilon^p(m), \varphi_\varepsilon^p(M)\big].$$

Finally, we show that φ_ε^p is contractive. For this, let $v, x \in [m, M]$ such that $v \neq x$. We denote $r_v^* := \mathrm{fix}(C_v^p)$ and $r_x^* := \mathrm{fix}(C_x^p)$. By using that A^p is contractive, it follows that

$$\begin{aligned}
\left|\varphi_\varepsilon^p(v) - \varphi_\varepsilon^p(x)\right| &= \left|r_v^* - r_x^*\right| = \left|C_v^p(r_v^*) - C_x^p(r_x^*)\right| = \left|A^p \circ \omega_v^p(r_v^*) - A^p \circ \omega_x^p(r_x^*)\right| \\
&< \left|\omega_v^p(r_v^*) - \omega_x^p(r_x^*)\right| = \left|w^p r_v^* + (1-w^p)v - \left(w^p r_x^* + (1-w^p)x\right)\right| \\
&= \left|w^p(r_v^* - r_x^*) + (1-w^p)(v-x)\right| \\
&< w^p|r_v^* - r_x^*| + (1-w^p)|v-x| \\
&= w^p\left|\varphi_\varepsilon^p(v) - \varphi_\varepsilon^p(x)\right| + (1-w^p)|v-x|
\end{aligned}$$

holds and thus we have (because $0 < w^p < 1$)

$$\begin{aligned}
&\left|\varphi_\varepsilon^p(v) - \varphi_\varepsilon^p(x)\right| < w^p\left|\varphi_\varepsilon^p(v) - \varphi_\varepsilon^p(x)\right| + (1-w^p)|v-x| \\
\Rightarrow\ &(1-w^p)\left|\varphi_\varepsilon^p(v) - \varphi_\varepsilon^p(x)\right| < (1-w^p)|v-x| \\
\Rightarrow\ &\left|\varphi_\varepsilon^p(v) - \varphi_\varepsilon^p(x)\right| < |v-x|.
\end{aligned}$$

□

As a consequence of φ_ε^p being contractive, the closed ε-ball centered at r_{p-1}^{**} is mapped to the open ε-ball centered at r_p^{**}. In this thesis, the ε-ball centered at $x_0 \in \mathbb{R}$ is denoted and defined by $B_\varepsilon(x_0) := \{x \in \mathbb{R} : |x - x_0| < \varepsilon\}$. The closed ε-ball centered at $x_0 \in \mathbb{R}$ is denoted by $\overline{B}_\varepsilon(x_0)$. Note that this notation is similar to that of the iteration function B_v^p. However, the two notations can be distinguished from each other by the superscript p.

Corollary 7.64 *If φ_ε^p exists, then $\varphi_\varepsilon^p\big(\overline{B}_\varepsilon(r_{p-1}^{**})\big) \subset B_\varepsilon(r_p^{**})$ holds.*

Proof. Let $p \in \{2, \ldots, N\}$ and let $\varepsilon > 0$. Recall from Lemma 7.42 that $r_p^{**} = \mathrm{fix}\big(C_{r_{p-1}^{**}}^p\big)$ and thus $\varphi_\varepsilon^p(r_{p-1}^{**}) = r_p^{**}$ holds by construction of φ_ε^p. Let $v \in \overline{B}_\varepsilon(r_{p-1}^{**})$. Because φ_ε^p is contractive (Theorem 7.63), we have

$$\left|\varphi_\varepsilon^p(v) - r_p^{**}\right| = \left|\varphi_\varepsilon^p(v) - \varphi_\varepsilon^p(r_{p-1}^{**})\right| < |v - r_{p-1}^{**}| \leq \varepsilon \ \Rightarrow\ \varphi_\varepsilon^p(v) \in B_\varepsilon(r_p^{**}).$$

□

The function φ_ε^p and the statement of Corollary 7.64 are demonstrated in the following example.

Example 7.65 *This example is an extension of Example 7.44, where a drift resistance super fixed point vector $\mathbf{r}^{**} = (r_1^{**}, r_2^{**}, r_3^{**})$ for the case $N = 3$ is determined. In particular, we reuse the function A^1, A^2 as well as ω_v^2 and we again assume that the corresponding domains are sufficiently large.*
With this, we have $A^1(r) := \frac{1}{2}r + \frac{1}{2}$ and thus $r_1^{**} = \mathrm{fix}(A^1) = 1$. Furthermore, we have

$$A^2(r) := \frac{1}{3}r \quad \text{and} \quad \omega_v^2(r) = \frac{1}{2}r + \frac{1}{2}v \ \Rightarrow\ C_v^2(r) = A^2 \circ \omega_v^2(r) = \frac{1}{6}r + \frac{1}{6}v \ \forall\ v \in V^2.$$

We consider φ_ε^p for $p = 2$. In this example, φ_ε^2 can be written as an explicit function. Recall from Definition 7.62 that φ_ε^2 maps certain drift resistance approximations v of ADA pair $p-1=1$ to the fixed points of the corresponding iteration functions C_v^p of ADA pair $p = 2$. These fixed points can be calculated by

$$C_v^2(r^*) = r^* \;\Leftrightarrow\; \frac{1}{6}r^* + \frac{1}{6}v = r^* \;\Leftrightarrow\; \frac{5}{6}r^* = \frac{1}{6}v \;\Leftrightarrow\; r^* = \frac{1}{5}v \;\Rightarrow\; \varphi_\varepsilon^2(v) = \frac{1}{5}v.$$

In particular, we have $r_1^{**} = 1$ and thus $r_2^{**} = \mathrm{fix}(C^2_{r_1^{**}}) = \frac{1}{5}$, see also Example 7.44.
To demonstrate Corollary 7.64, let $\varepsilon > 0$. Then, we have $\overline{B}_\varepsilon(r_1^{**}) = [1-\varepsilon, 1+\varepsilon]$ and thus

$$\varphi_\varepsilon^2\big(\overline{B}_\varepsilon(r_1^{**})\big) = [\frac{1}{5} - \frac{\varepsilon}{5}, \frac{1}{5} + \frac{\varepsilon}{5}] = [r_2^{**} - \frac{\varepsilon}{5}, r_2^{**} + \frac{\varepsilon}{5}] \subset (r_2^{**} - \varepsilon, r_2^{**} + \varepsilon) = B_\varepsilon(r_2^{**}).$$

We continue with an auxiliary lemma, which considers an ADA pair p, $p \geq 2$. The lemma states that if there is a sequence of drift resistance approximations of the upper neighbor of p, i.e., a sequence of drift resistance approximations of ADA pair $p-1$, that converges to the drift resistance super fixed point r_{p-1}^{**}, then the sequence of corresponding iteration functions converges pointwise to $C^p_{r_{p-1}^{**}}$.

Lemma 7.66 *Let $\boldsymbol{i}^{**} \in \mathbb{R}^N_{>0}$ and let $\boldsymbol{r}^{**} = (r_1^{**}, \ldots, r_N^{**})$ be the corresponding drift resistance super fixed point vector. Let $p \in \{2, \ldots, N\}$ and let A^p be contractive. Furthermore, let $m, M \in V^p$ such that $m < r_{p-1}^{**} < M$ and let $(v^n)_{n\in\mathbb{N}} \subset [m, M]$ be a sequence such that $\lim\limits_{n\to\infty} v^n = r_{p-1}^{**}$. Then, the following holds:*

$$\lim_{n\to\infty} C^p_{v^n}(r) = C^p_{r_{p-1}^{**}}(r) \;\forall\; r \in \hat{R}^p_m \cap \hat{R}^p_M.$$

Proof. According to Lemma 7.57, $\hat{R}^p_m \cap \hat{R}^p_M \subset \hat{R}^p_v$ holds for all $v \in [m, M]$. Therefore, the function evaluation $C^p_{v^n}(r)$ is well-defined for all $r \in \hat{R}^p_m \cap \hat{R}^p_M$ and for all $n \in \mathbb{N}$. Because $C_v^p = A^p \circ \omega_v^p$ (Definition 7.36) and A^p is contractive by assumption, we have

$$\begin{aligned}\big|C^p_{v^n}(r) - C^p_{r_{p-1}^{**}}(r)\big| &= \big|A^p \circ \omega^p_{v^n}(r) - A^p \circ \omega^p_{r_{p-1}^{**}}(r)\big| \\ &< \big|\omega^p_{v^n}(r) - \omega^p_{r_{p-1}^{**}}(r)\big| = \big|w^p r + (1-w^p)v^n - \big(w^p r + (1-w^p)r_{p-1}^{**}\big)\big| \\ &= (1-w^p)\big|v^n - r_{p-1}^{**}\big|\end{aligned}$$

and thus for $(n \to \infty)$ we have

$$v^n \to r_{p-1}^{**} \;\Rightarrow\; \big|v^n - r_{p-1}^{**}\big| \to 0 \;\Rightarrow\; \big|C^p_{v^n}(r) - C^p_{r_{p-1}^{**}}(r)\big| \to 0 \;\Rightarrow\; C^p_{v^n}(r) \to C^p_{r_{p-1}^{**}}(r).$$

□

As a final preparation, the following statement is considered. If the $(p-1)$th component of the resistance based ADA iterates converges to the $(p-1)$th component of the drift resistance super fixed point vector r_{p-1}^{**}, then the p-th component of the resistance based ADA iterates converges to r_p^{**} under certain conditions. This statement is required in the induction step of the proof of the major convergence Theorem 7.68 below.

Theorem 7.67 *Let $\boldsymbol{i}^{**} \in \mathbb{R}^N_{>0}$ and let $\boldsymbol{r}^{**} = (r_1^{**}, \ldots, r_N^{**})$ be the corresponding drift resistance super fixed point vector. Let $p \geq 2$.*

- *Let A^p be contractive.*
- *Let there exist $\delta > 0$ such that $[r_{p-1}^{**} - \delta, r_{p-1}^{**} + \delta] \subset V^p$ and $C^p_{r_{p-1}^{**}-\delta}$ as well as $C^p_{r_{p-1}^{**}+\delta}$ are selfmaps.*
- *Let u be a sufficiently well distributed ADA update sequence and $\hat{\boldsymbol{i}}_{\boldsymbol{t},\text{in}} = (i_1^{\text{in}}, \ldots, i_N^{\text{in}})$ be a given input vector such that $\hat{\boldsymbol{i}}_{\boldsymbol{t},\text{in}}$ and u are a feasible input combination.*

For $n \in \mathbb{N}$ let $\boldsymbol{r}^n(\hat{\boldsymbol{i}}_{\boldsymbol{t},\text{in}}, u) = (r_1^n, \ldots, r_N^n)$ be the corresponding n-th resistance based ADA iterate. Then, the following holds:

$$\lim_{n\to\infty} r_{p-1}^n = r_{p-1}^{**} \;\Rightarrow\; \lim_{n\to\infty} r_p^n = r_p^{**}.$$

Proof. Let $\lim_{n\to\infty} r_{p-1}^n = r_{p-1}^{**}$. Let $\varepsilon > 0$ arbitrary but fixed. Without loss of generality, let $\varepsilon \leq \delta$, where $\delta > 0$ is the constant from the theorem's requirements. Then, there exists $\bar{n} \in \mathbb{N}$ such that $|r_{p-1}^n - r_{p-1}^{**}| < \varepsilon$ for all $n \geq \bar{n}$. Aiming at a better readability, we suppose without loss of generality that $\bar{n} = 1$, i.e., $|r_{p-1}^n - r_{p-1}^{**}| < \varepsilon$ for all $n \in \mathbb{N}$. Furthermore, we denote $m := r_{p-1}^{**} - \varepsilon$ and $M := r_{p-1}^{**} + \varepsilon$. Because $\varepsilon \leq \delta$, we have

$$r_{p-1}^n \in [m, M] = \bar{B}_\varepsilon(r_{p-1}^{**}) \subseteq [r_{p-1}^{**} - \delta, r_{p-1}^{**} + \delta] \;\forall\; n \in \mathbb{N}. \tag{7.6}$$

Recall from Lemma 7.45 that in the $(n+1)$st iteration the p-th component of the resistance based ADA iterate is either updated by $r_p^{n+1} = C^p_{r_{p-1}^n}(r_p^n)$ (if $u_{n+1} = p$) or it remains unchanged, i.e., $r_p^{n+1} = r_p^n$ (if $u_{n+1} \neq p$). The following argumentation allows to assume without loss of generality that $u_n = p$ for all $n \in \mathbb{N}$ and simultaneously $\lim_{n\to\infty} r_{p-1}^n = r_{p-1}^{**}$. This is assumed to avoid a corresponding case distinction between $u_{n+1} = p$ and $u_{n+1} \neq p$. Then, we have

$$r_p^{n+1} = C^p_{r_{p-1}^n}(r_p^n) \;\forall\; n \in \mathbb{N} \tag{7.7}$$

according to Lemma 7.45. The assumption without loss of generality is valid for the following three reasons. First, we consider a sufficiently well distributed ADA update sequence and thus there exist infinite many updates with ADA pair p. Second, we have $\lim_{n\to\infty} r_{p-1}^n = r_{p-1}^{**}$ by assumption. In particular, we have $r_{p-1}^n \in [m, M]$ for all $n \in \mathbb{N}$ by construction. Therefore, we can execute the updates with ADA pair $p-1$ only implicitly and focus only on the updates with ADA pair p. Finally, an ADA iteration with an ADA pair q, $q > p$ or $q < p-1$, does not affect ADA pair p and thus such ADA iterations can be omitted in this proof, see also Lemma 7.45.
The road map for this proof is to show that:

1. There exists $k \in \mathbb{N}$ such that $r_p^k \in \hat{R}_m^p \cap \hat{R}_M^p$.
2. If $r_p^k \in \hat{R}_m^p \cap \hat{R}_M^p$ then $\left(C_m^p\right)^\ell(r_p^k) \leq r_p^{k+\ell} \leq \left(C_M^p\right)^\ell(r_p^k) \;\forall\; \ell \in \mathbb{N}$.

3. If $r_p^k \in \hat{R}_m^p \cap \hat{R}_M^p$ then there exists $\bar{\ell} \in \mathbb{N}$ such that $\left|\left(C_m^p\right)^\ell(r_p^k) - \operatorname{fix}(C_m^p)\right| < \varepsilon$ and $\left|\left(C_M^p\right)^\ell(r_p^k) - \operatorname{fix}(C_M^p)\right| < \varepsilon$ for all $\ell \geq \bar{\ell}$.
4. $|\operatorname{fix}(C_m^p) - r_p^{**}| < \varepsilon$ and $|\operatorname{fix}(C_M^p) - r_p^{**}| < \varepsilon$.

By combining Items 1 to 4 at the end of this proof, we obtain $|r_p^\ell - r_p^{**}| < 2\varepsilon$ for all $\ell \geq \bar{\ell}$ and the statement is shown.
First, we make some considerations that are relevant throughout the proof. Because $\hat{\boldsymbol{i}}_{\boldsymbol{t},\text{in}}$ and u are a feasible input combination, all considered ADA iterates $\boldsymbol{r}^n(\hat{\boldsymbol{i}}_{\boldsymbol{t},\text{in}}, u)$ exist and the corresponding function evaluations are well-defined for all $n \in \mathbb{N}$.
Furthermore, A^p is contractive and $C^p_{r_{p-1}^{**}-\delta}$ as well as $C^p_{r_{p-1}^{**}+\delta}$ are selfmaps by assumption. Therefore, C_v^p is a contractive selfmap and the unique fixed point $\operatorname{fix}(C_v^p)$ exists for all $v \in [r_{p-1}^{**} - \delta, r_{p-1}^{**} + \delta]$ (Theorem 7.58 and Corollary 7.47). In particular, C_m^p and C_M^p are contractive selfmaps. In addition, C_v^p is strictly increasing for all $v \in V^p$ (Lemma 7.46) and thus Lemma 4.45 can be applied to all C_v^p with $v \in [m, M]$, i.e., for all $r \in \hat{R}_v^p$

$$r < \operatorname{fix}(C_v^p) \;\Rightarrow\; r < C_v^p(r) < \operatorname{fix}\big(C_v^p(r)\big) \quad \text{and} \quad r > \operatorname{fix}(C_v^p) \;\Rightarrow\; r > C_v^p(r) > \operatorname{fix}\big(C_v^p(r)\big). \tag{7.8}$$

Now, we begin with Item 1. Because the domains are closed intervals, let $\hat{R}_m^p = [r_m^{\min}, r_m^{\max}]$ and $\hat{R}_M^p = [r_M^{\min}, r_M^{\max}]$ and thus $\hat{R}_m^p \cap \hat{R}_M^p = [r_m^{\min}, r_M^{\max}]$ (Lemma 7.59). Then, we have for all $n \in \mathbb{N}$

$$r_p^n < r_m^{\min} \;\Rightarrow\; r_p^n < r_p^{n+1} \quad \text{and} \quad r_p^n > r_M^{\max} \;\Rightarrow\; r_p^n > r_p^{n+1}. \tag{7.9}$$

Equation (7.9) holds, because

- $m \leq r_{p-1}^n \leq M \;\Rightarrow\; \operatorname{fix}(C_m^p) \leq \operatorname{fix}(C^p_{r_{p-1}^n}) \leq \operatorname{fix}(C_M^p)$ (Lemma 7.56) and
- $\operatorname{fix}(C_m^p) \in \hat{R}_m^p = [r_m^{\min}, r_m^{\max}]$, i.e., $r_m^{\min} \leq \operatorname{fix}(C_m^p)$, and thus

  $$r_p^n < r_m^{\min} \;\Rightarrow\; r_p^n < \operatorname{fix}(C_m^p) \leq \operatorname{fix}(C^p_{r_{p-1}^n}) \;\Rightarrow\; r_p^n < C^p_{r_{p-1}^n}(r_p^n) = r_p^{n+1} < \operatorname{fix}(C^p_{r_{p-1}^n}),$$

  where the last implication follows from (7.8).
- Analogously, we have $\operatorname{fix}(C_M^p) \in \hat{R}_M^p = [r_M^{\min}, r_M^{\max}]$, i.e., $\operatorname{fix}(C_M^p) \leq r_M^{\max}$, and thus

  $$r_p^n > r_M^{\max} \;\Rightarrow\; r_p^n > \operatorname{fix}(C_M^p) \geq \operatorname{fix}(C^p_{r_{p-1}^n}) \;\Rightarrow\; r_p^n > C^p_{r_{p-1}^n}(r_p^n) = r_p^{n+1} > \operatorname{fix}(C^p_{r_{p-1}^n}).$$

We use (7.9) to show that there exists $k \in \mathbb{N}$ such that $r_p^k \in \hat{R}_m^p \cap \hat{R}_M^p$. There are three cases: $r_m^{\min} \leq r_p^1 \leq r_M^{\max}$, $r_p^1 < r_m^{\min}$ and $r_p^1 > r_M^{\max}$. In the first case, there is nothing to show.
So let $r_p^1 < r_m^{\min}$. Let us suppose that there exists no $k \in \mathbb{N}$ such that $r_p^k \geq r_m^{\min}$, i.e., $r_p^n < r_m^{\min}$ for all $n \in \mathbb{N}$. Then, the sequence $(r_p^n)_{n\in\mathbb{N}}$ is strictly increasing according to (7.9) and it is bounded by $r_m^{\min}$. Therefore, there exists $r^* \leq r_m^{\min}$ such that $\lim_{n\to\infty} r_p^n = r^*$. In the following, we show that this leads to a contradiction. By construction, we have

$m = r_{p-1}^{**} - \varepsilon < r_{p-1}^{**}$ and thus $\mathrm{fix}(C_m^p) < \mathrm{fix}\big(C_{r_{p-1}^{**}}^p\big)$ (Lemma 7.56). Furthermore, because C_m^p is a selfmap on its domain $\hat{R}_m^p$, $\mathrm{fix}(C_m^p) \in \hat{R}_m^p = [r_m^{\min}, r_m^{\max}]$ holds, and thus

$$r_m^{\min} \leq \mathrm{fix}(C_m^p) < \mathrm{fix}\big(C_{r_{p-1}^{**}}^p\big) \Rightarrow\ r_m^{\min} < C_{r_{p-1}^{**}}^p(r_m^{\min}) < \mathrm{fix}\big(C_{r_{p-1}^{**}}^p\big),$$

where the last implication follows from (7.8) with $C_v^p = C_{r_{p-1}^{**}}^p$ and $r = r_m^{\min}$. Therefore, $C_{r_{p-1}^{**}}^p(r_m^{\min}) \neq r_m^{\min}$ holds and we set

$$\bar{\varepsilon} := \frac{1}{2}\big|C_{r_{p-1}^{**}}^p(r_m^{\min}) - r_m^{\min}\big| > 0.$$

By considering that $m \leq r_{p-1}^n \leq M$ for all $n \in \mathbb{N}$, $\lim\limits_{n\to\infty} r_{p-1}^n = r_{p-1}^{**}$ and $r_m^{\min} \in \hat{R}_m^p \cap \hat{R}_M^p$, we have $\lim\limits_{n\to\infty}\big(C_{r_{p-1}^n}^p(r_m^{\min})\big) = C_{r_{p-1}^{**}}^p(r_m^{\min})$ (Lemma 7.66) and thus

$$\exists\ n_1 \in \mathbb{N} : \big|C_{r_{p-1}^n}^p(r_m^{\min}) - C_{r_{p-1}^{**}}^p(r_m^{\min})\big| < \bar{\varepsilon}\ \forall\ n \geq n_1.$$

Let $n \geq n_1$, then

$$\begin{aligned}\bar{\varepsilon} + \big|C_{r_{p-1}^n}^p(r_m^{\min}) - C_{r_{p-1}^{**}}^p(r_m^{\min})\big| &< 2\bar{\varepsilon} = \big|C_{r_{p-1}^{**}}^p(r_m^{\min}) - r_m^{\min}\big| \\ &\leq \big|C_{r_{p-1}^{**}}^p(r_m^{\min}) - C_{r_{p-1}^n}^p(r_m^{\min})\big| + \big|\big(C_{r_{p-1}^n}^p(r_m^{\min})\big) - r_m^{\min}\big|\end{aligned}$$

and thus

$$\bar{\varepsilon} < \big|C_{r_{p-1}^n}^p(r_m^{\min}) - r_m^{\min}\big|\ \forall\ n \geq n_1. \tag{7.10}$$

Furthermore, $(r_p^n)_{n\in\mathbb{N}}$ is convergent and thus it is a Cauchy sequence. Therefore,

$$\exists\ n_2 \in \mathbb{N} : \big|r_p^n - r_p^{n+1}\big| < \bar{\varepsilon}\ \forall\ n \geq n_2. \tag{7.11}$$

Because $C_{r_{p-1}^n}^p$ is contractive for all $n \in \mathbb{N}$ and $C_{r_{p-1}^n}^p(r_p^n) = r_p^{n+1}$, we have

$$\big|C_{r_{p-1}^n}^p(r_m^{\min}) - r_p^{n+1}\big| = \big|C_{r_{p-1}^n}^p(r_m^{\min}) - C_{r_{p-1}^n}^p(r_p^n)\big| < \big|r_m^{\min} - r_p^n\big|. \tag{7.12}$$

Recall that we suppose that $r_p^n < r_m^{\min}$ for all $n \in \mathbb{N}$ and thus $|r_m^{\min} - r_p^n| = r_m^{\min} - r_p^n$. Furthermore, because $C_{r_{p-1}^n}^p$ is strictly increasing (Lemma 7.46), we have $C_{r_{p-1}^n}^p(r_m^{\min}) > C_{r_{p-1}^n}^p(r_p^n) = r_p^{n+1}$ and thus $\big|C_{r_{p-1}^n}^p(r_m^{\min}) - r_p^{n+1}\big| = C_{r_{p-1}^n}^p(r_m^{\min}) - r_p^{n+1}$ for all $n \in \mathbb{N}$. Therefore, we have

$$(7.12)\ \Rightarrow C_{r_{p-1}^n}^p(r_m^{\min}) - r_p^{n+1} < r_m^{\min} - r_p^n\ \Rightarrow\ C_{r_{p-1}^n}^p(r_m^{\min}) - r_m^{\min} < r_p^{n+1} - r_p^n. \tag{7.13}$$

By considering that $(r_p^n)_{n\in\mathbb{N}}$ is strictly increasing, we have $r_p^{n+1} - r_p^n = |r_p^{n+1} - r_p^n|$. Furthermore, because $m \leq r_{p-1}^n$ and thus $\mathrm{fix}(C_m^p) \leq \mathrm{fix}(C_{r_{p-1}^n}^p)$ (Lemma 7.56) as well as

$\text{fix}(C_m^p) \in \hat{R}_m^p = [r_m^{\min}, r_m^{\max}]$, we have $r_m^{\min} \leq \text{fix}(C_m^p) \leq \text{fix}(C_{r_{p-1}^n}^p)$. By applying (7.8) with $C_v^p = C_{r_{p-1}^n}^p$ and $r = r_m^{\min}$, we obtain $r_m^{\min} \leq C_{r_{p-1}^n}^p(r_m^{\min}) \leq \text{fix}(C_{r_{p-1}^n}^p)$, and thus

$$(7.13) \;\Rightarrow\; \left|C_{r_{p-1}^n}^p(r_m^{\min}) - r_m^{\min}\right| < \left|r_p^{n+1} - r_p^n\right| \;\forall\; n \in \mathbb{N}. \tag{7.14}$$

Finally, by considering (7.14) together with (7.10) and (7.11) we obtain

$$\bar{\varepsilon} < \left|\left(C_{r_{p-1}^n}^p(r_m^{\min})\right) - r_m^{\min}\right| < \left|r_p^{n+1} - r_p^n\right| < \bar{\varepsilon} \;\forall\; n \geq \max\{n_1, n_2\}.$$

This is a contradiction and thus there exists $k \in \mathbb{N}$ such that $r_p^k \geq r_m^{\min}$.
Recall that our goal is to show that there exists $k \in \mathbb{N}$ such that $r_p^k \in [r_m^{\min}, r_M^{\max}]$. Therefore, it remains to show that $r^k \leq r_M^{\max}$. For this, let $k \in \mathbb{N}$ such that $r_p^{k-1} < r_m^{\min}$ and $r_p^k \geq r_m^{\min}$, which exists as shown above and because we are in the case $r_p^1 < r_m^{\min}$. Because $m \leq r_{p-1}^{k-1} \leq M$ (Equation (7.6)), we have $\text{fix}(C_m^p) \leq \text{fix}\big(C_{r_{p-1}^{k-1}}^p\big) \leq \text{fix}(C_M^p)$ (Lemma 7.56). Furthermore, $\text{fix}(C_m^p) \in \hat{R}_m^p = [r_m^{\min}, r_m^{\max}]$ and $\text{fix}(C_M^p) \in [r_M^{\min}, r_M^{\max}]$ holds and thus

$$r_p^{k-1} < r_m^{\min} \leq \text{fix}(C_m^p) \leq \text{fix}\big(C_{r_{p-1}^{k-1}}^p\big) \leq \text{fix}(C_M^p) \leq r_M^{\max}.$$

By applying (7.8) with $C_v^p = C_{r_{p-1}^{k-1}}^p$ and $r = r_p^{k-1}$, we obtain

$$\begin{aligned} r_p^{k-1} < \text{fix}\big(C_{r_{p-1}^{k-1}}^p\big) \;&\Rightarrow\; r_p^{k-1} < C_{r_{p-1}^{k-1}}^p(r_p^{k-1}) < \text{fix}\big(C_{r_{p-1}^{k-1}}^p\big) \\ &\Rightarrow\; r_p^k = C_{r_{p-1}^{k-1}}^p(r_p^{k-1}) < \text{fix}\big(C_{r_{p-1}^{k-1}}^p\big) \leq r_M^{\max}. \end{aligned}$$

In total $r_p^k \in [r_m^{\min}, r_M^{\max}] = \hat{R}_m^p \cap \hat{R}_M^p$ holds, i.e., Item 1 of the proof's road map holds in the case $r_p^1 < r_m^{\min}$. The case $r_p^1 > r_M^{\max}$ can be shown analogously by swapping the roles of $r_m^{\min}$ and $r_M^{\max}$ as well as considering $>$ and $\geq$ instead of $<$ and $\leq$, respectively.
Next, we prove Item 2 of the proof's road map. We show by induction over ℓ that

$$\exists\; k \in \mathbb{N} : r_p^k \in \hat{R}_m^p \cap \hat{R}_M^p \;\Rightarrow\; \left(C_m^p\right)^\ell(r_p^k) \leq r^{k+\ell} \leq \left(C_M^p\right)^\ell(r_p^k) \;\forall\; \ell \in \mathbb{N}. \tag{7.15}$$

By assumption, A^p is contractive and $C_{r_{p-1}^{**}-\delta}^p$ as well as $C_{r_{p-1}^{**}+\delta}^p$ are selfmaps. Therefore, C_v^p is a contractive selfmap and the unique fixed point $\text{fix}(C_v^p)$ exists for all $v \in [r_{p-1}^{**} - \delta, r_{p-1}^{**} + \delta]$ (Theorem 7.58 and Corollary 7.47). In particular, C_m^p and C_M^p are contractive selfmaps. As a consequence, $\hat{R}_m^p \cap \hat{R}_M^p \subset \hat{R}_v^p$ holds for all $v \in [m, M]$ (Lemma 7.57) and thus $C_v^p(r)$ is well-defined for all $v \in [m, M]$ and for all $r \in \hat{R}_m^p \cap \hat{R}_M^p$. With this, we begin the induction over ℓ. So, let there exist $k \in \mathbb{N}$ such that $r_p^k \in \hat{R}_m^p \cap \hat{R}_M^p$.
Base case: Let $\ell = 1$. According to (7.6), we have $r_{p-1}^k \in [m, M]$. Then, according to Lemma 7.52 and according to (7.7),

$$C_m^p(r_p^k) \leq C_{r_{p-1}^k}^p(r_p^k) = r_p^{k+1} \leq C_M^p(r_p^k)$$

holds and the base case is proved.
Induction hypothesis: For a certain $j \in \mathbb{N}$ let (7.15) hold for all $\ell \leq j$.
Induction step: We show that (7.15) holds for $\ell = j+1$. According to Corollary 7.55, we have $\left\{\left(C_m^p\right)^j(r_p^k), \left(C_M^p\right)^j(r_p^k)\right\} \subset \hat{R}_m^p \cap \hat{R}_M^p$. Because $\hat{R}_m^p \cap \hat{R}_M^p$ is the intersection of two closed intervals, $\hat{R}_m^p \cap \hat{R}_M^p$ is a closed interval as well and thus $\left[\left(C_m^p\right)^j(r_p^k), \left(C_M^p\right)^j(r_p^k)\right] \subset \hat{R}_m^p \cap \hat{R}_M^p$ holds. According to the induction hypothesis, we have $\left(C_m^p\right)^j(r_p^k) \leq r_p^{k+j} \leq \left(C_M^p\right)^j(r_p^k)$ and thus $r_p^{k+j} \in \hat{R}_m^p \cap \hat{R}_M^p$.
Furthermore, C_m^p and C_M^p are both strictly increasing (Lemma 7.46). By considering the induction hypothesis again, we have

$$\left(C_m^p\right)^j(r_p^k) \leq r_p^{k+j} \;\Rightarrow\; C_m^p\Big(\left(C_m^p\right)^j(r_p^k)\Big) \leq C_m^p(r_p^{k+j}) \;\Rightarrow\; \left(C_m^p\right)^{j+1}(r_p^k) \leq C_m^p(r_p^{k+j})$$

and analogously $C_M^p(r_p^{k+j}) \leq \left(C_M^p\right)^{j+1}(r_p^k)$.
According to (7.6), we have $m \leq r_{p-1}^{k+j} \leq M$. By applying Lemma 7.52 and considering that $r_p^{k+j} \in \hat{R}_m^p \cap \hat{R}_M^p$, we have $C_m^p(r_p^{k+j}) \leq C_{r_{p-1}^{k+j}}^p(r_p^{k+j}) \leq C_M^p(r_p^{k+j})$. By combining everything, we have

$$\left(C_m^p\right)^{j+1}(r_p^k) \leq C_m^p(r_p^{k+j}) \leq C_{r_{p-1}^{k+j}}^p(r_p^{k+j}) = r_p^{k+j+1} \leq C_M^p(r_p^{k+j}) \leq \left(C_M^p\right)^{j+1}(r_p^k)$$

and the induction step is completed.
Next, we show that Item 3 holds. Since C_m^p and C_M^p are contractive selfmaps, the Picard iteration associated to C_m^p converges to the unique fixed point $\mathrm{fix}(C_m^p)$ for an arbitrary starting point in $\hat{R}_m^p$ and the Picard iteration associated to C_M^p converges to $\mathrm{fix}(C_M^p)$ for an arbitrary starting point in $\hat{R}_M^p$. Let $k \in \mathbb{N}_0$ such that $r_p^k \in \hat{R}_m^p \cap \hat{R}_M^p$, which exists according to Item 1. Then, there exists $n_m \in \mathbb{N}$ and $n_M \in \mathbb{N}$ such that

$$\left|\left(C_m^p\right)^n(r_p^k) - \mathrm{fix}(C_m^p)\right| < \varepsilon \;\forall\; n \geq n_m \quad \text{and} \quad \left|\left(C_M^p\right)^n(r_p^k) - \mathrm{fix}(C_M^p)\right| < \varepsilon \;\forall\; n \geq n_M.$$

By setting $\bar{\ell} := \max\{n_m, n_M\}$, Item 3 holds.
We continue with Item 4. Recall that $m := r_{p-1}^{**} - \varepsilon$ and $M := r_{p-1}^{**} + \varepsilon$ with $\varepsilon \leq \delta$. Because A^p is contractive, $[m, M] \subset V^p$ and C_m^p as well as C_M^p are selfmaps by assumption, the requirements of Definition 7.62 are met and thus the function $\varphi_\varepsilon^p : [m, M] \to \left[\mathrm{fix}(C_m^p), \mathrm{fix}(C_M^p)\right]$ exists. According to Corollary 7.64, we have

$$\varphi_\varepsilon^p(m) = \mathrm{fix}(C_m^p) \in B_\varepsilon(r_p^{**}) \;\Rightarrow\; |\mathrm{fix}(C_m^p) - r_p^{**}| < \varepsilon$$

and analogously $|\mathrm{fix}(C_M^p) - r_p^{**}| < \varepsilon$.
Finally, we combine all four statements. Let $k \in \mathbb{N}$ such that $r_p^k \in \hat{R}_m^p \cap \hat{R}_M^p$, which exists according to Item 1. Let $\bar{\ell} \in \mathbb{N}$ such that $\left|\left(C_m^p\right)^\ell(r_p^k) - \mathrm{fix}(C_m^p)\right| < \varepsilon$ and $\left|\left(C_M^p\right)^\ell(r_p^k) - \mathrm{fix}(C_M^p)\right| < \varepsilon$ for all $\ell \geq \bar{\ell}$, which exists according to Item 3. Furthermore, we have $|\mathrm{fix}(C_m^p) - r_p^{**}| < \varepsilon$ and $|\mathrm{fix}(C_M^p) - r_p^{**}| < \varepsilon$ according to Item 4. With this, we obtain

$$\left|\left(C_m^p\right)^n(r_p^k) - r_p^{**}\right| = \left|\left(C_m^p\right)^n(r_p^k) - \mathrm{fix}(C_m^p) + \mathrm{fix}(C_m^p) - r_p^{**}\right|$$

$$\begin{aligned}&\leq \left|\left(C_m^p\right)^n(r_p^k) - \operatorname{fix}(C_m^p)\right| + \left|\operatorname{fix}(C_m^p) - r_p^{**}\right| \\ &< \varepsilon + \varepsilon = 2\varepsilon \ \forall\ n \geq \bar{\ell}\end{aligned}$$

and $\left|\left(C_M^p\right)^n(r_p^k) - r_p^{**}\right| < 2\varepsilon$ for all $n \geq \bar{\ell}$ analogously. This result is combined with Item 2, which yields

$$r_p^{**} - 2\varepsilon < \left(C_m^p\right)^n(r_p^k) \leq r_p^{k+n} \leq \left(C_M^p\right)^n(r_p^k) < r_p^{**} + 2\varepsilon \ \Rightarrow\ |\, r_p^{k+n} - r_p^{**}| < 2\varepsilon \ \forall\ n \geq \bar{\ell},$$

i.e., $\lim\limits_{n\to\infty} r_p^n = r_p^{**}$. □

Finally, we can present the main convergence statement if the ADA Algorithm 5.2 is considered with a plurality of ADA pairs.

Theorem 7.68 *Let $\boldsymbol{i}^{**} \in \mathbb{R}^N_{>0}$ and let $\boldsymbol{r}^{**} = (r_1^{**}, \ldots, r_N^{**})$ be the corresponding drift resistance super fixed point vector.*

- *Let A^p be contractive for all $p \in [N]$.*
- *Let A^1 be a selfmap.*
- *Let there exist $\delta > 0$ such that $[r_{p-1}^{**} - \delta, r_{p-1}^{**} + \delta] \subset V^p$ and $C^p_{r_{p-1}^{**}-\delta}$ as well as $C^p_{r_{p-1}^{**}+\delta}$ are selfmaps for all $p \in \{2, \ldots, N\}$.*
- *Let u be an infinite and sufficiently well distributed ADA update sequence and let $\hat{\boldsymbol{i}}_{\boldsymbol{t},\text{in}} = (i_1^{\text{in}}, \ldots, i_N^{\text{in}})$ be a given input vector such that $\hat{\boldsymbol{i}}_{\boldsymbol{t},\text{in}}$ and u are a feasible input combination.*

Then, the following holds:

$$\lim_{n\to\infty} \hat{\boldsymbol{i}}_{\boldsymbol{t},\text{out}}\left(\hat{\boldsymbol{i}}_{\boldsymbol{t},\text{in}}, u(n)\right) = \boldsymbol{i}^{**}.$$

Proof. Let $\boldsymbol{r}^n(\hat{\boldsymbol{i}}_{\boldsymbol{t},\text{in}}, u) = (r_1^n, \ldots, r_N^n)$ be the corresponding n-th ADA iterate according to Definition 7.28. We show that $\lim\limits_{n\to\infty} \boldsymbol{r}^n(\hat{\boldsymbol{i}}_{\boldsymbol{t},\text{in}}, u) = \boldsymbol{r}^{**} = (r_1^{**}, \ldots, r_N^{**})$ by induction over the numbering of the ADA pairs. For this, let $\varepsilon > 0$ arbitrary but fixed.

Base case:

We consider ADA pair $p = 1$. Because A^1 is a contractive selfmap by assumption and $\hat{\boldsymbol{i}}_{\boldsymbol{t},\text{in}}$ as well as u are a feasible input combination, the Picard iteration associated to A^1 starting at $r_1^0 := \beta^1(i_1^{\text{in}})$ converges to the fixed point $\operatorname{fix}(A^1)$. Recall that $\operatorname{fix}(A^1) = r_1^{**}$ (Lemma 7.42). Since u is sufficiently well distributed, there exists a subsequence of u whose entries are all one and thus $\lim\limits_{n\to\infty} r_1^n = r_1^{**}$ holds (Lemma 7.45.). In particular, there exists $n_1 \in \mathbb{N}$ such that $|r_1^n - r_1^{**}| < \varepsilon$ for all $n \geq n_1$.

Induction hypothesis:

There exists $k < N$ such that $\lim\limits_{n\to\infty} r_p^n = r_p^{**}$ for all $p \in [k]$. Furthermore, there exists $n_k \in \mathbb{N}$ such that $|r_p^n - r_p^{**}| < \varepsilon$ for all $p \in [k]$ and for all $n \geq n_k$.

Induction step:
We consider ADA pair $p = k + 1$. According to the induction hypothesis, $\lim_{n\to\infty} r_k^n = r_k^{**}$ holds. Note that all requirements to apply Theorem 7.67 are met and thus $\lim_{n\to\infty} r_{k+1}^n = r_{k+1}^{**}$ holds as well. In particular, there exists $n_{k+1} \geq n_k$ such that $|r_{k+1}^n - r_{k+1}^{**}| < \varepsilon$ for all $n \geq n_{k+1}$ and the induction is completed.
In total, we have

$$\|(r_1^n, \ldots, r_N^n) - \boldsymbol{r}^{**}\|_{\max} < \varepsilon \ \forall\ n \geq n_N \ \Rightarrow \ \lim_{n\to\infty} \boldsymbol{r}^n(\hat{\boldsymbol{i}}_{\boldsymbol{t},\text{in}}, u) = \lim_{n\to\infty} (r_1^n, \ldots, r_N^n) = \boldsymbol{r}^{**}.$$

We apply Theorem 7.30 as well as Definition 7.32 and obtain

$$\lim_{n\to\infty} \boldsymbol{i}^n(\hat{\boldsymbol{i}}_{\boldsymbol{t},\text{in}}, u) = \left((\beta^1)^{-1}(r_1^{**}), \ldots, (\beta^N)^{-1}(r_N^{**})\right) = (i_1^{**}, \ldots, i_N^{**}) = \boldsymbol{i}^{**}.$$

□

The importance of Theorem 7.68 is that the super fixed point vector can be considered as the fixed point of the output of Algorithm 5.2 in the sense that every feasible input vector $\hat{\boldsymbol{i}}_{\boldsymbol{t},\text{in}}$ eventually converges to $\boldsymbol{i}^{**}$ if a sufficiently well distributed ADA update sequence u is considered. However, if an infinite ADA update sequence u is considered that is not sufficiently well distributed, then $\lim_{n\to\infty} \boldsymbol{i}^n(\hat{\boldsymbol{i}}_{\boldsymbol{t},\text{in}}, u) = \boldsymbol{i}^{**}$ does not hold in general, as demonstrated in the following example.

Example 7.69 *Let there be a feasible scenario, i.e., let* $\boldsymbol{i}^{**} = (i_1^{**}, \ldots, i_N^{**}) \in \mathbb{R}_{>0}^N$.

- *Let* $u = (u_n)_{n\in\mathbb{N}}$ *be the infinite ADA update sequence whose entries are all one, i.e.,* $u_n = 1$ *for all* $n \in \mathbb{N}$.
- *Let* $\hat{\boldsymbol{i}}_{\boldsymbol{t},\text{in}} = (i_1^{\text{in}}, \ldots, i_N^{\text{in}})$ *be an input vector with* $i_1^{\text{in}} \in \hat{I}^1$ *and such that there exists* $p \in \{2, \ldots, N\}$ *with* $i_p^{\text{in}} \neq i_p^{**}$.
- *Let* $\hat{\boldsymbol{i}}_{\boldsymbol{t},\text{in}}$ *and* u *be a feasible input combination.*
- *Let* A_i^1 *be a contractive selfmap.*

Because $u_n = 1$ *for all* $n \in \mathbb{N}$*, only the incumbent drifted test ioni current approximation of ADA pair* $p = 1$ *is updated. The approximations of the other ADA pairs remain at the input values. Therefore, the n-th ADA iterate is* $\boldsymbol{i}^n(\hat{\boldsymbol{i}}_{\boldsymbol{t},\text{in}}, u) = \left(\left(A_i^1\right)^n(i_1^{\text{in}}), i_2^{\text{in}}, \ldots, i_N^{\text{in}}\right)$ *for all* $n \in \mathbb{N}$ *according to Lemma 7.27. Because* A_i^1 *is a contractive selfmap and* $i_1^{\text{in}} \in \hat{I}^1$, $\lim_{n\to\infty} \left(A_i^1\right)^n(i_1^{\text{in}}) = \text{fix}(A_i^1) = i_1^{**}$ *holds and thus we have*

$$\lim_{n\to\infty} \boldsymbol{i}^n(\hat{\boldsymbol{i}}_{\boldsymbol{t},\text{in}}, u) = (i_1^{**}, i_2^{\text{in}}, \ldots, i_N^{\text{in}}) \neq (i_1^{**}, i_2^{**}, \ldots, i_n^{**}) = \boldsymbol{i}^{**}.$$

The inequality follows from the requirement that there exists $p \in \{2, \ldots, N\}$ *such that* $i_p^{\text{in}} \neq i_p^{**}$.

We can summarize that, depending on the ADA update sequence u and the input vector $\hat{\boldsymbol{i}}_{\boldsymbol{t},\text{in}}$, different limits can exist for the output of Algorithm 5.2. However, in practice, the ADA update sequences are usually sufficiently well distributed. Of course, all ADA update sequences are finite in practice. But as stated in Section 3.4.5, the ADA update sequence is automatically selected by the IoniDetect system [WHB, Item 4228]. In particular, if an ADA pair was not update for a longer period of time, a corresponding ADA update is forced [PHE, Item 12678]. Therefore, it is reasonable to assume that in practice sufficiently many updates with each ADA pair are performed and that the resulting sequence of updates is sufficiently mixed.
A further requirement of Theorem 7.68 is that $\hat{\boldsymbol{i}}_{\boldsymbol{t},\text{in}}$ and u are a feasible input combination. If that is not the case, the output vector of Algorithm 5.2 eventually becomes NaN in all components to indicate that the sequence of ADA iterations could not be successfully carried out. From a practical point of view, such a situation usually occurs if the range of feasible combustion states is left, see also Remark 5.33. In the optimization later on, this is avoided by specifying appropriate constraints.
So far, we know that if the iteration functions have certain "nice" properties according to the requirements of Theorem 7.68 and the inputs are "feasible", then the output of Algorithm 5.2 converges to the super fixed point vector $\boldsymbol{i}^{**}$. Recall that the goal of ADA is to approximate the drifted test ioni current i^p_{t,r_D} for each ADA pair $p \in [N]$. Therefore, the following section addresses the question under which conditions $i^{**}_p = i^p_{t,r_D}$ or equivalently $r^{**}_p = r_D$ holds for all $p \in [N]$.

7.4. Approximation Quality: Relation Between the Drift Resistance and the Super Fixed Point Vector

As detailed in Section 3.3 above, the ADA procedure ideally returns the drifted test ioni current i^p_{t,r_D} for each ADA pair $p \in [N]$. Because in this case the approximated drift resistance at the test fan speed t^p equals the sought drift resistance r_D for all $p \in [N]$ according to Equation (3.9) and the corresponding drift resistance approximation function is $\alpha_{\hat{\boldsymbol{i}}_{t,\text{out}}}(\text{fs}) = r_D$ for all fs $\in$ FS according to Definition 3.38. Therefore, we are interested in conditions under which the components of the super fixed point vector $\boldsymbol{i}^{**}$ correspond to the drifted test ioni currents, i.e., under which $i^{**}_p = i^p_{t,r_D}$ for all $p \in [N]$.
The following lemma states that this is the case if and only if $r^{**}_p = r_D$ for all $p \in [N]$, where $\boldsymbol{r}^{**} = (r^{**}_1, \ldots, r^{**}_N)$ is the drift resistance super fixed point vector corresponding to $\boldsymbol{i}^{**}$ according to Definition 7.32.

Lemma 7.70 *Let $r_D \geq 0$. Furthermore, let there be a feasible scenario, i.e., let $\boldsymbol{i}^{**} = (i^{**}_1, \ldots, i^{**}_N) \in \mathbb{R}^N_{>0}$, and let $\boldsymbol{r}^{**} = (r^{**}_1, \ldots, r^{**}_N)$ be the corresponding drift resistance super fixed point vector. Then, the following holds for all $p \in [N]$:*

$$i^{**}_p = i^p_{t,r_D} \;\Leftrightarrow\; r^{**}_p = r_D.$$

Proof. Let $p \in [N]$. Recall from Definition 3.27 that $i^p_{t,r_D} = \iota_{t^p,r_D}(g^p_t)$ with $g^p_t = \iota^{-1}_{t^p}(i^p_t)$. By applying (3.4), we obtain

$$\iota_{t^p,r_D}(g^p_t) = \frac{U\iota_{t^p}(g^p_t)}{r_D\iota_{t^p}(g^p_t)+U} = \frac{U\iota_{t^p}\circ\iota^{-1}_{t^p}(i^p_t)}{r_D\iota_{t^p}\circ\iota^{-1}_{t^p}(i^p_t)+U} = \frac{Ui^p_t}{r_D i^p_t+U}.$$

Furthermore, we have $r^{**}_p = \beta^p(i^{**}_p)$ (Definition 7.32) and thus

$$i^{**}_p = i^p_{t,r_D} \;\Leftrightarrow\; r^{**}_p = \beta_p(i^p_{t,r_D}) = \frac{U}{i_{t^p,r_D}} - \frac{U}{i^p_t} = \frac{r_D i^p_t + U}{i^p_t} - \frac{U}{i^p_t} = r_D.$$

□

Therefore, we focus on the relation between the drift resistance r_D and the components r^{**}_p, $p \in [N]$, of the drift resistance super fixed point vector. Recall from Lemma 7.42 that $r^{**}_p = \mathrm{fix}\big(C^p_{r^{**}_{p-1}}\big)$, i.e., there is a recursive relation between the components of $\boldsymbol{r}^{**}$. However, it is possible to decouple the elements r^{**}_{p-1} and r^{**}_p to a certain degree by considering the iteration function A^p instead of the iteration function $C^p_{r^{**}_{p-1}}$ for $p \in \{2,\dots,N\}$. Recall from Definition 6.21 that A^p is the corresponding drift resistance iteration function if the ADA pair p is considered individually. The following lemma states how the fixed point of A^p and that of C^p_v, $v \in V^p$, are related (if they exist).

Lemma 7.71 *Let $p \in \{2,\dots,N\}$ and let $v \in V^p$. Let A^p and C^p_v be both contractive selfmaps and let $\mathrm{fix}(A^p) \in \hat{R}^p$ be the fixed point of A^p as well as $\mathrm{fix}(C^p_v) \in \hat{R}^p_v$ be the fixed point of C^p_v (existence and uniqueness are guaranteed according to Lemma 6.35 and Corollary 7.47). Then,*

1. $v < \mathrm{fix}(A^p) \;\Leftrightarrow\; \mathrm{fix}(C^p_v) < \mathrm{fix}(A^p)$,
2. $v > \mathrm{fix}(A^p) \;\Leftrightarrow\; \mathrm{fix}(C^p_v) > \mathrm{fix}(A^p)$ *and*
3. $v = \mathrm{fix}(A^p) \;\Leftrightarrow\; \mathrm{fix}(C^p_v) = \mathrm{fix}(A^p)$.

Proof. As a preliminary step, we show that the fixed point of A^p is an element of $\hat{R}^p_v$, which is the domain of C^p_v. Because $\mathrm{fix}(A^p) \in \hat{R}^p$ and $\hat{R}^p_v := \big(\omega^p_v\big)^{-1}(\hat{R}^p)$ (Definition 7.4), we have $\bar{r} := \big(\omega^p_v\big)^{-1}\big(\mathrm{fix}(A^p)\big) \in \hat{R}^p_v$, i.e., $C^p_v(\bar{r})$ is well-defined. Furthermore, $C^p_v : \hat{R}^p_v \to \hat{R}^p_v$ is a selfmap by assumption and $C^p_v = A^p \circ \omega^p_v$ (Definition 7.36) and thus

$$C^p_v(\bar{r}) = A^p \circ \omega^p_v \circ \big(\omega^p_v\big)^{-1}\big(\mathrm{fix}(A^p)\big) = A^p\big(\mathrm{fix}(A^p)\big) = \mathrm{fix}(A^p) \in \hat{R}^p_v. \tag{7.16}$$

With this, we show the statements. We show the implications "⇒" of Items 1 to 3 first. Thereafter, the implications "⇐" are proved. Aiming at a better readability, we denote $r^* := \mathrm{fix}(A^p)$.
We begin with Item 1, so let $v < r^*$. Because $0 < w^p < 1$, we have

$$\begin{aligned} v < r^* \;&\Rightarrow\; (1-w^p)v < (1-w^p)r^* \\ &\Rightarrow\; \omega^p_v(r^*) = w^p r^* + (1-w^p)v < w^p r^* + (1-w^p)r^* = r^*. \end{aligned}$$

According to Equation (7.16), $r^* \in \hat{R}_v^p$ holds and thus $C_v^p(r^*)$ exists. By considering that A^p is strictly increasing, we have

$$\omega_v^p(r^*) < r^* \;\Rightarrow\; C_v^p(r^*) = A^p \circ \omega_v^p(r^*) < A^p(r^*) = r^*.$$

This implies that the Picard iteration associated to C_v^p starting at r^* is strictly decreasing (Lemma 4.47). According to Corollary 7.47, the Picard iteration associated to C_v^p converges for every starting point to the unique fixed point $\mathrm{fix}(C_v^p)$. Therefore, the fixed point $\mathrm{fix}(C_v^p)$ has to be smaller than r^*, i.e., $\mathrm{fix}(C_v^p) < r^* = \mathrm{fix}(A^p)$ holds.
Item 2, i.e., the case $v > r^*$, is shown analogously by

$$v > r^* \;\Rightarrow\; \omega_v^p(r^*) > r^* \;\Rightarrow\; C_v^p(r^*) > A^p(r^*) = r^* \;\Rightarrow\; \mathrm{fix}(C_v^p) > r^*.$$

To show Item 3, let $v = r^*$. Then, we have

$$\begin{aligned} C_v^p(r^*) &= A^p \circ \omega_v^p(r^*) = A^p\big(w^p r^* + (1-w^p)v\big) = A^p\big(w^p r^* + (1-w^p)r^*\big) = A^p(r^*) \\ &= r^*, \end{aligned}$$

i.e., r^* is a fixed point of C_v^p. Because the fixed point of C_v^p is unique, $\mathrm{fix}(C_v^p) = r^*$ holds. With this, we can show the implications "$\Leftarrow$" of all three items by contradiction. Let $\mathrm{fix}(C_v^p) < r^*$ and let us suppose that $v \geq r^*$. According to "$\Rightarrow$" of Items 2 and 3, $v \geq r^*$ implies $\mathrm{fix}(C_v^p) \geq r^*$, which is a contradiction. Thus, $v < r^*$ holds. The implications "$\Leftarrow$" of Items 2 and 3 are shown analogously. □

The statement of Lemma 7.71 is a bit counterintuitive, because the element v corresponds to the drift resistance approximation of ADA pair $p-1$ while $\mathrm{fix}(A^p)$ is related to ADA pair p, i.e., we compare drift resistance approximations of two different ADA pairs. However, this reflects the entanglement of neighbored ADA pairs. With Lemma 7.71 we get a criterion to check if $r_p^{**} = r_D$ holds for all $p \in [N]$ by considering the fixed points of the iteration functions A^p.

Theorem 7.72 *Let $r_D \geq 0$. Let $\boldsymbol{i}^{**} \in \mathbb{R}_{>0}^N$ and let $\boldsymbol{r}^{**} = (r_1^{**}, \ldots, r_N^{**})$ be the corresponding drift resistance super fixed point vector. Furthermore, let A^p be a contractive selfmap for all $p \in [N]$. Then, the following holds:*

$$\mathrm{fix}(A^p) = r_D \;\forall\; p \in [N] \;\Leftrightarrow\; r_p^{**} = r_D \;\forall\; p \in [N].$$

Proof. "$\Rightarrow$" Let $\mathrm{fix}(A^p) = r_D$ for all $p \in [N]$. We perform an induction over p.
Base case: According to Lemma 7.42, we have $r_1^{**} = \mathrm{fix}(A^1)$. Because $\mathrm{fix}(A^1) = r_D$ by assumption, $r_1^{**} = r_D$ holds.
Induction hypothesis: For a certain $k < N$ let $r_p^{**} = r_D$ for all $p \in [k]$.
Induction step: Let us consider $p = k+1$. We have $r_k^{**} = r_D$ (induction hypothesis), $\mathrm{fix}(A^{k+1}) = r_D$ (by assumption) and $r_{k+1}^{**} = \mathrm{fix}\big(C_{r_k^{**}}^{k+1}\big)$ (Lemma 7.42). By applying Item 3 of Lemma 7.71, we obtain

$$r_k^{**} = r_D = \mathrm{fix}(A^{k+1}) \;\Rightarrow\; r_{k+1}^{**} = \mathrm{fix}\big(C_{r_k^{**}}^{k+1}\big) = \mathrm{fix}(A^{k+1}) = r_D.$$

"$\Leftarrow$" Let $r_p^{**} = r_D$ for all $p \in [N]$. We consider $p = 1$ first. We have $r_1^{**} = \mathrm{fix}(A^1)$ (Lemma 7.42) and $r_1^{**} = r_D$ (by assumption) and thus $\mathrm{fix}(A^1) = r_D$.
Now, let $p \in \{2, \dots, N\}$. Because $r_{p-1}^{**} = r_p^{**} = r_D$ (by assumption) and $r_p^{**} = \mathrm{fix}\big(C^p_{r_{p-1}^{**}}\big)$ (Lemma 7.42), we have

$$\begin{aligned} r_D = r_p^{**} &\Rightarrow r_D = \mathrm{fix}\big(C^p_{r_{p-1}^{**}}\big) = \mathrm{fix}\big(C^p_{r_D}\big) \Rightarrow C^p_{r_D}(r_D) = r_D \\ &\Rightarrow r_D = A^p \circ \omega^p_{r_D}(r_D) = A^p(w^p r_D + (1 - w^p) r_D) = A^p(r_D) \\ &\Rightarrow \mathrm{fix}(A^p) = r_D. \end{aligned}$$

□

The benefit of Theorem 7.72 is two-fold. First, if $\mathrm{fix}(A^p) = r_D$ for all $p \in [N]$, then the ADA pairs are decoupled and we can deal with each ADA pair p individually. Second, the iteration function A^p has already been thoroughly analyzed in Section 6.3 and we can reuse some results of this analysis. Under which conditions $\mathrm{fix}(A^p) = r_D$ holds is analyzed in Section 6.3.2 above, where the impact of tolerances is discussed. With this, we show that the relation between $\boldsymbol{r}^{**}$ and r_D is closely related to the impact of tolerances.

7.4.1. Impact of Tolerances

Corollary 6.41 states that $\mathrm{fix}(A^p) = r_D$ if and only if the considered HE model $\mathcal{H}$ and the ADA pair p are nominal. Recall from Definition 6.39 that $\mathcal{H}$ and the ADA pair $(s^{p,p}, i_s^p, i_t^p)$ are called nominal if and only if $\iota_{s^p}^{-1}(i_s^p) = \iota_{t^p}^{-1}(i_t^p)$. If that is not the case, $\mathcal{H}$ and the ADA pair p are called non-standard and we have $\mathrm{fix}(A^p) \neq r_D$. A non-standard situation is usually caused by tolerances. This issue is discussed in detail in Example 6.38.
In total, we have the following criterion to check whether the super fixed point vector $\boldsymbol{i}^{**}$ corresponds to the sought drifted test ioni currents.

Theorem 7.73 *Let $r_D \geq 0$. Let an HE model $\mathcal{H}$ be given such that we have a feasible scenario, i.e., $\boldsymbol{i}^{**} = (i_1^{**}, \dots, i_N^{**}) \in \mathbb{R}^N_{>0}$, and let $\boldsymbol{r}^{**} = (r_1^{**}, \dots, r_N^{**})$ be the corresponding drift resistance super fixed point vector. Furthermore, let A^p be a contractive selfmap for all $p \in [N]$. Then, the following statements are equivalent:*

1. $i_p^{**} = i^p_{t,r_D}$ $\forall\ p \in [N]$,
2. $r_p^{**} = r_D$ $\forall\ p \in [N]$,
3. $\mathrm{fix}(A^p) = r_D$ $\forall\ p \in [N]$,
4. *the HE model $\mathcal{H}$ and ADA pair p are nominal, i.e.,* $\iota_{s^p}^{-1}(i_s^p) = \iota_{t^p}^{-1}(t^p)$ $\forall\ p \in [N]$.

Proof. The statement follows from Lemma 7.70, Theorem 7.72 and Corollary 6.41. □

The statement of Theorem 7.73 as well as the impact of tolerances with a plurality of ADA pairs are demonstrated in the following example.

Example 7.74 *As in Example 7.44, the functions and values considered in this example are artificial and we assume that all domains and required sets are sufficiently large such that all considered function evaluations are well-defined. Therefore, no domains or other sets are specified in this example.*
We consider a situation with three ADA pairs and no drift, i.e., we have $N = 3$ *and* $r_D = 0$*. Furthermore, let the iteration functions corresponding to the three ADA pairs be* $A^1(r) = A^2(r) = A^3(r) = \frac{1}{2}r$*, i.e., all ADA pairs have the same ADA iteration function in this example. It is apparent, that* $\mathrm{fix}(A^1) = \mathrm{fix}(A^2) = \mathrm{fix}(A^3) = 0$*. Note that* $\mathrm{fix}(A^p) = r_D$ *holds for all* $p \in [3]$*. Therefore, all three ADA pairs and* $\mathcal{H}$ *are nominal according to Corollary 6.41.*
Recall that the functions A^p*,* $p \in [3]$*, are the correct iteration functions if the ADA pairs are considered individually. However, we are interested in the case with a plurality of ADA pairs and thus we require the weights* w^2 *and* w^3 *in addition. In this example, let* $w^2 = w^3 = \frac{1}{2}$*. This gives us* $C_v^2(r) = A^2 \circ \omega_v^2(r) = A^2\big(w^2 r + (1 - w^2)v\big) = \frac{1}{2}\big(\frac{1}{2}r + \frac{1}{2}v\big) = \frac{1}{4}r + \frac{1}{4}v$ *and analogously* $C_v^3(r) = \frac{1}{4}r + \frac{1}{4}v$*.*
We construct the drift resistance super fixed point vector $\boldsymbol{r}^{**} = (r_1^{**}, \ldots, r_N^{**})$ *analogously to Example 7.44. In the first component, we have* $r_1^{**} = \mathrm{fix}(A^1) = 0$*. Regarding the second component, we have*

$$C^2_{r_1^{**}}(r) = \frac{1}{4}r + \frac{1}{4}r_1^{**} = \frac{1}{4}r \;\Rightarrow\; r_2^{**} = \mathrm{fix}\big(C^2_{r_1^{**}}\big) = 0 \text{ and analogously } r_3^{**} = \mathrm{fix}\big(C^3_{r_2^{**}}\big) = 0.$$

In total, $r_p^{**} = 0 = r_D$ *holds for all* $p \in [3]$*, which is in accordance with Theorem 7.73, since* $\mathrm{fix}(A^p) = r_D$ *for all* $p \in [3]$*. In particular,* $\alpha_{i^{**}}(\mathrm{fs}) = r_D$ *holds for all* $\mathrm{fs} \in \mathrm{FS}$*.*
Now, let us assume that we have a second HE model $\overline{\mathcal{H}}$ *that belongs to a specimen of the same HE type as* $\mathcal{H}$*, but this time the ioni electrode's position differs slightly because of manufacturing tolerances. All functions and fixed points related to* $\overline{\mathcal{H}}$ *are denoted by an overline in the following. Let the corresponding iteration function of ADA pair one be altered to* $\bar{A}^1(r) = \frac{1}{2}r + 1$*, while the iteration functions of ADA pair two and three remain unchanged, i.e.,* $\bar{A}^2(r) = A^2(r)$ *and* $\bar{A}^3(r) = A^3(r)$*. Because the iteration functions of ADA pairs two and three are unchanged, the corresponding iteration functions given* v *remain also unchanged, i.e.,* $\bar{C}_v^p(r) = \bar{A}^p \circ \omega_v^p(r) = A^p \circ \omega_v^p(r) = C_v^p(r) = \frac{1}{4}r + \frac{1}{4}v$ *for* $p \in \{2, 3\}$*.*
We have $\mathrm{fix}(\bar{A}^1) = 2$*, because* $\bar{A}^1(2) = \frac{1}{2}2 + 1 = 2$*. Note that* $\mathrm{fix}(\bar{A}^1) \neq r_D$*. Therefore, in contrast to* r^{**}*, the drift resistance super fixed point* $\overline{\boldsymbol{r}}^{**}$ *has components that are not equal to* r_D *according to Theorem 7.73. This is illustrated by determining* $\overline{\boldsymbol{r}}^{**}$*. Its first component is* $\bar{r}_1^{**} = \mathrm{fix}(\bar{A}^1) = 2$*. Regarding the second and third component, we have*

$$\bar{C}^2_{\bar{r}_1^{**}}(r) = \frac{1}{4}r + \frac{1}{4}\bar{r}_1^{**} = \frac{1}{4}r + \frac{1}{4}2 = \frac{1}{4}r + \frac{1}{2} \;\Rightarrow\; \bar{r}_2^{**} = \mathrm{fix}\big(\bar{C}^2_{\bar{r}_1^{**}}\big) = \frac{2}{3}$$

and

$$\bar{C}^3_{\bar{r}_2^{**}}(r) = \frac{1}{4}r + \frac{1}{4}\bar{r}_2^{**} = \frac{1}{4}r + \frac{1}{4}\frac{2}{3} = \frac{1}{4}r + \frac{1}{6} \;\Rightarrow\; \bar{r}_3^{**} = \mathrm{fix}\big(\bar{C}^3_{\bar{r}_2^{**}}\big) = \frac{2}{9},$$

respectively. It is particularly noteworthy that $\bar{r}_2^{**} \neq r_D$ *and* $\bar{r}_3^{**} \neq r_D$ *although* $\mathrm{fix}(\bar{A}_2) = \mathrm{fix}(\bar{A}_3) = r_D$ *holds. This is in accordance with Lemma 7.71, because*

$$2 = \bar{r}_1^{**} > \mathrm{fix}(\overline{A}^2) = r_D = 0 \;\Rightarrow\; \bar{r}_2^{**} = \mathrm{fix}\big(\bar{C}^2_{\bar{r}_1^{**}}\big) > \mathrm{fix}(\overline{A}^2) = r_D$$

and analogously $\bar{r}_2^{**} > \mathrm{fix}(\overline{A}^3)$ *implies* $\bar{r}_3^{**} = \mathrm{fix}\big(\bar{C}^3_{\bar{r}_2^{**}}\big) > \mathrm{fix}(\overline{A}^3)$.

As demonstrated in Example 7.74, we can distinguish two cases as a consequence of Theorem 7.73. These two cases play a central role when formulating the ADA optimization problems Chapter 8 below.

- If $\mathrm{fix}(A^p) = r_D$ holds for all $p \in [N]$, then the ADA pairs can be considered individually in order to determine the components of the drift resistance super fixed point vector. Such a situation is also referred to as the nominal case.

- If there exists $p \in [N]$ such that $\mathrm{fix}(A^p) \neq r_D$, then some components of the drift resistance super fixed point are not equal to the sought r_D. In particular, it is not possible to consider the ADA pairs individually in order to determine $\boldsymbol{r}^{**}$, i.e., the components of $\boldsymbol{r}^{**}$ have to be calculated recursively according to Lemma 7.42. It is important to emphasize that an individual consideration of the ADA pairs is misleading in this case as demonstrated in Example 7.74. Such a situation is also referred to as the non-standard case and is usually caused by tolerances.

Regarding the fixed points we can consider the ADA pairs individually if we have a nominal situation. However, in general the rates of convergence are different if the ADA pairs are considered individually and not as a plurality.

7.4.2. Comparison of Rates of Convergence in the Nominal Case

Let us suppose a nominal situation. Then, we have $\mathrm{fix}(A^1) = r_D$ and $\mathrm{fix}(A^p) = \mathrm{fix}(C^p_{r^{**}_{p-1}}) = r_D$ for all $p \in \{2, \ldots, N\}$ according to Theorem 7.73. Because A^p and $C^p_{r^{**}_{p-1}}$ have an identical fixed point for $p \geq 2$, we can compare their rates of convergence in this case.

Lemma 7.75 *Let* $\boldsymbol{i}^{**} \in \mathbb{R}^N_{>0}$ *and let* $\boldsymbol{r}^{**} = (r_1^{**}, \ldots, r_N^{**})$ *be the corresponding drift resistance super fixed point vector. Let this be a nominal situation, i.e.,* $r_p^{**} = r_D = \mathrm{fix}(A^p)$ *holds for all* $p \in [N]$. *Let* $p \in \{2, \ldots, N\}$, *then*

$$|C^p_{r^{**}_{p-1}}(r) - r_D| < |A^p(r) - r_D| \;\forall\; r \in \hat{R}^p \cap \hat{R}^p_{r^{**}_{p-1}},\; r \neq r_D.$$

Proof. Let $r \in \hat{R}^p \cap \hat{R}^p_{r^{**}_{p-1}}$, i.e., we can evaluate $A^p(r)$ and $C^p_{r^{**}_{p-1}}(r)$. Furthermore, let $r \neq r_D$. We consider the case $r < r_D$ first. Because $0 < w^p < 1$, we have

$$r < r_D \;\Rightarrow\; w^p r + (1 - w^p) r < w^p r + (1 - w^p) r_D \;\Rightarrow\; r < \omega^p_{r_D}(r) < r_D.$$

By considering that A^p is strictly increasing and that r_D is the fixed point of A^p by assumption, we obtain

$$A^p(r) < A^p \circ \omega^p_{r_D}(r) < A^p(r_D) \;\Rightarrow\; A^p(r) < C^p_{r_D}(r) < r_D \;\Rightarrow\; |C^p_{r_D}(r) - r_D| < |A^p(r) - r_D|.$$

Because $r^{**}_{p-1} = r_D$, $|C^p_{r^{**}_{p-1}}(r) - r_D| < |A^p(r) - r_D|$ holds in this case.
The case $r > r_D$ is shown analogously. □

Remark 7.76 *The interpretation of Lemma 7.75 is as follows. Let us suppose that ADA pair $p-1$ has already converged to its fixed point, which is the drift resistance in the nominal case. Then, the Picard iteration associated to $C^p_{r^{**}_{p-1}}$ starting at r converges faster to r_D than the Picard iteration associated to A^p starting at r (if both functions are contractive selfmaps). I.e., ADA pair p has a faster rate of convergence if a plurality of ADA pairs is considered and not the pair p individually under the condition that the approximation of ADA pair $p-1$ is already at (or close to) r_D.*

The faster rate of convergence of $C^p_{r^{**}_{p-1}}$ can be quantified to a certain degree. For this, we look at the relation between the Lipschitz constants of A^p and C^p_v.

Lemma 7.77 *Let A^p be L-Lipschitzian. Then, C^p_v is $(L \cdot w^p)$-Lipschitzian.*

Proof. Let A^p be L-Lipschitzian and let $x, y \in \hat{R}^p_v$ such that $x \neq y$. Then, the following holds:

$$\begin{aligned}\left|C^p_v(x) - C^p_v(y)\right| &= \left|A^p \circ \omega^p_v(x) - A^p \circ \omega^p_v(y)\right| \\ &\leq L\left|\omega^p_v(x) - \omega^p_v(y)\right| = L\left|w^p x + (1-w^p)v - \left(w^p y + (1-w^p)v\right)\right| \\ &= L\left|w^p x - w^p y\right| = L w^p \left|x - y\right|.\end{aligned}$$

□

As a consequence, if C^p_v is a contractive selfmap, we can state an upper bound for the rate of convergence of the Picard iteration associated to C^p_v.

Lemma 7.78 *Let A^p be L-Lipschitzian and let C^p_v be a contractive selfmap. For an arbitrary starting point $r_0 \in \hat{R}^p_v$, the estimation*

$$\left|r_n - \mathrm{fix}(C^p_v)\right| \leq L w^p \cdot \left|r_n - r_{n-1}\right| \leq (L w^p)^n \cdot \left|r_0 - \mathrm{fix}(C^p_v)\right| \;\forall\; n \in \mathbb{N}$$

holds, where $r_n := \left(C^p_v\right)^n(r_0)$.

Proof. Because C^p_v is Lw^p-Lipschitzian (Lemma 7.77), the statement follows from Banach's fixed point Theorem 4.39. □

Remark 7.79 *The statement of Lemma 7.78 holds for arbitrary $v \in V^p$, i.e., also for $v \neq r_D$. However, if $v \neq r_D = \mathrm{fix}(A^p)$, then A^p and C^p_v have different fixed points according to Lemma 7.71. Thus, the better bound for the rate of convergence of C^p_v*

might come at the price of a "worse" fixed point in the sense that the fixed point of C_v^p might have a non-negligible distance to r_D if $v \neq r_D$. This is typical for a non-standard situation, as demonstrated in Example 7.74.
The actual relation between the rate of convergence of the iteration functions and their Lipschitz constants is discussed in detail in Section 8.3 below.

As a summary of this subsection, the super fixed point vector can be determined by considering the ADA pairs individually in the nominal case. To be precise, the super fixed point vector is known in advance in the nominal case. In contrast, the recursion of Lemma 7.42 has to be applied to determine the super fixed point vector in the non-standard case. In addition, particular attention must be paid whether the super fixed point vector stays within feasible limits if we optimize the ADA parameters with a plurality of ADA pairs in the non-standard case, because in this case the resulting drift resistance approximations can significantly differ from the true drift resistance as demonstrated in Example 7.74. The convergence rate, on the other hand, is of secondary importance in the sense that it has better bounds if the plurality of ADA pairs is considered.

This concludes the analysis of the ADA procedure with a plurality of ADA pairs. The results of this chapter are summarized in the following section.

7.5. Conclusion and Considerations for Optimization

The following list briefly recaps the results and findings of this chapter.

- The difficulty with a plurality of ADA pairs is that an update of ADA pair p, $p \geq 2$, depends on the incumbent ioni currents i_p and i_{p-1} (Line 11 of Algorithm 5.2). To deal with this dependency, a set of feasible upper neighbor drift resistances $V_{r_D}^p$ (Definition 7.4) and a corresponding ioni current based iteration function $B_{r_D,v}^p$ with $v = \beta^{p-1}(i_{p-1}) \in V_{r_D}^p$ (Definition 7.8) are introduced for $p \geq 2$.

- Based on A_{i,r_D}^1 and on iteration functions of the type $B_{r_D,v}^p$ for $p \geq 2$, the (ioni current based) super fixed point vector $\boldsymbol{i}^{**}$ is recursively defined (Definition 7.14). If all components of $\boldsymbol{i}^{**}$ are not NaN, then $\boldsymbol{i}^{**}$ is called feasible and the underlying HE model $\mathcal{H}$, the N ADA pairs and the drift resistance r_D are called a feasible scenario.

- The major result of this chapter is that the output of Algorithm 5.2 converges to $\boldsymbol{i}^{**}$ under certain conditions (Theorem 7.68). Because this holds for all feasible input combinations $\hat{\boldsymbol{i}}_{\boldsymbol{t},\text{in}}$ and u, where u is a sufficiently well distributed ADA update sequence, $\boldsymbol{i}^{**}$ can be interpreted as the fixed point of (the output of) Algorithm 5.2. However, there can exist different limits for the output of Algorithm 5.2 if not sufficiently well distributed ADA update sequences are considered (Example 7.69).

- Because the output of Algorithm 5.2 converges to $\boldsymbol{i}^{**} = (i_1^{**}, \ldots, i_N^{**})$ (under certain conditions), we are interested in whether $i_p^{**} = i_{t,r_D}^p$ holds for all $p \in [N]$, i.e., whether

the drifted test ioni currents are perfectly approximated. This is the case if and only if $\mathrm{fix}(A^p_{r_D}) = r_D$ holds for all $p \in [N]$, which corresponds to the nominal situation (Theorem 7.73).
The case that there exists $p \in [N]$ such that $\mathrm{fix}(A^p_{r_D}) \neq r_D$ is called non-standard situation. A non-standard situation is usually caused by tolerances (Example 7.74).

- As a consequence, the ADA pairs can be considered individually in a nominal situation. In particular, the super fixed point vector is known in advance in this case ($i^{**}_p = i^p_{t,r_D}$ for all $p \in [N]$).
- In the case of a non-standard situation, the super fixed point vector must be calculated by the recursion of Lemma 7.27. In particular, the resulting drift resistance approximations can differ significantly from r_D even if $\mathrm{fix}(A^p) = r_D$ holds for all but one ADA pair (Example 7.74).
- The rate of convergence is usually faster if the plurality of ADA pairs is considered and not each ADA pair individually. However, this faster rate of convergence might come at the price of a "worse" super fixed point vector in the non-standard situation (Remark 7.79).

In the case of a single ADA pair, the found convergence characteristics of Algorithm 5.2 are compared to the results and documentation provided by Siemens in Section 6.3.4 above. However, Siemens has not published a documentation for the case of a plurality of ADA pairs. Therefore, the results in this chapter are new and they close a research gap in the context of the ADA parameterization.

Based on the analysis and the results from this and the previous chapter, two optimization models for the ADA parameterization are proposed in the following Chapter 8, one optimization model for the nominal case and one optimization model for the case with tolerances. The two cases are dealt with separately, because in the nominal case the ADA pairs can be considered individually to a certain degree, which makes the optimization less complex. In contrast, in the non-standard case, the plurality of ADA pairs has to be considered, which makes the optimization more complicated.

Part III.

Optimization of the ADA Parameters

8. Optimization Models

The optimization of the ADA parameters is divided into two parts. First, corresponding mathematical optimization models are proposed in this chapter. Thereafter, optimization algorithms to solve these models are proposed in the following Chapter 9.
Modeling an optimization problem means to convert "the description of an optimization problem" to a "mathematical representation of the problem" [Sán20, p. 13]. This representation is referred to as the optimization model [Sán20, p. 13]. An optimization model is composed of data, decision variables, constraints and objective functions [Sán20, p. 3]. Our goal in this chapter is to formulate the optimization of the ADA parameters as an optimization model. This requires a description of the ADA optimization problem in the first place, which is presented in the following Section 8.1. Two optimization models are then derived step by step from this description. One optimization model for the nominal case without tolerances and one model for the case with tolerances, which are presented in Sections 8.6 and 8.7, respectively.
These models have conflicting objectives, which puts us in the field of multiobjective optimization and decision making. Because the objectives are conflicting, not all objectives can be simultaneously optimized. Rather, one obtains a set of Pareto optimal solutions, see also Section 4.1. Therefore, usually two parties are involved in the multiobjective optimization process, which are a decision maker (DM) and an analyst [Bra+08, p. 2].
"In general, the DM is a person who is assumed to know the problem considered and be able to provide preference information related to the objectives and/or different solutions in some form. ... An analyst is a person or a computer program responsible for the mathematical modeling and computing sides of the solution process." [Bra+08, p. 2]. Based on preference information specified by the DM a "preference model is built from preference information and this model is exploited in order to find solutions that better fit the DM's preferences." [Bra+08, p. 2].
In the context of the ADA optimization, the decision makers are the two Vaillant engineers who were responsible for the ADA parameterization of the HEs at Vaillant during the period of writing this thesis. The role of the analyst was assumed by the author of this thesis.
In the following section a description of the ADA optimization problem is specified that corresponds to the preferences of the decision makers. The subsequent mathematical modeling is the work of the author of this thesis.

8.1. Description of the ADA Optimization Problem

For the description of the ADA optimization problem, the terms *specifications* and *objective criterion* introduced in *Modelling in Mathematical Programming* [Sán20] are used. *Specifications* are "regulations, impositions or limitations that must be fulfilled" and that "give rise to the constraints of the problem" [Sán20, p. 15]. The difference between specifications and constraints is that a constraint is "a single mathematical expression, whereas the specification is a characteristic ... that is implemented in one or more constraints" [Sán20, p. 15]. *Objective criterion* is an additional specification "expressing the criteria that guide the resolution" of the problem [Sán20, p. 15]. In particular, the objective criterion leads to the objective function(s) [Sán20, p. 191]. However, it might "also lead to ... the definition of specific constraints" [Sán20, p. 15].
The following description of the ADA optimization problem is the result of an interactive process with the decision makers. Together with the decision makers an initial draft of the description of the optimization problem and a corresponding optimization model were created. These were gradually developed further in iterative loops until the decision makers were satisfied with the optimized ADA parameters. This process is similar to the conventional design cycle presented in [MN22, pp. 3–4]. The following description is the final result of this process.

The decision makers want N ADA pairs (s^p, t^p, i_s^p, i_t^p), $p \in [N]$, that fulfill the following objective criterion (O) and the specifications (S1) to (S7).

(O) The ADA Algorithm 5.2 shall have good convergence characteristics in the scenarios specified by the decision makers.

(S1) The CO emissions during an ADA iteration must never exceed a limit specified by the decision makers, which is denoted by $\mathrm{co}_{\max}$ in the following. A common value used by Vaillant is $\mathrm{co}_{\max} = 150\mathrm{ppm}$ [PHE, Item 15498].

(S2) The equivalence AFR during an ADA iteration must never fall below a lower bound specified by the decision makers, which is denoted by $\lambda_{\min}$. A common value used by Vaillant is $\lambda_{\min} = 1.05$ [PHE, Item 15498]. This specification is given for two reasons. First, a combustion with an equivalence AFR close to one usually has a high flame temperature, which places a great strain on the material of the heating device and is therefore undesirable. Second, the ioni current as a function of λ has a maximum close to $\lambda = 1$. In Figure 2.6(b) this property is illustrated by the dashed curve. However, the ADA algorithm and the HE model require that the ioni current functions are strictly decreasing, see also Definition 2.18. The bound $\lambda_{\min}$ serves as a safety margin to $\lambda \approx 1$.

(S3) The equivalence AFR during an ADA iteration must never exceed an upper bound specified by the decision makers, which is denoted by $\lambda_{\max}$. A common value used by Vaillant is $\lambda_{\max} = 1.6$ [PHE, Item 15498]. This is done to limit the start point

increment in order to avoid too large time spans for an ADA iteration. The start point increment is introduced and discussed in Section 8.4 below. Furthermore, a large equivalence AFR corresponds to a small ioni current. At a certain point, the ioni current is too small and can no longer be measured reliably.

(S4) The start and test ioni currents must be feasible in the sense that they must be selected from the appropriate sets according to the HE model, i.e., $i_s^p \in \iota_{s^p}(G_{s^p}) = I_{s^p}$ and $i_t^p \in \iota_{t^p}(G_{t^p}) = I_{t^p}$, see also Definitions 5.2 and 2.22.

(S5) The decision makers want that the start ioni current is larger or equal to the corresponding point on the control curve and that the test ioni current is smaller or equal to the corresponding point on the control curve [PHE, Item 15498]. The control curve is introduced in Section 2.3.3. In other words, the test point shall stay in a more fuel-rich range and the start point shall stay in a more fuel-lean range compared to the desired equivalence AFR. This is supposed to provide a certain robustness with respect to tolerances of the position of the ioni electrode and to avoid too large time spans for an ADA iteration.

(S6) The equivalence AFRs of the (undrifted) start and test point shall have a minimum distance, denoted by $\Delta\lambda_{\min}$. This is necessary in order to have a clear distinction between the start and the test point, which is also supposed to provide a certain robustness with respect to tolerances of the position of the ioni electrode. A common value used by Vaillant is $\Delta\lambda_{\min} = 0.1$ [PHE, Item 3280].

(S7) The start and the test fan speeds must be selected as follows [PHE, Item 3280]:

- The test fan speeds follow a descending order, i.e., $t_1 > t_2 > \cdots > t_N$,
- the start fan speed of an ADA pair must be larger than the corresponding pair's test fan speed, i.e., $t^p < s^p$ for all $p \in [N]$,
- ADA pairs must not be overlapping, i.e., $s^p < t^{p-1}$ for all $p \in \{2, \ldots, N\}$,
- the test fan speed of ADA pair N must not be smaller than the HE's minimum fan speed, i.e., $t^N \geq \mathrm{fs}_{\min}$, and
- the start fan speed of ADA pair one must not be larger than the HE's maximum fan speed, i.e., $s^1 \leq \mathrm{fs}_{\max}$.

These restrictions are in accordance with the considerations made in Section 3.4 as well as with Definition 5.2.

Therefore, we can already state that the decision variables of the optimization models are the ADA parameters (s^p, t^p, i_s^p, i_t^p), $p \in [N]$.

The objective criterion (O) is composed of the two aspects "good convergence characteristics" and "scenarios specified by the decision makers", which are analyzed in more detail in this subsection. The specifications (S1) to (S7) and their corresponding constraints are detailed in Section 8.5.

8.1.1. Scenarios Specified by the Decision Makers

From a practical point of view, only certain scenarios are of interest. The decision makers decided to consider only scenarios, where all of the following items (Sc1) to (Sc3) are fulfilled, which reduces the complexity of the optimization problems to a certain degree.

(Sc1) Only a nonnegative and fixed drift resistance r_D is considered, i.e., r_D is not supposed to change over time or to be negative. This is in accordance with the assumptions made in Section 3.1.2. Vaillant typically considers $r_D = 140\Omega$ [PHE, Item 1618]. Two other common values are $r_D = 80k\Omega$ and $r_D = 200k\Omega$ [PHE, Item 1618].

(Sc2) Only the vector $\hat{\boldsymbol{i}}_{t,\text{in}} = (i_1^{\text{in}}, \ldots, i_N^{\text{in}})$ with $i_p^{\text{in}} = i_t^p$ for all $p \in [N]$, i.e., the vector that is composed of the (undrifted) test ioni currents, is considered as a starting vector for the ADA Algorithm 5.2 [PHE, Item 1618]. This vector corresponds to the situation in which no correction has yet been determined. It is a typical starting vector, see also Remark 5.34.

(Sc3) The decision makers specify the test fan speeds t^p, $p \in [N]$, in advance.

While (Sc1) and (Sc2) are straightforward, (Sc3) requires further explanation. What distinguishes the test fan speeds from the other ADA parameters, i.e., why do the decision makers specify the test fan speeds in advance? Recall from Section 3.4.2 that ADA provides N data points $(t^p, \hat{r}_D^p(i_p))$ for the approximation of the drift resistance function $r_D(\text{fs})$, see also Definition 3.38 and Figure 3.7. Depending on the situation, the decision makers prefer data points that have a certain distribution in the set of feasible fan speeds [PHE, Item 3280]. Usually, the decision makers want that:

- An ADA iteration can be performed when the burner is close to its minimum load. Thus, the smallest test fan speed should be close to the considered HE's minimum fan speed.
- An ADA iteration can be performed when the burner is close to its maximum load. Thus, the largest test fan speed shall be close to the considered HE's maximum fan speed fs_{max}. But not too close, because the corresponding start fan speed, which is larger than the test fan speed, must not be larger than fs_{max} according to (S7).
- The test fan speeds in between are uniformly distributed in order to have a good distribution of the test points in the set of fan speeds, i.e., $t^p - t^{p+1} = \frac{1}{N-1}(t^1 - t^N)$ for all $p \in [N-1]$.

Note that these three items with respect to the test fan speeds are not mandatory. For instance, in one use case it turned out that ADA pairs with the test fan speed in a particular range of the fan speeds have a too slow rate of convergence for a certain type of HE. The decision makers decided to not place an ADA pair in this fan speed range for this type of HE [PHE, Item 3855].

Because all test fan speeds must be within the HE model's set of feasible fan speeds $[\mathrm{fs}_{\min}, \mathrm{fs}_{\max}]$ and because they must follow a descending order according to (S7), the following definition of the set of feasible test fan speeds is provided.

Definition 8.1 *Let* $\mathcal{H} = \left(\mathrm{FS}, (G_{\mathrm{fs}})_{\mathrm{fs}\in\mathrm{FS}}, (\iota_{\mathrm{fs}})_{\mathrm{fs}\in\mathrm{FS}}, (\Lambda_{\mathrm{fs}})_{\mathrm{fs}\in\mathrm{FS}}, (\zeta_{\mathrm{fs}})_{\mathrm{fs}\in\mathrm{FS}}\right)$ *be an HE model. A set* $T := \{t^1, \ldots, t^N\} \subset \mathbb{R}_{>0}$ *is called* set of feasible test fan speeds with respect to $\mathcal{H}$, *if*

$$\mathrm{fs}_{\min} \leq t^N < t^{N-1} < \cdots < t^1 < \mathrm{fs}_{\max}\,.$$

Remark 8.2 *In an early phase of the modeling process, the test fan speeds were not considered as fixed. Rather, they were also a part of the decision variables. But the results were not satisfactory. Furthermore, it has been observed in practice that small changes in the test fan speed of an ADA pair only cause small changes in the ADA convergence characteristics of the corresponding ADA pair. This means that a test fan speed a few percent larger or smaller makes only a small difference to the rate of convergence. With this observation in mind, the decision makers decided to select the N test fan speeds first and keep them fixed during the optimization process.*

Remark 8.3 *It is an empirical finding that small changes in the test fan speed of an ADA pair usually cause only small changes in the corresponding rate of convergence, which cannot be proved with the properties of the HE model. Rather, this seems to be a property of the considered HE type itself. In general, it is thinkable that there are HE types such that this property does not hold. If it turns out that an HE type is such that the rates of convergence are sensitive to small changes in the test fan speeds, it may make sense to revise the optimization model and also include the optimization of the test fan speeds.*

It is important to emphasize that because the test fan speeds are provided by the decision makers, the selection of the test fan speeds is not a part of the proposed optimization models. This has the advantage, that the ADA pairs are decoupled and can be considered individually, see also Remark 8.50 below. This reduces the complexity of the optimization model and simplifies the decision making process.
For the remainder of this chapter, only the case where (Sc1), (Sc2) and (Sc3) hold is considered. In particular, the proposed optimization models require that (Sc1), (Sc2) and (Sc3) hold.
With these considerations in mind, the second aspect of (O) is discussed and we analyze what good convergence characteristics of Algorithm 5.2 are.

8.1.2. Good Convergence Characteristics

As stated in Section 7.4, the ADA Algorithm 5.2 ideally returns the drifted test ioni current i^p_{t,r_D} for each ADA pair $p \in [N]$. Recall from Definition 3.27 that $i^p_{t,r_D} = \iota_{t^p,r_D} \circ \iota^{-1}_{t^p}(i^p_t)$, $p \in [N]$. In addition, the ADA pairs should be chosen such that each ADA pair $p \in [N]$ has a fast rate of convergence to i^p_{t,r_D}. This allows us to break down the objective criterion (O) further. Ideally:

(O1) The super fixed point vector $\boldsymbol{i}^{**} = (i_1^{**}, \ldots, i_N^{**})$ approximates the drifted test ioni currents perfectly, i.e., $i_p^{**} = i_{t,r_D}^p$ holds for all $p \in [N]$.

(O2) For the input vector $\hat{\boldsymbol{i}}_{\boldsymbol{t},\text{in}} = (i_t^1, \ldots, i_t^N)$, which is the only relevant input vector according to (Sc2), and for all sufficiently well distributed ADA update sequences u, we have $\lim_{n\to\infty} \boldsymbol{i}^n(\hat{\boldsymbol{i}}_{\boldsymbol{t},\text{in}}, u) = \boldsymbol{i}^{**}$, i.e., the corresponding sequences of ADA iterates and thus the corresponding output of Algorithm 5.2 converge to $\boldsymbol{i}^{**}$.

(O3) The sequence $\boldsymbol{i}^n(\hat{\boldsymbol{i}}_{\boldsymbol{t},\text{in}}, u)$, where $\hat{\boldsymbol{i}}_{\boldsymbol{t},\text{in}} = (i_t^1, \ldots, i_t^N)$ and u is a sufficiently well distributed ADA update sequence, has a high rate of convergence in the sense that only a few ADA iterations with each ADA pair are required to get close to $\boldsymbol{i}^{**}$.

Items (O1) and (O2) can be considered as mandatory. Hence, they become a part of the constraints of the optimization models. They are dealt with in detail in the following section. Under all the ADA pairs that fulfill (O1) and (O2), we are interested in those that have the fastest rate of convergence. Therefore, (O3) becomes a part of the optimization goals. Item (O3) is dealt with in detail in Sections 8.3 and 8.4.
However, the final optimization models contain more constraints according to the specifications (S1) to (S7), which are detailed in Section 8.5. All objectives and constraints are then combined to the proposed optimization model for the nominal case without tolerances in Section 8.6. Finally, Section 8.7 extends the nominal optimization model for the case with tolerances.

8.2. Convergence Related Requirements

In this section, we first derive requirements such that (O1) and (O2) are satisfied. Corresponding constraints for the optimization model are then derived from these requirements. According to Theorem 7.73, (O1) is satisfied if and only if $\text{fix}(A_{r_D}^p) = r_D$ for all $p \in [N]$. Therefore, the following requirement guarantees that (O1) is satisfied.

(R1) $\text{fix}(A_{r_D}^p) = r_D$ for all $p \in [N]$.

However, finding requirements such that (O2) is satisfied is more complicated and is divided into two steps. First, we derive conditions such that $\hat{\boldsymbol{i}}_{\boldsymbol{t},\text{in}} = (i_t^1, \ldots, i_t^N)$ and an arbitrary update sequence u are a feasible input combination for Algorithm 5.2. Thereafter, we derive conditions such that $\lim_{n\to\infty} \boldsymbol{i}^n(\hat{\boldsymbol{i}}_{\boldsymbol{t},\text{in}}, u) = \boldsymbol{i}^{**}$ for all sufficiently well distributed ADA update sequences u.

8.2.1. Feasible Input Combination for the ADA Algorithm

Let $\hat{\boldsymbol{i}}_{\boldsymbol{t},\text{in}} = (i_t^1, \ldots, i_t^N)$ and let u be an arbitrary ADA update sequence. Without loss of generality, let u be an infinite sequence. This is done to avoid case distinctions with respect to the length of u. The input vector $\hat{\boldsymbol{i}}_{\boldsymbol{t},\text{in}}$ and u are a feasible input combination if and only if the ioni current based ADA iterates $\boldsymbol{i}^n(\hat{\boldsymbol{i}}_{\boldsymbol{t},\text{in}}, u) = (i_1^n, \ldots, i_N^n)$ are contained in $\mathbb{R}^N$ for all $n \in \mathbb{N}$ according to Definition 7.24.

The approach to show that $\hat{\boldsymbol{i}}_{\boldsymbol{t},\text{in}}$ and u are a feasible input combination is to show that the corresponding resistance based ADA iterates $\boldsymbol{r}^n(\hat{\boldsymbol{i}}_{\boldsymbol{t},\text{in}}, u) = (r_1^n, \ldots, r_N^n)$ are contained in the set $[0, r_D]^N$ for all $n \in \mathbb{N}$. Because $r_p^n = \beta^p(i_p^n)$ and $r_p^n \in [0, r_D]$, we have $i_p^n = (\beta^p)^{-1}(r_p^n) \in \mathbb{R}$ for all $p \in [N]$ in this case, see also Definitions 7.28 and 5.9.
The following lemmas are auxiliary statements that are needed to prove the following Theorem 8.10 about $\hat{\boldsymbol{i}}_{\boldsymbol{t},\text{in}}$ and u being feasible inputs. First, we state conditions such that the ADA iteration function $A_{r_D}^p$ is a selfmap on the interval $[0, r_D]$. For this, recall that $\hat{R}_{r_D}^p$ is the domain of $A_{r_D}^p$, see also Definition 6.21.

Lemma 8.4 *Let $r_D \geq 0$ and let $p \in [N]$. Furthermore, let $A_{r_D}^p$ be contractive, let $\text{fix}(A_{r_D}^p) = r_D$ and let $0 \in \hat{R}_{r_D}^p$. Then,*

$$r \in [0, r_D] \;\Rightarrow\; A_{r_D}^p(r) \in [0, r_D].$$

Proof. Because $\hat{R}_{r_D}^p$ is a closed interval (Lemma 6.11) and $0 \in \hat{R}_{r_D}^p$ as well as $r_D \in \hat{R}_{r_D}^p$ (by assumption), we have $[0, r_D] \subset \hat{R}_{r_D}^p$, i.e., $A_{r_D}^p(r)$ is well-defined for all $r \in [0, r_D]$. If $r_D = 0$, then $[0, r_D] = \{0\}$ and $A_{r_D}^p(r) = r_D = 0$ for all $r \in [0, r_D]$. Next, let $r_D > 0$. Because $A_{r_D}^p$ is strictly increasing (Lemma 6.34) and $A_{r_D}^p$ is contractive, we can apply Lemma 4.45 and obtain

$$0 \leq r \leq r_D = \text{fix}(A_{r_D}^p) \;\Rightarrow\; 0 < A_{r_D}^p(r) \leq \text{fix}(A_{r_D}^p) = r_D.$$

□

A similar relation exists for the weighted sum function ω_v^p according to Definition 7.1.

Lemma 8.5 *Let $r_D \geq 0$ and let $p \in \{2, \ldots, N\}$, then*

$$r \in [0, r_D] \text{ and } v \in [0, r_D] \;\Rightarrow\; \omega_v^p(r) \in [0, r_D].$$

Proof. Let $r \in [0, r_D]$ and let $v \in [0, r_D]$. Because $0 < w^p < 1$ (Lemma 5.13), we have

$$\begin{aligned}
&0 \leq r \leq r_D \text{ and } 0 \leq v \leq r_D \\
\Rightarrow\; &0 \leq w^p r \leq w^p r_D \text{ and } 0 \leq (1 - w^p)v \leq (1 - w^p)r_D \\
\Rightarrow\; &0 \leq w^p r + (1 - w^p)v \leq w^p r_D + (1 - w^p)r_D \\
\Rightarrow\; &0 \leq \omega_v^p(r) = w^p r + (1 - w^p)v \leq r_D.
\end{aligned}$$

□

With this, we can state conditions such that $C_{r_D,v}^p$ is a selfmap on $[0, r_D]$.

Lemma 8.6 *Let $r_D \geq 0$ and let $p \in \{2, \ldots, N\}$. Furthermore, let $A_{r_D}^p$ be contractive, let $\text{fix}(A_{r_D}^p) = r_D$ and let $0 \in \hat{R}_{r_D}^p$. Then,*

$$r \in [0, r_D] \text{ and } v \in [0, r_D] \;\Rightarrow\; C_{r_D,v}^p(r) \in [0, r_D].$$

In particular $C_{r_D,v}^p(r)$ is well-defined.

Proof. Let $r \in [0, r_D]$ and let $v \in [0, r_D]$. Then, $\omega_v^p(r) \in [0, r_D]$ (Lemma 8.5) and thus $A_{r_D}^p \circ \omega_v^p(r)$ is well-defined and $A_{r_D}^p \circ \omega_v^p(r) \in [0, r_D]$ holds (Lemma 8.4). With this, the statement follows from $C_{r_D,v}^p := A_{r_D}^p \circ \omega_v^p$ (Definition 7.36). □

An analogous statement exists for the ioni current based iteration function defined in Definition 7.8.

Corollary 8.7 *Let $r_D \geq 0$ and let $p \in \{2, \ldots, N\}$. Furthermore, let $A_{r_D}^p$ be contractive, let $\operatorname{fix}(A_{r_D}^p) = r_D$ and let $0 \in \hat{R}_{r_D}^p$. Then,*

$$i \in (\beta^p)^{-1}\big([0, r_D]\big) \text{ and } v \in [0, r_D] \;\Rightarrow\; B_{r_D,v}^p(i) \in (\beta^p)^{-1}\big([0, r_D]\big).$$

In particular $B_{r_D,v}^p(i)$ is well-defined in this case.

Proof. Because $r_t^p > 0$ (Remark 5.8), $(\beta^p)^{-1}(r) = \frac{U}{r + r_t^p}$ is well-defined for all $r \in [0, r_D]$, i.e., the set $(\beta^p)^{-1}\big([0, r_D]\big)$ is well-defined.
Let $i \in (\beta^p)^{-1}\big([0, r_D]\big)$ and let $v \in [0, r_D]$. By applying Lemma 8.6, we have

$$\begin{aligned} i \in (\beta^p)^{-1}\big([0, r_D]\big) &\;\Rightarrow\; \beta^p(i) \in [0, r_D] \;\Rightarrow\; C_{r_D,v}^p \circ \beta^p(i) \in [0, r_D] \\ &\;\Rightarrow\; (\beta^p)^{-1} \circ C_{r_D,v}^p \circ \beta^p(i) \in (\beta^p)^{-1}\big([0, r_D]\big), \end{aligned}$$

i.e., $(\beta^p)^{-1} \circ C_{r_D,v}^p \circ \beta^p(i)$ is well-defined and thus $B_{r_D,v}^p(i)$ is also well-defined according to Lemma 7.40. □

Remark 8.8 *In Definition 7.4, the set $V_{r_D}^p$, $p \in \{2, \ldots, N\}$, is introduced to make sure that the functions $B_{r_D,v}^p$ and $C_{r_D,v}^p$ are well-defined under all circumstances (Lemma 7.10). According to Lemma 8.6 and Corollary 8.7, we know that under certain conditions $v \in [0, r_D]$ implies that $B_{r_D,v}^p$ and $C_{r_D,v}^p$ are well-defined. This is independent of v being an element of $V_{r_D}^p$. Therefore, the set $V_{r_D}^p$ is considered as superfluous in this section. Rather, it is replaced by the condition $v \in [0, r_D]$ in the following. This does not impair any result from the previous chapter, because in all corresponding proofs the set $V_{r_D}^p$ is only required to make sure that $B_{r_D,v}^p$ and $C_{r_D,v}^p$ are well-defined, which is guaranteed by Lemma 8.6 and Corollary 8.7 if $v \in [0, r_D]$ and $r \in [0, r_D]$ are considered.*

Corollary 8.9 *Let $r_D \geq 0$ and let $p \in \{2, \ldots, N\}$. Furthermore, let $A_{r_D}^p$ be contractive, let $\operatorname{fix}(A_{r_D}^p) = r_D$ and let $0 \in \hat{R}_{r_D}^p$. Then,*

$$v \in [0, r_D] \;\Rightarrow\; C_{r_D,v}^p|_{[0,r_D]} \text{ is a contractive selfmap and } \operatorname{fix}(C_{r_D,v}^p) \in [0, r_D].$$

Proof. Let $v \in [0, r_D]$. Because $A_{r_D}^p$ is contractive (by assumption), $C_{r_D,v}^p$ is contractive as well (Lemma 7.48). Furthermore, we have $r \in [0, r_D]$ implies $C_{r_D,v}^p(r) \in [0, r_D]$ (Lemma 8.6) and thus $C_{r_D,v}^p$ restricted to $[0, r_D]$ is a selfmap.
As a strictly increasing and contractive selfmap, $C_{r_D,v}^p$ restricted to $[0, r_D]$ has the unique fixed point $\operatorname{fix}(C_{r_D,v}^p)$ (Corollary 7.47). Furthermore, $\operatorname{fix}(C_{r_D,v}^p)$ has to be an element of $[0, r_D]$. If not, this would be a contradiction to being a selfmap on $[0, r_D]$. □

Finally, we can show that $\hat{\boldsymbol{i}}_{\boldsymbol{t},\text{in}} = (i_t^1, \ldots, i_t^N)$ and an arbitrary ADA update sequence u are a feasible input combination.

Theorem 8.10 *Let $r_D \geq 0$. Let $A_{r_D}^p$ be contractive, let $\text{fix}(A_{r_D}^p) = r_D$ and let $0 \in \hat{R}_{r_D}^p$ for all $p \in [N]$. Then, $\hat{\boldsymbol{i}}_{\boldsymbol{t},\text{in}} := (i_t^1, \ldots, i_t^N)$ and u are a feasible input combination, where u is an arbitrary (finite or infinite) ADA update sequence.*

Proof. Aiming at a better readability, the subscript r_D of $\hat{R}_{r_D}^P$, $A_{r_D}^p$ and $C_{r_D,v}^p$ is omitted throughout the proof.
Let u be an arbitrary ADA update sequence. Without loss of generality, let u be infinite, i.e., $u = (u_n)_{n\in\mathbb{N}}$. Let $\boldsymbol{i}^n(\hat{\boldsymbol{i}}_{\boldsymbol{t},\text{in}}, u) = (i_1^n, \ldots, i_N^n)$ be the n-th ioni current based ADA iterate according to Definition 7.22. To show that $\hat{\boldsymbol{i}}_{\boldsymbol{t},\text{in}}$ and u are a feasible input combination, we have to guarantee that for all $n \in \mathbb{N}$ and for all $p \in [N]$ $i_p^n \neq \text{NaN}$ holds, see also Definition 7.24. For this, we consider the corresponding resistance based ADA iterates $\boldsymbol{r}^n(\hat{\boldsymbol{i}}_{\boldsymbol{t},\text{in}}, u) = (r_1^n, \ldots, r_N^n)$ defined by $r_p^n := \beta^p(i_p^n)$ according to Definition 7.28. They can be recursively calculated by

$$\boldsymbol{r}^n(\hat{\boldsymbol{i}}_{\boldsymbol{t},\text{in}}, u) = \begin{cases} \left(A^1(r_1^{n-1}), r_2^{n-1}, \ldots, r_N^{n-1}\right) & \text{if } u_n = 1, \\ \left(r_1^{n-1}, \ldots, r_{p-1}^{n-1}, C_{r_{p-1}^{n-1}}^p(r_p^{n-1}), r_{p+1}^{n-1}, \ldots, r_N^{n-1}\right) & \text{if } u_n =: p \geq 2. \end{cases} \tag{8.1}$$

with $r_p^0 := \beta^p(i_p^{\text{in}})$ for all $p \in [N]$ (Lemma 7.45). We show by induction over n that $r_p^n \in [0, r_D]$ for all $p \in [N]$ and for all $n \in \mathbb{N}_0$.
Base case: Let $n = 0$. By construction, we have

$$r_p^0 = \beta^p(i_p^{\text{in}}) = \beta^p(i_t^p) = \frac{U}{i_t^p} - \frac{U}{i_t^p} = 0 \;\forall\; p \in [N].$$

Induction hypothesis: For a certain $k \in \mathbb{N}$ let $r_p^\ell \in [0, r_D]$ for all $p \in [N]$ and for all $\ell \in [k]$.
Induction step: Let $n = k + 1$. According to (8.1), we have $r_p^n = r_p^{n-1} = r_p^k$ for all $p \in [N] \setminus \{u_n\}$. Because $r_p^k \in [0, r_D]$ according to the induction hypothesis, $r_p^n \in [0, r_D]$ holds for all $p \in [N] \setminus \{u_n\}$. It remains to show that $r_{u_n}^n \in [0, r_D]$.
If $u_n = 1$, then $r_1^n = A^1(r_1^{n-1})$ according to (8.1). Because $r_1^{n-1} \in [0, r_D]$ (induction hypothesis), we have $r_1^n = A^1(r_1^{n-1}) \in [0, r_D]$ (Lemma 8.4).
If $u_n =: p \in \{2, \ldots, N\}$, then $r_p^n = C_{r_{p-1}^{n-1}}^p(r_p^{n-1})$ according to (8.1). Because $r_{p-1}^{n-1} \in [0, r_D]$ as well as $r_p^{n-1} \in [0, r_D]$ (induction hypothesis), we have $r_p^n = C_{r_{p-1}^{n-1}}^p(r_p^{n-1}) \in [0, r_D]$ (Lemma 8.6) and the induction is completed.
Because $i_p^n = (\beta^p)^{-1}(r_p^n)$ and $r_p^n \in [0, r_D]$ and $[0, r_D] \subset \hat{R}^p$ (which is the domain of $(\beta^p)^{-1}$), we have $i_p^n \in (\beta^p)^{-1}([0, r_D])$ for all $p \in [N]$ and for all $n \in \mathbb{N}$. In particular $i_p^n \neq \text{NaN}$ for all $p \in [N]$ and for all $n \in \mathbb{N}$ and thus $\hat{\boldsymbol{i}}_{\boldsymbol{t},\text{in}}$ and u are a feasible input combination. □

According to the proof of Theorem 8.10, all components of all resistance based ADA iterates are contained in the interval $[0, r_D]$.

Corollary 8.11 *Let $r_D \geq 0$. Let $A^p_{r_D}$ be contractive, let $\mathrm{fix}(A^p_{r_D}) = r_D$ and let $0 \in \hat{R}^p_{r_D}$ for all $p \in [N]$. Let $\hat{\boldsymbol{i}}_{\boldsymbol{t},\mathrm{in}} := (i_t^1, \ldots, i_t^N)$, let u be an arbitrary (infinite) ADA update sequence and let $\boldsymbol{r}^n(\hat{\boldsymbol{i}}_{\boldsymbol{t},\mathrm{in}}, u) = (r_1^n, \ldots, r_N^n)$ be the corresponding n-th resistance based ADA iterate. Then, $r_p^n \in [0, r_D]$ for all $p \in [N]$ for all $n \in \mathbb{N}$.*

With this, we can prove that ADA Algorithm 5.2 given the inputs $\hat{\boldsymbol{i}}_{\boldsymbol{t},\mathrm{in}} = (i_t^1, \ldots, i_t^N)$ and a sufficiently well distributed ADA update sequence u converges to the super fixed point vector $\boldsymbol{i}^{**}$.

8.2.2. Convergence of the ADA Algorithm

The following theorem states conditions such that the ADA Algorithm 5.2 converges to the super fixed point vector $\boldsymbol{i}^{**} = (i_1^{**}, \ldots, i_N^{**})$ with $i_p^{**} = i^p_{t,r_D}$ for all $p \in [N]$. From the theorem's requirements we then derive conditions such that (O2) is satisfied.

Theorem 8.12 *Let $r_D \geq 0$. For all $p \in [N]$ let $A^p_{r_D}$ be contractive, $\mathrm{fix}(A^p_{r_D}) = r_D$ and $0 \in \hat{R}^p_{r_D}$. Then,*

- *$\boldsymbol{i}^{**} = (i_1^{**}, \ldots, i_N^{**})$ with $i_p^{**} = i^p_{t,r_D}$ for all $p \in [N]$ and*
- *$\lim_{n\to\infty} \boldsymbol{i}^n(\hat{\boldsymbol{i}}_{\boldsymbol{t},\mathrm{in}}, u) = \boldsymbol{i}^{**}$, where $\hat{\boldsymbol{i}}_{\boldsymbol{t},\mathrm{in}} = (i_t^1, \ldots, i_t^N)$ and u is an arbitrary sufficiently well distributed ADA update sequence.*

Proof. Let u be an arbitrary sufficiently well distributed ADA update sequence. To show the statement, we apply Theorem 7.68. We check the necessary prerequisites for this.

- Feasible scenario: Because $\mathrm{fix}(A^p_{r_D}) = r_D$ for all $p \in [N]$ by assumption, we have $i_p^{**} = i^p_{t,r_D}$ for all $p \in [N]$ (Theorem 7.73) and thus $i_p^{**} \in \mathbb{R}$ for all $p \in [N]$. In particular, the corresponding resistance based super fixed point vector is $\boldsymbol{r}^{**} = (r_1^{**}, \ldots, r_N^{**})$ with $r_p^{**} = r_D$ for all $p \in [N]$.
- The iteration function $A^p_{r_D}$ is contractive for all $p \in [N]$ by assumption.
- The starting vector $\hat{\boldsymbol{i}}_{\boldsymbol{t},\mathrm{in}} = (i_t^1, \ldots, i_t^N)$ and u are a feasible input combination according to Theorem 8.10.
- It remains to show that "there exists $\delta > 0$ such that $[r_{p-1}^{**} - \delta, r_{p-1}^{**} + \delta] \subset V^p_{r_D}$ and $C^p_{r_D, r_{p-1}^{**} - \delta}$ as well as $C^p_{r_D, r_{p-1}^{**} + \delta}$ are selfmaps for all $p \in \{2, \ldots, N\}$" (third requirement of Theorem 7.68).
  According to Corollary 8.11, all resistance based ADA iterates are elements of $[0, r_D]$. Therefore, we always have the situation "$v \in [0, r_D]$" (recall that v is the incumbent drift resistance approximation of ADA pair $p-1$ for $p \in \{2, \ldots, N\}$, see also Remark 7.3). As a consequence, we can safely assume that $C^p_{r_D,v}(r)$ is well-defined for all $p \in \{2, \ldots, N\}$ and for all $r \in [0, r_D]$, i.e., the set $V^p_{r_D}$ is not required in this case, see also Remark 8.8.
  We select $\delta := r_D$. According to the first item of this proof, we have $r_{p-1}^{**} = r_D$ for all

$p \in \{2, \ldots, N\}$ and thus $C^p_{r_D,v}|_{[0,r_D]}$ is a selfmap for all $v \in [0, r_D] = [r^{**}_{p-1} - \delta, r^{**}_{p-1}]$ (Corollary 8.9). However, we cannot make a statement about the iteration function $C^p_{r_D, r^{**}_{p-1}+\delta}$. We do not even know whether this function is well-defined. The following argumentation shows that it is sufficient to consider the iteration functions $C^p_{r_D,v}|_{[0,r_D]}$ with $v \in [0, r_D] = [r^{**}_{p-1} - \delta, r^{**}_{p-1}]$ in the specific case considered in this theorem, where we have $v \in [0, r_D]$.
Because $A^1_{r_D}$ is a selfmap on $[0, r_D]$ (Lemma 8.4) as well as $C^p_{r_D,v}|_{[0,r_D]}$, $p \in \{2, \ldots, N\}$, are selfmaps, the components of all ADA iterates are in the interval $[0, r_D]$. Therefore, a situation with $v > r_D$ never occurs under the conditions of this theorem. In visual terms, all drift resistance approximations of ADA pair p stay "left of r_D" (or are equal to r_D) for all $p \in [N]$. Thus, no information about what "happens right of r_D" is required.

With this, all requirements to apply Theorem 7.68 are met and thus $\lim_{n\to\infty} \boldsymbol{i}(\hat{\boldsymbol{i}}_{\boldsymbol{t},\text{in}}, u) = \boldsymbol{i}^{**}$. Furthermore, $i^{**}_p = i^p_{t,r_D}$ holds for all $p \in [N]$ □

Remark 8.13 *Note that all considerations made so far in this section are also valid if $A^p_{r_D}$ is only contractive over $[0, r_D]$, i.e., if only $A^p_{r_D}|_{[0,r_D]}$ is contractive. Therefore, the requirement "$A^p_{r_D}$ being contractive" is more restrictive than necessary. However, practical experience has shown that $A^p_{r_D}|_{[0,r_D]}$ being contractive usually implies that $A^p_{r_D}$ is contractive over its whole domain $\hat{R}^p_{r_D}$. Furthermore, from a practical point of view, it is convenient if $A^p_{r_D}$ is contractive over a larger set than $[0, r_D]$, because this leaves some room for the case that a drift resistance approximation $r \in \hat{R}^p_{r_D} \setminus [0, r_D]$ is considered for some reason. Therefore, the more general requirement $A^p_{r_D}$ being contractive over $\hat{R}^p_{r_D}$ is considered in the following.*

Item (O2) is satisfied if the requirements of Theorem 8.12 are met. Note that $r_D \geq 0$ and $\text{fix}(A^p_{r_D}) = r_D$ for all $p \in [N]$ are already covered by (Sc1) and (R1), respectively. The remaining requirements are:

(R2) $A^p_{r_D}$ is contractive for all $p \in [N]$.

(R3) $0 \in \hat{R}^p_{r_D}$ for all $p \in [N]$.

In conclusion, if (R1) to (R3) (as well as (Sc1)) hold, then (O1) and (O2) are satisfied. However, (R1) to (R3) are not constraints from a mathematical modeling point of view, because constraints "are functions of the design[1] variables that we want to restrict in some way" [MN22, p. 12]. In the following, we reformulate (R1) to (R3) and express them in dependence of the ADA parameters (s^p, t^p, i^p_s, i^p_t), $p \in [N]$. With this, we obtain constraints such that (O1) and (O2) are covered.

Remark 8.14 *Usually, strict inequalities are not allowed as constraints [Sán20, p. 9]. Because if a strict inequality is used and it is the active constraint, then there might be*

[1] The term "design variable" is synonymous to the term "decision variable" used in this work.

no optimal solution [MN22, p. 12]. Therefore, we follow the recommendation in [Sán20, p. 9]: Whenever we derive a constraint that is a strict inequality, we add (or subtract) an arbitrary small $\varepsilon > 0$ and transform the strict inequality to a not-strict inequality. Furthermore, for a better overview and simplification, we consider only equalities and less than or equal to inequalities as constraints in this work.

8.2.3. Derived Constraints for the Optimization Models

Let $r_D \geq 0$ be a given drift resistance and let $T = \{t^1, \ldots, t^N\}$ be a given set of feasible test fan speeds.

Requirement (R1)**:** We want that $\text{fix}(A^p_{r_D}) = r_D$ for all $p \in [N]$. According to Theorem 7.73, we have

$$\text{fix}(A^p_{r_D}) = r_D \ \forall\ p \in [N] \ \Leftrightarrow\ \iota^{-1}_{s^p}(i^p_s) = \iota^{-1}_{t^p}(i^p_t) \ \forall\ p \in [N].$$

The condition $\iota^{-1}_{s^p}(i^p_s) = \iota^{-1}_{t^p}(i^p_t)$ is already expressed in dependence of the ADA parameters and can be used as a constraint. Thus, in order to satisfy (R1), we include the constraint

(C-R1) $\iota^{-1}_{s^p}(i^p_s) - \iota^{-1}_{t^p}(i^p_t) = 0$ for all $p \in [N]$.

Requirement (R2)**:** We want that $A^p_{r_D}$ is contractive for all $p \in [N]$. Whether $A^p_{r_D}$ is contractive depends on its Lipschitz constant, which is denoted as follows.

Notation 8.15 *Let $p \in [N]$ and let $A^p_{r_D}$ be Lipschitzian. Then, the Lipschitz constant of $A^p_{r_D}$ is denoted by L^p.*

If $L^p < 1$, then $A^p_{r_D}$ is contractive. Thus, we are interested in ADA parameters (s^p, t^p, i^p_s, i^p_t) such that $L^p < 1$.

Remark 8.16 *There exist functions that are contractive whose Lipschitz constant is $L = 1$. However, the rate of convergence of a Picard iteration associated to such a function is usually slow, which is why this special case is not considered in the optimization model.*

Therefore, we define a function that maps the ADA parameters (s^p, t^p, i^p_s, i^p_t), for a given $p \in [N]$, with t^p taken from T, to the Lipschitz constant of the corresponding ADA iteration function $A^p_{r_D}$ (if it exists).

Definition 8.17 *Let $T = \{t^1, \ldots, t^N\}$ be a set of feasible test fan speeds and let $r_D \geq 0$ be given. For $p \in [N]$, we define $\mathcal{L}^p_{T,r_D} : \mathbb{R}^3 \to \mathbb{R}_{\geq 0} \cup \{\infty\}$ by*

$$\mathcal{L}^p_{T,r_D}(s^p, i^p_s, i^p_t) := \begin{cases} L^p \text{ (Lipschitz constant of } A^p_{r_D}) & \text{if } A^p_{r_D} \text{ is Lipschitzian,} \\ \infty & \text{else,} \end{cases}$$

where

$$A^p_{r_D}(r) = \sigma^-_{r^p_t} \circ \rho_{t^p, r_D} \circ \rho^{-1}_{s^p, r_D} \circ \sigma^+_{r^p_s}(r) = \rho_{t^p, r_D} \circ \rho^{-1}_{s^p, r_D}\big(r + \frac{U}{i^p_s}\big) - \frac{U}{i^p_t},$$

see also Definition 6.21.

Remark 8.18 *The function* $\mathcal{L}^p_{t^p,r_D}(s^p, i_s^p, i_t^p)$ *is well-defined by construction.*

In order to satisfy (R2), $\mathcal{L}^p_{t^p,r_D}(s^p, i_s^p, i_t^p) < 1$ for all $p \in [N]$ is a suitable constraint. However, no strict inequalities are allowed as constraints according to Remark 8.14. Therefore, we make us of an arbitrary small $\varepsilon > 0$ to transform the strict inequality to a not-strict inequality and we include the following constraint.

(C-R2) $\mathcal{L}^p_{T,r_D}(s^p, i_s^p, i_t^p) \leq 1 - \varepsilon$ for all $p \in [N]$, where $\varepsilon > 0$ is arbitrary small and fixed.

Requirement (R3): We want that $0 \in \hat{R}^p_{r_D}$ for all $p \in [N]$.

Lemma 8.19 *Let* $r_D \geq 0$ *and let* $p \in [N]$*, then*

$$\begin{aligned} 0 \in \hat{R}^p_{r_D} &\Leftrightarrow \frac{i_s^p U}{-i_s^p r_D + U} \in \iota_{s^p}(G_{s^p} \cap G_{t^p}) \\ &\Leftrightarrow \min \iota_{s^p}(G_{s^p} \cap G_{t^p}) \leq \frac{i_s^p U}{-i_s^p r_D + U} \leq \max \iota_{s^p}(G_{s^p} \cap G_{t^p}). \end{aligned}$$

Proof. By applying Definitions 5.19 and 6.14 as well as Lemma 6.20, we have

$$\hat{R}^p_{r_D} = \rho_{s^p,r_D}(G_{s^p} \cap G_{t^p}) + r_s^p = \rho_{s^p}(G_{s^p} \cap G_{t^p}) + r_D + r_s^p = \frac{U}{\iota_{s^p}(G_{s^p} \cap G_{t^p})} + r_D - r_s^p$$

and thus

$$\begin{aligned} 0 \in \hat{R}^p_{r_D} &\Leftrightarrow 0 \in \frac{U}{\iota_{s^p}(G_{s^p} \cap G_{t^p})} + r_D - r_s^p \Leftrightarrow \frac{U}{r_s^p - r_D} \in \iota_{s^p}(G_{s^p} \cap G_{t^p}) \\ &\Leftrightarrow \frac{U}{\frac{U}{i_s^p} - r_D} = \frac{i_s^p U}{-i_s^p r_D + U} \in \iota_{s^p}(G_{s^p} \cap G_{t^p}). \end{aligned}$$

Furthermore, $\iota_{s^p}(G_{s^p} \cap G_{t^p})$ is a closed and nonempty interval, because G_{s^p} and G_{t^p} are closed intervals and ι_{s^p} is a homeomorphism (Definition 2.18) as well as $G_{s^p} \cap G_{t^p} \neq \emptyset$ (Definition 5.2). □

Thus, in order to satisfy (R3), we include the following constraints, where we denote $G^p_{st} := G_{s^p} \cap G_{t^p}$.

(C-R3) $\min \iota_{s^p}(G^p_{st}) - \frac{i_s^p U}{-i_s^p r_D + U} \leq 0$ and $\frac{i_s^p U}{-i_s^p r_D + U} - \max \iota_{s^p}(G^p_{st}) \leq 0 \ \forall \ p \in [N]$.

At this point, we have made sure that (O1) and (O2) are covered and that optimized ADA parameters have a good approximation quality. But according to (O3), we also want a fast rate of convergence, which is dealt with below.

8.3. Optimization Objective: Fast Rate of Convergence

In this section, we deal with the remaining item (O3) and discuss how a fast rate of convergence can be modeled for the ADA optimization. Since (O1) and (O2) are considered as mandatory, we can restrict our considerations to situations where the corresponding requirements (R1) to (R3) are fulfilled. I.e., for all $p \in [N]$ we assume that $\mathrm{fix}(A^p_{r_D}) = r_D$, $L^p < 1$ and $0 \in \hat{R}^p_{r_D}$. Then, $r^n_p \in [0, r_D]$ for all $p \in [N]$ and for all $n \in \mathbb{N}$, where $\boldsymbol{r}^n(\hat{\boldsymbol{i}}_{\boldsymbol{t},\mathrm{in}}, u) = (r^n_1, \ldots, r^n_N)$ is the n-th resistance based ADA iterate with respect to $\hat{\boldsymbol{i}}_{\boldsymbol{t},\mathrm{in}} = (i^1_t, \ldots, i^N_t)$ and an arbitrary (infinite) ADA update sequence u (Corollary 8.11). Therefore, for each ADA pair it is sufficient to consider only drift resistance approximations in the interval $[0, r_D]$ in this case. If in addition u is sufficiently well distributed, then $\lim_{n\to\infty} \boldsymbol{r}^n(\hat{\boldsymbol{i}}_{\boldsymbol{t},\mathrm{in}}, u) = (r_D, \ldots, r_D)$ (Theorem 8.12).
In the following, we show that for all $p \in [N]$ a small Lipschitz constant L^p of the iteration function $A^p_{r_D}$ is an indicator for a fast rate of convergence regarding the drift resistance approximation by ADA pair p. As in the previous chapters, we make a case distinction with respect to p, because the iteration function of ADA pair $p = 1$ is different to those of the remaining ADA pairs.

8.3.1. Rate of Convergence of ADA Pair $p = 1$

Let r_1 be the incumbent drift resistance approximation of ADA pair $p = 1$. Then, an ADA iteration with ADA pair $p = 1$ corresponds to evaluating $A^1_{r_D}(r_1)$. A sequence of ADA iterations with ADA pair $p = 1$ starting at r_1 corresponds to the Picard iteration associated to $A^1_{r_D}$ starting at r_1, as delineated in Chapter 6. Therefore, we can apply Banach's fixed point Theorem 4.39 to estimate the rate of convergence in this case.

Lemma 8.20 *Let* $\mathrm{fix}(A^1_{r_D}) = r_D$ *and let* $A^1_{r_D}$ *be* L^1*-Lipschitzian with* $L^1 < 1$*, then*

$$\left|r_D - \left(A^1_{r_D}\right)^n(r_1)\right| \leq \left(L^1\right)^n \left|r_D - r_1\right| \;\forall\; r_1 \in \hat{R}^1_{r_D}.$$

Proof. Because $A^1_{r_D}$ is contractive and has a fixed point, it is also a selfmap (Lemma 6.35). Thus, we can apply Theorem 4.39. □

Therefore, a small Lipschitz constant L^1 is an indicator for a fast rate of convergence regarding the drift resistance approximation by ADA pair $p = 1$.

8.3.2. Rate of Convergence of ADA Pair p, $p \geq 2$

Regarding the rate of convergence of ADA pair p, $p \geq 2$, things are more complicated. Recall that an iteration with pair p, $p \geq 2$, corresponds to evaluating $C^p_{r_D,v}(r)$, where r and v are the incumbent drift resistance approximations of the ADA pairs p and $p-1$, respectively, see also Definition 7.36 and Remark 7.3.

Remark 8.21 *Aiming at a better readability, the subscript* r_D *of* $\hat{R}^p_{r_D}$, $A^p_{r_D}$ *and* $C^p_{r_D,v}$ *is omitted in this subsection.*

As in the case $p = 1$, we are interested in an estimate of the relation between $\left|r_D - C_v^p(r)\right|$ and $|r_D - r|$, i.e., we want to estimate how much closer $C_v^p(r)$ is to r_D than r is to r_D. Since we consider the specific case where we assume that (R1) to (R3) hold, it is sufficient to consider only $v \in [0, r_D]$ and $r \in [0, r_D]$ according to Corollary 8.11 and as delineated at the beginning of this Section 8.3.
First, we estimate how close the fixed point of C_v^p is to r_D, because $\operatorname{fix}(C_v^p) \neq r_D$ in general. Note that the fixed point of C_v^p exists for all $v \in [0, r_D]$ and that $\operatorname{fix}(C_v^p) \in [0, r_D]$ according to Corollary 8.9. Furthermore, recall that $0 < w^p < 1$ according to Lemma 5.13.

Lemma 8.22 *Let $p \in \{2, \dots, N\}$, let A^p be L^p-Lipschitzian with $L^p < 1$, let $\operatorname{fix}(A^p) = r_D$, let $0 \in \hat{R}^p$ and let $v \in [0, r_D]$. Then, the following inequality holds:*

$$|\operatorname{fix}(C_v^p) - r_D| \leq \frac{(1 - w^p)L^p}{1 - L^p w^p} |v - r_D|. \tag{8.2}$$

Proof. Let $v \in [0, r_D]$, then $\operatorname{fix}(C_v^p) \in [0, r_D]$ (Corollary 8.9). Because A^p is L^p-Lipschitzian, C_v^p is $L^p w^p$-Lipschitzian (Lemma 7.77). Furthermore, $\operatorname{fix}(A^p) = r_D$ by assumption. With this, we obtain

$$\begin{aligned}
\left|\operatorname{fix}(C_v^p) - r_D\right| &= \left|C_v^p\big(\operatorname{fix}(C_v^p)\big) - A^p(r_D)\right| \\
&\leq \left|C_v^p\big(\operatorname{fix}(C_v^p)\big) - C_v^p(r_D)\right| + \left|C_v^p(r_D) - A^p(r_D)\right| \\
&= \left|C_v^p\big(\operatorname{fix}(C_v^p)\big) - C_v^p(r_D)\right| + \left|A^p \circ \omega_v^p(r_D) - A^p(r_D)\right| \\
&\leq L^p w^p \left|\operatorname{fix}(C_v^p) - r_D\right| + L^p \left|\omega_v^p(r_D) - r_D\right| \\
&= L^p w^p \left|\operatorname{fix}(C_v^p) - r_D\right| + L^p \left|w^p r_D + (1 - w^p)v - r_D\right| \\
&= L^p w^p \left|\operatorname{fix}(C_v^p) - r_D\right| + L^p (1 - w^p) \left|v - r_D\right|
\end{aligned}$$

and thus

$$\begin{aligned}
(1 - L^p w^p) \left|\operatorname{fix}(C_v^p) - r_D\right| &\leq L^p (1 - w^p) \left|v - r_D\right| \\
\Rightarrow \quad \left|\operatorname{fix}(C_v^p) - r_D\right| &\leq \frac{L^p (1 - w^p)}{1 - L^p w^p} \left|v - r_D\right|.
\end{aligned}$$

□

The inequality in (8.2) is tight, which is demonstrated in Example 8.25 below. But first, we use Lemma 8.22 to estimate the distance between r_D and $C_v^p(r)$ for $r \in [0, \operatorname{fix}(C_v^p)]$.

Lemma 8.23 *Let $p \in \{2, \dots, N\}$, let A^p be L^p-Lipschitzian with $L^p < 1$, let $\operatorname{fix}(A^p) = r_D$, let $0 \in \hat{R}^p$ and let $v \in [0, r_D]$. If $r \in [0, \operatorname{fix}(C_v^p)]$, then*

$$r_D - C_v^p(r) \leq L^p r_D - L^p \big(w^p r + (1 - w^p)v\big). \tag{8.3}$$

Proof. Let $0 \leq v \leq r_D$ and let $0 \leq r \leq \operatorname{fix}(C_v^p)$. Note that $\operatorname{fix}(C_v^p) \leq r_D$ (Corollary 8.9), which implies $r \in [0, r_D]$. Therefore $C_v^p(r)$ is well-defined (Lemma 8.6). Because C_v^p is

strictly increasing, we have $C_v^p(r) \leq C_v^p\big(\mathrm{fix}(C_v^p)\big) = \mathrm{fix}(C_v^p)$ (Lemma 4.45). Furthermore, C_v^p is $L^p w^p$-Lipschitzian (Lemma 7.77). With this, we have

$$\begin{aligned}\mathrm{fix}(C_v^p) - C_v^p(r) = C_v^p\big(\mathrm{fix}(C_v^p)\big) - C_v^p(r) = \big|C_v^p\big(\mathrm{fix}(C_v^p)\big) - C_v^p(r)\big| &\leq L^p w^p \big|\mathrm{fix}(C_v^p) - r\big| \\ &= L^p w^p \big(\mathrm{fix}(C_v^p) - r\big)\end{aligned}$$

and thus

$$(1 - L^p w^p)\,\mathrm{fix}(C_v^p) + L^p w^p r \leq C_v^p(r). \tag{8.4}$$

We use the bound for $|\mathrm{fix}(C_v^p) - r_D|$ according to Lemma 8.22, c.f. (8.2), and we obtain (note that $0 < w^p < 1$ and $0 < L^p < 1$)

$$r_D - \mathrm{fix}(C_v^p) = |r_D - \mathrm{fix}(C_v^p)| \leq \frac{(1-w^p)L^p}{1 - L^p w^p}|v - r_D| = \frac{(1-w^p)L^p}{1 - L^p w^p}(r_D - v)$$

and thus

$$\begin{aligned}(1 - L^p w^p)\,\mathrm{fix}(C_v^p) &\geq (1 - L^p w^p) r_D + (1 - w^p) L^p (v - r_D) \\ &= r_D - L^p w^p r_D + (1 - w^p) L^p v - L^p r_D + w^p L^p r_D \\ &= (1 - L^p) r_D + (1 - w^p) L^p v. \end{aligned} \tag{8.5}$$

Finally, we combine (8.4) and (8.5), which yields

$$C_v^p(r) \geq (1 - L^p) r_D + (1 - w^p) L^p v + L^p w^p r = (1 - L^p) r_D + L^p\big(w^p r + (1 - w^p) v\big)$$

and thus

$$r_D - C_v^p(r) \leq L^p r_D - L^p\big(w^p r + (1 - w^p) v\big).$$

□

Remark 8.24 *Lemma 8.23 requires that $r \in [0, \mathrm{fix}(C_v^p)]$. It can be shown, that the case $r > \mathrm{fix}(C_v^p)$ never happens in the specific case considered where* (R1) *to* (R3) *hold and thus the requirement $r \in [0, \mathrm{fix}(C_v^p)]$ is not restrictive. However, the proof is lengthy and omitted for the following reason.*
If $r > \mathrm{fix}(C_v^p)$ (which never happens in the specific case considered), we can also estimate $r_D - C_v^p(r)$, because $r > \mathrm{fix}(C_v^p)$ implies $\mathrm{fix}(C_v^p) < C_v^p(r) < r$ according to Lemma 4.45 and thus $r_D - C_v^p(r) < r_D - \mathrm{fix}(C_v^p)$ and $r_D - \mathrm{fix}(C_v^p)$ can be estimated by (8.2) *according to Lemma 8.22.*

The following example demonstrates that the inequalities (8.2) and (8.3) are tight.

Example 8.25 *Let $r_D \geq 0$. Let us suppose that*

$$A^p : [0, r_D] \to \mathbb{R}, \quad A^p(r) := L^p(r - r_D) + r_D \text{ with } 0 < L^p < 1.$$

Note that (R1) *to* (R3) *hold. In particular, A^p is contractive with $L^p < 1$ and $A^p(r_D) = r_D$, i.e., $\mathrm{fix}(A^p) = r_D$. We are interested in the fixed point of $C_v^p = A^p \circ \omega_v^p$ for $v \in [0, r_D]$. Let $r^* := \mathrm{fix}(C_v^p)$, which exists according to Corollary 8.9. Then,*

$$\begin{aligned} r^* = C_v^p(r^*) = A^p \circ \omega_v^p(r^*) &= L^p\big(w^p r^* + (1-w^p)v - r_D\big) + r_D \\ &= L^p w^p r^* + (1-w^p)L^p v + (1-L^p)r_D \\ \Rightarrow\ r^* &= \frac{(1-w^p)L^p v + (1-L^p)r_D}{1-L^p w^p} \end{aligned}$$

and thus

$$\begin{aligned} r_D - r^* &= \frac{(1-L^p w^p)r_D - \big((1-w^p)L^p v + (1-L^p)r_D\big)}{1-L^p w^p} \\ &= \frac{r_D - L^p w^p r_D - (1-w^p)L^p v - r_D + L^p r_D}{1-L^p w^p} = \frac{(1-L^p)w^p(r_D - v)}{1-L^p w^p}. \end{aligned}$$

Therefore, the inequality (8.2) *is tight in this case.*
Next, we consider a function evaluation of C_v^p *with an arbitrary* $r \in [0, r^*]$. *We have*

$$C_v^p(r) = L^p\big(w^p r + (1-w^p)v - r_D\big) + r_D = (1-L^p)r_D + L^p w^p r + L^p(1-w^p)v$$

and thus $r_D - C_v^p(r) = L^p r_D - L^p\big(w^p r + (1-w^p)v\big)$, *i.e., the lower bound in* (8.3) *is also tight.*

Finally, we can state how much the approximation of r_D by ADA pair p, $p \geq 2$, improves with a single ADA iteration. For this, we consider the two cases $r \leq v$ and $r > v$ separately. Both cases are then interpreted and discussed with regard to a fast rate of convergence.

Lemma 8.26 *Let* $p \in \{2, \dots, N\}$, *let* A^p *be* L^p*-Lipschitzian with* $L^p < 1$, *let* $\mathrm{fix}(A^p) = r_D$ *and let* $0 \in \hat{R}^p$. *If* $v \in [0, r_D]$ *and* $r \in [0, \mathrm{fix}(C_v^p)]$, *then*

$$r \leq v \ \Rightarrow\ r_D - C_v^p(r) \leq L^p(r_D - r).$$

Proof. We have

$$r \leq v \ \Rightarrow\ w^p r + (1-w^p)v \geq w^p r + (1-w^p)r = r \ \Rightarrow\ -\big(w^p r + (1-w^p)v\big) \leq -r$$

and thus

$$(8.3) \ \Rightarrow\ r_D - C_v^p(r) \leq L^p r_D - L^p\big(w^p r + (1-w^p)v\big) \leq L^p r_D - L^p r = L^p(r_D - r).$$

□

In the case $r > v$, we cannot apply the estimation according to Lemma 8.26. But at least we can estimate the distance to the fixed point of C_v^p. The following statement holds for all $r \in [0, \mathrm{fix}(C_v^p)]$, i.e., it is not restricted to $r > v$.

Lemma 8.27 *Let* $p \in \{2, \dots, N\}$, *let* A^p *be* L^p*-Lipschitzian with* $L^p < 1$, *let* $\mathrm{fix}(A^p) = r_D$ *and let* $0 \in \hat{R}^p$. *If* $v \in [0, r_D]$ *and* $r \in [0, \mathrm{fix}(C_v^p)]$, *then*

$$\mathrm{fix}(C_v^p) - C_v^p(r) \leq L^p w^p\big(\mathrm{fix}(C_v^p) - r\big).$$

Proof. The statement follows from the fact that C_v^p is $L^p w^p$-Lipschitzian (Lemma 7.77) and because $r \leq \mathrm{fix}(C_v^p)$ implies $C_v^p(r) \leq \mathrm{fix}(C_v^p)$ (Lemma 4.45). □

Interpretation and Discussion of the Results with Regard to a Fast Rate of Convergence

In Section 8.3.1, a clear statement regarding the rate of convergence of the approximation of r_D by ADA pair $p = 1$ is given. This is not possible for the case $p \geq 2$, because in this case an iteration with ADA pair p depends on r and v. Recall that r and v are the incumbent approximations of r_D by ADA pairs p and $p-1$, respectively, as stated at the beginning of this Subsection 8.3.2. The difficulty in the case $p \geq 2$ is that two subsequent ADA iterations with ADA pair p are not done with the same iteration function C_v^p in general, because the value of v might change between these two iterations. For instance this is the case if the considered ADA update sequence is $u = (\dots, p, p-1, p, \dots)$. Therefore, two subsequent iterations with p cannot be calculated by $\left(C_v^p\right)^2(r)$ in general. Rather, because the incumbent approximation of the drift resistance by ADA pair $p-1$ might have changed between the two iterations with ADA pair p, we have two different incumbent approximations by ADA pair $p-1$, denoted by v^1 and v^2 for the moment, and one calculates $C_{v^2}^p\left(C_{v^1}^p(r)\right)$.
However, as long as the incumbent values are such that $r \leq v$ in each ADA iteration with ADA pair p, the approximation error of the approximation by ADA pair p is reduced by the factor L^p according to Lemma 8.26. Therefore, a small Lipschitz constant of A^p is an indicator for a fast rate of convergence in this case.
In the case $r > v$ things are different. In this case, we can only state that the approximation error to the fixed point of C_v^p (and not to r_D) is reduced by $L^p w^p$ according to Lemma 8.27. However, if the distance between $\operatorname{fix}(C_v^p)$ and r_D is small, ADA pair p can still approximate r_D with a small approximation error in this case. According to Lemma 8.22, we have

$$|\operatorname{fix}(C_v^p) - r_D| \leq \frac{(1-w^p)L^p}{1-L^p w^p}|v - r_D| = \frac{1-w^p}{\frac{1}{L^p} - w^p}|v - r_D|. \tag{8.6}$$

Because $L^p > 0$ is fixed and $w^p < 1$ is fixed, ADA pair p has the chance to approximate r_D with an arbitrarily small approximation error only if v gets close to r_D. Since we assume sufficiently well distributed ADA update sequences, v will eventually converge to r_D and ADA pair p will eventually approximate r_D arbitrary well. Nevertheless. a small Lipschitz constant L^p is advantageous with regard to the rate of convergence in the case $p \geq 2$ for two reasons. First, a small L^p guarantees a fast convergence to $\operatorname{fix}(C_v^p)$. Second, a smaller L^p reduces the distance between $\operatorname{fix}(C_v^p)$ and r_D according to (8.6), which improves the approximation quality by ADA pair p even if $v << r_D$ (the extreme case is $v = 0$).

In total, a small L^p can be considered as an indicator for a fast rate of convergence in all cases, i.e., if $p = 1$ and $p \geq 2$. Therefore, one goal of the ADA optimization is to reduce the Lipschitz constants of all iteration functions A^p, $p \in [N]$.

Remark 8.28 *Analogously to Remark 8.13, it is sufficient to consider the Lipschitz constant of A^p over $[0, r_D]$. However, in order to have some margin, the Lipschitz constant of A^p over its whole domain $\hat{R}^p$ is considered in the following. If it turns out that this is too restrictive, it may make sense to consider the Lipschitz constant of A^p over $[0, r_D]$ only.*

(G1) Minimize the Lipschitz constant L^p of A^p for all $p \in [N]$.

Note that (G1) is not an objective function. Rather, this is an interim result that leads to an objective function in the course of this chapter. The corresponding objective function is defined in Section 8.6.2 below when the nominal optimization model is defined.
In order to reduce L^p, Vaillant uses a method called "start point increment". However, this method causes conflicting objectives, which is shown next.

8.4. Conflicting Objectives: Small L^p Versus a Small Start Point Increment of ADA Pair p

In the previous section, the optimization goal (G1) is identified, which is to minimize the Lipschitz constant L^p for all $p \in [N]$. In this section, we show that L^p can be reduced by making the start point of the considered ADA pair more fuel-lean, i.e., the ratio of fuel to air is decreased or equivalently the AFR is increased, i.e., λ at the start point is increased. Therefore, this method is called "start point increment". However, an increased start point also has some disadvantages. Accordingly, the decision makers are interested in a good trade-off between a fast rate of convergence (small L^p) and a small start point increment. In the following, the start point increment method and its influence on L^p are detailed. Thereafter, its disadvantages are delineated, which results in a further optimization goal. Because we are only interested in the case where (Sc1) to (Sc3) as well as the requirements (R1) to (R3) are satisfied, we assume that $r_D \geq 0$ and that the corresponding constraints (C-R1) to (C-R3) are satisfied for the remainder of this section.

8.4.1. Working Principle of the Start Point Increment

If $A^p_{r_D}$ is differentiable, then L^p is equal to the maximum of the absolute value of the derivative of $A^p_{r_D}$, i.e., $L^p = \max_{r \in \hat{R}^p_{r_D}} \left(\left| \frac{d A^p_{r_D}}{dr}(r) \right| \right)$ (Lemma 4.44). Therefore, we can reduce L^p by reducing the maximum of the derivative of $A^p_{r_D}$ (recall that $A^p_{r_D}$ is strictly increasing and thus its derivative is always greater than zero).
The derivative of $A^p_{r_D}$ is determined in Section 6.3.3. Let ι_{s^p} and ι_{t^p} be differentiable. Then $A^p_{r_D}$ is also differentiable and for all $\bar{r} \in \hat{R}^p_{r_D}$ we have

$$\frac{d}{dr} A^p_{r_D}(\bar{r}) = \frac{\frac{d}{dg} \iota_{t^p}\big(g(\bar{r})\big)}{\frac{d}{dg} \iota_{s^p}\big(g(\bar{r})\big)} \cdot \frac{\iota^2_{s^p}\big(g(\bar{r})\big)}{\iota^2_{t^p}\big(g(\bar{r})\big)}, \tag{8.7}$$

where

$$g(\bar{r}) = \rho^{-1}_{s^p}(\bar{r} + r^p_s - r_D) = \iota^{-1}_{s^p}\Big(\frac{U}{\bar{r} + r^p_s - r_D}\Big) = \iota^{-1}_{s^p}\Big(\frac{i^p_s U}{i^p_s(\bar{r} - r_D) + U}\Big) \tag{8.8}$$

according to Theorem 6.42 and Lemma 6.17. The basic idea to reduce L^p is to reduce $\iota_{s^p}\big(g(\bar{r})\big)$ while keeping the other values in (8.7) (approximately) constant.

To illustrate how $\iota_{s^p}\big(g(\bar{r})\big)$ can be reduced, let us suppose that we want to parameterize ADA pair p and that we have already selected a test point, i.e., t^p and i_t^p are already selected. Let g_0 denote the corresponding gas valve position, i.e., $g_0 := \iota_{t^p}^{-1}(i_t^p)$. Because we assume that the constraint (C-R1) is satisfied, we have

$$\iota_{s^p}^{-1}(i_s^p) = \iota_{t^p}^{-1}(i_t^p) \;\Rightarrow\; \iota_{s^p}^{-1}(i_s^p) = g_0 \;\Rightarrow\; i_s^p = \iota_{s^p}(g_0),$$

i.e., the start point has the same gas valve position as the test point. Therefore, we must select the start fan speed s^p and the start ioni current i_s^p such that $\iota_{s^p}(g_0) = i_s^p$ holds. Such a situation is depicted in Figure 8.1, which is based on real HE measurement data. The left part of Figure 8.1 shows the ioni current as a function of the fan speed with the gas valve position fixed at g_0. The blue dot marks the already selected test point. Note that $\iota_{t^p}(g_0) = i_t^p$. The start point must be selected such that it is an element of this curve, because it must have the same gas valve position as the test point. It is apparent that the ioni current decreases with increasing fan speed. Therefore, the larger the selected start fan speed s^p is, the smaller is the corresponding start ioni current i_s^p. Let us suppose that we have three candidates for the start point of ADA pair p, denoted by a, b and c. Let their fan speeds be $s^{p,a}$, $s^{p,b}$ and $s^{p,c}$, respectively, such that $t^p < s^{p,a} < s^{p,b} < s^{p,c}$. They are depicted in Figure 8.1 by the turquoise, the yellow and the orange dot, respectively. Since our goal is to obtain a small start ioni current, we would select a large start fan speed, i.e., we would select candidate c with the fan speed $s^{p,c}$ and the ioni current $i_s^{p,c}$ (and the gas valve position g_0).

However, a small start ioni current comes at the prize of a large start equivalence AFR. The right part of Figure 8.1 shows the equivalence AFR as a function of the fan speed with the gas valve position fixed at g_0. Again, the blue dot marks the already selected test point. It is apparent that the equivalence AFR is strictly increasing with the fan speed. This is consistent with the physics of combustion, because an increased fan speed results in an increased air volume flow while the fixed gas valve position results in an (approximately) constant gas volume flow and thus the AFR increases. Because the AFR increases when a smaller (but usually better) start ioni current is selected, this method is called "start point increment" [PHE, Item 3280].

Remark 8.29 *The given explanation of the working principle of the start point increment so far is rudimentary. For instance, we are not only interested in the one value of the ioni current at the start fan speed s^p and at the gas valve position g_0. Rather, we are interested in the ioni currents for all gas valve positions $g(r) = \iota_{s^p}^{-1}\Big(\frac{i_s^p U}{i_s^p (r - r_D) + U}\Big)$ for $r \in [0, r_D]$ according to* (8.8) *and Corollary 8.11. This is demonstrated in more detail in Example 8.36.*

The start point increment is essential for the ADA optimization problem. Therefore, a corresponding definition is provided in the following.

8.4.2. Definition of the Start Point Increment

For the definition of the start point increment, we need a baseline, i.e., a condition that corresponds to a start point increment of zero. For this, we make use of the control curve,

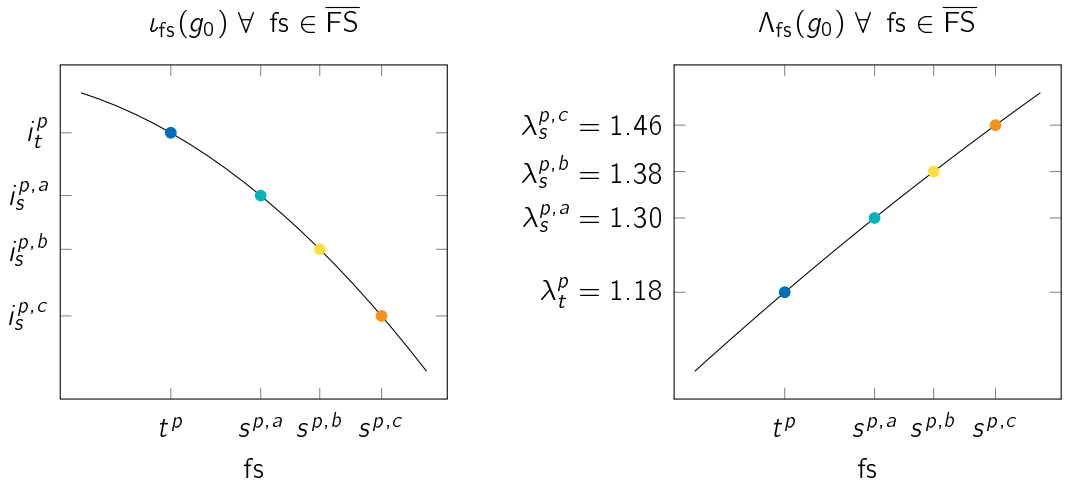

Figure 8.1.: The ioni current and the equivalence AFR are shown as a function of the fan speed with the gas valve position fixed at g_0 in the left and in the right part, respectively. The set $\overline{\mathrm{FS}}$ denotes the considered fan speeds. The blue dot marks an already selected test point with the fan speed t^p, the gas valve position g_0, the ioni current i_t^p and the equivalence AFR λ_t^p. Three start point candidates a, b and c, marked by the turquoise, the yellow and the orange dot, respectively, are also shown. With increasing start fan speed $s^{p,k}$, $k \in \{a, b, c\}$, the corresponding ioni current $i_s^{p,k}$ decreases and the corresponding equivalence AFR $\lambda_s^{p,k}$ increases.

which is introduced in Section 2.3.3. Recall that the control curve is a function that maps every feasible fan speed $\mathrm{fs} \in [\mathrm{fs}_{\min}, \mathrm{fs}_{\max}]$ to an ioni current setpoint $i_{\mathrm{set}}(\mathrm{fs})$ and that the control curve is used to control the combustion process during normal boiler operation. An exemplary control curve is depicted in the right part of Figure 2.7. Because it is essential for the start point increment, we provide a formal definition of the control curve with respect to the HE model.

Definition 8.30 *Let* $\mathcal{H} = \left(\mathrm{FS}, (G_{\mathrm{fs}})_{\mathrm{fs}\in\mathrm{FS}}, (\iota_{\mathrm{fs}})_{\mathrm{fs}\in\mathrm{FS}}, (\Lambda_{\mathrm{fs}})_{\mathrm{fs}\in\mathrm{FS}}, (\zeta_{\mathrm{fs}})_{\mathrm{fs}\in\mathrm{FS}}\right)$ *be an HE model. A* control curve with respect to $\mathcal{H}$ *is a function* i_{set} *that maps every feasible fan speed to a feasible ioni current setpoint, i.e.,* $i_{\mathrm{set}} : \mathrm{FS} \to \mathbb{R}_{>0}$ *such that* $i_{\mathrm{set}}(\mathrm{fs}) \in I_{\mathrm{fs}}$ *for all* $\mathrm{fs} \in \mathrm{FS}$. *The corresponding* operating point equivalence AFR *is defined by*

$$\lambda_{\mathrm{op}}(\mathrm{fs}) := \Lambda_{\mathrm{fs}} \circ \iota_{\mathrm{fs}}^{-1} \circ i_{\mathrm{set}}(\mathrm{fs})\ \forall\ \mathrm{fs} \in \mathrm{FS}\,.$$

Lemma 8.31 *The operating point equivalence AFR is well-defined for all* $\mathrm{fs} \in \mathrm{FS}$.

Proof. Let $\mathrm{fs} \in \mathrm{FS}$. According to Definitions 2.18 and 2.22, we have $\iota_{\mathrm{fs}}^{-1} : I_{\mathrm{fs}} \to G_{\mathrm{fs}}$ and $\Lambda_{\mathrm{fs}} : G_{\mathrm{fs}} \to L_{\mathrm{fs}}$. Because $i_{\mathrm{set}}(\mathrm{fs}) \in I_{\mathrm{fs}}$ (Definition 8.30), $\lambda_{\mathrm{op}}(\mathrm{fs}) := \Lambda_{\mathrm{fs}} \circ \iota_{\mathrm{fs}}^{-1} \circ i_{\mathrm{set}}(\mathrm{fs})$ is well-defined. □

Remark 8.32 *The operating point equivalence AFR corresponds to the equivalence AFR during normal HE operation. For instance, let us suppose that we have a heat demand that*

corresponds to a certain fan speed $\mathrm{fs} \in \mathrm{FS}$. *Then, IoniDetect sets the fan speed to* fs *and moves the gas valve such that the resulting ioni current equals* $i_{\mathrm{set}}(\mathrm{fs})$. *This in turn results in the equivalence AFR* $\lambda_{\mathrm{op}}(\mathrm{fs})$. *Ideally,* $\lambda_{\mathrm{op}}(\mathrm{fs})$ *equals the desired target equivalence AFR at the fan speed* fs, *see also Section 2.3.3 and Remark 2.12.*

Usually, the start point's ioni current is placed on the control curve, because in this case an ADA iteration can be started out of normal boiler operation with (almost) no delay [PHE, Item 3280]. Thus, a good baseline for the start point's ioni current is the value of the control curve that corresponds to the start fan speed s^p, i.e., $i_s^p = i_{\mathrm{set}}(s^p)$. However, regarding combustion physics, the start point's equivalence AFR and not its ioni current is the relevant physical quantity, see also Sections 2.2 and 2.3. Therefore, the operating point equivalence AFR at the start fan speed is the relevant size and thus $\lambda_{\mathrm{op}}(s^p)$ serves as the baseline for the start point increment.
For the following definition, keep in mind that the gvp of the start point is $g_s^p = \iota_{s^p}^{-1}(i_s^p)$ and thus the equivalence AFR at the start point is $\lambda_s^p = \Lambda_{s^p}(g_s^p) = \Lambda_{s^p} \circ \iota_{s^p}^{-1}(i_s^p)$. Furthermore, we assume that (C-R1) is satisfied and thus $\iota_{s^p}^{-1}(s^p) = \iota_{t^p}^{-1}(t^p)$ holds. In this case, the equivalence AFR at the start point is $\lambda_s^p = \Lambda_{s^p} \circ \iota_{t^p}^{-1}(t^p)$.

Definition 8.33 *Let* $\mathcal{H} = \big(\mathrm{FS}, (G_{\mathrm{fs}})_{\mathrm{fs}\in\mathrm{FS}}, (\iota_{\mathrm{fs}})_{\mathrm{fs}\in\mathrm{FS}}, (\Lambda_{\mathrm{fs}})_{\mathrm{fs}\in\mathrm{FS}}, (\zeta_{\mathrm{fs}})_{\mathrm{fs}\in\mathrm{FS}}\big)$ *be an HE model and let* i_{set} *be a corresponding control curve. Let* $p \in [N]$ *and let* (s^p, t^p, i_s^p, i_t^p) *be the ADA parameters of ADA pair p such that* $\iota_{s^p}^{-1}(s^p) = \iota_{t^p}^{-1}(t^p)$.
The start point increment *of ADA pair p is defined by*

$$\lambda_{s,\mathrm{incr}}^p(s^p, t^p, i_s^p, i_t^p) := \lambda_s^p - \lambda_{\mathrm{op}}(s^p) = \Lambda_{s^p} \circ \iota_{t^p}^{-1}(i_t^p) - \Lambda_{s^p} \circ \iota_{s^p}^{-1} \circ i_{\mathrm{set}}(s^p).$$

Remark 8.34 *Note that the start point increment is only defined for ADA parameters* (s^p, t^p, i_s^p, i_t^p) *such that* $\iota_{s^p}^{-1}(s^p) = \iota_{t^p}^{-1}(t^p)$ *holds.*

Lemma 8.35 *The start point increment is well-defined. Furthermore,*

$$i_s^p = i_{\mathrm{set}}(s^p) \;\Leftrightarrow\; \lambda_{s,\mathrm{incr}}^p(s^p, t^p, i_s^p, i_t^p) = 0.$$

Proof. By assumption, we have $\iota_{s^p}^{-1}(i_s^p) = \iota_{t^p}^{-1}(i_t^p) =: g_0$ and thus $g_0 \in G_{s^p} \cap G_{t^p}$. Because G_{s^p} is the domain of Λ_{s^p} (Definition 2.18), $\Lambda_{s^p}\big(\iota_{t^p}^{-1}(i_t^p)\big)$ is well-defined. Since $\Lambda_{s^p} \circ \iota_{s^p}^{-1} \circ i_{\mathrm{set}}(s^p)$ is well-defined as well (Lemma 8.31), $\lambda_{s,\mathrm{incr}}^p(s^p, t^p, i_s^p, i_t^p)$ is also well-defined. Furthermore, by considering that $\iota_{s^p}^{-1}(i_s^p) = \iota_{t^p}^{-1}(i_t^p)$, we have

$$\begin{aligned} i_s^p = i_{\mathrm{set}}(s^p) \;&\Leftrightarrow \Lambda_{s^p} \circ \iota_{t^p}^{-1}(i_t^p) = \Lambda_{s^p} \circ \iota_{s^p}^{-1}(i_s^p) = \Lambda_{s^p} \circ \iota_{s^p}^{-1} \circ i_{\mathrm{set}}(s^p) \\ &\Leftrightarrow\; \lambda_{s,\mathrm{incr}}^p(s^p, t^p, i_s^p, i_t^p) = \Lambda_{s^p} \circ \iota_{t^p}^{-1}(i_t^p) - \Lambda_{s^p} \circ \iota_{s^p}^{-1} \circ i_{\mathrm{set}}(s^p) = 0. \end{aligned}$$

□

The following example demonstrates the start point increment.

Example 8.36 *To demonstrate the start point increment, we consider the situation depicted in Figure 8.1. I.e., we have a test point defined by t^p and i_t^p as well as the three start point candidates a, b and c. Their fan speeds are $s^{p,a}$, $s^{p,b}$ and $s^{p,c}$, respectively. Since we assume that* (C-R1) *is satisfied, i.e., $\iota_{s^p}^{-1}(s^p) = \iota_{t^p}^{-1}(t^p)$, the gvp of the start point is already defined by the test point. The corresponding gvp is $g_0 = \iota_{t^p}^{-1}(i_t^p)$. This gives us the start point candidates' equivalence AFRs, which are $\lambda_s^{p,a} := \Lambda_{s^{p,a}}(g_0) = 1.3$, $\lambda_s^{p,b} := \Lambda_{s^{p,b}}(g_0) = 1.38$ and $\lambda_s^{p,c} := \Lambda_{s^{p,c}}(g_0) = 1.46$ according to the right part of Figure 8.1.*
In order to determine the start point increment of a, b and c, we also need the corresponding control curve equivalence AFRs according to Definition 8.33. For simplicity, let us suppose that $\lambda_{\mathrm{op}}(s^{p,a}) = \lambda_{\mathrm{op}}(s^{p,b}) = \lambda_{\mathrm{op}}(s^{p,c}) = 1.3$, i.e., the three start point candidates have an identical operating point equivalence AFR of 1.3, which is a common value. With this, we obtain $\lambda_{s,\mathrm{incr}}^{p,a} = \lambda_s^{p,a} - \lambda_{\mathrm{op}}(s^{p,a}) = 1.3 - 1.3 = 0$ and analogously $\lambda_{s,\mathrm{incr}}^{p,b} = 1.38 - 1.3 = 0.08$ as well as $\lambda_{s,\mathrm{incr}}^{p,c} = 1.46 - 1.3 = 0.16$. In particular, we have $\lambda_{s,\mathrm{incr}}^{p,a} < \lambda_{s,\mathrm{incr}}^{p,b} < \lambda_{s,\mathrm{incr}}^{p,c}$.
However, regarding the start ioni currents of a, b and c, we have $i_s^{p,a} > i_s^{p,b} > i_s^{p,c}$ according to the left part of Figure 8.1. Therefore, a smaller start ioni current comes at the price of a larger start point increment in this example.

Remark 8.37 *As in Example 8.36, the start ioni current and the start point increment are usually inversely proportional. But most likely, this does not hold in general. However, this is not required for the optimization model. Rather, optimized ADA parameters should have a small start ioni current and a small start point increment, which is explained in Section 8.4.3 below.*

Recall that we are interested in small start ioni currents in order to reduce L^p. This is demonstrated in the following example.

Example 8.38 *This example is based on the same HE measurement data as Figure 8.1 and Example 8.36. To be precise, this example continues Example 8.36, in which the start point increments of the three start point candidates a, b and c are determined.*
In this example, we consider the corresponding ADA iteration functions $A_{r_D}^{p,a}$, $A_{r_D}^{p,b}$ and $A_{r_D}^{p,c}$, respectively. We are particularly interested in their Lipschitz constants. For this, we use the drift resistance $r_D = 140k\Omega$, which is a typical value used by Vaillant as already mentioned before in (Sc1).
As with previous examples, most details of the measurement data are omitted for reasons of confidentiality. Therefore, the iteration functions are presented without specifying any parameters or HE model functions in the following. However, the considered HE model, the test point's ADA parameters (t^p, i_t^p) as well as the start point candidates' ADA parameters $(s^{p,a}, i_s^{p,a})$, $(s^{p,b}, i_s^{p,b})$ and $(s^{p,c}, i_s^{p,c})$ are identical to those in Figure 8.1 and in Example 8.36.
This gives us three candidates for ADA pair p, which are $(s^{p,k}, t^p, i_s^{p,k}, i_t^p)$, $k \in \{a, b, c\}$.

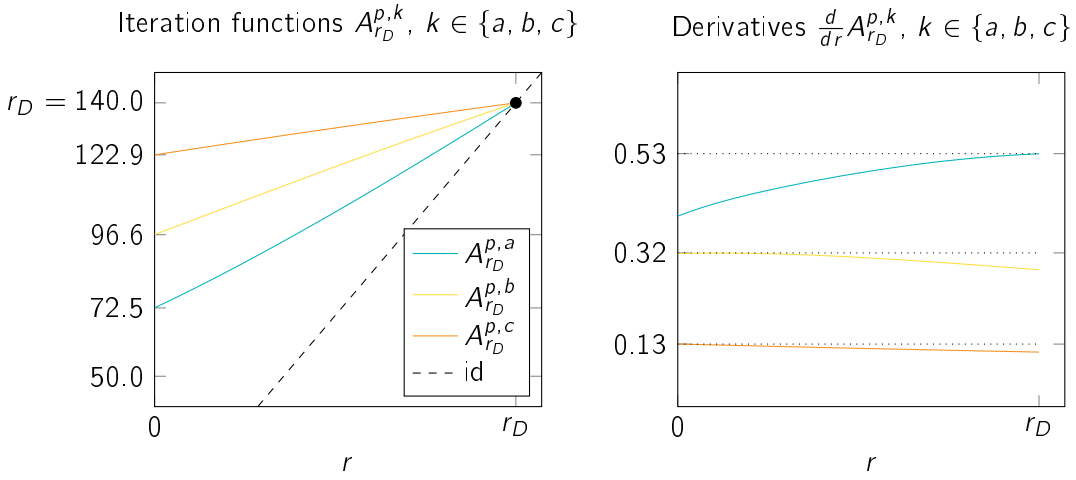

Figure 8.2.: In the left part, three ADA iteration functions restricted to the interval $[0, r_D]$ are shown. They correspond to the ADA pairs that are presented in Example 8.36 and in Figure 8.1, i.e., they correspond to the three start point candidates a, b and c together with the same test point (t^p, i^p_t). The fixed point of all three functions is r_D, which is marked by the black dot. The iteration function $A^{p,c}_{r_D}$ has the fastest rate of convergence and the iteration function $A^{p,a}_{r_D}$ has the slowest rate of convergence, because $A^{p,c}_{r_D}(r) > A^{p,b}_{r_D}(r) > A^{p,c}_{r_D}(r)$ for all $r \in [0, r_D)$.
In the right part, the corresponding derivatives are shown. The maximum of each derivative, which corresponds to the Lipschitz constant of the considered iteration function in the considered interval, is marked by a dotted line. The iteration function with the fastest rate of convergence has the smallest Lipschitz constant (over $[0, r_D]$) and vice versa.

The corresponding (resistance based) ADA iteration functions are

$$A^{p,k}_{r_D} = \sigma^-_{r^p_t} \circ \rho_{t^p, r_D} \circ \rho^{-1}_{s^{p,k}, r_D} \circ \sigma^+_{r^{p,k}_s}, \quad k \in \{a, b, c\},$$

according to Definition 6.21. Since we consider the specific case where we assume that (R1) *to* (R3) *hold, we can restrict their domains without loss of generality to the interval* $[0, r_D]$ *according to Corollary 8.11 and as delineated at the beginning of Section 8.3.*

The three iteration functions are shown in the left part of Figure 8.2, where the turquoise curve corresponds to $A^{p,a}_{r_D}$*, the yellow curve to* $A^{p,b}_{r_D}$ *and the orange curve to* $A^{p,c}_{r_D}$*. In addition, the identity function is shown by the dashed line. Because* $\mathrm{fix}(A^{p,k}_{r_D}) = r_D$ *for* $k \in \{a, b, c\}$*, all three iteration functions intersect the identity at* r_D*. Furthermore, it is apparent that the three iteration functions are strictly increasing and that the identity has a steeper slope, i.e., the derivatives of all three iteration functions are positive and smaller than one for all* $r \in [0, r_D]$*.*

This can be verified with the right part of Figure 8.2, which shows the corresponding derivatives $\frac{d}{dr}A^{p,k}_{r_D}$ *over* $[0, r_D]$*,* $k \in \{a, b, c\}$*. The black dotted lines are used to visualize the maxima of the derivatives. These maxima correspond to the Lipschitz constants* $L^{p,k}$ *over* $[0, r_D]$*,* $k \in \{a, b, c\}$*. We have* $L^{p,a} \approx 0.53$*,* $L^{p,b} \approx 0.32$ *and* $L^{p,c} \approx 0.13$*. That*

the derivatives' maxima are at the boundary of the interval $[0, r_D]$ *results from the fact that we consider* $A_{r_D}^{p,k}$ *over* $[0, r_D]$ *only and not over the whole domain* $\hat{R}_{r_D}^{p,k}$, $k \in \{a, b, c\}$. *Nevertheless, it is thinkable that a function* $A_{r_D}^{p}$ *exists whose derivative's maximum is in the interior of* $[0, r_D]$.
To summarize this example, the ADA pair with the start point candidate c has the smallest Lipschitz constant, i.e., we would prefer candidate c according to (G1). *However, this comes at the price of the largest start point increment, which is* $\lambda_{s,\text{incr}}^{p,c} = 0.16$, *whereas* $\lambda_{s,\text{incr}}^{p,b} = 0.08$ *and* $\lambda_{s,\text{incr}}^{p,a} = 0$ *according to Example 8.36.*

As demonstrated in Example 8.38, the Lipschitz constant L^p can be reduced (and thus the rate of convergence can be increased) by increasing the start point. However, an increased start point also has disadvantages.

8.4.3. Disadvantages of the Start Point Increment Lead to Conflicting Objectives

Increasing the start point has two main disadvantages. As explained in Section 2.2, beyond $\lambda \approx 1.4$ the emission of carbon monoxide (CO) increases with increasing equivalence AFR. Therefore, an increased equivalence AFR of the start point results in larger CO emissions during the execution of an ADA iteration. These emissions are permissible as long as certain limit values are not exceeded. However, it is generally desirable for an appliance to emit as few pollutants as possible. In addition, getting closer to a CO limit means less robustness in the case of tolerances, i.e., the margin to the lean CO limit is reduced.
Furthermore, an increased start point means that an ADA iteration with the corresponding ADA pair requires a larger time span. Recall that in practice an ADA iteration is started from normal heating operation. If the start point of ADA pair p is selected such that it is close to the normal operating point at the start fan speed s^p, i.e., the start point is on or close to the control curve, then the ADA procedure can be (almost) immediately started. However, if a start point increment is used, the appliance must leave the range of normal operation and drive to the more fuel-lean start point at the beginning of an ADA iteration, which takes some time. This additional required time reduces the chance that an ADA iteration can be successfully completed. For instance, this is the case if the heat demand reduces while an ADA iteration is executed, see also Section 3.4. Therefore, a short duration of the ADA iteration is desired, which is contrary to a large start point increment. Thus, a second optimization goal is introduced for each ADA pair p, $p \in [N]$:

(G2) Minimize the start point increment $\lambda_{s,\text{incr}}^{p}$ for all $p \in [N]$.

Just like (G1), (G2) is also not an objective function. Rather, (G2) is an interim result that leads to an objective function in the course of this chapter. The corresponding objective function is defined in Definition 8.59 in Section 8.6.2.
With this, we have the conflicting optimization goals minimize L^p and minimize $\lambda_{s,\text{incr}}^{p}$ for all $p \in [N]$ and the resulting optimization models are multiobjective.

Remark 8.39 *Even if the start point increment usually reduces the Lipschitz constant of the corresponding iteration function, this characteristic is not guaranteed by the properties of the HE model. However, since we optimize both goals, this is not a problem. In the extreme case that L^p and $\lambda^p_{s,\text{incr}}$ can be minimized simultaneously, there is a single nondominated point, which is the ideal point (if the problem is feasible).*

As demonstrated in Example 8.36, the start point increment can significantly reduce L^p and thus improve the rate of convergence of the ADA algorithm with respect to the p-th ADA pair. Of course, there are limits to the start point increment.
On the one hand, the equivalence AFR at the start point is limited by the CO emissions as already mentioned at the beginning of this subsection. Since CO is lethal, there exist strict limits for the emission of CO, which is covered by specification (S1). On the other hand, because ADA pairs must not be overlapping, the start fan speed of ADA pair p is limited by the test fan speed of its upper neighbor $p-1$ for $p \in \{2,\dots,N\}$, i.e., $s^p < t^{p-1}$, see also Lemma 3.44. In the case $p = 1$, the start fan speed is limited by the HE's maximum fan speed fs_{max}, see also Definition 5.2. These limitations are covered by the specification (S7).
All specifications (S1) to (S7) are discussed in detail in the following section, where corresponding constraints are derived.

8.5. Constraints

So far, we have considered the objective criterion (O) in detail. In this section, the specifications (S1) to (S7) are covered and converted to corresponding constraints.
The specifications (S1) to (S3) are closely related, because they all depend on the same gas valve position. Due to monotonicity properties with respect to the gas valve position, it is sufficient to check that the bounds according to (S1) to (S3) are satisfied only for certain situations, which makes solving the optimization problem more efficient. This is delineated in the following. Thereafter, corresponding constraints are derived.

8.5.1. Monotonicity with Respect to the Gas Valve Position

We are interested in the λ and CO values during the ADA iterations. Recall from Definition 2.18 that the λ values are represented by the function $\Lambda_{\text{fs}}(g)$ and the CO values are represented by the function $\zeta_{\text{fs}}(g)$, where $\text{fs} \in \text{FS}$ and $g \in G_{\text{fs}}$. In an ADA iteration with ADA pair p, $p \in [N]$, the start and the test fan speed, s^p and t^p, respectively, are the relevant fan speeds. The relevant gvp during an ADA iteration is determined in step (A3) presented in Section 5.1. According to Lines 9 and 11 of Algorithm 5.2, this gvp is

$$g_A = \iota^{-1}_{s^p,r_D} \circ \gamma^p \circ \begin{cases} \beta^1(i_1), & \text{if } p = 1 \\ \omega^p\big(\beta^p(i_p), \beta^{p-1}(i_{p-1})\big), & \text{if } p \in \{2,\dots,N\}, \end{cases} \tag{8.9}$$

where $\hat{\boldsymbol{i}}_{t,r_D} = (i_1, \ldots, i_N)$ is the incumbent vector of drifted test ioni current approximations. By plugging $g = g_A$ into the HE model's equivalence AFR function and CO function with respect to the start fan speed s^p, i.e., by calculating $\Lambda_{s^p}(g_A)$ and $\zeta_{s^p}(g_A)$, we obtain the λ value and the CO value, respectively, of the start point during the ADA iteration with ADA pair p. Analogously, $\Lambda_{t^p}(g_A)$ is the λ value and $\zeta_{t^p}(g_A)$ is the CO value of the test point during this ADA iteration.
Because the gvp g_A is essential for the following considerations, we provide a definition of the gas valve position that is used in the n-th ADA iteration based on (8.9). This definition requires the resistance based ADA iterates according to Definition 7.28. Just as in the previous sections, we implicitly assume that an HE model $\mathcal{H}$, a drift resistance $r_D \geq 0$ and N ADA pairs (s^p, t^p, i_s^p, i_t^p), $p \in [N]$, are given for the remainder of this section.

Definition 8.40 *Let $\hat{\boldsymbol{i}}_{\boldsymbol{t},\text{in}} = (i_1^{\text{in}}, \ldots, i_N^{\text{in}})$ be an input vector and let $u = (u_n)_{n\in\mathbb{N}}$ be an infinite ADA update sequence such that $\hat{\boldsymbol{i}}_{\boldsymbol{t},\text{in}}$ and u are a feasible input combination. For $n \in \mathbb{N}$ let $\boldsymbol{r}^n(\hat{\boldsymbol{i}}_{\boldsymbol{t},\text{in}}, u) = (r_1^n, \ldots, r_N^n)$ be the corresponding n-th resistance based ADA iterate. The corresponding* n-th gas valve position iterate *is defined by*

$$g^n(\hat{\boldsymbol{i}}_{\boldsymbol{t},\text{in}}, u) := \begin{cases} \rho_{s^1}^{-1}(r_1^{n-1} + r_s^1 - r_D), & \text{if } u_n = 1 \\ \rho_{s^p}^{-1}\big(\omega^p_{r_{p-1}^{n-1}}(r_p^{n-1}) + r_s^p - r_D\big) & \text{if } p := u_n \in \{2, \ldots, N\}, \end{cases}$$

where $r_p^0 := \beta^p(i_p^{\text{in}})$ for all $p \in [N]$, see also Lemma 7.45.

Lemma 8.41 *The gas valve position iterate $g^n(\hat{\boldsymbol{i}}_{\boldsymbol{t},\text{in}}, u)$ corresponds to the gas valve position during the n-th iteration with Algorithm 5.2 given the inputs $\hat{\boldsymbol{i}}_{\boldsymbol{t},\text{in}}$ and u. In particular, $g^n(\hat{\boldsymbol{i}}_{\boldsymbol{t},\text{in}}, u)$ is well-defined.*

Proof. Because $\hat{\boldsymbol{i}}_{\boldsymbol{t},\text{in}} = (i_1^{\text{in}}, \ldots, i_N^{\text{in}})$ and u are a feasible input combination, all corresponding ADA iterates (ioni current based and resistance based) and the corresponding function evaluations are well-defined.
Let $n \in \mathbb{N}$ and let $\boldsymbol{i}^n(\hat{\boldsymbol{i}}_{\boldsymbol{t},\text{in}}, u) = (i_1^n, \ldots, i_N^n)$ be the corresponding n-th ioni current based ADA iterate. According to Corollary 7.23, $\boldsymbol{i}^n(\hat{\boldsymbol{i}}_{\boldsymbol{t},\text{in}}, u)$ corresponds to the incumbent drifted test ioni current vector after the n-th iteration with the for-loop of Algorithm 7.1 given the inputs $\hat{\boldsymbol{i}}_{\boldsymbol{t},\text{in}}$ and u. Therefore, the gas valve position during the n-th ADA iteration with ADA pair p is

$$g_A = \iota^{-1}_{s^p,r_D} \circ \gamma^p \circ \begin{cases} \beta^1(i_1^{n-1}), & \text{if } p = 1 \\ \omega^p\big(\beta^p(i_p^{n-1}), \beta^{p-1}(i_{p-1}^{n-1})\big), & \text{if } p \in \{2, \ldots, N\}, \end{cases}$$

according to (8.9), where $i_p^0 := i_p^{\text{in}}$ for all $p \in [N]$. By considering that

- $r_p^n = \beta^p(i_p^n)$ for all $p \in [N]$ (Definition 7.28),
- $\omega^p\big(\beta^p(i_p^n), \beta^{p-1}(i_{p-1^n})\big) = \omega^p_{r_{p-1}^n}(r_p^n)$ for $p \in \{2, \ldots, N\}$ (Definition 7.1) and

- $\iota^{-1}_{s^p,r_D} \circ \gamma^p(r) = \rho^{-1}_{s^p,r_D} \circ \sigma^+_{r_s^p}(r) = \rho^{-1}_{s^p}(r + r_s^p - r_D)$ for all $r \in \hat{R}^p_{r_D}$ (Lemmas 6.23 and 6.20),

we obtain for the gas valve position in the n-th ADA iteration with ADA pair p

$$g_A = \begin{cases} \rho^{-1}_{s^1}(r_1^{n-1} + r_s^1 - r_D), & \text{if } p = 1 \\ \rho^{-1}_{s^p}\big(\omega^p_{r_{p-1}^{n-1}}(r_p^{n-1}) + r_s^p - r_D\big) & \text{if } p \in \{2, \dots, N\}. \end{cases}$$

□

Since we consider only the input vector $\hat{\boldsymbol{i}}_{\boldsymbol{t},\text{in}} = (i_t^1, \dots, i_t^N)$ and situations where the requirements (R1) to (R3) are met, we have $r_p^n \in [0, r_D]$ for all $p \in [N]$ and for all $n \in \mathbb{N}_0$ according to Corollary 8.11. Under these circumstances, we can state a lower and an upper bound for the gas valve position iterates. For the following definition, recall that ρ^{-1}_{fs} is strictly decreasing for all fs $\in$ FS (Lemma 6.17).

Definition 8.42 *Let $r_D \geq 0$ and let $0 \in \hat{R}^p_{r_D}$ as well as $r_D \in \hat{R}^p_{r_D}$. For all $p \in [N]$, we define*

$$g^p_{\min} := \rho^{-1}_{s^p}(r_s^p) \quad \text{and} \quad g^p_{\max} := \rho^{-1}_{s^p}(r_s^p - r_D).$$

Lemma 8.43 *Let $r_D \geq 0$. Let $A^p_{r_D}$ be contractive, let $\text{fix}(A^p_{r_D}) = r_D$ and let $0 \in \hat{R}^p_{r_D}$ for all $p \in [N]$. Furthermore, let $\hat{\boldsymbol{i}}_{\boldsymbol{t},\text{in}} := (i_t^1, \dots, i_t^N)$ and let u be an arbitrary (infinite) ADA update sequence. Then,*

$$u_n = p \;\Rightarrow\; g^p_{\min} \leq g^n(\hat{\boldsymbol{i}}_{\boldsymbol{t},\text{in}}, u) \leq g^p_{\max} \;\forall\, n \in \mathbb{N}.$$

In particular, $g^p_{\min}$ and $g^p_{\max}$ are well-defined.

Proof. Let $p \in [N]$. By assumption, we have $0 \in \hat{R}^p_{r_D}$ as well as $r_D \in \hat{R}^p_{r_D}$ and thus $[0, r_D] \subset \hat{R}^p_{r_D}$, i.e., $A^p_{r_D}(r) = \sigma^-_{r_t^p} \circ \rho_{t^p,r_D} \circ \rho^{-1}_{s^p,r_D} \circ \sigma^+_{r_s^p}(r)$ is well-defined for all $r \in [0, r_D]$. Therefore, $\rho^{-1}_{s^p,r_D} \circ \sigma^+_{r_s^p}(r) = \rho^{-1}_{s^p}(r + r_s^p - r_D)$ is well-defined for all $r \in [0, r_D]$ and thus $g^p_{\min} := \rho^{-1}_{s^p}(r_s^p)$ as well as $g^p_{\max} := \rho^{-1}_{s^p}(r_s^p - r_D)$ are well-defined.
For the following, recall that $r_p^n \in [0, r_D]$ for all $n \in \mathbb{N}$ (Corollary 8.11) and that $\rho^{-1}_{s^p}$ is strictly decreasing for all $p \in [N]$ (Lemma 6.17). Furthermore, $r_p^0 = \beta^p(i_t^p) = \frac{U}{i_t^p} - \frac{U}{i_t^p} = 0$ for all $p \in [N]$. Let $n \in \mathbb{N}$. First, let $p = 1$. Then,

$$\begin{aligned} 0 \leq r_1^{n-1} \leq r_D \;&\Rightarrow\; 0 + r_s^1 - r_D \leq r_1^{n-1} + r_s^1 - r_D \leq r_D + r_s^1 - r_D = r_s^1 \\ &\Rightarrow\; \rho^{-1}_{s^1}(r_s^1 - r_D) \geq \rho^{-1}_{s^1}(r_1^{n-1} + r_s^1 - r_D) \geq \rho^{-1}_{s^1}(r_s^1) \\ &\Rightarrow\; g^1_{\max} \geq g^n(\hat{\boldsymbol{i}}_{\boldsymbol{t},\text{in}}, u) \geq g^1_{\min}. \end{aligned}$$

Next, let $p \in \{2, \dots, N\}$. Because $0 < w^p < 1$ (Lemma 5.13), we have

$$
\begin{aligned}
& 0 \leq r_p^{n-1} \leq r_D \text{ and } 0 \leq r_{p-1}^{n-1} \leq r_D \\
\Rightarrow\ & 0 \leq w^p r_p^{n-1} \leq w^p r_D \text{ and } 0 \leq (1-w^p) r_{p-1}^{n-1} \leq (1-w^p) r_D \\
\Rightarrow\ & 0 \leq w^p r_p^{n-1} + (1-w^p) r_{p-1}^{n-1} \leq w^p r_D + (1-w^p) r_D = r_D \\
\Rightarrow\ & 0 \leq \omega^p_{r_{p-1}^{n-1}}(r_p^{n-1}) \leq r_D \\
\Rightarrow\ & 0 + r_s^p - r_D \leq \omega^p_{r_{p-1}^{n-1}}(r_p^{n-1}) + r_s^p - r_D \leq r_D + r_s^p - r_D = r_s^p \\
\Rightarrow\ & \rho_{s^p}^{-1}(r_s^p - r_D) \geq \rho_{s^p}^{-1}\big(\omega^p_{r_{p-1}^{n-1}}(r_p^{n-1}) + r_s^p - r_D\big) \geq \rho_{s^p}^{-1}(r_s^p) \\
\Rightarrow\ & g^p_{\min} \geq g^n(\hat{\boldsymbol{i}}_{\boldsymbol{t},\text{in}}, u) \geq g^p_{\min}.
\end{aligned}
$$

□

With the bounds for the gas valve position according to Lemma 8.43, we can formulate constraints corresponding to the specifications (S1) to (S3) in the following.

8.5.2. Combustion Related Constraints

In this subsection, we derive constraints corresponding to the specifications (S1) to (S3). The remaining specifications (S4) to (S7) are dealt with in the following Subsection 8.5.3.

Specification (S1): The CO emissions during all ADA iterations must never exceed $\text{co}_{\max}$. As delineated at the beginning of the preceding Subsection 8.5.1, the CO emissions at the start and at the test point during an ADA iteration result from the gas valve position that is defined in Definition 8.40. Because the CO emission is represented by $\zeta_{\text{fs}}(g)$ (Definition 2.18) the CO emissions during an ADA iteration are as follows.

Definition 8.44 *Let $\hat{\boldsymbol{i}}_{\boldsymbol{t},\text{in}}$ and $(u_n)_{n\in\mathbb{N}}$ be a feasible input combination. For $n \in \mathbb{N}$, the corresponding n-th* start and test CO iterate *are defined by*

$$
\text{co}_s^n(\hat{\boldsymbol{i}}_{\boldsymbol{t},\text{in}}, u) := \zeta_{s^p}\big(g^n(\hat{\boldsymbol{i}}_{\boldsymbol{t},\text{in}}, u)\big) \quad \textit{and} \quad \text{co}_t^n(\hat{\boldsymbol{i}}_{\boldsymbol{t},\text{in}}, u) := \zeta_{t^p}\big(g^n(\hat{\boldsymbol{i}}_{\boldsymbol{t},\text{in}}, u)\big),
$$

respectively, where $p := u_n$.

Corollary 8.45 *Let $\hat{\boldsymbol{i}}_{\boldsymbol{t},\text{in}}$ and $(u_n)_{n\in\mathbb{N}}$ be a feasible input combination. During the n-th ADA iteration with Algorithm 5.2 given the inputs $\hat{\boldsymbol{i}}_{\boldsymbol{t},\text{in}}$ and u, the CO emission at the start point is $\text{co}_s^n(\hat{\boldsymbol{i}}_{\boldsymbol{t},\text{in}}, u)$ and the CO emission at the test point is $\text{co}_t^n(\hat{\boldsymbol{i}}_{\boldsymbol{t},\text{in}}, u)$.*

Proof. The statement follows from Lemma 8.41 and from Definition 2.18 of the HE model. □

According to the HE model, ζ_{fs} is convex (Definition 2.18). Therefore, it is sufficient to check that $\text{co}_{\max}$ is not exceeded at the minimum and at the maximum gas valve position of the start and of the test point (if $\hat{\boldsymbol{i}}_{\boldsymbol{t},\text{in}} = (i_t^1, \ldots, i_t^N)$, $r_D \geq 0$ and the requirements (R1) to (R3) are met).

Lemma 8.46 *Let $r_D \geq 0$. Let $A^p_{r_D}$ be contractive, let $\mathrm{fix}(A^p_{r_D}) = r_D$ and let $0 \in \hat{R}^p_{r_D}$ for all $p \in [N]$. Furthermore, let $\hat{\boldsymbol{i}}_{\boldsymbol{t},\mathrm{in}} := (i_t^1, \ldots, i_t^N)$ and let u be an arbitrary (infinite) ADA update sequence. Then, the following holds for all $n \in \mathbb{N}$:*

$$u_n = p \;\Rightarrow\; \mathrm{co}_s^n(\hat{\boldsymbol{i}}_{\boldsymbol{t},\mathrm{in}}, u) \leq \max\left\{\zeta_{s^p}(g^p_{\min}), \zeta_{s^p}(g^p_{\max})\right\}$$

and

$$u_n = p \;\Rightarrow\; \mathrm{co}_t^n(\hat{\boldsymbol{i}}_{\boldsymbol{t},\mathrm{in}}, u) \leq \max\left\{\zeta_{t^p}(g^p_{\min}), \zeta_{t^p}(g^p_{\max})\right\}.$$

Proof. The statement follows from Lemma 8.43, from Corollary 8.45 and from the fact that ζ_{fs} is convex for all $\mathrm{fs} \in [\mathrm{fs}_{\min}, \mathrm{fs}_{\max}]$ (Definition 2.18). □

Lemma 8.46 implies that it is sufficient to check that the CO limit at the start and at the test fan speed is not exceeded for $g^p_{\min}$ and $g^p_{\max}$ only. It is not required to check the CO emissions for each ADA iteration separately. By considering that $g^p_{\min} = \rho^{-1}_{s^p}(\frac{U}{i^p_s})$ and that $g^p_{\max} = \rho^{-1}_{s^p}(\frac{U}{i^p_s} - r_D)$ (Definition 8.42), we obtain the following constraints.

(C-S1) For all $p \in [N]$:

$$\zeta_{s^p} \circ \rho^{-1}_{s^p}(\frac{U}{i^p_s}) \leq \mathrm{co}_{\max}, \quad \zeta_{s^p} \circ \rho^{-1}_{s^p}(\frac{U}{i^p_s} - r_D) \leq \mathrm{co}_{\max} \text{ and}$$
$$\zeta_{t^p} \circ \rho^{-1}_{s^p}(\frac{U}{i^p_s}) \leq \mathrm{co}_{\max}, \quad \zeta_{t^p} \circ \rho^{-1}_{s^p}(\frac{U}{i^p_s} - r_D) \leq \mathrm{co}_{\max}\,.$$

Specification (S2)**:** The equivalence AFR during an ADA iteration must never fall below $\lambda_{\min}$. Because Λ_{fs} is strictly decreasing (Definition 2.18), it is sufficient to check that $\lambda_{\min} \leq \Lambda_{s^p}(g)$ and that $\lambda_{\min} \leq \Lambda_{t^p}(g)$ for the gas valve position bounds $g_{\min}$ and $g_{\max}$ only. Analogous to the CO emissions, the equivalence AFRs during an ADA iteration are as follows.

Definition 8.47 *Let $\hat{\boldsymbol{i}}_{\boldsymbol{t},\mathrm{in}}$ and $(u_n)_{n\in\mathbb{N}}$ be a feasible input combination. For $n \in \mathbb{N}$, the corresponding n-th* start-λ and test-λ iterate *are defined by*

$$\lambda_s^n(\hat{\boldsymbol{i}}_{\boldsymbol{t},\mathrm{in}}, u) := \Lambda_{s^p}\big(g^n(\hat{\boldsymbol{i}}_{\boldsymbol{t},\mathrm{in}}, u)\big) \quad \text{and} \quad \lambda_t^n(\hat{\boldsymbol{i}}_{\boldsymbol{t},\mathrm{in}}, u) := \Lambda_{t^p}\big(g^n(\hat{\boldsymbol{i}}_{\boldsymbol{t},\mathrm{in}}, u)\big),$$

respectively, where $p := u_n$.

Corollary 8.48 *Let $\hat{\boldsymbol{i}}_{\boldsymbol{t},\mathrm{in}}$ and $(u_n)_{n\in\mathbb{N}}$ be a feasible input combination. During the n-th ADA iteration with Algorithm 5.2 given the inputs $\hat{\boldsymbol{i}}_{\boldsymbol{t},\mathrm{in}}$ and u, the equivalence AFR of the start point is $\lambda_s^n(\hat{\boldsymbol{i}}_{\boldsymbol{t},\mathrm{in}}, u)$ and the equivalence AFR of the test point is $\lambda_t^n(\hat{\boldsymbol{i}}_{\boldsymbol{t},\mathrm{in}}, u)$.*

Proof. The statement follows from Lemma 8.41 and from Definition 2.18 of the HE model. □

According to the HE model, $\Lambda_{s^p}(g)$ and $\Lambda_{t^p}(g)$ are strictly decreasing (Definition 2.18). This allows us to state bounds for the equivalence AFR during the ADA iterations.

Lemma 8.49 *Let $r_D \geq 0$. Let $A^p_{r_D}$ be contractive, let $\mathrm{fix}(A^p_{r_D}) = r_D$ and let $0 \in \hat{R}^p_{r_D}$ for all $p \in [N]$. Furthermore, let $\hat{\boldsymbol{i}}_{\boldsymbol{t},\mathrm{in}} := (i_t^1, \ldots, i_t^N)$ and let u be an arbitrary (infinite) ADA update sequence. Then, the following holds for all $n \in \mathbb{N}$:*

$$u_n = p \;\Rightarrow\; \Lambda_{s^p}(g^p_{\max}) \leq \lambda^n_s(\hat{\boldsymbol{i}}_{\boldsymbol{t},\mathrm{in}}, u) \leq \Lambda_{s^p}(g^p_{\min})$$

and

$$u_n = p \;\Rightarrow\; \Lambda_{t^p}(g^p_{\max}) \leq \lambda^n_t(\hat{\boldsymbol{i}}_{\boldsymbol{t},\mathrm{in}}, u) \leq \Lambda_{t^p}(g^p_{\min}).$$

Proof. Let $n \in \mathbb{N}$ and let $u_n = p$. Then $g^p_{\min} \leq g^n(\hat{\boldsymbol{i}}_{\boldsymbol{t},\mathrm{in}}, u) \leq g^p_{\max}$ (Lemma 8.43). Because Λ_{s^p} and Λ_{t^p} are strictly decreasing (Definition 2.18), we have

$$\Lambda_{\mathrm{fs}}(g^p_{\min}) \geq \Lambda_{\mathrm{fs}}\big(g^n(\hat{\boldsymbol{i}}_{\boldsymbol{t},\mathrm{in}}, u)\big) \geq \Lambda_{\mathrm{fs}}(g^p_{\max}), \quad \mathrm{fs} \in \{s^p, t^p\}.$$

According to Definition 8.47, we have $\lambda^n_s(\hat{\boldsymbol{i}}_{\boldsymbol{t},\mathrm{in}}, u) = \Lambda_{s^p}\big(g^n(\hat{\boldsymbol{i}}_{\boldsymbol{t},\mathrm{in}}, u)\big)$ and $\lambda^n_t(\hat{\boldsymbol{i}}_{\boldsymbol{t},\mathrm{in}}, u) = \Lambda_{t^p}\big(g^n(\hat{\boldsymbol{i}}_{\boldsymbol{t},\mathrm{in}}, u)\big)$ and the statement is proved. □

Lemma 8.49 implies that it is sufficient to check that the equivalence AFR does not fall below $\lambda_{\min}$ for the actuator positions $(s^p, g_{\max})$ and $(t^p, g_{\max})$ (if $\hat{\boldsymbol{i}}_{\boldsymbol{t},\mathrm{in}} = (i_t^1, \ldots, i_t^N)$, $r_D \geq 0$ and the requirements (R1) to (R3) are met). It is not required to check the equivalence AFR for each ADA iteration separately. By considering that $g^p_{\max} = \rho^{-1}_{s^p}(\frac{U}{i^p_s} - r_D)$ (Definition 8.42), we obtain the following constraints.

(C-S2) For all $p \in [N]$: $-\Lambda_{s^p} \circ \rho^{-1}_{s^p}(\frac{U}{i^p_s} - r_D) \leq -\lambda_{\min}$ and $-\Lambda_{t^p} \circ \rho^{-1}_{s^p}(\frac{U}{i^p_s} - r_D) \leq -\lambda_{\min}$.

Specification (S3)**:** The equivalence AFR during an ADA iteration must never exceed $\lambda_{\max}$. Analogous to (S2) and (C-S2), it is sufficient to check that the equivalence AFR does not exceed $\lambda_{\max}$ for the actuator positions $(s^p, g_{\min})$ and $(t^p, g_{\min})$ (if $\hat{\boldsymbol{i}}_{\boldsymbol{t},\mathrm{in}} = (i_t^1, \ldots, i_t^N)$, $r_D \geq 0$ and the requirements (R1) to (R3) are met) according to Lemma 8.49. By considering that $g^p_{\min} = \rho^{-1}_{s^p}(\frac{U}{i^p_s})$ (Definition 8.42), we obtain the following constraints.

(C-S3) For all $p \in [N]$: $\Lambda_{s^p} \circ \rho^{-1}_{s^p}(\frac{U}{i^p_s}) \leq \lambda_{\max}$ and $\Lambda_{t^p} \circ \rho^{-1}_{s^p}(\frac{U}{i^p_s}) \leq \lambda_{\max}$.

In total, if the constraints (C-S1) to (C-S3) are met, then the specifications (S1) to (S3) are satisfied.

8.5.3. General Feasibility Constraints

In this subsection, we derive constraints corresponding to the specifications (S4) to (S7).

Specification (S4)**:** It is required that $i^p_s \in \iota_{s^p}(G_{s^p})$ and $i^p_t \in \iota_{t^p}(G_{t^p})$. Because G_{fs} is a closed interval and ι_{fs} is a homeomorphism, $\iota_{\mathrm{fs}}(G_{\mathrm{fs}})$ is a closed interval as well for all fan speeds $\mathrm{fs} \in \mathrm{FS}$. Therefore, it is sufficient to check that i^p_s and i^p_t are within the boundaries of the corresponding intervals and we obtain the following constraints.

(C-S4) For all $p \in [N]$:

$$\begin{aligned} \min \iota_{s^p}(G_{s^p}) - i^p_s \leq 0, \quad & -\max \iota_{s^p}(G_{s^p}) + i^p_s \leq 0 \quad \text{and} \\ \min \iota_{t^p}(G_{t^p}) - i^p_t \leq 0, \quad & -\max \iota_{t^p}(G_{t^p}) + i^p_t \leq 0. \end{aligned}$$

Specification (S5): The start ioni current shall be on or below the control curve and the test ioni current shall be on or above the control cure. Expressed with the control curve function $i_{\text{set}}(\text{fs})$ according to Definition 8.30, this corresponds to $i_s^p \leq i_{\text{set}}(s^p)$ and $i_{\text{set}}(t^p) \leq i_t^p$. Thus, we include the following constraints.

(C-S5) $i_s^p - i_{\text{set}}(s^p) \leq 0$ and $i_{\text{set}}(t^p) - i_t^p \leq 0$ for all $p \in [N]$.

Specification (S6): The distance between the equivalence AFR at the undrifted start point and the equivalence AFR at the undrifted test point must be at least $\Delta\lambda_{\text{min}}$. The term "undrifted" refers to a situation with $r_D = 0$. In this case we can use the HE model functions without drift according to Definition 2.18. Therefore, the gvp at the start point is $g_{s^p} = \iota_{s^p}^{-1}(i_s^p)$ and the corresponding equivalence AFR is $\lambda_s^p := \Lambda_{s^p} \circ \iota_{s^p}^{-1}(i_s^p)$. Analogously, we have $\lambda_t^p := \Lambda_{t^p} \circ \iota_{t^p}^{-1}(i_t^p)$. With $\lambda_s^p - \lambda_t^p \geq \Delta\lambda_{\text{min}}$, we obtain the following constraints.

(C-S6) $-\Lambda_{s^p} \circ \iota_{s^p}^{-1}(i_s^p) + \Lambda_{t^p} \circ \iota_{t^p}^{-1}(i_t^p) \leq -\Delta\lambda_{\text{min}}$ for all $p \in [N]$.

Specification (S7): The specification (S7) corresponds to the restrictions with respect to the start fan speeds and to the test fan speeds. Because we consider only sets of feasible test fan speeds $T = \{t^1, \ldots, t^N\}$ according to (Sc3), the conditions $t^1 > t^2 > \cdots > t^N$ as well as $t^1 \geq \text{fs}_{\text{min}}$ are already satisfied according to Definition 8.1. The remaining restrictions are $t^p < s^p$ for all $p \in [N]$, $s^p < t^{p-1}$ for all $p \in \{2, \ldots, N\}$ and $s^1 \leq \text{fs}_{\text{max}}$. Recall that strict inequalities are not allowed in the optimization model according to Remark 8.14. Thus, we make once more use of an arbitrary small but fixed $\varepsilon > 0$. Because the test fan speeds t^p are taken from the set T, they are considered as constants and not as a part of the decision variables. Therefore, they are placed on the right hand side of the following inequalities. With this, we include the following constraints.

(C-S7) $-s^p \leq -(t^p + \varepsilon)\ \forall\ p \in [N]$, $s^p \leq t^{p-1} - \varepsilon\ \forall\ p \in \{2, \ldots, N\}$ and $s^1 \leq \text{fs}_{\text{max}}$.

To summarize this section, if the constraints (C-S1) to (C-S7) are satisfied, then the specifications (S1) to (S7) are satisfied as well. With this, we have all the parts together to define the feasible set of the optimization model for the case without tolerances in the following section.

8.6. Optimization Model for the Nominal Case Without Tolerances

In this section, an optimization model for the nominal case without tolerances is proposed based on the considerations made in this chapter so far. This means that we want to optimize the ADA parameters of N ADA pairs with the goals (G1) and (G2) given the scenarios (Sc1) to (Sc3) and under the constraints (C-R1) to (C-R3) as well as (C-S1) to (C-S7). As already mentioned in Section 8.1, the decision variables are the parameters (s^p, t^p, i_s^p, i_t^p) of each ADA pair p, $p \in [N]$.

The test fan speed t^p can be considered as given and fixed, because the decision makers specify the set of feasible test fan speeds $T = \{t^1, \ldots, t^N\}$ in advance according to (Sc3). Therefore, the three parameters s^p, i_s^p and i_t^p are left as decision variables for each ADA pair p, $p \in [N]$. This gives us a total of $3N$ decision variables.
However, it is possible to optimize each ADA pair individually. In a certain sense, the ADA pairs can be considered as decoupled, which results in N optimization problems each with a three-dimensional decision space.
Why is it possible to consider the ADA pairs individually? Regarding ADA pair p, $p \in [N]$, each constraint (C-R1) to (C-R3) as well as (C-S1) to (C-S6) depends only on the ADA parameters of ADA pair p, i.e., these constraints depend only on s^p, i_s^p, i_t^p and t^p. In particular, they do not depend on s^q, i_s^r, i_t^m for all $q, r, m \in [N] \setminus \{p\}$.
Constraint (C-S7) is a little different, because in addition to s^p and t^p this constraint depends also on t^{p-1} if $p \geq 2$, which is the only coupling of the ADA pairs. However, t^p and t^{p-1} are specified in advance, which cancels out the coupling of the ADA pairs in this case.
The same holds for the objective functions corresponding to the goals (G1) and (G2), because the Lipschitz constant L^p as well as the start point increment of ADA pair p, $p \in [N]$, depend only on s^p, i_s^p, i_t^p and t^p. The objective functions is defined and detailed in Section 8.6.2 below after the feasible set is defined.

Remark 8.50 *The ADA pairs can be considered individually for two reasons. First, the test fan speeds are specified by the decision makers in advance, as already delineated. Secondly, we only consider situations where* $\operatorname{fix}(A_{r_D}^p) = r_D$ *for all* $p \in [N]$ *according to* (R1). *With this, the drift resistance super fixed point vector is* $\boldsymbol{r}^{**} = (r_1^{**}, \ldots, r_N^{**})$ *with* $r_p^{**} = r_D$ *for all* $p \in [N]$ *(Theorem 7.73). I.e., the super fixed point vector is already known and it is not required to determine it with the recursion according to Lemma 7.42 in this case. Therefore, the coupling of the ADA pairs related to the super fixed point vector is not relevant in this case.*

Remark 8.51 *As stated in the preceding Remark 8.50, the requirement* (R1) *is essential for the decoupling of the ADA pairs. The corresponding constraints is* (C-R1). *It is equivalent to* $\iota_{s^p}^{-1}(i_s^p) = \iota_{t^p}^{-1}(i_t^p)$, *which is the nominal condition according to Definition 6.39. Therefore, the optimization problem proposed in this section is called the nominal optimization problem.*
However, as delineated in Section 7.4.1 and as demonstrated in Example 7.74, because of tolerances with respect to the position of the ioni electrode the nominal condition is not always fulfilled. In such a case it is not possible to satisfy (R1) *and the ADA pairs cannot be optimized individually anymore, because the super fixed point vector* $\boldsymbol{r}^{**}$ *has to be determined with the recursion according to Lemma 7.42. This is discussed in detail in Section 8.7, where a corresponding optimization model to optimize the ADA parameters in the case with tolerances is proposed.*

In the following, a set of feasible ADA parameters for the ADA pair p, $p \in [N]$, with

respect to T and $r_D \geq 0$ is defined. Thereafter, the objective functions are discussed and finally the corresponding optimization model is presented.

8.6.1. Set of Feasible Solutions with Respect to ADA Pair p

As already mentioned, for a fixed $p \in [N]$ the decision space under the conditions specified at the beginning of Section 8.6 is three-dimensional. Its dimensions are the three ADA parameters s^p, i_s^p and i_t^p. The fourth ADA parameter t^p is already specified in the set T. The definition of the feasible set is straightforward. A solution is defined as feasible, if the ADA parameters (s^p, t^p, i_s^p, i_t^p) fulfill all constraints (C-R1) to (C-R3) as well as (C-S1) to (C-S7).

Definition 8.52 *Let $\mathcal{H} = \big(\mathrm{FS}, (G_{\mathrm{fs}})_{\mathrm{fs}\in\mathrm{FS}}, (\iota_{\mathrm{fs}})_{\mathrm{fs}\in\mathrm{FS}}, (\Lambda_{\mathrm{fs}})_{\mathrm{fs}\in\mathrm{FS}}, (\zeta_{\mathrm{fs}})_{\mathrm{fs}\in\mathrm{FS}}\big)$ be a given HE model. Let $T = \{t^1, \ldots, t^N\}$ be a set of feasible test fan speeds, let $r_D \geq 0$ and let $\lambda_{\min}$, $\lambda_{\max}$, $\mathrm{co}_{\max}$ as well as $\Delta\lambda_{\min}$ be the combustion limits specified by the decision makers. Furthermore, let $\varepsilon > 0$ be small and fixed. For $p \in [N]$, the* set of the feasible ADA parameters of ADA pair p with respect to T and r_D, *denoted by X^p_{T,r_D}, contains exactly all vectors $x = (s^p, i_s^p, i_t^p) \in \mathbb{R}^3$ that fulfill all of the following constraints:*

(C-R1) $\iota_{s^p}^{-1}(i_s^p) - \iota_{t^p}^{-1}(i_t^p) = 0,$

(C-R2) $\mathcal{L}^p_{T,r_D}(s^p, i_s^p, i_t^p) \leq 1 - \varepsilon,$

(C-R3) $\min \iota_{s^p}(G^p_{st}) - \dfrac{i_s^p U}{-i_s^p r_D + U} \leq 0, \qquad \dfrac{i_s^p U}{-i_s^p r_D + U} - \max \iota_{s^p}(G^p_{st}) \leq 0,$

(C-S1) $\zeta_{s^p} \circ \rho_{s^p}^{-1}\left(\dfrac{U}{i_s^p}\right) \leq \mathrm{co}_{\max}, \qquad \zeta_{s^p} \circ \rho_{s^p}^{-1}\left(\dfrac{U}{i_s^p} - r_D\right) \leq \mathrm{co}_{\max},$

$\zeta_{t^p} \circ \rho_{s^p}^{-1}\left(\dfrac{U}{i_s^p}\right) \leq \mathrm{co}_{\max}, \qquad \zeta_{t^p} \circ \rho_{s^p}^{-1}\left(\dfrac{U}{i_s^p} - r_D\right) \leq \mathrm{co}_{\max},$

(C-S2) $-\Lambda_{s^p} \circ \rho_{s^p}^{-1}\left(\dfrac{U}{i_s^p} - r_D\right) \leq -\lambda_{\min}, \qquad -\Lambda_{t^p} \circ \rho_{s^p}^{-1}\left(\dfrac{U}{i_s^p} - r_D\right) \leq -\lambda_{\min},$

(C-S3) $\Lambda_{s^p} \circ \rho_{s^p}^{-1}\left(\dfrac{U}{i_s^p}\right) \leq \lambda_{\max}, \qquad \Lambda_{t^p} \circ \rho_{s^p}^{-1}\left(\dfrac{U}{i_s^p}\right) \leq \lambda_{\max},$

(C-S4) $\min \iota_{s^p}(G_{s^p}) - i_s^p \leq 0, \qquad -\max \iota_{s^p}(G_{s^p}) + i_s^p \leq 0,$

$\min \iota_{t^p}(G_{t^p}) - i_t^p \leq 0, \qquad -\max \iota_{t^p}(G_{t^p}) + i_t^p \leq 0,$

(C-S5) $i_s^p - i_{\mathrm{set}}(s^p) \leq 0, \qquad i_{\mathrm{set}}(t^p) - i_t^p \leq 0,$

(C-S6) $\Lambda_{t^p} \circ \iota_{t^p}^{-1}(i_t^p) - \Lambda_{s^p} \circ \iota_{s^p}^{-1}(i_s^p) \leq -\Delta\lambda_{\min},$

(C-S7) $-s^p \leq -(t^p + \varepsilon)\ \forall\ p \in [N], \qquad s^p \leq \begin{cases} \mathrm{fs}_{\max} & \text{if } p = 1, \\ t^{p-1} - \varepsilon & \text{if } p \in \{2, \ldots, N\}. \end{cases}$

Remark 8.53 *According to Definition 8.52, the set X^p_{T,r_D} of feasible ADA parameters of ADA pair p implicitly depends on the HE model $\mathcal{H}$, on ε as well as on the limits $\lambda_{\min}$, $\lambda_{\max}$, $\mathrm{co}_{\max}$ and $\Delta\lambda_{\min}$ specified by the decision makers. For better readability, these are not shown in the notation of this set. Rather, they are implicitly assumed to be given.*

Remark 8.54 *Definition 8.52 of* X^p_{T,r_D} *contains redundancies. Constraint* (C-R1) *implies that* $\iota^{-1}_{s^p}(i^p_s)$ *and* $\iota^{-1}_{t^p}(i^p_t)$ *are well-defined. This in turn implies that* $i^p_s \in \iota_{s^p}(G_{s^p})$ *and* $i^p_t \in \iota_{t^p}(G_{t^p})$*, which is equivalent to the constraint* (C-S4)*. Thus,* (C-S4) *in Definition 8.52 can be omitted. But aiming at a better overview, it is still listed in Definition 8.52.*

Remark 8.55 *The set* X^p_{T,r_D} *is bounded. According to* (C-S7)*, the start fan speed* s^p *is bounded from below by* $t^p + \varepsilon$ *and from above by* $t^{p-1} - \varepsilon$ *(if* $p \geq 2$*) or by* $\mathrm{fs}_{\max}$ *(if* $p = 1$*). Furthermore, we have* $i^p_s \in \iota_{s^p}(G_{s^p})$ *and* $i^p_t \in \iota_{t^p}(G_{t^p})$ *according to* (C-S4)*, where* $\iota_{s^p}(G_{s^p})$ *and* $\iota_{t^p}(G_{t^p})$ *are closed intervals according to Lemma 2.21.*
Whether the set X^p_{T,r_D} *is compact or not is not easy to answer and remains an open question in this work. If it is not compact, then the set of Pareto optimal points and the Pareto front might be empty, see also Section 4.1.1. However, from a practical point of view, a good approximation of the nondominated set in the closure of the image of* X^p_{T,r_D} *under the objective functions is sufficient.*

Remark 8.56 *Note that* $X^p_{T,r_D} \subset \mathbb{R}^3_{>0}$*. This follows from Definition 2.18 of the HE model, because* $s^p \in [\mathrm{fs}_{\min}, \mathrm{fs}_{\max}] \subset \mathbb{R}_{>0}$*,* $i^p_s \in \iota_{s^p}(G_{s^p}) = I_{s^p} \subset \mathbb{R}_{>0}$ *and* $i^p_t \in \iota_{t^p}(G_{t^p}) = I_{t^p} \subset \mathbb{R}_{>0}$*.*

Remark 8.57 *That the feasible set* X^p_{T,r_D} *is continuous is a relaxation. In practice, the ADA parameters, i.e., the start and the test fan speed as well as the start and the test ioni current, have to be integers. Therefore, the components of an optimized* $x \in X^p_{T,r_D}$ *must be rounded to their nearest integer. However, the resulting difference in the objective function values usually has the order of magnitude of measurement errors and the decision makers are satisfied with the rounded relaxed solutions [PHE, Items 3124 and 7082].*

The following theorem summarizes some properties if the N ADA pairs p, $p \in [N]$, are all obtained from the feasible sets X^p_{T,r_D}, $p \in [N]$.

Theorem 8.58 *Let* $T = \{t^1, \ldots, t^N\}$ *be a set of feasible test fan speeds and let* $r_D \geq 0$*. Furthermore, let* (s^p, t^p, i^p_s, i^p_t) *be the ADA parameters of ADA pair* p*,* $p \in [N]$*.*
If $(s^p, i^p_s, i^p_t) \in X^p_{T,r_D}$ *for all* $p \in [N]$ *and* $\hat{\boldsymbol{i}}_{\boldsymbol{t},\mathrm{in}} = (i^1_t, \ldots, i^p_t)$*, then the following holds:*

- $\boldsymbol{i}^{**} = (i^1_{t,r_D}, \ldots, i^N_{t,r_D})$*, where* i^p_{t,r_D} *is the drifted test ioni current according to Definition 3.27 for all* $p \in [N]$*,*
- *if* u *is a sufficiently well distributed ADA update sequence, then* $\lim_{n\to\infty} \boldsymbol{i}^n(\hat{\boldsymbol{i}}_{\boldsymbol{t},\mathrm{in}}, u) = \boldsymbol{i}^{**}$*,*
- *the equivalence AFRs are in the interval* $[\lambda_{\min}, \lambda_{\max}]$ *and the CO emissions do not exceed* $\mathrm{co}_{\max}$ *during all iterations with the ADA Algorithm 5.2 given the inputs* $\hat{\boldsymbol{i}}_{\boldsymbol{t},\mathrm{in}}$ *and* u*, where* u *is an arbitrary ADA update sequence, and*
- *all start and test fan speeds are in the interval* $\mathrm{FS} = [\mathrm{fs}_{\min}, \mathrm{fs}_{\max}]$ *and the ADA pairs are not overlapping.*

Proof. The statement follows from the construction of the sets X^p_{T,r_D} for all $p \in [N]$. □

Next, we consider the objective functions.

8.6.2. Objective Functions

When optimizing ADA pair p, $p \in [N]$, we have the two optimization goals (G1) and (G2), which are a small Lipschitz constant L^p and a small start point increment $\lambda^p_{s,\text{incr}}$, respectively.

A function that maps the ADA parameters (s^p, t^p, i_s^p, i_t^p), where t^p is taken from T, to the corresponding Lipschitz constant L^p (if it exists) has already been defined in Definition 8.17. This function is denoted by $\mathcal{L}^p_{T,r_D}$. Therefore, to satisfy (G1) the first objective is to minimize $\mathcal{L}^p_{T,r_D}(x)$ with $x \in X^p_{T,r_D}$.

Regarding (G2), we define a corresponding objective function in the following. The start point increment $\lambda^p_{s,\text{incr}}(s^p, t^p, i_s^p, i_t^p)$ has already been defined in Definition 8.33. Because t^p can be considered as given and fixed, we define a function that maps the remaining three ADA parameters s^p, i_s^p and i_t^p to the corresponding start point increment $\lambda^p_{s,\text{incr}}(s^p, t^p, i_s^p, i_t^p)$.

Definition 8.59 *Let $\mathcal{H} = \big(\text{FS}, (G_{\text{fs}})_{\text{fs}\in\text{FS}}, (\iota_{\text{fs}})_{\text{fs}\in\text{FS}}, (\Lambda_{\text{fs}})_{\text{fs}\in\text{FS}}, (\zeta_{\text{fs}})_{\text{fs}\in\text{FS}}\big)$ be an HE model and let i_{set} be a corresponding control curve. Let $T = \{t^1, \dots, t^N\}$ be a set of feasible test fan speeds and let $r_D \geq 0$. The* start point increment function of ADA pair p with respect to T and r_D *is the function $\mathcal{S}^p_{T,r_D} : X^p_{T,r_D} \to \mathbb{R}$ defined by*

$$\mathcal{S}_{T,r_D}(s^p, i_s^p, i_t^p) := \lambda^p_{s,\text{incr}}(s^p, t^p, i_s^p, i_t^p) = \Lambda_{s^p} \circ \iota^{-1}_{t^p}(i_t^p) - \Lambda_{s^p} \circ \iota^{-1}_{s^p} \circ i_{\text{set}}(s^p).$$

Lemma 8.60 *The start point increment function is well-defined and nonnegative, i.e., $\mathcal{S}^p_{T,r_D}(x) \geq 0$ for all $x \in X^p_{T,r_D}$.*

Proof. Let $x = (s^p, i_s^p, i_t^p) \in X^p_{T,r_D}$. Then, we have $\iota^{-1}_{t^p}(i_t^p) = \iota^{-1}_{s^p}(i_s^p)$ according to (C-R1) and thus $\mathcal{S}^p_{T,r_D}(x)$ is well-defined (Definition 8.33 and Lemma 8.35).
To show that $\mathcal{S}^p_{T,r_D}(x) \geq 0$, we use that $i_s^p \leq i_{\text{set}}(s^p)$ according to (C-S5), that $\iota^{-1}_{s^p}$ is strictly increasing (Definition 2.18), that Λ_{s^p} is strictly decreasing (Definition 2.18) and that $\iota^{-1}_{t^p}(i_t^p) = \iota^{-1}_{s^p}(i_s^p)$, which gives us

$$\begin{aligned} i_s^p \leq i_{\text{set}}(s^p) \;&\Rightarrow\; \iota^{-1}_{s^p}(i_s^p) \leq \iota^{-1}_{s^p}\big(i_{\text{set}}(s^p)\big) \;\Rightarrow\; \Lambda_{s^p}\big(\iota^{-1}_{s^p}(i_s^p)\big) \geq \Lambda_{s^p}\Big(\iota^{-1}_{s^p}\big(i_{\text{set}}(s^p)\big)\Big) \\ &\Rightarrow\; \mathcal{S}_{T,r_D}(s^p, i_s^p, i_t^p) = \Lambda_{s^p}\big(\iota^{-1}_{t^p}(i_t^p)\big) - \Lambda_{s^p}\Big(\iota^{-1}_{s^p}\big(i_{\text{set}}(s^p)\big)\Big) \geq 0. \end{aligned}$$

□

Therefore, to satisfy (G2) the second objective is to minimize $\mathcal{S}^p_{T,r_D}(x)$ with $x \in X^p_{T,r_D}$. This completes the specification of the objective functions and we can combine everything to the proposed nominal optimization model.

8.6.3. The Optimization Model

We want to optimize the ADA parameters of ADA pair p, $p \in [N]$. For this, we assume that a set of feasible test fan speeds $T = \{t^1, \ldots, t^N\}$ and a drift resistance $r_D \geq 0$ are given. I.e., we want to find optimal parameters s^p, i_s^p and i_t^p given the test fan speed $t^p \in T$ and the drift resistance r_D. As stated in Remark 8.51, the set of feasible solutions X^p_{T,r_D} contains the constraint $\iota_{s^p}^{-1}(i_s^p) = \iota_{t^p}^{-1}(i_t^p)$, which is the nominal condition according to Definition 6.39, and thus the corresponding optimization problem is called the nominal optimization problem.

Definition 8.61 *Let $\mathcal{H} = \left(\mathrm{FS}, (G_{\mathrm{fs}})_{\mathrm{fs}\in\mathrm{FS}}, (\iota_{\mathrm{fs}})_{\mathrm{fs}\in\mathrm{FS}}, (\Lambda_{\mathrm{fs}})_{\mathrm{fs}\in\mathrm{FS}}, (\zeta_{\mathrm{fs}})_{\mathrm{fs}\in\mathrm{FS}}\right)$ be an HE model and let i_{set} be a corresponding control curve. Let $N \in \mathbb{N}$ be the number of ADA pairs to be parameterized. Let $T = \{t^1, \ldots, t^N\}$ be a set of feasible test fan speeds and let $r_D \geq 0$. The* nominal optimization problem for ADA pair p, $p \in [N]$, *is defined by*

$$\min_{x \in X^p_{T,r_D}} \quad f^{\mathrm{nom},p}(x) := \left(f_1^{\mathrm{nom},p}(x) = \mathcal{L}^p_{T,r_D}(x), f_2^{\mathrm{nom},p}(x) = \mathcal{S}^p_{T,r_D}(x)\right) \qquad (\text{nom-}P^p_{T,r_D})$$

Remark 8.62 *The nondominated set with respect to* (nom-P^p_{T,r_D}) *is not convex in general. An example is illustrated in Figure 9.2 below. The purple curve segments in the right part of Figure 9.2 correspond to the nondominated set of a problem of the type* (nom-P^p_{T,r_D})*, which is not convex in this case.*

If we want to optimize all N ADA pairs, which is usually the case, we have to solve the problem (nom-P^p_{T,r_D}) for each $p \in [N]$, i.e., we have to solve N biobjective optimization problems. A huge advantage of this approach is that the ADA pairs can be optimized individually (once the set T is fixed). A method how to approximate the Pareto front of the problem (nom-P^p_{T,r_D}) is proposed in Section 9.1 below.

As already mentioned, all ADA pairs optimized with (nom-P^p_{T,r_D}) fulfill the nominal condition according to Definition 6.39. However, as delineated in Section 7.4.1 and as demonstrated in Example 7.74, because of tolerances with respect to the position of the ioni electrode the nominal condition is not always fulfilled. In such a case, the ADA pairs cannot be optimized individually anymore, because the super fixed point vector $\boldsymbol{i}^{**}$ has to be determined with the recursion according to Definition 7.14 (or equivalently $\boldsymbol{r}^{**}$ has to be determined with the recursion according to Lemma 7.42) and thus (nom-P^p_{T,r_D}) cannot be applied. Therefore, an optimization model to optimize the ADA parameters with tolerances is proposed in the following section.

8.7. Optimization Model for the Case with Tolerances

According to the objective criterion (O1), the optimized ADA parameters shall approximate the drifted test ioni currents exactly, i.e., the super fixed point vector $\boldsymbol{i}^{**} = (i_1^{**}, \ldots, i_N^{**})$ shall satisfy $i_p^{**} = i^p_{t,r_D}$ for all $p \in [N]$. This is the case if and only if $\iota_{s^p}^{-1}(i_s^p) = \iota_{t^p}^{-1}(t^p)$ for

all $p \in [N]$ according to Theorem 7.73. Therefore, the constraint (C-R1) is included in the definition of the feasible set X^p_{T,r_D} of (nom-P^p_{T,r_D}) (Definition 8.52).
If an HE model $\mathcal{H}$ and an ADA pair (s^p, t^p, i^p_s, i^p_t) are such that $\iota^{-1}_{sp}(i^p_s) = \iota^{-1}_{tp}(t^p)$ holds, this situation is called nominal. But as demonstrated in Example 7.74, tolerances with respect to the ioni electrode's position might cause that this condition is not fulfilled anymore. Then, such a situation is called non-standard according to Definition 6.39.
Therefore, in the non-standard situation, i.e., in the case with tolerances, we have to relax the objective criterion (O1). A corresponding optimization model that deals with non-standard situations is proposed in this section. It is closely related to the approach taken by Vaillant how to deal with tolerances with respect to the ioni electrode's position, which is detailed in the following.

8.7.1. Approach by Vaillant to Deal with Tolerances of the Ioni Electrode's Position

For confidentiality reasons, the following explanations are kept at a general level and without explicitly specifying parameters. Vaillant defines the position of the ioni electrode by two dimensions. The first dimension is the distance between the tip of the ioni electrode and a reference point in the burning chamber, denoted by d in the following. The second dimension is an angle between the axis of the ioni electrode and a reference axis, denoted by α in the following.
With this, Vaillant defines an ideal or nominal position $(d_{\text{nom}}, \alpha_{\text{nom}})$ of the ioni electrode. Furthermore, they specify a maximal allowable deviation from the nominal distance and from the nominal angle that may be caused by tolerances. They are denoted by $\Delta d_{\max}$ and $\Delta\alpha_{\max}$, respectively. The maximal allowable deviations are used to define four extreme cases with respect to the ioni electrode's position, which are $(d_{\text{nom}} - \Delta d_{\max}, \alpha_{\text{nom}} - \Delta\alpha_{\max})$, $(d_{\text{nom}} + \Delta d_{\max}, \alpha_{\text{nom}} - \Delta\alpha_{\max})$, $(d_{\text{nom}} - \Delta d_{\max}, \alpha_{\text{nom}} + \Delta\alpha_{\max})$ and $(d_{\text{nom}} + \Delta d_{\max}, \alpha_{\text{nom}} + \Delta\alpha_{\max})$. These extreme cases can be considered as worst case scenarios in the sense that Vaillant makes the assumption that if a set of N ADA pairs "works" for all four extreme ioni electrode positions, then these ADA pairs also work for an arbitrary intermediate position.
In order to deal with the tolerances with respect to the ioni electrode's position, HE measurement data for each of the four extreme positions is determined in the lab. This gives us four corresponding HE models, which form a scenario set for the ADA optimization with tolerances. In the field of robust optimization, the scenario set is also called uncertainty set and is usually denoted by $\mathcal{U}$ [DZG18, p. 147]. Since the considerations made in this section are closely related to robust optimization, the term uncertainty set is used in this work.
The following definition of an uncertainty set with respect to tolerances considers the more general case with k sets of measurement data with respect to tolerances, where $k \in \mathbb{N}_0$.

Definition 8.63 *Let there be k, $k \in \mathbb{N}_0$, sets of measurement data related to k scenarios with respect to tolerances. The corresponding HE models are called* tolerance HE models

and are denoted by $\mathcal{H}_{\text{tol}}^j = \left(\text{FS}^j, (G_{\text{fs}}^j)_{\text{fs}\in\text{FS}}, (\iota_{\text{fs}}^j)_{\text{fs}\in\text{FS}}, (\Lambda_{\text{fs}}^j)_{\text{fs}\in\text{FS}}, (\zeta_{\text{fs}}^j)_{\text{fs}\in\text{FS}}\right)$, $j \in [k]$.
The corresponding uncertainty set with respect to tolerances *is the collection of the tolerance HE models. It is defined by*

$$\mathcal{U}_{\text{tol}} := \bigcup_{j\in[k]} \{\mathcal{H}_{\text{tol}}^j\}.$$

In addition to the uncertainty set $\mathcal{U}_{\text{tol}}$ that contains the tolerance HE models we also require an HE model that corresponds to the nominal case.

Notation 8.64 *The HE model that is based on nominal measurement data is called* nominal HE model *and is denoted by* $\mathcal{H}_{\text{nom}} = \left(\text{FS}, (G_{\text{fs}})_{\text{fs}\in\text{FS}}, (\iota_{\text{fs}})_{\text{fs}\in\text{FS}}, (\Lambda_{\text{fs}})_{\text{fs}\in\text{FS}}, (\zeta_{\text{fs}})_{\text{fs}\in\text{FS}}\right)$.

Remark 8.65 *Usually, in addition to a nominal HE model there are four tolerance HE models that correspond to the four extreme positions of the ioni electrode, i.e., the case* $k = 4$ *is common in practice. However,* k *can be arbitrary and depends on the use case. Even the case* $k = 0$ *is allowed, which corresponds to the situation that there is only a nominal HE model and no tolerance HE model. This is done to avoid corresponding case distinctions in the course of this section.*

How are the tolerance HE models and the uncertainty set $\mathcal{U}_{\text{tol}}$ related to the ADA optimization? According to (O1), the decision makers want that the super fixed point vector $\boldsymbol{i}^{**} = (i_1^{**}, \ldots, i_N^{**})$ satisfies $i_p^{**} = i_{t,r_D}^p$ for all $p \in [N]$. However, the super fixed point vector depends on the HE model and on the ADA parameters according to Definition 7.14. If the same N ADA pairs (s^p, t^p, i_s^p, i_t^p), $p \in [N]$, are considered with different HE models, we obtain in general different fixed point vectors and (O1) cannot be simultaneously satisfied for different HE models. Therefore, we have to adapt the ADA optimization model if we consider tolerances with respect to the ioni electrode's position.
For this, we introduce a notation that reflects the dependency of the super fixed point vector on the considered ADA parameters and on the considered HE model. The underlying definition of the super fixed point vector is not changed.

Notation 8.66 *Let* $\mathcal{A} := \left\{(s^p, t^p, i_s^p, i_t^p) : p \in [N]\right\}$ *be a set of* N *ADA pairs and let* $\mathcal{H}$ *be an HE model. The corresponding super fixed point vector according to Definition 7.14 is denoted by* $\boldsymbol{i}^{**}(\mathcal{A}, \mathcal{H})$.

A common approach to optimize the ADA pairs with respect to tolerances would be to find a set of ADA parameters $\mathcal{A}$ such that the corresponding super fixed point vectors come as close as possible to the vector of drifted test ioni currents. For instance, this could be modeled by

$$\min_{\mathcal{A} \text{ feasible}} \max_{\mathcal{H}\in\mathcal{U}} \left\| \boldsymbol{i}^{**}(\mathcal{A}, \mathcal{H}) - (i_{t,r_D}^1, \ldots, i_{t,r_D}^N) \right\|_\infty,$$

which corresponds to the concept of strict robustness in the field of robust optimization [DZG18, p. 149].

However, the decision makers argue that the nominal situation is the common case and that convergence characteristics should be designed for this. They do not want that the convergence characteristics of nominal HEs are worsened in order to improve the convergence characteristics of HEs with tolerances. Rather, it is sufficient to check that in the worst case scenarios the ADA Algorithm 5.2 has a certain minimum approximation quality and a certain minimum rate of convergence as well as that certain combustion limits are not exceeded. From the perspective of robust optimization, one may argue that the optimization goals are related to the mean position of the ioni electrode, i.e., to the nominal position, while the constraints are related to the worst-case scenarios. This is the approach that the decision-makers ultimately opted for [PHE, Item 3280].
In the following, an optimization model is proposed that corresponds to this approach. We begin with the corresponding specifications provided by the decision makers.

8.7.2. Specifications with Respect to Tolerances

Regarding the nominal HE model, the objective criteria (O1) to (O3) as well as the specifications (S1) to (S7) remain valid according to the approach presented in the preceding Subsection 8.7.1. Also, again only the case where the scenarios (Sc1) to (Sc3) hold is considered.
Regarding the tolerance HE models contained in $\mathcal{U}_{\text{tol}}$, we introduce additional scenarios and specifications. The following consideration motivates the introduction of the additional scenario (Sc-T1) below. In contrast to the nominal case, we cannot guarantee that the components of all resistance based ADA iterates related to the tolerance HE models stay in the interval $[0, r_D]$. It might be computationally expensive (or even impossible) to check that the incumbent solutions of Algorithm 5.2 given the inputs $\hat{\boldsymbol{i}}_{\boldsymbol{t},\text{in}} = (i_t^1, \dots, i_t^N)$ and an arbitrary sufficiently well distributed ADA update sequence u stay within certain bounds.Therefore, the approach taken is that the decision makers specify a single sufficiently well distributed ADA update sequence $\tilde{u}$, which they consider very likely, and that the optimization specifications are related only to $\tilde{u}$ and not to all sufficiently well distributed ADA update sequences u.
If the ADA parameters are designed manually, only the specific ADA update sequence $(1, \dots, N, 1, \dots, N, \dots)$ is considered for technical reasons [PHE, Item 15936]. In addition, the decision makers consider this sequence likely. Therefore, the decision makers decided to use it for the optimization model with respect to tolerances. In this thesis, it is called the periodic ADA update sequence and it is denoted as follows.

Notation 8.67 *The* periodic ADA update sequence with N ADA pairs *is denoted by*

$$\tilde{u} := \{1, 2, \dots, N, 1, 2, \dots, N, \dots\}.$$

The corresponding scenario is:

(Sc-T1) Regarding the tolerance HE models $\mathcal{H} \in \mathcal{U}_{\text{tol}}$, Algorithm 5.2 is only considered with the sequence $\tilde{u}$ (and the input vector $\hat{\boldsymbol{i}}_{\boldsymbol{t},\text{in}} = (i_t^1, \dots, i_t^N)$ according to (Sc2)).

In addition to the scenario (Sc-T1), the decision makers want that the optimized set of ADA pairs $\mathcal{A}$ satisfies the following tolerance related counterparts to the objective criteria (O1) to (O3) as well as to the specifications (S1) to (S4).

(S-T1) For all $\mathcal{H} \in \mathcal{U}_{\text{tol}}$ the super fixed point vector $\boldsymbol{i}^{**}(\mathcal{A}, \mathcal{H})$ is feasible and the ADA Algorithm 5.2 given the inputs $\hat{\boldsymbol{i}}_{\boldsymbol{t},\text{in}} = (i_t^1, \ldots, i_t^N)$ and $\tilde{u}$ converges to $\boldsymbol{i}^{**}(\mathcal{A}, \mathcal{H})$ at a certain minimum rate of convergence [PHE, Item 15936]. This can be considered as the tolerance related counterpart to (O2) and (O3).

(S-T2) A drift compensation with the super fixed point vector $\boldsymbol{i}^{**}(\mathcal{A}, \mathcal{H})$ guarantees a minimum combustion quality for all $\mathcal{H} \in \mathcal{U}_{\text{tol}}$ [PHE, Items 3280 and 15500]. This can be considered as the relaxed counterpart to (O1).

(S-T3) For all $\mathcal{H} \in \mathcal{U}_{\text{tol}}$ the following must hold. During all iterations with ADA Algorithm 5.2 given the inputs $\hat{\boldsymbol{i}}_{\boldsymbol{t},\text{in}} = (i_t^1, \ldots, i_t^N)$ and $\tilde{u}$ the CO values must not exceed co_{max}, the equivalence AFR must never fall below λ_{min} and the equivalence AFR must never exceed λ_{max} [PHE, Item 3280]. This is analogous to the specifications (S1), (S2) and (S3) for the nominal case. In particular, the bounds co_{max}, λ_{min} and λ_{max} are the same as for (S1), (S2) and (S3).

(S-T4) The start and the test ioni currents must be feasible in the sense that they must be contained in the corresponding sets of the tolerance HE models, i.e., $i_s^p \in \iota_{s^p}(G_{s^p})$ and $i_t^p \in \iota_{t^p}(G_{t^p})$ for all $\mathcal{H} = \big(\text{FS}, (G_{\text{fs}})_{\text{fs}\in\text{FS}}, (\iota_{\text{fs}})_{\text{fs}\in\text{FS}}, (\Lambda_{\text{fs}})_{\text{fs}\in\text{FS}}, (\zeta_{\text{fs}})_{\text{fs}\in\text{FS}}\big) \in \mathcal{U}_{\text{tol}}$. This is analogous to the specification (S4) for the nominal case.

Remark 8.68 *So far, we have specified tolerance related counterparts to* (O1) *to* (O3) *as well as to* (S1) *to* (S4). *The specifications* (S5) *and* (S7) *are independent of tolerances in the sense that they are satisfied for the nominal HE model if and only if they are satisfied for the tolerance HE models. Therefore, corresponding specifications with respect to tolerances are not required.*
The specification (S6) *is not applicable in the case with tolerances, because in the case with tolerances the start and the test point do not have a common gas valve position in general. Thus, it is not possible to compare the equivalence AFR at the start and at the test point in a meaningful way in this case. Therefore, a specification with respect to tolerances corresponding to* (S6) *is not given.*

Before we derive constraints corresponding to the specifications (S-T1) to (S-T4), we need to specify the decision space.

8.7.3. Decision Space in the Case with Tolerances

In the nominal case, i.e., with the problem (nom-P^p_{T,r_D}), we consider the ADA pairs individually and the corresponding decision space is three-dimensional. In the case with tolerances this is not possible in general, because the super fixed point vector has to be determined with the recursion according to Definition 7.14, i.e., all N ADA pairs must be

simultaneously considered. Therefore, the decision space is $3N$-dimensional in this case and its elements are vectors of the form

$$x = (s^1, i_s^1, i_t^1, \ldots, s^N, i_s^N, i_t^N) \in \mathbb{R}^{3N}.$$

As a consequence, we need a transformation from the $3N$-dimensional decision space and a given vector of feasible test fan speeds T to the N ADA pairs, which is defined as follows.

Definition 8.69 *Let $x = (s^1, i_s^1, i_t^1, \ldots, s^N, i_s^N, i_t^N) \in \mathbb{R}^{3N}$ and let $T = \{t^1, \ldots, t^N\}$ be a set of feasible test fan speeds. The set of corresponding ADA pairs is defined by*

$$\mathcal{A}_T(x) := \left\{(s^1, t^1, i_s^1, i_t^1), \ldots, (s^N, t^N, i_s^N, i_t^N)\right\}.$$

Based on this, we can formulate the specifications (S-T1) to (S-T4) as inequalities that depend on the decision variables x.

8.7.4. Constraints with Respect to Tolerances

As a preliminary step, we introduce a notation that reflects the dependency of the ioni current based ADA iterates and of the resistance based ADA iterates on the set of ADA pairs $\mathcal{A}$ and on the considered HE model $\mathcal{H}$, see also Definitions 7.22 and 7.28. This is done analogously to Notation 8.66 of $\boldsymbol{i}^{**}(\mathcal{A}, \mathcal{H})$. The underlying Definitions 7.22 and 7.28 of the ADA iterates are not changed.

Notation 8.70 *Let $\mathcal{A} := \left\{(s^p, t^p, i_s^p, i_t^p) : p \in [N]\right\}$ be a set of N ADA pairs and let $\mathcal{H}$ be an HE model. Furthermore, let $\hat{\boldsymbol{i}}_{\boldsymbol{t},\text{in}}$ be an input vector and let u be an infinite ADA update sequence such that $\hat{\boldsymbol{i}}_{\boldsymbol{t},\text{in}}$ and u are a feasible input combination with respect to $\mathcal{A}$ and $\mathcal{H}$, see also Remark 7.25.*
The n-th ioni current based and resistance based ADA iterate with respect to $\hat{\boldsymbol{i}}_{\boldsymbol{t},r_D}$, u, $\mathcal{A}$ and $\mathcal{H}$ are denoted by $\boldsymbol{i}^n(\hat{\boldsymbol{i}}_{\boldsymbol{t},\text{in}}, u, \mathcal{A}, \mathcal{H})$ and $\boldsymbol{r}^n(\hat{\boldsymbol{i}}_{\boldsymbol{t},\text{in}}, u, \mathcal{A}, \mathcal{H})$, respectively, for all $n \in \mathbb{N}$.

Analogously, we introduce a notation for the iteration functions $A^p_{r_D}$, $p \in [N]$, according to Definition 6.21.

Notation 8.71 *Let $r_D \geq 0$, let $\mathcal{A} := \left\{(s^p, t^p, i_s^p, i_t^p) : p \in [N]\right\}$ be a set of N ADA pairs and let $\mathcal{H}$ be an HE model. The corresponding drift resistance ADA iteration functions are denoted by $A^p_{r_D,\mathcal{A},\mathcal{H}}$ for all $p \in [N]$.*

With this, we derive constraints such that the specifications (S-T1) to (S-T4) are satisfied.

Specification (S-T1) Let $\mathcal{A}$ be a set of N ADA pairs. We want that $\boldsymbol{i}^{**}(\mathcal{A}, \mathcal{H}) \in \mathbb{R}^N$ and that Algorithm 5.2 given the inputs $\hat{\boldsymbol{i}}_{\boldsymbol{t},\text{in}} = (i_t^1, \ldots, i_t^N)$ and $\tilde{u}$ converges to $\boldsymbol{i}^{**}(\mathcal{A}, \mathcal{H})$ with a certain minimum rate of convergence for all $\mathcal{H} \in \mathcal{U}_{\text{tol}}$. The convergence characteristics of Algorithm 5.2 are thoroughly analyzed in Chapter 7 above. One major result of this

analysis is Theorem 7.68, which states conditions for the convergence of Algorithm 5.2 to $\boldsymbol{i}^{**}(\mathcal{A}, \mathcal{H})$, i.e., conditions such that $\lim_{n\to\infty} \boldsymbol{i}^n(\hat{\boldsymbol{i}}_{\boldsymbol{t},\text{in}}, u, \mathcal{A}, \mathcal{H}) = \boldsymbol{i}^{**}(\mathcal{A}, \mathcal{H})$. However, in practice it is difficult to check some of the requirements of Theorem 7.68. For instance, Theorem 7.68 requires that $\boldsymbol{i}^{**}(\mathcal{A}, \mathcal{H})$ is known in advance, which is in general not applicable in the case with tolerances.
The idea to overcome this problem is to approximate $\boldsymbol{i}^{**}(\mathcal{A}, \mathcal{H})$ by simply applying Algorithm 5.2 with the inputs $\hat{\boldsymbol{i}}_{\boldsymbol{t},\text{in}} = (i_t^1, \ldots, i_t^N)$ and $\tilde{u}$ as well as the considered set of ADA pairs $\mathcal{A}$ and the considered tolerance HE model $\mathcal{H}$. As a by-product, we also receive the information whether $\hat{\boldsymbol{i}}_{\boldsymbol{t},\text{in}}$ and $\tilde{u}$ are a feasible input combination with respect to $\mathcal{A}$ and $\mathcal{H}$. If they are not, Algorithm 5.2 will abort at some point and eventually return the vector whose components are all NaN.
Because $\tilde{u}$ is an infinite sequence, we have to manually terminate Algorithm 5.2 at a suitable point. For this, we specify a maximum number of iterations $n_{\max}$. Furthermore, we specify a small threshold value $i_{\text{thr}} > 0$ to check if Algorithm 5.2 can be considered as sufficiently well converged after $n_{\max}$ iterations. Recall from Corollary 7.23 that the intermediate result after the n-th iteration of Algorithm 5.2 given the inputs $\hat{\boldsymbol{i}}_{\boldsymbol{t},\text{in}}$ and $\tilde{u}$ corresponds to the n-th ADA iterate $\boldsymbol{i}^n(\hat{\boldsymbol{i}}_{\boldsymbol{t},\text{in}}, \tilde{u}, \mathcal{A}, \mathcal{H})$. With this, the approach is as follows:
If $\left\|\boldsymbol{i}^{n_{\max}}(\hat{\boldsymbol{i}}_{\boldsymbol{t},\text{in}}, \tilde{u}, \mathcal{A}, \mathcal{H}) - \boldsymbol{i}^{n_{\max}+N}(\hat{\boldsymbol{i}}_{\boldsymbol{t},\text{in}}, \tilde{u}, \mathcal{A}, \mathcal{H})\right\|_\infty \leq i_{\text{thr}}$ and $A^p_{r_D,\mathcal{A},\mathcal{H}}$ is contractive for all $p \in [N]$, then we assume that

$$\lim_{n\to\infty} \boldsymbol{i}^n(\hat{\boldsymbol{i}}_{\boldsymbol{t},\text{in}}, \tilde{u}, \mathcal{A}, \mathcal{H}) = \boldsymbol{i}^{**}(\mathcal{A}, \mathcal{H}) \quad \text{and} \quad \boldsymbol{i}^{**}(\mathcal{A}, \mathcal{H}) \approx \boldsymbol{i}^{n_{\max}+N}(\hat{\boldsymbol{i}}_{\boldsymbol{t},\text{in}}, \tilde{u}, \mathcal{A}, \mathcal{H}).$$

The condition $\left\|\boldsymbol{i}^{n_{\max}}(\hat{\boldsymbol{i}}_{\boldsymbol{t},\text{in}}, \tilde{u}, \mathcal{A}, \mathcal{H}) - \boldsymbol{i}^{n_{\max}+N}(\hat{\boldsymbol{i}}_{\boldsymbol{t},\text{in}}, \tilde{u}, \mathcal{A}, \mathcal{H})\right\|_\infty \leq i_{\text{thr}}$ is an indicator for the convergence of Algorithm 5.2 given the inputs $\hat{\boldsymbol{i}}_{\boldsymbol{t},\text{in}}$ and $\tilde{u}$. The condition that $A^p_{r_D,\mathcal{A},\mathcal{H}}$ is contractive for all $p \in [N]$ ensures the uniqueness of the super fixed point vector, see also Lemma 6.35, Lemma 7.48 and Corollary 7.47. In particular, we assume that $\hat{\boldsymbol{i}}_{\boldsymbol{t},\text{in}}$ and $\tilde{u}$ are a feasible input combination in this case, because Algorithm 5.2 did not abort early.

Remark 8.72 *It is not sufficient to compare $\boldsymbol{i}^{n_{\max}}(\hat{\boldsymbol{i}}_{\boldsymbol{t},\text{in}}, \tilde{u}, \mathcal{A}, \mathcal{H})$ with $\boldsymbol{i}^{n_{\max}+1}(\hat{\boldsymbol{i}}_{\boldsymbol{t},\text{in}}, \tilde{u}, \mathcal{A}, \mathcal{H})$. Indeed, according to Lemma 7.27, in the $(n_{\max}+1)$st iteration only the p-th component of the ADA iterate $\boldsymbol{i}^n(\hat{\boldsymbol{i}}_{\boldsymbol{t},\text{in}}, \tilde{u}, \mathcal{A}, \mathcal{H})$ is updated, where $p = \tilde{u}_{n_{\max}+1}$ is the $(n_{\max}+1)$st entry of the update sequence $\tilde{u}$.*
But we want to make sure that each of the N components of $\boldsymbol{i}^{n_{\max}}(\hat{\boldsymbol{i}}_{\boldsymbol{t},\text{in}}, \tilde{u}, \mathcal{A}, \mathcal{H})$ is changed by at most i_{thr} in its next update. By construction of the ADA update sequence $\tilde{u}$, after N iterations with $\tilde{u}$ each component of the ADA iterate was updated exactly once (Notation 8.67). Therefore, we have to compare $\boldsymbol{i}^{n_{\max}}(\hat{\boldsymbol{i}}_{\boldsymbol{t},\text{in}}, \tilde{u}, \mathcal{A}, \mathcal{H})$ with $\boldsymbol{i}^{n_{\max}+N}(\hat{\boldsymbol{i}}_{\boldsymbol{t},\text{in}}, \tilde{u}, \mathcal{A}, \mathcal{H})$.

Of course this is only a heuristic. It is neither guaranteed that $\boldsymbol{i}^{n_{\max}+N}(\hat{\boldsymbol{i}}_{\boldsymbol{t},\text{in}}, \tilde{u}, \mathcal{A}, \mathcal{H})$ is close to the real super fixed point vector (if it even exists), nor that Algorithm 5.2 given the inputs $\hat{\boldsymbol{i}}_{\boldsymbol{t},\text{in}}$ and $\tilde{u}$ converges at all. However, this approach worked well in the considered use cases.
In order to formalize this approach and to formulate corresponding constraints, we need a

function that maps an element x of the decision space and a set of feasible test fan speeds T to the Lipschitz constants of the function $A^p_{r_D,\mathcal{A},\mathcal{H}}$, $p \in [N]$.

Definition 8.73 *Let $r_D \geq 0$, let T be a set of feasible test fan speeds and let $\mathcal{H}$ be an HE model. For $p \in [N]$ and $x \in \mathbb{R}^{3N}$, we define the function $\bar{\mathcal{L}}^p_{T,r_D,\mathcal{H}} : \mathbb{R}^{3N} \mapsto \mathbb{R} \cup \{\infty\}$ by*

$$\bar{\mathcal{L}}^p_{T,r_D,\mathcal{H}}(x) := \begin{cases} \text{Lipschitz constant of } A^p_{r_D,\mathcal{A}_T(x),\mathcal{H}} & \text{if } A^p_{r_D,\mathcal{A}_T(x),\mathcal{H}} \text{ is Lipschitzian,} \\ \infty & \text{else.} \end{cases}$$

Remark 8.74 *The function $\bar{\mathcal{L}}^p_{T,r_D,\mathcal{H}}$ is well-defined by construction. The overline notation is used to distinguish it from the function $\mathcal{L}^p_{T,r_D}$ according to Definition 8.17 used in the nominal case.*

With this, we can finally specify constraints such that (S-T1) is "approximately" satisfied.

(C-T1.1) $\left\| \boldsymbol{i}^{n_{\max}}(\hat{\boldsymbol{i}}_{\boldsymbol{t},\text{in}}, \tilde{u}, \mathcal{A}_T(x), \mathcal{H}) - \boldsymbol{i}^{n_{\max}+N}(\hat{\boldsymbol{i}}_{\boldsymbol{t},\text{in}}, \tilde{u}, \mathcal{A}_T(x), \mathcal{H}) \right\|_\infty \leq i_{\text{thr}}$ for all $\mathcal{H} \in \mathcal{U}_{\text{tol}}$.

(C-T1.2) $\bar{\mathcal{L}}^p_{T,r_D,\mathcal{H}}(x) \leq 1 - \varepsilon \ \forall\, p \in [N] \ \forall\, \mathcal{H} \in \mathcal{U}_{\text{tol}}$ (with a certain $\varepsilon > 0$ small but fixed).

Remark 8.75 *With the parameters $n_{\max}$ and i_{thr} a minimum rate of convergence as well as the accuracy of the super fixed point vector approximation are controlled. In the use cases, $n_{\max} = 50N$, i.e., 50 iterations with each ADA pair, and $i_{\text{thr}} = 10^{-4}$ were a good compromise between required computation time and accuracy.*
The components of the super fixed point vector usually have values in the range from 6000 to 8000. Therefore, a difference of $i_{\text{thr}} = 10^{-4}$ usually corresponds to a relative difference of approximately $1.25 \cdot 10^{-8}$ to $1.67 \cdot 10^{-8}$.

Specification (S-T2) We need an indicator for the "quality" of $\boldsymbol{i}^{**}(\mathcal{A}, \mathcal{H})$. For this, the control curve and the λ-target curve are used. Recall from Section 2.3.3 that the control curve maps every feasible fan speed fs $\in$ FS to an ioni current setpoint $i_{\text{set}}(\text{fs})$ and that the corresponding desired equivalence AFR is called λ-target and is denoted by $\lambda_{\text{target}}(\text{fs})$. An exemplary λ-target curve and control curve are shown in Figure 2.7. The control curve is formally defined in Definition 8.30 above.
Furthermore, recall from Sections 3.2.2 and 3.4.2 that the incumbent vector of drifted test ioni current approximations $\hat{\boldsymbol{i}}_{t,r_D}$ is used to correct the control curve for the influence of the drift resistance. For this, let fs $\in$ FS. First, $\hat{\boldsymbol{i}}_{t,r_D}$ is used to approximate the drift resistance at the fan speed fs according to Definition 3.38, i.e., $\hat{r}_D := \alpha_{\hat{\boldsymbol{i}}_{t,r_D}}(\text{fs})$ is determined. The ioni current setpoint $i_{\text{set}}(\text{fs})$ is then corrected by plugging $i_{\text{set}}(\text{fs})$ and $\hat{r}_D$ into (3.10), see also Definition 3.40.
The idea to indicate whether the approximation quality of $\boldsymbol{i}^{**}(\mathcal{A}, \mathcal{H})$ is sufficient is as follows: If the control curve is corrected with $\hat{\boldsymbol{i}}_{t,r_D} = \boldsymbol{i}^{**}(\mathcal{A}, \mathcal{H})$, then the resulting equivalence AFRs are allowed to differ only by a certain fixed tolerance $\lambda_{\text{wp,tol}}$ from $\lambda_{\text{target}}(\text{fs})$ for all fs $\in$ FS and for all $\mathcal{H} \in \mathcal{U}_{\text{tol}}$ [PHE, Item 3280]. A common value used by Vaillant is

$\lambda_{\text{wp,tol}} = 0.1$ [PHE, Item 15500].
For this, we define the λ-working-point function $\lambda_{\text{wp}}(\text{fs}, \hat{\boldsymbol{i}}_{t,r_D}, \mathcal{H})$, whose image corresponds to the equivalence AFR that results from correcting the ioni current setpoint at the fan speed fs with the incumbent vector $\hat{\boldsymbol{i}}_{t,r_D}$ while the HE model $\mathcal{H}$ is considered.

Definition 8.76 *Let $r_D \geq 0$. Let $\mathcal{H} = \big(\text{FS}, (G_{\text{fs}})_{\text{fs}\in\text{FS}}, (\iota_{\text{fs}})_{\text{fs}\in\text{FS}}, (\Lambda_{\text{fs}})_{\text{fs}\in\text{FS}}, (\zeta_{\text{fs}})_{\text{fs}\in\text{FS}}\big)$, $\mathcal{H} \in \mathcal{U}_{\text{tol}}$, be a tolerance HE model and let $i_{\text{set}}(\text{fs})$ be a given control curve. Let $\hat{\boldsymbol{i}}_{t,r_D}$ be an incumbent vector of drifted test ioni current approximations and let $\alpha_{r_D}(\text{fs})$ be the corresponding drift resistance approximation function according to Definition 3.38.*
Let fs $\in$ FS. *The* working point equivalence AFR at the fan speed fs related to r_D, $\hat{\boldsymbol{i}}_{t,r_D}$ and $\mathcal{H}$ *is defined by*

$$\lambda_{\text{wp}}(\text{fs}, \hat{\boldsymbol{i}}_{t,r_D}, \mathcal{H}) \coloneqq \Lambda_{\text{fs}} \circ \iota^{-1}_{\text{fs},r_D}\Big(\frac{U i_{\text{set}}(\text{fs})}{\hat{r}_D\, i_{\text{set}}(\text{fs}) + U}\Big) \text{ with } \hat{r}_D = \alpha_{\hat{\boldsymbol{i}}_{t,r_D}}(\text{fs}). \tag{8.10}$$

Remark 8.77 *The working point equivalence AFR is closely related to the operating point equivalence AFR $\lambda_{\text{op}}(\text{fs}) = \Lambda_{\text{fs}} \circ \iota^{-1}_{\text{fs}} \circ i_{\text{set}}(\text{fs})$ defined in Definition 8.30. In deed, if $\hat{r}_D = r_D$ (and the same $\mathcal{H}$ is considered), then $\lambda_{\text{wp}}(\text{fs}, \hat{\boldsymbol{i}}_{t,r_D}, \mathcal{H}) = \lambda_{\text{op}}(\text{fs})$. By applying Lemmas 6.17 and 6.20, we have*

$$\iota^{-1}_{\text{fs},r_D}(i) = \rho^{-1}_{\text{fs},r_D}\Big(\frac{U}{i}\Big) = \rho^{-1}_{\text{fs}}\Big(\frac{U}{i} - r_D\Big)$$

and thus (with $\hat{r}_D = r_D$)

$$\begin{aligned}\iota^{-1}_{\text{fs},r_D}\Big(\frac{U i_{\text{set}}(\text{fs})}{\hat{r}_D\, i_{\text{set}}(\text{fs}) + U}\Big) &= \rho^{-1}_{\text{fs}}\Big(\frac{\hat{r}_D\, i_{\text{set}}(\text{fs}) + U}{i_{\text{set}}(\text{fs})} - r_D\Big) = \rho^{-1}_{\text{fs}}\Big(\frac{U}{i_{\text{set}}(\text{fs})} + \hat{r}_D - r_D\Big)\\ &= \rho^{-1}_{\text{fs}}\Big(\frac{U}{i_{\text{set}}(\text{fs})}\Big) = \iota^{-1}_{\text{fs}}\big(i_{\text{set}}(\text{fs})\big).\end{aligned}$$

Remark 8.78 *A statement about $\lambda_{\text{wp}}(\text{fs}, \hat{\boldsymbol{i}}_{t,r_D}, \mathcal{H})$ being well-defined is not provided. This is not necessary, because ADA parameters such that evaluating* (8.10) *is not well-defined are considered to be infeasible in the optimization model with tolerances.*

With this, the corresponding condition to satisfy (S-T2) is

$$\big|\lambda_{\text{wp}}(\text{fs}, \hat{\boldsymbol{i}}_{t,r_D}, \mathcal{H}) - \lambda_{\text{target}}(\text{fs})\big| \leq \lambda_{\text{wp,tol}} \;\forall\; \text{fs} \in \text{FS} \;\; \forall\, \mathcal{H} \in \mathcal{U}_{\text{tol}}. \tag{8.11}$$

However, in practice it is usually not possible to check whether (8.11) holds for all fs $\in$ FS, because the function $\lambda_{\text{wp}}(\text{fs}, \hat{\boldsymbol{i}}_{t,r_D}, \mathcal{H})$ is not available in an explicit form in general, nor does it have a certain monotonic behavior in general. Therefore, we have to fall back on a sample set of FS, i.e., we only check for certain fan speed samples whether (8.11) holds. This sample set is denoted by $\text{FS}_{\text{sample}}$ in the following. In the use cases, a sample set with 100 equidistantly distributed points between fs_{min} and fs_{max} worked well.
With this, we have all the parts together to specify a constraint such that (S-T2) is "approximately" satisfied. For this, recall that the super fixed point vector $\boldsymbol{i}^{**}\big(\mathcal{A}_T(x), \mathcal{H}\big)$ is approximated by $\boldsymbol{i}^{n_{\text{max}}+N}\big(\hat{\boldsymbol{i}}_{t,\text{in}}, \tilde{u}, \mathcal{A}_T(x), \mathcal{H}\big)$.

(C-T2) $\Big|\lambda_{\text{wp}}\Big(\text{fs}, \boldsymbol{i}^{n_{\text{max}}+N}\big(\hat{\boldsymbol{i}}_{t,\text{in}}, \tilde{u}, \mathcal{A}_T(x), \mathcal{H}\big), \mathcal{H}\Big) - \lambda_{\text{target}}(\text{fs})\Big| \leq \lambda_{\text{wp,tol}}$ for all fs $\in \text{FS}_{\text{sample}}$ and for all $\mathcal{H} \in \mathcal{U}_{\text{tol}}$.

Specification (S-T3) This specification is related to combustion limits with respect to the CO emission and to the equivalence AFR. The corresponding constraints for the case with tolerances are derived analogously to the nominal case by considering the CO iterates and the λ iterates, see also Section 8.5.2. For this, we adapt the notation of the CO iterates (Definition 8.44) and of the λ iterates (Definition 8.47) such that the dependency on the set of ADA pairs $\mathcal{A}$ and on the HE model $\mathcal{H}$ is reflected. As with all adapted notations in this section, the underlying definitions are not changed. In particular, the statements of Corollaries 8.45 and 8.48 remain valid.

Notation 8.79 *Let $\mathcal{A} := \{(s^p, t^p, i_s^p, i_t^p) : p \in [N]\}$ be a set of N ADA pairs and let $\mathcal{H}$ be an HE model. Furthermore, let $\hat{\boldsymbol{i}}_{\boldsymbol{t},\mathrm{in}}$ be an input vector and let u be an infinite ADA update sequence.*
The corresponding n-th start and test CO iterates according to Definition 8.44 are denoted by $\mathrm{co}_s^n(\hat{\boldsymbol{i}}_{\boldsymbol{t},\mathrm{in}}, u, \mathcal{A}, \mathcal{H})$ and $\mathrm{co}_t^n(\hat{\boldsymbol{i}}_{\boldsymbol{t},\mathrm{in}}, u, \mathcal{A}, \mathcal{H})$, respectively.
The corresponding n-th start and test λ iterates according to Definition 8.47 are denoted by $\lambda_s^n(\hat{\boldsymbol{i}}_{\boldsymbol{t},\mathrm{in}}, u, \mathcal{A}, \langle\rangle)$ and $\lambda_t^n(\hat{\boldsymbol{i}}_{\boldsymbol{t},\mathrm{in}}, u, \mathcal{A}, \mathcal{H})$, respectively.

In contrast to the nominal case, in the case with tolerances it is in general not sufficient to check the combustion limits for certain inputs only. Rather, for each tolerance HE model $\mathcal{H}$, $\mathcal{H} \in \mathcal{U}_{\mathrm{tol}}$, we have to check that $\mathrm{co}_{\max}$ and $\lambda_{\max}$ are never exceeded and that the equivalence AFR never falls below $\lambda_{\min}$ in each ADA iteration. Recall from Remark 8.72 that we are only interested in the first $n_{\max} + N$ ADA iterations. Therefore, it is sufficient to check that the CO and λ iterates are within the specified limits for the first $n_{\max} + N$ iterations. The corresponding constraints are as follows.

(C-T3) For all $\mathcal{H} \in \mathcal{U}_{\mathrm{tol}}$ and for all $n \in [n_{\max} + N]$:

$$\begin{aligned} &\mathrm{co}_s^n\big(\hat{\boldsymbol{i}}_{\boldsymbol{t},\mathrm{in}}, \tilde{u}, \mathcal{A}_T(x), \mathcal{H}\big) \le \mathrm{co}_{\max}, \quad && \mathrm{co}_s^n\big(\hat{\boldsymbol{i}}_{\boldsymbol{t},\mathrm{in}}, \tilde{u}, \mathcal{A}_T(x), \mathcal{H}\big) \le \mathrm{co}_{\max}, \\ &-\lambda_s^n\big(\hat{\boldsymbol{i}}_{\boldsymbol{t},\mathrm{in}}, \tilde{u}, \mathcal{A}_T(x), \mathcal{H}\big) \le -\lambda_{\min}, \quad && \lambda_s^n\big(\hat{\boldsymbol{i}}_{\boldsymbol{t},\mathrm{in}}, \tilde{u}, \mathcal{A}_T(x), \mathcal{H}\big) \le \lambda_{\max}, \\ &-\lambda_t^n\big(\hat{\boldsymbol{i}}_{\boldsymbol{t},\mathrm{in}}, \tilde{u}, \mathcal{A}_T(x), \mathcal{H}\big) \le -\lambda_{\min}, \quad && \lambda_t^n\big(\hat{\boldsymbol{i}}_{\boldsymbol{t},\mathrm{in}}, \tilde{u}, \mathcal{A}_T(x), \mathcal{H}\big) \le \lambda_{\max}. \end{aligned}$$

Specification (S-T4) This specification is related to the set of feasible gas valve positions G_{fs} and to the ioni current functions ι_{fs}, $\mathrm{fs} \in \mathrm{FS}$, of the tolerance HE models $\mathcal{H}$, $\mathcal{H} \in \mathcal{U}_{\mathrm{tol}}$. The corresponding constraints are analogous to (C-S4).

(C-T4) For all $\mathcal{H} = \big(\mathrm{FS}, (G_{\mathrm{fs}})_{\mathrm{fs}\in\mathrm{FS}}, (\iota_{\mathrm{fs}})_{\mathrm{fs}\in\mathrm{FS}}, (\Lambda_{\mathrm{fs}})_{\mathrm{fs}\in\mathrm{FS}}, (\zeta_{\mathrm{fs}})_{\mathrm{fs}\in\mathrm{FS}}\big) \in \mathcal{U}_{\mathrm{tol}}$ and for all ADA pairs $(s^p, t^p, i_s^p, i_t^p) \in \mathcal{A}_T(x)$, $p \in [N]$:

$$\begin{aligned} &\min \iota_{s^p}(G_{s^p}) - i_s^p \le 0, \quad -\max \iota_{s^p}(G_{s^p}) + i_s^p \le 0 \quad \text{and} \\ &\min \iota_{t^p}(G_{t^p}) - i_t^p \le 0, \quad -\max \iota_{t^p}(G_{t^p}) + i_t^p \le 0. \end{aligned}$$

8.7.5. Feasible Set

As stated at the beginning of Section 8.7.2, the objective criteria (O1) to (O3) as well as the specifications (S1) to (S7) from the nominal case must still be satisfied with respect

to the nominal HE model. Therefore, regarding the nominal HE model $\mathcal{H}_{\text{nom}}$ the feasible sets X^p_{T,r_D}, $p \in [N]$, from (nom-P^p_{T,r_D}) are reused. To make clear that the sets X^p_{T,r_D}, $p \in [N]$ refer to a certain HE model the following notation is introduced.

Notation 8.80 *Let $\mathcal{H} = \big(\text{FS}, (G_{\text{fs}})_{\text{fs}\in\text{FS}}, (\iota_{\text{fs}})_{\text{fs}\in\text{FS}}, (\Lambda_{\text{fs}})_{\text{fs}\in\text{FS}}, (\zeta_{\text{fs}})_{\text{fs}\in\text{FS}}\big)$ be an HE model and let $p \in [N]$. We denote by $X^p_{T,r_D}(\mathcal{H})$ the situation where the functions Λ_{fs}, ι_{fs} and ζ_{fs} of $\mathcal{H}$ specify the considered feasible set X^p_{T,r_D} according to Definition 8.52.*

With this, we have all the parts together to define the set of feasible solutions for the optimization model with tolerances.

Definition 8.81 *Let $N \in \mathbb{N}$ be fixed. Let $T = \{t^1, \dots, t^N\}$ be a set of feasible test fan speeds and let $r_D \geq 0$. Let λ_{min}, λ_{max}, co_{max}, $\Delta\lambda_{\text{min}}$, $\lambda_{\text{wp,tol}}$, n_{max}, i_{thr} and $\text{FS}_{\text{sample}}$ be the combustion limits and approximation parameters specified by the decision makers. Let $\mathcal{H}_{\text{nom}}$ be a nominal HE model and let $\mathcal{U}_{\text{tol}}$ be a collection of k tolerance HE models, $k \in \mathbb{N}_0$. Furthermore, let $\hat{\boldsymbol{i}}_{\boldsymbol{t},\text{in}} = (i_t^1, \dots, i_t^N)$ and let $\tilde{u} = (1, \dots, N, 1 \dots, N, \dots)$ be the periodic ADA update sequence as defined in Notation 8.67.*
The corresponding set of feasible solutions with respect to tolerances, *which is denoted by $X^{\text{tol}}_{T,r_D}(\mathcal{H}_{\text{nom}}, \mathcal{U}_{\text{tol}})$, is defined as the set of all vectors*

$$x = (s^1, i_s^1, i_t^1, \dots, s^N, i_s^N, i_t^N) \in \mathbb{R}^{3N}$$

such that all of the following constraints are satisfied:

(C-R1) – (C-R3) *and* (C-S1) – (C-S7) $\quad (s^p, i_s^p, i_t^p) \in X^p_{T,r_D}(\mathcal{H}_{\text{nom}})\ \forall\ p \in [N]$

and for all $\mathcal{H} \in \mathcal{U}_{\text{tol}}$:

(C-T1.1) $\quad \big\| \boldsymbol{i}^{n_{\text{max}}}(\hat{\boldsymbol{i}}_{\boldsymbol{t},\text{in}}, \tilde{u}, \mathcal{A}_T(x), \mathcal{H}) - \boldsymbol{i}^{n_{\text{max}}+N}(\hat{\boldsymbol{i}}_{\boldsymbol{t},\text{in}}, \tilde{u}, \mathcal{A}_T(x), \mathcal{H}) \big\|_\infty \leq i_{\text{thr}},$

(C-T1.2) $\quad \bar{\mathcal{L}}^p_{T,r_D,\mathcal{H}}(x) \leq 1 - \varepsilon\ \forall\ p \in [N] \quad (\varepsilon > 0 \text{ small but fixed}),$

(C-T2) $\quad \Big| \lambda_{\text{tol}}\Big(\text{fs}, \boldsymbol{i}^{n_{\text{max}}+N}\big(\hat{\boldsymbol{i}}_{\boldsymbol{t},\text{in}}, \tilde{u}, \mathcal{A}_T(x), \mathcal{H}\big), \mathcal{H}\Big) - \lambda_{\text{target}}(\text{fs}) \Big| \leq \lambda_{\text{wp,tol}}\ \forall\ \text{fs} \in \text{FS}_{\text{sample}},$

(C-T3) $\quad \text{co}^n_k\big(\hat{\boldsymbol{i}}_{\boldsymbol{t},\text{in}}, \tilde{u}, \mathcal{A}_T(x), \mathcal{H}\big) \leq \text{co}_{\text{max}}\ \forall\ n \in [n_{\text{max}} + N],\ k \in \{s, t\},$
$\quad -\lambda^n_k\big(\hat{\boldsymbol{i}}_{\boldsymbol{t},\text{in}}, \tilde{u}, \mathcal{A}_T(x), \mathcal{H}\big) \leq -\lambda_{\text{min}}\ \forall\ n \in [n_{\text{max}} + N],\ k \in \{s, t\},$
$\quad \lambda^n_k\big(\hat{\boldsymbol{i}}_{\boldsymbol{t},\text{in}}, \tilde{u}, \mathcal{A}_T(x), \mathcal{H}\big) \leq \lambda_{\text{max}}\ \forall\ n \in [n_{\text{max}} + N],\ k \in \{s, t\},$

(C-T4) $\quad \min \iota_{k^p}(G_{k^p}) - i^p_k \leq 0\ \forall\ p \in [N], k \in \{s, t\},$
$\quad -\max \iota_{k^p}(G_{k^p}) + i^p_k \leq 0\ \forall\ p \in [N], k \in \{s, t\}.$

With the set of feasible solutions defined, we detail the objective functions next.

8.7.6. Objective Functions

As delineated at the end of Section 8.7.1, the decision makers argue that optimal convergence characteristics of the ADA pairs with the nominal HE model is most important.

They do not want to improve convergence characteristics with tolerance HE models at the prize of worsened convergence characteristics for the nominal HE model. Therefore, the objective functions remain unchanged, i.e., we minimize the Lipschitz constant of $A^p_{r_D}$ and the start point increment $\lambda^p_{s,\text{incr}}$ of each ADA pair p, $p \in [N]$, with respect to the nominal HE model $\mathcal{H}_{\text{nom}}$.
However, because we cannot consider the ADA pairs individually anymore, we have to minimize both objective functions for all N ADA pairs simultaneously, i.e., we have $2N$ objective functions and not two as in (nom-P^p_{T,r_D}). Furthermore, we have to slightly modify the definitions of the objective functions $\mathcal{L}^p_{T,r_D}$ (Definition 8.17) and $\mathcal{S}^p_{T,r_D}$ (Definition 8.59) to make them compatible with the feasible set with respect to tolerances $X^{\text{tol}}_{T,r_D}(\mathcal{H}_{\text{nom}}, \mathcal{U}_{\text{tol}})$.

Definition 8.82 *For $x = (s^1, i_s^1, i_t^1, \ldots, s^N, i_s^N, i_t^N) \in X^{\text{tol}}_{T,r_D}(\mathcal{H}_{\text{nom}}, \mathcal{U}_{\text{tol}})$ and $p \in [N]$, we define*

$$\overline{\mathcal{L}}^p_{T,r_D}(x) \coloneqq \mathcal{L}^p_{T,r_D}(s^p, i_s^p, i_t^p) \quad \text{and} \quad \overline{\mathcal{S}}^p_{T,r_D}(x) \coloneqq \mathcal{S}^p_{T,r_D}(s^p, i_s^p, i_t^p),$$

where $\mathcal{L}^p_{T,r_D}$ and $\mathcal{S}^p_{T,r_D}$ are related to the nominal HE model $\mathcal{H}_{\text{nom}}$.

Lemma 8.83 *The functions $\overline{\mathcal{L}}^p_{T,r_D}$ and $\overline{\mathcal{S}}^p_{T,r_D}$ are well-defined for all $p \in [N]$.*

Proof. Let $x = (s^1, i_s^1, i_t^1, \ldots, s^N, i_s^N, i_t^N) \in X^{\text{tol}}_{T,r_D}(\mathcal{H}_{\text{nom}}, \mathcal{U}_{\text{tol}})$. By construction, we have $(s^p, i_s^p, i_t^p) \in X^p_{T,r_D}(\mathcal{H}_{\text{nom}})$ for all $p \in [N]$ (Definition 8.81). Because $X^p_{T,r_D}(\mathcal{H}_{\text{nom}})$ is the domain of $\mathcal{S}^p_{T,r_D}$ (Definition 8.59) and $\mathbb{R}^3$ is the domain of $\mathcal{L}^p_{T,r_D}$ (Definition 8.17), $\overline{\mathcal{L}}^p_{T,r_D}(x)$ and $\overline{\mathcal{S}}^p_{T,r_D}(x)$ are well-defined for all $p \in [N]$. □

With this, we can finally formulate the ADA optimization model with respect to tolerances.

8.7.7. The Optimization Model with Respect to Tolerances

The proposed optimization model to optimize the ADA parameters with respect to tolerances is as follows.

Definition 8.84 *Let $N \in \mathbb{N}$ be fixed. Let $T = \{t^1, \ldots, t^N\}$ be a set of feasible test fan speeds and let $r_D \geq 0$. Let λ_{min}, λ_{max}, co_{max}, $\Delta\lambda_{\text{min}}$, $\lambda_{\text{wp,tol}}$, n_{max}, i_{thr} and $\text{FS}_{\text{sample}}$ be the combustion limits and approximation parameters specified by the decision makers. Let $\mathcal{H}_{\text{nom}}$ be a nominal HE model and let $\mathcal{U}_{\text{tol}}$ be a collection of k tolerance HE models, $k \in \mathbb{N}_0$.*
The corresponding ADA optimization problem with respect to tolerances *is defined by*

$$\min_{x \in X^{\text{tol}}_{T,r_D}(\mathcal{H}_{\text{nom}}, \mathcal{U}_{\text{tol}})} f^{\text{tol}}(x) \coloneqq \left(f_1^{\text{tol}}(x), \ldots, f_{2N}^{\text{tol}}(x)\right) \qquad \text{(tol-}P_{T,r_D}\text{)}$$

with

$$f_k^{\text{tol}}(x) \coloneqq \begin{cases} \overline{\mathcal{L}}^k_{T,r_D}(x) & \text{if } k \in \{1, \ldots, N\} \\ \overline{\mathcal{S}}^{(k-N)}_{T,r_D}(x) & \text{if } k \in \{N+1, \ldots, 2N\}. \end{cases}$$

Remark 8.85 *Note that the order of the objective functions is irrelevant with respect to Pareto optimality.*

A method how to approximate the Pareto front of (tol-P_{T,r_D}) is proposed in the following Chapter 9. But before that, the differences and similarities between the two optimization models (nom-P^p_{T,r_D}) and (tol-P_{T,r_D}) are briefly discussed.

8.8. Comparison of the Two Optimization Models

Let us suppose that we want to optimize N ADA pairs. Because the super fixed point vector has to be determined with the recursion according to Definition 7.14 in the case of tolerances, we cannot decouple the ADA pairs in the optimization model with tolerances (tol-P_{T,r_D}). Accordingly, the problem (tol-P_{T,r_D}) is much more complex than (nom-P^p_{T,r_D}). In (tol-P_{T,r_D}), the decision space is $3N$-dimensional and the objective space is $2N$-dimensional. In contrast, the decision space and the objective space of the problems (nom-P^p_{T,r_D}) are three-dimensional and two-dimensional, respectively, for $p \in [N]$. However, we have to solve the problem (nom-P^p_{T,r_D}) for all $p \in [N]$, i.e., we have to solve N biobjective optimization problems in the nominal case.
The totality of all N problems (nom-P^p_{T,r_D}), $p \in [N]$, can be interpreted as a special case of the more complex problem (tol-P_{T,r_D}). If the uncertainty set $\mathcal{U}_{\text{tol}}$ is empty, i.e., if we only have a nominal HE model but no tolerance HE models, then every combination of exactly one Pareto optimal solution from each (nom-P^p_{T,r_D}), $p \in [N]$, can be combined to a Pareto optimal solution of (tol-P_{T,r_D}) and vice versa.
For this, we first show that the Pareto optimal solutions of (nom-P^p_{T,r_D}) and (tol-P_{T,r_D}) correspond to each other in a certain sense if $\mathcal{U}_{\text{tol}} = \emptyset$.

Lemma 8.86 *Let a nominal HE model $\mathcal{H}_{\text{nom}}$ be given and let $\mathcal{U}_{\text{tol}} = \emptyset$. Furthermore, let $T = \{t^1, \dots, t^N\}$ be a set of feasible test fan speeds and let $r_D \geq 0$. Let $X^{\text{tol}}_{T,r_D}(\mathcal{H}_{\text{nom}}, \mathcal{U}_{\text{tol}})$ be the corresponding feasible set with respect to tolerances. Then,*

$$(s^p, i_s^p, i_t^p) \in X^p_{T,r_D}(\mathcal{H}_{\text{nom}}) \ \forall\ p \in [N] \ \Leftrightarrow\ (s^1, i_s^1, i_t^1, \dots, s^N, i_s^N, i_t^N) \in X^{\text{tol}}_{T,r_D}(\mathcal{H}_{\text{nom}}, \mathcal{U}_{\text{tol}}).$$

Proof. The statement follows from the constraint $(s^p, i_s^p, i_t^p) \in X^p_{T,r_D}(\mathcal{H}_{\text{nom}})$ for all $p \in [N]$ in Definition 8.81 and from the fact that the remaining constraints (C-T1.1) to (C-T4) in Definition 8.81 do not apply in the case $\mathcal{U}_{\text{tol}} = \emptyset$. □

With this, we can show that the totality of Pareto optimal solutions of (nom-P^p_{T,r_D}), $p \in [N]$, and the Pareto optimal solutions of (tol-P_{T,r_D}) correspond to each other in the case $\mathcal{U}_{\text{tol}} = \emptyset$.

Theorem 8.87 *Let a nominal HE model $\mathcal{H}_{\text{nom}}$ be given and let $\mathcal{U}_{\text{tol}} = \emptyset$. Furthermore, let $T = \{t^1, \dots, t^N\}$ be a set of feasible test fan speeds and let $r_D \geq 0$.*
If (nom-P^p_{T,r_D}) *is related to $\mathcal{H}_{\text{nom}}$ for all $p \in [N]$ and* (tol-P_{T,r_D}) *is related to $\mathcal{H}_{\text{nom}}$ as well as to $\mathcal{U}_{\text{tol}}$, then the following two statements are equivalent:*

1. $x^{p,*} = (s^{p,*}, i_s^{p,*}, i_t^{p,*})$ *is Pareto optimal with respect to* (nom-P^p_{T,r_D}) $\forall\ p \in [N]$.

2. $x^* = (s^{1,*}, i_s^{1,*}, i_t^{1,*}, \ldots, s^{N,*}, i_s^{N,*}, i_t^{N,*})$ *is Pareto optimal with respect to* (tol-P_{T,r_D}).

Proof. "1. $\Rightarrow$ 2." For all $p \in [N]$ let $x^{p,*} = (s^{p,*}, i_s^{p,*}, i_t^{p,*})$ be Pareto optimal with respect to (nom-P^p_{T,r_D}). Let $x^* := (s^{1,*}, i_s^{1,*}, i_t^{1,*}, \ldots, s^{N,*}, i_s^{N,*}, i_t^{N,*})$. According to Lemma 8.86, $x^* \in X^{\text{tol}}_{T,r_D}(\mathcal{H}_{\text{nom}}, \mathcal{U}_{\text{tol}})$, i.e., x^* is feasible with respect to (tol-P_{T,r_D}).
Let us suppose that x^* is not Pareto optimal with respect to (tol-P_{T,r_D}). Then, there exists $\bar{x} = (\bar{s}^1, \bar{i}_s^1, \bar{i}_t^1, \ldots, \bar{s}^N, \bar{i}_s^N, \bar{i}_t^N) \in X^{\text{tol}}_{T,r_D}(\mathcal{H}_{\text{nom}}, \mathcal{U}_{\text{tol}})$ such that $f^{\text{tol}}(\bar{x}) \leq f^{\text{tol}}(x^*)$, i.e., $f_i^{\text{tol}}(\bar{x}) \leq f_i^{\text{tol}}(x^*)$ for all $i \in [2N]$ and there exists $j \in [2N]$ such that $f_j^{\text{tol}}(\bar{x}) < f_j^{\text{tol}}(x^*)$. Without loss of generality, let $j = 1$. Then, $f_1^{\text{tol}}(\bar{x}) < f_1^{\text{tol}}(x^*)$ and $f_{N+1}^{\text{tol}}(\bar{x}) \leq f_{N+1}^{\text{tol}}(x^*)$. According to Definitions 8.84 and 8.82, we have

$$\mathcal{L}^1_{T,r_D}(\bar{s}^1, \bar{i}_s^1, \bar{i}_t^1) < \mathcal{L}^1_{T,r_D}(s^{1,*}, i_s^{1,*}, i_t^{1,*}) \quad \text{and} \quad \mathcal{S}^1_{T,r_D}(\bar{s}^1, \bar{i}_s^1, \bar{i}_t^1) \leq \mathcal{S}^1_{T,r_D}(s^{1,*}, i_s^{1,*}, i_t^{1,*}).$$

Because $\bar{x}^1 := (\bar{s}^1, \bar{i}_s^1, \bar{i}_t^1) \in X^1_{T,r_D}$ (Lemma 8.86), this implies $f^{\text{nom},1}(\bar{x}^1) \leq f^{\text{nom},1}(x^{1,*})$ (Definition 8.61). This is a contradiction to $x^{1,*}$ being Pareto optimal with respect to (nom-P^p_{T,r_D}) with $p = 1$. Thus, x^* has to be Pareto optimal with respect to (tol-P_{T,r_D}).
"2. $\Rightarrow$ 1." Let $x^* := (s^{1,*}, i_s^{1,*}, i_t^{1,*}, \ldots, s^{N,*}, i_s^{N,*}, i_t^{N,*})$ be Pareto optimal with respect to (tol-P_{T,r_D}). Then, $x^{p,*} := (s^{p,*}, i_s^{p,*}, i_t^{p,*}) \in X^p_{T,r_D}$ for all $p \in [N]$ (Lemma 8.86).
Let us suppose that there exists $p \in [N]$ such that $x^{p,*}$ is not Pareto optimal with respect to (nom-P^p_{T,r_D}). Without loss of generality, let $p = 1$. Then, there exists $\bar{x}^1 = (\bar{s}^1, \bar{i}_s^1, \bar{i}_t^1) \in X^1_{T,r_D}$ such that $f^{\text{nom},1}(\bar{x}^1) \leq f^{\text{nom},1}(x^{1,*})$. We set

$$\bar{x} := (\bar{s}^1, \bar{i}_s^1, \bar{i}_t^1, s^{2,*}, i_s^{2,*}, i_t^{2,*}, \ldots, s^{N,*}, i_s^{N,*}, i_t^{N,*}).$$

Then, $\bar{x} \in X^{\text{tol}}_{T,r_D}(\mathcal{H}_{\text{nom}}, \mathcal{U}_{\text{tol}})$ (Lemma 8.86) and $f^{\text{tol}}(\bar{x})$ is well-defined. By construction, and because $f^{\text{nom},1}(\bar{x}^1) \leq f^{\text{nom},1}(x^{1,*})$, we have $f_i^{\text{tol}}(\bar{x}) \leq f_i^{\text{tol}}(x^*)$ for all $i \in [2N]$. Furthermore, by considering Definitions 8.61, 8.82 and 8.84 as well as $f^{\text{nom},1}(\bar{x}^1) \leq f^{\text{nom},1}(x^{1,*})$, we have $f_1^{\text{tol}}(\bar{x}) < f_1^{\text{tol}}(x^*)$ or $f_{N+1}^{\text{tol}}(\bar{x}) < f_{N+1}^{\text{tol}}(x^*)$. In total, $\bar{x}$ dominates x^*. This is a contradiction to x^* being Pareto optimal with respect to (tol-P_{T,r_D}) and thus $x^{p,*} = (s^{p,*}, i_s^{p,*}, i_t^{p,*})$ has to be Pareto optimal with respect to (nom-P^p_{T,r_D}) for all $p \in [N]$. □

This concludes the chapter on modeling the optimization of the ADA parameters. In the following chapter, two methods to approximate the Pareto fronts of the ADA optimization problems are proposed, one for (nom-P^p_{T,r_D}) and one for (tol-P_{T,r_D}).

9. Solving the ADA Optimization Problems

In this chapter, algorithms to solve the problems (nom-P^p_{T,r_D}) and (tol-P_{T,r_D}) are proposed. Recall that both problems are multiobjective optimization problems. In the book *Multiobjective Optimization* [Bra+08], several desirable properties of multiobjective optimization methods are listed. Among others, "the method should generate Pareto optimal solutions reliably, it should help the DM to get an overview of the set of Pareto optimal solutions, it should not require too much time from the DM ... and the method should support the DM in finding the most preferred solution as the final one so that the DM could be convinced of its relative goodness." [Bra+08, p. 2]. These requirements were kept in mind when developing and selecting the algorithms presented in this chapter.
Two common approaches in multiobjective optimization are *a priori* methods and *a posteriori* methods [Bra+08, p. 3]: "In a priori methods, the DM first articulates preference information and one's aspirations and then the solution process tries to find a Pareto optimal solution satisfying them as well as possible. This is a straightforward approach but the difficulty is that the DM does not necessarily know the possibilities and limitations of the problem beforehand and may have too optimistic or pessimistic expectations." In contrast, in a posteriori methods "a representation of the set of Pareto optimal solutions is first generated and then the DM is supposed to select the most preferred one among them" [Bra+08, p. 3]. The a posteriori approach has the advantage that the DMs have the information about the trade-offs between different solutions available and can select the best compromise according to their preferences. However, "if there are more than two objectives in the problem, it may be difficult for the DM to analyze the large amount of information ... and, on the other hand, generating the set of Pareto optimal solutions may be computationally expensive." [Bra+08, p. 3].
Because the DMs are interested in the trade-off information and they cannot specify aspiration levels in advance, only the a posteriori approach is considered here. Therefore, we are interested in finding good representations of the sets of Pareto optimal solutions of (nom-P^p_{T,r_D}) and (tol-P_{T,r_D}) [Bra+08, p. 15].

9.1. Solving the Nominal ADA Optimization Problem

The problem (nom-P^p_{T,r_D}) is a constrained, continuous, nonlinear, biobjective optimization problem. Furthermore, we have to consider the following aspects.

- In general, the Pareto front of (nom-P^p_{T,r_D}) is not convex, which is demonstrated in Subsection 9.1.4 below.

- Multimodality cannot be excluded.

- Depending on the regression/interpolation method used for the HE model, the objective functions and the constraints of (nom-P^p_{T,r_D}) are not differentiable everywhere in general. For instance, this is the case if an interpolation method is used that is based on a piecewise linear interpolation. Even if the HE model consists of differentiable functions, the objective functions and the constraints will usually be not available as an analytical expressions. Rather, they can be considered as black box functions. Therefore, a symbolic differentiation or automatic differentiation of the functions is not possible in general. However, numerical differentiation by finite differences can usually be applied.

Taking all these aspects into account, only derivative-free methods are investigated, i.e., gradient-based methods are not considered in this work.

Two common derivative-free approaches in multiobjective optimization are direct search methods and evolutionary multiobjective optimization algorithms [CEM12, p. 3]. Another common approach to solve multiobjective optimization problems, which can be combined with derivative-free methods, is based on scalarization [Eic21, p. 3]. As delineated in Section 4.1, a scalarization combines all objective functions of a multiobjective problem into a single objective function.
Two of the most popular scalarization methods are the weighted-sum scalarization and the ε-constraint scalarization [Eic21, p. 4]. Both methods are introduced and discussed in Sections 4.1.2 and 4.1.3, respectively. As stated in Remark 4.23, the weighted-sum scalarization generally does not find all Pareto optimal solutions if the multiobjective optimization problem is nonconvex. Because the Pareto front of (nom-P^p_{T,r_D}) is not convex in general, the weighted-sum scalarization is not used in this work. In contrast, the ε-constraint scalarization can find Pareto optimal solutions in the nonconvex part of the Pareto front. However, a difficulty with the ε-constraint scalarization is to chose suitable ε-vectors [Deb01, p. 58], [Eic21, p. 13]. The ε-vectors must be selected such that their components are within the corresponding objective functions' minimum and maximum value. In particular, with an increased number of objectives it might become more difficult to specify suitable ε-vectors [Deb01, p. 58].
In the course of this section, we show that the biobjective problem (nom-P^p_{T,r_D}) has a certain structure, which allows to specify tight bounds for its second objective function. With this, a combination of a simple direct search method and a modified ε-constraint scalarization is proposed to solve (nom-P^p_{T,r_D}), which is presented in the following.

9.1.1. Idea Behind the Proposed Method to Solve (nom-P^p_{T,r_D})

The idea behind the proposed algorithm to solve (nom-P^p_{T,r_D}) is based on two observations. For this, let $p \in [N]$. Recall that for a given set of feasible test fan speeds T and a drift

resistance $r_D \geq 0$ the feasible set to optimize ADA pair p is X^p_{T,r_D} according to Definition 8.52. I.e., the decision space is three-dimensional with the three decision variables s^p, i^p_s and i^p_t.
The first observation is that as soon as the start fan speed s^p and one of the two ioni currents are selected, the remaining ioni current follows from the feasibility condition $\iota^{-1}_{s^p}(i^p_s) = \iota^{-1}_{t^p}(i^p_t)$ according to (C-R1) in Definition 8.52. We have

$$s^p \text{ and } i^p_s \text{ given } \Rightarrow\ i^p_t = \iota_{t^p} \circ \iota^{-1}_{s^p}(i^p_s) \quad \text{as well as} \quad s^p \text{ and } i^p_t \text{ given } \Rightarrow\ i^p_s = \iota_{s^p} \circ \iota^{-1}_{t^p}(i^p_t). \tag{9.1}$$

It is therefore possible to consider a two-dimensional search space, even though the decision space is three-dimensional.
The second observation is related to the second objective function of (nom-P^p_{T,r_D}). Recall from Definitions 8.59 and 8.61 that for $x = (s^p, i^p_s, i^p_t) \in X_{T,r_D}$, we have

$$\begin{aligned} f_2^{\text{nom},p}(x) = \mathcal{S}^p_{T,r_D}(s^p, i^p_s, i^p_t) &= \Lambda_{s^p}\big(\iota^{-1}_{t^p}(i^p_t)\big) - \Lambda_{s^p}\Big(\iota^{-1}_{s^p}\big(i_{\text{set}}(s^p)\big)\Big) \\ &= \Lambda_{s^p}\big(\iota^{-1}_{s^p}(i^p_s)\big) - \Lambda_{s^p}\Big(\iota^{-1}_{s^p}\big(i_{\text{set}}(s^p)\big)\Big), \end{aligned} \tag{9.2}$$

where the second line follows from the feasibility condition $\iota^{-1}_{s^p}(i^p_s) = \iota^{-1}_{t^p}(i^p_t)$. According to (9.2), the second objective function depends on s^p and i^p_s only, i.e., it is independent of t^p and i^p_t. Furthermore, because Λ_{s^p} is a homeomorphism, the corresponding start ioni current $x_2 = i^p_s$ can be calculated from $x_1 = s^p$ and from the function value $f_2^{\text{nom},p}(x)$. This allows us to define a two-dimensional set whose components are the start fan speed and the start point increment that is equivalent to X^p_{T,r_D} in the sense that there exists a bijection between the two-dimensional set and X^p_{T,r_D}. This is formalized in the following definition. Because the second objective function corresponds to the start point increment, its function value is denoted by $\lambda^p_{s,\text{incr}}$ in the following, see also Definition 8.33 above.

Definition 9.1 *Let $p \in [N]$ and let a set of feasible test fan speeds T as well as a drift resistance $r_D \geq 0$ be given. The corresponding* set of feasible start points *is defined by*

$$X^{p,s}_{T,r_D} := \big\{(s^p, \lambda^p_{s,\text{incr}}) \in \mathbb{R}^2 : \exists\, x = (s^p, i^p_s, i^p_t) \in X^p_{T,r_D} \text{ s.t. } f_2^{\text{nom},p}(x) = \lambda^p_{s,\text{incr}}\big\}.$$

The corresponding transformation function is defined by

$$\tau^p : X^p_{T,r_D} \to X^{p,s}_{T,r_D}, \quad x = (s^p, i^p_s, i^p_t) \mapsto \big(s^p, f_2^{\text{nom},p}(x)\big).$$

Lemma 9.2 *The set $X^{p,s}_{T,r_D}$ and the function τ^p are well-defined. Furthermore, τ^p is bijective. If $x = (\tau^p)^{-1}(s^p, \lambda^p_{s,\text{incr}})$, then*

$$x_1 = s^p, \quad x_2 = \iota_{s^p} \circ \Lambda^{-1}_{s^p}\Big(\lambda^p_{s,\text{incr}} + \Lambda_{s^p}\Big(\iota^{-1}_{s^p}\big(i_{\text{set}}(s^p)\big)\Big)\Big) \quad \text{and} \quad x_3 = \iota_{t^p} \circ \iota^{-1}_{s^p}(x_2) \tag{9.3}$$

for all $(s^p, \lambda_{s,\text{incr}}) \in X^{p,s}_{T,r_D}$.

Proof. According to Definitions 8.59 and 8.61, the set X^p_{T,r_D} is the domain of the second objective function $f_2^{\text{nom},p}$. In particular, $f_2^{\text{nom},p}$ is well-defined (Lemma 8.60). Therefore, $X^{p,s}_{T,r_D}$ and τ^p are well-defined. Next, we show that τ^p is bijective.
Surjective: τ^p is surjective by construction of the set $X^{p,s}_{T,r_D}$.
Injective: Let $x^1 = (s^{p,1}, i_s^{p,1}, i_t^{p,1})$ and $x^2 = (s^{p,2}, i_s^{p,2}, i_t^{p,2})$ such that $x^1, x^2 \in X^p_{T,r_D}$ and $\tau^p(x^1) = \tau^p(x^2)$. Then, we have $s^{p,1} = s^{p,2}$ and $f_2^{\text{nom},p}(x^1) = f_2^{\text{nom},p}(x^2)$. By applying (9.2), we have

$$\Lambda_{s^{p,1}}\big(\iota^{-1}_{s^{p,1}}(i_s^{p,1})\big) - \Lambda_{s^{p,1}}\Big(\iota^{-1}_{s^{p,1}}\big(i_{\text{set}}(s^{p,1})\big)\Big) = \Lambda_{s^{p,2}}\big(\iota^{-1}_{s^{p,2}}(i_s^{p,2})\big) - \Lambda_{s^{p,2}}\Big(\iota^{-1}_{s^{p,2}}\big(i_{\text{set}}(s^{p,2})\big)\Big).$$

With additional consideration of $s^{p,1} = s^{p,2}$, we obtain

$$\begin{aligned} s^{p,1} = s^{p,2} &\Rightarrow \Lambda_{s^{p,1}}\Big(\iota^{-1}_{s^{p,1}}\big(i_{\text{set}}(s^{p,1})\big)\Big) = \Lambda_{s^{p,2}}\Big(\iota^{-1}_{s^{p,2}}\big(i_{\text{set}}(s^{p,2})\big)\Big) \\ &\Rightarrow \Lambda_{s^{p,1}}\big(\iota^{-1}_{s^{p,1}}(i_s^{p,1})\big) = \Lambda_{s^{p,2}}\big(\iota^{-1}_{s^{p,2}}(i_s^{p,2})\big) \\ &\Rightarrow i_s^{p,1} = i_s^{p,2}, \end{aligned}$$

where the last implication follows from the fact that $\Lambda_{s^{p,1}}$ and $\iota_{s^{p,1}}$ are bijections.
Finally, by applying (9.1), we have

$$i_t^{p,1} = \iota_{t^p} \circ \iota^{-1}_{s^{p,1}}(i_s^{p,1}) = \iota_{t^p} \circ \iota^{-1}_{s^{p,2}}(i_s^{p,2}) = i_t^{p,2}.$$

In total, $x^1 = x^2$ holds and τ^p is injective.
It remains to show that (9.3) is correct. Let $(s^p, \lambda^p_{s,\text{incr}}) \in X^{p,s}_{T,r_D}$. Because τ^p is bijective, there exists a unique $x = (s^p, i_s^p, i_t^p) \in X^p_{T,r_D}$ such that $f_2^{\text{nom},p}(x) = \lambda^p_{s,\text{incr}}$. Note that $x_1 = s^p$ by construction. By applying (9.2), we have

$$\begin{aligned} & f_2^{\text{nom},p}(x) = f_2^{\text{nom},p}\big((s^p, i_s^p, i_t^p)\big) = \Lambda_{s^p}\big(\iota^{-1}_{s^p}(i_s^p)\big) - \Lambda_{s^p}\Big(\iota^{-1}_{s^p}\big(i_{\text{set}}(s^p)\big)\Big) = \lambda^p_{s,\text{incr}} \\ \Leftrightarrow\ & x_2 = i_s^p = \iota_{s^p} \circ \Lambda^{-1}_{s^p}\Big(\lambda^p_{s,\text{incr}} + \Lambda_{s^p}\Big(\iota^{-1}_{s^p}\big(i_{\text{set}}(s^p)\big)\Big)\Big). \end{aligned}$$

Finally, $x_3 = i_t^p = \iota_{t^p} \circ \iota^{-1}_{s^p}(i_s^p)$ follows from (9.1). □

With this, we can reformulate (nom-P^p_{T,r_D}) to an optimization problem that is in a certain sense equivalent but less complex, which is thus called the simplified nominal model. For this, we define two objective functions that correspond to the nominal objective functions $f_1^{\text{nom},p}$ and $f_2^{\text{nom},p}$ but that have the domain $X^{p,s}_{T,r_D}$ instead of X^p_{T,r_D}.

Definition 9.3 *Let $T = \{t^1, \dots, t^N\}$ be a set of feasible test fan speeds and let $r_D \geq 0$. For $p \in [N]$, we define*

$$f_1^{\text{sim},p} : X^{p,s}_{T,r_D} \to \mathbb{R}, \quad f_1^{\text{sim},p}(s^p, \lambda^p_{s,\text{incr}}) := f_1^{\text{nom},p} \circ (\tau^p)^{-1}(s^p, \lambda^p_{s,\text{incr}}),$$

$$f_2^{\text{sim},p} : X^{p,s}_{T,r_D} \to \mathbb{R}, \quad f_2^{\text{sim},p}(s^p, \lambda^p_{s,\text{incr}}) := \lambda^p_{s,\text{incr}}$$

and

$$f^{\text{sim},p} : X^{p,s}_{T,r_D} \to \mathbb{R}^2, \quad f^{\text{sim},p} := \big(f_1^{\text{sim},p}, f_2^{\text{sim},p}\big).$$

Lemma 9.4 *Let $T = \{t^1, \dots, t^N\}$ be a set of feasible test fan speeds, let $r_D \geq 0$ and let $p \in [N]$. Then,*

$$f^{\text{nom},p} = f^{\text{sim},p} \circ \tau^p \quad \textit{and} \quad f^{\text{sim},p} = f^{\text{nom},p} \circ (\tau^p)^{-1}.$$

In particular, the functions $f_1^{\text{sim},p}$, $f_2^{\text{sim},p}$ and $f^{\text{sim},p}$ are well-defined.

Proof. That $f_1^{\text{sim},p}$ is well-defined follows from the facts that $(\tau^p)^{-1} : X_{T,r_D}^{p,s} \to X_{T,r_D}^{p}$ is well-defined and that X_{T,r_D}^{p} is the domain of $f_1^{\text{nom},p}$. The function $f_2^{\text{sim},p}$ is the second projection map, which is well-defined even on $\mathbb{R}^2$. With this, $f^{\text{sim},p}$ is also well-defined.
Next, we show component-wise that $f^{\text{sim},p} = f^{\text{nom},p} \circ (\tau^p)^{-1}$. We have $f_1^{\text{sim},p} = f_1^{\text{nom},p} \circ (\tau^p)^{-1}$ by construction (Definition 9.3). To show that $f_2^{\text{sim},p} = f_2^{\text{nom},p} \circ (\tau^p)^{-1}$, let $(s^p, \lambda_{s,\text{incr}}^p) \in X_{T,r_D}^{p,s}$. According to Lemma 9.2, we have $(\tau^p)^{-1}((s^p, \lambda_{s,\text{incr}}^p)) = (s^p, i_s^p, i_t)$ with

$$i_s^p = \iota_{s^p} \circ \Lambda_{s^p}^{-1}\left(\lambda_{s,\text{incr}}^p + \Lambda_{s^p}\left(\iota_{s^p}^{-1}\left(i_{\text{set}}(s^p)\right)\right)\right) \quad \text{and} \quad i_t^p = \iota_{t^p} \circ \iota_{s^p}(i_s^p).$$

By plugging (s^p, i_s^p, i_t^p) into $f_2^{\text{nom},p}$ and by considering that $\iota_{t^p}^{-1}(i_t^p) = \iota_{s^p}^{-1}(i_s^p)$, we obtain with Definitions 8.59 and 8.61

$$\begin{aligned}
f_2^{\text{nom},p}(s^p, i_s^p, i_t^p) &= \Lambda_{s^p}\left(\iota_{t^p}^{-1}(i_t^p)\right) - \Lambda_{s^p}\left(\iota_{s^p}^{-1}\left(i_{\text{set}}(s^p)\right)\right) = \Lambda_{s^p}\left(\iota_{s^p}^{-1}(i_s^p)\right) - \Lambda_{s^p}\left(\iota_{s^p}^{-1}\left(i_{\text{set}}(s^p)\right)\right) \\
&= \Lambda_{s^p} \circ \iota_{s^p}^{-1} \circ \iota_{s^p} \circ \Lambda_{s^p}^{-1}\left(\lambda_{s,\text{incr}}^p + \Lambda_{s^p}\left(\iota_{s^p}^{-1}\left(i_{\text{set}}(s^p)\right)\right)\right) - \Lambda_{s^p}\left(\iota_{s^p}^{-1}\left(i_{\text{set}}(s^p)\right)\right) \\
&= \lambda_{s,\text{incr}}^p + \Lambda_{s^p}\left(\iota_{s^p}^{-1}\left(i_{\text{set}}(s^p)\right)\right) - \Lambda_{s^p}\left(\iota_{s^p}^{-1}\left(i_{\text{set}}(s^p)\right)\right) = \lambda_{s,\text{incr}}^p \\
&= f_2^{\text{sim},p}(s^p, \lambda_{s,\text{incr}}^p).
\end{aligned}$$

Therefore, $f_2^{\text{sim},p} = f_2^{\text{nom},p} \circ (\tau^p)^{-1}$ holds and thus $f^{\text{sim},p} = f^{\text{nom},p} \circ (\tau^p)^{-1}$ holds as well. With this, we finally have $f^{\text{nom},p} = f^{\text{nom},p} \circ (\tau^p)^{-1} \circ \tau^p = f^{\text{sim},p} \circ \tau^p$. □

Definition 9.5 *Let $T = \{t^1, \dots, t^N\}$ be a set of feasible test fan speeds and let $r_D \geq 0$. The* simplified nominal optimization problem for ADA pair *p, $p \in [N]$, is defined by*

$$\min_{(s^p, \lambda_{s,\text{incr}}^p) \in X_{T,r_D}^{p,s}} \left(f_1^{\text{sim},p}(s^p, \lambda_{s,\text{incr}}^p), f_2^{\text{sim},p}(s^p, \lambda_{s,\text{incr}}^p) = \lambda_{s,\text{incr}}^p\right). \qquad \text{(simple-}P_{T,r_D}^p\text{)}$$

Remark 9.6 *The problem* (simple-P_{T,r_D}^p) *may be expected to be less complex than the problem* (nom-P_{T,r_D}^p)*, because its feasible set is two-dimensional and its second objective function is simply the projection of a feasible solution to its second component.*
However, evaluating the first objective function $f_1^{\text{sim},p}(s^p, \lambda_{s,\text{incr}}^p)$ (and also evaluating $f_1^{\text{nom},p}(s^p, i_s^p, i_t^p)$) is expected to be computationally expensive. Recall that these objective functions correspond to the determination of the Lipschitz constant L^p of the ADA iteration function A^p. Since A^p is usually not available as an analytical expression, we have to approximate L^p by finite differences, i.e., we have to evaluate A^p several times. The computational costs to evaluate A^p in turn depend on the selected HE model, because A^p

is composed of the two HE model functions $\iota^{-1}_{s^p,r_D}$ and ι_{t^p,r_D}. Therefore, the computational costs of evaluating the HE model are crucial for the computational costs of the proposed ADA optimization methods.
With this, (simple-P^p_{T,r_D}) is a so-called heterogeneous problem [Eic21, p. 4]. Its first objective function is computationally expensive to evaluate, while an evaluation of its second objective function as a projection is computationally cheap (almost for free).

The following lemma and corollary state how the Pareto optimal solutions and the Pareto fronts of (nom-P^p_{T,r_D}) and (simple-P^p_{T,r_D}) are related.

Lemma 9.7 *Let $T = \{t^1, \dots, t^N\}$ be a set of feasible test fan speeds, let $r_D \geq 0$ and let $p \in [N]$.*
Then, $x^* \in X^p_{T,r_D}$ is Pareto optimal with respect to (nom-P^p_{T,r_D}) if and only if $\tau^p(x^*)$ is Pareto optimal with respect to (simple-P^p_{T,r_D}).

Proof. By considering that $f^{\text{nom},p} = f^{\text{sim},p} \circ \tau^p$ (Lemma 9.4), we have

$$
\begin{aligned}
& x^* \text{ Pareto optimal wrt. (nom-}P^p_{T,r_D}\text{)} \\
\Leftrightarrow\ & \nexists\, x \in X^p_{T,r_D} : f^{\text{nom},p}(x) \leq f^{\text{nom},p}(x^*) \\
\Leftrightarrow\ & \nexists\, x \in X^p_{T,r_D} : f^{\text{sim},p} \circ \tau^p(x) \leq f^{\text{sim},p} \circ \tau^p(x^*) \\
\Leftrightarrow\ & \nexists\, \bar{x} \in X^{p,s}_{T,r_D} = \tau^p(X^p_{T,r_D}) : f^{\text{sim},p}(\bar{x}) \leq f^{\text{sim},p} \circ \tau^p(x^*) \\
\Leftrightarrow\ & \tau^p(x^*) \text{ Pareto optimal wrt. (simple-}P^p_{T,r_D}\text{)}.
\end{aligned}
$$

□

Corollary 9.8 *Let $Y^p_N(X^p_{T,r_D})$ be the Pareto front of (nom-P^p_{T,r_D}) and let $Y^p_N(X^{p,s}_{T,r_D})$ be the Pareto front of (simple-P^p_{T,r_D}). Then, $Y^p_N(X^p_{T,r_D}) = Y^p_N(X^{p,s}_{T,r_D})$.*

Proof. This follows directly from Lemma 9.7. "$\subset$" Let $y \in Y^p_N(X^p_{T,r_D})$. Then, there exists Pareto optimal $x \in X^p_{T,r_D}$ such that $f^{\text{nom},p}(x) = y$. By applying Lemma 9.7, we know that $\tau^p(x)$ is Pareto optimal with respect to (simple-P^p_{T,r_D}). Therefore, $f^{\text{sim},p} \circ \tau^p(x) = f^{\text{nom},p}(x) = y$ must be in the Pareto front of (simple-P^p_{T,r_D}).
"$\supset$" Let $y \in Y^p_N(X^{p,s}_{T,r_D})$. Then, there exists Pareto optimal $x \in X^{p,s}_{T,r_D}$ such that $f^{\text{sim},p}(x) = y$. By applying Lemma 9.7, we know that $(\tau^p)^{-1}(x)$ is Pareto optimal with respect to (nom-P^p_{T,r_D}). Therefore, $f^{\text{nom},p} \circ (\tau^p)^{-1}(x) = f^{\text{sim},p}(x) = y$ must be in the Pareto front of (nom-P^p_{T,r_D}). □

Lemma 9.7 and Corollary 9.8 justify the approach to focus on (simple-P^p_{T,r_D}) in order to solve (nom-P^p_{T,r_D}). The approach taken in this work is to approximate the Pareto front of (simple-P^p_{T,r_D}) with a variant of the ε-constraint scalarization. We keep the first objective function $f^{\text{sim},p}_1$ and move the second objective function as an equality constraint for certain start point increment samples $\lambda^p_{s,\text{incr}}$ to the constraint set. This method differs from the classical ε-constraint scalarization, which is presented in Section 4.1.3, in that the restriction of $f^{\text{sim},p}_2$ is formulated as an equation and not as an inequality. The advantage

of adding $f_2^{\text{sim},p}$ as an equality constraint is that the corresponding scalarized problem has a one-dimensional search space, see also Remark 9.12 below. In contrast, if $f_2^{\text{sim},p}$ is added as an inequality constraint, then the scalarized problem's search space is two-dimensional. However, this comes at the price that an optimal solution of a scalarized problem with $f_2^{\text{sim},p}$ as an equality constraint is in general not Pareto optimal with respect to (simple-P^p_{T,r_D}). In Lemma 9.18 below, it is shown that an optimal solution of such a scalarized problem is Pareto optimal with respect to (simple-P^p_{T,r_D}) if the Pareto front of (simple-P^p_{T,r_D}) is connected and the equality constraint with respect to $f_2^{\text{sim},p}$ is selected such that the value of $f_2^{\text{sim},p}$ is between the ideal point and the nadir point.
The corresponding algorithm is presented first. It is then demonstrated in a use case. Thereafter, its advantages and disadvantages are discussed.

9.1.2. Proposed Algorithm to Solve (nom-P^p_{T,r_D})

First, we define the scalarized problem.

Definition 9.9 *For a given $\varepsilon_2 \in \mathbb{R}$, we define the corresponding scalarized variant of* (simple-P^p_{T,r_D}) *by*

$$\min_{(s^p,\varepsilon_2)\in X^{p,s}_{T,r_D}} f_1^{\text{sim},p}(s^p,\varepsilon_2). \qquad \text{(simple-}P^p_{T,r_D}(\varepsilon_2)\text{)}$$

Remark 9.10 *An equivalent but less concise variant of* (simple-$P^p_{T,r_D}(\varepsilon_2)$) *is*

$$\min_{(s^p,\lambda^p_{s,\text{incr}})\in X^{p,s}_{T,r_D}} f_1^{\text{sim},p}(s^p,\lambda^p_{s,\text{incr}}) \quad s.t. \quad \lambda^p_{s,\text{incr}} = \varepsilon_2.$$

Remark 9.11 *Depending on the selection of ε_2, the problem* (simple-$P^p_{T,r_D}(\varepsilon_2)$) *might not be feasible. A mitigation of this issue is discussed in Remark 9.14 below.*

Remark 9.12 *The problem* (simple-$P^p_{T,r_D}(\varepsilon_2)$) *has a one-dimensional search space in the sense that the only free decision variable is s^p.*

Because we want to solve (simple-$P^p_{T,r_D}(\varepsilon_2)$) for several values of ε_2, we need a corresponding sample set.

Notation 9.13 *The* start point increment sample set *is denoted by $S_{\lambda^p_{s,\text{incr}}}$. It is implicitly assumed that the sample set is finite and that its elements are in strictly increasing order, i.e., $S_{\lambda^p_{s,\text{incr}}} = \{\lambda^{p,1}_{s,\text{incr}},\dots,\lambda^{p,n}_{s,\text{incr}}\}$ with $\lambda^{p,i}_{s,\text{incr}} < \lambda^{p,i+1}_{s,\text{incr}}$ for all $i \in [n-1]$, where n is the cardinality of $S_{\lambda^p_{s,\text{incr}}}$.*

Remark 9.14 *It is possible to state "good" bounds for the sample set $S_{\lambda^p_{s,\text{incr}}}$ such that the risk of infeasibilty of* (simple-$P^p_{T,r_D}(\varepsilon_2)$) *is reduced without being too restrictive. According to Lemma 8.60, we have $\lambda^p_{s,\text{incr}} = \mathcal{S}^p_{T,r_D}(x) \geq 0$ for all $x \in X^p_{T,r_D}$. Therefore, it is suggested to select $S_{\lambda^p_{s,\text{incr}}}$ such that $\min S_{\lambda^p_{s,\text{incr}}} = 0$.*
Regarding the maximal element of $S_{\lambda^p_{s,\text{incr}}}$, recall from Lemma 8.35 that a start point

increment of zero corresponds to the equivalence AFR that results from the control curve and the start fan speed s^p. For all fan speeds, the AFR corresponding to the control curve is usually greater or equal to $\lambda = 1.3$, see also Sections 2.2 and 2.3.3. On the other hand, the equivalence AFR must not be greater than $\lambda_{\max}$ according to (C-S3) *in Definition 8.52. Usually, we have $\lambda_{\max} = 1.6$ according to* (S3)*. Therefore, it is suggested to select $S_{\lambda^p_{s,\text{incr}}}$ such that $\max S_{\lambda^p_{s,\text{incr}}} = \lambda_{\max} - 1.3 = 0.3$.*
Note that these suggestions do not guarantee feasibility of (simple-$P^p_{T,r_D}(\varepsilon_2)$) *for $\varepsilon_2 \in S_{\lambda^p_{s,\text{incr}}}$. Rather, feasibility is more likely for such ε_2 compared to the general cases $\varepsilon_2 \in \mathbb{R}$ or $\varepsilon_2 \in \mathbb{R}_{\geq 0}$. Of course, if a different $\lambda_{\max}$ is considered or if the control curve is changed, it may make sense to revise the upper bound of the sample set.*

Remark 9.15 *The exploration of the Pareto front of* (simple-P^p_{T,r_D}) *(and thus also of* (nom-P^p_{T,r_D})*) with respect to the second objective can be controlled with the selection of the set $S_{\lambda^p_{s,\text{incr}}}$. This is possible, because the elements of $S_{\lambda^p_{s,\text{incr}}}$ are used as additional equality constraints for the second objective. For instance, if a uniform exploration of the Pareto front with respect to the second objective is desired, a uniform spacing in $S_{\lambda_{s,\text{incr}}}$ is suggested. Or if one is particularly interested in a solution with a small start point increment, the spacing of $S_{\lambda_{s,\text{incr}}}$ could be selected such that it is dense for small start point increments and sparse for larger start point increments.*
In all cases, the selected spacing is a compromise between accuracy and computation time. A good compromise for a uniform spacing is $\Delta\lambda_{s,\text{incr}} = 0.001$ to $\Delta\lambda_{s,\text{incr}} = 0.005$.

With this, Algorithm 9.1 to find an approximation of the set of Pareto optimal solutions of (simple-P^p_{T,r_D}) is proposed. The framework of Algorithm 9.1 is straightforward. For each $\lambda^p_{s,\text{incr}} \in S_{\lambda^p_{s,\text{incr}}}$, the scalarized problem (simple-$P^p_{T,r_D}(\varepsilon_2)$) is solved with $\varepsilon_2 = \lambda^p_{s,\text{incr}}$. Because we are in the biobjective case and the elements in $S_{\lambda^p_{s,\text{incr}}}$ follow an increasing order, we can simultaneously filter the results for Pareto nondominance.

Remark 9.16 *If the problem* (simple-$P^p_{T,r_D}(\varepsilon_2)$) *has an optimal solution that is not unique, then one arbitrary solution of the set of optimal solutions may be selected and added to the set of approximated efficient solutions in Line 9 of Algorithm 9.1. However, the case that the optimal solution of* (simple-$P^p_{T,r_D}(\varepsilon_2)$) *is not unique is considered very unlikely in practice for numerical reasons alone.*

Algorithm 9.1 is rather a heuristic and only approximates the set of efficient solutions of (simple-P^p_{T,r_D}). Nevertheless, some theoretical statements about its output with respect to Pareto nondominance as well as Pareto optimality are possible.

Lemma 9.17 *Let $\tilde{X}^p_{\text{eff}}$ be the output of Algorithm 9.1. If $\tilde{X}^p_{\text{eff}}$ is nonempty, then all elements in $f^{\text{sim},p}(\tilde{X}^p_{\text{eff}})$ are (within this set) nondominated.*

Proof. Let $\tilde{X}^p_{\text{eff}}$ be nonempty. Let us suppose there exists $x = (s^p, \lambda^p_{s,\text{incr}}) \in \tilde{X}^p_{\text{eff}}$ such that $f^{\text{sim},p}(x)$ is dominated in $f^{\text{sim},p}(\tilde{X}^p_{\text{eff}})$. Then there exists $x^* = (s^{p,*}, \lambda^{p,*}_{s,\text{incr}}) \in \tilde{X}^p_{\text{eff}}$ such that $f^{\text{sim},p}(x^*) \leq f^{\text{sim},p}(x)$, i.e., $f_1^{\text{sim},p}(x^*) \leq f_1^{\text{sim},p}(x)$ and $f_2^{\text{sim},p}(x^*) \leq f_2^{\text{sim},p}(x)$

Algorithm 9.1 Algorithm to Approximate the Set of Efficient Solutions of (simple-P^p_{T,r_D})

Input:

1: $S_{\lambda^p_{s,\text{incr}}} = \{\lambda^{p,1}_{s,\text{incr}}, \ldots, \lambda^{p,n}_{s,\text{incr}}\}$ // *start point increment sample set in increasing order*

Calculations:

2: $\widetilde{X}^p_{\text{eff}} \leftarrow \emptyset$ // *set of approximated efficient solutions*
3: $f_1^{\text{best}} \leftarrow \infty$ // *incumbent best value of first objective function*
4: **for all** $i = 1$ to n **do**
5: $\quad \varepsilon_2 \leftarrow \lambda^{p,i}_{s,\text{incr}}$
6: $\quad$ solve (simple-$P^p_{T,r_D}(\varepsilon_2)$)
7: $\quad$ **if** (simple-$P^p_{T,r_D}(\varepsilon_2)$) has an optimal solution $s^{p,*}$ with the function value f_1^* **then**
8: $\quad\quad$ **if** $f_1^* < f_1^{\text{best}}$ **then**
9: $\quad\quad\quad \widetilde{X}^p_{\text{eff}} \leftarrow \widetilde{X}^p_{\text{eff}} \cup \{(s^{p,*}, \lambda^{p,i}_{s,\text{incr}})\}$
10: $\quad\quad\quad f_1^{\text{best}} \leftarrow f_1^*$
11: $\quad\quad$ **end if**
12: $\quad$ **end if**
13: **end for**

Output:

14: $\widetilde{X}^p_{\text{eff}}$ // *approximated efficient solutions of* (simple-P^p_{T,r_D})

and $f^{\text{sim},p}(x^*) \neq f^{\text{sim},p}(x)$. Because $f_2^{\text{sim},p}(x^*) = \lambda^{p,*}_{s,\text{incr}}$ and $f_2^{\text{sim},p}(x) = \lambda^p_{s,\text{incr}}$, we have $\lambda^{p,*}_{s,\text{incr}} \leq \lambda^p_{s,\text{incr}}$. Note that $\lambda^{p,*}_{s,\text{incr}}$ and $\lambda^p_{s,\text{incr}}$ must be contained in the sample set $S_{\lambda^p_{s,\text{incr}}}$, because otherwise they cannot be a part of the output of Algorithm 9.1.
Let us suppose that $\lambda^{p,*}_{s,\text{incr}} < \lambda^p_{s,\text{incr}}$. In the for-loop in Line 4 of Algorithm 9.1 the elements of $S_{\lambda^p_{s,\text{incr}}}$ are selected in increasing order, thus $\lambda^{p,*}_{s,\text{incr}}$ is selected before $\lambda^p_{s,\text{incr}}$ in this case. But then $(s^p, \lambda^p_{s,\text{incr}})$ can only be added to $\tilde{X}^p_{\text{eff}}$ if $f_1^{\text{sim},p}(x) < f_1^{\text{sim},p}(x^*)$ according to Line 8 of Algorithm 9.1. This is a contradiction to $f_1^{\text{sim},p}(x^*) \leq f_1^{\text{sim},p}(x)$.
Next, let us suppose that $f_1^{\text{sim},p}(x^*) < f_1^{\text{sim},p}(x)$. Then, $(s^{p,*}, \lambda^{p,*}_{s,\text{incr}})$ is added to $\tilde{X}^p_{\text{eff}}$ after the point $(s^p, \lambda^p_{s,\text{incr}})$ according to Line 8 of Algorithm 9.1. Because in the for-loop in Line 4 of Algorithm 9.1 the elements of $S_{\lambda^p_{s,\text{incr}}}$ are taken in a strictly increasing order, we have $\lambda^p_{s,\text{incr}} < \lambda^{p,*}_{s,\text{incr}}$. This is a contradiction to $\lambda^{p,*}_{s,\text{incr}} \leq \lambda^p_{s,\text{incr}}$.
Since all cases lead to a contradiction, there cannot be a dominated point in $f^{\text{sim},p}(\tilde{X}^p_{\text{eff}})$. □

If the samples in $S_{\lambda^p_{s,\text{incr}}}$ are selected such that they are between the ideal and the nadir point and if the Pareto front of (simple-P^p_{T,r_D}) is connected, then all points in the output of Algorithm 9.1 are efficient with respect to (simple-P^p_{T,r_D}).

Lemma 9.18 *Let* $(s^{p,I}, \lambda^{p,I}_{s,\text{incr}})$ *be the ideal point and let* $(s^{p,N}, \lambda^{p,N}_{s,\text{incr}})$ *be the nadir point of* (simple-P^p_{T,r_D}). *Let* $S_{\lambda^p_{s,\text{incr}}}$ *be such that* $\lambda^{p,I}_{s,\text{incr}} \leq \min S_{\lambda^p_{s,\text{incr}}}$ *and* $\max S_{\lambda^p_{s,\text{incr}}} \leq \lambda^{p,N}_{s,\text{incr}}$. *Let* $\tilde{X}^p_{\text{eff}}$ *be the corresponding output of Algorithm 9.1.*

If the Pareto front of (simple-P^p_{T,r_D}) *is connected, then* $\tilde{X}^p_{\text{eff}}$ *is a subset of the efficient solutions of* (simple-P^p_{T,r_D}).

Proof. Let the Pareto front of (simple-P^p_{T,r_D}) be connected. Let us suppose that there exists $x^* = (s^{p,*}, \lambda^{p,*}_{s,\text{incr}}) \in \tilde{X}^p_{\text{eff}}$ that is not Pareto optimal with respect to (simple-P^p_{T,r_D}). Because $x^* \in \tilde{X}^p_{\text{eff}}$, we have $\lambda^{p,*}_{s,\text{incr}} \in S_{\lambda^p_{s,\text{incr}}}$ and thus $\lambda^{p,I}_{s,\text{incr}} \leq \lambda^{p,*}_{s,\text{incr}} \leq \lambda^{p,N}_{s,\text{incr}}$. Because the Pareto front is connected, for all $\lambda_{s,\text{incr}} \in [\lambda^{p,I}_{s,\text{incr}}, \lambda^{p,N}_{s,\text{incr}}]$ there exists a Pareto optimal solution $x \in X^{p,s}_{T,r_D}$ whose second component is $\lambda^{p,*}_{s,\text{incr}}$ according to Lemma 4.18. Therefore, there exists a Pareto optimal solution $\bar{x} = (\bar{s}^p, \bar{\lambda}^p_{s,\text{incr}})$ with $\bar{\lambda}^p_{s,\text{incr}} = \lambda^{p,*}_{s,\text{incr}}$. Because $\bar{x}$ is Pareto optimal and x^* is not and because $\bar{\lambda}^p_{s,\text{incr}} = \lambda^{p,*}_{s,\text{incr}}$, i.e., $f_2^{\text{sim},p}(\bar{x}) = f_2^{\text{sim},p}(x^*)$, we have $f_1^{\text{sim},p}(\bar{x}) < f_1^{\text{sim},p}(x^*)$. This means that $\bar{x}$ is an optimal solution of (simple-$P^p_{T,r_D}(\varepsilon_2)$) for $\varepsilon_2 := \bar{\lambda}^p_{s,\text{incr}} = \lambda^{p,*}_{s,\text{incr}}$ and x^* is not (Definition 9.9). But then the solution $\bar{x}$ and not the solution x^* is added to $\tilde{X}^p_{\text{eff}}$ according to Line 7 of Algorithm 9.1, i.e., $x^* \notin \tilde{X}^p_{\text{eff}}$. This is a contradiction to $x^* \in \tilde{X}^p_{\text{eff}}$. □

In practice, the requirements of Lemma 9.18 are not always satisfied. On the one hand, the ideal point and the nadir point are not known in advance in general and thus it may be difficult to specify the sample set $S_{\lambda^p_{s,\text{incr}}}$ accordingly. On the other hand, the Pareto front of (simple-P^p_{T,r_D}) is not always connected. This is illustrated in Subsection 9.1.4, where Algorithm 9.1 is demonstrated in a use case.
But first, another aspect of Algorithm 9.1 is considered. In Line 6 of Algorithm 9.1, the scalarized problem (simple-$P^p_{T,r_D}(\varepsilon_2)$) must be solved and we need a corresponding solver. This is briefly discussed in the following subsection.

9.1.3. Solver for the Scalarized Problems

The problem (simple-$P^p_{T,r_D}(\varepsilon_2)$) is constrained, nonlinear and multimodal (and thus non-convex) in general. Two exemplary objective functions $f_1^{\text{sim},p}(s^p, \varepsilon_2)$ are shown in Figure 9.1. Their global minimum is each marked by a black dot. Both shown objective functions are determined with the same HE model, which is based on a piecewise linear interpolation. The HE model's underlying measurement data is provided by Vaillant and corresponds to [PHE, Item 6371]. In the left part of Figure 9.1, the scalarized objective function for the case with $t^p = 6000$ and $\varepsilon_2 = \lambda_{s,\text{incr}} = 0.12$ is shown. This function is "nice" in the sense that it is convex (and unimodal) and a variety of solvers is suited to find its minimum.
The right part of Figure 9.1 shows the scalarized objective function for the case with $t^p = 2500$ and $\varepsilon_2 = \lambda_{s,\text{incr}} = 0.12$. In contrast to the objective function shown in the left part, this function has multiple local minima, i.e., it is multimodal. In such a situation, it might happen that an optimization method finds only a local minimum but not the global minimum. Therefore, a global method to solve (simple-$P^p_{T,r_D}(\varepsilon_2)$) is required that does not get stuck in a local minimum.

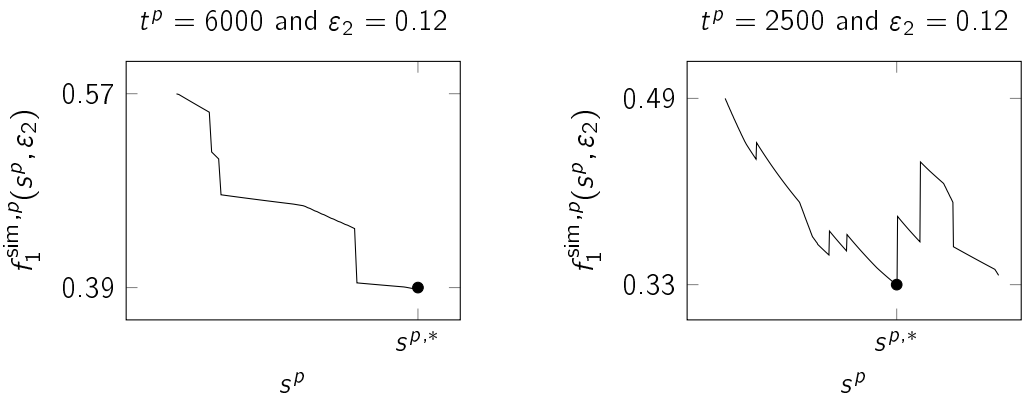

Figure 9.1.: Two exemplary objective functions of the scalarized problem (simple-$P^p_{T,r_D}(\varepsilon_2)$) are shown. Both functions were determined with the same HE model based on a piecewise linear interpolation of measurement data provided by Vaillant. The function in the right part is multimodal and thus a global solver that does not get stuck in local minima is required.

Remark 9.19 *The "roughness" of the function depicted in the right part of Figure 9.1 might be caused by the HE model, which is based on a piecewise linear interpolation. If a smoother regression method, for instance a local weighted linear regression, is used, the objective function might be smoother. Nevertheless, it can be expected that the function is also multimodal in this case.*

In the following, we propose a direct search method to solve the scalarized problems (simple-$P^p_{T,r_D}(\varepsilon_2)$). Direct search methods are a common class of derivative-free methods to solve constrained single objective optimization problems [CSV09, p. 242] [CEM12, p. 5]. They are iterative procedures, whose iterations are composed of a search step, a poll step and a parameter update. In the search step, the objective function is evaluated at a finite set of sample points. The poll step is a subsequent local search at the sample point with the best function value from the preceding search step. Depending on the results of the search and/or the poll step, some parameters like the step size or the search directions are updated at the end of each iteration [CEM12, p. 7]. The search step is optional and usually introduced to improve efficiency [CSV09, p. 117]. Finally, when a stopping criterion is reached, the procedure is terminated. There exists a variety of strategies for the search step, the poll step, the parameter updates and the stopping criterion. These strategies as well as a corresponding framework are covered in detail in the book *Introduction to Derivative-Free Optimization* [CSV09].
In order to reduce the risk that only a local minimum and not the global minimum is approximated, we propose an initial search step with an equidistant spacing in the sample set to solve (simple-$P^p_{T,r_D}(\varepsilon_2)$). This initial sample set of start fan speeds is denoted by S_{s^p} in the following.

Remark 9.20 *From an empirical point of view, solutions with a small start fan speed ($s^p \approx t^p$) or a large start fan speed ($s^p > 1.4t^p$) are usually infeasible due to some of*

the combustion limits according to Definition 8.52. Therefore, $\min S_{s^p} = 1.05t^p$ *and* $\max S_{s^p} = \min\{1.4t^p, t^{p-1} - \varepsilon\}$ *(*$\max S_{s^1} = \min\{1.4t^1, \mathrm{fs}_{\max}\}$*) are proposed, which is in accordance with* (C-S7) *in Definition 8.52.*

The step size of the equidistant spacing depends on the desired accuracy and on the allowed maximum computation time. In the considered use cases, $\Delta s^p = 0.002t^p$ was a good compromise. For instance, if $t^p = 6000$, then the step size $\Delta s^p = 12$ is suggested. The initial search step is straightforward. Let S_{s^p} have the cardinality n. For every $s^{p,i} \in S_{s^p}$, $i \in [n]$, we check whether $(s^{p,i}, \varepsilon_2)$ is feasible, i.e., if $(s^{p,i}, \varepsilon_2) \in X^{p,s}_{T,r_D}$. If $(s^{p,i}, \varepsilon_2) \notin X^{p,s}_{T,r_D}$ for all $i \in [n]$, then the problem is considered to be infeasible. Of all feasible solutions, the start fan speed $s^{p,i}$ with the smallest function value $f_1^{\mathrm{sim},p}(s^{p,i}, \varepsilon_2)$ is used as the incumbent approximation of the optimal solution of (simple-$P^p_{T,r_D}(\varepsilon_2)$). In the subsequent poll step, a local search at the incumbent solution is performed.
In practice, it has been found that the incumbent solution after the initial search step approximates the optimal solution of (simple-$P^p_{T,r_D}(\varepsilon_2)$) sufficiently well and that subsequent poll steps are not necessarily required. Therefore, it is proposed to just perform the initial search step with an appropriate sample set S_{s^p} to approximate the optimal solution of (simple-$P^p_{T,r_D}(\varepsilon_2)$).

Remark 9.21 *As a supplement or as an alternative to the sampling approach, a warm start strategy could be used. For this, let* $S_{\lambda^p_{s,\mathrm{incr}}} = \{\lambda^{p,1}_{s,\mathrm{incr}}, \ldots, \lambda^{p,n}_{s,\mathrm{incr}}\}$ *be the sample set of start point increments in increasing order, which is the set from which the* ε_2*-values are taken for the scalarization according to Algorithm 9.1. Let us suppose that we have approximated the optimal solution of* (simple-$P^p_{T,r_D}(\varepsilon_2)$) *for the first element in* $S_{\lambda^p_{s,\mathrm{incr}}}$*, i.e., for* $\varepsilon_2 = \lambda^{p,1}_{s,\mathrm{incr}}$*. This approximation of the optimal solution is denoted by* $s^{p,1,*}$ *for the moment. Then, to solve* (simple-$P^p_{T,r_D}(\varepsilon_2)$) *for the subsequent* $\varepsilon_2 = \lambda^{p,2}_{s,\mathrm{incr}}$*, we can perform a warm start with* $s^{p,1,*}$*. I.e., instead of performing the search step with a start fan speed sample set* S_{s^p}*, we perform a local search around* $s^{p,1,*}$*.*
However, this warm start method has not been tested in practice and is left for future research.

In the following subsection, Algorithm 9.1 together with the proposed sampling approach to solve the scalarized problems is demonstrated in a use case.

9.1.4. Demonstration of Algorithm 9.1 in a Use Case

In this use case, we want to find optimal ADA parameters for the Vaillant HE with the measurement data corresponding to [PHE, Item 6371]. For this, we consider an HE model that is based on a piecewise linear interpolation. Let us suppose that the decision makers want to optimize two ADA pairs, i.e., we are in the case $N = 2$. Furthermore, we suppose that the decision makers specified the set of feasible test fan speeds by $T = \{t^1 = 10000, t^2 = 6000\}$. The drift resistance is specified by $r_D = 140k\Omega$. The problem's parameters are specified by the common values $\lambda_{\min} = 1.05$, $\lambda_{\max} = 1.6$,

$\mathrm{co}_{\max} = 150$ and $\Delta\lambda_{\min} = 0.1$. Our goal is to find the Pareto optimal solutions of (nom-P^p_{T,r_D}) for $p = 1$ and $p = 2$.
For this, we approximate a subset of the Pareto optimal solutions of (simple-P^p_{T,r_D}) for each $p \in [2]$ with Algorithm 9.1. These approximated sets are denoted by $\widetilde{X}^p_{\text{eff}}$, $p \in [2]$, in the following. Then, $(\tau^p)^{-1}(\widetilde{X}^p_{\text{eff}})$ is an approximation of the set of Pareto optimal solutions of (nom-P^p_{T,r_D}), $p \in [2]$, according to Lemma 9.7.
All results presented in the course of this subsection are determined with corresponding implementations in Matlab evaluated on an AMD Ryzen 5800x system.

We begin with the smaller test fan speed, i.e., we consider the case $p = 2$ first. In order to apply Algorithm 9.1, we need a start point increment sample set $S_{\lambda^2_{s,\text{incr}}}$. In addition, we need a start fan speed sample set S_{s^2} to solve the scalarized problems (simple-$P^p_{T,r_D}(\varepsilon_2)$), $p = 2$.

Start point increment sample set: We specify the sample set $S_{\lambda^2_{s,\text{incr}}}$ according to Remarks 9.14 and 9.15, i.e., we select $S_{\lambda^2_{s,\text{incr}}}$ such that $\min S_{\lambda^2_{s,\text{incr}}} = 0$ and $\max S_{\lambda^2_{s,\text{incr}}} = 0.3$. Let us suppose that we are interested in a uniform exploration of the Pareto front. Therefore, we select a uniform spacing. In this use case, we select $\Delta\lambda^2_{s,\text{incr}} = 0.01$. This is a rather large spacing, but it enables a clear visualization of the set of sample points and of the approximation of the Pareto front in Figure 9.2 below. The resulting sample set is $S_{\lambda^2_{s,\text{incr}}} := \{0, 0.01, 0.02, \ldots, 0.3\}$ and contains 31 samples.

Start fan speed sample set: As suggested in Remark 9.20, we select S_{s^2} such that $\min S_{s^2} = 1.05t^2 = 6300$ and $\max S_{s^2} = 1.4t^2 = 8400$. Analogous to the selected spacing in the start point increment sample set, we consider a rather coarse start fan speed sample set. For illustration purposes, we select the spacing such that S_{s^2} is composed of 30 equidistant points, which results in a spacing of $\Delta s^2 \approx 72.4$.
Note that we use the same start fan speed sample set S_{s^2} to solve every instance of (simple-$P^p_{T,r_D}(\varepsilon_2)$), $p = 2$, i.e., for all $\varepsilon_2 = \lambda^{2,i}_{s,\text{incr}} \in S_{\lambda^2_{s,\text{incr}}}$. Using the same sample set S_{s^p} to approximate the optimal solution of each scalarized problem (simple-$P^p_{T,r_D}(\varepsilon_2)$), $\varepsilon_2 \in S_{\lambda^p_{s,\text{incr}}}$, is not restricted to this use case. This is possible, because in practice a sample set S_{s^p} with the suggested minimum $\min S_{s^p} = 1.05t^p$ and maximum $\max S_{s^p} = 1.4t^p$ covers the feasible set for all $\lambda^p_{s,\text{incr}} \in S_{\lambda^p_{s,\text{incr}}} \subset [0, 0.3]$ sufficiently without being too restrictive.

In total, this approach corresponds to considering a sample set of solutions for (simple-P^p_{T,r_D}), $p = 2$, that is the Cartesian product $G := S_{s^2} \times S_{\lambda^2_{s,\text{incr}}}$. The set G is a square grid in the $(s^2, \lambda^2_{s,\text{incr}})$ plane and consists of $|S_{s^2}| \cdot |S_{\lambda^2_{s,\text{incr}}}| = 30 \cdot 31 = 930$ sample points. In other words, Algorithm 9.1 in combination with the sampling approach to solve the scalarized problems corresponds to determine the nondominated points in the set $G \cap X^{2,s}_{T,r_D}$.
This situation is depicted in Figure 9.2. The left part of Figure 9.2 shows the decision space of (simple-P^p_{T,r_D}), $p = 2$. The region within the green curve corresponds to

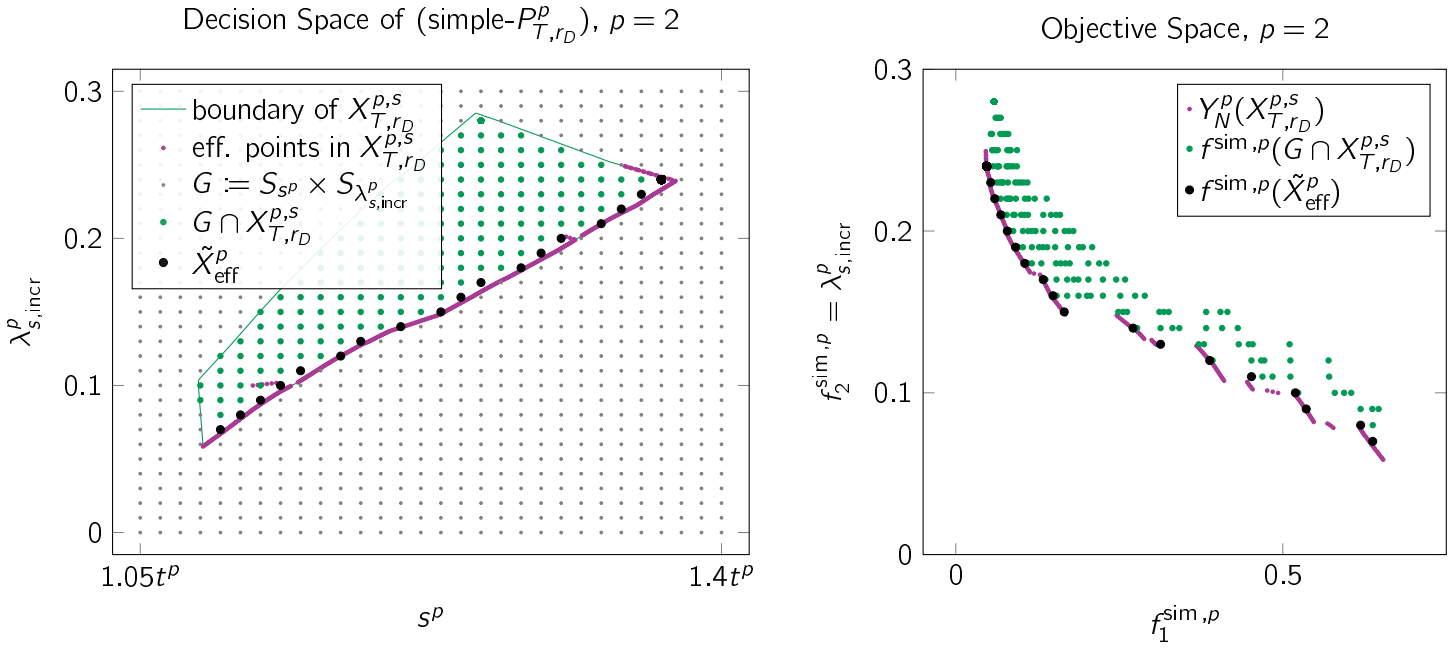

Figure 9.2.: In the left part the decision space of the use case problem (simple-P^p_{T,r_D}) delineated in Section 9.1.4 for the case $p = 2$ is shown. The region within the green curve corresponds to the feasible set $X^{p,s}_{T,r_D}$. The purple curve segments correspond to the efficient points in $X^{p,s}_{T,r_D}$. The small gray dots correspond to the sample points of the grid $G := S_{s^p} \times S_{\lambda^p_{s,\text{incr}}}$ and the green dots are the feasible points of G. The black dots correspond to the output of Algorithm 9.1, which are the feasible and nondominated points in G.
In the right part the problem's objective space is shown in the same color scheme. I.e., the images of the aforementioned sets under the objective function $f^{\text{sim},2}$ are shown.
Because the second component of the objective function is just the projection to the second coordinate, the decision space and the objective space both have the same y-axis and thus a point of the Pareto front can be directly identified with its efficient solution(s) in the decision space.

the feasible set $X^{2,s}_{T,r_D}$. The purple curve segments correspond to all efficient solutions in $X^{2,s}_{T,r_D}$. The sample points, i.e., the set G, are represented by the gray dots. The feasible sample points, i.e., the set $G \cap X^{2,s}_{T,r_D}$, are represented by the green dots. The black dots correspond to the output of Algorithm 9.1, which is denoted by $\tilde{X}^2_{\text{eff}}$. Note that these points are the nondominated solutions in $G \cap X^{2,s}_{T,r_D}$. The run time required to determine $\tilde{X}^2_{\text{eff}}$ was approximately 0.79 seconds.
The right part of Figure 9.2 shows the corresponding objective space in the same color scheme. The green dots correspond to $f^{\text{sim},2}(G \cap X^{2,s}_{T,r_D})$, the black dots correspond to $f^{\text{sim},2}(\tilde{X}^2_{\text{eff}})$ and the purple curve segments correspond to the Pareto front of the problem (simple-P^p_{T,r_D}), $p = 2$. The approximated nondominated points $f^{\text{sim},2}(\tilde{X}^2_{\text{eff}})$ are not a subset of the Pareto front of (simple-P^p_{T,r_D}), $p = 2$, in this case. The approximation quality should improve when refining the grid, but beyond that we generally have no information about the approximation quality of the output of Algorithm 9.1. However, most of the points in $f^{\text{sim},2}(\tilde{X}^2_{\text{eff}})$ are close to the Pareto front in this case. In addition, the set $f^{\text{sim},2}(\tilde{X}^2_{\text{eff}})$ provides a uniform representation of the Pareto front of (simple-P^p_{T,r_D}), $p = 2$, with respect to the second objective function.

Remark 9.22 *The boundary of the feasible set and the Pareto front shown in the left and in the right part of Figure 9.2, respectively, are only approximations. They were determined with sample sets* S_{s^2} *and* $S_{\lambda^2_{s,\text{incr}}}$ *that each contains* 1000 *equidistant elements, i.e., the corresponding grid was composed of one million* $(s^2, \lambda^2_{s,\text{incr}})$ *samples. The required run time was approximately* 507.6 *seconds.*

Next, we approximate the Pareto optimal solutions of (simple-P^p_{T,r_D}) for the case $p = 1$. This is done analogously to the case $p = 2$. In particular, we select the same set of start point increment samples, i.e., we select $S_{\lambda^1_{s,\text{incr}}} := S_{\lambda^2_{s,\text{incr}}}$. Regarding the start fan speed sample set, we select S_{s^1} such that $\min S_{s^1} = 1.05t^1 = 10500$ and such that $\max S_{s^1} = \min\{1.4t^1, \text{fs}_{\max}\} = \text{fs}_{\max} = 12200$. Analogously to S_{s^2}, the spacing is selected such that we have 30 equidistant points in S_{s^1}, which corresponds to a spacing of $\Delta s^1 \approx 58.6$.

This situation is depicted in Figure 9.3. It is analogous to Figure 9.2, i.e., it uses the same color scheme and the same legend. The left part of Figure 9.3 shows the decision space and the right part shows the objective space. The depicted boundary of the feasible set as well as the depicted Pareto front are approximations that were again determined by 1000 by 1000 search grid, which required a run time of approximately 706.4 seconds.
As in the case $p = 2$, it is apparent that the approximated nondominated points are not a subset of the Pareto front of (simple-P^p_{T,r_D}), $p = 1$. However, they can be considered as a good approximation of the Pareto front of (simple-P^p_{T,r_D}), $p = 1$. The run time required to determine $\tilde{X}^1_{\text{eff}}$ was approximately 0.6 seconds.
In contrast to the case $p = 2$, a uniform exploration of the Pareto front with respect to the second objective is not given in this case. This can be seen in the right part of Figure 9.3. The vertical distance between the second and the third black dot (counted from left to

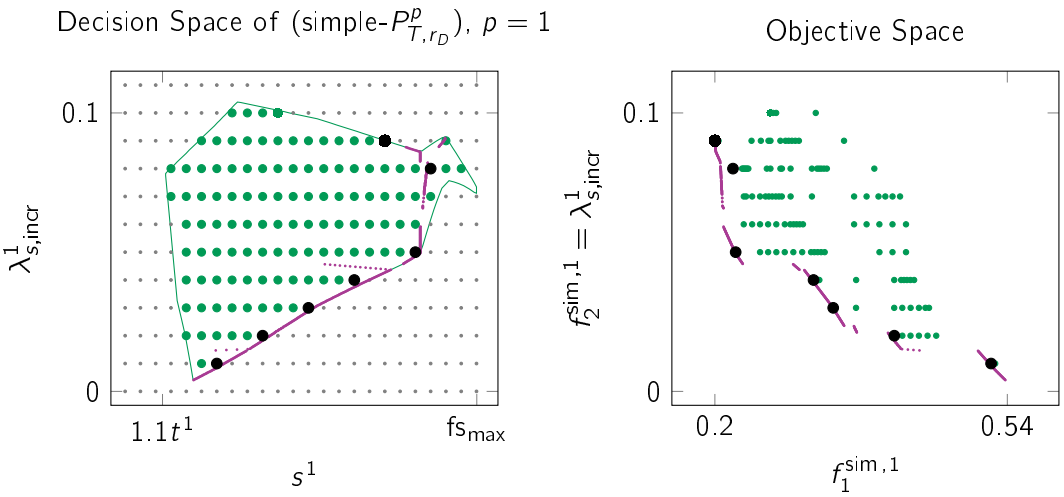

Figure 9.3.: In the left part the decision space and in the right part the objective space of (simple-P^p_{T,r_D}) for the case $p = 1$ are shown. The color scheme and the legend are identical to those of Figure 9.2

right) is $3\Delta\lambda^1_{s,\text{incr}} = 0.03$. In contrast, all remaining black dots have a vertical distance of $1\Delta\lambda^1_{s,\text{incr}} = 0.01$ to their neighbors.

Since we follow an a posteriori method, the next step in the optimization and decision making process would be the selection of the final solutions by the decision makers. I.e, for each $p \in [2]$ the decision makers select a solution from $\tilde{X}^p_{\text{eff}}$ based on the approximated Pareto front of (simple-P^p_{T,r_D}) (and thus also of (nom-P^p_{T,r_D}) according to Corollary 9.8) that best fits their preferences. This concludes the use case and the demonstration of Algorithm 9.1.
As a final remark, regarding the problem (simple-P^p_{T,r_D}), the considered use case shows that the efficient solutions can lie in the interior and on the boundary of the feasible set, that the Pareto front is not convex and that the Pareto front is not connected in general.

Some advantages and disadvantages of Algorithm 9.1 and of the sampling approach to solve (simple-$P^p_{T,r_D}(\varepsilon_2)$) have already been mentioned in this subsection. These are discussed in detail in the following.

9.1.5. Discussion of the Proposed Grid Search Method

The advantages and disadvantages of Algorithm 9.1 are discussed first. Thereafter, it is assessed from a practical point of view.

Advantages The major advantage of Algorithm 9.1 is that the problem (nom-P^p_{T,r_D}) is not required to have a special structure. In particular, the Pareto front is not required to

be convex and the problem may be multimodal. As a consequence, the proposed method is robust in the sense that it works with a variety of HE types and HE models.
A further advantage is that by the selection of the sample points in $S_{\lambda^p_{s,\text{incr}}}$ the exploration of the Pareto front with respect to the second objective of (nom-P^p_{T,r_D}) can be controlled to a certain degree. For instance, in the use case presented in Section 9.1.4 a uniform spacing in $S_{\lambda^2_{s,\text{incr}}}$ was selected, which resulted in a uniform spacing of the approximated Pareto front as shown in the right part of Figure 9.2. This provides a good overview of the set of Pareto optimal solutions to the decision makers. However, this does not hold in general as demonstrated in the use case with the case $p = 1$, see also Figure 9.3.
Furthermore, Algorithm 9.1 has a simple structure and is rather easy to implement. This is also reflected by the fact that Algorithm 9.1 requires only a few parameters to be specified, which are the specifications of the sample set(s). In addition, with the selected size of the sample set(s) the computational effort of Algorithm 9.1 can be directly controlled.
Finally, Algorithm 9.1 is easy to parallelize, because the scalarized problems that must be solved in each iteration of the for-loop in Algorithm 9.1 are independent of each other.

Disadvantages If the Pareto front of (nom-P^p_{T,r_D}) is connected and the start point increment sample set $S_{\lambda^p_{s,\text{incr}}}$ is selected such that its bounds are between the second components of the ideal and of the nadir point, then Algorithm 9.1 returns a subset of the Pareto optimal solutions according to Corollary 9.8 (if the scalarized optimization problems (simple-$P^p_{T,r_D}(\varepsilon_2)$) are solved exactly in Line 6 of Algorithm 9.1). But as demonstrated in the use case in Section 9.1.4, the Pareto front of (nom-P^p_{T,r_D}) is not connected in general. Furthermore, in general the scalarized problem (simple-$P^p_{T,r_D}(\varepsilon_2)$) is multimodal and its objective function and constraints are not differentiable and thus one usually has to fall back on approximation methods to solve (simple-$P^p_{T,r_D}(\varepsilon_2)$).
The major disadvantage of Algorithm 9.1 is that its approximation quality is unknown in general. The objective functions and the constraint functions depend on the structure of the measurement data, which in turn depends on the considered HE type and the measuring instruments used. Furthermore, they depend on the considered regression/interpolation method of the HE model as well as on HE parameters like the control curve. This results in an unmanageable number of cases that need to be considered in order to determine the approximation quality.
Because the approximation quality is unclear, the optimal size and spacing of the sample set(s) are unclear as well. In particular, it is not clear by how much the approximation quality improves when the number of sample points is increased or the sample set's boundaries are adjusted. In the worst case, the computational effort increases without increasing the approximation quality.

Assessment from a practical point of view In the introduction to this Chapter 9, some desired properties of a multiobjective optimization method are listed. The method should provide reliable results, should give the decision makers a good overview of the Pareto

optimal set, should not require too much time and should support the decision makers in finally selecting the preferred solution [Bra+08, p. 2]. In the use case in Section 9.1.4, the outputs of Algorithm 9.1 provide a good approximation and representation of the Pareto fronts even with a rather small sample grid. Furthermore, the calculations were not very time consuming. For instance, an approximation of the Pareto optimal set with a 30 by 31 sample grid in the presented use case took approximately 0.6 to 0.8 seconds on an AMD Ryzen 5800x system. A similar characteristic was observed in all other use cases by Vaillant. Therefore, in the opinion of the author of this thesis, the above mentioned desired properties of a multiobjective optimization method are fulfilled by Algorithm 9.1 in combination with the sampling approach to solve (simple-$P^p_{T,r_D}(\varepsilon_2)$). But the approach's blind spot in terms of approximation quality remains a disadvantage and must be kept in mind.
Because the decision-makers are satisfied with the optimization process based on Algorithm 9.1, no further methods to solve (nom-P^p_{T,r_D}) were investigated. However, if the approximation quality is considered to be not sufficient, subsequent poll steps, i.e., a local search, could be used to obtain better approximations, see also Section 9.1.3. Furthermore, a warm start in combination with a local search could improve the efficiency as well as the approximation quality as delineated in Remark 9.21. Finally, if one is interested in a completely different approach, evolutionary multiobjective optimization algorithms could be a good alternative to solve (nom-P^p_{T,r_D}).

This concludes the optimization of the ADA parameters in the nominal case. An approach based on evolutionary multiobjective optimization to solve the ADA optimization problem with tolerances is presented and discussed in the following section.

9.2. Solving the ADA Optimization Problem with Tolerances

The ADA optimization problem with tolerances (tol-P_{T,r_D}) has a $2N$-dimensional objective space according to Definition 8.84. Usually, up to seven ADA pairs are optimized, i.e., we usually have $N = 7$. In this case the objective space is 14-dimensional. Such a high-dimensional objective space makes the decision making more difficult, because it is difficult to visualize the trade-offs between the individual objectives. Furthermore, higher-dimensional optimization problems are usually harder to solve [Bra+08, p. 3].
Because the decision makers are mostly interested in minimizing the largest Lipschitz constant and minimizing the largest start point increment, it is proposed to aggregate all Lipschitz constants to a single objective function and to aggregate all start point increments to a single objective function where the largest values are weighted over proportionally. Then, the resulting problem is always biobjective, regardless of N.
This biobjective problem is detailed in the following subsection. A method how to solve the biobjective problem is then proposed, which is demonstrated in a subsequent use case. Finally, the results of this section are briefly discussed.

9.2.1. Aggregate Objectives to Reduce Dimension of Objective Space

The aggregated objective functions and the corresponding optimization model are defined as follows.

Definition 9.23 *Let $\alpha_L \in (0,1)$ and let $\alpha_{\lambda_{s,\text{incr}}} \in (0,1)$. The* aggregated Lipschitz constant function *is defined for all $x \in X^{\text{tol}}_{T,r_D}(\mathcal{H}_{\text{nom}}, \mathcal{U}_{\text{tol}})$ by*

$$\overline{\mathcal{L}}^{\text{agg}}_{T,r_D}(x) := \alpha_L \overline{\mathcal{L}}^{j}_{T,r_D}(x) + \frac{1-\alpha_L}{N-1} \sum_{p \in [N]\setminus\{j\}} \overline{\mathcal{L}}^{p}_{T,r_D}(x),$$

where $j \in [N]$ such that $\overline{\mathcal{L}}^{j}_{T,r_D}(x) \geq \overline{\mathcal{L}}^{p}_{T,r_D}(x)$ for all $p \in [N]$.
The aggregated start point increment function *is defined for all $x \in X^{\text{tol}}_{T,r_D}(\mathcal{H}_{\text{nom}}, \mathcal{U}_{\text{tol}})$ by*

$$\overline{\mathcal{S}}^{\text{agg}}_{T,r_D}(x) := \alpha_{\lambda_{s,\text{incr}}} \overline{\mathcal{S}}^{k}_{T,r_D}(x) + \frac{1-\alpha_{\lambda_{s,\text{incr}}}}{N-1} \sum_{p \in [N]\setminus\{k\}} \overline{\mathcal{S}}^{p}_{T,r_D}(x),$$

where $k \in [N]$ such that $\overline{\mathcal{S}}^{k}_{T,r_D}(x) \geq \overline{\mathcal{S}}^{p}_{T,r_D}(x)$ for all $p \in [N]$.
The ADA optimization model with respect to tolerances with aggregated objective functions *is defined by*

$$\min_{x \in X^{\text{tol}}_{T,r_D}(\mathcal{H}_{\text{nom}}, \mathcal{U}_{\text{tol}})} f^{\text{tol,agg}}(x) := \left(\overline{\mathcal{L}}^{\text{agg}}_{T,r_D}(x), \overline{\mathcal{S}}^{\text{agg}}_{T,r_D}(x)\right). \qquad \text{(tol-agg-}P\text{)}$$

Remark 9.24 *Note that the indices j and k in Definition 9.23 are not necessarily unique. However, the aggregated functions $\overline{\mathcal{L}}^{\text{agg}}_{T,r_D}$ and $\overline{\mathcal{S}}^{\text{agg}}_{T,r_D}$ are also well-defined in such a case.*

Remark 9.25 *Definition 9.23 is rather general and also allows small factors α_L and $\alpha_{\lambda_{s,\text{incr}}}$. In order to weight the largest Lipschitz constant over proportionally, one has to select $\alpha_L > \frac{1}{N}$, which is equivalent to $\alpha_L > \frac{1-\alpha_L}{N-1}$, because (with $0 < \alpha_L < 1$ and $N \geq 2$)*

$$\alpha_L > \frac{1}{N} \;\Leftrightarrow\; N > \frac{1}{\alpha_L} \;\Leftrightarrow\; N-1 > \frac{1}{\alpha_L} - 1 = \frac{1-\alpha_L}{\alpha_L} \;\Leftrightarrow\; \alpha_L > \frac{1-\alpha_L}{N-1}.$$

The same is true for the start point increment.
In the use case with $N = 6$ presented in Section 9.2.4 below, the factors $\alpha_L = 0.8$ and $\alpha_{\lambda_{s,\text{incr}}} = 0.8$ are selected.

A solution that is Pareto optimal with respect to (tol-agg-P) is also Pareto optimal with respect to (tol-P_{T,r_D}).

Lemma 9.26 *If x^* is efficient with respect to* (tol-agg-P)*, then x^* is also efficient with respect to* (tol-P_{T,r_D}).

Proof. Let x^* be efficient with respect to (tol-agg-P) and let us suppose that x^* is not efficient with respect to (tol-P_{T,r_D}). Then, there exists $\tilde{x} \in X^{\text{tol}}_{T,r_D}(\mathcal{H}_{\text{nom}}, \mathcal{U}_{\text{tol}})$ such that $f^{\text{tol}}(\tilde{x}) \leq f^{\text{tol}}(x^*)$, i.e.,

$$f^{\text{tol}}_i(\tilde{x}) \leq f^{\text{tol}}_i(x^*) \;\forall\; i \in [2N] \quad \text{and} \quad \exists\; \ell \in [2N] : f^{\text{tol}}_\ell(\tilde{x}) < f^{\text{tol}}_\ell(x^*).$$

In particular, we have $\overline{\mathcal{L}}^p_{T,r_D}(\tilde{x}) \leq \overline{\mathcal{L}}^p_{T,r_D}(x^*)$ and $\overline{\mathcal{S}}^p_{T,r_D}(\tilde{x}) \leq \overline{\mathcal{S}}^p_{T,r_D}(x^*)$ for all $p \in [N]$. Note that the indices j and k according to Definition 9.23 might be different for $x = x^*$ and for $x = \tilde{x}$.
As an intermediate result we show that $\overline{\mathcal{L}}^{\text{agg}}_{T,r_D}(\tilde{x}) \leq \overline{\mathcal{L}}^{\text{agg}}_{T,r_D}(x^*)$ and $\overline{\mathcal{S}}^{\text{agg}}_{T,r_D}(\tilde{x}) \leq \overline{\mathcal{S}}^{\text{agg}}_{T,r_D}(x^*)$. For this, let $\tilde{j} \in [N]$ such that $\overline{\mathcal{L}}^p_{T,r_D}(\tilde{x}) \leq \overline{\mathcal{L}}^{\tilde{j}}_{T,r_D}(\tilde{x})$ for all $p \in [N]$ and let $j^* \in [N]$ such that $\overline{\mathcal{L}}^p_{T,r_D}(x^*) \leq \overline{\mathcal{L}}^{j^*}_{T,r_D}(x^*)$ for all $p \in [N]$. Then,

$$\overline{\mathcal{L}}^{j^*}_{T,r_D}(\tilde{x}) \leq \overline{\mathcal{L}}^{\tilde{j}}_{T,r_D}(\tilde{x}) \leq \overline{\mathcal{L}}^{\tilde{j}}_{T,r_D}(x^*) \leq \overline{\mathcal{L}}^{j^*}_{T,r_D}(x^*)$$

holds. For the following, recall that $\alpha_L > 0$ and $\frac{1-\alpha_L}{N-1} > 0$. If $\tilde{j} \neq j^*$, then

$$\begin{aligned}
\overline{\mathcal{L}}^{\text{agg}}_{T,r_D}(\tilde{x}) &= \alpha_L \overline{\mathcal{L}}^{\tilde{j}}_{T,r_D}(\tilde{x}) + \frac{1-\alpha_L}{N-1}\overline{\mathcal{L}}^{j^*}_{T,r_D}(\tilde{x}) + \frac{1-\alpha_L}{N-1}\sum_{p\in[N]\setminus\{\tilde{j},j^*\}} \overline{\mathcal{L}}^p_{T,r_D}(\tilde{x}) \\
&\leq \alpha_L \overline{\mathcal{L}}^{j^*}_{T,r_D}(x^*) + \frac{1-\alpha_L}{N-1}\overline{\mathcal{L}}^{\tilde{j}}_{T,r_D}(x^*) + \frac{1-\alpha_L}{N-1}\sum_{p\in[N]\setminus\{\tilde{j},j^*\}} \overline{\mathcal{L}}^p_{T,r_D}(x^*) \\
&= \overline{\mathcal{L}}^{\text{agg}}_{T,r_D}(x^*).
\end{aligned}$$

If $\tilde{j} = j^*$, then

$$\begin{aligned}
\overline{\mathcal{L}}^{\text{agg}}_{T,r_D}(\tilde{x}) &= \alpha_L \overline{\mathcal{L}}^{\tilde{j}}_{T,r_D}(\tilde{x}) + \frac{1-\alpha_L}{N-1}\sum_{p\in[N]\setminus\{\tilde{j}\}} \overline{\mathcal{L}}^p_{T,r_D}(\tilde{x}) \\
&\leq \alpha_L \overline{\mathcal{L}}^{\tilde{j}}_{T,r_D}(x^*) + \frac{1-\alpha_L}{N-1}\sum_{p\in[N]\setminus\{\tilde{j}\}} \overline{\mathcal{L}}^p_{T,r_D}(x^*) = \overline{\mathcal{L}}^{\text{agg}}_{T,r_D}(x^*).
\end{aligned}$$

In particular, if there exists $m \in [N]$ such that $\overline{\mathcal{L}}^m_{T,r_D}(\tilde{x}) < \overline{\mathcal{L}}^m_{T,r_D}(x^*)$, then $\overline{\mathcal{L}}^{\text{agg}}_{T,r_D}(\tilde{x}) < \overline{\mathcal{L}}^{\text{agg}}_{T,r_D}(x^*)$ (in both cases $\tilde{j} = j^*$ and $\tilde{j} \neq j^*$).
The inequality $\overline{\mathcal{S}}^{\text{agg}}_{T,r_D}(\tilde{x}) \leq \overline{\mathcal{S}}^{\text{agg}}_{T,r_D}(x^*)$ is shown analogously.
Next, we perform a case distinction with respect to ℓ (the index such that $f^{\text{tol}}_\ell(\tilde{x}) < f^{\text{tol}}_\ell(x^*)$). If $\ell \in [N]$, then

$$\overline{\mathcal{L}}^\ell_{T,r_D}(\tilde{x}) < \overline{\mathcal{L}}^\ell_{T,r_D}(x^*) \;\Rightarrow\; \overline{\mathcal{L}}^{\text{agg}}_{T,r_D}(\tilde{x}) < \overline{\mathcal{L}}^{\text{agg}}_{T,r_D}(x^*).$$

Because $\overline{\mathcal{S}}^{\text{agg}}_{T,r_D}(\tilde{x}) \leq \overline{\mathcal{S}}^{\text{agg}}_{T,r_D}(x^*)$, we have $f^{\text{tol,agg}}(\tilde{x}) \leq f^{\text{tol,agg}}(x^*)$ in this case. But this is a contradiction to x^* being efficient with respect to (tol-agg-P).
If $\ell \in \{N+1, \ldots, 2N\}$, then

$$\overline{\mathcal{S}}^{\ell-N}_{T,r_D}(\tilde{x}) < \overline{\mathcal{S}}^{\ell-N}_{T,r_D}(x^*) \;\Rightarrow\; \overline{\mathcal{S}}^{\text{agg}}_{T,r_D}(\tilde{x}) < \overline{\mathcal{S}}^{\text{agg}}_{T,r_D}(x^*).$$

Because $\overline{\mathcal{L}}^{\text{agg}}_{T,r_D}(\tilde{x}) \leq \overline{\mathcal{L}}^{\text{agg}}_{T,r_D}(x^*)$, $f^{\text{tol,agg}}(\tilde{x}) \leq f^{\text{tol,agg}}(x^*)$ also applies in this case. Again, this is a contradiction to x^* being efficient with respect to (tol-agg-P). Therefore, x^* must also be efficient with respect to (tol-P_{T,r_D}). □

Remark 9.27 *The converse is not true in general, i.e., x^* efficient with respect to* (tol-P_{T,r_D}) *does not imply x^* efficient with respect to* (tol-agg-P). *For this, we consider the following brief counterexample with $N = 2$. Let us suppose that we have two solutions x^* and $\tilde{x}$ that are efficient with respect to* (tol-P_{T,r_D}). *Let us further suppose that*

$$\overline{\mathcal{L}}^1_{T,r_D}(x^*) = 0.6,\ \overline{\mathcal{L}}^2_{T,r_D}(x^*) = 0.6 \quad \textit{and} \quad \overline{\mathcal{L}}^1_{T,r_D}(\tilde{x}) = 0.8,\ \overline{\mathcal{L}}^2_{T,r_D}(\tilde{x}) = 0.1$$

as well as $\overline{\mathcal{S}}^p_{T,r_D}(x^*) = \overline{\mathcal{S}}^p_{T,r_D}(\tilde{x}) =: \lambda^p_{s,\text{incr}}$ for $p \in [2]$. Then, we have

$$f^{\text{tol}}(x^*) = (0.6, 0.6, \lambda^1_{s,\text{incr}}, \lambda^2_{s,\text{incr}}) \quad \textit{and} \quad f^{\text{tol}}(\tilde{x}) = (0.8, 0.1, \lambda^1_{s,\text{incr}}, \lambda^2_{s,\text{incr}}).$$

Note that $f^{\text{tol}}(x^*) \not\leq f^{\text{tol}}(\tilde{x})$ and that $f^{\text{tol}}(\tilde{x}) \not\leq f^{\text{tol}}(x^*)$, which is consistent with x^* and $\tilde{x}$ being efficient with respect to (tol-P_{T,r_D}).
However, regarding the aggregated objective functions with $\alpha_L = 0.8$, we have

$$\overline{\mathcal{L}}^{\text{agg}}_{T,r_D}(x^*) = 0.8 \cdot 0.6 + 0.2 \cdot 0.6 = 0.6 \quad \textit{and} \quad \overline{\mathcal{L}}^{\text{agg}}_{T,r_D}(\tilde{x}) = 0.8 \cdot 0.8 + 0.2 \cdot 0.1 = 0.66$$

as well as $\overline{\mathcal{S}}^{\text{agg}}_{T,r_D}(x^*) = \overline{\mathcal{S}}^{\text{agg}}_{T,r_D}(\tilde{x})$, i.e., $f^{\text{tol,agg}}(x^*) \leq f^{\text{tol,agg}}(\tilde{x})$ and thus $\tilde{x}$ cannot be efficient with respect to (tol-agg-P).

According to Remark 9.27, by solving (tol-agg-P) we do not find all Pareto optimal solutions of (tol-P_{T,r_D}) in general. However, because the decision makers are particularly interested in solutions where the largest Lipschitz constant as well as the largest start point increment are small and in order to make decision making easier, it is proposed to solve the aggregated problem (tol-agg-P) instead of the problem (tol-P_{T,r_D}), which provides a subset of the Pareto optimal solutions of (tol-P_{T,r_D}).
In the following subsection, a method based on evolutionary multiobjective optimization algorithms is proposed to solve (tol-agg-P).

9.2.2. Proposed Method to Solve (tol-agg-P)

To solve the problem (tol-agg-P), we again focus on derivative-free methods, because

- non-convexity of the Pareto front of (tol-agg-P) cannot be excluded,
- multimodality cannot be excluded,
- in general, gradients are not available.

This is analogous to the nominal problem (nom-P^p_{T,r_D}), see also Section 9.1. To solve (nom-P^p_{T,r_D}), a grid search method is proposed. However, this method is not suited to solve (tol-agg-P) for the following reason:
In the nominal case, the decision space has the dimension three. In contrast, the decision space of (tol-agg-P) has the dimension $3N$ according to Definitions 9.23 and 8.81. For instance, in the common case $N = 7$, the decision space has the dimension 21 and it is practically impossible to build a dense search grid. This phenomenon is also called the *curse of dimensionality* [HTF09, p. 22].

Because it is a "major challenge" allowing direct search methods "to tackle higher dimensional problems" [CEM12, p. 8], direct search methods to solve (tol-agg-P) are not investigated in this work. Rather, we focus on evolutionary algorithms, which are "relatively robust and flexible for solving nonlinear optimization problems" [CEM12, p. 14]. One of the most popular evolutionary multiobjective optimization algorithms, in particular for two- and three-dimensional problems, is the NSGA-II [Coe+20, p. 223]. Therefore, it is proposed to use NSGA-II to solve (tol-agg-P).
NSGA-II and its working principle are presented in Section 4.2.2. Because NSGA-II assumes that the underlying problem is unconstrained, we also need a constraint handling technique (CHT). A CHT that was designed for NSGA-II is the constrained dominance principle (CDP), which is detailed in Section 4.2.3. Therefore, it is proposed to combine NSGA-II with CDP for solving (tol-agg-P).
In the following, some details and particularities of a corresponding implementation are covered. Thereafter, solving (tol-agg-P) with NSGA-II and CDP is demonstrated in a use case.

9.2.3. Details and Particularities of the Implementation

NSGA-II is a popular algorithm and there already exists a variety of implementations. To solve (tol-agg-P), the Matlab implementation by Seshadri [Ses09] is used. The key points of this implementation are as follows.

Box constraints: Because an evolutionary optimization algorithm needs a space from which the considered solutions are drawn and generated, box constraints are "usually trivially enforced" in an evolutionary algorithm [DD15, p. 3]. This also applies to the implementation by Seshadri. Therefore, we have to specify suitable box constraints such that the feasible set $X^{\text{tol}}_{T,r_D}(\mathcal{H}_{\text{nom}},\mathcal{U}_{\text{tol}})$ is covered without being too relaxed.

Remark 9.28 *A box constraint with respect to the i-th variable x_i is of the form $x_i^L \leq x_i \leq x_i^U$ [DD15, p. 3].*

According to Definition 8.81 of the feasible set $X^{\text{tol}}_{T,r_D}(\mathcal{H}_{\text{nom}},\mathcal{U}_{\text{tol}})$, we have

$$(s^1, i_s^1, i_t^1, \ldots, s^N, i_s^N, i_t^N) \in X^{\text{tol}}_{T,r_D}(\mathcal{H}_{\text{nom}},\mathcal{U}_{\text{tol}}) \;\Rightarrow\; (s^p, i_s^p, i_t^p) \in X^{p}_{T,r_D}(\mathcal{H}_{\text{nom}}) \;\forall\; p \in [N].$$

Therefore, we can select the box constraints for each ADA pair individually. Furthermore, one may consider only the sets $X^{p}_{T,r_D}(\mathcal{H}_{\text{nom}})$, $p \in [N]$, when selecting the box constraints. The set $X^{p}_{T,r_D}(\mathcal{H}_{\text{nom}})$ is the feasible set of the nominal ADA optimization problem (nom-P^{p}_{T,r_D}), $p \in [N]$, and thus it has already been analyzed in the preceding Section 9.1.
Let $p \in [N]$. As delineated in Section 9.1.1, there exists a two-dimensional set $X^{p,s}_{T,r_D}$ and a bijection τ^p such that $\tau^p\big(X^{p}_{T,r_D}\big) = X^{p,s}_{T,r_D}$. Recall from Definition 9.1 that the two components of the set $X^{p,s}_{T,r_D}$ are the start fan speed s^p and the start point increment $\lambda^p_{s,\text{incr}}$.

Remark 9.20 states that $1.05t^p$ and $\min\{1.4t^p, t^{p-1} - \varepsilon\}$ ($\min\{1.4t^1, \mathrm{fs}_{\max}\}$ if $p = 1$) are suitable lower and upper bounds, respectively, for s^p. Remark 9.14 states that 0 and 0.3 are suitable lower and upper bounds, respectively, for $\lambda^p_{s,\mathrm{incr}}$.
Therefore, we select the box constraints for the two-dimensional sets $X^{p,s}_{T,r_D}$, $p \in [N]$, as follows. For each $p \in [N]$, we select $s^{p,L} = 1.05t^p$ and $s^{p,U} = \min\{1.4t^p, t^{p-1} - \varepsilon\}$ ($s^{1,U} = \min\{1.4t^1, \mathrm{fs}_{\max}\}$) as well as $\lambda^{p,L}_{s,\mathrm{incr}} = 0$ and $\lambda^{p,U}_{s,\mathrm{incr}} = 0.3$.
The resulting approach is straightforward. The search space consists of all elements $(s^1, \lambda^1_{s,\mathrm{incr}}, \ldots, s^N, \lambda^N_{s,\mathrm{incr}}) \in \mathbb{R}^{2N}$ such that $s^{p,L} \leq s^p \leq s^{p,U}$ and $\lambda^{p,L}_{s,\mathrm{incr}} \leq \lambda^p_{s,\mathrm{incr}} \leq \lambda^{p,U}_{s,\mathrm{incr}}$ for all $p \in [N]$. By applying $(\tau^p)^{-1}$ to $(s^p, \lambda^p_{s,\mathrm{incr}})$ for all $p \in [N]$ and concatenating the images, we obtain the corresponding $x = (s^1, i^1_s, i^1_t, \ldots, s^N, i^N_s, i^N_t)$ at which the constraints and the objective functions of (tol-agg-P) are evaluated.

Remark 9.29 *According to Definition 9.1, the function $(\tau^p)^{-1}$ is only defined for elements $(s^p, \lambda^p_{s,\mathrm{incr}}) \in X^{p,s}_{T,r_D}$. Therefore, one has to pay attention that all transformations from the box constrained search space to $X^{\mathrm{tol}}_{T,r_D}(\mathcal{H}_{\mathrm{nom}}, \mathcal{U}_{\mathrm{tol}})$ via $(\tau^p)^{-1}$ are well-defined.*
The same is true for evaluating the objective functions, because the obtained x is not necessarily an element of $X^{\mathrm{tol}}_{T,r_D}(\mathcal{H}_{\mathrm{nom}}, \mathcal{U}_{\mathrm{tol}})$ (otherwise we would not require a constraint handling technique at all).

A major advantage of this approach is that the search space is $2N$-dimensional. In contrast, the original feasible set $X^{\mathrm{tol}}_{T,r_D}(\mathcal{H}_{\mathrm{nom}}, \mathcal{U}_{\mathrm{tol}})$ is $3N$-dimensional.

Used genetic operators: As delineated in Section 4.2, as a genetic algorithm NSGA-II requires a reproduction, a crossover and a mutation operator. The implementation by Seshadri uses tournament selection, simulated binary crossover and polynomial mutation, respectively, which is a common choice [Deb+02, p. 178] [Bra+08, p. 76]. These operators are detailed in Section 4.2.1.

Meaningful objective function values of infeasible solutions: Regarding infeasible solutions, we have to consider two aspects. First, we have to make sure that infeasible solutions can be evaluated, i.e., that the constraints and the objective functions are well-defined for all infeasible solutions within the box constraints, see also Remark 9.29. For instance, this can be done by artificially extending the domains of the constraints and the objective functions. However, this must be done in a meaningful way.
This is the second aspect we have to consider. It is required because the selected CHT is CDP. With CDP it may happen that two infeasible solutions are compared with each other for "less infeasibility". Therefore, it is required that infeasible solutions get an indicator for their degree of infeasibility. This has to be taken into account when the domains of constraints and of objective functions are artificially extended.

This concludes the details of the implementation used to solve (tol-agg-P). Next, the implementation is demonstrated in a use case.

9.2.4. Use Case

We want to find optimal ADA parameters for a Vaillant HE. In contrast to the use case presented in Section 9.1.4, we also consider tolerances with respect to the position of the ioni electrode this time. As in Section 9.1.4, the nominal HE measurement data corresponds to [PHE, Item 6371] and all HE models considered in this use case are based on a piecewise linear interpolation. The HE's tolerance measurement data corresponds to [PHE, Item 6168], [PHE, Item 6177], [PHE, Item 6200], [PHE, Item 6327] and [PHE, Item 6344], i.e., the considered uncertainty set $\mathcal{U}_{\text{tol}}$ consists of five tolerance HE models. Let us suppose that the decision makers want to optimize six ADA pairs, i.e., we are in the case $N = 6$. Furthermore, we suppose that the decision makers specified the set of feasible test fan speeds by $T = \{t^1 = 10000, t^2 = 8500, t^3 = 7000, t^4 = 5500, t^5 = 4000, t^6 = 2500\}$. The drift resistance is specified by $r_D = 140k\Omega$. Our goal is to find the Pareto optimal solutions of (tol-agg-P). The problem's parameters are specified by the common values $\lambda_{\text{min}} = 1.05$, $\lambda_{\text{max}} = 1.6$, $\text{co}_{\text{max}} = 150$, $\Delta\lambda_{\text{min}} = 0.1$, $\lambda_{\text{wp,tol}} = 0.1$, $n_{\text{max}} = 50$ and $i_{\text{thr}} = 3 \cdot 10^{-4}$. The set $\text{FS}_{\text{sample}}$ consists of 100 equidistant points between the HE's minimum and maximum fan speed $\text{fs}_{\text{min}} = 2200$ and $\text{fs}_{\text{max}} = 12000$, respectively. To solve this instance of (tol-agg-P), we use an implementation of NSGA-II as proposed and described in Sections 9.2.2 and 9.2.3.
The used implementation of NSGA-II also requires some parameters, which are selected as follows:

- **Population size:** The population size indicates how many individuals are considered at the beginning of each generation. In this use case, a population size of 200 is selected.
- **Number of generations:** The number of generations indicates how many iterations with the NSGA-II are executed. In this use case, we consider 300 generations.
- **Mating pool size:** The mating pool size indicates how often the reproduction operator is executed. A common value is half of the population size. In this use case this corresponds to a mating pool size of 100.
- **Simulated binary crossover parameter η_c:** In this use case we use $\eta_c = 20$, which is a common value. For details of η_c see Section 4.2.1.
- **Mutation parameter η_m:** In this use case we use $\eta_m = 20$, which is a common value. For details of η_m see Section 4.2.1.

We perform a single run of the NSGA-II implementation with these parameters. In each generation, the genetic operators are applied and the resulting population is sorted for nondominance. Figure 9.4 shows the corresponding set of nondominated points in the objective space of (tol-agg-P) after 20, 50, 100, 200, and 300 generations. It is apparent that with increasing number of iterations the approximation quality of the Pareto front improves. Note that the difference between the nondominated sets after 200 and after

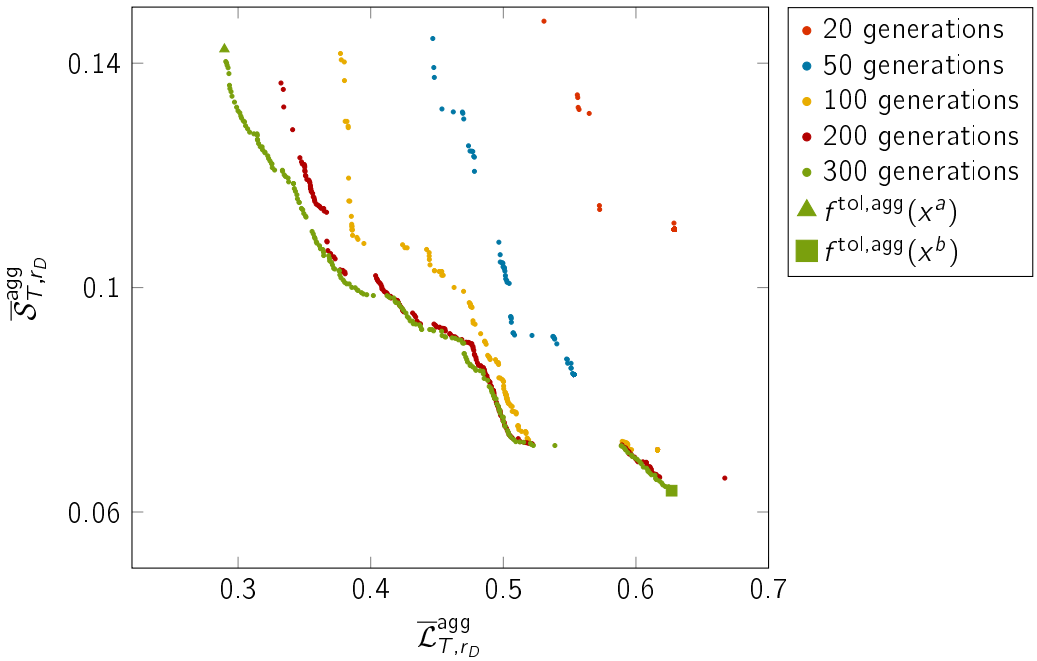

Figure 9.4.: The nondominated sets in the objective space of the aggregated problem (tol-agg-P) after 20, 50, 100, 200 and 300 generations with the NSGA-II are displayed. The point with the smallest aggregated Lipschitz constant is highlighted by the green triangle. The point with the smallest aggregated start point increment is highlighted by the green square.

300 generations is rather small, in particular in regions with a small second objective function value. It can therefore be assumed that beyond 300 generations the approximation quality improves only slightly, if at all. However, the true Pareto front and therefore the true approximation quality remain unknown.
The required computation time for 20, 50, 100, 200 and 300 generations on a system with an AMD Ryzen 5800x was 81.7 seconds, 297.2 seconds, 652.4 seconds, 1344.9 seconds and 1991.3 seconds, respectively.
Recall that a point in the objective space of (tol-agg-P) represents the aggregated objective functions $\overline{\mathcal{L}}^{\text{agg}}_{T,r_D}$ and $\overline{\mathcal{S}}^{\text{agg}}_{T,r_D}$. Ultimately, however, we are interested in the Lipschitz constant and in the start point increment of each ADA pair individually. We therefore take a closer look at the two extreme solutions after 300 generations as examples. Let $x^a \in X^{\text{tol}}_{T,r_D}(\mathcal{H}_{\text{nom}}, \mathcal{U}_{\text{tol}})$ be the solution such that $f^{\text{tol,agg}}(x^a)$ corresponds to the nondominated point with the smallest aggregated Lipschitz constant after 300 generations. Analogously, let $x^b \in X^{\text{tol}}_{T,r_D}(\mathcal{H}_{\text{nom}}, \mathcal{U}_{\text{tol}})$ be the solution such that $f^{\text{tol,agg}}(x^b)$ corresponds to the nondominated point with the smallest aggregated start point increment after 300 generations. Their images are marked in Figure 9.4 by the green triangle and by the green square, respectively. The corresponding aggregated objective function values as well as the corresponding ADA pairs' individual Lipschitz constant and start point increment are

x	$\overline{\mathcal{L}}^{\text{agg}}_{T,r_D}(x)$	$\overline{\mathcal{L}}^{1}_{T,r_D}(x)$	$\overline{\mathcal{L}}^{2}_{T,r_D}(x)$	$\overline{\mathcal{L}}^{3}_{T,r_D}(x)$	$\overline{\mathcal{L}}^{4}_{T,r_D}(x)$	$\overline{\mathcal{L}}^{5}_{T,r_D}(x)$	$\overline{\mathcal{L}}^{6}_{T,r_D}(x)$
x^a	0.2897	**0.2914**	0.2914	0.2586	0.2830	0.2859	0.2889
x^b	0.6269	0.3622	0.3732	**0.6513**	0.6469	0.5279	0.6156
	$\overline{\mathcal{S}}^{\text{agg}}_{T,r_D}(x)$	$\overline{\mathcal{S}}^{1}_{T,r_D}(x)$	$\overline{\mathcal{S}}^{2}_{T,r_D}(x)$	$\overline{\mathcal{S}}^{3}_{T,r_D}(x)$	$\overline{\mathcal{S}}^{4}_{T,r_D}(x)$	$\overline{\mathcal{S}}^{5}_{T,r_D}(x)$	$\overline{\mathcal{S}}^{6}_{T,r_D}(x)$
x^a	0.1425	0.0606	0.0815	0.1151	0.1384	0.1037	**0.1511**
x^b	0.0638	0.0458	0.0636	0.0650	0.0625	**0.0651**	0.0505

Table 9.1.: This table compares the aggregated objective function values of two exemplary solutions with the Lipschitz constant and the start point increment of each individual ADA pair p, $p \in [6]$. The considered solutions x^a and x^b correspond to the two nondominated extreme points in Figure 9.4. The largest Lipschitz constant and the largest start point increment of the two solutions are highlighted in bold.

shown in Table 9.1. The largest Lipschitz constant and the largest start point increment of x^a and x^b are highlighted in bold.
The aggregated function values are smaller than but close to the largest individual function values, which is to be expected since we weighted the largest values with a factor of $\alpha_L = 0.8$ and $\alpha_{\lambda_{s,\text{incr}}} = 0.8$. However, the individual function values can differ from the aggregated value significantly. For instance, the aggregated Lipschitz constant of x^b is $\overline{\mathcal{L}}^{\text{agg}}_{T,r_D}(x^b) = 0.6269$ while the corresponding Lipschitz constant of ADA pair one is $\overline{\mathcal{L}}^{1}_{T,r_D}(x^b) = 0.3622$.
This concludes the use case. The advantages and disadvantages of the approach with aggregated function values and of the selected solution method based on NSGA-II are discussed next.

9.2.5. Discussion of the Proposed Approach

We discuss the approach to solve the aggregated problem (tol-agg-P) in order to obtain Pareto optimal solutions of the original problem (tol-P_{T,r_D}) first. Using NSGA-II to solve (tol-agg-P) is then discussed.

The aggregated Problem (tol-agg-P)**:** Our goal is to solve the tolerance ADA optimization problem (tol-P_{T,r_D}), which has $2N$ objectives, where N is the number of ADA pairs to be optimized. In order to make the decision making easier, the aggregated problem (tol-agg-P) is introduced, which is always biobjective. It is true that the trade-off between two solutions of the aggregated problem (tol-agg-P) can be presented clearly. But this comes at a price.
The aggregated objective function values contain no information about the variance of the individual objective function values. This is briefly mentioned at the end of the preceding subsection, where the function values listed in Table 9.1 represent a corresponding

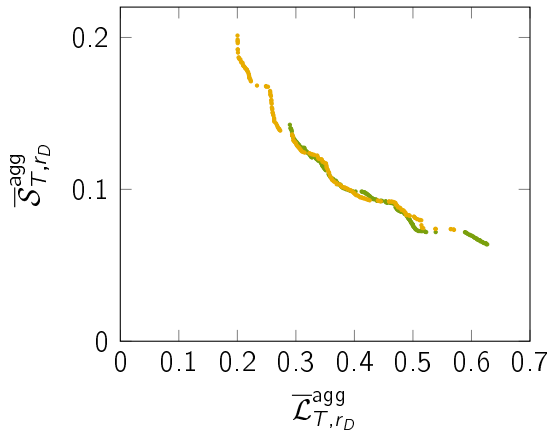

Figure 9.5.: The nondominated sets after 300 generations with NSGA-II for two different random starting populations are displayed. The randomness in the evolutionary algorithm causes the outputs to differ significantly.

example. Furthermore, because a nondominated point in the objective space represents N ADA pairs at once, it is unclear how each ADA pair is affected if a different solution is selected. For instance, two neighbored points in the objective space might have significantly different ADA parameters, i.e., the ADA pairs and their Lipschitz constants as well as their start point increments might differ significantly. Therefore, the decision maker has less possibilities to fine-tune the solution in the selection process.
If the decision makers are not satisfied with the decision making process using the aggregated problem (tol-agg-P), it may make sense to revise the aggregated problem (tol-agg-P) or to even solve the original problem (tol-P_{T,r_D}).

NSGA-II: As an evolutionary algorithm, NSGA-II has some randomness by intention. However, from a user's perspective this might be disturbing, because it is (almost) impossible to reproduce solutions that were once obtained in a different run with NSGA-II. In particular, two different runs with NSGA-II might produce two significantly different approximations of the Pareto front. This is illustrated in Figure 9.5. The yellow dots correspond to the nondominated set after a single run of NSGA-II with 300 generations. The green dots also correspond to the nondominated set after a single run with 300 generations but with a different (randomly generated) starting population. Both runs were performed with the same parameters as selected in the use case presented in Section 9.2.4. In the run corresponding to the yellow solutions smaller aggregated Lipschitz constants were explored. In contrast, in the run corresponding to the green solutions smaller aggregated start point increments were explored.
However, having significantly different nondominated sets offers potential for obtaining a better approximation of the true Pareto front. For this, the nondominated sets of several runs with NSGA-II are combined into a single set. This combined set is filtered for Pareto nondominance to obtain the corresponding set of nondominated points, which is usually

larger than each of the original nondominated sets. In Figure 9.5, this nondominated set corresponds to all nondominated points in the union of the yellow and the green points (not explicitly illustrated). Therefore, instead of increasing the number of generations or the population size in order to obtain a better approximation of the Pareto front, it might be more effective to start several runs with different starting populations. However, for the special case that (single-objective) additively separable functions are considered, an analytical study suggests that "for difficult problems ... the best alternative is to use a single run with the largest population possible" [CG03, p. 811].
Selecting a suitable population size and number of generations as well as selecting suitable other parameters for NSGA-II (pool size, crossover factor and mutation factor) might be challenging, because the true Pareto front is unknown in general. I.e., it is hard to assess whether the selected parameters are appropriate. However, the results obtained with the parameters selected in the use case in Section 9.2.4 are satisfactory for the practitioners. The same is true for the selected constraint handling technique. The constrained dominance principle performed well in the use case. After approximately 100 generations all found solutions are feasible and stay feasible in the subsequent generations (because NSGA-II is an elitist algorithm). However, it cannot be excluded that other constraint handling techniques perform even better, since we do not know how close we are to the true Pareto front. In particular, it is not guaranteed that the selected methods find a feasible solution at all. This may be further analyzed in future research.
Another aspect regarding the constraint handling is that the HE model must provide meaningful outputs for certain infeasible solutions, as stated at the end of Section 9.2.3. In the use case, this was achieved by artificially extending the domains of the HE model functions such that their monotonicity properties are preserved.
Finally, depending on the population size and on the number of generations, the required computation time is rather large. In the use case, the NSGA-II required 1991.3 seconds for 300 generations with a population size of 200. Because the optimization is run only once during the design process, the required computation time is acceptable.
To summarize this discussion, the selected combination of NSGA-II and constrained dominance principle is suited to solve the aggregated tolerance problem (tol-agg-P). However, its approximation quality remains hard to assess. Furthermore, the randomness of the evolutionary algorithm on the one hand may be disturbing to the decision makers. On the other hand, by combining the results of several runs it can be used to improve the approximation quality in some cases.
For future research, it might be of interest to investigate how methods other than NSGA-II perform when solving (tol-agg-P). An interesting alternative could be the so-called Multi-Objective Evolutionary Algorithm based on Decomposition [Coe+20, p. 224].

By proposing, demonstrating and discussing methods for solving the ADA optimization problems (nom-P^p_{T,r_D}) and (tol-P_{T,r_D}), the remaining research question from the introductory Chapter 1 was addressed in this chapter. The following chapter concludes this thesis by summarizing the most important results.

10. Conclusion

This chapter concludes the thesis by summarizing the main findings in relation to the research aims and research questions. The contributions of this work as well as its limitations are then reviewed and further research is suggested.

This thesis analyzes the ADA procedure from a mathematical point of view and assists in finding optimized ADA parameters by computer simulation. The analysis shows that the convergence properties of the ADA Algorithm 5.2 depend strongly on the drift resistance ADA iteration functions $A^p_{r_D}$, $p \in [N]$, from Definition 6.21. Because $A^p_{r_D}$ depends on the ADA parameters (s^p, t^p, i^p_t, i^p_s), $p \in [N]$, the selection of suitable ADA parameters is essential for the ADA procedure to function properly.

If the ADA parameters are selected such that $A^p_{r_D}$ is a contractive selfmap and such that $\iota^{-1}_{s^p}(i^p_s) = \iota^{-1}_{t^p}(i^p_t)$ holds for all $p \in [N]$, then the ADA Algorithm 5.2 converges to the sought vector of drifted test ioni currents, i.e., the drift resistance is perfectly approximated by all ADA pairs. The rate of convergence depends on the Lipschitz constants of the functions $A^p_{r_D}$, $p \in [N]$. Small Lipschitz constants of the iteration functions guarantee a high rate of convergence. Therefore, one goal of the ADA optimization is to find ADA parameters such that the iteration functions' Lipschitz constants are small.
However, as delineated in Section 8.4, this goal usually conflicts with the requirement that the duration of a single ADA iteration should be short. An indicator for the duration required for an ADA iteration is the so-called start point increment defined in Section 8.4.2. A small start point increment corresponds to a short duration of an ADA iteration. As a consequence, the proposed optimization models are multiobjective, where the objectives are to minimize the iteration functions' Lipschitz constants as well as the corresponding start point increments simultaneously.
A further finding is that the condition $\iota^{-1}_{s^p}(i^p_s) = \iota^{-1}_{t^p}(i^p_t)$ for all $p \in [N]$ is usually not satisfied if tolerances with respect to the position of the ioni electrode are present. Then, the limit of the ADA Algorithm 5.2 does not correspond to the sought drifted test ioni currents (if the limit exits at all). In this case, it must be ensured that the algorithm's limit does not result in combustion states that exceed permissible limits. This was taken into account when developing the optimization models by considering the two cases "tolerances are not present" and "tolerances are present" separately. The resulting models are (nom-P^p_{T,r_D}) and (tol-P_{T,r_D}), respectively. A particularity of (nom-P^p_{T,r_D}) is that the ADA pairs are considered individually. In contrast, in the case with tolerances this is not possible and thus the problem (tol-P_{T,r_D}) considers all ADA pairs simultaneously.
Finally, this thesis proposes to solve (nom-P^p_{T,r_D}) with a grid search combined with a vari-

ant of the ε-constraint scalarization and to solve (tol-P_{T,r_D}) with NSGA-II. Regarding the constraint handling, it is proposed to combine NSGA-II with the constrained dominance principle. Both methods are demonstrated in a use case.

This thesis provides a deeper insight into the properties of the ADA procedure. In the literature, i.e., in the technical documentation of IoniDetect, the ADA procedure is only considered in the special case with a single ADA pair and without tolerances. In this thesis, also the cases with a plurality of ADA pairs as well as with tolerances are analyzed, which fills this gap. Furthermore, understanding the multiobjective character of the ADA parameterization might assist the decision makers to select ADA parameters that fit their preferences best. Finally, the use cases provide examples of applying the ε-constraint scalarization and NSGA-II in practice.
The practical contribution of this work is that the developed models and proposed methods support the engineers at Vaillant in the ADA parameterization. In particular, the ADA parameters can be selected by computer simulation, which reduces required lab capacities and development time. Moreover, optimized ADA parameters yield better convergence characteristics and are more robust with respect to tolerances of the position of the ioni electrode.

Although the decision makers are satisfied with the ADA parameters optimized according to the results of this work and the methods presented, there is still a discrepancy between simulation results and measured values when the optimized ADA parameters are verified in the lab. The discrepancy might result from limitations of the HE model defined in Section 2.4. The HE model does not take dynamic behavior into account. Furthermore, the HE model assumes continuous gas valve positions, ioni currents and fan speeds. Assuming a continuous gas valve position is particularly disputable, because the outputs of an HE system corresponding to two neighboring discrete gas valve positions (with the same fan speed) can differ significantly. This might be problematic, because the gas valve position plays a central role in the ADA iteration function and in the ADA procedure. Although this is a potential shortcoming, a continuous HE model facilitates the convergence analysis of the ADA procedure, because the considered iteration functions have continuous domains and images in this case.
That the HE model disregards dynamic HE behavior is a consequence of the measurement data provided by Vaillant. However, practical experience indicates that dynamics might influence the results of the ADA procedure. Furthermore, the influence of environmental and atmospheric conditions such as the air pressure and humidity or the gas pressure and temperature are not considered in the HE model.
A further limitation related to the modeling aspect is that the drift resistance is considered to be constant. It cannot be excluded in practice that the drift resistance is a function of the fan speed and/or the equivalence AFR.
Finally, regarding the proposed optimization models and methods, there are two major limitations. First, the proposed optimization methods are heuristics and not exact methods, i.e., we have no information about the "degree of optimality" of a found solution.

Secondly, the proposed optimization models are relaxations. But at least in the simulation, a relaxed solution has barely better objective function values than its rounded to nearest integer counterpart.

Further modeling work will have to be conducted in order to understand and reduce the discrepancy between simulation results and measured values in the lab. This could include considering discrete gas valve positions, dynamics of the HE systems and influence of environmental conditions. In addition, further research should be undertaken to analyze the influence of a discrete gas valve position and a variable drift resistance on the convergence characteristics of the ADA procedure. Furthermore, it might be of interest to investigate the precise mechanism by which tolerances with respect to the position of the ioni electrode influence the resulting ioni current. If this is better understood, it might be possible to simulate the influence of tolerances which helps to further reduce required lab capacities. A further study could assess whether discrete optimization models and methods obtain (significantly) better ADA parameters than the relaxed continuous models and methods proposed in this thesis. Finally, further research might explore how other deposits than the oxide layer on the ioni electrode influence the ioni current. For example, at the time of writing, Vaillant engineers are investigating the influence of silicates deposited on the ioni electrode. The silicates come from detergents used in washing machines.

In summary, despite its limitations, this work significantly contributes to the understanding of the ADA procedure and provides practical support for the ADA parameterization.

Bibliography

[Ada22] Michael Adams. *Signal and Systems*. 4th ed. Department of Electrical and Computer Engineering, University of Victoria, 2022. ISBN: 9780987919779.

[ÅM09] Karl Johan Åström and Richard M. Murray. *Feedback Systems. An Introduction for Scientists and Engineers*. Princeton University Press, 2009. ISBN: 9780691135762.

[AR24] Andre Autermann and Andreas Reinert. "Verfahren zur Inbetriebnahme eines Heizgerätes, Computerprogramm, Regel- und Steuergerät und Heizgerät". DE 10 2022 133 191 A1. 2024.

[BDH23] BDH. *Marktentwicklung Wärmemarkt 2023*. Accessed on September 30, 2024. 2023. URL: https://www.bdh-industrie.de/fileadmin/user_upload/Pressemeldungen/Absatzzahlen_Waermemarkt_Deutschland_2023-12.pdf.

[BDH24] BDH. *Gesamtbestand zentraler Wärmeerzeuger in Deutschland 2023*. Accessed on September 30, 2024. 2024. URL: https://www.bdh-industrie.de/fileadmin/user_upload/Pressegrafiken/Infografik_Gesamtbestand_zentraler_Waermeerzeuger_DE_082024.pdf.

[Ber07] V. Berinde. *Iterative Approximation of Fixed Points*. Ed. by J.-M. Morel, F. Takens, and B. Teissier. Vol. 1912. Lecture Notes in Mathematics. Springer, 2007. DOI: 10.1007/978-3-540-72234-2.

[BK16] Hans Dieter Baehr and Stephan Kabelac. *Thermodynamik. Grundlagen und technische Anwendungen*. 16th ed. Springer Vieweg, 2016. DOI: 10.1007/978-3-662-49568-1.

[Bra+08] Jürgen Branke et al., eds. *Multiobjective Optimization. Interactive and Evolutionary Approaches*. Lecture Notes in Computer Science. Springer Berlin, Heidelberg, 2008. DOI: 10.1007/978-3-540-88908-3.

[Car+18] Stéphane Carpentier et al. *Self-regulated gas boilers able to cope with gas quality variation. State of the art and performances*. Research rep. GERG, 2018. DOI: 10.1007/3-540-45105-6_94.

[CEM12] Ana Luísa Custódio, Michael Emmerich, and José Firmino Aguilar Madeira. "Recent Developments in Derivative-Free Multiobjective Optimisation". In: *Computational Technology Reviews* 5 (2012). DOI: 10.4203/ctr.5.1.

[CG03] Erick Cantú-Paz and David E. Goldberg. "Are Multiple Runs of Genetic Algorithms Better than One?" In: *Genetic and Evolutionary Computation — GECCO 2003*. Ed. by Erick Cantú-Paz et al. Springer Berlin Heidelberg, 2003, pp. 801–812. DOI: 10.1007/3-540-45105-6_94.

[CL17] Günther Cerbe and Benno Lendt. *Grundlagen der Gastechnik*. 8th ed. Carl Hanser Verlag München, 2017. DOI: 10.1007/978-3-446-44966-4.

[Coe+20] Carlos A. Coello Coello et al. "Evolutionary Multiobjective Optimization: Open Research Areas and Some Challenges Lying Ahead". In: *Complex & Intelligent Systems* 6 (July 1, 2020), pp. 221–236. DOI: 10.1007/s40747-019-0113-4.

[CSV09] Andrew R. Conn, Katya Scheinberg, and Luis N. Vicente. *Introduction to Derivative-Free Optimization*. Society for Industrial and Applied Mathematics, 2009. DOI: 10.1137/1.9780898718768.

[DD15] Rituparna Datta and Kalyanmoy Deb, eds. *Evolutionary Constrained Optimization*. Infosys Science Foundation Series. 2015. DOI: 10.1007/978-81-322-2184-5.

[Deb+02] Kalyanmoy Deb et al. "A fast and elitist multiobjective genetic algorithm: NSGA-II". In: *IEEE Transactions on Evolutionary Computation* 6.2 (2002), pp. 182–197. DOI: 10.1109/4235.996017.

[Deb01] Kalyanmoy Deb. *Multi-Objective Optimization using Evolutionary Algorithms*. Wiley, 2001. ISBN: 978-0-471-87339-6.

[DFT90] John Doyle, Bruce A. Francis, and Allen Tannenbaum. *Feedback Control Theory*. Macmillan Publishing Company, 1990.

[DZG18] Michael Doumpos, Constantin Zopounidis, and Evangelos Grigoroudis, eds. *Robustness Analysis in Decision Aiding, Optimization, and Analytics*. International Series in Operations Research & Management Science. Springer Cham, 2018. DOI: 10.1007/978-3-319-33121-8.

[Ehr05] Matthias Ehrgott. *Multicriteria Optimization*. 2nd ed. Springer Berlin Heidelberg, 2005. DOI: 10.1007/3-540-27659-9.

[Eic21] Gabriele Eichfelder. "Twenty years of continuous multiobjective optimization in the twenty-first century". In: *EURO Journal on Computational Optimization* 9 (2021). DOI: 10.1016/j.ejco.2021.100014.

[Eur22] European Standard. *Safety and control devices for burners and appliances-burning gaseous or liquid fuels - Control functions inelectronic systems - Part 2: Fuel/air ratiocontrol/supervision of the electronic type; EN 12067-2:2022*. 2022.

[For23] Otto Forster. *Analysis 1. Differential- und Integralrechnung einer Veränderlichen*. 13th ed. Grundkurs Mathematik. Springer Spektrum Wiesbaden, 2023. DOI: 10.1007/978-3-658-40130-6.

[FSK08] Alexander I. J. Forrester, András Sóbester, and Andy J. Keane. *Engineering Design via Surrogate Modelling. A Practical Guide*. John Wiley & Sons Ltd., 2008. DOI: 10.1002/9780470770801.

[Gar13] D. J. H. Garling. *A Course in Mathematical Analysis. Volume 1: Foundations and Elementary Real Analysis*. Vol. 1. Cambridge University Press, 2013. DOI: 10.1017/CBO9781139424493.

[Gol14] Victor Gold. *Compendium of Chemical Terminology*. International Union of Pure and Applied Chemistry, 2014. DOI: 10.1351/goldbook.

[HTF09] Trevor Hastie, Robert Tibshirani, and Jerome Friedman. *The Elements of Satistical Learning. Data Mining, Inference, and Prediction*. 2nd ed. Springer Series in Statistics. Springer Science+Business Media, 2009. DOI: 10.1007/978-0-387-84858-7.

[Joh03] Don H. Johnson. "Origins of the equivalent circuit concept: the voltage-source equivalent". In: *Proceedings of the IEEE*. Vol. 91. 2003, pp. 636–640. DOI: 10.1109/JPROC.2003.811716.

[Kie+12] Martin Kiefer et al. "Combustion Control Based on Flame Ionization". In: *25th World Gas Conference*. 2012.

[Lia+23] Jing Liang et al. "A Survey on Evolutionary Constrained Multiobjective Optimization". In: *IEEE Transactions on Evolutionary Computation* 27.2 (2023), pp. 201–221. DOI: 10.1109/TEVC.2022.3155533.

[LJ19] Fernando Puente León and Holger Jäkel. *Signale und Systeme*. 7th ed. De Gruyter, 2019.

[Loc16] Rainer Lochschmied. *ADA. Besuch Fa. Vaillant*. Tech. rep. Siemens (confidential), 2016.

[Loc18] Rainer Lochschmied. *Funktionsweise ADA*. Siemens AG (confidential), 2018.

[LS17] Rainer Lochschmied and Bernd Schmiederer. "Control Facility For a Burner System". US 9,651,255 B2. 2017.

[MCF11] Sara McAllister, Jyh-Yuan Chen, and A. Carlos Fernandez-Pello. *Fundamentals of Combustion Processes*. Ed. by Frederick F. Ling. Mechanical Engineering Series. Springer New York, 2011. DOI: 10.1007/978-1-4419-7943-8.

[Mer+06] Günter P. Merker et al. *Simulating Combustion. Simulation of combustion and pollutant formation for engine-development*. Springer, 2006. DOI: 10.1007/3-540-30626-9.

[Mie98] Kaisa Miettinen. *Nonlinear Multiobjective Optimization*. International Series in Operations Research & Management Science. Springer Science+Business Media New York, 1998. DOI: 10.1007/978-1-4615-5563-6.

[MN22] Joaquim R. R. A. Martins and Andrew Ning. *Engineering Design Optimization*. Cambridge University Press, 2022. DOI: 10.1017/9781108980647. URL: https://mdobook.github.io.

[PHE] Vaillant. *Polarion: Platform Heat Engine (confidential)*. Application Lifecycle Management Tool. Vaillant, 2024.

[Res19] Sabrina Resch. "Voruntersuchungen für eine mechatronische Produktentwicklung von elektronischen Gas-Luft-Verbünden". PhD thesis. Bergische Universität Wuppertal, 2019.

[Sán20] José Manuel García Sánchez. *Modelling in Mathematical Programming*. International Series in Operations Research & Management Science. 2020. DOI: 10.1007/978-3-030-57250-1.

[Sch15] Bernd Schmiederer. *Konzept Sitherm Pro*. Tech. rep. Siemens (confidential), 2015.

[Ses09] Aravind Seshadri. *NSGA - II: A multi-objective optimization algorithm, Version 1.8.0.0*. Accessed on September 20, 2024. 2009. URL: https://de.mathworks.com/matlabcentral/fileexchange/10429-nsga-ii-a-multi-objective-optimization-algorithm.

[Son23] Julian Sonnenschein. "Entwicklung eines Verfahrens zur Kalibrierung der Ionisationsstrommessung in Gas-Brennwertgeräten". PhD thesis. Bergische Universität Wuppertal, 2023.

[Tan14] Zhongchao Tan. *Air Pollution and Greenhouse Gases. From Basic Concepts to Engineering Applications for Air Emission Control*. Springer Singapore, 2014. DOI: 10.1007/978-981-287-212-8.

[Vai24] Vaillant Group. *AT A Glance*. Accessed on September 20, 2024. 2024. URL: https://www.vaillant-group.com/our-company/at-a-glance/.

[Wes06] Tim Wescott. *Applied Control Theory for Embedded Systems*. Elsevier, 2006. DOI: 10.1016/B978-0-7506-7839-1.X5000-4.

[WHB] Vaillant. *Polarion: Wall Hanging Boiler (confidential)*. Application Lifecycle Management Tool. Vaillant, 2024.

[Wic19] Jens Wichtermann. *Vaillant launches next generation of gas-fired condensing boilers*. Accessed on September 20, 2024. 2019. URL: https://www.vaillant-group.com/news-stories/the-new-ecotec-exclusive-works-as-efficiently-as-possible-at-all-times.html.

[Wis19] Wissenschaftliche Dienste. *Grenzwerte für Wasserstoff (H2) in der Erdgasinfrastruktur, Aktenzeichen WD 8 - 3000 - 066/19*. Deutscher Bundestag, 2019.

A. Examples with Respect to the ADA Iteration Functions

Example A.1 *This example shows that there exists an ADA iteration function A^p_{i,r_D} that is not contractive but that still has a unique fixed point i^* and the Picard iteration associated to A^p_{i,r_D} converges to i^* for every starting point $i \in \hat{I}^p_{r_D}$. The example is based on artificial data and uses only the properties of the HE model according to Definition 2.18.*
The idea behind this example is as follows. We construct a drift resistance iteration function $A^p_{r_D}$ according to Definition 6.21 such that $A^p_{r_D}$ is a contractive selfmap but its ioni current based counterpart A^p_{i,r_D} is not contractive. Then, $A^p_{r_D}$ has a unique fixed point r^* and the Picard iteration associated to $A^p_{r_D}$ converges to r^* for all starting points $r \in \hat{R}^p_{r_D}$ (Lemma 6.35). According to Theorems 6.31 and 6.32, the Picard iteration associated to A^p_{i,r_D} converges to $i^* := \beta^{-1}(r^*)$ for all starting points $i \in \hat{I}^p_{r_D}$ and i^* is the unique fixed point of A^p_{i,r_D}.
Aiming at a better readability, the superscript p is omitted throughout this example. Furthermore, we consider $r_D = 0$. First, we construct linear start and test resistance functions $\rho_s(g) := m_s g + d_s$ and $\rho_t = m_t g + d_t$ such that $A_{r_D}(r) = \sigma^-_{r_t} \circ \rho_{t,r_D} \circ \rho^{-1}_{s,r_D} \circ \sigma^+_{r_s}(r)$ is contractive. Note that $r_D = 0$ implies that $\rho_{s,r_D} = \rho_s$ and $\rho_{t,r_D} = \rho_t$. We select

$$m_s = -0.105,\ d_s = 3 \quad \text{and} \quad m_t = -0.1,\ d_t = 1.$$

With these selections, ρ_s and ρ_t are both strictly decreasing, which is in accordance with Lemma 6.17. As linear functions, ρ_s and ρ_t are defined on $\mathbb{R}$. The domains of ρ_s and ρ_t are implicitly specified in the course of this example, when the set $\hat{R}_{r_D}$ is specified below. To obtain A_{r_D}, we are interested in the inverse of ρ_s and consider

$$\rho_s(g) = m_s g + d_t \ \Leftrightarrow\ \rho_s^{-1}(r) = \frac{1}{m_s}(r - d_s).$$

Therefore, the drift resistance iteration function is

$$\begin{aligned} A_{r_D}(r) &= \sigma^-_{r_t} \circ \rho_{t,r_D} \circ \rho^{-1}_{s,r_D} \circ \sigma^+_{r_s}(r) = \sigma^-_{r_t} \circ \rho_t \circ \rho_s^{-1} \circ \sigma^+_{r_s}(r) \\ &= \sigma^-_{r_t} \circ \rho_{t,r_D}\big(\frac{1}{m_s}(r - d_s + r_s)\big) = \frac{m_t}{m_s}(r - d_s + r_s) + d_t - r_t \\ &= m(r - d_s + r_s) + d_t - r_t,\ \text{with } m := \frac{m_t}{m_s}. \end{aligned}$$

Because $m = \frac{m_t}{m_s} = \frac{-0.1}{-0.105} = \frac{100}{105} < 1$, the drift resistance function $A_{r_D}(r)$ is contractive. In particular, it is Lipschitz with the Lipschitz constant $L := m < 1$. Note that $A_{r_D}(r)$ is

strictly increasing, which is in accordance with Lemma 6.34. The fixed point of $A_{r_D}(r)$ *is determined by*

$$A_{r_D}(r^*) = r^* \;\Leftrightarrow\; m(r^* - d_s + r_s) + d_t - r_t = r^* \;\Leftrightarrow\; m(r_s - d_s) + d_t - r_t = (1-m)r^*$$
$$\Leftrightarrow\; r^* = \frac{m(r_s - d_s) + d_t - r_t}{1-m}.$$

In this example, we specify the parameters r_s *and* r_t *by*

$$r_s := \rho_s(g_s) \text{ with } g_s = 2.6 \text{ and } r_t := \rho_t(g_t) \text{ with } g_t = 2.4 \;\Rightarrow\; r_s = 2.727 \text{ and } r_t = 0.76,$$

which results in the fixed point $r^* = -0.42$.
Although this particular iteration function A_{r_D} *is defined on* $\mathbb{R}$*, we must make sure that its domain* $\hat{R}_{r_D}$ *satisfies* $\hat{R}_{r_D} \subset (-r_t, \infty)$ *to be consistent with the assumptions made in this thesis (Lemma 6.4). Let us suppose that the domains* G_s *and* G_t *of the functions* ρ_s *and* ρ_t*, respectively, are selected such that* $\hat{R}_{r_D} = [-r_t + 0.1, -r_t + 5]$*. In particular,* $\hat{R}_{r_D} \subset (-r_t, \infty)$ *is satisfied in this case. Furthermore, we have* $r^* \in \hat{R}_{r_D}$*. In total,* A_{r_D} *is a contractive function on* $\hat{R}_{r_D}$ *with the fixed point* $r^* \in \hat{R}_{r_D}$ *and thus the Picard iteration associated to* A_{r_D} *starting at* r *converges to* r^* *for all* $r \in \hat{R}_{r_D}$ *(Lemma 6.35).*
Next, we consider the corresponding ioni current iteration function A_{i,r_D}*. Recall from Definition 5.9 that* $\beta(i) = \frac{U}{i} - r_t$ *and thus* $\beta^{-1}(r) = \frac{U}{r + r_t}$*. By applying Lemma 6.25, we obtain*

$$A_{i,r_D}(i) = \beta^{-1} \circ A_{r_D} \circ \beta(i) = \beta^{-1} \circ A_{r_D}\left(\frac{U}{i} - r_t\right) = \beta^{-1}\left(m\left(\frac{U}{i} - r_t - d_s + r_s\right) + d_t - r_t\right)$$
$$= \frac{U}{m\left(\frac{U}{i} - r_t - d_s + r_s\right) + d_t - r_t + r_t} = \frac{U}{m\left(\frac{U}{i} - r_t - d_s + r_s\right) + d_t} \;\forall\; i \in \hat{I}_{r_D}. \tag{A.1}$$

Let us suppose that $U = 1$ *in this example. By plugging the values for* U, m, r_s, r_t, d_s *and* d_t *into* (A.1)*, we have*

$$A_{i,r_D}(i) = \frac{1}{\frac{100}{105}\left(\frac{1}{i} - 0.76 - 3 + 2.727\right) + 1} = \frac{105}{100\left(\frac{1}{i} - 1.033\right) + 105} = \frac{105}{\frac{100}{i} + 1.7} \;\forall\, i \in \hat{I}_{r_D}.$$

Recall further, that $\hat{I}_{r_D} = \beta^{-1}(\hat{R}_{r_D})$ *(Definition 6.3), i.e., for all* $i \in \hat{I}_{r_D}$ *there exists (a unique)* $r \in \hat{R}_{r_D}$ *such that* $i = \frac{U}{r + r_t}$.
With this, we can finally select to elements to show that the Lipschitz constant L *of* A_{i,r_D} *is greater than one. Let us consider* $r_1 := 5 - r_t$ *and* $r_2 := 4 - r_t$*. Because* $\hat{R}_{r_D} = [-r_t + 0.1, -r_t + 5]$*, we have* $r_1 \in \hat{R}_{r_D}$ *and* $r_2 \in \hat{R}_{r_D}$ *and thus* $i_1 := \beta^{-1}(r_1) = \frac{U}{r_1 + r_t} = \frac{1}{5 - r_t + r_t} = \frac{1}{5} \in \hat{I}_{r_D}$ *and analogously* $i_2 := \beta^{-1}(r_2) = \frac{1}{4} \in \hat{I}_{r_D}$*. We have*

$$|i_1 - i_2| = \frac{1}{20} \quad \text{as well as} \quad |A_{i,r_D}(i_1) - A_{i,r_D}(i_2)| = \left|\frac{105}{501.7} - \frac{105}{401.7}\right| > 0.052$$

and thus

$$L \geq \frac{|A_{i,r_D}(i_1) - A_{i,r_D}(i_2)|}{|i_1 - i_2|} > 0.052 \cdot 20 = 1.04,$$

i.e., the Lipschitz constant of A_{i,r_D} is greater than one and A_{i,r_D} cannot be contractive. In particular, this example demonstrates that A_{r_D} being contractive does not imply that A_{i,r_D} is contractive.

Example A.2 *This example shows that A^p_{i,r_D} being contractive does not imply that the corresponding drift resistance based ADA iteration function $A^p_{r_D}$ is contractive. Aiming at a better readability, the superscript p is omitted throughout this example. The approach in this example is very similar to that in the preceding Example A.1. We again consider the case $r_D = 0$ and construct linear resistance functions ρ_s and ρ_t. But this time, these are constructed such that A_{r_D} is not contractive but A^p_{i,r_D} is. Furthermore, the construction is more complicated, because this time ρ_t is composed of two piecewise linear functions. We specify the required gvp sets by $G_s = G_t = [-4, 2]$, which is in accordance with Definition 2.18. With this, we define for all $g \in G_s = G_t$*

$$\rho_s(g) := m_s g + d_s \quad \text{and} \quad \rho_t(g) := \begin{cases} m_{t,\ell} g + d_t & \text{if } g \leq 0 =: g_x, \\ m_{t,r} g + d_t & \text{if } g > 0 \end{cases}$$

with

$$m_s = -0.1,\ d_s = 3 \quad \text{as well as} \quad m_{t,\ell} = -0.05,\ m_{t,r} = -0.103 \text{ and } d_t = 2.$$

Furthermore, we select

$$r_s = \rho_s(g_A) \text{ and } r_t = \rho_t(g_A) \text{ with } g_A = -1 \ \Rightarrow\ r_s = 3.1 \text{ and } r_t = 2.05.$$

We are interested in the drift resistance ADA iteration function $A_{r_D}(r) = \sigma^-_{r_t} \circ \rho_{t,r_D} \circ \rho^{-1}_{s,r_D} \circ \sigma^+_{r_s}(r) = \sigma^-_{r_t} \circ \rho_t \circ \rho_s^{-1} \circ \sigma^+_{r_s}(r)$. We consider its domain first. Because $\hat{R}_{r_D} = \rho_s(G_s \cap G_t) - r_s$ (Definitions 5.19 and 6.14), we have $\hat{R}_{r_D} = [-0.3, 0.3]$. Because ρ_t is a piecewise linear function with two segments and the changepoint g_x, the iteration function A_{r_D} consists of two segments as well. For this, we define $r_x := \rho_s(g_x) - r_s = \rho_s(0) - r_s = d_s - r_s = -0.1$. Note that $r_x \in \hat{R}_{r_D}$ and by construction $\rho_s^{-1}(r_x + r_s) = \rho_s^{-1}\big(\rho_s(0) - r_s + r_s\big) = \rho_s^{-1}\big(\rho_s(0)\big) = 0 = g_x$. Therefore, r_x is the changepoint of the two segments of A_{r_D}. Because ρ_s^{-1} is strictly decreasing (Lemma 6.17), we have for all $r \in \hat{R}_{r_D}$

$$r \leq r_x \ \Leftrightarrow\ r + r_s \leq r_x + r_s \ \Leftrightarrow\ \rho_s^{-1}(r + r_s) \geq \rho_s^{-1}(r_x + r_s) = 0,$$

i.e., if $r \leq r_x$, we have to consider the "right segment" of ρ_t and vice versa. Thus, analogously to Example A.1, the drift resistance ADA iteration function is

$$A_{r_D}(r) = \begin{cases} \frac{m_{t,r}}{m_s}(r - d_s + r_s) + d_t - r_t & \text{if } r \leq r_x, \\ \frac{m_{t,\ell}}{m_s}(r - d_s + r_s) + d_t - r_t & \text{if } r > r_x \end{cases}$$

for all $r \in \hat{R}_{r_D}$. Because $\frac{m_{t,r}}{m_s} = \frac{-0.103}{-0.1} = \frac{103}{100} > 1$, the Lipschitz constant of A_{r_D} is greater than one and thus A_{r_D} is not contractive.
Next, we consider the corresponding ioni current based ADA iteration function A_{i,r_D}. Our

goal is to show that A_{i,r_D} *is contractive. We begin with its domain, which is* $\hat{I}_{r_D} = \beta^{-1}(\hat{R}_{r_D}) = \frac{U}{\hat{R}_{r_D}+r_t} = [i_{\min} := \frac{1}{2.35}, i_{\max} := \frac{1}{1.75}]$. *Beacause* A_{r_D} *is composed of two segments and* $A_{i,r_D}(i) = \beta^{-1} \circ A_{r_D} \circ \beta(i)$ *(Lemma 6.25),* A_{i,r_D} *is composed of two segments as well. The changeover point is* $i_x := \beta^{-1}(r_x) = \frac{U}{r_x+r_t} = \frac{1}{1.95} \in \hat{I}_{r_D}$. *Note that for all* $i \in \hat{I}_{r_D}$

$$i \leq i_x \;\Leftrightarrow\; \beta(i) = \frac{U}{i} - r_t \geq \frac{U}{i_x} - r_t = \beta(i_x) = r_x,$$

i.e., if $i \leq i_x$, *we have to consider the "right segment" of* A_{r_D} *and vise versa. Thus, analogously to Example A.1, we have*

$$A_{i,r_D}(i) = \begin{cases} \frac{U}{m_\ell(\frac{U}{i} - r_t - d_s + r_s) + d_t} & \text{if } i \leq i_x, \\ \frac{U}{m_r(\frac{U}{i} - r_t - d_s + r_s) + d_t} & \text{if } i > i_x \end{cases}$$

with $m_\ell := \frac{m_{t,\ell}}{m_s}$ *and* $m_r := \frac{m_{t,r}}{m_s}$ *for all* $i \in \hat{I}_{r_D}$. *By considering* $c_\ell := m_\ell(-r_t - d_s + r_s) + d_t$ *and* $c_r := m_r(-r_t - d_s + r_s) + d_t$, *we can bring* A_{i,r_D} *into a more concise form, which is*

$$A_{i,r_D}(i) = \begin{cases} \frac{U}{m_\ell \frac{U}{i} + c_\ell} = U\big(m_\ell \frac{U}{i} + c_\ell\big)^{-1} & \text{if } i \leq i_x, \\ \frac{U}{m_r \frac{U}{i} c_r} = U\big(m_r \frac{U}{i} + c_r\big)^{-1} & \text{if } i > i_x \end{cases}$$

for $i \in \hat{I}_{r_D}$. *Since we are interested in the Lipschitz constant of* A_{i,r_D}, *we consider the derivatives of the two segments. We apply the chain rule to the left segment of* A_{i,r_D} *to obtain its derivative, which is*

$$\begin{aligned} \frac{d}{di}A_{i,r_D}(i) &= U(-1)\big(m_\ell \frac{U}{i} + c_\ell\big)^{-2} m_\ell U(-1)\frac{1}{i^2} = m_\ell \frac{U^2}{i^2}\frac{1}{\big(m_\ell \frac{U}{i} + c_\ell\big)^2} \\ &= \frac{m_\ell}{\big(m_\ell + \frac{c_\ell}{U} i\big)^2} \;\forall\; i \in \hat{I}_{r_D} \cap (-\infty, i_x). \end{aligned}$$

Analogously, we have

$$\frac{d}{di}A_{i,r_D}(i) = \frac{m_r}{\big(m_r + \frac{c_r}{U} i\big)^2} \;\forall\; i \in \hat{I}_{r_D} \cap (i_x, \infty).$$

We determine the maximum of each derivative, which corresponds to the Lipschitz constant of the corresponding segment of A_{i,r_D}. *We consider the left part first, i.e., we consider the case that* $i \leq i_x$. *For this, we require the value of* c_ℓ, *which is*

$$c_\ell = m_\ell(-r_t - d_s + r_s) + d_t = \frac{-0.05}{-0.1}(-2.05 - 3 + 3.1) + 2 = \frac{1}{2}(-1.95) + 2 = 1.025.$$

Because $c_\ell > 0$, *we have for all* $i \in \hat{I}_{r_D} = [i_{\min}, i_{\max}]$

$$0 < i_{\min} \leq i \;\Rightarrow\; 0 < m_\ell + \frac{c_\ell}{U} i_{\min} \leq m_\ell + \frac{c_\ell}{U} i \;\Rightarrow\; 0 < \big(m_\ell + \frac{c_\ell}{U} i_{\min}\big)^2 \leq \big(m_\ell + \frac{c_\ell}{U} i\big)^2$$

$$\Rightarrow \quad \frac{m_\ell}{\left(m_\ell + \frac{c_\ell}{U} i\right)^2} \leq \frac{m_\ell}{\left(m_\ell + \frac{c_\ell}{U} i_{\min}\right)^2} = \frac{1}{2} \frac{1}{\left(\frac{1}{2} + 1.025 \frac{1}{2.35}\right)^2} = \frac{2209}{3872} =: L_\ell < 1.$$

In other words, $\frac{d}{di} A_{i,r_D}(i) \leq L_\ell < 1$ *for all* $i \in [i_{\min}, i_x)$.
We proceed analogously with the right side and consider

$$c_r = m_r(-r_t - d_s + r_s) + d_t = \frac{103}{100}(-2.05 - 3 + 3.1) + 2 = \frac{103}{100}(-1.95) + 2 = -0.0085.$$

In particular, we have $c_r < 0$. *Furthermore, we have*

$$m_\ell + \frac{c_\ell}{U} i_{\max} = \frac{103}{100} + \frac{-0.0085}{1.75} = \frac{897}{875} > 0.$$

and thus for all $i \in \hat{I}_{r_D} = [i_{\min}, i_{\max}]$

$$\begin{aligned} i \leq i_{\max} \quad &\Rightarrow \quad c_r i \geq c_r i_{\max} \quad \Rightarrow \quad m_r + \frac{c_r}{U} i \geq m_r + \frac{c_r}{U} i_{\max} > 0 \\ &\Rightarrow \quad \left(m_r + \frac{c_r}{U} i\right)^2 \geq \left(m_r + \frac{c_r}{U} i_{\max}\right)^2 > 0 \\ &\Rightarrow \quad \frac{m_r}{\left(m_r + \frac{c_r}{U} i\right)^2} \leq \frac{m_r}{\left(m_r + \frac{c_r}{U} i_x\right)^2} = \frac{103}{100}\left(\frac{875}{897}\right)^2 = \frac{3154375}{3218436} =: L_r < 1. \end{aligned}$$

In other words, $\frac{d}{di} A_{i,r_D}(i) \leq L_r < 1$ *for all* $i \in (i_x, i_{\max}]$. *Because* A_{i,r_D} *is continuous in* i_x, *the Lipschitz constant of* A_{i,r_D} *is* $L = \max\{L_\ell, L_r\} = L_r < 1$ *and thus* A_{i,r_D} *is contractive. In total* A_{i,r_D} *is contractive while its counterpart* A_{r,r_D} *is not.*
To conclude this example, we consider the fixed points of the iteration functions. First, we show that the fixed point of the drift resistance iteration function A_{r_D} *is* $r^* = 0$. *Recall that* $r_D = 0$, $g_A = 0$ *and* $r_s = \rho_s(g_A)$ *as well as* $r_t = \rho_t(g_A)$. *Therefore, we have*

$$A_{r_D}(0) = \sigma_{r_t}^- \circ \rho_t \circ \rho_s^{-1} \circ \sigma_{r_s}^+(0) = \sigma_{r_t}^- \circ \rho_t \circ \rho_s^{-1} \circ \rho_s(g_A) = \sigma_{r_t}^- \circ \rho_t(g_A) = r_t - r_t = 0.$$

According to Theorem 6.31, $i^* := \beta^{-1}(r^*)$ *is the fixed point of* A_{i,r_D}. *Therefore, the Picard iteration associated to* A_{i,r_D} *starting at* i *converges to* i^* *for all* $i \in \hat{I}_{r_D}$ *(Lemma 6.35). Then, the Picard iteration associated to* A_{r_D} *starting at* r *converges to* r^* *for all* $r \in \hat{R}_{r_D}$ *(Theorem 6.32). This is noteworthy, because* A_{r,r_D} *is not contractive.*

Notation Cheat Sheet Dissertation Tobias Suszka

Constants

$U \in \mathbb{R}_{>0} := \{x \in \mathbb{R} : x > 0\}$: DC voltage (is fixed and constant)
$r_D \in \mathbb{R}_{\geq 0} := \{x \in \mathbb{R} : x \geq 0\}$: drift resistance (Assumption 3.10)

HE model (without drift and with drift)

Def. 2.18: $\mathcal{H} = \big(\mathrm{FS}, (G_{\mathrm{fs}})_{\mathrm{fs}\in\mathrm{FS}}, (\iota_{\mathrm{fs}})_{\mathrm{fs}\in\mathrm{FS}}, (\Lambda_{\mathrm{fs}})_{\mathrm{fs}\in\mathrm{FS}}, (\zeta_{\mathrm{fs}})_{\mathrm{fs}\in\mathrm{FS}}\big)$
$\mathrm{FS} = [\mathrm{fs}_{\min}, \mathrm{fs}_{\max}]$: set of feasible fan speeds
G_{fs}: set of feasible gas valve positions wrt. $\mathrm{fs} \in \mathrm{FS}$; is closed and bounded interval
$\iota_{\mathrm{fs}} : G_{\mathrm{fs}} \to I_{\mathrm{fs}} \subset \mathbb{R}_{>0}$: ioni current function wrt. fs; is strictly increasing homeomorphism
$\Lambda_{\mathrm{fs}} : G_{\mathrm{fs}} \to L_{\mathrm{fs}} \subset \mathbb{R}_{>0}$: equivalence AFR function wrt. fs; is strictly decreasing homeomorphism
$\zeta_{\mathrm{fs}} : G_{\mathrm{fs}} \to \mathbb{R}_{>0}$: CO emission function wrt. fs; is convex and continuous
$I_{\mathrm{fs}} := \iota_{\mathrm{fs}}(G_{\mathrm{fs}})$, $L_{\mathrm{fs}} := \Lambda_{\mathrm{fs}}(G_{\mathrm{fs}})$; both are closed and bounded intervals (Def. 2.22)
$\iota_{\mathrm{fs},r_D} := \frac{U\iota_{\mathrm{fs}}}{r_D\iota_{\mathrm{fs}}+U}$: drifted ioni current function wrt. fs; is strictly increasing homeo. (Def. 3.12)
$I_{\mathrm{fs},r_D} := \iota_{\mathrm{fs},r_D}(G_{\mathrm{fs}}) \subset \mathbb{R}_{>0}$: set of drifted ioni currents wrt. fs (Notation 3.17)

ADA Parameters / ADA pairs

$[N] := \{1, \dots, N\}$ for fixed $N \in \mathbb{N}$
$s^p, t^p \in \mathrm{FS}$: start and test fan speed of the p-th ADA pair (Notation 5.1)
$i_s^p \in I_{s^p}$ and $i_t^p \in I_{t^p}$: start and test ioni current, respectively, of pair p (Notation 5.1)
(s^p, t^p, i_s^p, i_t^p): ADA parameters of the p-th ADA pair, $p \in [N]$ (Def. 5.2)
$r_s^p := \frac{U}{i_s^p}$, $r_t^p = \frac{U}{i_t^p}$: start and test resistance, respectively, of the p-th ADA pair (Def. 5.7)
$i_{s,r_D}^p := \frac{i_s^p U}{i_s^p r_D+U}$, $i_{t,r_D}^p := \frac{i_t^p U}{i_t^p r_D+U}$: drifted start and test ioni current, respectively (Def. 3.27)
$\hat{\boldsymbol{i}}_{t,r_D} = (i_1, \dots, i_N) \subset \mathbb{R}_{>0}^N$: vector of drifted test ioni current approximations (Alg. 5.1)
$\alpha_{\hat{\boldsymbol{i}}_{t,r_D}} : \mathrm{FS} \to \mathbb{R}$: drift resistance approximation function given the vector $\hat{\boldsymbol{i}}_{t,r_D}$, maps a fan speed to the corresponding drift resistance approximation (Def. 3.38)
w^p: weight with $0 < w^p < 1$, s.t. $s^p = w^p t^p + (1 - w^p)t^{p-1}$ (Def. 5.12 and Lemma 5.13)

Formalism: sets and functions

$\hat{R}_{r_D}^p := \frac{U}{\iota_{s^p,r_D}(G_{s^p} \cap G_{t^p})} - r_s^p$: set of feasible drift resistance approximations of pair p (Def. 5.19)
$\beta^p : \mathbb{R}_{>0} \to (-r_t^p, \infty)$, $\beta^p(i) := \frac{U}{i} - \frac{U}{i_t^p}$: transforms approximation of i_{t,r_D}^p to corresponding approximation of r_D at the test fan speed t^p; is decreasing homeomorphism (Def. 5.9 and L. 5.11)
$\hat{I}_{r_D}^p := (\beta^p)^{-1}(\hat{R}_{r_D}^p)$: set of feasible drifted test ioni current approximations of pair p (Def. 6.3)
$\gamma^p : \hat{R}^p \to \iota_{s^p,r_D}\big(G_{s^p} \cap G_{t^p}\big)$, $\gamma^p(r) := i_s^p \frac{U}{i_s^p \cdot r+U}$: maps approximation of r_D to the corresponding approximation of i_{s,r_D}^p; is strictly decreasing (Def. 5.22)
$\omega^p(x, y) = w^p x + (1 - w^p)y$: weighted sum of x and y with weight w^p (Def. 5.17)

ADA procedure with a single ADA pair: ioni current based

$A_{i,r_D}^p : \hat{I}_{r_D}^p \to \mathbb{R}$, $\quad A_{i,r_D}^p := \iota_{t^p,r_D} \circ \iota_{s^p,r_D}^{-1} \circ \gamma^p \circ \beta^p$: ioni current based ADA iteration function of the p-th ADA pair (Def. 6.5)

ADA procedure with a single ADA pair: resistance based

$R_{\mathrm{fs}} := \frac{U}{I_{\mathrm{fs}}}$: set of resistances wrt. fs, $\mathrm{fs} \in \mathrm{FS}$ (Def. 6.14)

$R_{\mathrm{fs},r_D} := \frac{U}{I_{\mathrm{fs},r_D}}$: set of drifted resistances at the fan speed fs (Def. 6.14)

$\sigma_c^+ : \mathbb{R} \to \mathbb{R}$, $\sigma_c^+(x) := x + c$: auxiliary function that adds the constant c (Def. 6.18)

$\rho_{\mathrm{fs}} : G_{\mathrm{fs}} \to R_{\mathrm{fs}}$, $\rho_{\mathrm{fs}} := \frac{U}{\iota_{\mathrm{fs}}}$: resistance function wrt. fs (Def. 6.14)

$\rho_{\mathrm{fs},r_D} : G_{\mathrm{fs}} \to R_{\mathrm{fs},r_D}$, $\rho_{\mathrm{fs},r_D} := \frac{U}{\iota_{\mathrm{fs},r_D}} = \sigma^+_{r_D} \circ \rho_{\mathrm{fs}}$: drifted resistance fct. wrt. fs (Def. 6.14 and L. 6.20)

$A^p_{r_D} : \hat{R}^p_{r_D} \to \mathbb{R}$, $A^p_{r_D} := \sigma^-_{r_t^p} \circ \rho_{t^p,r_D} \circ \rho^{-1}_{s^p,r_D} \circ \sigma^+_{r_s^p}$: drift resistance iteration function of the p-th ADA pair (Def. 6.21)

ADA procedure with a plurality of pairs (following definitions are only valid for $p \geq 2$)

$\omega^p_v(r) := w^p r + (1 - w^p)v$: "one-dimensional" weighted sum function (Def. 7.1)

$V^p_{r_D}$: set of feasible upper neighbor drift resistance approximations of ADA pair p, i.e., $v \in V^p_{r_D}$ corresponds to the drift resistance approximation of pair $p-1$ (Def. 7.4)

$\hat{R}^p_{r_D,v} := \left(\omega^p_v\right)^{-1}(\hat{R}^p_{r_D})$: set of feasible drift resistance approximations of pair p given v (Def. 7.4)

$\hat{I}^p_{r_D,v} := \left(\beta^p\right)^{-1}(\hat{R}^p_{r_D,v})$: set of feasible drifted test ioni current approximations of pair p given v (Def. 7.4)

$B^p_{r_D,v} : \hat{I}^p_{r_D,v} \to \mathbb{R}$, $B^p_{r_D,v} := \iota_{t^p,r_D} \circ \iota^{-1}_{s^p,r_D} \circ \gamma^p \circ \omega^p_v \circ \beta^p$: ioni current based iteration function of ADA pair p given v with $v = \beta^{p-1}(i_{p-1}) \in V^p_{r_D}$ (Def. 7.8)

$C^p_{r_D,v} : \hat{R}^p_{r_D,v} \to \mathbb{R}$, $C^p_{r_D,v} := A^p_{r_D} \circ \omega^p_v = \sigma^-_{r_t^p} \circ \rho_{t^p,r_D} \circ \rho^{-1}_{s^p,r_D} \circ \sigma^+_{r_s^p} \circ \omega^p_v$: resistance based iteration function of ADA pair p given v, $v \in V^p_{r_D}$ (Def. 7.36)

$u(n)$: ADA subsequence that contains first n entries of u (Def. 7.20)

$\boldsymbol{i}^n(\hat{\boldsymbol{i}}_{\boldsymbol{t},\mathrm{in}}, u) = (i_1^n, \ldots, i_N^n) := \hat{\boldsymbol{i}}_{\boldsymbol{t},\mathrm{out}}\big(\hat{\boldsymbol{i}}_{\boldsymbol{t},\mathrm{in}}, u(n)\big)$: n-th (ioni current based) ADA iterate (Def. 7.22), corresponds to output of Algorithm 5.2 after n-th iteration (Corollary 7.23)

$\boldsymbol{r}^n(\hat{\boldsymbol{i}}_{\boldsymbol{t},\mathrm{in}}, u) = (r_1^n, \ldots, r_N^n)$, with $r_p^n := \beta^p(i_p^n)$: n-th resistance based ADA iterate (Def. 7.28)

$\boldsymbol{i}^{**} = (i_1^{**}, \ldots, i_N^{**})$: (ioni current based) super fixed point vector recursively defined by $i_1^{**} = \mathrm{fix}(A^1_{\cdot})$ and $i_p^{**} = \mathrm{fix}\big(B^p_{\beta^{p-1}(i^{**}_{p-1})}\big)$ for $p \geq 2$ (Def. 7.14)

$\boldsymbol{r}^{**} = (r_1^{**}, \ldots, r_N^{**})$: drift resistance super fixed point vector defined by $r_p^{**} = \beta^p(i_p^{**})$ (Def. 7.32) and recursively calculated by $r_1^{**} = \mathrm{fix}(A^1)$ and $r_p^{**} = \mathrm{fix}\big(C^p_{r^{**}_{p-1}}\big)$ for $p \geq 2$ (Lemma 7.42)

feasible super fixed point vector: if $\boldsymbol{i}^{**} \in \mathbb{R}^N$ holds (Def. 7.14)

feasible scenario: we consider (s^p, t^p, i_s^p, i_t^p), $p \in [N]$, $\mathcal{H}$ and $r_D \geq 0$ s.t. $\boldsymbol{i}^{**} \in \mathbb{R}^N_{>0}$ (Def. 7.16)

feasible input combination: input vector $\hat{\boldsymbol{i}}_{\boldsymbol{t},\mathrm{in}}$ and ADA update sequence u such that for all $n \in \mathbb{N}$ (or $n \in [\ell]$) $\boldsymbol{i}^n(\hat{\boldsymbol{i}}_{\boldsymbol{t},\mathrm{in}}, u) \in \mathbb{R}^N_{>0}$ holds (Def. 7.24)

Optimization models

$T = \{t^1, \ldots, t^N\}$ s.t. $\mathrm{fs}_{\min} \leq t^N < \cdots < t^1 < \mathrm{fs}_{\max}$: set of feasible test fan speeds (Def. 8.1)

$\mathcal{L}^p_{T,r_D}(s^p, i_s^p, i_t^p)$: Lipschitz constant of $A^p_{r_D}$ wrt. ADA pair (s^p, t^p, i_s^p, i_t^p) (Def. 8.17)

$\mathcal{S}_{T,r_D}(s^p, i_s^p, i_t^p) = \Lambda_{s^p} \circ \iota^{-1}_{t^p}(i_t^p) - \Lambda_{s^p} \circ \iota^{-1}_{s^p} \circ i_{\mathrm{set}}(s^p)$: start point increment of pair p (Def. 8.59)

X^p_{T,r_D}: set of feasible ADA parameters of ADA pair p wrt. T and r_D (Def. 8.52)

(nom-P^p_{T,r_D}): nominal optimization problem for ADA pair p (Def. 8.61)

$X^{\mathrm{tol}}_{T,r_D}(\mathcal{H}_{\mathrm{nom}}, \mathcal{U}_{\mathrm{tol}})$: set of feasible solutions with respect to tolerances (Def. 8.81)

(tol-P_{T,r_D}): ADA optimization problem with respect to tolerances (Def. 8.84)